NASA-CP-3201 19930021759

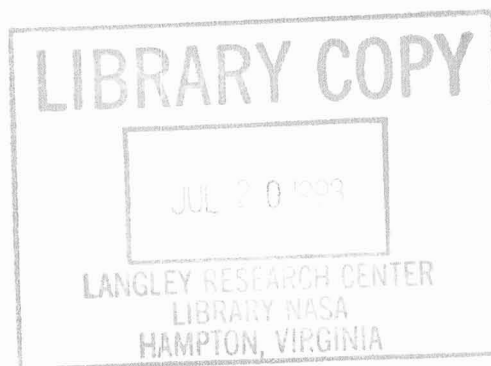*NASA Conference Publication 3201*

National Educators' Workshop: Update 92

Standard Experiments in Engineering Materials Science and Technology

Proceedings of a workshop held in Oak Ridge, Tennessee November 11–13, 1992

NIST   NSU   DEPARTMENT OF ENERGY · UNITED STATES OF AMERICA   NASA

NASA Conference Publication 3201

National Educators' Workshop: Update 92

Standard Experiments in Engineering Materials Science and Technology

Compiled by
James E. Gardner
NASA Langley Research Center
Hampton, Virginia

James A. Jacobs
Norfolk State University
Norfolk, Virginia

Douglas F. Craig
Oak Ridge National Laboratory
Oak Ridge, Tennessee

NASA

National Aeronautics and
Space Administration

Office of Management

Scientific and Technical
Information Program

1993

PREFACE

NEW:Update 92 was held during the anniversaries of two of our sponsors: Oak Ridge National Laboratory (ORNL) celebrating 50 years and NASA Langley Research Center (NASA LaRC) celebrating 75 years. The workshop was held November 11-13, 1992, at Oak Ridge National Laboratory (ORNL) in Oak Ridge, Tennessee. As with previous workshops, the theme was strengthening materials education. Participants witnessed demonstrations of experiments, discussed issues of materials science and engineering (MS&E) with people from education, industry, government, and technical societies and heard about new MS&E developments. Faculty in attendance represented community colleges, smaller colleges, and major universities.

Marking the 7th annual **NEW:Update**, we continue to see an increase in the quantity and quality of experiments and demonstrations related to materials science through the efforts of the presenters and writers of the materials enclosed in this notebook. This year we added a set of half day mini workshops utilizing the facilities and expertise at ORNL.

Through the invaluable coordination of Mr. James Gardner, of NASA, announcements, mailings, and the production of the this **NEW:Update 92** publication are possible. Dr. Linda Horton, with involvement of Mr. Edward Aebischer and Ms. Bonnie Reesor, provided the key link in making arrangements at ORNL and with the Department of Energy. Dr. Robert Berrettini, of the Materials Education Council, arranged for a distinguished review panel to provide peer review of the experiments. At Norfolk State University Ms. Diana LaClaire, Dr. Heidi Ries and Mr. Todd Winters have kept the workshop activities on track. We also wish to recognize all of you for continuing to support these on-going efforts to strengthen materials education. We received continual praise, input, and requests for the products of the **NEW:Update** series from around the nation and world.

As with past **NEW:Updates**, we developed this year's workshop based on the input from participants of previous workshops. An extensive peer review process of experiments was followed. After submission of abstracts, selected authors were notified of their acceptance and given the format for submission of experiments. Experiments were reviewed by a panel of specialists through the cooperation of the Materials Education Council. Authors received comments from the panel prior to NEW:Update 92, allowing them to make necessary adjustments prior to demonstrating their experiments. Participants at **NEW:Update 92** also provided verbal and written comments to authors/presenters. Finally, the NASA LaRC editorial staff provided a quality check of the documents for grammar, spelling, etc.

NEW:Update 92, as with previous NEW:Updates, resulted from considerable cooperative efforts among individuals in government, education, and industry. The workshops' goals are to maintain the network of participants and to continue to collect these ideas and resources to bring them together in a comprehensive collection of experiments and demonstrations in materials science, engineering and technology.

The three-stage review process coupled with field testing, promotes useful experiments and demonstrations. With this publication, we will have produced 139 experiments and demonstrations. For past issues see ordering information on page v.

With involvement of the Materials Education Council and the Materials Division of the American Society for Engineering Education, we have begun steps to select experiments and demonstrations from previous NEW:Updates to produce a new publication for distribution throughout the materials education community.

We hope that the material presented in this publication will assist you in teaching about materials science, engineering and technology. We would like to have your comments on their value and means of improving them. Please send comments to James A. Jacobs, School of Technology, Norfolk State University, Norfolk, Virginia 23504.

NEW:Update 93 is being planned for November 2-5, 1993, at NASA Langley Research Center (LaRC) in Hampton, Virginia. As with this year, we plan to spend a part of a day with small groups in various labs at NASA LaRC.

The use of trademarks or manufacturers' names in this publication does not constitute endorsement, either expressed or implied, by the National Aeronautics and Space Administration.

Workshop Co-Directors

Douglas F. Craig
Metals and Ceramics Division
Oak Ridge National Laboratory

James A. Jacobs
Professor of Engineering Technology
Norfolk State University

Liaisons

James E. Gardner, NASA-LaRC
Roy Bunnell, ASM International
Robert Berrettini, Materials Education Council
Linda Horton, Oak Ridge National Laboratory
Edward Aebischer, Oak Ridge National Laboratory

Director's Assistant
Diana P. LaClaire
Norfolk State University

Organization Committee Members

Seth Bates, San Jose State University
William Callister, Materials Div., ASEE
David Werstler, Materials Div., ASEE
Jonice Harris, NIST
William Winn, Department of Energy
Woodrow W. Leake, ASEE
Robert J. Sullivan, WMCO

Peggy Weeks, Corning Community College
John W. Patterson, Iowa State Univ.
Heidi Ries, Norfolk State University
Thomas F. Kilduff, Thomas Nelson Community College
F. Xavier Spiegel, Loyola College
Jennifer Taylor, NYS College of Ceramics at Alfred
James Thomas, American Society for Testing & Materials

CONTENTS

REVIEWERS FOR NEW:Update 92

Nicholas Akinkuoye
Assistant Professor
Dept. of Industrial Education and
Technology
Iowa State University

Else Breval
Senior Research Associate
Materials Research Laboratory
Pennsylvania State University

Witold Brostow
Professor of Materials Science
Center for Materials Characterization
University of North Texas

Paul Brown
Associate Professor of Ceramic Science
and Engineering
Materials Research Laboratory
Pennsylvania State University

William D. Callister
Materials Science and Engineering
University of Utah

Wenwu Cao
Research Associate
Materials Research Laboratory
Pennsylvania State University

James A. Clum
Mechanical & Industrial Engineering
T. J. Watson School of Engineering
State University of N.Y. at Binghamton

Thomas Gorman
Assistant Professor
Department of Forest Products
University of Idaho

Girish Harshe
Postdoctoral Fellow, MRL
Pennsylvania State University

Sue Hayle
Research Associate
Materials Research Laboratory
Pennsylvania State University

James Provan
Dean of Engineering
University of Victoria
British Columbia, Canada

Jerzy Ruzyllo
Associate Professor of Electrical
Engineering
Pennsylvania State University

Mary Shaw
Assistant Professor, Engineering
Science and Mechanics Department
Pennsylvania State University

M. S. Wang
Professor of Civil Engineering
Pennsylvania State University

PARTICIPANTS

==

Edward Aebischer
Manager, University & Educational Programs
Martin Marietta Energy Systems, Inc.
Oak Ridge National Laboratory
P. O. Box 2008
Oak Ridge, TN 37831
615-574-0762

Abayomi Ajayi-Majebi
Central State University
114-A Jenkins
Wilberforce, OH 45384
513-376-6525

Robert Berrettini
Materials Education Council
Materials Research Laboratory
University Park, PA 16802
814-865-1643

Peter J. Blau
Martin Marietta Energy Systems, Inc.
Oak Ridge National Laboratory
P. O. Box 2008
Oak Ridge, TN 37831-6063
615-574-5377

W. V. Brewer
1031 Voorhees Avenue
Jackson State University
Jackson, MS 39209
601-968-2466

Robert J. Brungraber
Bucknell University
Lewisburg, PA 17837
908-879-4174 (home)

L. Roy Bunnell
Battelle
Pacific Northwest Laboratories
P. O. Box 999 MSIN P8-44
Richland, WA 99352
509-376-2799

Douglas F. Craig
Director, Metals & Ceramics Division
Oak Ridge National Laboratory
Martin Marietta Energy Systems, Inc.
P. O. Box 2008
Oak Ridge, TN 37831-6263
615-574-4065

Jai N. Dahiya
Southeast Missouri State University
One University Plaza
Cape Girardeau, MO 63701
314-651-2390

C. Ray Diez
University of North Dakota
P.O. Box 8057
Grand Forks, ND 58202
701-777-2249 ext. 2198

Ravinder Diwan
Southern University
Mechanical Engineering Department
Baton Rouge, LA 70813
504-771-4705

Russell Eng
Portland Community College
12000 SW 49th Avenue
Portland, OR 97219-0990
503-244-6111 Ext. 4653

William D. Forgeng
California Polytechnic State University
Materials Engineering Department
San Luis Obispo, CA 83407
805-756-1537

James E. Gardner
NASA Langley Research Center
11 Langley Boulevard MS-118
Hampton, VA 23681-0001
804-864-6003

Robert J. Gray
Metals & Ceramics Division
ORNL, P.O. Box 2008
Oak Ridge, TN 37831-6139
615-574-4069

George T. Hahn
Vanderbilt University
Box 1593 Sta B
Nashville, TN 37235
615-322-3594

Ian W. Hall
University of Delaware
Spencer Laboratory
Newark, DE 19716
302-831-1295

John M. Henshaw, P.E.
Dept. of Mechanical Engineering
University of Tulsa
Tulsa, OK 74104
918-631-3002

Astor Y. Herrell
Winston-Salem State University
P. O. Box 13236
Winston-Salem, NC 27110
919-750-2543

David Hinaman
Westinghouse Environmental Management
Co. of Ohio
P. O. Box 398704
Cincinnati, OH 45239-8704

Linda Horton
Oak Ridge National Laboratory
Martin Marietta Energy Systems, Inc.
P. O. Box 2008
Oak Ridge, TN 37831-6263
615-574-5081

Matthew Hsu
Materials Research Center
Northwestern University
2145 Sheridan Road
Evanston, IL 60208-3116
708-491-3607

Emil H. Isaacson
University of District of Columbia
39 Great Pines Court
Rockville, MD 20850
301-762-1277

James A. Jacobs
Norfolk State University
2401 Corprew Avenue
Norfolk, VA 23504
804-683-8109

Thomas J. Jenkins
Dept. of Electrical & Computer Engr.
(AFIT/ENG Bldg. 640 Area B)
Air Force Institute of Technology
Wright-Patterson Air Force Base
Ohio 45433-6583
513-255-3708; 4960; 6027

Norman Johnston
NASA Langley Research Center
MS-226
Hampton, VA 23681-0001
804-864-4260

Lisa Ketron
Hocking Tech. College
3301 Hocking Parkway
Nelsonville, OH 45764
614-753-3591

Thomas F. Kilduff
504 Brafferton Circle
Hampton, VA 23663-1921
804-851-0272

Howard A. Kuhn, Program Director
National Center for Excellence
Metalworking Processing Technology
1450 Scalp Avenue
Johnstown, PA 15904
814-269-2426

Nikhil K. Kundu
Purdue University
Statewide Technology
2424 California Road
Elkhart, IN 46514
219-264-3111

Woodrow W. Leake
Deputy Executive Director
American Society for Engineering Education
Suite 200 Eleven Dupont Circle
Washington, DC 20036
202-293-7080

Stephen Lin
Department of Chemistry
North Carolina Central
3116 Annandale Road
Durham, NC 27707
919-560-6100

Ping Liu
Eastern Illinois University
School of Technology
101 Klehm Hall
Charleston, IL 61920
217-581-6267

Jed S. Lyons
Dept. of Mechanical Engineering-Sumwalt
University of South Carolina
Columbia, SC 29208
803-777-9552

Pat L. Mangonon
Florida Institute of Technology
150 W. University Blvd.
Melbourne, FL 32901
407-768-8000/8068/7560

Mark I. Marpet
St. John's University
Staten Island Campus
300 Howard Avenue
Staten Island, NY 10301
718-390-4545

Donald H. Martin
Tri State University
Manufacturing Technology
Angola, IN 46703-0307
219-665-4100

James V. Masi
Western New England College
Dept. of Electrical Engineering
Springfield, MA 01119
413-782-1344

Harvey E. Miller
Oral Roberts University
7777 S. Lewis Avenue
Tulsa, OK 74171
918-495-6952

David Needham
Duke University
Department Mechanical Engineering
    & Materials Science
Durham, NC 27706
919-660-5329

Thomas Nunnelley
Tarrant County Junior College
5301 Campus Drive
Fort Worth, TX 76119
817-531-4779

Matthew A. Panhans
Milwaukee School of Engineering
1025 N. Milwaukee
Milwaukee, WI 53202
414-277-7277

Edwin J. Prior
NASA-Langley Research Center
MS- 400
Hampton, VA 23681-0001

Mansur Rastani, P.E., CMfgE
Department of Manufacturing Systems
NC A&T State University
Greensboro, NC 27411
919-334-7585

Bonnie Reesor
Oak Ridge National Laboratory
Martin Marietta Energy Systems, Inc.
P. O. Box 2008
Oak Ridge, TN 37831
615-574-5984

Heidi·Ries
Norfolk State University
2401 Corprew Avenue
Norfolk, VA 23504
804-683-8020

William Ross
Muskegon Community College
221 S. Quarterline
Muskegon, MI 49442
616-777-0367

Rustum Roy
The Materials Research Laboratory
The Pennsylvania State University
University Park, PA 16802
814-865-9951

Hui-Ru Shih
Department of Technology
Jackson State University
1400 J. R. Lynch Street
Jackson, MS 39217
601-968-2466

Ram N. Singh
St. Louis Community College
3400 Pershall Road
St. Louis, MO 63135-1499
314-595-2311

Alphonso C. Smith
Hampton University
Department of Engineering   1F
Hampton, VA 23668
804-727-5292

Carl Smith
Kanawha Manufacturing Co.
and WVU at Parkersburg
1520 Dixie Street
Charleston, WV 25311
304-342-6127

F. Xavier Spiegel
Department of Engineering
Loyola College
4501 N. Charles Street
Baltimore, MD 21210
410-617-2515

A. F. Sprecher
Dept of Materials Science & Engineering
North Carolina State University
Raleigh, NC 27695-7907
919-515-2377

Patrick M. Stephan
Norton Diamond Film
Goddard Road
Northboro, MA 01532-1545
508-351-7600

Ali Taba-Tabai
Don Bosco Technical Institute
1151 San Gabriel Boulevard
Rosemead, CA 91770
818-280-0451

A. H. Tabrizi
Evergreen Valley College
3095 Yerba Buena Road
San Jose, CA 95135
408-274-7900

H. Richard Thornton
Texas A&M University
Department of Mechanical Engineering
College Station, TX 77843-3123
409-845-6151

Steven M. Tipton
The University of Tulsa
Mechanical Engineering Department
600 S. College
Tulsa, OK 74104
918-631-3000

Jeffrey Wagner
Westinghouse Environmental Management
Co. of Ohio
P. O. Box 398704
Cincinnati, OH 45239-8704
513-738-6084

Tom Waskom
Eastern Illinois University
School of Technology - Klehm Hall
Charleston, IL 61920
217-581-5762

Martin Weiser
Mechanical Engineering Department and
Center for Micro-Engineéred Ceramics
University of New Mexico
Albuquerque, NM 87131
505-277-2831

David Werstler
Western Washington University
Technology Department
Bellingham, WA 98225-9086
206-676-3447

Harvey A. West
Dept of Materials Science & Engineering
North Carolina State University
Raleigh, NC 27695-7907
919-515-2377

Jerry L. Wickman
Plastics Research and
Education Center
Ball State University
College of Applied Sciences and Technology
Department of Industry and Technology
Muncie, IN 47306-0255
317-285-5641

Edward L. Widener
MET Department
Purdue University
Knoy Hall - Room 119
West Lafayette, IN 47907
317-494-7521

Todd A. Winters
Norfolk State University
2401 Corprew Avenue
Norfolk, VA 23504
804-683-8109

LISTING OF EXPERIMENTS FROM NEW:UPDATES

EXPERIMENTS & DEMONSTRATIONS IN TESTING AND EVALUATION

NEW:Update 88   **NASA Conference Publication 3060**
Sastri, Sankar. "Fluorescent Penetrant Inspection"
Sastri, Sankar. "Magnetic Particle Inspection"
Sastri, Sankar. "Radiographic Inspection"

NEW:Update 89   **NASA Conference Publication 3074**
Chowdhury, Mostafiz R. and Chowdhury, Farida. "Experimental Determination of Material Damping
        Using Vibration Analyzer"
Chung, Wenchiang R. "The Assessment of Metal Fiber Reinforced Polymeric Composites"
Stibolt, Kenneth A. "Tensile and Shear Strength of Adhesives"

NEW:Update 90   **NIST Special Publication 822**
Azzara, Drew C. "ASTM: The Development and Application of Standards"
Bates, Seth P. "Charpy V-Notch Impact Testing of Hot Rolled 1020 Steel to Explore Temperature Impact
        Strength Relationships"
Chowdhury, Mostafiz R. "A Nondestructive Testing Method to Detect Defects in Structural Members"
Cornwell, L. R., Griffin, R. B., and Massarweh, W. A. "Effect of Strain Rate on Tensile Properties of
        Plastics"
Gray, Stephanie L., Kern, Kristen T., Harries, Wynford L., and Long, Sheila Ann T.
        "Improved Technique for Measuring Coefficients of Thermal Extension for Polymer Films"
Halperin, Kopl. "Design Project for the Materials Course: To Pick the Best Material for a Cooking Pot"
Kundu, Nikhil. "Environmental Stress Cracking of Recycled Thermoplastics"
Panchula, Larry and Patterson, John W. "Demonstration of a Simple Screening Strategy for Multifactor
        Experiments in Engineering"
Taylor, Jenifer A. T. "How Does Change in Temperature Affect Resistance?"
Wickman, Jerry L. and Corbin, Scott M. "Determining the Impact of Adjusting Temperature Profiles on
        Photodegradability of LDPE/Starch Blown Film"
Widener, Edward L. "It's Hard to Test Hardness"
Widener, Edward L. "Unconventional Impact-Toughness Experiments"

NEW:Update 91   **NASA Conference Publication 3151**
Bunnell, L. Roy. "Tempered Glass and Thermal Shock of Ceramic Materials"
Lundeen, Calvin D. "Impact Testing of Welded Samples"
Gorman, Thomas M. "Designing, Engineering, and Testing Wood Structures"
Strehlow, Richard R. "ASTM - Terminology for Experiments and Testing"
Karplus, Alan K. "Determining Significant Material Properties, A Discovery Approach"
Spiegel, F. Xavier and Weigman, Bernard J. "An Automated System for Creep Testing"
Denton, Nancy L. and Hillsman, Vernon S. "Isotropic Thin-Walled Pressure Vessel Experiment"
Allen, David J. "Stress-Strain Characteristics of Rubber-Like Materials: Experiment and
        Analysis"
Dahl, Charles C. "Computer Integrated Lab Testing"
Cornwell, L. R. "Mechanical Properties of Brittle Material"

Bunnell, L. Roy. "Temperature-Dependent Electrical Conductivity of Soda-Lime Glass and Construction and Testing of Simple Airfoils to Demonstrate Structural Design, Materials Choice, and Composite Concepts"

Marpet, Mark I. "Walkway Friction: Experiment and Analysis"

Martin, Donald H. "Application of Hardness Testing in Foundry Processing Operations: A University and Industry Partnership"

Masi, James V. "Experiments in Corrosion for Younger Students By and For Older Students"

Needham, David. "Micropipet Manipulation of Lipid Membranes: Direct Measurement of the Material Properties of a Cohesive Structure That is Only Two Molecules Thick"

Perkins, Steven W. "Direct Tension Experiments on Compacted Granular Materials"

Shih, Hui-Ru. "Development of an Experimental Method to Determine the Axial Rigidity of a Strut-Node Joint"

Spiegel, F. Xavier. "An Automated Data Collection System For a Charpy Impact Tester"

Tipton, Steven M. "A Miniature Fatigue Test Machine"

Widener, Edward L. "Tool Grinding and Spark Testing"

EXPERIMENTS & DEMONSTRATIONS IN METALS

NEW:Update 88   NASA Conference Publication 3060

Nagy, James P. "Sensitization of Stainless Steel"

Neville, J. P. "Crystal Growing"

Pond, Robert B. "A Demonstration of Chill Block Melt Spinning of Metal"

Shull, Robert D. "Low Carbon Steel: Metallurgical Structure vs. Mechanical Properties"

NEW:Update 89   NASA Conference Publication 3074

Balsamel, Richard. "The Magnetization Process - Hysteresis"

Beardmore, Peter. "Future Automotive Materials - Evolution or Revolution"

Bunnell, L. Roy. "Hands-On Thermal Conductivity and Work-Hardening and Annealing in Metals"

Kazem, Sayyed M. "Thermal Conductivity of Metals"

Nagy, James P. "Austempering"

NEW:Update 90   NIST Special Publication 822

Bates, Seth P. "Charpy V-Notch Impact Testing of Hot Rolled 1020 Steel to Explore Temperature Impact Strength Relationships"

Chung, Wenchiang R. and Morse, Margery L. "Effect of Heat Treatment on a Metal Alloy"

Rastani, Mansur. "Post Heat Treatment in Liquid Phase Sintered Tungsten-Nickel-Iron Alloys"

Spiegel, F. Xavier. "Crystal Models for the Beginning Student"

Yang, Y. Y. and Stang, R. G. "Measurement of Strain Rate Sensitivity in Metals"

NEW:Update 91   NASA Conference Publication 3151

Cowan, Richard L. "Be-Cu Precipitation Hardening Experiment"

Kazem, Sayyed M. "Elementary Metallography"

Krepski, Richard P. "Experiments with the Low Melting Indium-Bismuth Alloy System"

Lundeen, Calvin D. "Impact Testing of Welded Samples"

McCoy, Robert A. "Cu-Zn Binary Phase Diagram and Diffusion Couples"

Patterson, John W. "Demonstration of Magnetic Domain Boundary Movement Using an Easily Assembled Videocam-Microscope System"

Widener, Edward L. "Heat-Treating of Materials"

Dahiya, Jai N. "Phase Transition Studies in Barium and Strontium Titanates at Microwave
      Frequencies"
Rastani, Mansur. "Improved Measurement of Thermal Effects on Microstructure"
Walsh, Daniel W. "Visualizing Weld Metal Solidification Using Organic Analogs"

EXPERIMENTS & DEMONSTRATIONS IN POLYMERS

NEW:Update 89   **NASA Conference Publication 3074**
Chung, Wenchiang R. "The Assessment of Metal Fiber Reinforced Polymeric Composites"
Greet, Richard and Cobaugh, Robert. "Rubberlike Elasticity Experiment"
Kern, Kristen T., Harries, Wynford L., and Long, Sheila Ann T. "Dynamic Mechanical Analysis of
      Polymeric Materials"
Kundu, Nikhil K. and Kundu, Malay. "Piezoelectric and Pyroelectric Effects of a Crystalline Polymer"
Kundu, Nikhil K. "The Effect of Thermal Damage on the Mechanical Properties of Polymer Regrinds"
Stibolt, Kenneth A. "Tensile and Shear Strength of Adhesives"
Widener, Edward L. "Industrial Plastics Waste: Identification and Segregation"
Widener, Edward L. "Recycling Waste-Paper"

NEW:Update 90   **NIST Special Publication 822**
Brostow, Witold and Kozak, Michael R. "Instruction in Processing as a Part of a Course in Polymer
      Science and Engineering"
Cornwell, L. R., Griffin, R. B., and Massarweh, W. A. "Effect of Strain Rate on Tensile Properties of
      Plastics"
Gray, Stephanie L., Kern, Kristen T., Harries, Wynford L., and Long, Sheila Ann T. "Improved Technique
      for Measuring Coefficients of Thermal Extension for Polymer Films"
Humble, Jeffrey S. "Biodegradable Plastics: An Informative Laboratory Approach"
Kundu, Nikhil. "Environmental Stress Cracking of Recycled Thermoplastics"
Wickman, Jerry L. and Corbin, Scott M. "Determining the Impact of Adjusting Temperature Profiles on
      Photodegradability of LDPE/Starch Blown Film"

NEW:Update 91   **NASA Conference Publication 3151**
Allen, David J. "Stress-Strain Characteristics of Rubber-Like Materials: Experiment and Analysis"
Chowdhury, Mostafiz R. "An Experiment on the Use of Disposable Plastics as a Reinforcement in
      Concrete Beams"
Gorman, Thomas M. "Designing, Engineering, and Testing Wood Structures"
Lloyd, Isabel K., Kolos, Kimberly R., Menegaux, Edmond C., Luo, Huy, McCuen, Richard H., and Regan,
      Thomas M. "Structure, Processing and Properties of Potatoes"
McClelland, H. T. "Laboratory Experiments from the Toy Store"
Sorensen, Carl D. "Measuring the Surface Tension of Soap Bubbles"
Wickman, Jerry L. and Plocinski, David. "A Senior Manufacturing Laboratory for Determining Injection
      Molding Process Capability"

NEW:Update 92   **NASA Conference Publication 3201**
Kundu, Nikhil K. "Performance of Thermal Adhesives in Forced Convection"
Liu, Ping. "Solving Product Safety Problem on Recycled High Density Polyethylene Container"
Wickman, Jerry L. "Thermoforming From a Systems Viewpoint"

EXPERIMENTS & DEMONSTRATIONS IN CERAMICS

NEW:Update 88   **NASA Conference Publication 3060**
Nelson, James A. "Glasses and Ceramics: Making and Testing Superconductors"
Schull, Robert D. "High T_c Superconductors: Are They Magnetic?"

NEW:Update 89   **NASA Conference Publication 3074**
Beardmore, Peter. "Future Automotive Materials - Evolution or Revolution"
Bunnell, L. Roy. "Hands-On Thermal Conductivity and Work-Hardening and Annealing in Metals"
Link, Bruce. "Ceramic Fibers"
Nagy, James P. "Austempering"
Ries, Heidi R. "Dielectric Determination of the Glass Transition Temperature"

NEW:Update 90   **NIST Special Publication 822**
Dahiya, J. N. "Dielectric Behavior of Superconductors at Microwave Frequencies"
Jordan, Gail W. "Adapting Archimedes' Method for Determining Densities and Porosities of Small Ceramic Samples"
Snail, Keith A., Hanssen, Leonard M., Oakes, David B., and Butler, James E. "Diamond Synthesis with a Commercial Oxygen-Acetylene Torch"

NEW:Update 91   **NASA Conference Publication 3151**
Bunnell, L. Roy. "Tempered Glass and Thermal Shock of Ceramic Materials"
Craig, Douglas F. "Structural Ceramics"
Dahiya, J. N. "Dielectric Behavior of Semiconductors at Microwave Frequencies"
Weiser, Martin W., Lauben, David N., and Madrid, Philip. "Ceramic Processing: Experimental Design and Optimization"

NEW:Update 92   **NASA Conference Publication 3201**
Bunnell, L. Roy. "Temperature-Dependent Electrical Conductivity of Soda-Lime Glass"
Henshaw, John M. "Fracture of Glass"
Stephan, Patrick M. "High Thermal Conductivity of Diamond"
Vanasupa, Linda S. "A $.69 Look at Thermoplastic Softening"

EXPERIMENTS & DEMONSTRATIONS IN COMPOSITES

NEW:Update 88   **NASA Conference Publication 3060**
Nelson, James A. "Composites: Fiberglass Hand Laminating Process"

NEW:Update 89   **NASA Conference Publication 3074**
Beardmore, Peter. "Future Automotive Materials - Evolution or Revolution"
Chung, Wenchiang R. "The Assessment of Metal Fiber Reinforced Polymeric Composites"
Coleman, J. Mario. "Using Template/Hotwire Cutting to Demonstrate Moldless Composite Fabrication"

NEW:Update 90   **NIST Special Publication 822**
Bunnell, L. R. "Simple Stressed-Skin Composites Using Paper Reinforcement"
Schmenk, Myron J. "Fabrication and Evaluation of a Simple Composite Structural Beam"
West, Harvey A. and Sprecher, A. F. "Fiber Reinforced Composite Materials"

NEW:Update 91   NASA Conference Publication 3151
Greet, Richard J. "Composite Column of Common Materials"

NEW:Update 92   NASA Conference Publication 3201
Thornton, H. Richard. "Mechanical Properties of Composite Materials"

EXPERIMENTS & DEMONSTRATIONS IN ELECTRONIC MATERIALS

NEW:Update 88   NASA Conference Publication 3060
Sastri, Sankar. "Magnetic Particle Inspection"

NEW:Update 89   NASA Conference Publication 3074
Kundu, Nikhil K. and Kundu, Malay. "Piezoelectric and Pyroelectric Effects of a Crystalline Polymer"
Molton, Peter M. and Clarke, Clayton. "Anode Materials for Electrochemical Waste Destruction"
Ries, Heidi R. "Dielectric Determination of the Glass Transition Temperature"

NEW:Update 90   NIST Special Publication 822
Dahiya, J. N. "Dielectric Behavior of Superconductors at Microwave Frequencies"

NEW:Update 91   NASA Conference Publication 3151
Dahiya, J. N. "Dielectric Behavior of Semiconductors at Microwave Frequencies"
Patterson, John W. "Demonstration of Magnetic Domain Boundary Movement Using an Easily Assembled
        Videocam-Microscope System"

NEW:Update 92   NASA Conference Publication 3201
Bunnell, L. Roy. "Temperature-Dependent Electrical Conductivity of Soda-Lime Glass
Dahiya, Jai N. "Phase Transition Studies in Barium and Strontium Titanates at Microwave
        Frequencies"

ORDERING INFORMATION FOR ADDITIONAL RESOURCES

NATIONAL EDUCATORS' WORKSHOP PUBLICATIONS AVAILABLE FROM:

Dr. James A. Jacobs
Department of Technology
Norfolk State University
2401 Corprew Avenue
Norfolk, VA 23504

Shipping and handling charges

1988	$17.00
1989	$27.00
1990	$31.00
1991	$39.00
1992	$43.00

All of the above $73.00
Any three of the above $55.00

BOB POND'S "FUN IN METALS" TAPE - AVAILABLE FROM:

Johns Hopkins University
Maryland Hall 210
3400 N. Charles Street
Baltimore, Maryland 21218

Cost $30.00

JOURNAL OF MATERIALS EDUCATION SUBSCRIPTIONS:

JME has two categories of subscription: Institutional and Secondary. The institutional subscription -- for university departments, libraries, government laboratories, industrial, or other multiple-reader agencies is $245.00 (US$) per year. Institutional two-year subscriptions are $398.00 (US$). When the institution is already a subscriber, secondary subscriptions for individuals and subdivisions are $40.00 (US$). (Secondary subscriptions may be advantageous where it is the desire to preserve one copy for reference and cut up the second copy for ease of duplication.) Two-year subscriptions for secondary for individual or subdivision are $70.00 (US$). Back issues of JME are $35 (US$).

Other Materials Education Council Publications available:

Classic Crystals: A Book of Models - Hands-on Morphology. Twenty-Four Common Crystal models to assemble and study. Aids in learning symmetry and Miller indices. $17.00.

A Set of Four Hardbound Volumes of Wood Modules - The Clark C. Heritage Memorial Series. Published by MEC in cooperation with the U.S.Forest Products Laboratory, Madison, Wisconsin. A compilation of nine modules entitled Wood: Its Structure and Properties (I), edited by Frederick F. Wangaard. A compilation of eight modules especially developed for architects and civil engineers entitled Wood As A Structural Material (II). Also, Adhesive Bonding of Wood and Other Structural Materials (III) and Wood: Engineering Design Concepts (IV). Each of the first three wood volumes costs $27.00; the fourth volume costs $37.00. The entire four-volume set is only $115.00 plus $3.50 shipping ($4.50 overseas).

The Crystallography Course - MEC's popular nine-unit course on crystallography. $37.00.

Instructional Modules in Cement Science - Five units prepared for civil engineering and ceramic materials science students and professionals. $19.00.

Laboratory Experiments in Polymer Synthesis and Characterization - A collection of fifteen peer-reviewed, student-tested, competency-based modules. $21.00. Topics include: bulk polycondensation and end-group analysis, interfacial polycondensation, gel permeation chromatography, x-ray diffraction and others.

Metallographic Atlas - Royal Swedish of Technology. $28.00. A brief introduction to the microstructures of metallic materials - how they appear and how they can be modified.

Please add $2.00 per book shipping charge.
Checks payable to The Pennsylvania State University

Managing Editor, JME
110 Materials Research Laboratory
The Pennsylvania State University
University Park, PA 16802

National Educators' Workshop 92

Left to Right, Rows Top (10) to Bottom (1)
Row 10: R. Diez, D. Craig, D. Needham, D. Forgeng, H. Miller
Row 9: J. Masi, I. Hall, D. Werstler, L. Ketron, T. Jenkins
Row 8: J. Wickman, H. Shih, E. Isaacson, A. Smith, A. Herrell
Row 7: T. Waskom, H. West, P. Liu, R. Diwan
Row 6: A. Sprecher, M. Hsu, D. Martin, R. Berrettini, T. Kilduff
Row 5: C. Smith, G. Hahn, S. Lyons, A. Ajayi-Majebi, A. Tabrizi
Row 4: R. Eng, S. Tipton, J. Gardner, R. Brungraber
Row 3: M. Weiser, R. Gray, P. Mangonon, L. Horton, M. Marpet
Row 2: T. Winters, R. Roy, E. Widener, A. Taba-Tabai, M. Panhans
Row 1: N. Johnston, X. Spiegel, W. Brewer, R. Singh, H. Ries, J. Jacobs, R. Bunnell

NATIONAL EDUCATORS' WORKSHOP

Update 92: Standard Experiments in Engineering Materials Science and Technology

November 11-13, 1992 - Oak Ridge, Tennessee

water reservoir

solenoid/valve

12 V battery

loading fixture
(metal)

water

test specimen

metal contact

insulating post
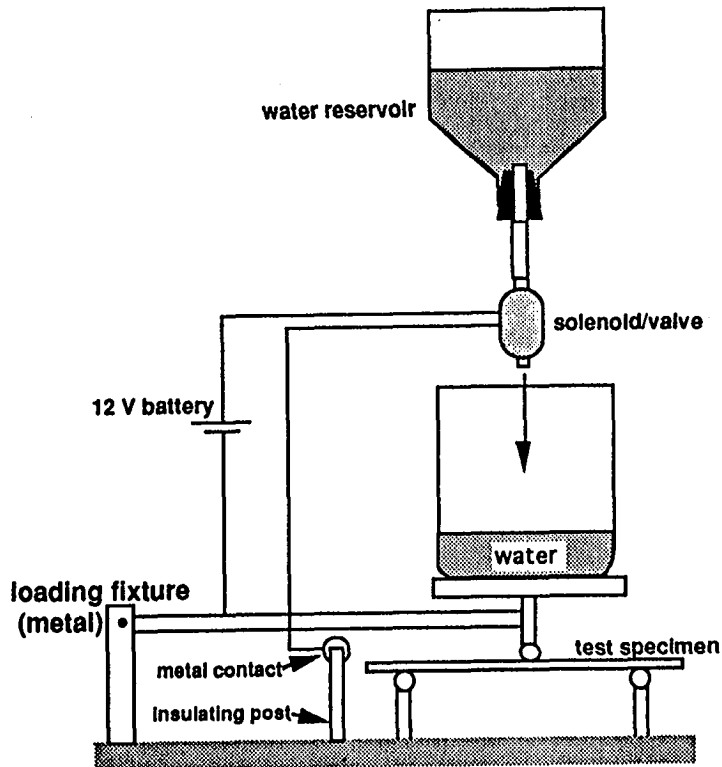
Sponsored by

United States
Department of Energy
FMPC and ORNL

National Aeronautics & Space Administration
Langley Research Center

Norfolk State University
School of Technology

National Institute of Standards
& Technology, Materials Science
& Engineering Laboratories

with the support of

American Society for Engineering Education
ASM International
Battelle, Pacific Northwest Laboratory
Martin Marietta Energy Systems, Inc.
Materials Education Council
Westinghouse Environmental Management Company of Ohio

NEAR NET SHAPE PROCESSING - A NECESSITY FOR ADVANCED MATERIALS APPLICATIONS

Howard A. Kuhn

Program Director
National Center for Excellence
Metalworking Processing Technology
1450 Scalp Avenue
Johnstown, Pennsylvania 15904

Telephone 814-269-2426

1

Near Net Shape Processing

— A Necessity for Advanced Materials Applications —

Howard A. Kuhn, P.E.
Concurrent Technologies Corporation
1450 Scalp Avenue
Johnstown, PA 15904

High quality discrete parts are the backbones for successful operation of equipment used in transportation, communication, construction, manufacturing and appliances. Traditional shapemaking for discrete parts is carried out predominantly by machining, or removing unwanted material to produce the desired shape. As the cost and complexity of modern materials escalates, coupled with the expense and environmental hazards associated with handling of scrap, it is increasingly important to develop near net shape processes for these materials. Such processes involve casting of liquid materials, consolidation of powder materials or deformation processing of simple solid shapes into the desired shape. Frequently, several of these operations may be used in sequence to produce a finished part. The processes for near net shape forming may be applied to any type of material, including metals, polymers, ceramics and their composites. The ability to produce shapes is the key to implementation of laboratory developments in materials science into real world applications. This seminar presents an overview of near net shapemaking processes, some application examples, current developments and future research opportunities.

Net Shape Processing

— A Necessity for Advanced Material Applications—

Howard A. Kuhn

Concurrent Technologies Corporation

Johnstown, PA

Outline

Overview and Historical Perspective

Taxonomy of Net Shape Forming

Examples of Processes

New Developments

    Powder Forging

    Powder Injection Molding

    Spray Forming

    Metal Matrix Composites

Process Modeling and Concurrent Engineering

Challenges

4

Ultimate Goal of Manufacturing

Generation of Wealth Through Production of Components and Systems

(i.e., Making "things" from "stuff")

Economic viability of the nation requires sharp focus on generation of wealth, with secondary attention to services and distribution of wealth.

High Quality

Components and Systems

are the keys to successful performance of equipment used in everyday activities:

Communication	Construction
Transportation	Manufacturing
Utilities	Appliances
Defense	Medicine

Materials Processing

- Materials in natural state are not useful as functional implements

  (exception: stones for throwing or hammering)

- Production of parts and components involves a series of transformations of materials from their natural or recycled state into a useful state

Useful State

- Shape   -   form, dimensions, tolerances

- Surface   -   finish, appearance, wear and corrosion resistance

- Structure -   determines properties, e.g. strength, toughness, conductivity

Transformations of materials to useful state:

Shapemaking
- Solidification of liquid material
- Forming of solid material
- Consolidation of powder material
- Removal of excess material

Structural Change
- Thermal treatments
- Radiation treatment

Surfacing
- Cladding and plating
- Implantation
- Grinding and polishing
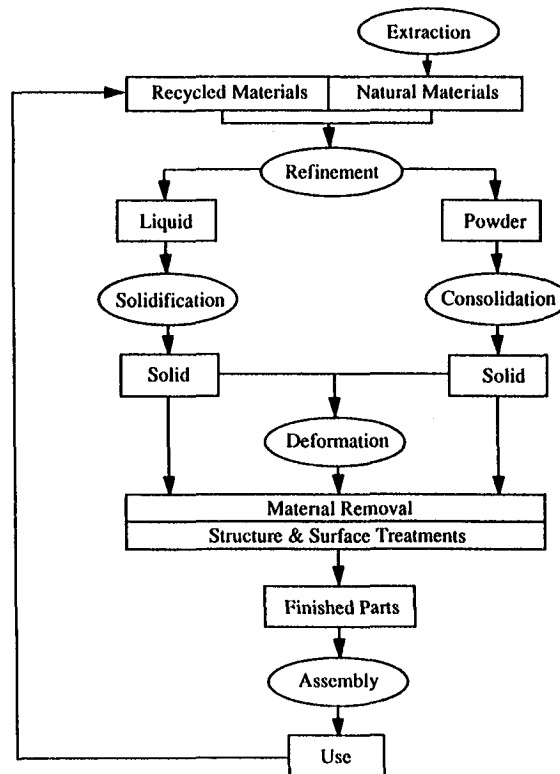
Material removal is most common process for making parts:

- Stone impact on stone for spear points, arrowheads

- Cutting of bark and twigs from tree branch to form club, spear, arrow shaft

- Machining with lathe, miller, grinder, plane, saw

- Electrodischarge machining, laser cutting, waterjet cutting

In modern times material removal has deleterious side effects:

- Chips and scrap must be recycled or disposed

- Cutting fluids cause pollution

- Airborne pollutants are generated

- Process is costly and time-consuming for production of complex shapes

Net Shape Processes

produce desired shape by solidification of liquid material, forming of solid material or consolidation of powder material, rather than material removal

Near-Net Shape Processes

require small amount of material removal to reach target shape, dimensions and tolerances.

(secondary objectives are net surface and net structure)

Solidification (metals & polymers)

- Cast Ingots ⟶ deformation processing

- Atomization of Powder ⟶ consolidation

- Casting of Shapes:

  Sand Mold

  Permanent Mold

  Injection Molding

  Die Casting

  Investment Casting

Forming (metals)

Bulk F

Forging

Rolling

Extrusion

Drawing

Sheetforming

Stretching

Bending

Deep Drawing

Consolidation (metals, polymers, ceramics)

Cold

Die Compaction
and Sintering

Slip Casting

Hot

Hot Pressing

Hot Isostatic Pressing

Powder Forging

Cost Comparisons of Forging vs. Machining
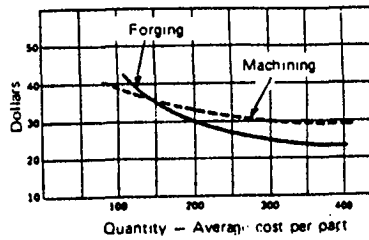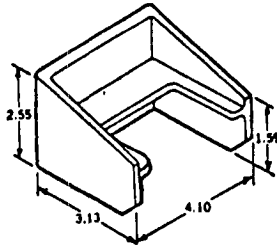
400 Pieces/Contract   50 Pieces/Release

Fabricating Method	Material (Part Cost)	Tooling Cost	Die Cost	Machining Cost	Set-Up Cost	Total Cost
Pressing	14.75	–	6.63	–	2.50	23.58
Machining	2.50	3.00	–	24.00	0.50	30.00

a.
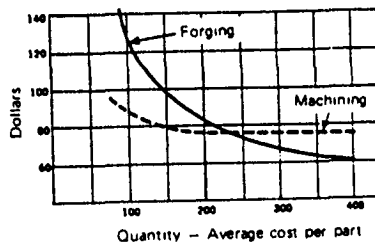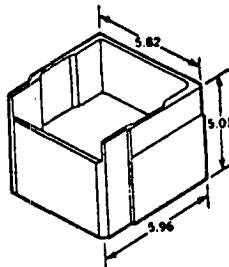
400 Pieces/Contract   50 Pieces/Release

Fabricating Method	Material (Part Cost)	Tooling Cost	Die Cost	Machining Cost	Set-Up Cost	Total Cost
Pressing	24.75	1.25	24.30	6.00	2.50	58.80
Machining	18.00	5.00	–	48.00	1.00	72.00

b.
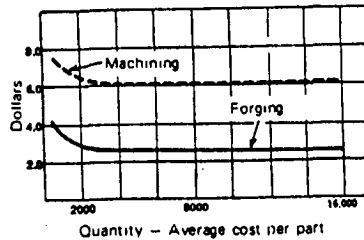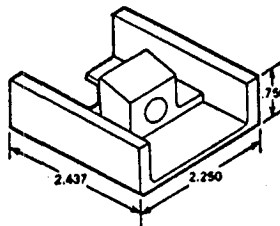
16,000 Pieces/Contract   500 Pieces/Release

Fabricating Method	Material (Part Cost)	Tooling Cost	Die Cost	Machining Cost	Set-Up Cost	Total Cost
Pressing	2.40	–	0.05	–	0.25	2.70
Machining	0.50	0.06	–	5.40	0.06	6.02

11

Example Sequences

Beverage Cans

Aluminum alloy 3004 production

Cast Ingot

Hot rolled to 0.120

Cold rolled to 0.011

Blank, deep, reverse draw cup

Iron wall

Trim & flange

Spark Plugs

Steel 1008	Al_2O_3	Copper
Continuously Cast Billet	HIP	Continuously Cast Billet
Hot roll to 1" dia.		Hot roll to wire
Cutoff slug		Cutoff roll thread
Back extrude		
Finish machine		
(Body)	(Insulator)	(Electrode)

Assemble Spark Plug

Semi-Solid Metalworking

- Emerging method for the manufacture of near-net shape discrete components

- Incorporates elements of both casting and forging

- Capable of producing parts essentially free of extensive porosity

- Components can be heat-treated to obtain mechanical properties superior to those achievable by die casting and permanent mold casting processes.

- Properties equivalent to those of forgings are obtainable at a significantly lower cost.

THE SEMI-SOLID METALWORKING PROCESS
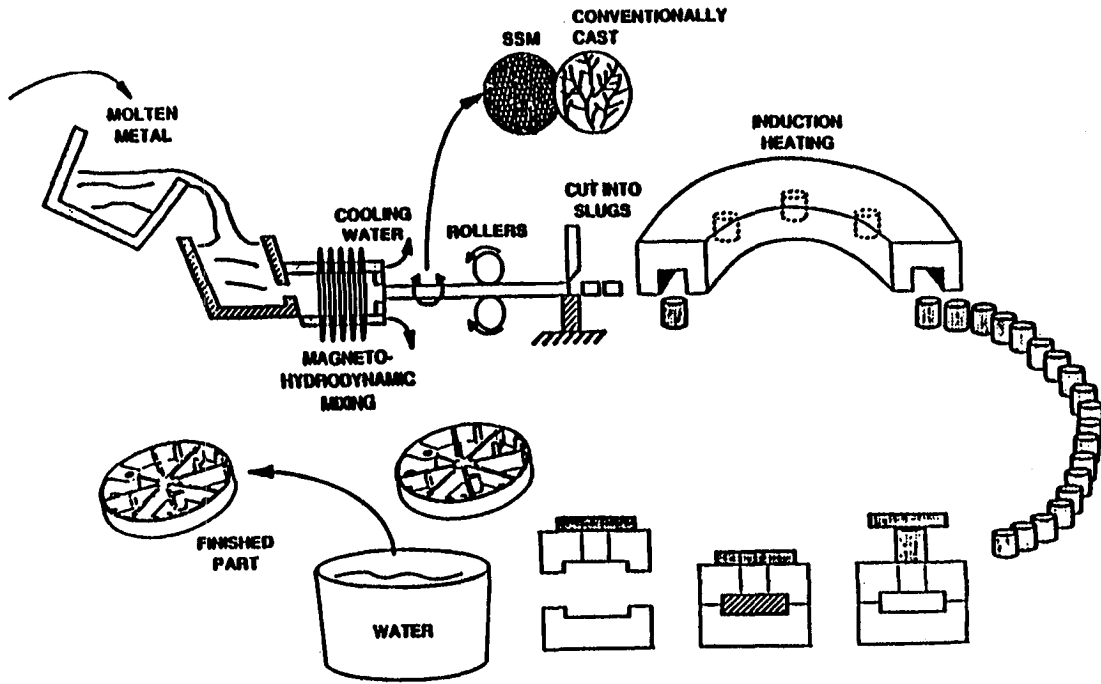
SCHEMATIC OF THE POWDER INJECTION MOLDING (PIM) PROCESS

powder   binder   lubricant

mixing

granulation

injection

debinding
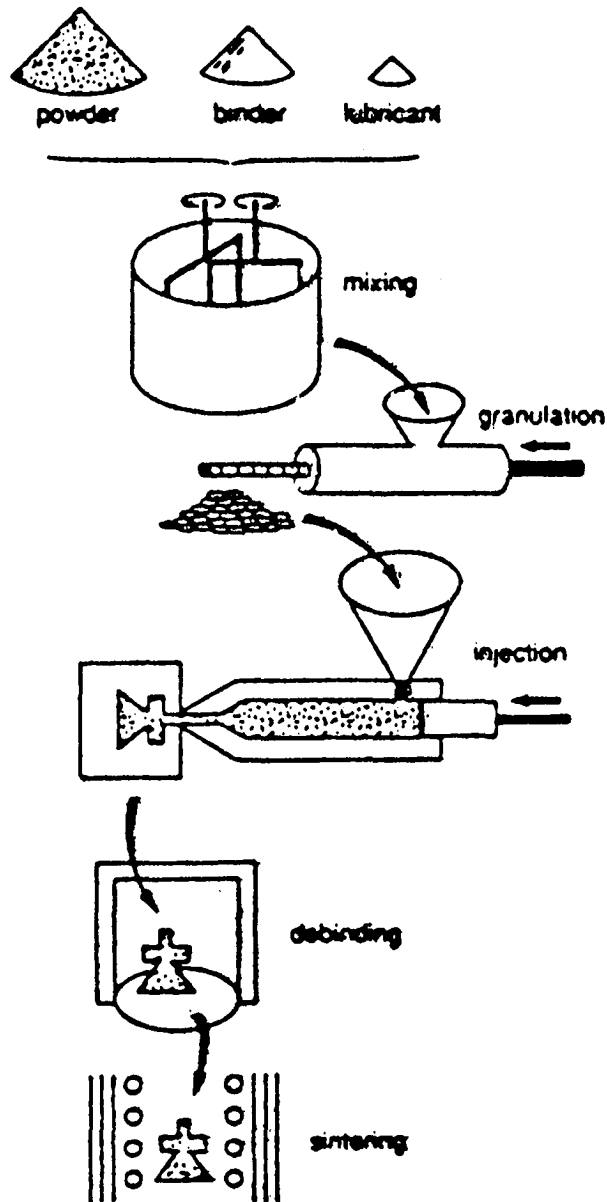
sintering

Criteria for PIM Processing

- size < 300 g or 100 mm (thickness)

- complex shape

- quantity over 10,000

- sinterable powder material

- +/ - 0.3% tolerances

Pseudo Isostatic Pressing

- Granular or soft material used as the pressure transmission medium in a conventional trap forging die

- Shorter cycle times than hot isostatic pressing

- Equipment less costly than hot isostatic pressing

Example: Ceracon Process

CERACON PROCESS

HEATED PREFORM

COMBINATION OF HEATED PART WITH HEATED GRAIN

CONSOLIDATION

EJECTION

SEPARATION

PARTS FOR FINISHING

GRAIN RECYCLED
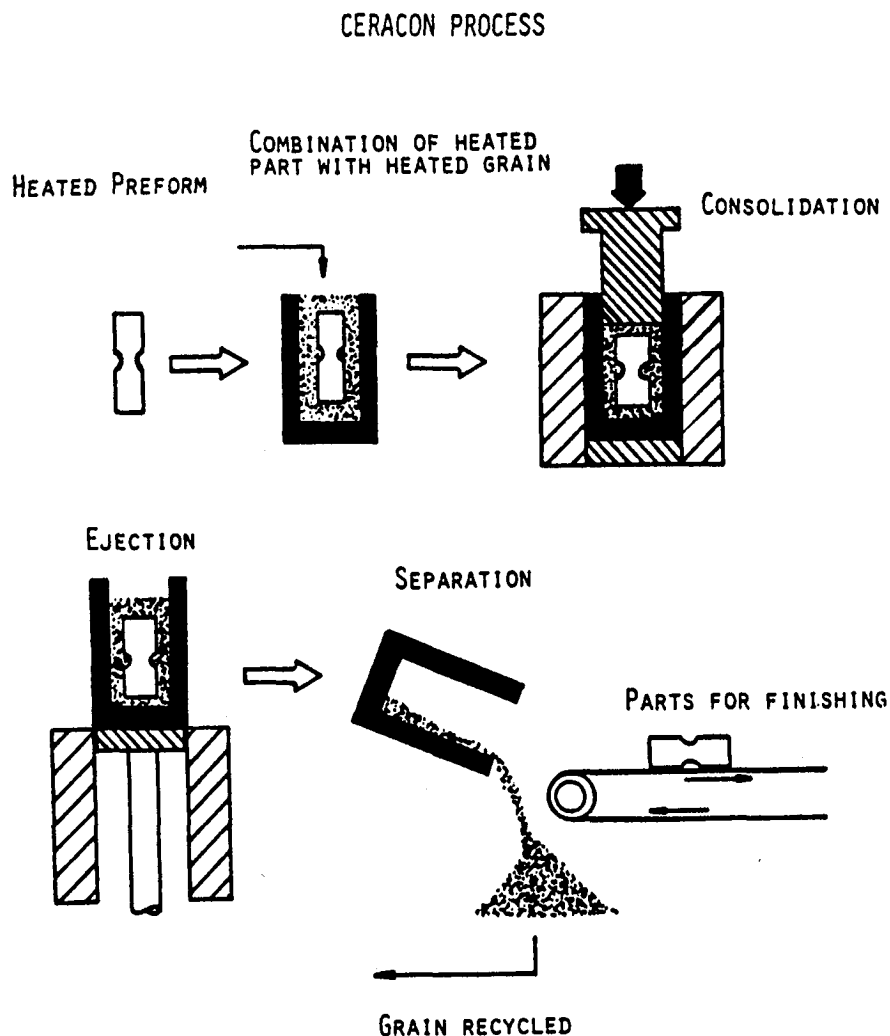
Powder Forging

- Die compaction and sintering of a preform
- Forging of the preform into a fully dense part
- Forging implies large amount of metal flow
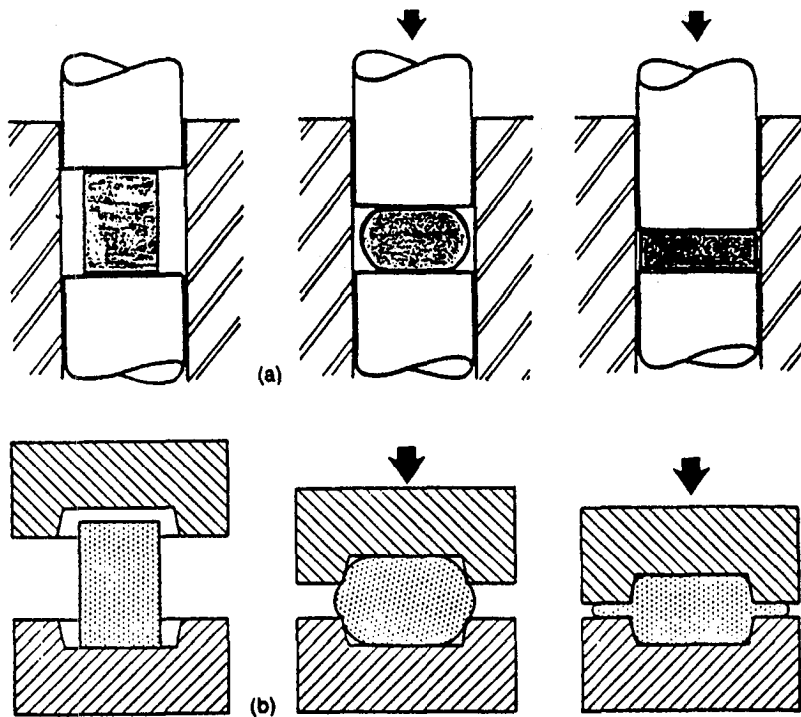
(a) Illustration of a trap die for powder forging and (b) an impression die with flash for conventional forging.
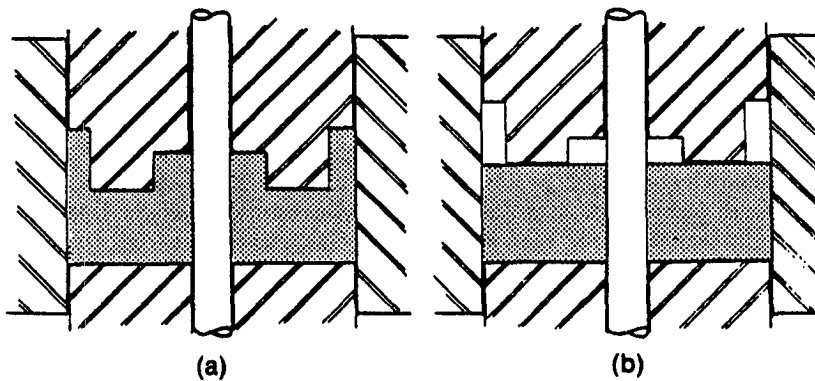
Comparison of (a) powder repressing and (b) powder forging.

Comparison of Powder Forging and Conventional Forging
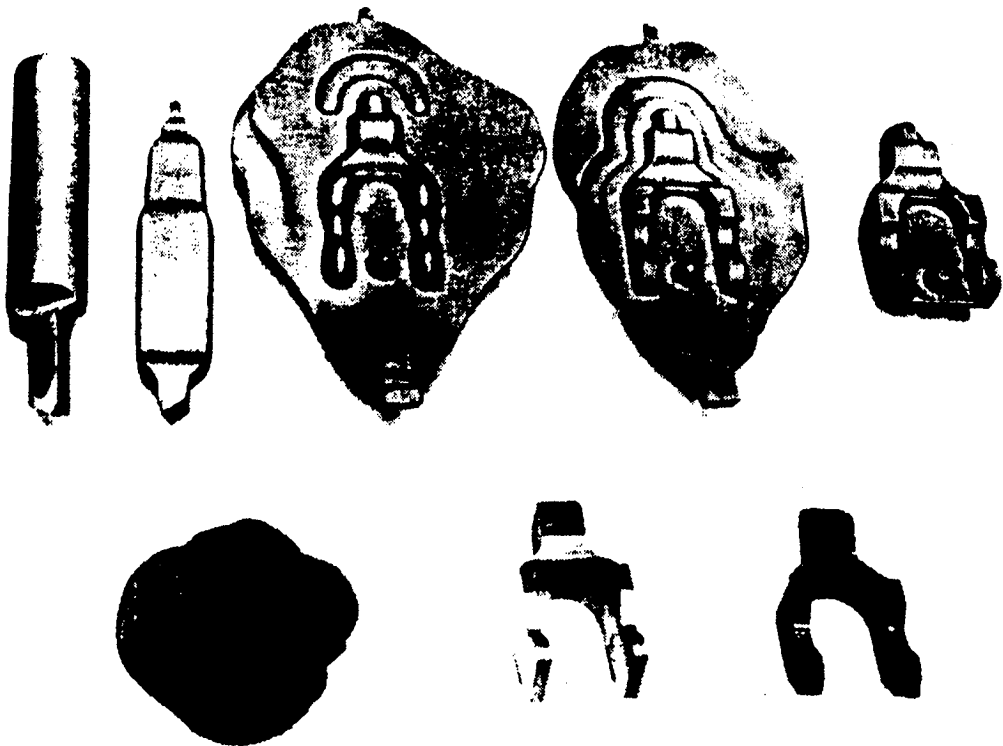
(Original Photo Not Available.)

Comparison of conventional forging practice and the powder forging process

Powder Forging

- ## Example: Torque converter clutch hub
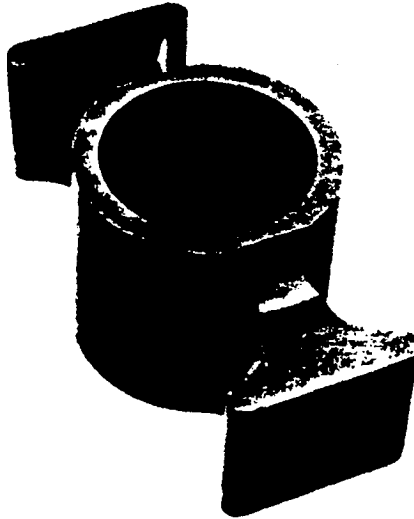
Torque converter clutch hub, forging preform, courtesy Imperial Clevite of Canada.

- ## All Ford automobile engine connecting rods made by powder forging
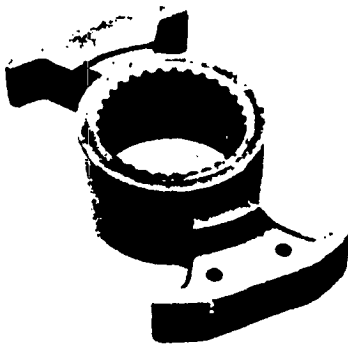
Torque converter clutch hub, forged blank, courtesy Imperial Clevite of Canada.

Torque converter clutch hub, finish machined, courtesy Imperial Clevite of Canada.

(Original Photos Not Available.)

Spray Forming

- Thermal spray of powder to form shapes

- Liquid particles impact substrate, flatten, solidify
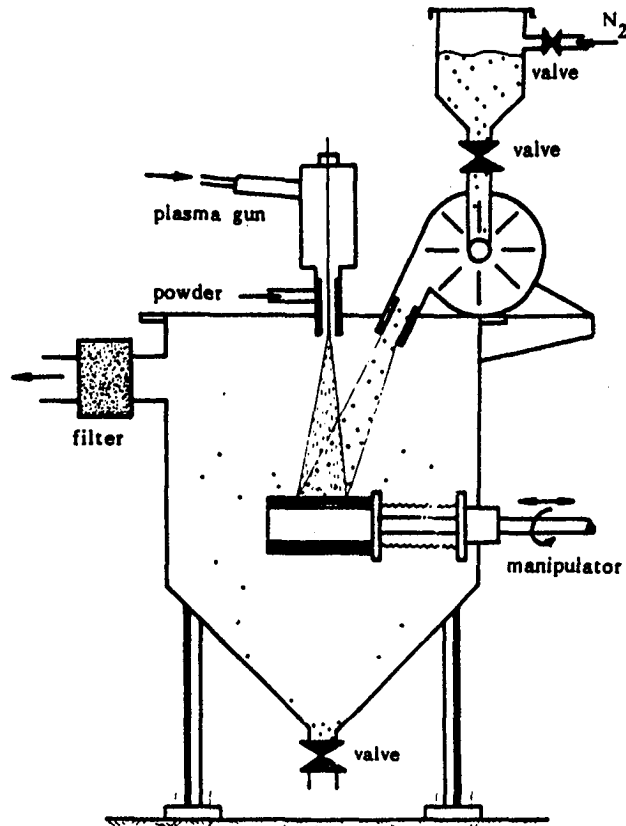
Typical structure of deposit made at low spray density

Metal Matrix Composites

Continuous fiber

- Forming of shapes by hot isostatic pressing of assembly in a canister

- Assembly may be foil/fiber/foil construction, or plasma sprayed fiber foils

- Variety of shapes, including tubes, sheet, hat sections

- Applications to aerospace structures, such as NASP
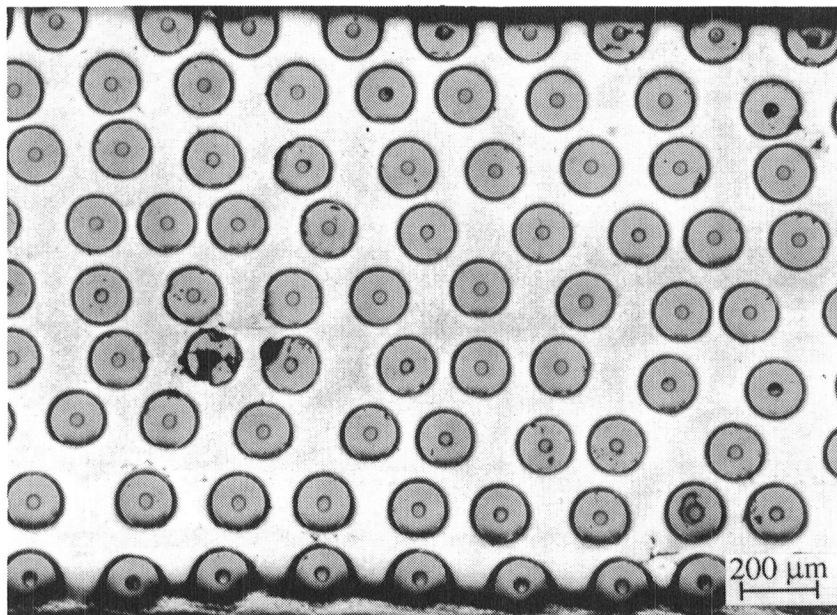
Cross-section of consolidated composite showing good consolidation at the central part of the specimen.

Process Variables: Temperature, T(t) Pressure, p(t)

HIP Cannister (e.g. Titanium)

Initial deformation at contact points

Interlaminar porosity arises due to surface roughness

Intermetallic Matrix (e.g. Ti_3Al)

Fiber (e.g. SiC, Al_2O_3) Fiber - induced anisotropy Fiber - matrix reactions Stress concentration

Internal porosity
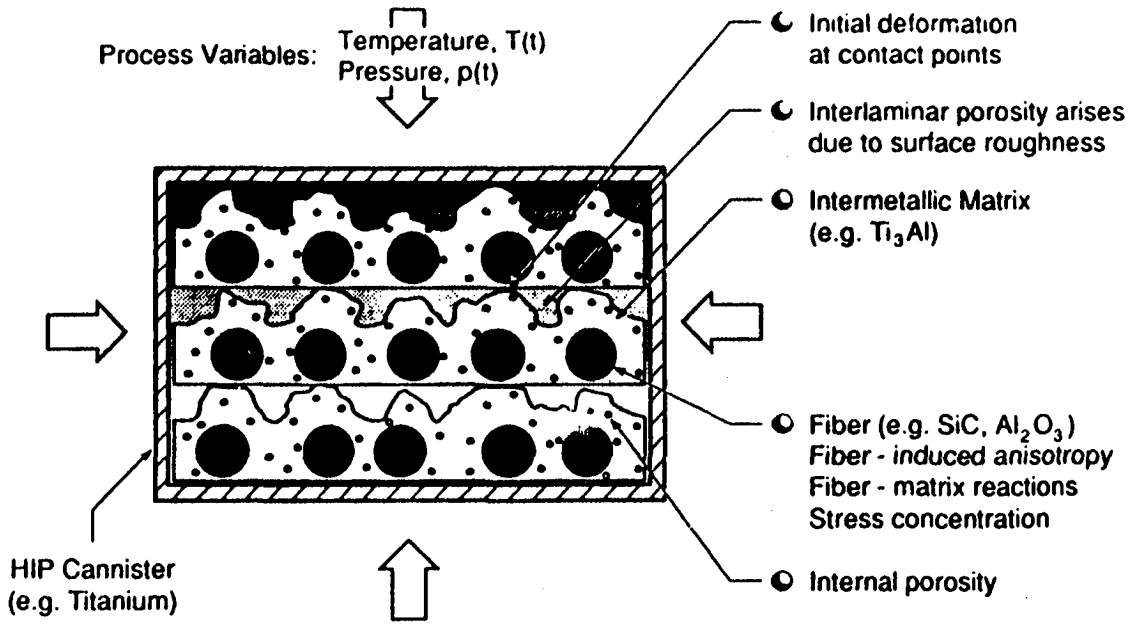
Schematic illustration of the HIP process as applied to the consolidation of plasma sprayed composite foils.
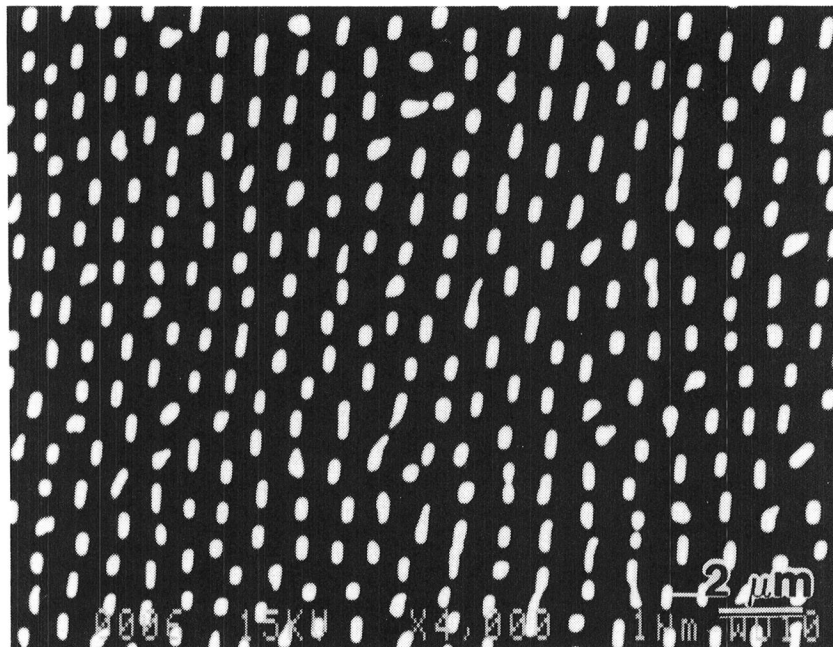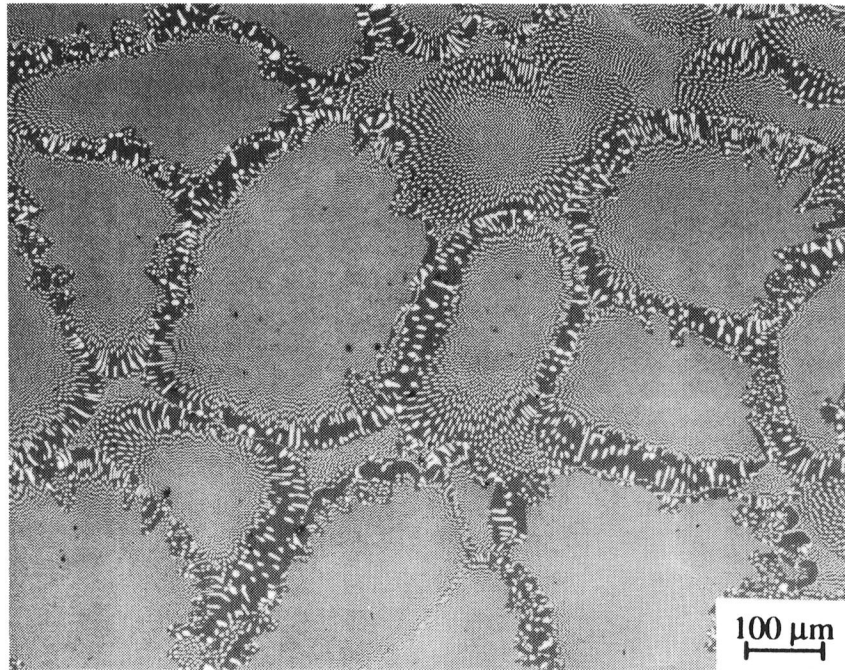
Backscattered SEM microstructures of a transverse section of a NiAl-10 at % Mo alloy directionally solidified at 0.5 mm/min.

(a) Eutectic colonies consisting of fine Mo filaments in a NiAl matrix.

(b) Uniform distribution of Mo filaments in the NiAl maxtrix.

R·P²D℠

PRODUCT PERFORMANCE REQUIREMENTS

GEOMETRY DATABASE

PRODUCT EXPERTISE

PROCESS EXPERTISE

ENVIRONMENTAL FACTORS

PRODUCT DESIGN MANAGEMENT

PROCESS DESIGN MANAGEMENT

MATERIAL CHARACTERIZATION

PRODUCT ANALYSIS

PROCESS MODELING

PRODUCT/PROCESS DESIGN
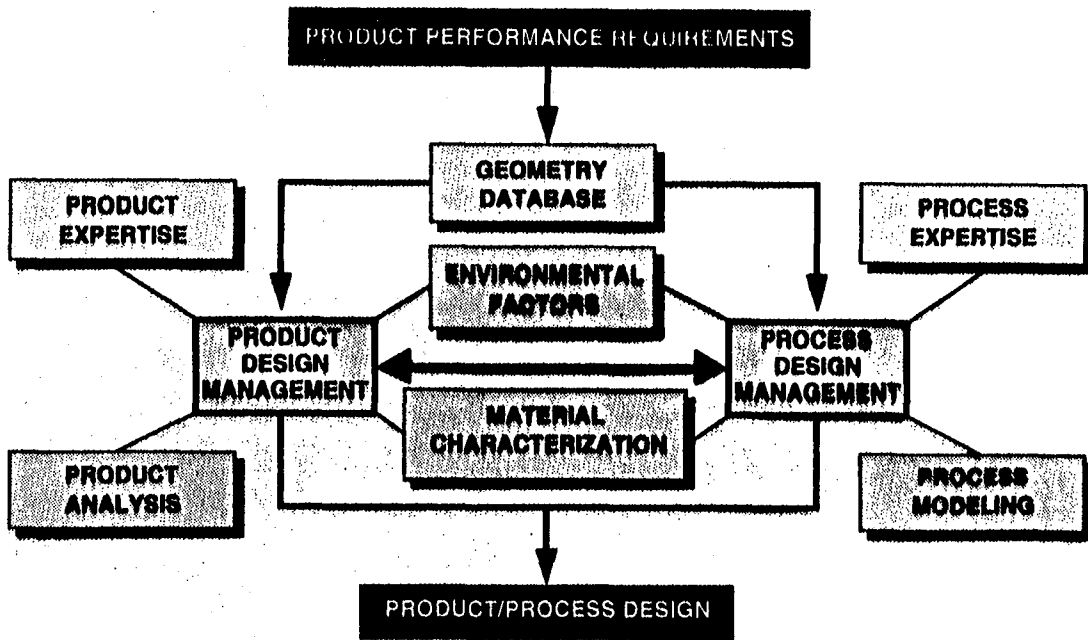
Concurrent Engineering

- Geometric data file serves as starting point (CAD wireframe or solid model)

- File is shared by Product Design group and Process Design group

- Experience knowledge bases as well as computer modeling are used

- Material behavior is measured to provide input to computer models and assure realistic predictions

- Environmental considerations are brought to design stage

Computer Modeling

Focus on:
- Shape and dimension predictions (Mold or die dimensions plus shrinkage)
- Structure and defect predictions
- Residual stress predictions

Integrates:
- Metallurgical factors (Structural evolution, void formation, ductile fracture)
- Continuum mechanics (Heat transfer, fluid flow, stress analysis)
- Computer graphics (Solid models, animation)

Formability of hard-to-work alloys is aided by the use of formability and workability diagrams

- Laboratory tests establish combinations of strains at fracture for a given material.

- These strains are plotted to produce a formability or workability map for the given material.

- Strains in actual process are compared with formability or workability maps.

- Process changes and/or material changes are determined to avoid defects.

KEELER-GOODWIN FORMING LIMIT DIAGRAM

Forming limit diagram
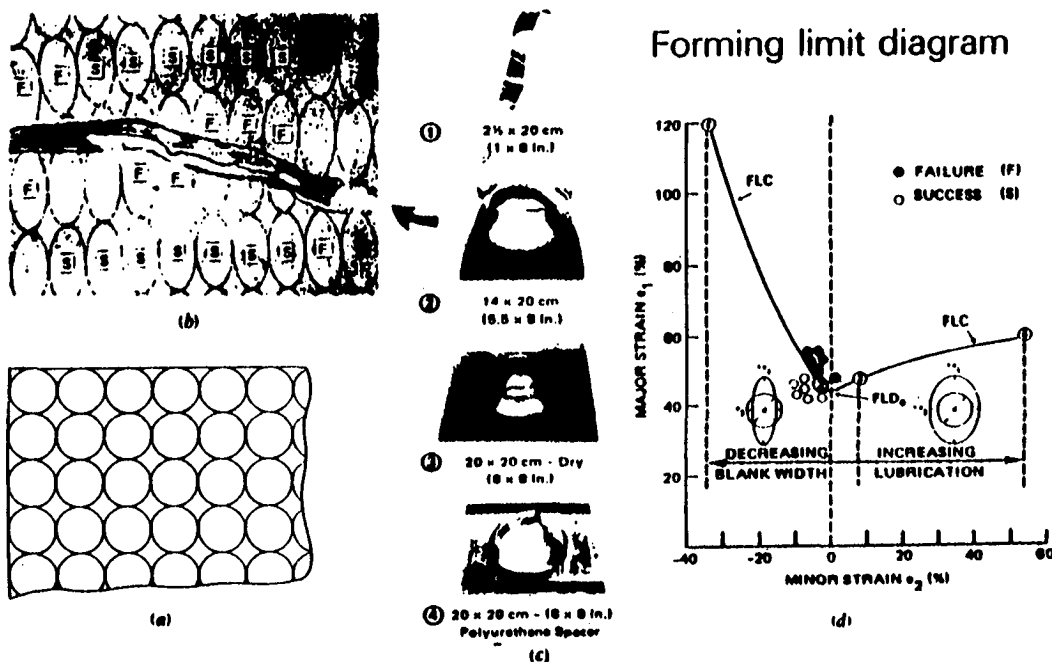
(Original Photos Not Available.)

Sheet Metal Forming Limit Diagrams

- Limiting strains at failure are determined through simple sheet metal tests
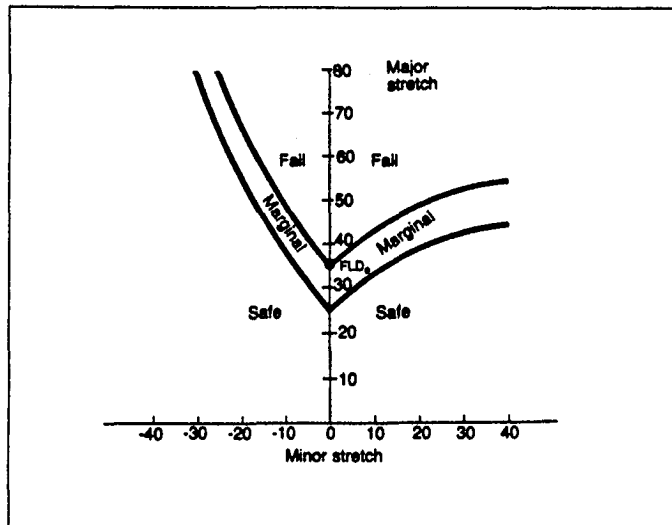
Establishing a safety margin with FLD_0. (*National Steel Corporation*)

- Strains in a formed part are measured from grid circles and compared with the forming limit diagram
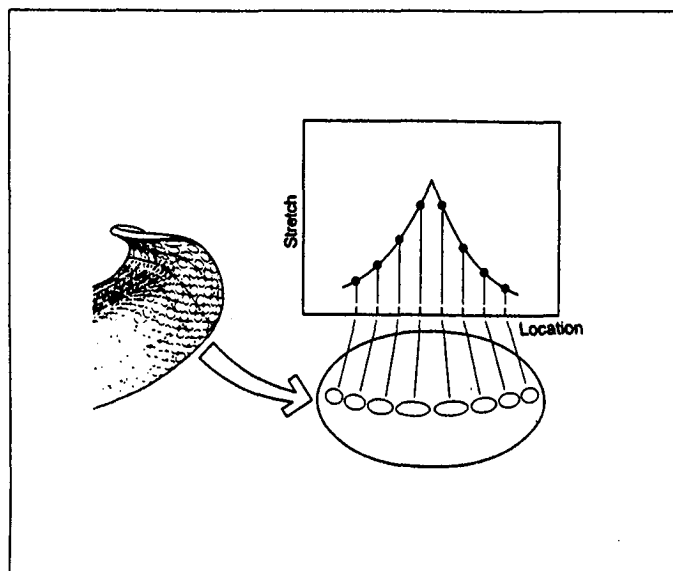
Rating forming severity by location. (*National Steel Corporation*)

27

Application of Forming Limit Concept

Floor pan reinforcement

Failure

Proposed design

Initial design
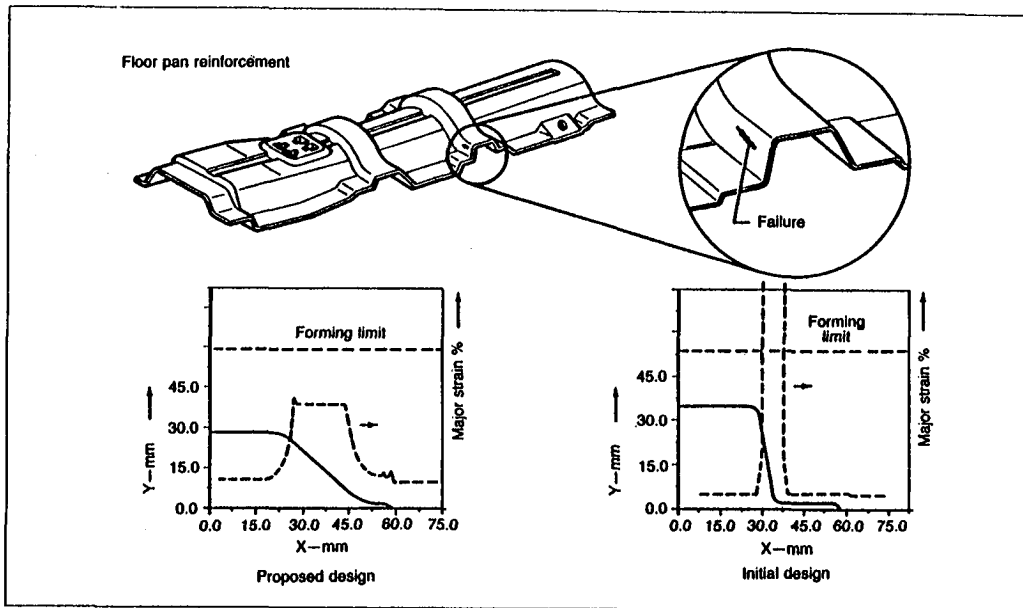
Upset Test
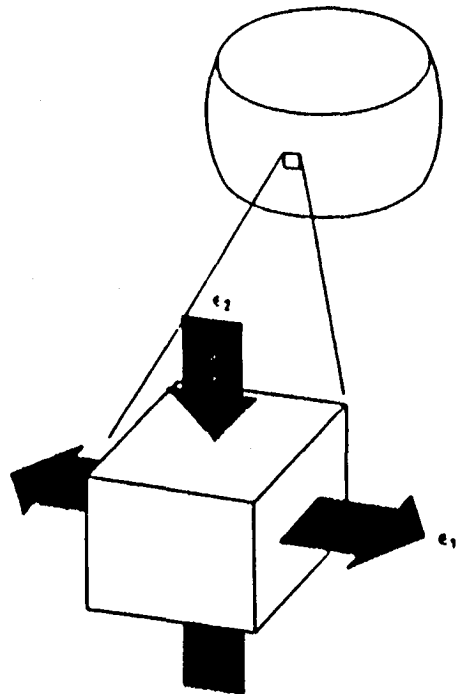
Fracture Strain Lines for 2024 Aluminum Alloy
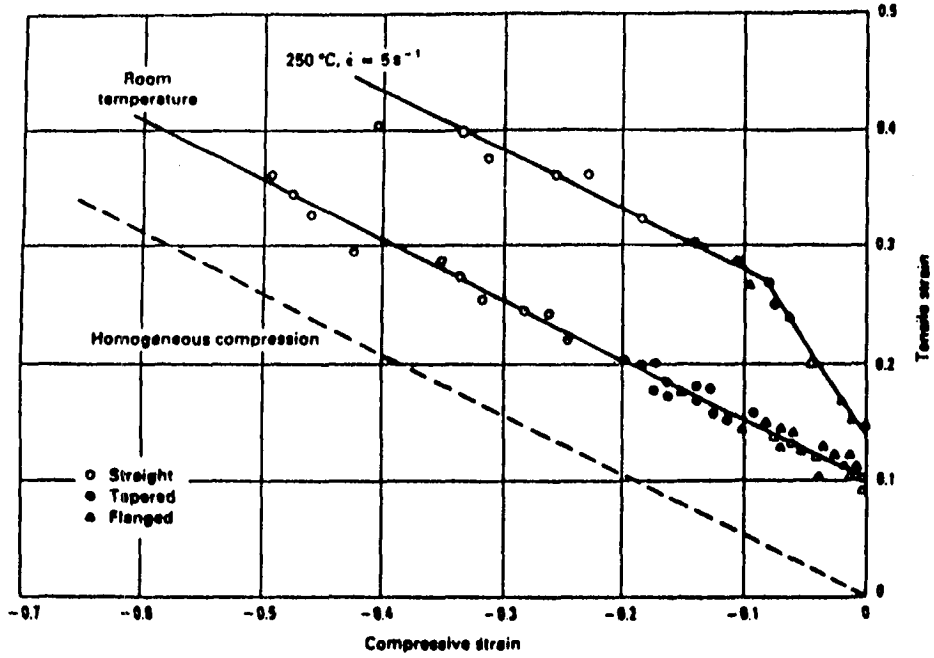
Upsetting
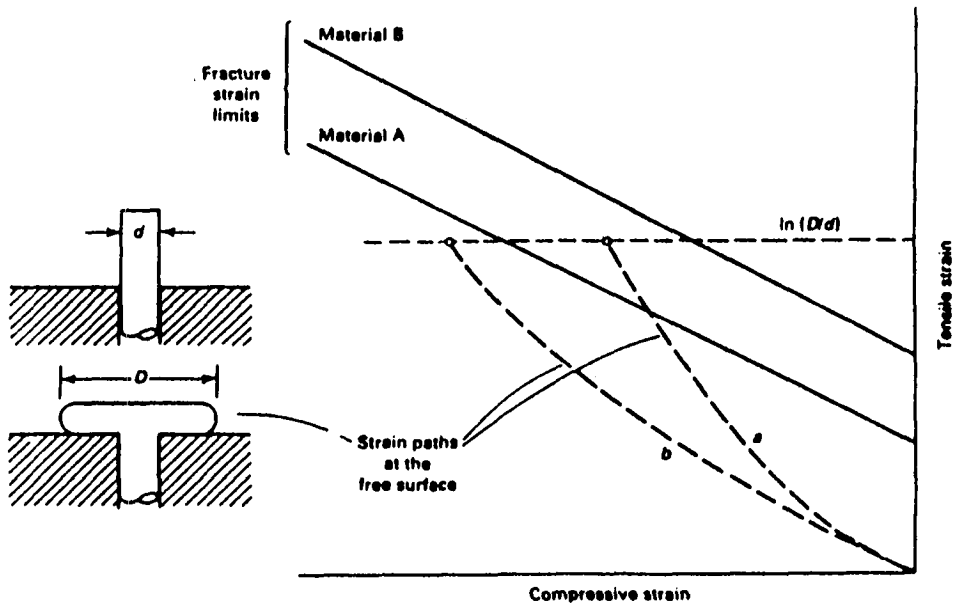
Material Fracture Strain Limits
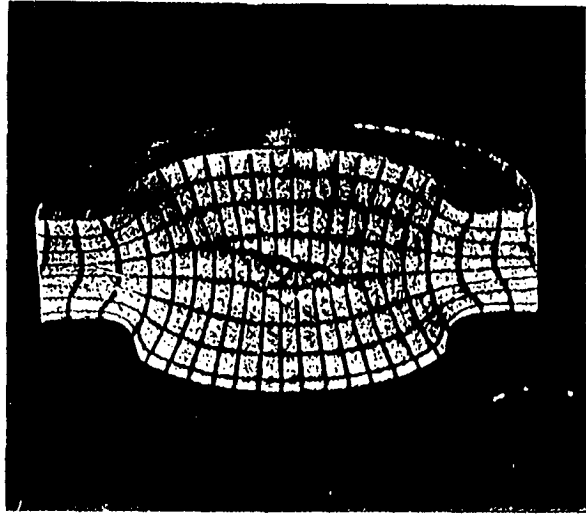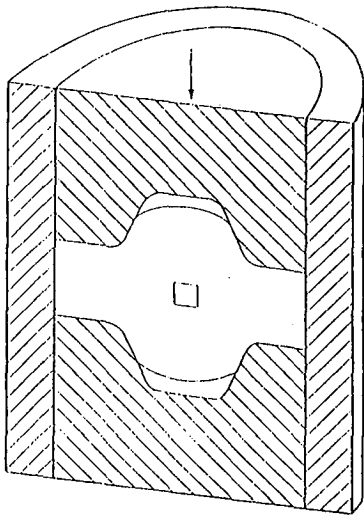
Cutaway view of double hub forging. Left figure shows a schematic of the tooling arrangement and the right figure shows a cross section of a forging containing a crack at the center.
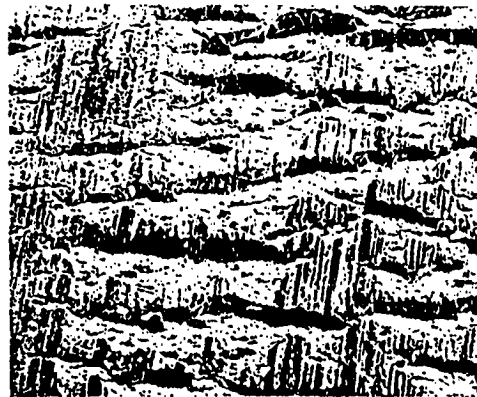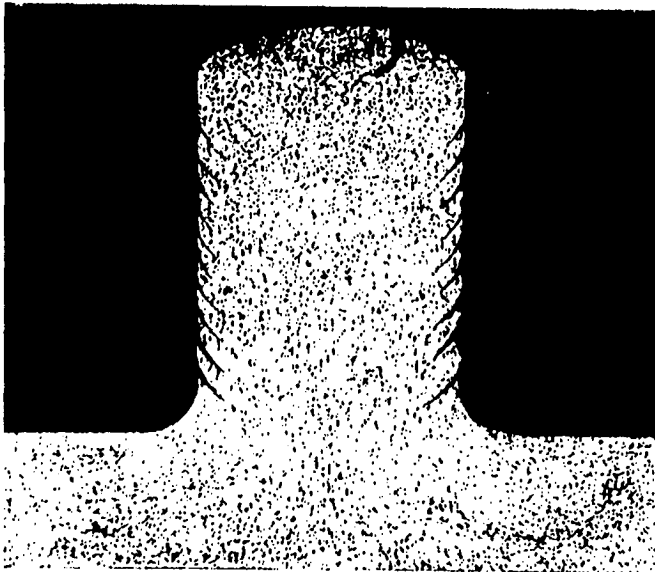
Surface cracking during extrusion forging.

(Original Photos Not Available.)
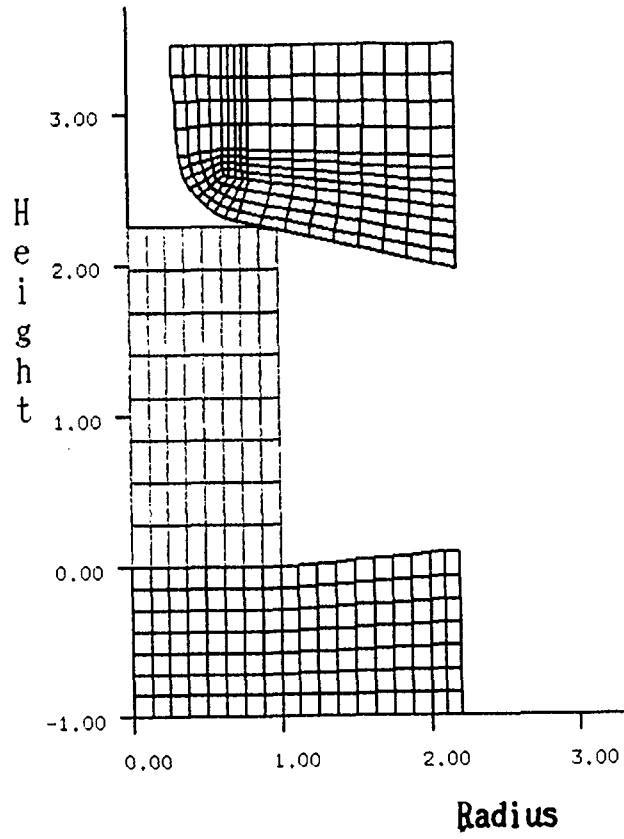
Finite element mesh for simulation of extrusion forging

3.00

Height 2.00

1.00

0.00

-1.00

0.00   1.00   2.00   3.00

Radius

Eff. Stn Rt
Object # 2
□ = 1.4112
△ = 0.32138E-
A= 0.00000E-
B= 0.17640
C= 0.35281
D= 0.52921
E= 0.70561
F= 0.88202
G= 1.0584
H= 1.2348
I= 1.4112

Object # 3
□ = 0.00000E
△ = 0.00000E
A= 0.00000E
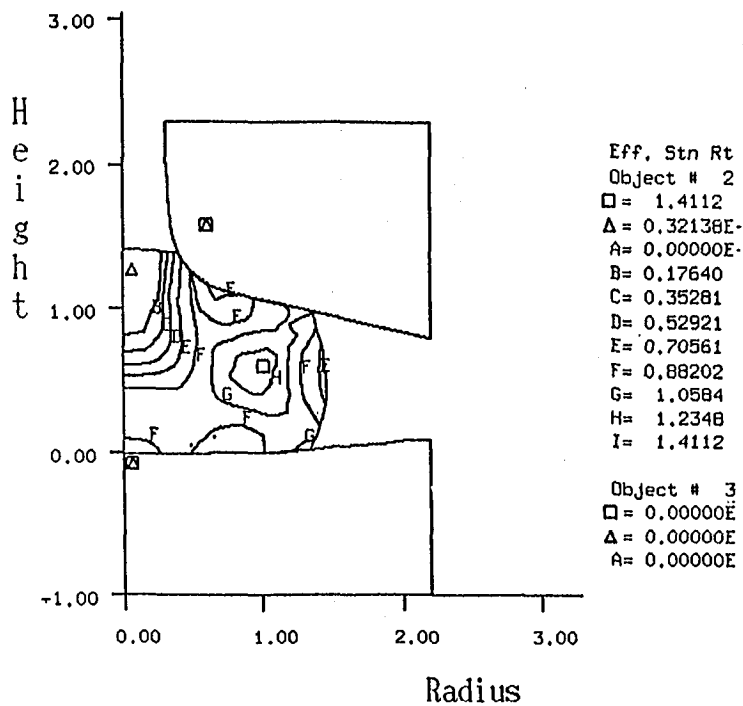
Contours of effective strain rate in finite element
simulation of extrusion - forging

Net Shape Forming Challenges

- Improve dimensional control

- Improve shape complexity

- Improve structure control

- Improve surfaces

- Reduce tooling costs

- Adapt to small batches
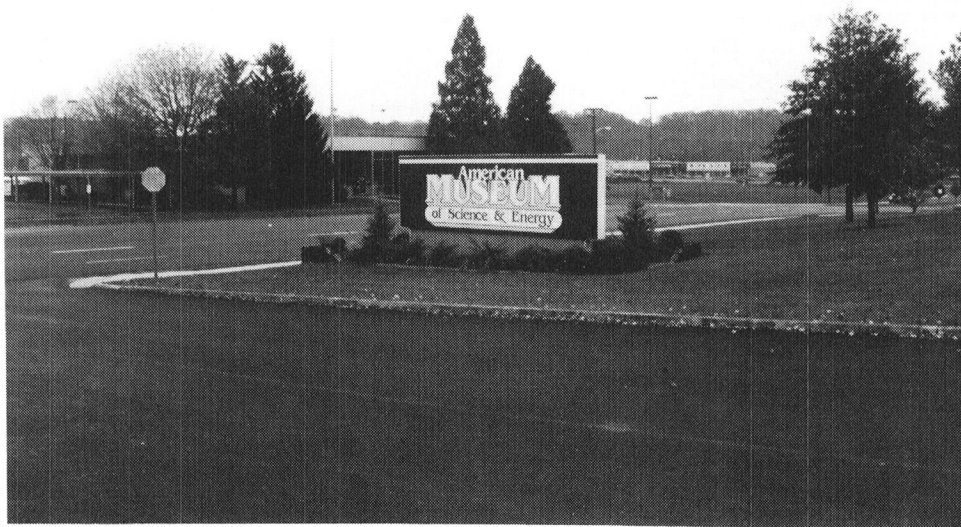
Workshop Location

Registration

Welcome
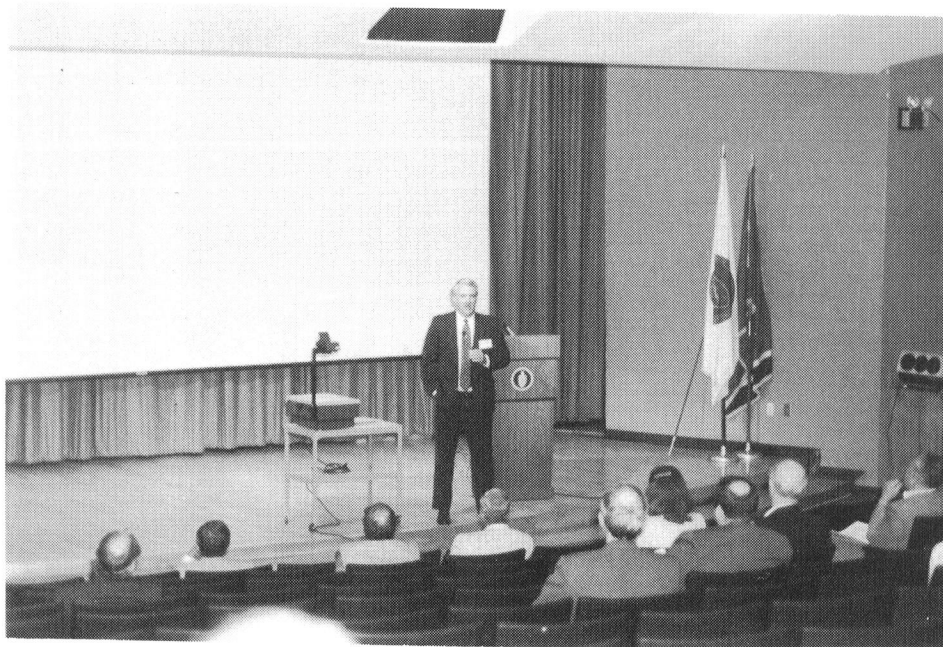
Keynote

DEVELOPMENT OF AN EXPERIMENTAL METHOD TO DETERMINE THE AXIAL RIGIDITY OF A STRUT-NODE JOINT

W. V. Brewer
and
Hui-Ru Shih

Department of Technology
Jackson State University
1400 J. R. Lynch Street
Jackson, Mississippi 39217

Telephone 601-968-2466

DEVELOPMENT OF AN EXPERIMENTAL METHOD TO DETERMINE THE AXIAL RIGIDITY OF A STRUT-NODE JOINT

W. V. Brewer and Hui-Ru Shih

Department of Technology
Jackson State University, Jackson, Mississippi

KEY WORDS: rigidity, torque, strut-node joint.

PREREQUISITE KNOWLEDGE: The concepts of force, deflection, and rigidity.

OBJECTIVES: To present: (i) the experimental procedure and the results that have been performed to determine the axial rigidity of the strut-node joint; and (ii) the method for modifying a simple testing machine to make it capable of performing more accurate tests over a specific load range and able to accept larger test assemblies.

EQUIPMENT AND SUPPLIES: Vega Universal Testing Machine, dial gage, strut and strut-node joint assembly, torque wrench, pressure gage, manual needle-stop valve, brake lines (the last three items were inserted into the hydraulic line of the testing machine).

PROCEDURE: In this experiment, the test specimen was a joint assembly consisting of a node with a strut half mounted on either side (figure 1). The strut is a hollow aluminum tube which has a hex-head bolt attacted to its one end by means of a bonded, interference fit aluminum plug. The node is a hollow steel sphere with eighteen threaded holes for strut attachment.

A simple "Vega Universal (VU) Testing Machine" was used to provide load in this experiment. This machine was intended to test small stout material specimens [1], rather than the bulkier less robust strut-node joint assembly we have. Space in both tensile and compressive frames was insufficient to accommodate our joint assembly. Lengthened frame posts of our own manufacture have been installed.

Loads which were applied to the strut-node system in the experimental procedure range from 0 to 1600 N. Whereas the load gage on the VU testing machine, which ranges from 0 to 89000 N (20000 lb), reads in 445 N (100 lb) increments with very little precision in the range of interest. In order to measure loads more accurately, a pressure gage of appropriate range has been inserted into the hydraulic line of the VU testing machine. The corresponding load is the gage pressure times the cross-sectional area of the hydraulic load piston. Available gages in the

range of interest have to be protected from higher pressure capabilities of the testing machine. To accomplish this, a manual needle-stop valve was used. This valve must be closed if the testing machine is used at pressures above the upper limit of the pressure gage.

The VU testing machine employs universal jaws with V grips to hold the test specimen. The end of each strut to be placed in the machine was fitted with a solid plug in order to prevent the strut from being crushed. Three dial gages were employed to measure the deflection of the specimen. These dial gages were around the test specimen and mounted between two mounting plates by using clamps and threaded rods. The deflections of three dial gages were averaged to compensate for any bending that occurred in the specimen [2].

In order to calibrate the system to ensure the experiment set-up was operating properly, a segment of a strut having the same length as the joint assembly was tested first to determine its axial rigidity. The load-deflection curve for the strut is shown in figure 2. From this curve, the experimentally determined rigidity is 4.449×10^6 N. This rigidity value is calculated by multiplying the slope of the load-deflection curve by the test specimen length, 355.6 mm (14.0 in.) [3], i.e.

$$EA = \frac{PL}{\delta} \tag{1}$$

where E is the Young's modulus, P is the applied load, δ is the deflection, and A and L are the cross-sectional area and the length of the test specimen, respectively. The product EA in equation (1) is known as the axial rigidity. The strut is a hollow aluminum tube, with a material Young's modulus of 70 GPa and a cross-sectional area of 62.97 mm^2 (22.05 mm outer diameter, 0.95 mm wall thickness). Thus, the predicted axial rigidity is 4.408×10^6 N. This represents a difference of only 0.923 percent from the experimentally determined value of 4.449×10^6 N and thus verifies the test procedure.

After verifying the test procedure, a strut-node joint assembly was loaded to determine its rigidity and the effect of the attachment bolt torque value on joint rigidity. To accomplish this, tests using two torque values, 3.39 N-m (30 lb-in.) and 16.95 N-m (150 lb-in.), were conducted. As shown in figure 3, the rigidity of the strut-node joint assembly increases as the attachment bolt torque value is increased. A comparison of the rigidity values for strut and strut-node joint assembly with different torque values is presented in table 1. An examination of table 1 reveals that the percent increase in rigidity of the strut-node joint assembly over that of the strut varies from 4.1 % for a torque value of 3.39 N-m to 7.8 % for a torque value of 16.95 N-m.

SAMPLE DATE SHEETS: Self-Evident.

INSTRUCTOR NOTES: An experimental method has been developed to determine the axial rigidity characteristics of a strut-node joint, and to compare that with the rigidity of a

similar length of strut without a joint. The experimental results have shown that the strut-node system is stiffer than the strut and the rigidity of the strut-node joint assembly increases as the attachment bolt torque value is increased. The structural performance of the strut-node joint assembly can be improved by increasing the pre-load in the threaded connections between the node and strut. This experiment was performed with a simple Vega Universal Testing Machine. Through the specialized modification, this testing machine could be used to test a strut-node joint or other larger assembly where the required measurable load range is much smaller.

REFERENCES:
1. Materials Technology Laboratory Manual, VEGA Enterprises Inc., Decatur, Illinois, 1980.
2. McGowan, D. M.; and Lake, M. S.: "Experimental Evaluation of Small-Scale Erectable Truss Hardware", NASA TM 89068, June 1987.
3. Gere, J. M.; and Timoshenko, S. P.: Mechanics of Materials, third edition, PWS-KENT Publishing Company, Boston, 1990.

SOURCES OF SUPPLY: The strut and strut-node joint assembly are provided by NASA Langley Research Center. Hardware stores can provide the rest of supplies.
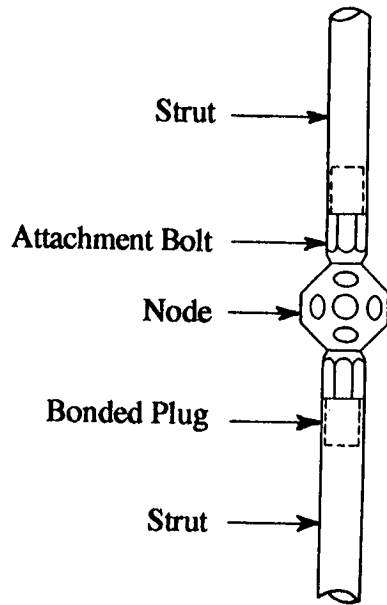
Figure 1. Strut-Node Joint Assembly
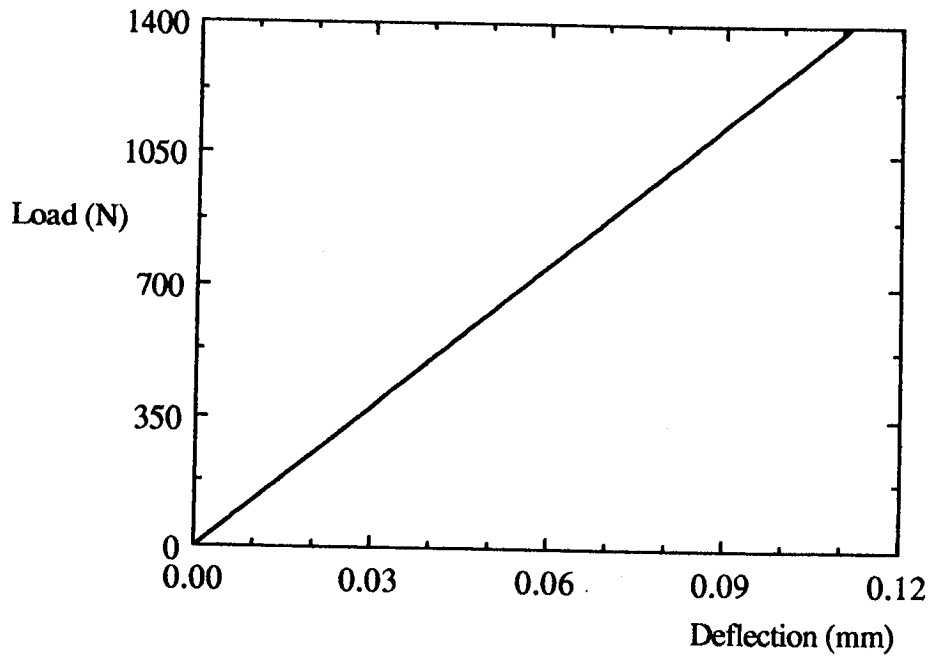
Figure 2. Load-Deflection Curve for Strut
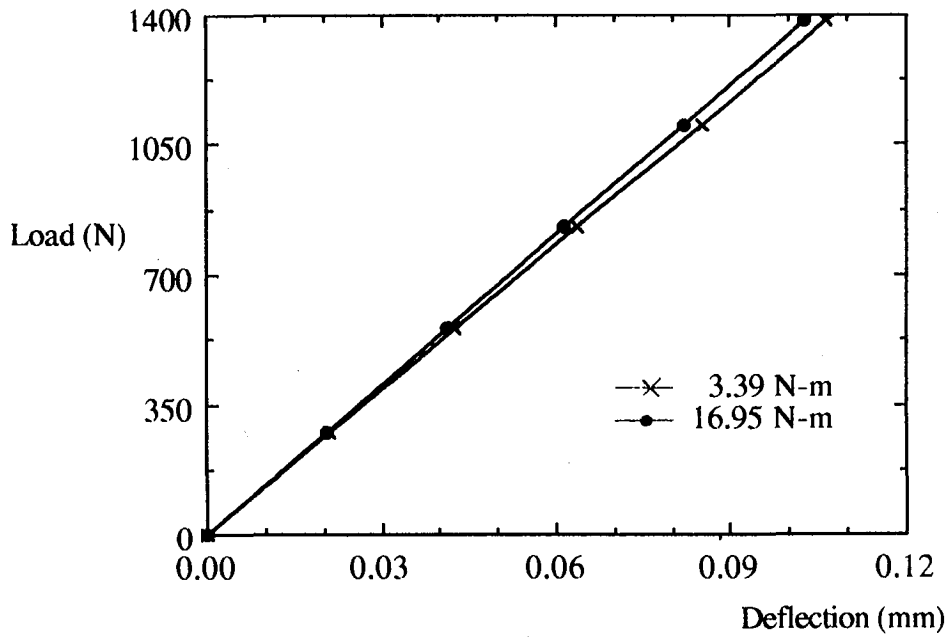
Figure 3. Load-Deflection Curves for Strut-Node Joint with 3.39 N-m
and 16.95 N-m Torque values

Table 1. Comparison of the Rigidity of Strut and Strut-Node Assemblies
for a Fixed Length of 355.6 mm (14.0 in)

Specimen	Rigidity $(N \times 10^6)$	% Difference with Strut
Strut	4.449	-----
Strut-Node 1	4.631	4.1
Strut-Node 2	4.798	7.8

Strut-Node 1 is a strut-node joint assembly with 3.39 N-m torque
Strut-Node 2 is a strut-node joint assembly with 16.95 N-m torque

Participants
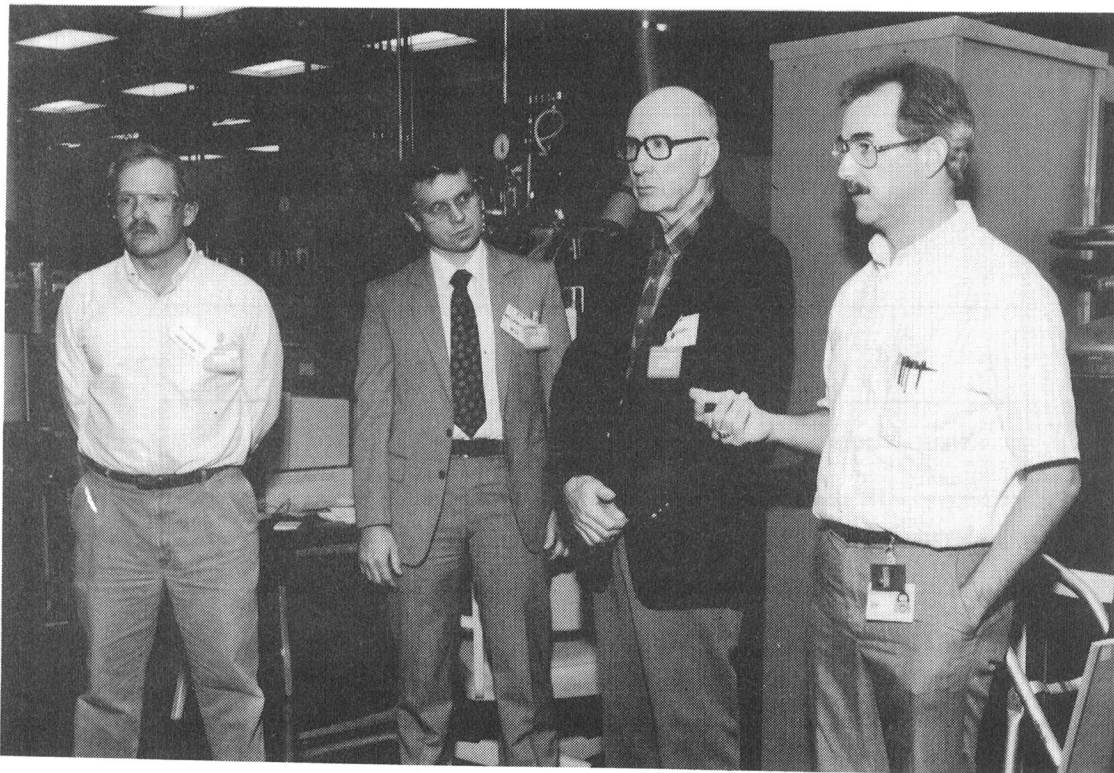
MECHANICAL PROPERTIES OF COMPOSITE MATERIALS

H. Richard Thornton

and

L. R. Cornwell

Department of Mechanical Engineering
Texas A&M University
College Station, Texas 77843-3123

Telephone 409-845-6151

MECHANICAL PROPERTIES OF
COMPOSITE MATERIALS

H.R. Thornton and L.R. Cornwell
Department of Mechanical Engineering
Texas A&M University
College Station, Texas 77843-31123

KEY WORDS: fiber reinforced composites, laminate, orthotropic, longitudinal, transverse, and shear stress, strain, modulus of elasticity, tensile test, "Laminate" analysis (computer).

PREREQUISITE KNOWLEDGE: The student should understand orthotropic characteristics and how off-angle plies are layed-up into fiber reinforced composite laminates. The understanding of orthotropic elastic properties is basic.

EQUIPMENT AND SUPPLIES: Universal testing machines such as Instron or MTS, Tabbed 0°, 90°, and off-angle composite laminate specimens, "Laminate" computer program on PC.

INTRODUCTION: A composite material incorporates high strength, high modulus fibers in a matrix (polymer, metal, or ceramic). The fibers may be oriented in a manner to give varying in-plane properties (longitudinal, transverse-stress, strain, modulus of elasticity). The lay-up of the composite laminates is such that a center line of symmetry and no bending moment exist through the thickness. The laminates are tabbed, with either aluminum or fiberglass, and are ready for tensile testing.

The determination of the tensile properties of resin matrix composites, reinforced by continuous fibers, is outlined in ASTM standard D 3039, "Tensile Properties of Oriented Fiber Composites." The tabbed flat tensile coupons are placed into the grips of a tensile machine and load-deformation curves plotted. The load-deformation data are translated into stress-strain curves for determination of mechanical properties (ultimate tensile strength and modulus of elasticity).

PROCEDURE: Composite test coupons (in our case graphite/epoxy) are fabricated in the following fiber orientations:

1. 0° laminate (all fibers oriented in 0° direction to applied load)

2. 90° laminate (all fibers oriented 90° to applied load)

3. laminates containing off-angle plies.

The flat coupons are tabbed on both ends (both sides) to accept the perforations from the grips on the tensile machine. The tensile coupons are shown in figure 1. The width and thickness are measured and the length is the distance between the tabs. The cross sectional area and the average ply thickness are calculated for each tensile coupon.
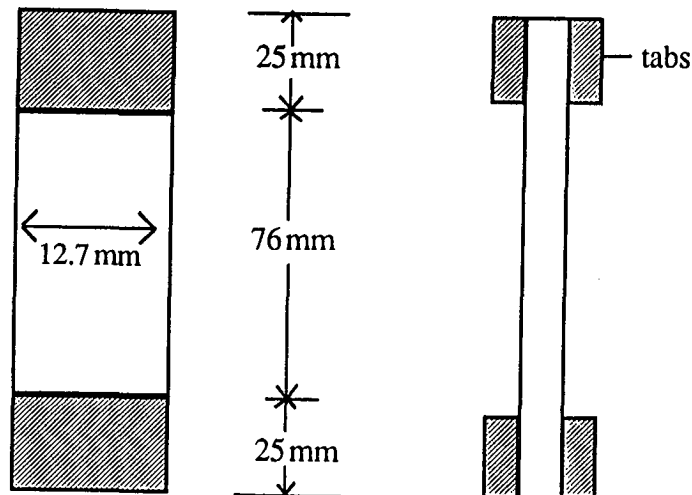
Figure 1. Tensile coupons

The tensile coupons are normally 12.7 mm wide and 1.4 mm in thickness. The thickness is normally 8 plies. The length is approximately 76 mm. These dimensions can vary as long as they adhere to ASTM standard 3039.

The mechanical properties of the 0°and 90° laminates are required for input into the "Laminate" computer program. The computer program also requires the number of plies through the thickness and the average ply thickness.

The tensile coupon is placed into the grips of the tensile test apparatus. Align the coupons and tighten the grips onto the tabbed ends of the specimen. A low strain rate (0.02 mm/mm/minute) is selected for test. Most fiber reinforced composites have limited deformation at fracture. The load vs displacement spectrum is recorded and mechanical property data calculated. 0° coupons provide longitudinal stress and modulus data and 90°coupons provide the transverse properties. The fracture surfaces are examined and failure modes determined. The laminates containing off-angle plies are tensile tested and data reduced.

COMPOSITE ANALYSIS-"LAMINATE": The theory for composite plate analysis considers constitutive equations (Jones, 1975). The "Laminate" computer program calculates mechanical properties of a given laminate considering constitutive [A] (extensional), [B] (coupling), and [D] (bending) stiffness matrices (Andrews, Killespies, Ochoa, 1992). Test data from 0° and 90° laminates define the longitudinal $(E_1)$and transverse (E_2) properties for the composite system. This assumes that the fiber volume

percent is the same in all cases.

The program requires the following data:

1. total number of lamina (plies)
2. E_1 - longitudinal modulus (0°)
3. E_2 - transverse modulus (90°)
4. G_{12} - shear modulus (not determined in test and given by instructor)
5. ultimate tensile strength
   S_1 - longitudinal (0°)
   S_2 - transverse (90°)

   T_{12} - shear (given by instructor)
6. ply orientation (degrees) of laminates with off-angle plies (i.e., +45, --45, 0 - - -)
7. ply thickness (mm).

The program will now calculate plate solutions for selected boundary conditions. Stress-strain valves can be calculated at either the lamina or the laminate level. This experiment will consider the laminate level as our students are not familiar with orthotropic materials at this point.

INITIAL EXPERIMENT: The mechanical properties of the 0° and 90° laminates and laminates with off-angle plies are determined by test. The initial experiment would consider the moduli of elasticity. The 0° and 90° laminates are required for analysis. The moduli of elasticity for the laminates containing off-angle plies are also determined from test. The input data are fed into the "Laminate" program and the moduli of elasticity for laminates with off-angle plies are calculated. An analysis can now be made between the test and analytical moduli of elasticity for laminates with off-angle plies.

This experiment can be used to introduce students to the mechanical properties of composite materials. Also, values can be compared with other materials with which the students are more familiar.

SECOND EXPERIMENT: More in depth information can be determined from the "Laminate" program. For students that are familiar with composite materials, stress-strain relationships can be calculated at the lamina level (ply). The composite plate analysis will determine "first ply failure" within the laminate. This would require that the student have a greater knowledge of the mechanics of composite materials. An understanding of the failure mechanism is required. Also, a failure theory is included in the "Laminate" program that the student should be aware of. The failure theory (Tsai-Hill, Tsai-Wu) should be explained to the student.

This experiment can be considered as a second step in the understanding of the

tensile properties of composite materials.

REFERENCE:

Jones, R.M., *Mechanics of Composite Materials*, McGraw-Hill Book Company, New York, 1975.

Andrews, S., Killespies, H. and Ochoa, O., *TAMULAM - Composite Plate Analysis*, Department of Mechanical Engineering Texas A&M University, College Station, Texas 77843, 1992.

NEW MATERIALS: FOUNTAINHEAD FOR NEW TECHNOLOGIES AND NEW SCIENCE

Rustum Roy

Evan Pugh Professor of the Solid State
Professor of Science, Technology and Society
The Pennsylvania State University
University Park, Pennsylvania 16802

Telephone 814-865-9951

NEW MATERIALS: FOUNTAINHEAD FOR NEW TECHNOLOGIES AND NEW SCIENCE

Rustum Roy
Materials Research Laboratory
The Pennsylvania State University

Abstract

The role of materials as the benchmark technologies which give epochs of human history their names continues into the present. The discovery of new materials has nearly always been the source of new materials science, and frequently of new technologies.

This paper analyzes the actual processes by which new materials are synthesized, i.e. whether driven by serendipitous observations, new knowledge pulled by the market, or integrated into a technological thrust. This analysis focuses on modern ceramic materials discoveries, since WW II, and uses 45 years experience in materials synthesis in the author's own laboratory as case studies.

A dozen different families of materials or processes are involved: hydrothermal reactions; sol-gel processing; clays and zeolites; electroceramics; zero expansion ceramics; diamond films; radioactive waste host phases. Nanocomposite concepts introduced by the author a decade ago offer an entire, large, new class of materials which will dominate synthesis for the next period.

The **future** of materials research for the next 25 years cannot be extrapolated from the past 25 years. We are near the asymptote for materials utilization in most metals. Likewise we are approaching saturation in improvement of many useful properties. Justifying much further "basic" R/D for incremental improvement in civilian-oriented industries will not be easy. In materials synthesis the near-term future is sure to emphasize not "new phases," but tailored micro- and nano-composites for chemical, electrical, optical and magnetic uses. Unexpected new discoveries such as the Lanxide process may offer rarer chances for step function advances.

The new structure of knowledge management will rely less on local research than on integration of worldwide inputs. Better scientific and technological opportunities will lie in designing knowledge intensive materials to meet the new environmental and conservation goals, and the human needs of the very large numbers at the bottom of the socio-economic structures of the world.

NEW MATERIALS: FOUNTAINHEAD FOR NEW TECHNOLOGIES AND NEW SCIENCE

THE ROLE OF MATERIALS IN HUMAN SOCIETY

This rather bold title has been chosen to call attention to the long-neglected pivotal role that the discovery of a new material or a new process for making—typically new—materials has played in the progress of humankind and the science of materials.

Figure 1 recalls that historical epochs have been named after materials. Today our post WW II epoch would be accurately named the silicon era. We will conclude this paper by claiming that the next era will be that of the nanocomposites. Figure 2 brings together some characteristics of all the materials that humankind uses. In national and world policy it is important to have a feel for the volumes of the different materials actually used. Many are surprised to find the rank order of the tonnages of these materials: wood; ceramics including cement; metals; polymers; and semiconductors. Another interesting comparison in Figure 3 introduces the importance of the comparative scale in very

---

- STONE AGE / *old* (paleo)

  \ *new* (neo)

  - Pottery

- BRONZE AGE

  - Cement

- IRON AGE

  - Aluminum

- SILICON AGE

  - (Nano) Composite

"FIDES SUBSTANTIA RES" Teilhard de Chardin   RES SUBSTANTIA SPEI
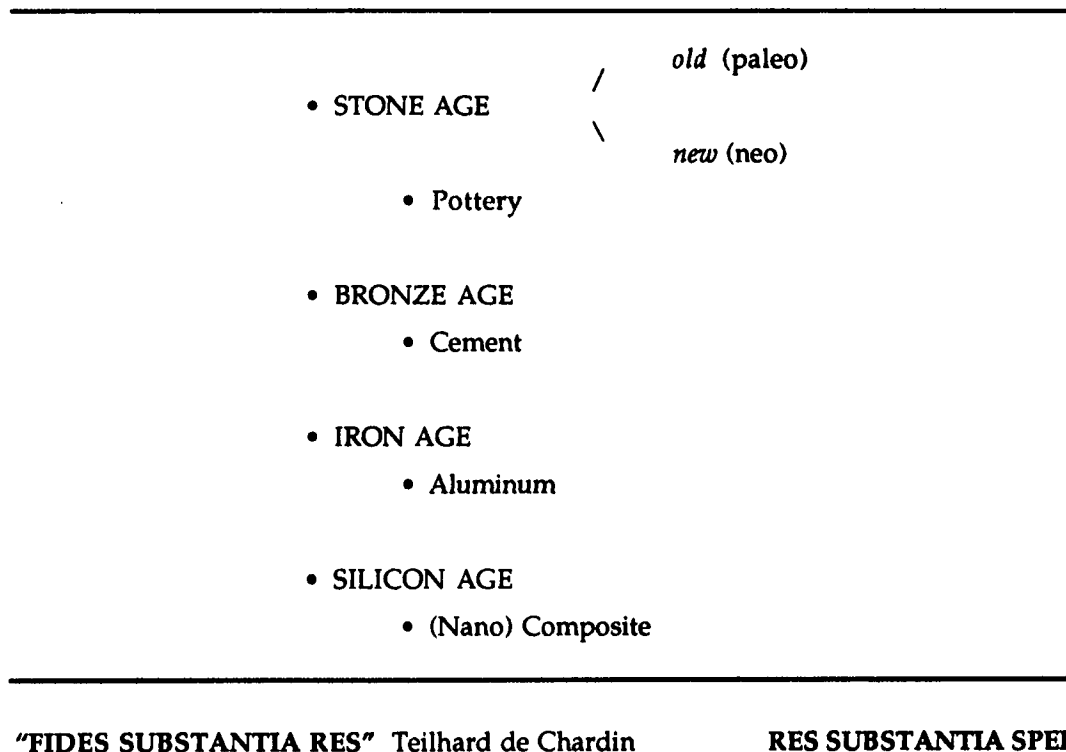
Figure 1.   The "progress" of human history has been marked by (new) materials. It is not an unreasonable index as the philosopher scientist Chardin observed "Faith is the substance of things." I have paraphrased the modern situation for many societies on the right, "Materials give substance to hope."

Use Started In	Millions of Tons/Year	Resources Needed	Products	Properties Utilized
WOOD 3,000,000 B.C. (natural composites)	1-10,000	renewable, but somewhat geographically limited	building	mechanical
CERAMICS <10,000 B.C. Incl. cement	1-10,000 1,000	SiO_2, Al_2O_3, CaO, MgO Fe_2O_3 universally available no resource problem for any nation	pottery glass - bulk - optical cement; refractories; cutting tools; diamonds; turbines	mechanical optical electrical
METALS 5,000 B.C.	iron = 500 others = <500	viable ores geographically very uneven	myriad products steel, copper, aluminum alloys	mechanical electrical
POLYMERS 1900	~100+	petroleum (now)	containers, furniture, textiles	mechanical (electrical)
SEMICONDUCTORS 1940	<<.001	no resource issue	small electrical devices	electrical
COMPOSITES 1950	1-10	not important	furniture to airplanes	mechanical (electrical)

Figure 2. The Material World.

53

Factor	Highway Materials Asphalt & Concrete	Superalloy	Microchip	Ceramic Matrix Composite
Tons/yr	1,000,000,000	50,000	100	10
Second phase	Stone, rebar, pores	γ'	Epitax layer	SiC
Size of second phase (nm)	From 1 up to 10^{10}	10^3	10^2	10^4
Cost, $/#	0.05	100	23,000	100
U.S. Research Effort	3×10^7 (1977)	10^8	10^{9+}	10^8

Figure 3. The enormous range in contemporary materials (after R. Decker), in volume, size, price, and total research effort which is not related to the business opportunity.

different parameters among different materials. Not only volumes and size and second phase are significant. One notes that the research effort bears some relation to the cost per pound, but none at all to the total volume of cost of the class of material. Figure 4 is a summary of the status of our ability today to **design to specification and synthesize materials,** by the size of the units involved in composite or single phases. The larger the size from meters to tens of micrometers, the more advanced our ability. At the unit cell or "atomic" level our synthesis ability is still very primitive indeed. It is a major thesis of this paper that the nanocomposite level provides the level of aggregation which will form the frontier for materials research worldwide in the immediate future.

Macro (cm-m)	Excellent	Materials for very large structures have been optimized; e.g. reinforced concrete, airframe alloys.
Micro (mm-μm)	Very good	Lab scale and small objects (GRP to graphite-epoxy composites; transparent Lucalox, composite transducers, etc.).
Nano (0.1 to 10 nm)	Primitive but new	New materials *designed* and made: intercalates, glass-ceramics, toughened zirconia, nanocomposite desiccants, etc.
Atomic (0.1 nm)	Poor	New materials found by serendipity: penicillin, teflon, magnetic garnets, R.I.B., 1:2:3 superconductors, etc.

Figure 4. A comparison of our contemporary capacity to prepare new materials or composites arranged as a hierarchy of size.

THE INNOVATION PROCESS

We turn now to the question of what the historical record teaches us on how innovation has occurred in science and technology.

In earlier reviews (1,2) I have referred to the work of J. D. de Solla Price (3), one of the great historians of science who shows definitively how much advances in all branches of sciences depended on new instruments. I argued by analogy (4) that "new materials" play exactly the analogous role in the materials sciences and technologies. The relationship is that shown in Figure 5. This figure makes several points. First it supports Price's contention (the title of his AAAS address) that by and large (contrary to the totally unsupported maxims of many scientists in academia), *science is largely applied technology*. From Galileo, applier of the telescope, to the modern particle accelerators, appliers of magnet and electronic technology, there is no room for argument that in most cases, as Price puts it, "the

Materials Technology   New Materials → New Science
      ↑ ↑   ↑
   Other Inputs   ↓
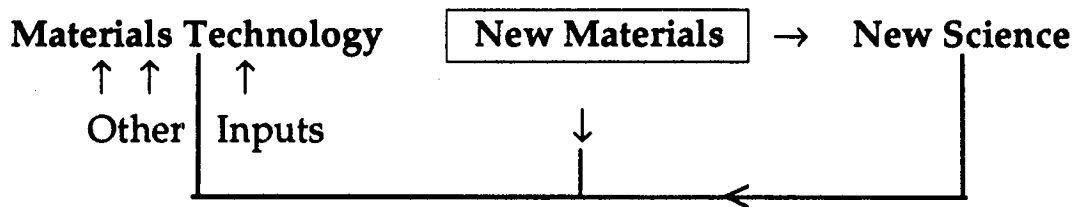
Figure 5. In parallel with de Solla Price's assigning of the key role to new instruments in advancing science and then technology, new materials can independently advance both materials science and materials technology. The science has not led to new materials, except increasingly in the design of composites.

arrow of causality" is from technology → science. Certainly particle physics CANNOT help the materials science of magnets; the latter is essential to the former. Second is the point that a new material, often discovered serendipitously, leads to new science. The extent to which this is true is illustrated by the case of new superconducting materials to BCS and other theories of superconductivity. The latter certainly did not give an iota of guidance on finding new materials. Yet the discovery by amateur chemistry of 1:2:3 oxide superconductors will provide activity and employment for hundreds of theorists in physics worldwide. Exactly analogous examples may be found in magnetic or ferroelectric materials. New materials certainly are the fountainhead for new materials science.

In the advancement of technology, the story is the same. The new material—teflon, polyethylene, the magnetic garnets, new zeolites—all lead rather directly to new technologies. The feedback loop going towards products requires, in addition, the major components of capital, labor,

entrepreneurship, etc. Any contributions from the science often comes later as an add-on in the second generation of products, new zeolites, magnetic bubbles, etc. Thus materials science often helps in the fine-tuning and optimization. But the discovery of the new material is the pivotal point. Had zeolite A not been discovered by Breck et al. (5) an entire industry of catalysts and separation might not exist.

Why then has materials synthesis been so neglected, especially in the U.S.? My analysis of this issue illustrates the necessity for understanding the human dimensions of scientific research. I attempt in this paper to interweave the science with the human and societal dimension. By omitting it I believe we give a false picture of how science really progresses. My studies of why scientists pursue particular topics show the following factors to be most significant in decreasing order of importance: Fashion (based on stories in the popular press), availability of money, local access to particular specialized equipment, the more specialized or exotic, the more powerful the influence. Other factors such as novelty of idea, significance to science, etc., have a very small impact. Few scientists today have even thought about their research in those terms. Thus, in the post WWII U.S., it was the agile and active physics community returning from the Manhattan project that saw the opportunity and took over the field of materials research. They brought with them the incredibly naive and totally spurious notion that basic science (the more the better) "leads automatically to technology and thence to prosperity." [This is a quote from G. A. Keyworth (6), President Reagan's science adviser for seven years]. This notion was built on similar simplistic, later to be proved totally erroneous (7), aphorisms such as "The A-bomb led to the defeat of Japan." And the greatest swindle of all, since Jacob outwitted Esau, that "The bomb was a triumph of science," and not of the incredible power of organized American technology.

Based on these erroneous precepts U.S. national science policy went off on a totally erroneous track as traced by Shapley and Roy in their book (8). Following the ruling paradigm of the day that the more "basic" the science the better, materials science was, in the fifties and sixties, equated to metal physics and solid state physics of idealized alkali halides and similar substances. By the fortunate coincidence of the discovery of transistor action in a new material—highly purified germanium—an ideal marriage of opportunity and availability appeared in the semiconductor world and appeared to support the value of such science. Ge, then Si, in the simple diamond structure, became available in extraordinarily pure and perfect form—thanks to a triumph of materials synthesis. And this opened up the enormous opportunity for the fantastic new science of semiconductors, and the new technologies underlying modern electronics.

In the meantime, in academia and the research-supporting agencies, synthesis of new materials, whether in metallic alloys, ceramics, or polymers was relegated to second class, or worse, status. Theory and phenomena ruled the day. In industry the situation was very different. All corporations remained very active in materials synthesis and processing: Bell Laboratories in Ge, Si, garnets, etc.; GE in new alloys; Lucalox, polymers; Corning in glass-ceramics, photoceramics, etc.; 3M in sol-gel fibers

and grains; Philips in ferrites, and so on. At Penn State, the Materials Research Laboratory was the lone exception among major universities with "Materials Preparation" (as the keystone of our clearly articulated research strategy). This put us closer to the kind of materials research regarded as most significant by industry. Hence it was no accident that the Laboratory has had for decades the highest percentage of support from industry among such U.S. laboratories. And for the thirty-year life of the Laboratory and a dozen years before it was formed, we have had at Penn State a major continuing research effort—with several striking successes—in materials synthesis. This long and broad track record was all focussed in the area of ceramic materials. And it is to an examination of the details of what we can learn from these results that we now turn.

DIFFERENT MODELS FOR DOING MATERIALS (SYNTHESIS) RESEARCH

In a lecture such as this I believe it is not productive merely to review the literature on synthesis, or to catalogue our own studies, but to conduct a meta-analysis of the latter to extract insights on the thought processes involved. Our goal here is not to invent new epistemologies, or come up with new theories of innovation or creativity. Rather it is to try to examine clearly the empirical data on 45 years of research on synthesis and see if one can find underneath some common patterns among the successful cases.

We start by making distinctions within the very fuzzy term "science" as it is used in our culture. At least the following three categories of science, S^1, S^2 and S^3, can be identified and defined below:

S^1 = Serendipitous discovery (careful observation by highly trained observer).

S^2 = Science for society (purposive, long-term basic science).

S^3 = Science for self and the institution of science.

Next, we turn to determining the relationship of these kinds of science to the motivation or context for the synthesis research. Here also we define three categories, of which the first two are well known:

S.P.: Science Push. This is the concept that the pursuit of knowledge in itself leads to (useful) discoveries.

M.P.: Market Pull. The concept that a need—either in a company or in society—in the "marketplace" for improving a product or finding a better one leads to the advancement. S^2 science based on such market pulls would tend to be narrow in scope and short term. Much new product development research in industry, today, would fit into this category.

T.T.: Technology Traction. This is my own term describing the linking of the new research to a societal need or private market *through* a specific application or technology. Such a "traction" from existing or new devices, hardware, etc., provides a feedback mechanism to the S^2 science from the real application. All such research also

utilizes all relevant "science on the shelf" which will have accumulated partly from S^3 science. It also maintains the S^2 focus for the longer-term science, and hence can, in turn, be sustained for longer periods because it is linked to an existing or definitely needed technology. Much of the *longer-term* research in industry, connected to, or directly relatable to a technology, fits into this category. And it is precisely *only* this T.T.-S^2 research within industry that is by far the most cost-effective and productive component of "research" or science. It was this fraction of the total research spectrum which led to the enormous U.S. technological prowess up through the seventies. It is not fully realized that it is Japan's clear-sighted focus on this T-T-S^2 research which has brought Japanese industry into a commanding position in so many technologies. Unfortunately during the fifties and sixties much of American industry, taking its miscue from U.S. academia, conflated its S^2 and its S^3 research. This muddle continues into the present. In the late eighties it became clear that S^3 research supported by industry was simply not justifiable. Regrettably, however, not only S^3 but much T.T.-S^2 research has now been eliminated in U.S. industry demonstration of the urgency for clarifying our terminology, and properly classifying particular research. Figure 6 is a schematic representation of the T.T. process. In many ways it is the realization of the U.S. Defense Department's "basic" or "6.1" research. The imminent downsizing of all industrial research will be followed, in my estimation, by appropriate similar reduction in S^3 academic research. But this will affect all T-T-S^2 research also unless we start making the distinctions very clearly now.

It is clear that these classifications are hardly sharp and watertight, but they are no less essential for that.

EMPIRICAL ANALYSIS OF LOCAL MATERIALS
SYNTHESIS RESEARCH USING THESE CATEGORIES

In earlier papers (1,2), I have alluded to the fact that the basic sciences necessary for a scientific approach to materials synthesis of inorganic nonmetallics are **phase equilibria and crystal chemistry**. In this respect the U.S. is at a substantial disadvantage compared to the U.K., Europe, the former U.S.S.R., India, etc., since these topics are ignored in chemistry and physics departments and in many materials departments.

This section of this paper is an attempt to analyze the processes by which successful materials synthesis research has actually been conducted in this Laboratory. It analyzes retrospectively using the lens of the categories defined above what actually happened in ten areas where significant

innovation in materials synthesis or processes actually took place. Table 1 gives an overview of the ten subject areas we deal with.
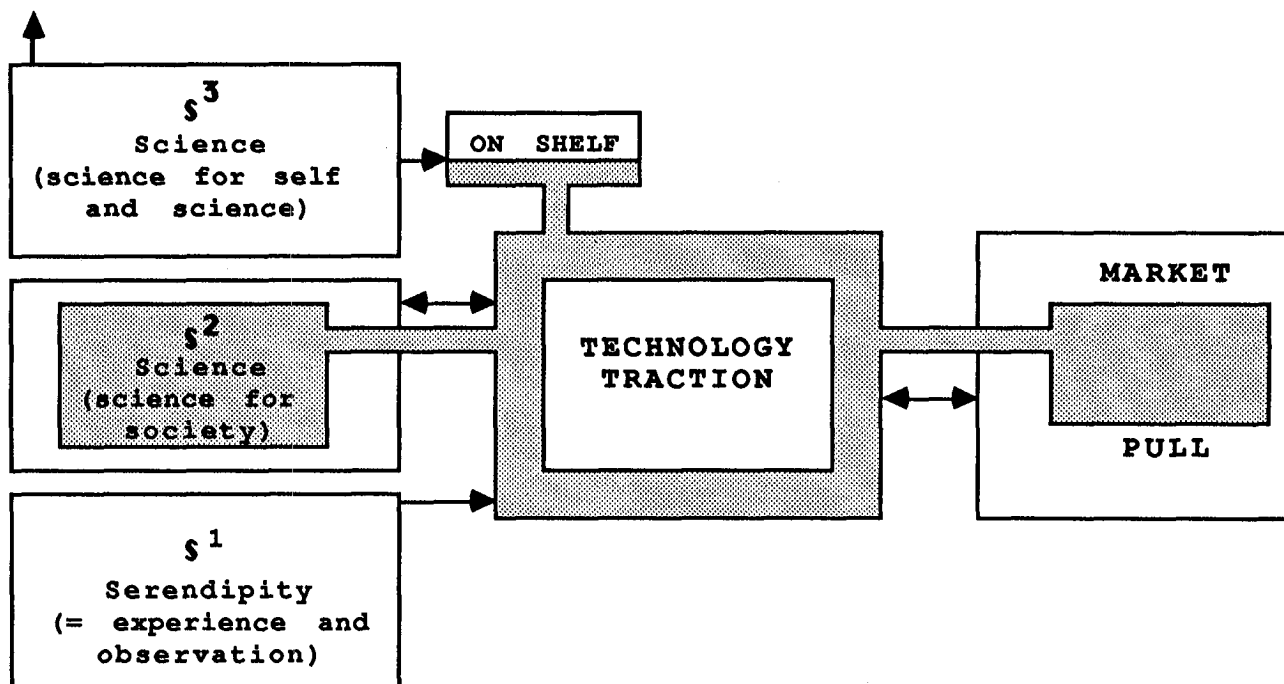
Figure 6.   Technology traction model of materials science. In many ways this represents the ideal of what is attempted in the U.S. defense departments 6.1 and 6.2 research.

1a. Hydrothermal Processing; 1b. Sol-Gel Process

These two processing innovations are dealt with together because in fact the basic advances and initial "reduction to practice" were completed in one year (July 1948-June 1949). Together they form a rather clear example of "S.P.," a science-push innovation.

In 1948, hydrothermal techniques had been known for a couple decades as a means of making hydrous phases. The principal "instrument" was the Morey bomb limited to about 400°-450°C and about 1 kbar H_2O pressure. The idea of using water pressure to catalyze anhydrous reactions per se or the hydration of anhydrous phases in the system Al_2O_3-SiO_2-H_2O called for new equipment which could reach higher temperatures. The design of the "test-tube bomb" and multiplexing of several of them with one pressure source created almost a perfect example of the kind of "instrument" to which de Solla Price attributes much of scientific advance. Based on this "instrument," Penn State became the world HQ for systematic hydrothermal synthesis and phase equilibria work for 2-3 decades. It is remarkable to note that this design of the hydrothermal "instrument" has not changed for forty years and the January 26, 1992 issue of *Chemical & Engineering News* carries on its back cover, a full-page

Table 1. Retrospective analysis of "context" of Roy's ceramic research, 1948-1991.

RESEARCH AREA	MOTIVATION		STATUS
• Hydrothermal processes	S.P.	To accelerate reactions among oxides at low temperatures	Widely adopted worldwide immediately
• Sol-gel process		To make *homogeneous* ceramics for all lab research	On the shelf (O.S.) for 15-20 years
• Glass Ceramics			
(a) phase diagram for Li$_2$O-Al$_2$O$_3$-SiO$_2$	S.P.	Basic studies in area *known*	Utilized by Corning
(b) metastable immiscibility	T.T.	To *be useful* in industry	Picked up very slowly
• New zero expansion ceramics	T.T.	Clear technology-market pull. Based on major science base.	Applications being explored on wide front after 5-year incubation.
• New methods for fine powders			
(a) EDS	S.P.	Improve options for lab powders	O.S. 10 years
(b) RESA			Unpredictable
• Clay mineral synthesis stability.	S.P.	Systematic basic work. Known to be useful to oil industry	Used immediately. Fed into industry.
• Zeolite synthesis	T.T.		
• BaO-TiO$_2$ phase diagram	T.T.	Value of basic science to tech. was clear	Universally utilized rapidly.
• Perovskite ×1 chemistry			
• High pressure materials synthesis/stability (anvils)	S.P.	Opportunity push (based on instrument) helped by diamond tech. pull.	No application for any results from huge worldwide effort.
• Design and synthesis of crystalline radioactive waste Ditto hazardous wastes.	M.P. T.T.	Apply basic science to obvious societal need	Strong worldwide impact via regulatory agencies.
• Theory and practice of glass formation in oxides	S.P.	Originally basic science of above	Enters general broad stream of activity.
• Thin films. Si, Ge; diamonds	T.T.	Pure tech traction	Enormous impact on industry
• Concept of SSG-derived nanocomposites	T.T.	New broad concept in our area of expertise	Very rapid entry into science and technology

advertisement for these vessels, still sold by a local firm, with the exact design we optimized within a year or two of its original development.

The sol-gel process was also born out of the community's needs in experimental work in oxide systems at low temperatures. The goal was simple and global: To make atomically homogeneous ceramic powders of essentially *any* composition. Without such intimate mixing, in the system being studied (Al_2O_3-SiO_2-H_2O), reaction rates were essentially zero. Necessity was the mother of invention.

It was clear that mixing via a *solution* step was the only way in which such atomic scale mixing could be achieved. This was already in use for precipitating or pyrolyzing to obtain powders, but gelling ions mixed in solution was the difficult step. To achieve this, I originally used organic precursors for the first time to mix in SiO_2, Al_2O_3, TiO_2, etc. Later inorganic sols with 20-100 nm particles proved to be equally efficacious. The conceptual advance was the use of a gel step instead of a glass step (then in common use in high temperature silicate equilibria studies, but limited to glass-forming compositions). Here again although it was S.P. research, there was a distinct generic experimental "need" which was being addressed at the same time. This makes a kind of connection to a T.T. type research. What is truly remarkable about the sol-gel process is, first, how completely successful it was. Within a decade our Laboratory files held vials of several thousand compositions in dozens of simple and complex oxide systems made by several different investigators and described in dozens of papers. Secondly, it was remarkable how long it took for the sol-gel method to be picked up by the ceramics community—nearly 15 years in industry and 25 years in academia. This, in spite of the fact that the large number of papers had been published by the Penn State groups and the world-wide geoscience community.

2. Glass-Ceramics: This is an Excellent Combination of S.P. and T.T.

My connection to glass ceramic research came about entirely serendipitously because my Ph.D. thesis was the detailed phase diagram for the system Li_2O-Al_2O_3-SiO_2, including the spodumene-eucryptite join. Simultaneously with this study my colleague, F. A. Hummel, discovered the extraordinary low and negative thermal expansion of the eucryptite and spodumene phases. Stookey at Corning, after his doubly serendipitous discovery of the glass ceramic process, of course, utilized Hummel and Roy's work in making the first commercial glass-ceramics, Corningware.

Thus our S.P. contribution was prior to Corning's discovery of the process, but our further contributions were strongly pulled by the T.T. process since many other corporations such as Pfaudler and PPG turned to us for collaboration in their glass-ceramic research. Their goals were met in a very short time. Our subsequent contribution to understanding the glass-ceramic process came from our phase equilibria studies on titano-silicate systems. Thus in pure S.P. research, DeVries, Roy and Osborn (8) first totally revised the phase diagram of the system TiO_2-SiO_2 from supposedly having zero liquid

immiscibility, to nearly 80% immiscibility. And their work on the CaO-TiO$_2$-SiO$_2$ (9) system outlined large areas of stable liquid-liquid immiscibility, bordered by large regions where enamel-like glasses formed. This led me to the key paper (10) on the role of **metastable liquid immiscibility** as the correct nucleation step (correcting Stookey's original and sometimes still reported, assignation of the nucleation step to "rutile" formation). The two highly relevant phase diagrams are shown in Figure 7. One of the issues in contemporary synthesis research is the general weakening in the materials community of the ability to interpret especially more complex phase diagrams and the absence of classical crystal chemical knowledge.
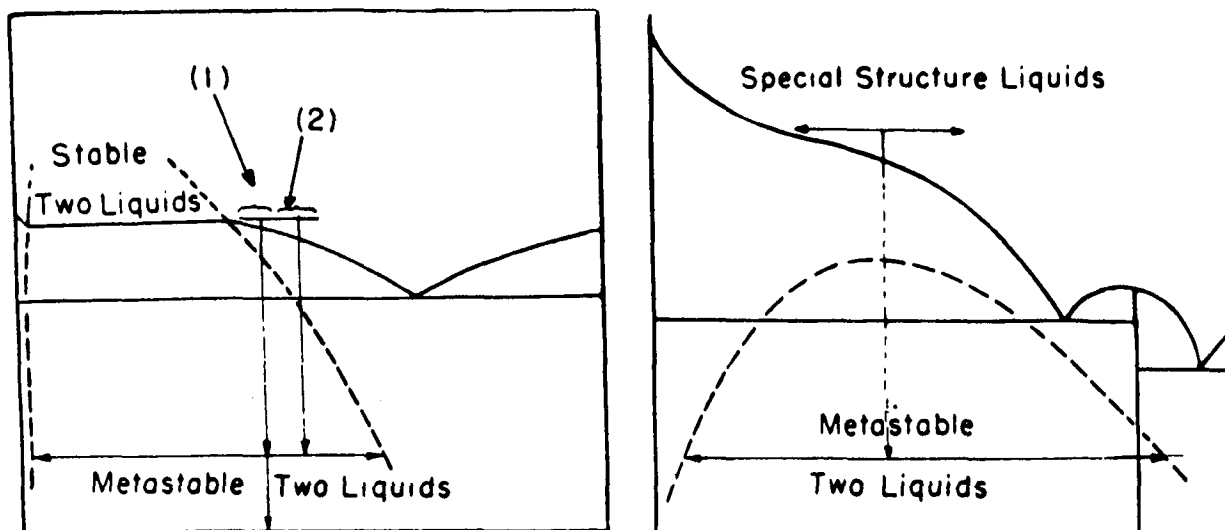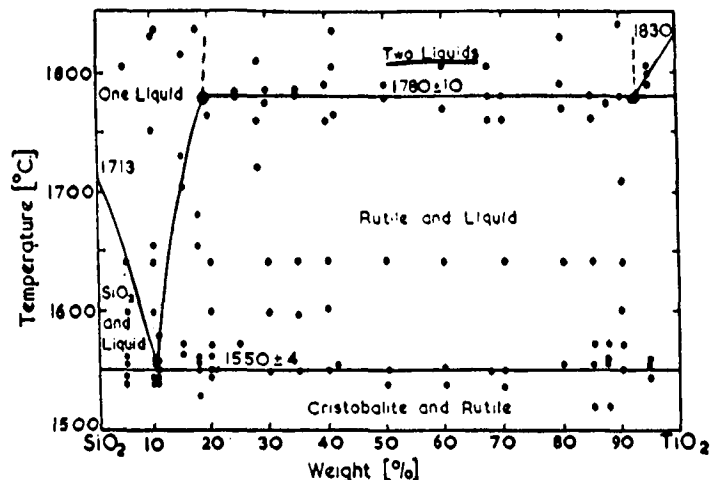
Figure 7. The role of liquid-immiscibility in TiO$_2$-rich silicate melts was hinted at from the phase diagram for the system TiO$_2$-SiO$_2$ (and CaO-TiO$_2$-SiO$_2$ not shown) and *metastable* mixing of two liquids explicitly identified as the nucleation step in such glass ceramics.

3. Zero-Expansion Ceramics: A Model T.T. Success in Synthesis

This is one of the clearest examples of a technology traction development. Because of our involvement with the initial discovery of the major zero expansion materials of commerce, the lithium aluminosilicates (LAS, see above), the Air Force Office of Scientific Research approached us to try to develop a new material with thermal expansions even closer to zero at $-100°C$ for space structures. Here was a clear market pull; well-established technologies existed that could use such materials and while much new data on new materials had been accumulated in the 40 years since the LAS discovery, no other crystal structure had even begun to compete. Our approach proceeded sequentially:

1. Modifying, compositionally, a known near-zero α material: cordierite. By using sol-gel processing we were able to introduce more Ge than hitherto achieved and obtained some very acceptable low α phases (see Ref. 11).

2. "Theory" was totally useless in helping locate an inherently anomalous structure. By serendipitous observation, using our own empirical guidelines (structures articulating strongly (4+ and 5+ valent cations), bonded polyhedra around large "holes") we discovered the low-α properties of a very well known structural family, the NZP $(NaZr_2P_3O_{12})$ or CTP $(Ca_{0.5}Ti_2P_3O_{12})$ family (Refs. 12-14). We were able to show that a dozen different compositions completely bracketed the low+ and low- α range, with extensive solid solution allowing every value in between (Figure 8).

THERMAL EXPANSION OF [NZP]-FAMILY
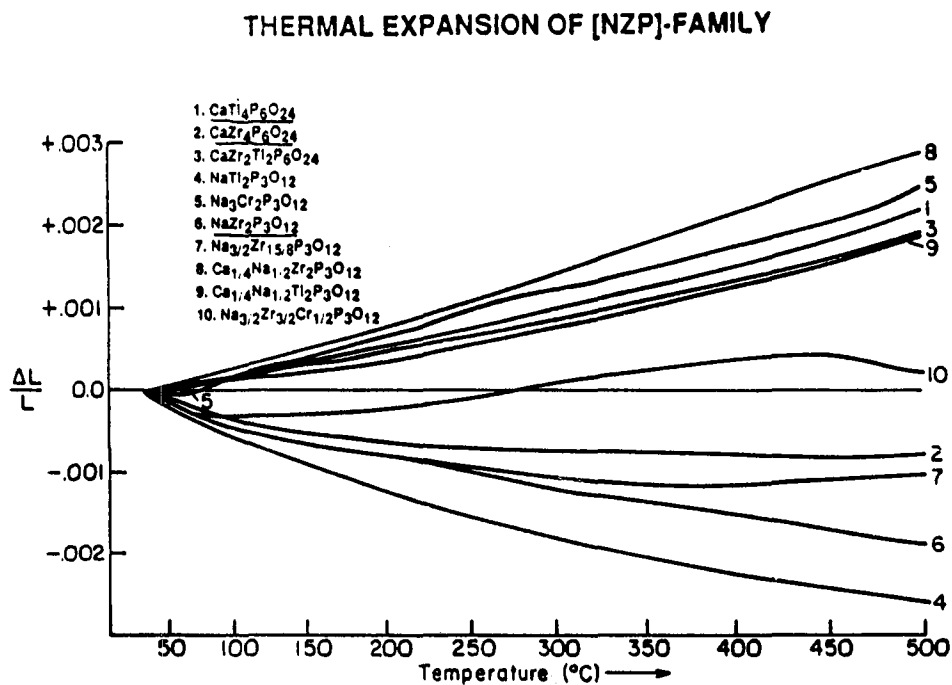
Figure 8.

Success with this objective led the AFOSR to set another: eliminate the anisotropy of α if possible. There appeared to be no rational process to eliminate the anisotropy of α in the hexagonal phase, since it is by averaging a negative α in "a" or "c" direction with a positive α in the "c" or "a" direction, that we get zero. But another **serendipitous observation** (that in $Sr_{0.5}Zr_2P_3O_{12}$ the "a" and "c" axes were reversed) led us to the "zero"-α, "zero"-anisotropy $Sr_{0.5}Ca_{0.5}Zr_4P_6O_{24}$ family which also turned out to have melting points above 1700°C (14).

3. The third objective given to us of making a ferrimagnetic NZP phase to absorb radar signals (market pull) appeared like a reasonable challenge due to the fact that most 3d and 4f ions can be accommodated in the structure. Yet, in spite of very extensive experimental substitution, this approach did NOT work. We were unable to synthesize any ferrimagnetic NZP phase. Instead, we had to design a microcomposite of two thermodynamically compatible (determined experimentally) phases, one with a negative α ($Na_4Zr_2Si_3O_{12}$) and a ferrimagnet (YIG) with a positive α.

    The NZP family of controllable low expansion ceramics is an outstanding example of systematic T.T. materials synthesis. There are obvious technological opportunities for such materials but the actual penetration into established markets will be decided by many other factors outside science. This example is almost a textbook case of T.T. practice at its best—which is, of course, NOT universally successful. It demonstrates the value of having access to an "on-the-shelf" science base—in our very long experience in the field. And it demonstrates that "theory" is not of much help in designing new materials. And finally, it proves the value of serendipity based on careful observation by experienced observers who can recognize anomalies and pick up hints in not directly related literature.

4. Processes for Making Fine Powders (S.P.)

In the early fifties in parallel with the sol-gel processes we had also experimented (15) with spray pyrolysis of the mixed solutions. By a decade later Ruthner (16) had exploited the same process and made it into a successful commercial process for making ferrite and alumina powders. We showed that the EDS or DMS (decomposition of misted solutions) process had both general and special applications in powder preparation in the laboratory also (17). However, in spite of the enormous interest in ceramic powders, few really new methods have appeared in decades. The laser pyrolysis approach had proved to be very limited in the range of ceramic powders which can be made and very costly. This "need" in science and technology provided the very diffuse pull for our work. The concept of the "reactive electrode submerged arc" (RESA) (modified after the classical work of Faraday on

making gold sols) works by striking an arc under water, solutions, organic liquids, silicones, etc. The apparatus is shown in Figure 9.

The RESA process has proved to be quite general (18) for making pure submicron powders of oxides, carbides, nitrides, and very recently (unpublished) of new crystalline carbons related to Buckyballs. It represents a successful science push development, not yet linked to a technology, but has obvious potential for special application. And a recent development, the so-called "combustion synthesis" developed in India, appears to be another really novel process (19) for making fine powders.
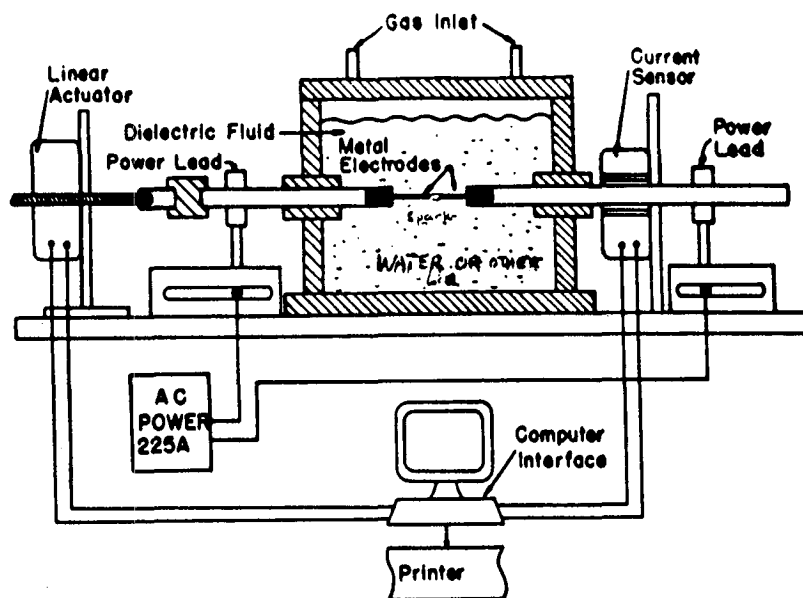
Figure 9.

In all such S.P. advances that we have made to date an important common characteristic is the discontinuous break with the past. S.P. advances in synthesis or processing occur far from mainstream activity and therefore are very likely to be missed and ignored for years. This again argues the case for scouring the literature on the periphery of one's interest to pick up hints or related advances which may have been already demonstrated in other connections.

5. Clay and Zeolite Synthesis (S.P. + T.T.)

We have noted that the first application of the hydrothermal instrumentation was to the system Al_2O_3-SiO_2-H_2O for the catalysis of subsolidus equilibria among anhydrous phases, and studies of the synthesis (and stability) of the hydrated clay minerals (kaolinite and pyrophyllite) in the system. With that beginning, we launched a ten-year emphasis on the synthesis and stability of all clay

minerals first in the system Al_2O_3-SiO_2-H_2O and later with the systematic, step at a time, addition of alkali (K, Na) and alkaline earth (Ca, Mg) oxides as an additional component.

Figure 10 gives but one example of two dozen of the kind of detailed phase equilibrium "maps" (this one for the system Na_2O-Al_2O_3-SiO_2-H_2O) which we produced, at enormous personnel cost by today's standards, as the permanent template to guide all such synthesis efforts. Alongside this S.P. science, we were able, for the first time, to create entire suites of di-octahedral (Mg) and tri-octahedral (Al) sets in the 7Å, 10Å and 14Å mica and clay mineral families. Both expanding and non-expanding

Na_2O-Al_2O_3-SiO_2-H_2O
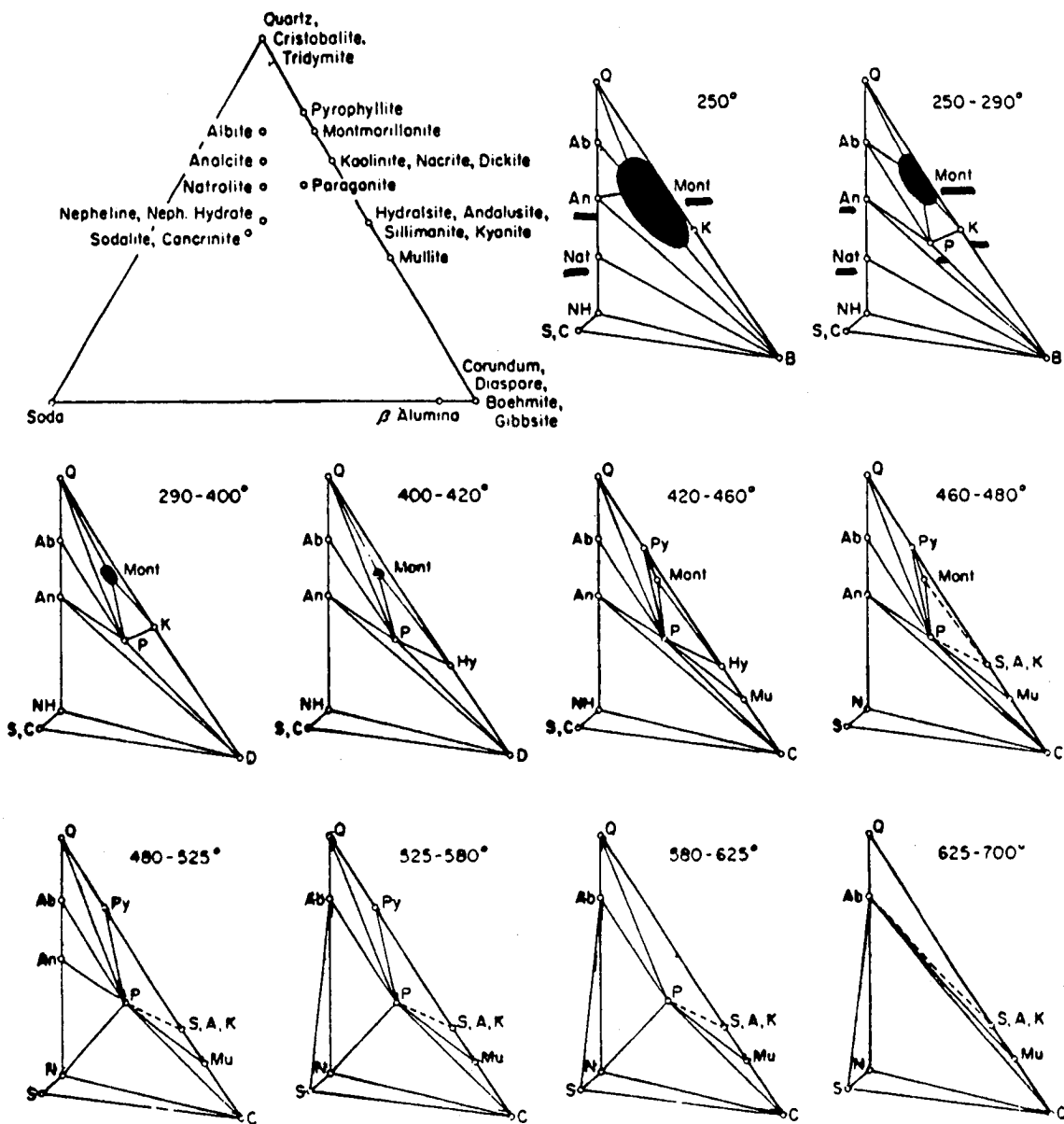
Figure 10.

10Å minerals of completely controlled charge density were synthesized in various systems including exotic ones involving Ni, Ga, Ge, Zn, etc. The demand for this depth of basic work was, of course, due to a T.T. linkage to the petroleum industry's interest in clay minerals both as stratigraphic markers and as drilling muds.

Even in the mid-fifties we were able to even control the morphology of micron size powders from high aspect ratio fibers, to equant hexagonal flakes [see Roy and Roy (20)] by compositional manipulation (i.e., Al^{IV} and Al^{VI} substitution for Mg^{VI} and Si^{IV}).

Following the *systematic* clay syntheses, we pursued the same strategy on the *known* major zeolite families. Systematic detailed studies of the synthesis and stability of the phillipsite, analcite and mordenite-wairakite families were carried out in the hydrothermal regime. Even after the Union Carbide discovery of zeolites A and X, due to the highly proprietary nature of the work, in spite of our obvious expertise, we were not invited by industry to be involved in the race to create new zeolites, i.e., there was an insufficient T.T. element to channel our synthesis capabilities into possibly fruitful directions. Our zeolite syntheses therefore "stayed on the shelf."

6. Perovskite Electroceramics (T.T. and S.P.)

This area constitutes a first-rate example of using all our knowledge base to put materials synthesis of an important new family of materials on an intellectually sound basis. The U.S. Army Electronics Command recognized the need (a) to grow single crystals of $BaTiO_3$ and (b) to look for similar phases which might be even more useful. In the early fifties there was enormous research activity in applications of such phases to capacitors and the technology traction feedback loops were active and *rapid*.

For task (a) it was realized that a reliable phase diagram was essential. Figure 11 shows the phase diagram for the system $BaO-TiO_2$ which was determined by us, the first such detailed high temperature equilibrium diagram of a titanate system with any degree of reliability. And it was on the basis of this diagram that Linz et al. at MIT were then able to grow the first reproducible large single crystals of $BaTiO_3$. Here was S.P.-T.T. coupling across institutions.

For task (b), we worked in the V. M. Goldschmidt tradition of empirically determining the structures of a large number of rationally engineered (with respect to composition) candidate phases. From the structural data we were able to provide structure field maps for future materials synthesizers in search of a particular phase. See the book by Muller and Roy (21) for a compilation of such SFM for all ternary ceramic structures. Our crystal chemical study on the perovskite structure (22), for example, besides lists of very much-used substitutions, shows the first of the phases $Ba_3NiTa_2O_9$ prototypical of the PMN ($Pb_3MgNb_2O_5$) or relaxor ferroelectric materials, which have now become possible successors of $BaTiO_3$ in certain applications.
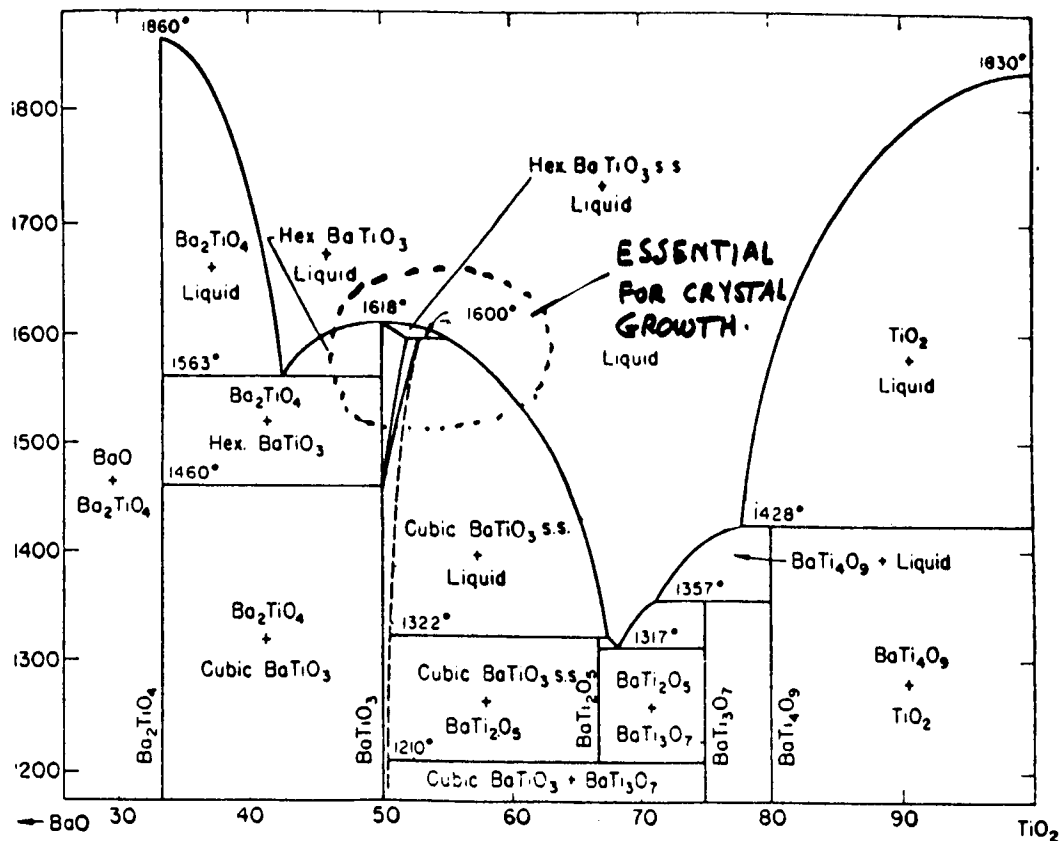
Figure 11. BaO, TiO₂.

7. High Pressure Materials Synthesis: Pure S.P. Syntheses with no Spin-off

Although in the mid-1950's we were the leading laboratory in the hydrothermal high pressure regime (up to a maximum of say 10 kbars) we had failed to synthesize any of the high pressure minerals (kyanite, jadeite, pyrope, and of course diamond) mineralogists had set their sights on. With the work of Coes at Norton and Hall at GE, two new kinds of apparatus—the piston-cylinder and belt—were developed which enabled one to reach the P-T regime for synthesis of all minerals occurring on the surface of the earth. Again, the "instrument" played the key role.

Yet these apparatuses were extremely expensive and time-consuming to operate. Hence we chose to develop instead Bridgman's simple and compound anvils as a simple "instrument" for use in materials *synthesis*, at very high pressures (≈200kbars) and modest (≈500°C) temperatures. Our

opposed-anvil apparatus proved to be a very effective and reliable tool in materials synthesis [see Dachille and Roy (23-25)] and also became widely used. Indeed later on the utilization of single crystal diamond as the anvils by van Valkenburg at the National Bureau of Standards led eventually to the work of Mao and Bell at the Geophysical Laboratory in reaching megabar pressures at ~2000°C temperatures to study in-situ transformations especially those related to the interior of the earth. The diamond anvils have not produced many new quenchable phases.

Our opposed-anvil apparatus allowed us to synthesize—by 1970—more new high pressure materials (which could be retained at ambient conditions) than all other laboratories combined. On the other hand, our own crystal chemical studies on the effects of pressure showed that there was no scientific reason why high pressure would lead us to new structures with extraordinary properties. The logic of each of our structure field maps showed that whatever structures could only be achieved with pressure at a certain composition, could often be created at 1 atm pressure merely by changing the composition. Hence nothing especially interesting should be expected among high pressure phases with the single exception of diamond which is the unique extremum in composition in the middle and top of the periodic table.

In any event, we were proved correct. No product of any value, no technology, has emerged from the extensive worldwide high pressure program. This was quintessential S.P. materials research which led only to "science on the shelf"; in geophysics the results proved to be very stimulating to new hypotheses about the mantle.

8. Materials for Radioactive Waste Immobilization; Excellent Example of M.P. (T.T.)

This area is an extraordinarily apt example to illustrate the relationship between society's needs, and universally expressed desires from the world of science and technology, and how the U.S. system of R/D actually responds.

Reading in the general press about the enormous public anxiety about nuclear waste and the national plans for the solidification of radioactive waste, it became clear to us before 1970 that modern ceramic materials research could be brought to bear on the problem. To our astonishment, in spite of the enormous public and vocal "market pull" in this very visible area, quite literally zero research was being done on examining alternative solids in which to contain the radionuclides. The design scenario in 1976 (more or less tacitly adopted by all nations worldwide) was to melt the radionuclide mixture into a borosilicate glass, fill the molten glass into steel canisters 3m × 1m diameter, and dispose of these in selected rock formations (either salt or shale) with equilibrium centerline temperatures of 500°C (or more).

In a few months of preliminary work we established two key facts:

1. That the projected glasses would totally decompose in times of about 1 week if exposed to any water at the proposed repository temperatures. The one-page paper we published in *Nature*

(26) had probably more *technological* impact than any single equivalent recent scientific paper. It forced every nation to redesign their waste form by diluting the radioactive content. Thus, this multiplied the volume of glass waste 3-4 times, and hence increased the *projected* repository area and cost proportionately by billions of dollars.

2. In the second paper [McCarthy et al. (27)] we proved that an ordinary multiphase crystalline *ceramic* (as in a porcelain or brick) could be made to incorporate all the radionuclides of reprocessing waste.

Only after this S.P. demonstration on two fronts was the M.P. strong enough to actually start a modest national research program on alternative solidification. Yet, and this is enormously significant, since there was no technology in place, the M.P. could only sustain the program for five years. This shortlived research effort (worldwide) on novel ceramic waste form synthesis produced notable successes including Oak Ridge's Fuetap cement, Penn State's first tailored ceramics and Australia's synroc subset of the tailored ceramics. (See Table 2 for details.) While it lasted, excellent science started to provide the kind of data the technical community and the public wanted, the scientific data on synthesis stability and leachability and the related data needed to make a judgment on quality of product and costs with these alternative forms [Roy (28,29)]. But the Reagan Administration decided—since alternatives would take time to study—to proceed with the most advanced-in-engineering form—borosilicate glass—in order to "complete the job" on a totally unrealistic time schedule. A decade later, in an area where the total costs will run into the hundreds of billions of dollars, no glass technology exists, no alternative waste forms are being studied nor waste form options for commercial waste. And we are no closer to acceptance of *any* solution and this materials component of the research is not yet done. So much for the efficacy of M.P. in the absence of T.T. in sustaining synthesis research.

9. Ceramic Thin Films From Glass Formation to Diamond Films (S.P. to T.T.)

When we started our research on thin films in the 1960's probably few ceramic thin films existed in technology; the science was non-existent. Sol-gel derived noncrystalline films were starting to appear as coatings on windows, and MgF_2 coated lenses were being modified by other oxide optical coatings on glass.

Our interest in the thin film form of ceramics derived from the vapor, was that it would offer a new way to create noncrystalline phases from compositions which could not normally be so rendered. By (splatting and) sputtering we were in fact able to create a wide range of such new glassy materials. But then the interest shifted to being able to prepare unique thin film glassy or crystalline ceramics (including Si, Ge, CdS, etc.) by utilizing RF sputtering onto virtually any substrate. This gave us the ability to create very interesting new materials such as hyperdense noncrystalline Ge (30-32) which could be crystallized "explosively" at room temperature by a mechanical or thermal trigger pulse. It also started the work to determine the processing conditions to yield thin film crystalline perovskites

Table 2. Ceramic radionuclide containment.

Structure Type	Illustrative Compositions	Possible Radionuclides and other f.p. incorporated		
		Total	Major	Minor

A. "Insoluble" Mineral-Modelled Phases

Structure Type	Illustrative Compositions	Total	Major	Minor
[Monazite]	$(Ln,Al^{3+})PO_4$ $An^{4+}SiO_4$ $(Ca_{0.5}An^{4+}_{0.5})PO_4$	Ln,An		
[Perovskite]	$(Sr,Ba)(Ti,Zr)O_3$	Sr	Ru,Tc^{4+}	Ti,Cs,An,Ln
[Pollucite]	$Cs,AlSi_2O_6$	Cs		
[Spinel]	$(Ni,Fe)(Al,Fe)_2O_4$		Tc^{4+}	Ru
[Apatite]	$(Ca,Sr)_5(PO_4)_3$	Sr		Ru
[Scheelite]	$(Sr,Ba)MoO_4$	Sr	Tc^{6+}	Ln,An,Ru,Te
[Feldspar]	$SrAl_2Si_2O_8$	Sr		
[Fluorite]	$(An,Ln,Zr)O_{2+x}$	Ln,An		Sr
[Zirconolite*] (ordered fluorite)	$CaZrTi_2O_7$	Sr	Ru	
[Rutile]	RuO_2	Ru,Te		
[Fcc Metal]	Pd			Pd
[Hollandite*]	$BaAl_2Ti_6O_{16}$		Cs	
[Nepheline]	$NaAlSiO_4$			$Cs(?)$
[Barium-aluminate* iron titanate]	$Ba(AlFe)_2Fe_8Ti_{13}O_{38}$		Cs	
[Magnetoplumbite*]	$BaFe_{12}O_{19}$	Sr	Cs	

B. Tailored Ceramic Assemblages to Accommodate PW-4b Waste Ions

High concentration of fission products	(i) + scheelite + fluorite + pollucite + apatite + corundum
	(ii) + scheelite + fluorite + pollucite + zircononia + monazite + corundum
	(iii) perovskite + fluorite + pollucite + monazite + spinel
Low Concentration of fission products	Zirconolite + perovskite + hollandite

(33)—especially high K materials such as $BaTiO_3$. Sputtering also provided an easy route to synthesize a whole range of crystalline or noncrystalline solutions of ceramics in one run simply by using two targets or mixed targets (32).

When the synthesis of BaBiPb oxide superconducting perovskite was announced by Sleight et al., we began the first systematic study to attempt to raise the T_c by crystalline substitution. The sputtering process for producing the first crystalline ceramic superconductors was described by Gilbert, Messier and Roy (33) nearly ten years before Geballe et al. (34) reported on similar sputtered films of the 1:2:3 composition perovskite.

Up to this point our substantial thin film effort had been driven mainly by S.P. Some T.T. work had been incorporated in attempts to apply these techniques to electrochromic films of WO_3. But it was in 1985 that a radical transformation occurred when I personally encountered the successful CVD diamond film work at NIRIM in Tsukuba, Japan, and at the Institute for Physical Chemistry in Moscow. After convincing skeptical agenices, and supported by the Office of Naval Research in a T.T. model, we drove the system into a major effort of understanding the process of making CVD diamond thin films (35,36) and transferring our knowledge about them effectively. Our diamond film synthesis effort has been comprehensive, to be able to compare all the methods for diamond film synthesis; and evaluative, not advocating one or other method or explanation or theory. This stance has allowed us to observe how slowly indeed real progress is made in materials synthesis. Today after hundreds of person years of research, the original Derjaguin and Fedoseev discovery (theory) of using atomic H to dissolve graphite and retain diamond (37) lies at the heart of every process in use (see Review 35). The original Japanese utilization of microwave plasma (and hot filaments) still is the standard method (38). The most novel addition has been Hirose's (39) utilization of the oxy-acetylene torch. The extensive theoretical and modelling research—as in all cases of materials synthesis—has proven to be so far without any redeeming social or scientific value. Research managers must face the empirical reality that here, as in 1:2:3 superconductors, in ferroelectrics, in new magnets: theory and models have provided zero guidance to any synthesizer.

Our local research contributions so far include the creation by Badzian et al. of rather perfect homoepitaxial diamond films which, when diamond was featured as the first "Molecular of the Year" in 1991 graced the cover of *Science*, and also some of the first diamond electronic devices (40) based on such films.

10. Nanocomposites and Their Formation Via the SSG Route (S.P. + T.T.)

In a series of presentations in 1983 and 1984 I presented (41) an approach to the synthesis of an entirely new *class* of materials which I termed nanocomposites. My argument ran as follows. All traditional materials synthesis and processing techniques—sintering, melting, etc., must allow enough kT energy to equilibrate the total composition involved on at least the scale of micrometers or tens of micrometers.

In other words, in known multicomponent-single phase and multiphasic materials (except certain alloys with post formation heat treatment) the size of the phases are at least on that scale. On these scales the two phases do not interact with each other with respect to chemical, structural, and most electrical, optical and magnetic properties. Bulk properties are averages or additions. If we could reduce the scale of mixing—I argued—to the nanometer dimension, we would be able to create a hybridization of properties of two phases. Moreover, if one could use low temperature processes to synthesize such "nanocomposites," radically different phases, very far from equilibrium with one

another, could be mixed with one another. This change of direction for SSG research has been described in context in a review (42). At approximately the same time E. Gleiter at Saarbrucken was reporting his own work on the very interesting advantages of simply reducing the size of particles of a single phase to nanometer dimensions (43).

Our earliest attempts to create such nanocomposites were to use two target sputtering, to combine Al_2O_3 with Au, or platinum with teflon or polyimids. These gave rise to interesting combinations of 1-2 nm size metal particles, some with 5-fold symmetry (44) in an insulator matrix. The process, however, was tedious and the only form which the materials appeared in was as thin films.

It was then in 1983 that I re-entered the world of solution-sol-gel research which worldwide was now addressing universally the goal I had set for myself in 1948, viz: to make **maximally homogeneous** ceramics. My new goal was to create **maximally heterogeneous** ceramics (i.e. with the maximum interface area of two or more phases) by the SSG route (see Ref. 42). In the next several years, making *nanocomposites* became a major research area in our laboratories (45-47). Our Japanese colleagues held the first international conference on the topic in 1989 (48) where very interesting new composites, created and studied, were reported on. Our original efforts and these results signal that nanocomposites may well have as substantial an impact on the field of ceramics as did the original sol-gel work.

Our own research in SSG-derived nanocomposites has demonstrated that—by the simple universally accessible expedient of mixing two sols—one can achieve the entire set of processing innovations shown in Table 3. Two interacting phenomena explain all these chemical-structural effects, the effects of chemical heterogeneity and structural heterogeneity (Table 3).

Table 3.   Nanocomposites will certainly offer a family of new materials with improved properties in various applications. Our work has demonstrated such improvements in the chemical/ structural area. The work of others has started to provide examples of real improvements in other properties.

What can nanoscale mixing achieve? In different properties?

Chemical/Structural	• Control of phases formed • Lowers reaction and sintering temperatures • Control of microstructure • Control of morphology • Via solid state epitaxy	Our studies
Mechanical	• Five-fold increase in strength as size goes from 100-20 nm • Suprahard (>diamond?) materials	
Optical	• Ten-fold increase in luminescence	Work of others
Electrical	• Change in fundamental conduction	
Magnetic	• New super-, para-, and ferri-magnets	

1. Compositional Heterogeneity

Such composites may make possible exothermic and rapid reactions of two intimately mixed phases far from equilibrium with each other. For example, one may contrast these classes of mixtures of, say, $Al_2O_3 + SiO_2$ at the mullite composition (or $ZrO_2 + SiO_2$ at the zircon composition):

(a) Mixed 325 mesh powders of Al_2O_3 and amorphous SiO_2.

(b) Single homogeneous liquid solution made into an atomic scale homogeneous (one phase) solid (xerogel) solution.

(c) A composite of 1-10 nm size particles of Al_2O_3 and SiO_2 (diphasic xerogel).

Mixture (a) heated at, say, 1250°C for 1 hr will show no measurable reaction by XRD, and little in TEM except perhaps in the reaction rim around some of the grains. Mixture (b) would show a high percentage of formation of mullite but mixture (c) would show the highest percentage of well-crystallized mullite.

The explanation lies in the fact that the diphasic xerogel has the advantage that the reaction of Al_2O_3 with SiO_2 is auto-catalytic because it is exothermic, due to the $\Delta H_{reaction}$. In the monophasic gel, the reaction rate is much slower because the only ΔG available to drive is the ΔH of the noncrystalline → crystalline transition. Generically compositionally heterogeneous nanocomposites utilize the heat of reaction of the metastable → stable assemblages.

2. Structural Heterogeneity

The idea of seeding gels with desirable structural templates goes back to the very first year (1948-49) of the discovery of the SSG process and hydrothermal process (49). We used 10-50μ size crystalline templates as one phase and noncrystalline xerogels as the other. In these early papers we demonstrated the successful overgrowth on such phases as diaspore, α-spodumene, benitoite, etc., in hydrothermal reactions. Here one could assume the second phase with the "right" crystallography was serving as an epitaxial substrate for material transported via the liquid phase. Thirty years later crystallographically seeded xerogel nanocomposites showed remarkable effects on the kinetics even of solid state reactions completed in minutes or hours.

3. Combined Structural and Compositional Homogeneity

An additional wrinkle in utilizing such composites is to make them tri- or tetraphasic and combine both the compositional and structural inhomogeneities in the composite.

In the last 8 years we have demonstrated the large effects which can be caused on materials synthesis by these simple experiments in many systems: alumina; mullite; zircon; thorite; cordierite. Figure 12 is a schematic summary of the temperatures to achieve equivalent formation of $ZrSiO_4$ from

various mono-, di- and triphasic xerogels. The advantage is clearly very substantial: lowerings of about 250°-300°C.

Solid-State Epitaxy

Finally, in the early diphasic work we unequivocally established the fact that the efficacy of structural di-phasicity (seeding) was due to crystallographic epitaxy. This was done by using seeds of different structure and demonstrating that only the one with the structure of the product phase was effective. The effects could *not* be associated with just overall heterogeneous nucleates (46,49). However, another approach provided complete proof of the phenomena of **solid state** epitaxy. In recent papers (50) we have grown very highly aligned crystals of the product phase (TiO_2, $SrTiO_3$, Al_2O_3, PZT, PMN, etc.) onto large (cm size) single crystal substrates of the same phase. Indeed utilizing the "solid" state epitaxy principle, it has been possible to crystallize *albite* ($NaAlSi_3O_8$) from a di-phasic gel made from its own glass with crystalline albite seeds. This is possibly one of the most difficult glasses in existence to crystallize (51).

We have also shown that by using the appropriate crystallographic template one can drive the reaction to different products—either metastable or stable assemblages (e.g., $ThSiO_4$ can be crystallized at 1400°C to either the huttonite or thorite structures. And by controlling the composition one can control the morphology of the final product phase (52).

Crystallization begins in $ZrSiO_4$ at

Compositionally

	Homogeneous	Nanocomposite
Homogeneous	1350°C	1175°C
Nanocomposite	1100°C	1075°C

(Structurally)

Figure 12. Efficacy of nanocompositing in starting material in lowering reaction temperatures in various mono- and di-phasic gels. The reaction of crystalline ZrO_2 and SiO_2 would be very small at these temperatures.

Outside our work on chemical structural effects we can see that compositional and structural engineering at the nanolevel is certain to become a routine powerful tool in ceramic processing from the results reported in Ref. 48. No better demonstration can be found than in the dramatic results achieved by Niihara et al. (53) in all the mechanical properties of engine ceramics (Al_2O_3, SiC, sialon) by the use of nanoscale dispersions of second-hard phases.

NEW MATERIALS SYNTHESIS: FUTURE DIRECTIONS

SOME BLIND ALLEYS: CONTROLLED DESIGN OF NEW MATERIALS

In Figure 4, I summarized the capability we have to create new materials. It is self-evident that in any mature technology, the combination of two or more materials always will do better than one. It is well established for all mechanical applications that composites do vastly better than single phases. The initial success of discrete silicon devices was soon eclipsed by composite structures on a micrometer scale of the chip technology. Optical fibers are all graded composites.

But what is the potential of synthesizing by design a completely new crystal structure, at the unit-cell level with desirable optical, magnetic, superconducting properties? Again, however hard it is for the scientist and the manager to accept, the empirical track record is unassailable. Our capacity is nearly zero. No better example can be found than the worldwide search for new superconductors. After the first public announcement by Zhao (54) of high T_c phases in the system Y_2O_3-BaO-CuO found by sheer empirical mixing and measuring, it was a matter of one or two person weeks of work in several different laboratories in IBM, AT&T and Bangalore to isolate the $YBa_2Cu_3O_7$ phase. But since then, after some **thousands of person years**, with full benefit of theory, with no shortage of equipment or money, the world's synthesis communities have found exactly zero really new structures outside the 'perovskite + Cu-O layers' family. The recent serendipitous discovery of superconductivity in Rb_3C_{60} and Cs_3C_{60} Buckyball compounds, confirms the total scientific ignorance in our theory of synthesis of really new phases with desirable properties.

The original serendipitous discovery of the magnetic rare earth garnets in 1954 by Keith and Roy (55) did not equip us or any of the enormous range of extremely competent magnetic materials groups in the world to design or even to find, in 40 years, any comparable 3 sub-lattice structural families with similar ferrimagnetism. The new rare earth iron borides again were·a unique and serendipitous discovery with little transferability of knowledge, and again, surprisingly, no follow-on success.

In 1992 we must therefore admit that it is not possible to synthesize any new phases with different crystal structures, with specifically desired properties, based on any theories or models. Even serendipitously discovered new materials provide but little empirical guidance for tinkering with neighboring compositions and obvious substitutions.

BLIND ALLEYS II: BIOMIMETICS; BIOGNOSIS

In the last year or two as the publicity surrounding quasi-crystals and cold fusion subsides, a wave of publicity has been created to suggest that one *might* make useful new materials by mimicking nature. The extraordinary gullibility of the present-day scientist community is evidenced in the reception to this idea since it is never presented based on a single, even modest, achievement. Yet, surprisingly no synthesis of any material with any extraordinary or useful property has been reported by all those who advocate the value of this route to new *biomimetic* materials (56). To the best of our knowledge, only one single useful material which can by any stretch of the language be called a biomimetic material, has ever been made. This is the replamine process by E. W. White et al. in this laboratory, who mimicked a South Sea coral in its key external morphology of a 3:3 connected structure. From this they made both biomaterials for dental and bone implants, and exactly mimicked the morphology of the same materials (see Fig. 13) using them as templates for making biological and electroceramic composites (see 57-59).

The implication in the oft-repeated appeals, that Nature, which optimized its materials for low temperatures (<50 °C) and aqueous environments, would provide some miraculous templates for mimicking to make materials for airframes, or superconductors, or magnetic or optical materials, smacks, as Professor Jonathan Black of Clemson (60) remarks, of a return to the philosophy of "vitalism." The empirical facts are exactly the reverse. Materials science and technology have
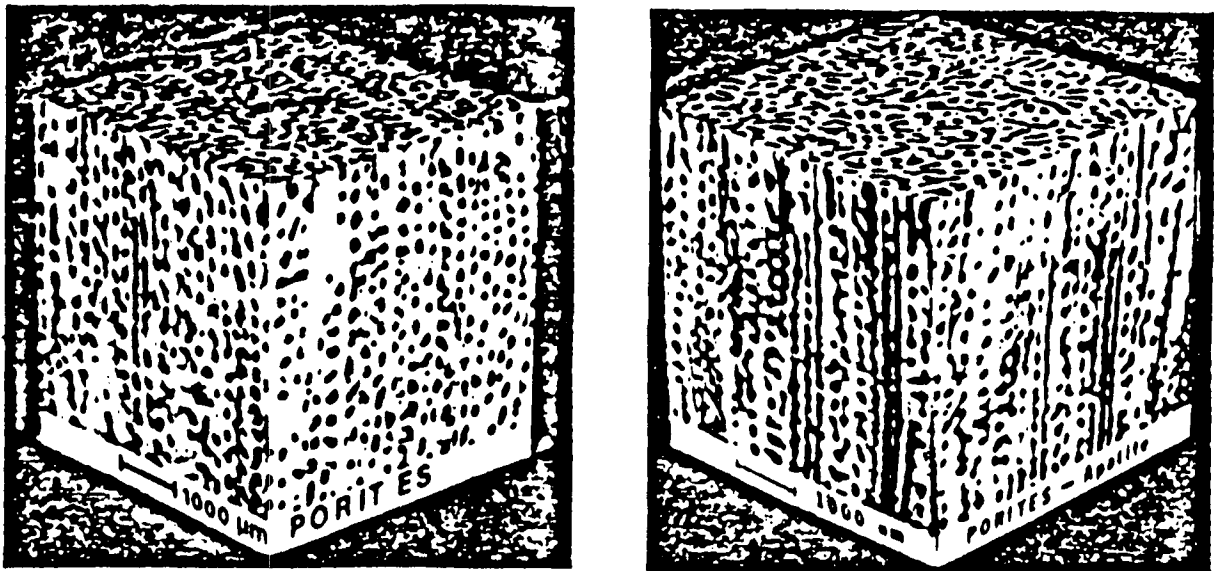

Figure 13.   Three-dimensional SEM photograph of original coral (var. Porites) made of $CaCO_3$ on the left, and the exactly copied biomaterial on the right after transformation under hydrothermal conditions to apatite. This is the only example of a commercialized biomimetic material known.

provided enormous help from non-bio-derived materials for the human biological system: Metal, polymer and ceramic parts for teeth and bones; polymers for skin and other soft tissue, etc., are ubiquitous and unlikely to be displaced to any large extent by bio-derived solids.

This is not to say that the materials designer and synthesizer may not have **much to learn from**—not necessarily to mimick—nature. I have termed this process **biognosis**. Here again one must note that the extraordinarily detailed studies by the three or four British schools, of Vincent, Currey, Mann, Birchall, etc., which have *described* biological hard tissue in great detail over the last 10-20 years have yet to synthesize their first novel material based on such learning. If biognosis is to offer any help in synthesizing materials, it is clear from the record that the experts have not found it. Very recently my colleague, R. E. Newnham (64), has ingeniously learned from the grunts generated in fish bladders, and the sound receiving systems of bats, to design and prepare successful composite transducers utilizing the same principles. These are the only **biognostic** derived "electronic" materials known to us. **Biomimetics** as a major design route for useful materials is not likely to be of significance outside of biomaterials, and excepting for White's work (op. cit.) has yet to record its first success.

SUCCESS STORIES: I. LANXIDE

The history of the development of the directed metal oxidation process by the Lanxide Corporation is one of the most interesting success stories of innovative materials synthesis. For the first time in human history a process involving a reaction of **Liq + vapor → solid** was used to make useful materials. The ceramic matrix composites produced were the largest, simplest to make, and had many unique properties. The degree of innovativeness of the discovery can be judged by the fact that the corporation has filed nearly 3,000 patents worldwide in about six years and most are issuing with little or no challenge. Yet more than five years after the public announcements of the process (61-63) it is an extraordinary phenomenon that no more than one or two other groups in the entire world seem to have embarked on research in this process. Why? The only sharp difference from other fields such as high T_c superconductors, cold fusion, quasi-crystals, Buckyballs, is the *total* absence of deliberate publicity in the science press or newspapers since the company did not want such.

Table 4 shows the range of compositions of metal, ceramics, and reinforcements which can be incorporated into Lanxide composites. Table 5 shows some of the properties attained in some of these CMC. The second generation development by Lanxide of the metal matrix composites also made by this method bodes well for directed liquid metal oxidation—one of the most significant single synthesis and processing discoveries of the post-war era.

Table 4. Examples of Lanxide™ ceramic matrix systems.

Parent Metal	Reaction Product
Aluminum	Oxide, nitride, boride, titanate
Silicon	Nitride, boride, carbide
Titanium	Nitride, boride, carbide
Zirconium	Nitride, boride, carbide
Hafnium	Boride, carbide
Tin	Oxide
Lanthanum	Boride

Table 5. Nicalon™/Al_2O_3 mechanical properties.

Temperature °C (°F)	Flexural Strength MPa (k.s.i.)	Fracture Toughness MPa$\sqrt{m}$ (k.s.i.$\sqrt{in.}$)
R.T.	461 ± 28 (8) (67)	27.8 ± 4.6 (3) (25.3)
1200 (2192)	488 ± 22 (12) (71)	23.3 ± 2.7 (3) (21.2)
1300 (2372)	400 ± 12 (4) (58)	19.2 ± 2.8 (3) (17.5)
1400 (2552)	340 ± 11 (4) (49)	15.6 ± 3.7 (3) (14.2)

SUCCESS STORIES: II. NANOCOMPOSITES: A MAJOR FUTURE ROLE IN SYNTHESIS

In the section above I referred to the real success story found in the chemical reactivity of nanocomposite powders themselves or when used as starting materials. This nanocomposite principle can be carried to the next hierarchical level of structure.

My argument above has been that we cannot purposively design new phases at the unit cell level. At the same time we have learned to design a whole world of composite materials. Initially the only application was for superior mechanical properties. In the 1950-80 period, a strong iterative process between technology and society has led to a more or less routinized capability to "synthesize" novel composites for structural uses.

However, the design of microcomposites for **electrical, magnetic and optical properties** was decades behind. While every semiconductor device is today a precisely architected composite, the different elements of the composite are used for their different properties. They do not interact to

enhance one property. In the last decade L. E. Cross and R. E. Newnham have designed from first principles and created whole families of electroceramic composites. These have been model examples of very fruitful T.T. research for over 15 years. The properties of such composites, e.g. the pioneering polymer-PZT transducer, are often orders of magnitude better than the separate components. The paper by Newnham (64) provides a magisterial overview of the state of this art and gives the theoretical basis for this new thrust. It shows clearly why the future of synthesis will belong to such micro-nano-composites in the near-term future. Although no other families of applications have been analyzed and treated so thoroughly, similar composite materials are now appearing in magnetic powders and optical intercalates (65).

LOOKING AHEAD IN CERAMIC SYNTHESIS RESEARCH

Some time ago C. F. von Weizsacker, the physicist-philosopher, made the case (66) that thermodynamics was not symmetrical with respect to time. We cannot extrapolate from the past into the future even in fundamental physics. Prognostication must be based on the past record and any known constraints in the future. I have made the case (67), following Victor Weisskopf of MIT and Gunther Stent of Caltech, that useful and utilizable overall fundamental "scientific knowledge" is finite and that humankind is rapidly approaching the asymptote. Recently David Mermin (68) has made a more radical case that little new fundamental physics has been discovered since quantum mechanics.

What do I foresee in the field of materials synthesis and processing which has suddenly been singled out for policy attention in the U.S.? First one must exclude the absolutely certain flux of serendipitous discoveries from any analysis. However, the distribution of the flux, number and significance of serendipitous events may not be compared to the number and size of meteorites striking the moon or earth, because scientists are more like beachcombers going over already well-combed beaches. Moreover, contrary to glib assertions about the great value of new analytical tools and new computer capabilities, these are of little use and almost certainly will prove to be of negative value in really new syntheses. The major recent "discoveries": 1:2:3 superconductors, the diamond films, Lanxide, Buckyballs, putative cold-fusion, required only the most modest apparatus available in most laboratories a century ago. Large instruments have historically proved to be idea-sinks, not idea sources. Of course, second generation materials engineering by, say, MBE machines, will be valuable.

The two spectacular successes in materials synthesis of the postwar era were the introduction of two active classes of materials: semiconductors and polymers. These step functions can never be repeated in scientific or technological significance. There are no more classes of materials left. The next set of discoveries will involve replacements of existing materials by others with superior performance. In the field of ceramics, since WW II, we have had entire industries such as the magnetic ceramic materials from the spinels to the garnets to $SmCO_5$ and the NdFe borides; the $BaTiO_3$ and PZT

capacitor and transducers, the various phosphors, the zeolite and other catalysts, and the optical fibers as the volume and dollar leaders. The field is much more crowded now, so that entirely new materials for new functions are doubly unlikely, and replacing an existing material is technologically very difficult indeed.

Hence in looking ahead one has to be very careful to analyze the impact of the new data one presents. In this connection, I will contrast two documents on the past and future of materials technology. The U.S. National Academies produced, after four years of committee work, the *Materials Science and Engineering Report* (69). In this report, we find a set of graphs depicting the enormous program which has been made in the improvement of the desirable properties of materials by serendipitous discovery or science-based engineering. Figure 14 shows four examples from superconductors, magnetic materials, etc. But a study of these figures forces one to a very important conclusion about future materials synthesis research: It has a very short life expectancy. In 1979 in my book, *Experimenting with Truth* (67), I first made the case that these "exploding exponentials" guaranteed a very major change in a very short time (<25 years). Obviously if research on high T_c superconductors continues to increase the T_c at the same rate as in the past we will be above the melting point of all materials soon. Similarly the BxH product in magnets will be infinite, etc. The optimistic upbeat suggestion of the great advances we have made in this report, is therefore totally unjustified in their future scenario which would be roughly: If we keep going at this pace there will be nothing left to discover in 20 years.

Turning to the other document (70) from the U.K., Professor A. Kelly looks at the utilization of bulk materials. Figure 15 reproduces some of his figures. Here are plotted the total world usage figures for all the major metals and a per-capita usage of steel. These data present a very different tone for any planner. They tell us that humankind is reaching a new and unexpected asymptote in the total consumption of materials. That with more and more producers the battle for "market share" will increase. Part of the slowdown is due to conservation and an understanding of the finitude of resources. This "sustainability" argument has in fact slowly come to dominate technological decisions. Agriculture research dominated for nearly 100 years by growth scenarios and the research and technologies derivative of those (supported unquestioningly by all university and agriculture colleges) now finds itself radically re-directed towards low-input sustainable agriculture. Moreover it is instructive to note that this revolution did not come from a university or major industry. Instead it was championed by a few individuals such as Robert Rodale, the CEO of the Rodale Press, and Lester Brown, President of Worldwatch Institute. Another societal impact example is the fact that in spite of the exaggerations both by the activists, and the apple industry, Alar is off the market and the apple industry is healthy—but again it was not done by the traditional research groups. What is instructive from those snapshots on current R/D trends is that societal and environmental concerns have totally reshaped the research directions and agenda of agriculture research.
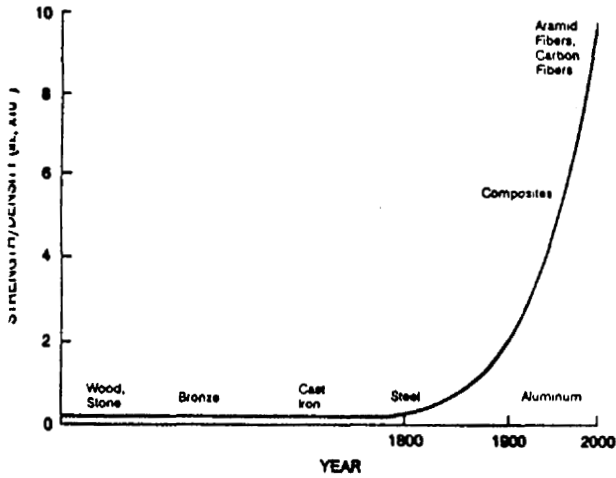
FIGURE 1.1 Progress in materials strength-to-density ratio as a function of time, showing 50-fold increase in the strength of today's advanced materials compared to that of primitive materials.
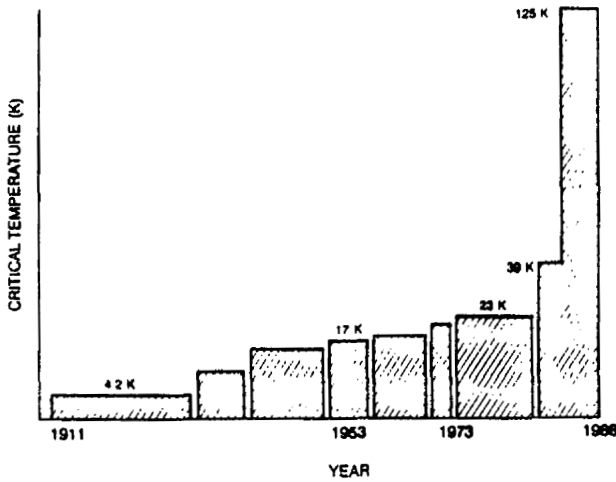
FIGURE 1.4 Progress of critical temperature of the best superconducting material as a function of time.
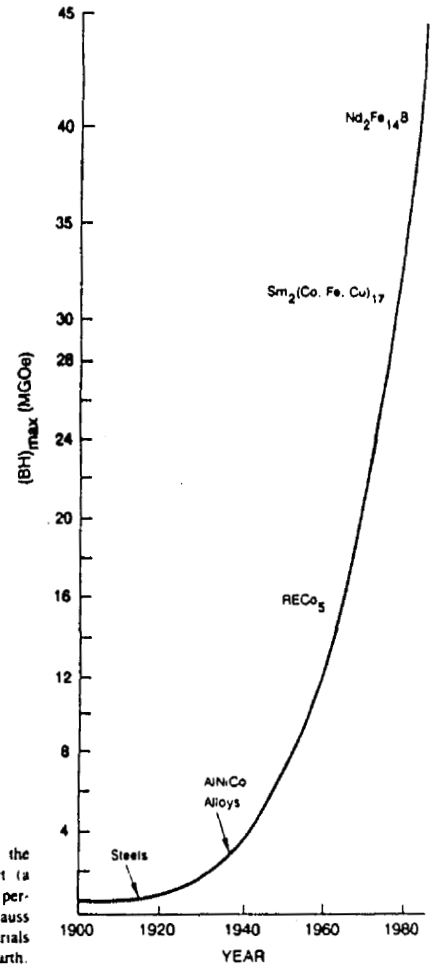
FIGURE 1.3 Progress in the flux-magnetization product (a measure of the strength of a permanent magnet in megagauss oersteds) of magnetic materials over time. Note: RE, rare earth.

Figure 14. Curves from MSE study by U.S. N.R.C. suggest that in a very short time we will have reached physical limits in property improvement.
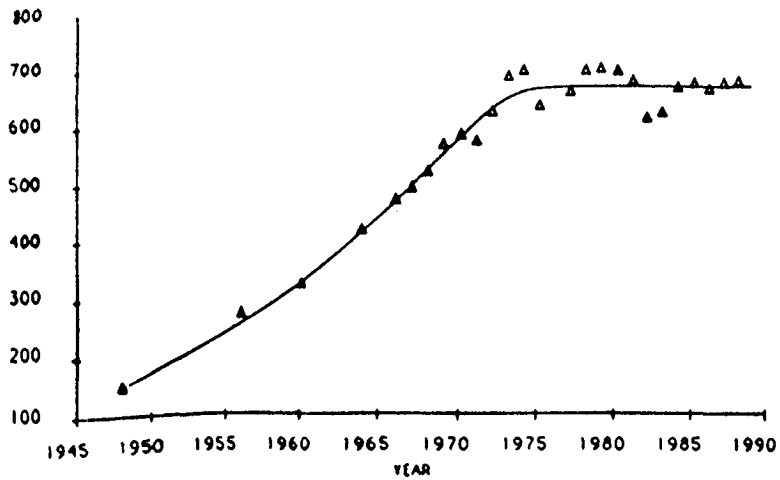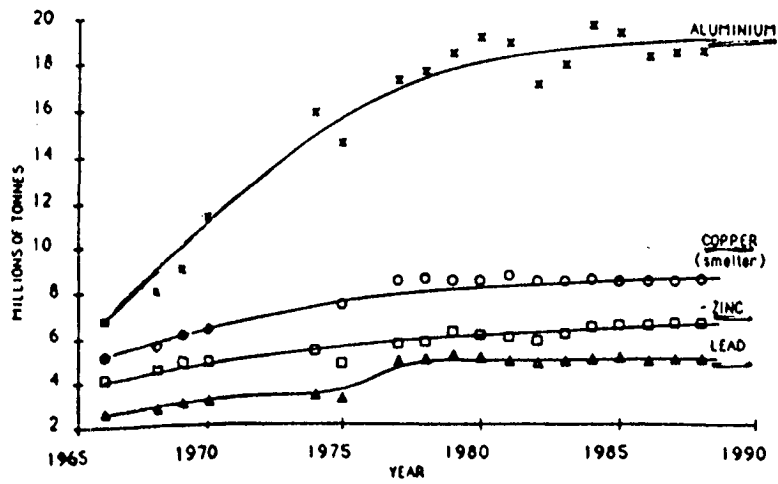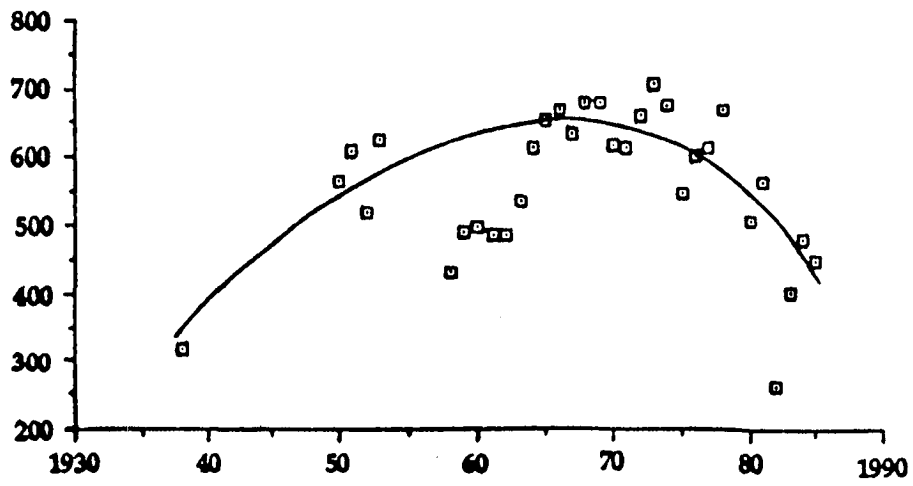
Figure 15.   The future (1975-90) was obviously not predictable from the past (1950-75).   World usage of all major classes of metals has plateaued after 1975.   Per capita use is declining (after A. Kelly).

83

It is certain that analogous societal pressures—whether they are scientifically "correct," or justifiable—will shape the future macro directions of *materials* research. It behooves the science community to anticipate such changes and start to reshape the directions of our research to match society's new priorities. In "looking ahead" I see a radical change from the situation in the last 25 years. In the past whatever was discovered by the science community's research set the directions for development and technology and thence the agenda for society. There was no countervailing force. That force has now appeared in the shape of the environmental demands of citizens translated into regulation by legislatures. It has appeared in the form of safety and "hypersafety" demands by the public. Hence the future research directions will be the resultant vector of one arising from societal constraints and the other from scientific discovery. I will end by treating each of these in turn.

Some Likely Directions for Discovery-Led Materials Synthesis Research

One cannot conceive of any materials developments which will come close to the enormous impact which the discovery and exploitation of semiconductors and of polymers has had on the materials industry. The functions which these new materials opened up in the communications and computer industries are now being fulfilled by third and fourth generation optimizations. Any new material will either be a drop-in improvement over the established ones—such as diamond over GaAs—or it will have a very hard time getting into the field. New functions for known materials based on new synthesis or processing will also have to compete against the existing technologies which are also constantly being improved. Twenty years ago the hope for ceramic turbines was very high. After enormous research expenditures the total role of ceramics in the engine area is now seen as being more modest.

On the other hand, the electroceramic area which was not much publicized has grown into a major industry. The high band gap and narrow gap materials are getting closer because of two advances in synthesis/processing. First is the ability to make, say, diamonds and/or ferroelectrics, as thin films to mate with traditional semiconductor processing. Second, the switching from electronics to optonics involves a whole new range of electro-optical materials most of which are transparent, and this will make the way for more ceramic involvement in the communications technologies.

Table 6 lists the families of "bulk" and thin film materials in which I believe the successful research drive will generate some new opportunities. The family of "chemically bonded ceramics", as I named cement and its cogeners, will offer continuing opportunities because these materials are needed worldwide for highways, buildings, waste disposal, i.e., for the entire population, and because these resources are geographically relatively uniformly distributed.

I have separated out the thin film form of ceramics as a special case because there is so far very little usage in this form, and hence specially attractive opportunities may present themselves. Just as metals have been widely used as a plated (or evaporated) thin film for electrical or chemical

applications, there appears to be no reason why ceramic phases and functionally graded materials may not make a major contribution here. The fact that ferroelectrics in thin film form are different from the bulk, and in fact one can modify the surface to change its properties, points to the kind of direction where there will be many opportunities for research.

Table 6. New ceramic materials.

(a) **New (Bulk) Ceramics (via New Processes)**
  - Functionally gradient materials
  - Lanxide as prototype of CMC
  - Chemically bonded ceramics (cements, clays, zeolites and other low temperature reaction products)
  - Nano-micro composites as substitutes in many fields

(b) **Ceramics in Thin Film Form**
  - Ultrahard and/or conducting coatings
    - diamond, cBN, DLC, ceramic metals
  - Ferroic materials
    - active surface modified
    - passive: key properties different from bulk
  - Functionally gradient materials

Societal Constraints on the Future of Materials Synthesis Research

The basic societal trends are not difficult to summarize and I have attempted to do this in tabular form in Table 7.

Table 7. The future: Asymptotes and limits of low input materials-inventive technology. (LIMIT is analogous to LISA in agriculture.)

- Minimize energy and materials usage.
- Minimize depredations on environment.
- Cope with absolute physical limits.
- Atomic scale inventions will continue to be serendipitous.
- Nanocomposites is the major opportunity for new materials.
- U.S. role in materials research will diminish rapidly.
- New high volume materials will be driven by needs of less industrialized countries.

In the developed world, energy and materials conservation and environmental issues will dominate R&D directions more than property improvements. Many of these improvements—as indicated earlier—are coming up against absolute physical limits in any case. This is similar to the communications industry where transmission speed and "useful" information (for the masses) have saturated.

Really new materials will appear from time to time as a result of serendipitous discovery, but the commercial significance of such discoveries will inexorably diminish because existing materials are not going to disappear. No new laws of physics can appear to explain most of what humans do and experience (i.e. of any significance to other sciences or society) for the simple reason that the laws of motion, of electromagnetism, of quantum mechanics, etc., are so completely verified and adequate. So also the major classes of materials are established and they have been optimized for a myriad applications. Of course, each application driven by the commercial and social factors will seek to improve on the present materials, in a technology traction mode. It is in these applications where I see the emphasis on tailored micro and nanocomposites as playing the central role in materials synthesis in the decades ahead. Furthermore, as the U.S. role in materials research and in most science diminishes the science-push model will be displaced—indeed it already has been as witness the existence of the thrust towards synthesis and processing—by the technology traction model which is central to Japanese R/D management. The extent to which this has occurred is evident from Fig. 16, after Roy and Silsbee,

TOTALS

NO. PUBLICATIONS

Topic:
Cement
Silicon Nitride
Zirconia
Zeolites
Sol Gel

	1965	1970	1975	1980	1985	1990
GERMANY	0	61	162	98	193	206
PRC	0	0	1	36	140	279
USSR	4	687	876	1028	738	719
JAPAN	3	49	496	1124	1941	2758
UK	0	0	0	21	220	228
USA	12	144	476	781	945	1422

PUBLICATION YEAR

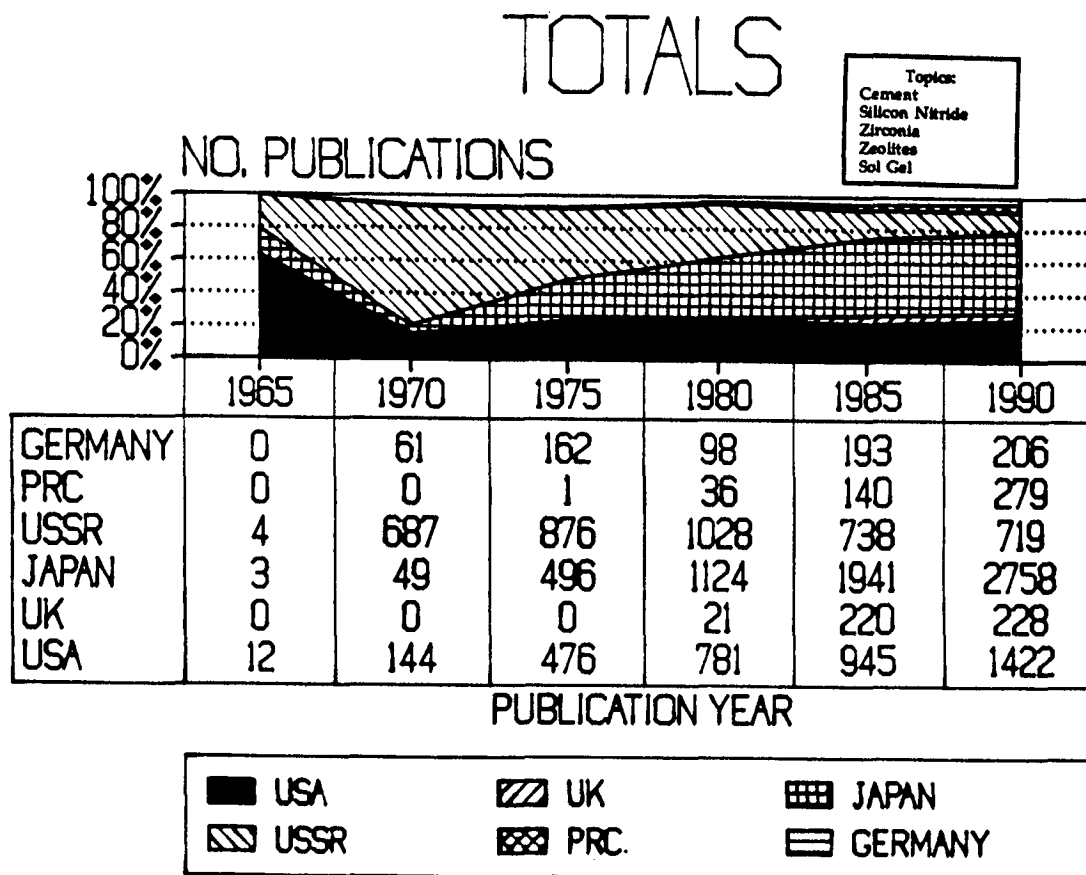■ USA   ▨ UK   ▦ JAPAN

▨ USSR   ▨ PRC.   ▤ GERMANY

Figure 16.

(unpublished) which shows the dominance of Japan in published American research. The emergence of second and third tier countries as substantial research centers will also slowly move the center of gravity of materials research towards the basic needs of the vast majority of humankind in shelter, transportation, etc.

Changing Role of Research in Knowledge Management

A major change has occurred—unnoticed by most policy makers—in the value of locally carried out research in the total management of knowledge. Figure 17, taken from my presentation (71) at a conference on comparison of U.S. and Japanese research practice, makes the following key points:

1. No local laboratory—even of the biggest industries—can produce more than a minuscule fraction of the total S^3 and S^1 discoveries being produced.

2. It is more cost effective by orders of magnitude to college knowledge (by carefully sifting through the literature, by visits to key laboratories, etc.) than to generate it.

3. That only experienced personnel in the S^2-T.T. mode can find the most usable knowledge available and both put it to work directly and typically use it to guide the S^2 research.

What this implies is revolutionary in its implication for the training of scientists (that breadth of training and critical thinking are much more important than specialization). It is also revolutionary for research in third tier countries. Instead of investing in large specialized instruments they should invest in all major literature data bases and train managers to collect and sift new knowledge rather than generate it.

Goals for Materials Research in the 21st Century

Most humanists and social scientists have not accepted the classical model of "disinterested" (S^3) science. Moreover, the support of S^3 science, increasingly accurately perceived as a luxury "consumption good," is certain to dwindle. The public will continue to demand more S^2 science. But can lofty goals be set for aspiring scientists in a partly globalized economy which on the one hand are sensitive to the new societal demands, and on the other encourage the inventiveness of the community? A recent Japanese document offers one such.

The Science and Technology Agency in Japan, in its February 1991 report to Prime Minister Kaifu, set as Japan's R/D policy goal: "Harmony among science and technology, humankind and society." In Fig. 18 I have combined this kind of universal goal for scientific research with.the S.P., T.T., and M.P. motifs for research, expressing the clear change in the vector by which society will now drive and pull its needed technology and in turn its science (see Ref. 72).
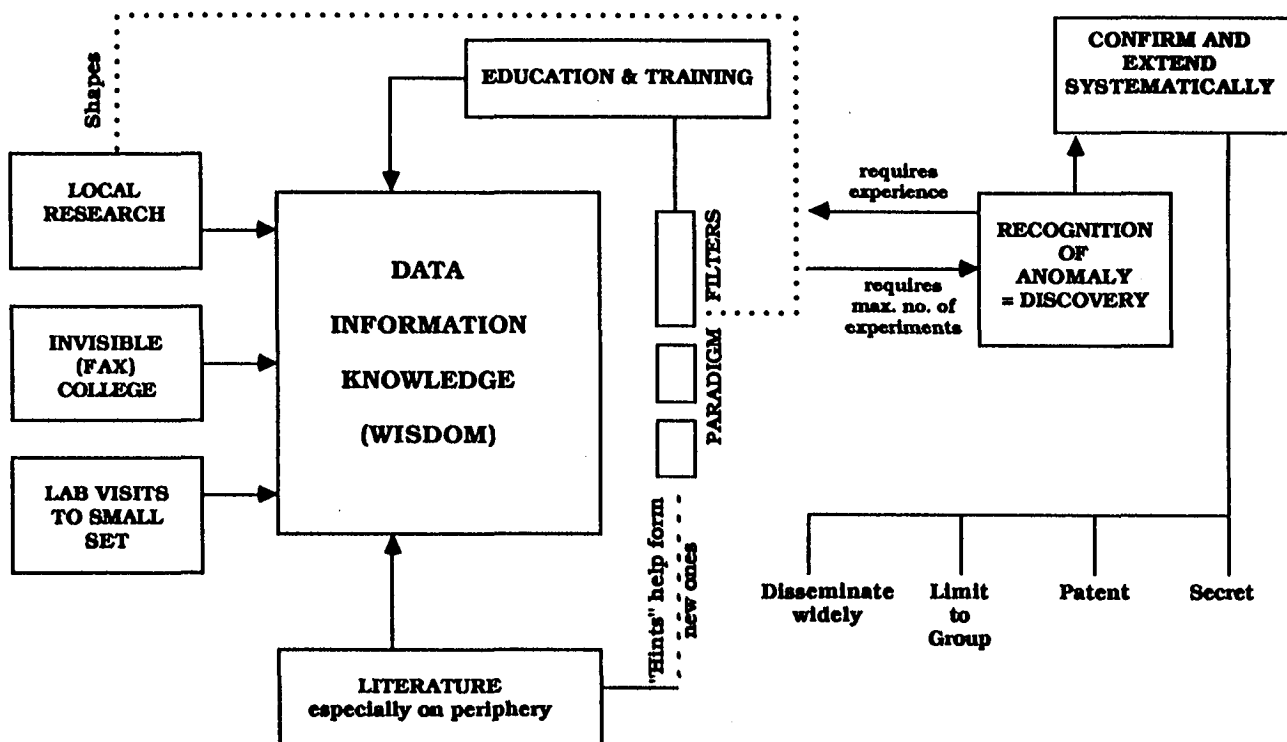
KNOWLEDGE MANAGEMENT

Figure 17. A new role for *local* research which radically diminishes significance is seen when it is placed in the context of the total flux of knowledge which universities or other agencies must learn to manage.
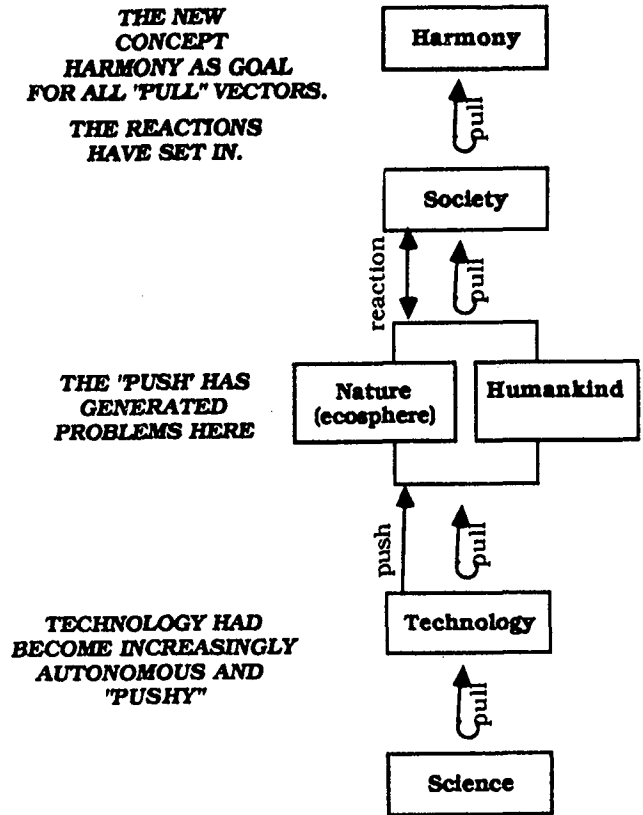
Figure 18.

89

REFERENCES

1. (a) R. Roy, Synthesizing New Materials to Specification, *Solid State Ionics* 32/33:3-22 (1989). (b) R. Roy, "Rational and Irrational Strategies for the Synthesis of New Materials," *Microelectronic Systems*, Am. Ceram. Soc., Washington, DC (1990), pp. 3-10.

2. R. Roy, in *Ceramics and Civilization*, Vol. 11, *High technology ceramics—past, present and future*, Ed. W. D. Kingery, Am. Ceram. Soc., Washington, DC, pp. 351-370 (1987).

3. D. de Solla Price, "Sealing Wax and String: A Philosophy of the Experimenter's Craft and Its Role in the Genesis of High Technology," Sarton Lecture, AAAS Meeting (May 1983).

4. R. Roy, "HTSC: Restoring Scientific and Policy Perspective," *Proc. World Superconductivity Congress*, World Scientific, Singapore, p. 27 (1988).

5. D. W. Breck, W. G. Eversole, R. M. Milton, T. B. Reed and T. L. Thomas, *J. Am. Ceram. Soc.* 78:5963 (1956).

6. G. A. Keyworth, quoted in *Physics Today* (April 1985).

7. G. Alperovitz, *Technology Review* (Aug/Sep 1990), p. 23 ff.

8. DeVries, R.C., Rustum Roy and E.F. Osborn. The System TiO_2-SiO_2, *Trans. Brit. Ceram. Soc.* 53:525-540 (1954).

9. R. C. DeVries, R. Roy and E. F. Osborn, "Phase Equilibria in the System CaO-TiO_2-SiO_2," *J. Am. Ceram. Soc.* 48:158-171 (1955).

10. R. Roy, "Metastable Liquid Immiscibility and Subsolidus Nucleation," *J. Am. Ceram. Soc.* 43:670-671 (1960).

11. D. K. Agrawal, V. S. Stubican and Y. Mehrotra, "Germanium-modified Cordierite Ceramics with Low Thermal Expansion," *J. Am. Ceram. Soc.* 67:847-51 (1986).

12. R. Roy, D. K. Agrawal, J. Alamo and R. A. Roy, "[CTP]: A New Structural Family of Near-Zero Expansion Ceramics. *Mat. Res. Bull.* 19:471-477 (1984).

13. Alamo, James and Rustum Roy, "Ultralow-Expansion Ceramics in the System Na_2O-O_2-P_2O_5-SiO_2," *Communications of the American Ceramic Society*, C-78-80 (May 1984).

14. S. Y. Limaye, D. K. Agrawal and Y. Mehrotra, "Synthesis, Sintering and Thermal Expansion of $Ca_{1-x}Sr_xZr_4P_6O_{24}$—An Ultra Low Thermal Expansion Material," *J. Mat. Sci.* 26:93-98 (1991).

15. A. J. Majumdar and Rustum Roy, "The System CaO-Al_2O_3-H_2O," *J. Am. Ceram. Soc.* 4: 434-442 (1956); R. Roy, *Proc. Conf. on the Silicate Industry*, Budapest, pp. 1005-1017 (1973); reprinted in *Powder Metal. Intl.* 6:25 (1974); *Keramische Z.* 26:386 (1974).

16. M. J. Ruthner, Third Roundtable Meeting, Internat. Team on Sintering, Herceg-Novi, Yugoslavia (September 1973).

17. T. P. O'Holleran, R. Roy and D. M. Roy, "Amorphous Powder and Sintered Nab-Al_2O_3 by DMS Process," *Powder Metallurgy International* 17(3):134-136 (1985).

18. (a) Amitabh Kumar and Rustum Roy, "Reactive-Electrode Submerged-Arc Process for Producing Fine Non-Oxide Powders," *J. Am. Ceram. Soc.* 72(2):354-356 (1989).

    (b) Amitabh Kumar and Rustum Roy, "RESA—A Wholly New Process for Fine Oxide Powder Preparation," *J. Mater. Res.* 3(6):1373-1377 (1988).

19. J. L. Kingsley and K. C. Patil, *Mat. Lett.* 6:427 (1988).

20. Della M. Roy and Rustum Roy, "An Experimental Study of the Formation and Properties of Synthetic Serpentines and Related Layer Silicate Minerals," *Am. Mineralogist* 39:957-975 (1954).

21. O. Muller and R. Roy, *The Major Ternary Structural Families*, Springer-Verlag, Heidelberg (1974).

22. R. Roy, "Multiple Ion Substitution in the Perovskite Lattice," *J. Am. Ceram. Soc.* 37:581-588 (1954).

23. Frank Dachille and Rustum Roy, "The Spinel-Olivine Inversion in Mg_2GeO_4," *Nature* 183:1257 (1959).

24. Frank Dachille and Rustum Roy," High Pressure Region of the Silica Isotypes," *Zeits. für Krist.* 3:451-461 (1959).

25. Mark Myers, Frank Dachille and Rustum Roy, "Contribution to Calibration of High Pressure Systems from Studies in Opposed-Anvil Apparatus," *High Pressure Measuremen*, Giardini and Lloyd, pp. 17-33 (1963).

26. G. J. McCarthy, W. B. White, R. Roy, B. E. Scheetz, S. Komarneni, D. K. Smith and D. M. Roy, "Interactions Between Nuclear Waste and Surrounding Rock," *Nature* 273:216-217 (1978).

27. G. McCarthy and M. T. Davidson, *Bull. Am. Ceram. Soc.* 54:782 (1975).

28. Roy, Rustum, *Radioactive Waste Disposal, Volume 1: The Waste Package*, Pergamon Press, New York, 1982. 232 pp.

29. Roy, Rustum, "Science Underlying Radioactive Waste Management: Status and Needs," *Scientific Basis for Nuclear Waste Management*, Vol. 1, pp. 1-20. Ed. G.J. McCarthy, Plenum Publishing Corp., New York (1979).

30. T. Takamori, R. Messier and Rustum Roy, "New Non-Crystalline Germanium which Crystallizes 'Explosively' at Room Temperature," *Appl. Phys. Lett.* 20:201-203 (1972).

31. Russell Messier and Rustum Roy, "Thermal Behavior of Noncrystalline Sputtered Films in the System Ge-Te," *Mat. Res. Bull.* 6:749-758 (1971).

32. Russell Messier, A.K. Sarkar and Rustum Roy, "New Metal-Rich Germanide and Carbide Non-Crystalline Solids," *Mat. Res. Bull.* 9:157-166 (1974).

33. L. R. Gilbert, R. Messier and R. Roy, "Superconducting $BaPb_{1-x}Bi_xO_3$ Ceramic Films Prepared by R.F. Sputtering," *Thin Solid Films* 54:129-136 (1978).

34. K. Char, A. D. Kent, A. Kapitulnik, M. R. Beasley and T. H. Geballe, "Reactive Magnetron Sputtering of Thin-Film Superconductor Yttrium Barium Copper Oxide ($YBa_2Cu_3O_{7-x}$)," *Appl. Phys. Lett.* 51(17):1370-1372 (1987).

35. A. R. Badzian and R. C. DeVries, *Mat. Res. Bull.* 23:385 (1988).

91

36. R. Roy, "CVD Diamond Science and Technology: One of Three Materials Revolutions," *Proc. 41st Annual National Conference on the Advancement of Research*, September 27-30, 1987, Technomic Publishing Company (1988).

37. B. V. Derjaguin and D. V. Fedoseev, "Growth of Diamond and Graphite from the Gas Phase," *Izd. Nauka*, Moscow (1977).

38. S. Matsumoto and N. Setaka, *Carbon* 17:485 (1979); *Carbon* 19:232 (1981).

39. Y. Matsui, A. Yuuki, M. Sahara and Y. Hirose, *Jpn. J. Appl. Phys.* 28(29):1718 (1989).

40. G. Gildenblatt, S. Grott and A. R. Badzian, "Electrical Properties and Device Applications of Homoepitaxial and Polycrystalline Diamonds," *Proc. IEEE* 79:647 (1991).

41. (a) R. Roy, "New Hybrid Materials Made by Sol-Gel Technique, " *Bull. Am. Ceram. Soc.* 61:374 (1982).

    (b) R. Roy, "Ceramics from Solutions: Retrospect and Prospect," *MRS Annual Meeting Abstracts*, p. 370 (1982).

    (c) R. Roy, "New Metal-Ceramic Hybrid Xerogels," *MRS Annual Meeting Abstracts*, p. 377 (1982).

42. R. Roy, "Ceramics by the Solution Sol-Gel Route," *Science* 238:1664 (1987).

43. H. Gleiter, *Mat. Sci. & Engr.* 52:92(1982); review in *Nanostructured Mat.* 1:1-19 (1992).

44. R. A. Roy, R. Messier and J. M. Cowley, "Fine Structure of Gold Particles in Thin Films Prepared by Metal-Insulator Co-Sputtering," *Thin Solid Films* 79(3):207-215 (1981).

45. David Hoffman Rustum Roy and S. Komarneni, "Diphasic Ceramic Composites via a Sol-Gel Method," *Mat. Lett.* 2(3):245-247 (1984).

46. R. Roy, S. Komarneni and D. M. Roy, "Multi-phasic Ceramic Composites Made by Sol-Gel Technique," *Better Ceramics Through Chemistry*, Proc., Mat. Res. Soc. Symp., Vol. 32. Ed. C. J. Brinker, D. E. Clark and D. R. Ulrich, Elsevier Science Publishing Co., Inc., NY. pp. 347-359 (1984).

47. R. Roy, S. Komarneni and W. Yarbrough, "Some New Advances with SSG-Derived Nanocomposites," Chapter 42, *Ultrastructure Processing of Advanced Ceramics*, John MacKenzie and Don Ulrich (eds.), Wiley Interscience, pp. 571-588 (1988).

48. Proc. Seventh Seminar on Frontier Technology — Nano-Hybridization and Creation of New Functions, Feb. 7-10 (1989), Oiso, Japan.

49. G. Ervin, thesis, Pennsylvania State College, University Park, PA (1949); E. F. Osborn, *J. Geol.* 59:381 (1951); V. G. Hill, R. Roy and E. F. Osborn, *J. Am. Ceram. Soc.* 35:135 (1952); R. Roy, D. M. Roy and E. F. Osborn, *ibid* (1950).

50. (a) U. Selvaraj, A. V. Prasadarao, S. Komarneni and R. Roy, "Sol-Gel Fabrication of Epitaxial and Oriented TiO_2 Thin Films," *J. Am. Ceram. Soc.* (in press).

    (b) U. Selvaraj, A. V. Prasadarao, S. Komarneni and R. Roy, "Epitaxial $SrTiO_3$ Thin Films by Sol-Gel Processing," *J. Mat. Res.* (in press).

51. U. Selvaraj, C. L. Liu, S. Komarneni and R. Roy, "Epitaxial Crystallization of Seeded Albite Glass," *J. Am. Ceram. Soc.* 74:1378-1381 (1991).

52. G. Vilmin, S. Komarneni and R. Roy, "Crystallization of ThSiO4 from Structurally or Compositionally Di-phasic Gels," *J. Mat. Res.* 2:489 (1987).

53. K. Niihara and A. Nakahira, "Structural Ceramic Nanocomposites," *Ceramics: Towards the 21st Century*, Ceramic Society of Japan, Tokyo (1991), p. 404 ff.

54. Z. Zhao, "Chinese Scientists Success in Highest T_c Superconductor," *Peoples Daily*, Beijing, February 25, 1987.

55. M. L. Keith and R. Roy, "Structural Relations Among Double Oxides of the Trivalent Elements," *Am. Min.* 39:1-23 (1954).

56. (a) A. H. Heuer, "Biological and Biomimetric Ceramics: A New Frontier," Orton Lecture, 93rd Ann. Mtg. of the American Ceramic Society, April 28-May 2, 1991, Cincinnati, OH, p. 338.
(b) I. Aksay, quoted by R. Eisner, *The Scientist*, July 8, 1991, p. 14.
(c) A. V. Srinivasan, G. Haritos and F. Hedberg, "Biomimetics: Naturally Evolved Systems as Paradigms for Advanced Aerospace Materials and Systems," Air Force Office of Scientific Research, Washington, DC (1990).

57. J. N. Weber, E. W. White and J. Liebiedzik, "New Porous Biomaterials by Replication of Echinoderm Skeletal Microstructure," *Nature* 233:337-339 (1971).

58. R. A. White, J. N. Weber and E. W. White, "Replamineform: A New Process for Preparing Ceramics, Metal, and Polymer Prosthetic Materials," *Science* 176:922-924 (1972).

59. E. W. White, J. N. Weber, D. M. Roy, E. L. Owen, R. T. Chiroff and R. A. White, "Replamineform Porous Biomaterials for Hard Tissue Implant Applications," *J. Biomed. Mat. Res. Symp.* 6:23-27 (1975).

60. Jonathan Black, personal communication.

61. M. Newkirk et al., *J. Mat. Res.* 1:81 (1986).

62. A. S. Fareed, B. Sonuparlak, C. T. Lee, A. J. Fortini and G. H. Schiroky, "Mechanical Properties of 2-D Nicalon™ Fiber Reinforced LANXIDE™ Aluminum Oxide and Aluminum Nitride Matrix Composites," *Ceram. Eng. Sci. Proc* 11[7-8]:782-794 (1990).

63. C. A. Andersson, P. Barron-Antolin, A. S. Fareed and G. H. Schiroky, "Properties of Fiber-reinforced Lanxide™ Alumina Matrix Composites," *ASM Proc. Int. Conf. Whisker- and Fiber-toughened Ceram.*, pp. 209-215 (1988).

64. R. E. Newnham and G. Ruschau, "Smart Electroceramics," *J. Am. Ceram. Soc.* 74:463 (1991).

65. N. Tsuya, Y. Saito, H. Nakamura, S. Hayano, A. Furugohri, K. Ohta, Y. Takui and T. Tokushima, "A Perpendicular Magnetic Recording Medium by Aluminte," *J. Mag. . Mat.* 54-57:1681-1682 (1986); T. Endo, T. Sato and M. Shimada, "Fluorescence Properties of the Dye-intercalated Smectite," *J.*

Phys. Chem. Sol. 47(8):1423-1428 (1988); R. E. Newnham and S. E. Trolier-McKinstry, "Structure-Property Relationships in Ferroic Nanocomposites," *Ceramic Trans.* 8:235-252 (1990).

66. C. F. von Weizsacker, *The Unity of Nature:* Farrar, Strauss and Giroux (1980).

67. R. Roy, *Experimenting With Truth*, Pergamon Press, NY (1973).

68. D. Mermin, *Physics Today* (November 1990), p. 9 ff.

69. Materials Science and Engineering for the 1990's, U.S. National Research Council, Washington, DC (1989).

70. A. Kelly, "The Future of Metals," *Min. Ind. Intnl. Bull.* 996:5-10 (1990).

71. Rustum Roy, "The Management of Knowledge and the Role of Culture in the R/D Enterprise," *Japanese/American Technolgical Innovation*, Elsevier Science Publishing Co., Inc., 253-257 (1991).

72. R. Roy, "Achieving Harmony Between Science and Technology and Humankind and Society," presented at The Kanagawa Academy of Science and Technology (May 29, 1991).

MATERIALS SYNTHESIS TODAY
ACHIEVEMENTS IN CERAMICS POST WW II

- Magnetic Materials: ferrites, garnets, $SmCO_5$,R.B.I.'s

- Glass Ceramic Process: Materials: Process: Understanding

- Low Expansion Ceramics: Cordierites, L-A-S, CZP

- Synthetic Diamonds, CBN.

- Sol-Gel Process: Maximizing homogeneity; now heterogeneity

- Float glass

- Strong Polycrystalline Ceramics: LAS--▸ SiC--▸ sialon

- Toughened Ceramics: Fibers, transition (ZrO_2); Lanxide

- Fine, Pure Powders: Solution, EDS, hydrothermal, RESA

- New Cements

LANDMARK MATERIALS SYNTHESES POST WW II
METALS

1. Ni-based superalloys

2. Basic oxygen process

3. Aircraft engine alloys-directioal solidification single crystal turbine blades

4. Amorphous metals (allied: 100 million lbs capacity)

5. Permanent magnets: $SmCo_5$, NdFe borides

The Historians of Science Have Shown the Critical Role
of Instruments in Advancing Science

Technology ⟶ Instruments ⟶ New Science

Other Inputs

Material Technology ⟶ New Materials ⟶ New Science

Other Inputs
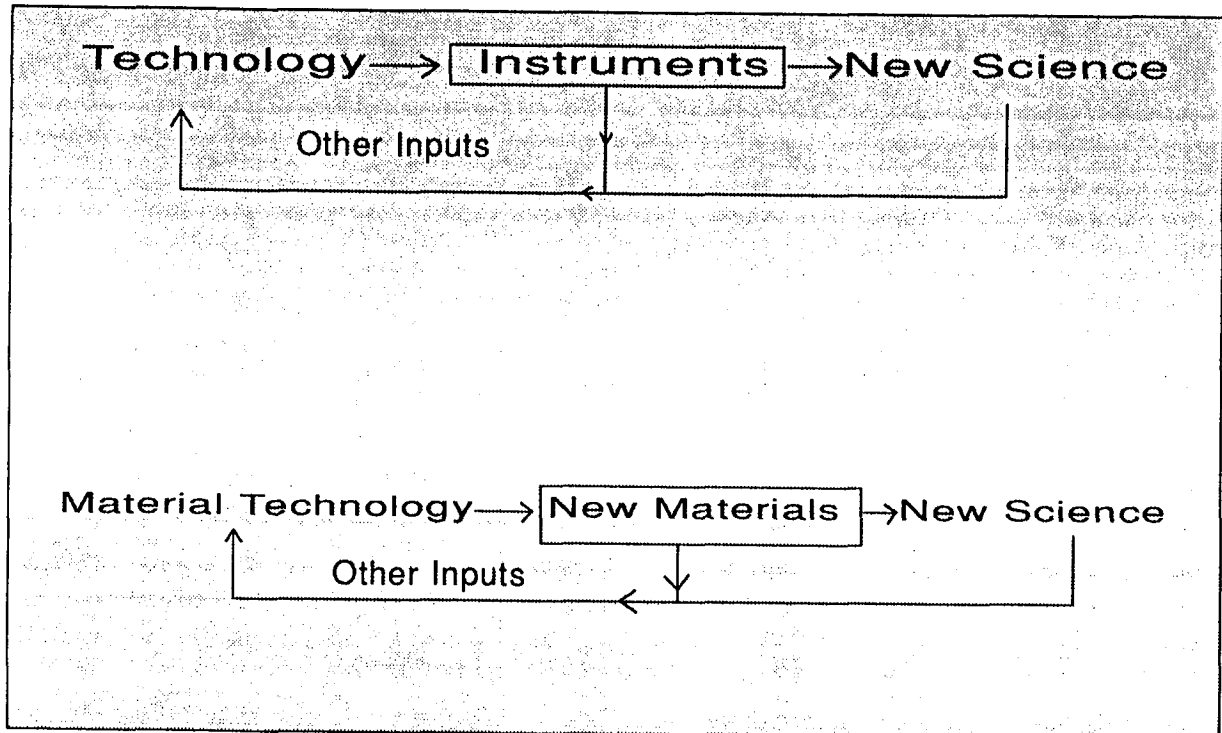
In exactly analogous ways "New Materials" coming out of "Technology" advance materials science
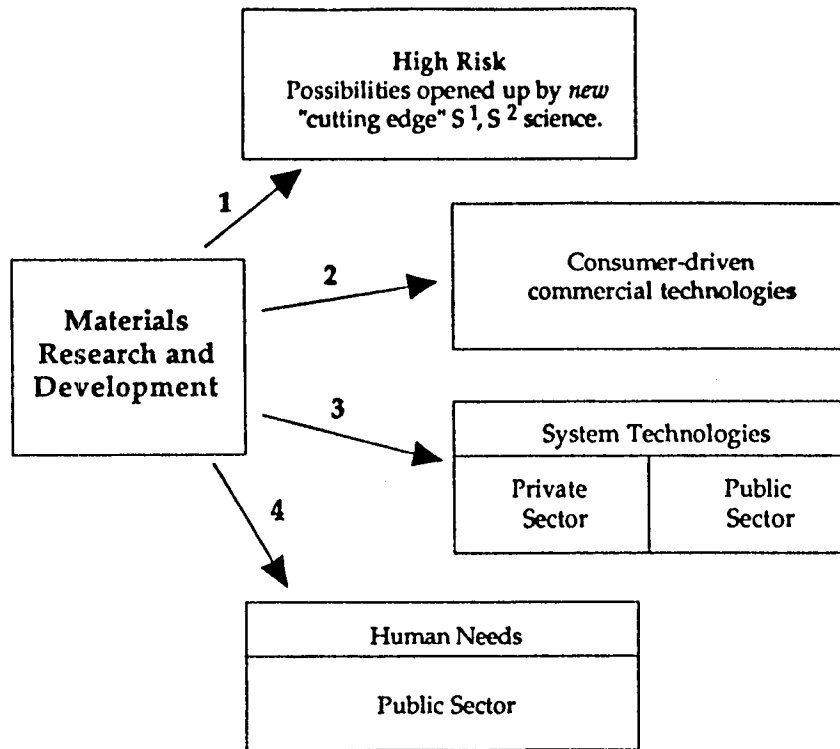
What drives technology?

WHAT DRIVES EFFECTIVE SYNTHESIS RESEARCH?

S.P. = SCIENCE PUSH

M.P. = MARKET PULL

NEW→ T.T. = "TECHNOLOGY TRACTION"
CONNECTION OF SCIENCE TO A
TECHNOLOGICAL GOAL (DETERMINED BY
PUBLIC OR PRIVATE SECTOR NEEDS)

THREE KINDS OF "SCIENCE"

S = SERENDIPITOUS DISCOVERY
(CAREFUL OBSERVATION BY HIGHLY TRAINED
OBSERVER)

S^2 = SCIENCE FOR SOCIETY (PURPOSIVE, LONG-TERM BASIC
SCIENCE)

S^3 = SCIENCE FOR SELF AND THE INSTITUTION OF SCIENCE

A. FURNACE
Raw materials are melted

B. MOLTEN METAL
Molten metal ready for delivery to casting system as needed

C. CASTING SYSTEM
Molten metal under pressure is sprayed from nozzle

F. MANIPULATOR Positions spray nozzle to vary amorphous metal ribbon thickness

D. HIGH SPEED ROTATING COPPER BELT
Molten metal sprayed on cooled copper belt forms amorphous metal ribbon

E. COOLING BOX Keeps temperature of belt near room temperature
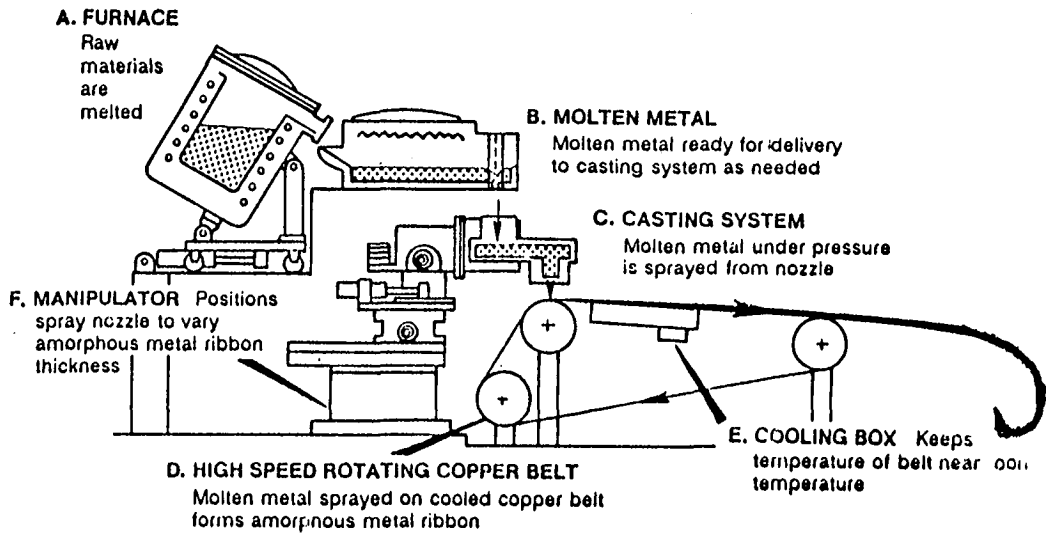
A REAL WINNER OF NEW MATERIALS SYNTHESIS
GLASSY METALS.
(S.P. & T.T)

MICROPIPET MANIPULATION OF LIPID MEMBRANES: DIRECT MEASUREMENT OF THE MATERIAL PROPERTIES OF A COHESIVE STRUCTURE THAT IS ONLY TWO MOLECULES THICK

David Needham

Department Mechanical Engineering & Materials Science
Duke University
Durham, North Carolina 27708-0300

Telephone 919-660-5329

MICROPIPET MANIPULATION OF LIPID MEMBRANES: DIRECT MEASUREMENT OF THE MATERIAL PROPERTIES OF A COHESIVE STRUCTURE THAT IS ONLY TWO MOLECULES THICK

David Needham

Department of Mechanical Engineering and Materials Science,

Duke University, Durham, NC 27708-0300

Key Words: lipid bilayer, stress, strain, elasticity, failure, biological cells.

Prerequisite Knowledge:

To appreciate this demonstration, students should have some understanding of the concepts of stress and strain, elasticity, tensile strength, strain energy and composites. A rudimentary familiarity with the chemical composition of surfactant-like molecules, in particular phospholipids, is also required.

Objectives:

The objectives are to demonstrate how we can make direct measurements of the mechanical properties of a special structure in biology, namely the lipid bilayer membrane, using a micromanipulation technique; and how these properties compare and contrast with "more traditional" technological/engineering materials. Given that the investment in equipment and expertise to carry out these experiments is probably beyond the scope of most teaching labs, the described experiment is not intended as one that can actually be demonstrated in a student laboratory class. The intention behind presenting this work is to begin to raise awareness in the Material Science community about the material properties of biological material that form a new (to us) category of soft engineering materials that have dimensions on the nanoscale.

Introduction:

Nature has chosen a specific state of matter and some exceptional materials with which to construct the biological world. She colonized the colloidal state of matter (material in the size range 10Å to 10μm) and has used the solvent, water, to great advantage in forming and maintaining the integrity of structures that have both hydrophilic and hydrophobic components. From a materials design perspective, 10^9 years of evolution have gone into Nature's design methodology; materials have been selected based on their availability, compatibility with a given system, and their ultimate performance in service. The systems that have survived, and that give good service performance, provide lessons

for scientists and engineers regarding materials selection and properties, especially for those concerned with designing artificial systems that must interface with biology's own materials.

Nature's materials are different to our usual notion of engineering materials, in that they and their interfaces are soft. The softness derives from the fact that, in water, the separation of polar and non-polar phases relies on entropy rather than enthalpy; the, so called, hydrophobic effect [1] excludes oil-like, non-polar material from the water phase. These separate, non-polar phases are not strongly bonded (attractive forces are weak van der Waals forces) and, consequently, biological material is soft and often liquid-like. The lipid bilayer membrane is a "classic" material that includes both hydrophilic and hydrophobic regions in a structure that is only 5nm thick.

The importance of the simple lipid bilayer is underscored when we realize that it is the structure that surrounds every cell on our planet.
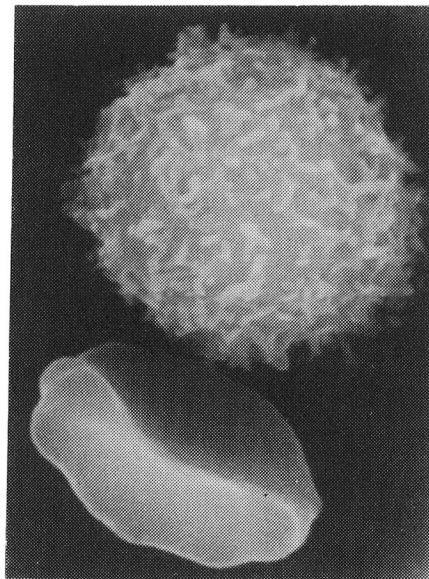

Figure 1. Scanning electron micrograph of a neutrophil (top) and an erythrocyte [2]. The erythrocyte has an excess of surface area compared to a sphere of the same volume and its smooth membrane is supported by a viscoelastic cytoskeleton. In contrast, the neutrophil is spherical and its 100% excess membrane area is supported in microvillious structures.

In addition to its many important functions of a chemical and biochemical nature, the lipid bilayer provides a mechanical, chemical and electrical barrier that isolates the cellular interior. It is also the structural matrix of the composite cell membrane to which, and in which, all the other, more "exotic", protein and carbohydrate molecules are located. This membrane defines the interface and site of communication between the cell and its surrounding medium. To give two common examples consider the electron micrograph in Figure 1. We see two different cells, a white blood cell and a red blood cell.

The red blood cell, or erythrocyte, is characterized by a smooth membrane and a discoid shape. The white blood cell, in this case a neutrophil, has a highly microvilliated surface. In addition to the lipid membrane experiments described here, we have used the micropipet method and devised experiments (large deformation and recovery after large deformation) that allow us to make measurements of the viscous and elastic properties of whole cells [2, 3, 4, 5, 6, 7].

When we look inside the neutrophil, as shown in Figure 2, we see that it is composed of a highly complex arrangement of microfilaments and granules.
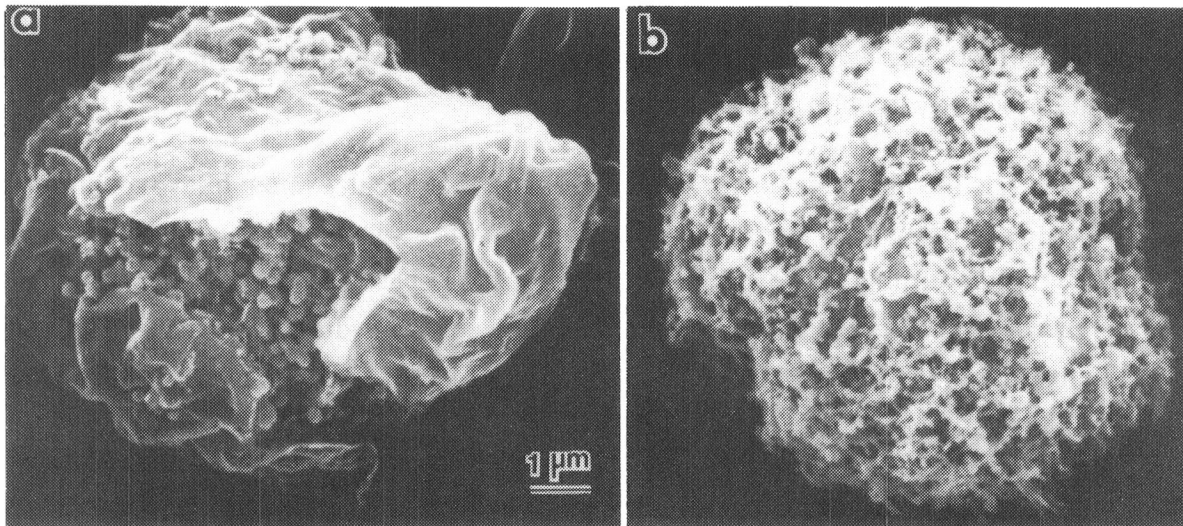
Figure 2 Scanning electron micrographs of an osmotically lysed and a detergent solubilized neutrophil.* By bursting a hole in the plasma membrane using osmotic stress or by dissolving away the whole membrane with gentle detergent the complex filamentous and particulate nature of the cytoplasm is revealed.

---

*Hochmuth, R. M., H. P. Ting-Beall, B. Beaty, D. Needham, R. Tran-Son-Tay, "The Viscosity of Passive Human Neutrophils Undergoing Small Deformations." Biophys. J., in press.

Having introduced the lipid membrane as a biological structure, let us now consider some basic material features of the lipid bilayer membrane and, through this discussion, demonstrate a special technique that allows us to make micromechanical measurements on these colloidal-sized, soft materials.

As a class of material, the lipid membrane is an association colloid made up of surfactant-like, phospholipid molecules that have both hydrophilic and hydrophobic parts. These molecules associate in aqueous media due to the operation of the hydrophobic effect and, to varying extent, to secondary attraction forces (van der Waals dispersion forces).
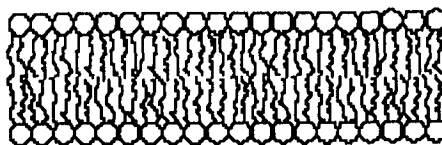
Figure 3. Schematic of bilayer arrangement of phospholipid molecules showing transverse section through the bimolecular lipid layer. The circles represent the polar phospholipid headgroups (e.g. phosphocholine) oriented towards the water interface, and the squiggles represent the long hydrocarbon chains (e.g., 18 carbons per chain; 2 chains per molecule) that form the hydrophobic interior of the bilayer.

The membrane is formed by the packing of molecules into a bilayer configuration with the hydrophobic acyl chains forming the core of the layer and the hydrophilic headgroups forming the interface with the aqueous phase, as shown in the schematic in Figure 3. The bilayer interior is essentially a liquid-like hydrocarbon and, in the plane of the membrane, molecules move about in a liquid-like manner, without significant shear rigidity.

In our micromechanical studies we have been and continue to be concerned with composition-structure-property relations in lipid bilayer membranes [8, 9, 10, 11]. We have found that the material properties of lipid bilayer membranes depend on the chemical structure of the constituent lipid molecules and the interaction of the lipids with cholesterol and other lipid-membrane-soluble components. We have used micropipet manipulation methods to measure the response of this membrane to several modes of deformation (bending, in-plane shear for solid bilayers and isotropic area dilation [8]). Here we will focus on area expansion, the elastic area expansion modulus and, the failure parameters, tensile strength, critical areal strain and strain energy.

Procedures:

Experimental Methods and Equipment

The preparation of lipid vesicles from lipid solutions and the procedures for carrying out thermomechanical studies on a range of lipid and mixed lipid systems are documented in several recent publications concerning the micromanipulation of such structures [8, 9, 12, 13, 14, 15]. In order to prepare lipid bilayer vesicles, that are suitable for micromanipulation using optical microscopy, an aqueous solution is added to dry the lipid (Avanti Polar Lipids Pelham, AL; Sigma, St. Louis, MO) and the lipid spontaneously hydrates to form spherical capsules, called lipid vesicles or liposomes. Depending on the level of imposed agitation during or after this hydration step these lipid vesicles can be made to vary in size from 250Å in diameter (e.g., by sonication), to 'Giant' liposomes of 20 μM to 50 μM in diameter, (formed by the gentlest of convective procedures). Preparation procedures can give varying degrees of multilamellarity to these lipid bilayer structures that can range from single membrane capsules, to multiwalled "onion-skin" liposomes, to unusable gobs of partially hydrated material. In our micropipet experiments we select single walled liposomes from the largely multilamellar population. (Note: other techniques that complement our mechanical measurements, such as x-ray methods, require detectable repeat periods of multiwalled liposomes and can yield information about the bilayer geometry, phase behavior and colloidal interaction between membranes [10, 16]). The lipid vesicle solution is diluted into a glucose solution and placed in a simple glass microchamber on a microscope stage.

With regard to the experimental set-up and equipment, details have also been fully documented in recent publications [15, 17, 18, 19]. The micromanipulation system is centered around an inverted microscope that has micromanipulators mounted directly on the microscope stage. Control over micropipet suction pressure is in the range of microatmospheres to tenths of atmospheres (1 dyn/cm^2 to 100,000 dyn/cm^2) and is achieved by a micrometer-driven manometer and recorded by in-line pressure transducers (Validyne). An essential part of the manipulation system is a glass micropipet of desired internal diameter (~8-10 μm) and flat tip that is used to apply the force to the aspirated vesicle during the vesicle deformation tests. Micropipets are made from 0.75 mm internal diameter glass capillary tubing (A-M Systems, Inc., Everett, WA), formed into microneedles by a heated pipet puller.
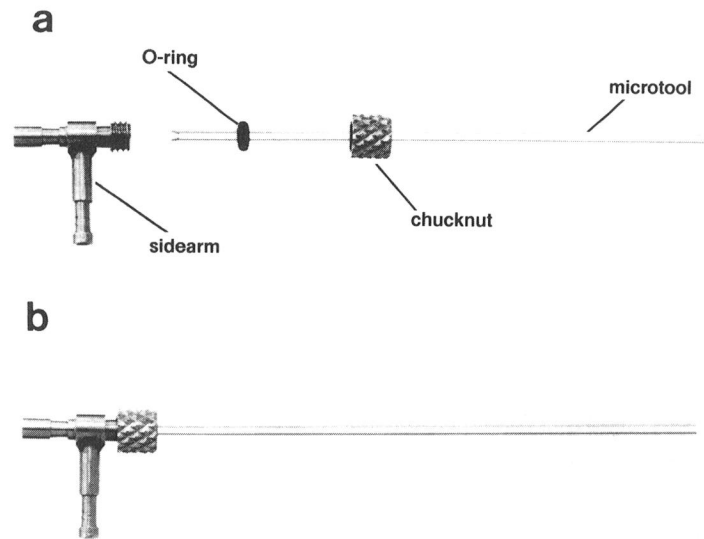
Figure 4. The chuck and micropipet arrangement. a) individual pieces; b) assembled chuck and micropipet. (Courtesy of Research Instruments Inc., Durham, NC)
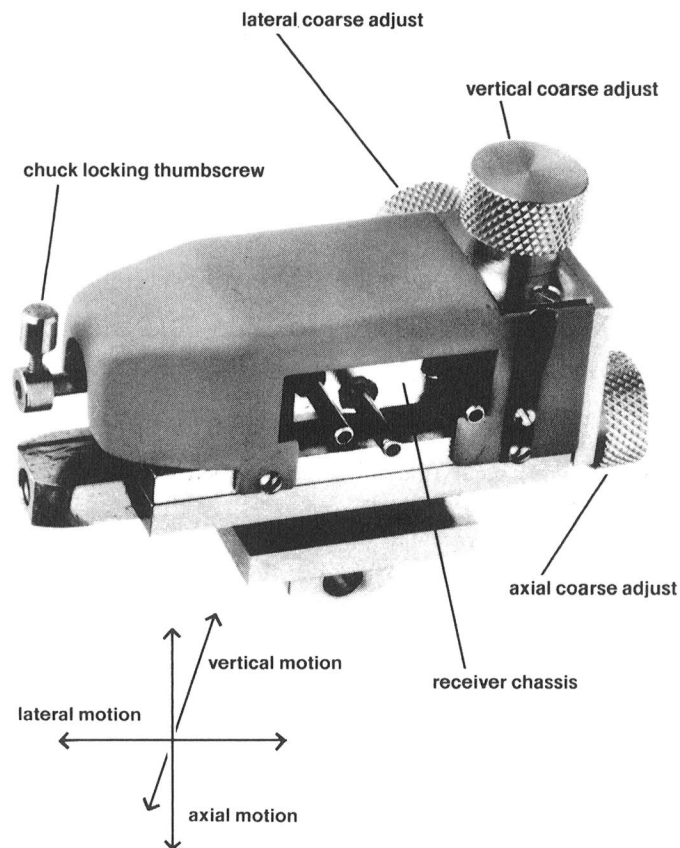
Figure 5. The manipulator (Courtesy of Research Instruments Inc., Durham, NC)

The flat pipet tips of desired diameter (1 μm to 15μm) are broken by quick fracture on a microforge. The pipets are filled with a NaCl solution that matches the osmolarity of the solution that the liposome properties are measured in. The measuring micropipet is inserted into a metal chuck (Research Instruments Inc., Durham, NC), as shown in Figure 4, that connects the pipet to the water-filled manometer system. The chuck with side-arm access, allows any suitable micro-tool to be rapidly sealed to the chuck with an "O"-ring compression seal.
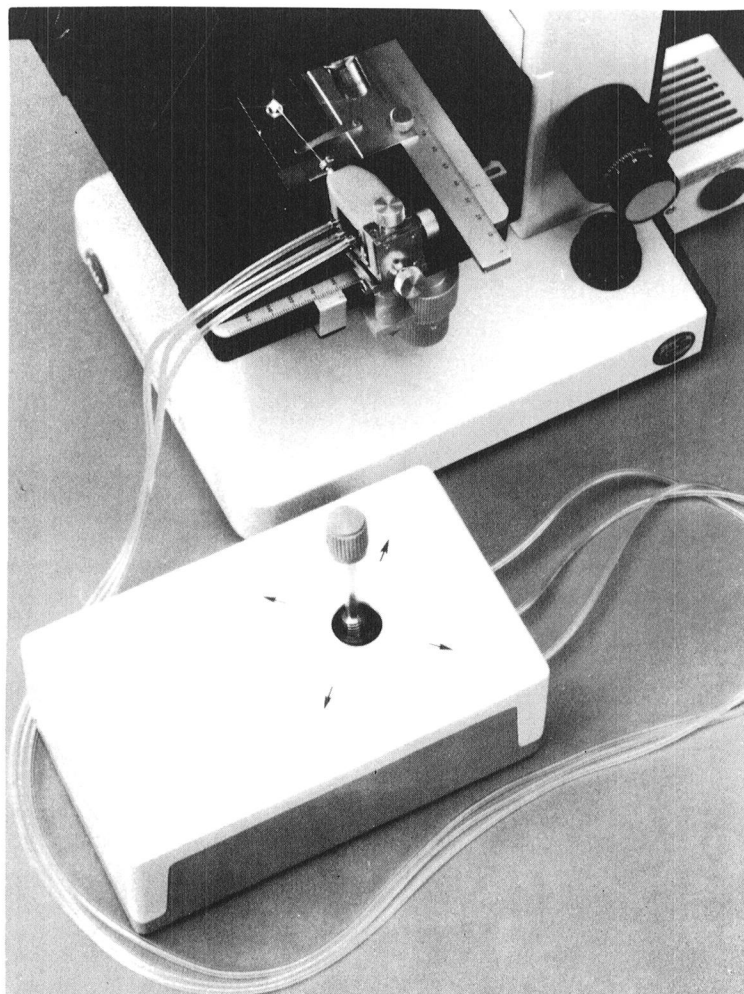
Figure 6. "Aerial" view of manipulator with micropipet mounted on the microscope stage connected to the joy stick that allows fine pneumatic control of micropipet position. (Courtesy of Research Instruments Inc., Durham, NC)

The pipet-chuck assembly is then mounted into a de Fonbrune-type micromanipulator, Figure 5, (Research Instruments Inc., Durham, NC) The manipulator has three course positioning knobs for making preliminary adjustments of the micropipet in

the axial, lateral and vertical directions. Fine adjustments are made by the transduction of three separate and variable air pressures provided by the joy stick via flexible transmission tubes. The whole assembly is then mounted on the microscope stage as shown in the "aerial" view in Figure 6 so that the pipet enters the microchamber horizontally (microchamber not shown). The small micromanipulators are pneumatically controlled by hand operated joy sticks that allow smooth motion in all three axes (axial, lateral and vertical), zero drift and control of position on the micron scale.
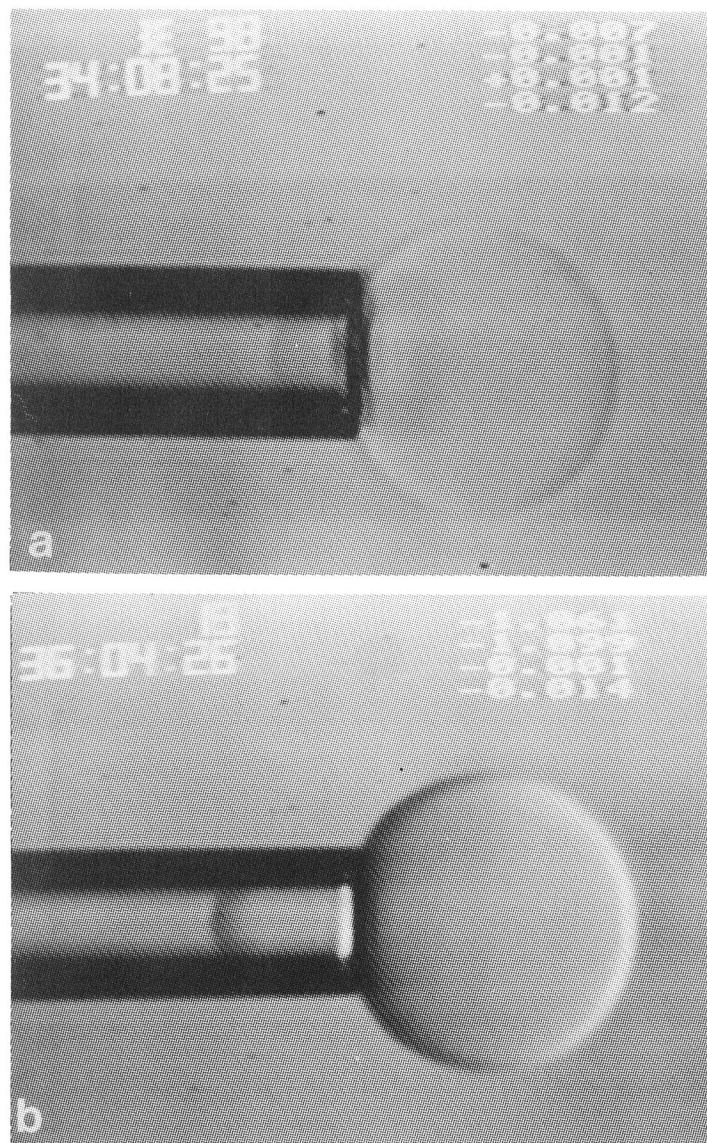
Figure 7. Videomicrographs of a giant lipid bilayer vesicle (30 μm diameter) aspirated by micropipet (8 μm diameter). a) lipid vesicle with the same solution inside and out. b) lipid vesicle in an external medium that has a different refractive index than the internal solution for ease of visibility and capture.

This micropipet manipulation system together with video interference microscopy then allows us to manipulate individual cell-sized lipid vesicles. Figure 7a shows a videomicrograph of a lipid vesicle that is being manipulated by a suction micropipet. Time and pipet pressures are multiplexed onto the video screen, as shown in the top of each micrograph. Pressurization of the liposome by the suction pipet induces an isotropic tension in the membrane and a corresponding expansion in lipid vesicle area. The pipet therefore acts as a means to manipulate individual vesicles, to apply suction pressure, and, by measuring changes in the length of the vesicle projection in the pipet, it also provides a sensitive measure of small changes in membrane area that may be as small as ~1-5%. The applied pipet suction pressure together with the pipet and vesicle geometry are used to calculate the induced isotropic membrane tension. The pipet diameter is 8 μm and the vesicle diameter is 30 μm. The lipid vesicle in Figure 7a contains the same medium inside and out and it is "seen" by virtue of its diffraction pattern in the interference contrast microscope (Leitz, inverted microscope equipped with Hoffman Modulation Optics). It is more usual for us to load the liposomes with a solution (e.g. 160 mM sucrose) that is more dense and has a different refractive index than the subsequent suspending solution (e.g., equiosmotic glucose or NaCl) so that the liposomes collect on the bottom of the microscope chamber and observation is easier, as shown in Figure 7b. Experiments are recorded on videotape and information such as time and pipet suction pressure are multiplexed directly onto the video using video multiplexing (Vista Electronics, 8226 Vista Dr. La Mesa CA). A series of experiments can then be carried out and recorded such that geometrical analyses (vesicle and pipet dimensions) can be made subsequent to the experiment using a video caliper system (Vista Electronics, CA).

Stress Strain Plot

In each experiment, area changes are derived from the projection length of the lipid vesicle in the micropipet as a function of membrane tension at constant temperature. Membrane tension (τ) is uniform over the entire vesicle surface and is given by the pipet suction pressure (P) and the pipet/vesicle geometry [12]:

$$\tau = PR_p/(2 - 2R_p/R_o) \tag{1}$$

where R_p is the pipet radius and R_o is the radius of the outer spherical segment of the vesicle. Changes in vesicle membrane projection length (ΔL) inside the pipet are a direct measure of the fractional change in total vesicle membrane area (ΔA):

$$\Delta A = 2PR_p(1 - R_p/R_o)\Delta L \tag{2}$$

This relationship is valid only if the volume of the vesicle is constant. Changes in volume (due to filtration of water by pipet suction) are in fact found to be negligible when a vesicle is held under maximum suction for periods well in excess of the duration of the experiment. Since the number of molecules in the membrane is fixed (due to extremely low lipid solubility in aqueous media), changes in vesicle area represent changes in surface area per lipid molecule. The mode of deformation that we examine in this micropipet experiment is area dilation and a simple relation between membrane tension and area change which characterizes the area elasticity in terms of an expansion modulus K. If A_0 is the reference area of the vesicle in the pipet at a low (~0.5 dyn/cm) initial membrane tension, then α, the relative, fractional change in vesicle membrane area ($\Delta A/A_0$) in response to a change in membrane tension at constant temperature, yields the compressibility modulus, K, from the constitutive relation,

$$K = \Delta\tau/\Delta\alpha \tag{3}$$

In the experiment we sequentially load and unload the membrane by increasing and decreasing the pipet suction pressure, and finally increase the suction pressure to a level that produces failure, as shown in Figure 8. The deformation is elastic (the motions of molecules are on the order of microseconds for this liquid-like membrane, so we don't see any viscous effects); there is no ductility and the failure is that of a liquid membrane.

By using this micropipet method then we can characterize lipid membranes in terms of several common material parameters:

1) Membrane area compressibility represents the resistance of the membrane to isotropic area dilation and is characterized by an elastic area compressibility (or expansion) modulus K;

2) tensile strength is given by the membrane tension at failure τ_s;

3) critical areal strain is the fractional increase in membrane area at failure α_c;

4) membrane strain energy (or toughness) E_s represents the work done on the membrane up to failure and is given by the area under the stress strain plot $K(\alpha_c)^2/2$.

These parameters were measured for several lipid and lipid/cholesterol mixtures, in particular for Stearoyloleoylphosphatidylcholine (SOPC) (18:0/18:1) alone and in combination with cholesterol. SOPC is a "standard lipid", equivalent to the average acyl chain composition of natural lipid membranes, and cholesterol is an almost ubiquitous

component that is present in natural cell membranes; for example, it is present at 40 mol% in red blood cell membranes.
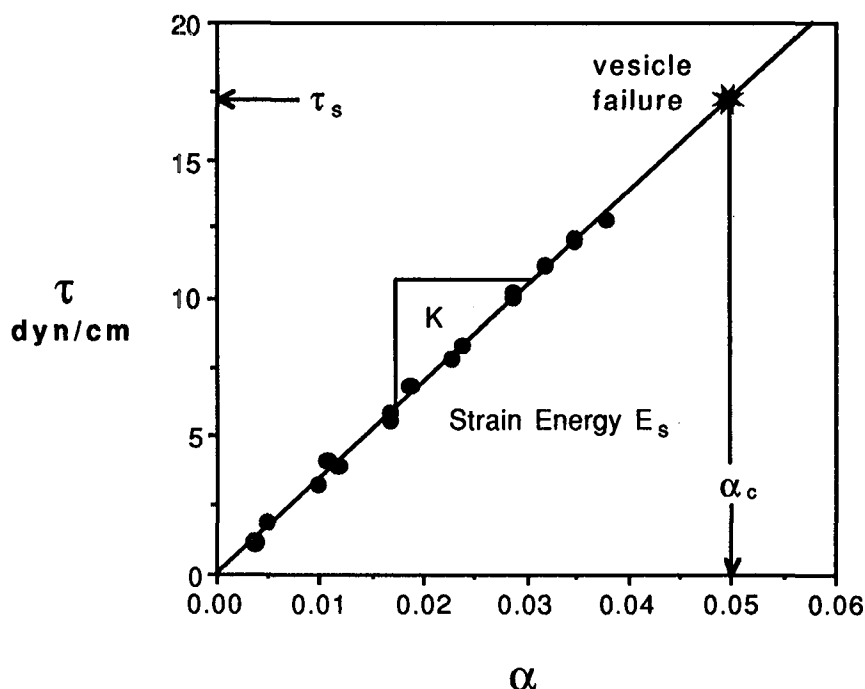
Figure 8. Stress vs strain plot for micropipet pressurization of a lipid vesicle. Vesicle membrane tension τ resulting from the applied micropipet suction pressure is plotted against the areal strain α (i.e., the observed increase in vesicle membrane area ΔA relative to an initial low stressed state A_0). The slope of the τ vs α plot is the elastic area compressibility modulus K. The star symbol represents the point of membrane failure at the critical areal strain α_c and tensile strength τ_s. The area under the plot represents the strain energy at membrane failure E_s.

Results:

Elastic Area Compressibility (Expansion) Modulus

The results for the SOPC/CHOL mixtures are shown in Figure 9. As the amount of cholesterol in the lipid bilayer is increased, the elastic modulus shows little change initially but then increases rapidly. At ~60mol% or slightly less the property saturates and reflects the chemical saturation of cholesterol in the bilayer phase. At greater stoichiometries, any excess cholesterol is present in aqueous suspension as cholesterol crystalites.
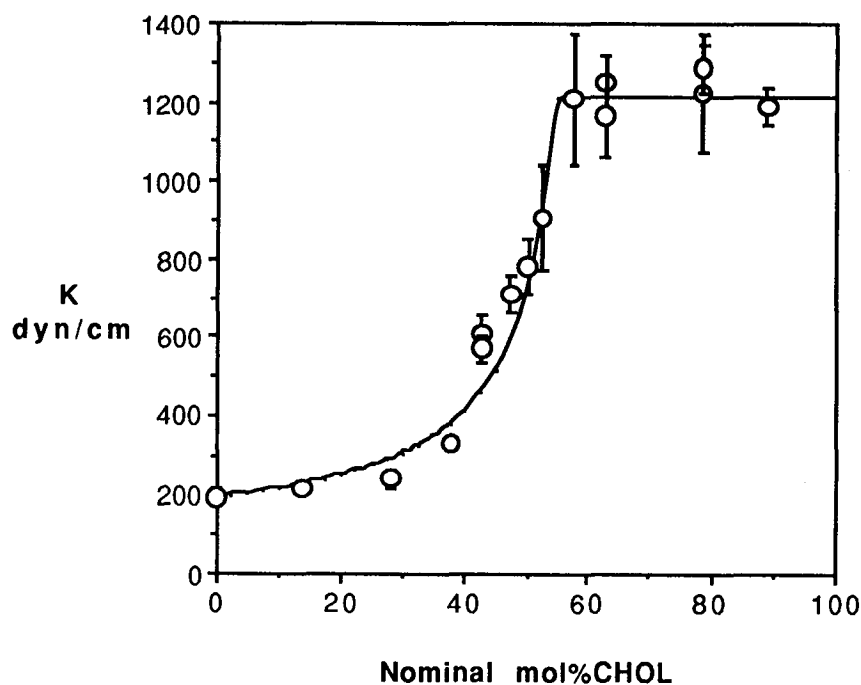
Figure 9. Area expansion modulus K versus Nominal Mol% Cholesterol in SOPC lipid bilayers. Also shown is the molecular composite model (solid line).

By analogy with common macroscopic composite theory for fiber- or particulate-reinforced materials (in which a matrix material is stiffened by the incorporation of particles of a higher modulus material), a simple 2 dimensional (isostress) molecular composite model was used to fit the data for the SOPC/CHOL system. Briefly, the simple equation for the composite bilayer is,

$$K_m = \left(\frac{a_L}{K_L} + \frac{a_{L/C}}{K_{L/C}}\right)^{-1}$$

(4)

in which the area compressibility modulus of the membrane K_m is a linear combination of the moduli of the two components, namely, free lipid K_L and a lipid/cholesterol molecular complex $K_{L/C}$ scaled by their area fractions a_L and $a_{L/C}$.

The area fractions of the two components (uncomplexed lipid a_L and lipid/cholesterol complex $a_{L/C}$) were calculated from experimental measures of the molecular areas of the free lipid 65 Å^2, the limiting value of 48Å^2 for lipid in a cholesterol saturated bilayer, and for cholesterol, from experiments involving spread monolayers

leading to a limiting area per molecule of 37Å^2. (i.e., $A_L = 65\text{Å}^2$ and $A_{L/C} = 93\text{Å}^2$). The theoretical value for the modulus thus obtained for the simple composite membrane as a function of mol%CHOL in the bilayer phase is also plotted in Figure 9 and matches the increase in bilayer area expansion modulus with increasing mol%CHOL.

Thus, when the mol% of cholesterol in the bilayer is increased, a simple property averaging theory can account for the non-linear increase in area modulus that is observed. In the model, no assumptions were made regarding size or shape of component domains. Whether homogeneously mixed or separated into component-rich domains the correlation with a macroscopic composite theory indicates that each molecular component brings to the bilayer phase its "characteristic modulus" and reflects its average interactions with its neighbors.

Membrane Failure: Critical Areal Strain, Tensile Strength and Failure Energy

Figures 10 a, b and c show the changes in critical areal strain α_c, membrane tension at vesicle lysis τ_s and energy per unit area at failure $K(a_c)^2/2$ plotted vs nominal mol%CHOL for the SOPC/CHOL system. If we look at these parameters, what do we learn about the failure mechanism?
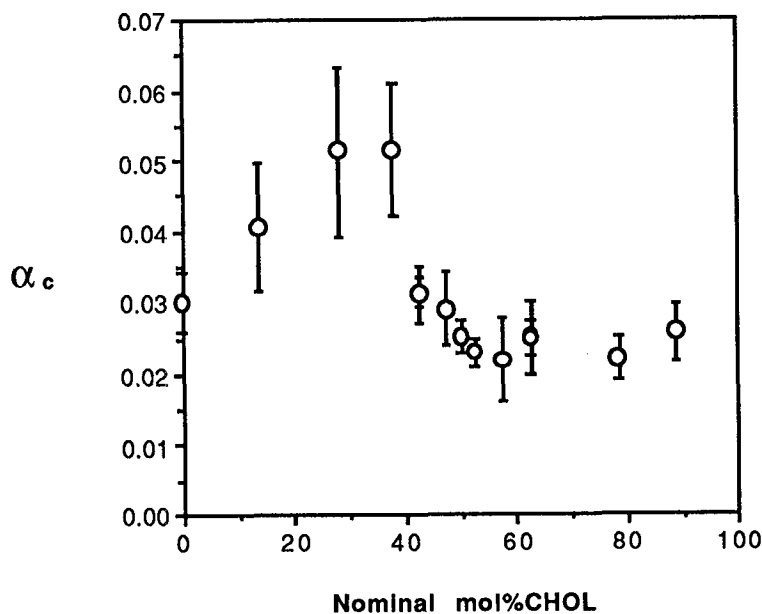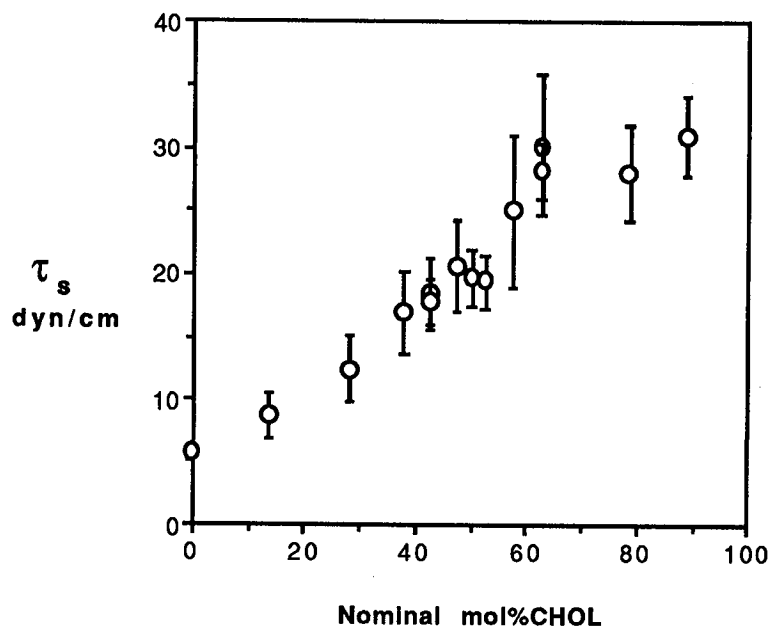

Figure 10 a Critical areal strain α_c

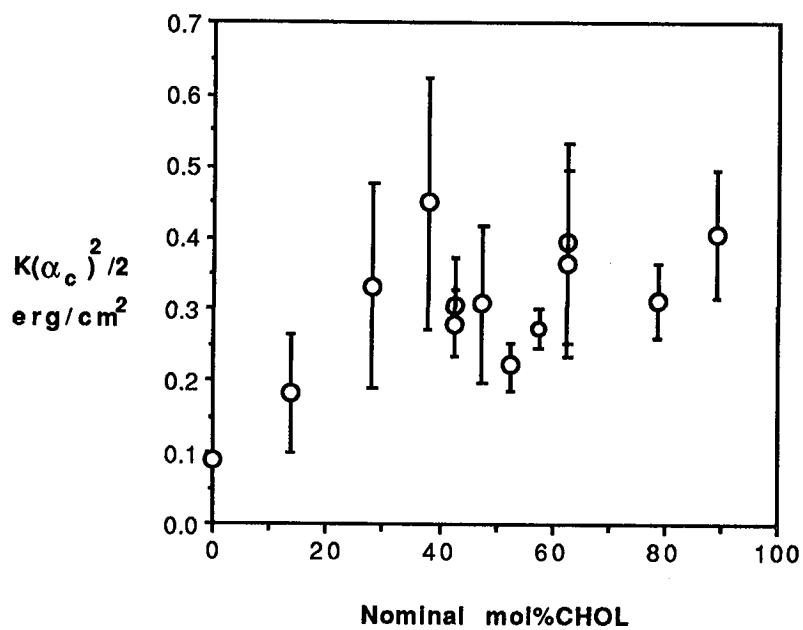**Figure 10 b** Membrane tension at vesicle lysis τ_s

Figure 10 c Energy per unit area at failure $K(a_c)^2/2$, stored in the bilayer membrane due to elastic deformation.

The fact that the critical areal strain increases then decreases (Figure 10a) demonstrates that bilayer failure per se (at least for two components) cannot be linked to an area criterion and a single value for critical strain, i.e a critical percent expansion in area per molecule. We have recently measured much stiffer membranes and the trend is for stiffer membranes to expand the least, sometimes as little as 1% at failure.

The increase in critical tension (Figure 10b) shows that the addition of cholesterol increases the strength of the bilayer, and points to an increase in cohesion that cannot be just due to the hydrophobic effect; cholesterol must increase the strength of the molecular interactions and create a more bonded material. The peak in critical areal strain and the steadily increasing tensile strength are combined in Figure 10c as $K(\alpha_c)^2/2$ to show that the lipid membrane is essentially "toughened" by the addition of cholesterol, but only up to a certain point, around 40 mol%CHOL.

If we are designing for "toughness" and not strength, then intermediate cholesterol concentrations give the best membranes. This may be coincidence, but it is interesting to note that the natural RBC membrane also contains ~40mol%CHOL. Red blood cells flow almost interminably (120 days) in the blood stream and must survive the rigors of fluctuating hydrodynamic forces. Were the membranes "designed/selected" for toughness and not strength? As with the modulus measurements, all these properties showed constancy above ~58 mol%CHOL, which again indicated a constant bilayer composition for nominal cholesterol concentrations above 58 mol%CHOL.

Our analysis can be taken a step further by converting the failure energy per unit area $K(\alpha_c)^2/2$ into an energy per mole of lipid by multiplying by Avogadro's number and the appropriate area per molecule. Interestingly, the amount of energy that is stored in the SOPC/CHOL membrane when it breaks ranges from 35 J/mol for the single component SOPC membrane to 130 J/mol for the 40 mol%CHOL membrane. When compared to RT (2400 J/mol), the thermal energy per mol, we see that a relatively small amount of energy is required to cause irreversible failure by applied tensile stresses. The energy stored in the membrane up to failure is only a small fraction of the available thermal energy per mole. This might be taken to imply that failure results from a defect that comprises many (~50-100) molecules. We are currently investigating defect formation and failure during electric field-induced breakdown of lipid bilayers and the formation of a pore-like defect made up of many molecules seems to be at the heart of bilayer failure [20, 21].

Finally, a simple thermodynamic interpretation along the lines of Whol, [22] can be made if we recognize that an increase in bilayer strain energy represents an increase in stability and may be correlated with a decrease in the overall free energy of the bilayer. A decrease in the excess Gibbs energy of the bilayer due to mixing the two membrane components, namely, uncomplexed lipid and the lipid/cholesterol complex, would make a stabilizing contribution to the overall free energy. This simple analysis indicates a maximum in overall stability of the bilayer structure for bilayer cholesterol concentrations around 35mol%CHOL. The experimental membrane strain energy shows approximately the same form as the excess mixing free energy and gives some credence to the hypothesis that simply mixing the two (postulated) bilayer components confers stability on the structure. The enhanced stability then, would appear to come from an increase in internal energy, i.e., an increase in the cohesive energy density of the material due to the mixing.

Concluding Remarks and Perspectives

The bulk elastic modulus of the lipid bilayer is $\sim 10^9$ Nm^{-2}, in the range found for normal incompressible fluids and high density polyethylene. However, because the membrane is a highly anisotropic structure the surface area compressibility at constant bilayer volume is expected to contrast markedly with the bulk elasticity. From our micromechanical measurements, the in-plane, elastic area compressibility modulus for normal phospholipids is found to be $\sim 10^{-1}$ Nm^{-1} and when this is converted to an equivalent bulk modulus by dividing by the membrane thickness of ~ 5 nm, we see that the surface compressibility is $\sim 10^7$ Nm^{-2}, i.e., in the surface plane, the structure has a compressibility somewhere between that of an ordinary liquid and a gas! This defines the softness of this nevertheless cohesive material. We can therefore view the membrane as a 2 dimensional cohesive liquid that (in-plane) can be about 100 times more compressible than its embedding, aqueous fluid.

Some of our more recent, as yet unpublished, results also show that this area elasticity can range over two orders of magnitude (50 - 4000 dyn/cm) depending on the lipid composition and alloying with cholesterol. Compare this behavior with that of metals, where the Young's elastic modulus for lead and tungsten varies by not quite 20 times, and for ceramics, where ice to diamond ranges by about two orders of magnitude. Thus, the lipid bilayer shows a very wide range of elasticity for any single type of material because it starts from a state of weakly bonded softness.

Before these measurements were made it was generally accepted that the cohesion in lipid membranes is approximated by twice the interfacial tension between hydrocarbon

and water, giving K ~ 100 dyn/cm; i.e., surface pressure is opposed by the hydrophobic effect between the lipid hydrocarbon chains and the bathing water at the membrane interface. Whilst the hydrophobic effect can be responsible for getting the lipids to assemble in aqueous media and sets the lower cohesive limit, the higher moduli for cholesterol-rich bilayers indicates that there are additional bonding forces responsible for bilayer integrity, and points to a specific interaction between phospholipids and cholesterol. These high modulus membranes are now showing expansion behavior like more traditional solid and liquid materials where the repulsive (thermal) forces between molecules are counteracted by the attractive, in this case van der Waals, forces between the hydrocarbon chains.

The phospholipid bilayer, then, presents to the Material Scientist a very accessible, versatile and simple liquid (or solid) structure with which to test models for elasticity, cohesion, and failure, including mixing relations. There are not many alternatives for energy storage and dissipation in this kind of structure and agreement between experimental data and simple theories is likely to be good.

Finally, these kinds of materials engineering studies are important to both fundamental and technological endeavors. They provide a basis for understanding the material properties of natural cell membranes and in formulating mechanisms of membrane breakdown and cell damage caused by disease or environmental insult. For example, in cancer, abnormalities in the biosynthetic regulation of cholesterol constitute early events in tumorigenesis and underlie many of the phenotypic hallmarks of cancer cells [23]. Altered cholesterol levels, particularly in membranes, lead to the development of a host of altered metabolic patterns within the affected tissue, since the normal function of integral membrane proteins often requires a specific lipid environment. Thus, membrane expansivity appears to be a very important regulator of cellular events. Our measurements of the material properties and colloidal interactions of lipid-based systems also provide much needed engineering design parameters for medical and other technologies that use lipid bilayers and similar organic thin films in, for example, encapsulated drug delivery, optics, tribology and biosensors. This is a new area of nanoengineering that uses self-assembling systems to form well ordered 2D arrays of molecules at surfaces. We are currently involved in the engineering of nanocarrier delivery systems (Stealth® liposome drug delivery [24]). These drug-carrying lipid capsules, upon intravenous injection, have the ability to evade the body's defenses and shift the distribution of toxic anti-cancer drug away from healthy organs and tissues and more towards the tumor [25, 26].

References:

1. Tanford, C. 1980. "The Hydrophobic Effect: Formation of Micelles and Biological Membranes." John Wiley and Sons, Inc.

2. Needham, D., H. P. Ting-Beall and R. Tran-Son-Tay, 1991. A physical characterization of GAP A3 hybridoma cells: morphology, geometry and mechanical properties. Biotech. and Bioeng. **38**, 838-852.

3. Needham, D., M. Armstrong, D. L. Hatchell and R. S. Nunn, 1989. Rapid deformation of "passive" polymorphonuclear leukocytes: the effects of pentoxifylline. J. Cell. Physiol. **140**, 549-557.

4. Hochmuth, R. M. and D. Needham, 1990. Viscosity of neutrophils and their transit times through small pores. Biorheology. **27**, 817-828.

5. Needham, D. and R. M. Hochmuth, 1990. Rapid flow of passive neutrophils into a $4\mu m$ pipet and measurement of cytoplasmic viscosity. J. Biomech. Eng. **112**, 269-276.

6. Tran-Son-Tay, R., D. Needham, A. Yeung and R. M. Hochmuth, 1991. Time dependent recovery of passive neutrophils after large deformation. Biophys. J. **60**, 856-866.

7. Needham, D. and R. M. Hochmuth, 1992. A sensitive measure of surface stress in the resting neutrophil. Biophys. J. **61**, 1664-1670.

8. Evans, E. and D. Needham, 1987. Physical properties of surfactant bilayer membranes: thermal transitions, elasticity, rigidity, cohesion, and colloidal interactions. J. Phys. Chem. **91**, 4219-4228.

9. Needham, D. and R. S. Nunn, 1990. Elastic deformation and failure of lipid bilayer membranes containing cholesterol. Biophys. J. **58**, 997-1009.

10. McIntosh, T. J., S. A. Simon, D. Needham and C.-h. Huang, 1992. Structure and Cohesive Properties of Sphingomyelin:Cholesterol Bilayers. Biochemistry. **31**, 2012-2020.

11. Simon, S. A., T. J. McIntosh, A. D. Magid and D. Needham, 1992. Modulation of interbilayer hydration pressure by the addition of dipoles at the hydrocarbon-water interface. Biophys. J. **61**, 786-799.

12. Kwok, R. and E. Evans, 1981. Thermoelasticity of large lecithin bilayer vesicles. Biophys. J. **35**, 637-652.

13. Needham, D. and E. Evans, 1988. Structure and mechanical properties of giant lipid (DMPC) vesicle bilayers from 20 C below to 10 C above the liquid crystal-crystalline phase transition at 24 C. Biochem. **27**, 8261-8269.

14. Needham, D., T. J. McIntosh and E. Evans, 1988. Thermomechanical and transition properties of dimyristoylphosphatidylcholine/cholesterol bilayers. Biochem. **27**, 4668-4673.

15. Needham, D., 1992. "Measurement of interbilayer adhesion energy." Membrane Fusion Techniques. Düzgünes ed. Academic Press. in press

16. McIntosh, T. J. and S. A. Simon, 1986. Hydration force and bilayer deformation: a reevaluation. Biochem. **25**, 4058-4066.

17. Evans, E., 1988. "Mechanics of cell deformation and cell-surface adhesion." Physical Basis of Cell-Cell Adhesion. Bongrand ed. CRC Press, Inc. Boca Raton, Fla.

18. Evans, E., 1988. "Micromethods for measurement of deformability and adhesivity properties of blood cells and synthetic membrane vesicles." Physical Basis of Cell-Cell Adhesion. Bongrand ed. CRC Press, Inc. Boca Raton, Fla.

19. Evans, E., 1989. "Structure and Deformation Properties of Red Blood Cells." Methods in Enzymology. Academic Press.

20. Needham, D. and R. M. Hochmuth, 1989. Electro-mechanical permeabilization of lipid vesicles: role of membrane tension and compressibility. Biophys. J. **55**, 1001-1009.

21. Zhelev, D. and D. Needham, 1992. Long-lived reversible pores in giant vesicle: determination of pore size and edge energy. Biochim. Biophys. Acta. submitted for publication.

22. Wohl, K., 1946. Thermodynamic Evaluation of Binary and Ternary Liquid Systems. AIChE. **42**, 215-249.

23. Coleman, P. S. and B. B. Lavietes, 1981. Membrane cholesterol, tumorigenesis, and the biochemical phenotype of neoplasia. CRC Crit. Rev. Biochem. 341-393.

24. Stealth®, "Stealth" is a registered trademark of Liposome Technology Inc.

25. Needham, D., T. J. McIntosh and D. D. Lasic., 1992. Repulsive interactions and mechanical stability of polymer-grafted lipid membranes. Biochim. Biophys. Acta. **1108**, 40-48.

26. Needham, D., K. Hristova, T. J. McIntosh, M. Dewhirst, N. Wu and D. D. Lasic, 1992. Polymer-grafted liposomes: physical basis for the "stealth" property. J. Liposome Res., Vol. 2, p. 411–430.

TOOL GRINDING AND SPARK TESTING

Edward L. Widener

MET Department
Purdue University
Knoy Hall - Room 119
West Lafayette, Indiana 47907

Telephone 317-494-7521

TOOL GRINDING AND SPARK TESTING

Edward L.Widener,PE
Mechanical Engineering Technology Dept.
Purdue University, West Lafayette, IN 47907-1252

KEY WORDS: sparking, non-sparking, grinding, testing, recycling.

PREREQUISITE KNOWLEDGE: Students should be familiar with the Standard Symbols to identify chemical elements (say Fe, C, Mn, Cr, Si); and with Standard Systems to identify metal alloys (say AISI 4340 low alloy steel; AISI 316 stainless steel; AISI/SAE M34 tool steel, i.e. UNS T11334; ASTM A242, HSLA steel; AA 6061-T6 aged aluminum; and CDA 122, i.e. UNS C12200). These letters designate the American Iron and Steel Institute; the Society of Automotive Engineers; the Unified Numbering System; the American Society for Testing and Materials; High Strength-Low Alloy; the Aluminum Association; and the Copper Development Association.

OBJECTIVES: To revive the neglected art of metal-sparking. To promote quality-assurance in the workplace. To avoid spark-ignited explosions of dusts or volatiles. To facilitate the salvage of scrap-metals. To summarize important references.

EQUIPMENT & SUPPLIES: (1) Grinding wheel, bench or portable type; e.g., the common "Dremel Moto-Tool Kit," keyless model 395, with 5-speeds, plus Si-carbide disk (#85422,grey) or Al-oxide disk (#8215,brown) is satisfactory and readily available at hardware stores. (2) Eye protection, safety glasses or goggles. (3) Samples of lo-alloy steels, with lo/med/hi-carbon contents. (4) Stainless-steels, including iron-crystal types of ferritic/martensitic/austenitic. (5) Cast-irons, including gray/white/malleable/ductile/wrought grades. (6) Tool-steels, including types with W/O/A/D heat-treatments. (7) Light-metals(Li,Mg,Al,Ti). (8) Copper and its brass/bronze alloys. (9) Classic sparkers, like Zirconium and Cerium. (10) Optional camera, instant-color preferred, to freeze motions and record observations.

BACKGROUND: After discovering fire, primitive peoples apparently learned to kindle flames from tinder and sparks, possibly with rocks struck by metal ores. Later on, hunters and soldiers of the 16th or 17th centuries replaced fire-locks (ignited by matches) with flint-locks (striking steel-steel) pistols or rifles. Today, we have cigarette- lighters and gas-igniters (using sparks from cerium, scratched by steel). Pouring molten steel or cutting structural steel can produce cascades of twinkling, scintillating sparkles. Driving behind a gasoline-truck, especially at night, we see sparks from a chain which discharges static-electricity to the pavement. Also, plastics and ceramics, although insulators, can collect static charges and may arc if grounded. Surely, the study of sparking materials is important for identifying metals, discerning alloy contents, and averting explosions.

PROCEDURE: Students must have proper eye-protection! They should not test non-ferrous metal-samples on a shop-grinder, normally used by the iron-workers; soft-metals may clog the wheel, requiring maintenance to re-dress the wheel and reduce its life.

Samples are then hand-held against the bench-mounted grinder; or a portable tool with attached grind-wheel can bear against the clamped sample. Students can stand back to observe sparkles and compare specimens, before grinding their own. Obviously, bearing-pressures and spark-arcs can vary, so consistent procedure is recommended for metal comparisons or contrasts. Although hand-held samples do not exceed 140 Fahrenheit (threshold of pain for bare skin), there is risk of injury to ungloved fingers; using tongs brings risks of over-hot samples or flying pieces; so be careful!

Materials may be identified or classified, referring to standard charts or tables. However, consult an experienced machinist to save time and improve diagnoses.

RESULTS: For plain steels, sparking has greater length/frequency/ complexity, as carbon content increases. The characteristic color is orange. Low-carbon/high-alloy steels, like stainless or magnet grades, may not spark much.

Grey cast-iron, with much higher carbon-content than steel,nevertheless has virtually no sparks. The graphite flakes in iron are soft and not dissolved in a matrix of iron atoms. However, wrought-iron pipe being cut by torch, may shower sparks profusely (although carbon is negligible in alpha-ferrite). White iron (chilled to transform graphite to cementite) sparks well.

Tool steels are traditionally characterized by their distinctive sparking. However, this is a dying art, practiced mainly by expert machinists.

Titanium is a real surprise, with its blue-white glow. In dull contrast, the light-weight aluminum and magnesium alloys produce no sparks at all! Similarly, copper and its alloys of brass or bronze have no sparks.

However, zirconium does give that amazing blue-white glow. Moreover, cerium literally sputters and smokes, if you merely strike it with a steel bar; it is ideal for cigarette-lighters.

CONCLUSIONS: This is a cheap & quick way to identify tools, predict carbon-content of steel, select non-sparking equipment, and salvage valuable metals. However, for unsophisticated eyes and unskilled hands, the subtle differences in alloy-compositions of tools and stocks are probably undetectable. Variations of hand-pressure and spark-flight are troublesome. Moreover, published tables and charts (by makers of abrasives and welders) tend to be inconsistent and contradictory.

For scrap dealers or maintenance workers, a set of standard samples may be collected or purchased; these are controls (benchmarks) for comparing (gaging) sparks. Another technique is to make or buy color-photos or dynamic video-tapes of major metals.

For large lots of costly metals, the modern techniques of DTA (Differential Thermal Analysis) or APS (Arc Plasma Spectrometer) are often more reliable. These could be used to train novices in spark-

grinding or to verify the preliminary assessments by veteran sparkers, as insurance against the day when hi-tech units are unavailable or unaffordable.

RECOMMENDATION: A lab experiment is enhanced by a written report. Students should explore why materials do or don't spark. Why do sparks differ in appearance and behavior? What is the size and shape of grinder dust? How does grinder-wheel composition affect the sparks and dusts? Apparently, the material hardness and grinder speed contribute to frictional heating; a material's oxidizing rate or melting temperature may be involved; consider oxygen concentration or static electricity. What causes sparks to twinkle or scintillate? Perhaps particles have blowouts, as the crust is solidified and/or the heat of fusion is released. Possibly the particles tumble, as they fly off the grinder, depending on shape variations. Use the references; search the literature; consult with mechanics; and find the experts may disagree. This could spark some research and development activity!

ACKNOWLEDGEMENTS: Prof.F.Xavier Spiegel, EE & ES Dept of Loyola College in Baltimore, MD, provided most of my references and exhibits. Like Newton, he claims only to stand on the shoulders of giants in the spark-testing field. Messrs.E.Bishop and E.Pitois may indeed be gurus, but to me Spiegel is special.
Prof.Marvin L.Sarapin, Dept.of Technology, Kean College of Union,NJ, introduced spark-tests while directing ten summer seminars to train welders and pipefitters of the United Association. The late W.Fred Stone conducted sparking demonstrations for the"Ed & Fred Show" in our lab sessions.
The late Prof.Sayyed M.Kazem, MET Dept, Purdue University, has been an important resource for team-teaching the metals lab these past 22-semesters.
Prof. David Werstler, Eng.Tech.Dept., MS 9086, W.Washington University, Bellingham,WA, sent the "Metal I.D." pages from an Allen & Mortensen lab manual.
Dr. L.Roy Bunnell, Materials Science Dept, Battelle Pacific Northwest Labs, Richland,WA, sent data and information sheets from the "Welding Engineer" files.

REFERENCES:
1) Bishop,Edsel E., "The Art of Spark Testing", Wyckoff Steel Co., Pittsburgh,PA, 1954.
2) Pitois,E., "Sparking of Steel", transl.by J.D.Gat, Chem.Publ.Co., Easton,PA, 1929.
3) Spiegel,F.X.et al, "Scrap-Metal Bibliography", U.S.Bureau of Mines, Avondale,MD, 1984.
4) Spiegel,F.X.et al, "Scrap-Metal Identification Based on Particles Generated During Spark-Testing", U.S.Bureau of Mines, Avondale,MD, 1984.
5) Palmer,F.R., "Tool-Steel Simplified", Carpenter Steel Co.,Reading,PA, 1937.
6) Aston,J. and Story,E.B., "Wrought Iron", A.M.Byers Co.,Pittsburgh,PA, 1944, p79.

7) Hildorf,W.G.and McCollam,C.H., "Metal Pellets, Produced by Spark Tests, to Identify Alloy Steels", The Iron Age, New York,NY; vol.126, no.1, p1.

8) Sarapin,M.L., "Properties & Characteristics of Metals", UL#38 Instructor Training Notebook, Purdue University, W.Lafayette,IN, 1988.

9) Allen,D.K. and Mortensen,K.S., "Materials Science Lab Manual", Am.Tech.Soc., Chicago,IL, 1992 , p59.

10) Norton Co., Spark Chart & Table, "Grits and Grinds", June 1940.

EDWARD L. WIDENER

Has taught mechanical engineering technology at Purdue University (since 1978), concentrating on statics, fluid mechanics, materials, labs and technical writing...Member ASME, ASEE, ASM, TAPPI. Registered P.E. in New York and Indiana...ABET visitor in 1983-92...B.S. M.E. from Purdue University and M.S. E.M. from the University of Kansas...Taught evenings at IUPU Indianapolis and Danville, IL. Worked as Mechanical Development Engineer for "Coria" collagen casing with Teepak Co., Continental Group (1976-78). Process Group Leader for mechanical contractor, Baker-McHenry-Welch, Indianapolis (1974-76). Project Leader for creped-wadding and secondary-fibers with Kimberly Clark Co., Memphis, TN (1968-74). Process Engineer for "Nomex" nylon with E.I. DuPont Co., Richmond, VA (1963-68). Associate Engineer for electro-furnace alloys with Union Carbide Co., Niagara Falls, NY (1952-60). Fuel Engineer with U.S. Steel Co., Gary IN,(1951-52).

EXPERIMENTS IN CORROSION FOR YOUNGER STUDENTS BY AND FOR OLDER STUDENTS

James V. Masi

Western New England College
Department of Electrical Engineering
Springfield, Massachusetts 01119

Telephone 413-782-1344

EXPERIMENTS IN CORROSION FOR YOUNGER STUDENTS BY AND FOR OLDER STUDENTS

James V. Masi, PhD
Western New England College
Dept. of Electrical Engineering
Springfield, MA 01119

THE COLLEGE EXPERIMENT

KEY WORDS: corrosion, batteries, electromotive force series, anode, cathode, plating.

PREREQUISITE KNOWLEDGE: The college student should understand the concepts of electrochemical potential through a basic chemistry course and a concurrent materials science course (usually third year level). The college student is first given his or her classroom lecture on corrosion, is shown the "Corrosion in Action" video from LaQue Center for Corrosion Technology, Inc. (Wrightsville Beach, NC), and performs a laboratory experiment. This allows the college student to be a mentor to the junior high school student. The junior high school student should have had a general science course and be in the upper half of his or her class.

OBJECTIVES: To illustrate the electrochemical nature of corrosion and to observe the location of anodes and cathodes (arising from differences in composition and cold work) of metals immersed in electrolyte solutions. The magnitudes of voltages and current densities on corroding couples is obtained.

EQUIPMENT AND SUPPLIES: College: Iron nails, three Petri dishes, 400 ml beaker, 3% NaCl electrolyte, agar gel, copper displacement plating cell, zinc electroplating cell, two high impedance multimeters, phenolphthalein in alcohol solution, potassium ferricyanide, deformed nails, zinc plated nails, and copper wires and sheets. Junior High: Two multimeters, small d.c. power supply with clip leads, 10X microscope, large and small area electrodes of zinc, platinum, calomel, graphite, aluminum, copper, 1018 steel, 300 series stainless steel, mercury/silver amalgams, lemons and potatoes, and nails of iron, copper, and aluminum.

PROCEDURE: The work is to be done by pairs of students. Each pair will observe three different, previously prepared corrosion specimens in Petri or glass dishes. Prepare one similar specimen, and observe two different specimens freshly prepared by other groups in the class. Also, each group will measure emf and corrosion current density for the following cells (all of which use the 3% NaCl solution as the electrolyte): iron vs cold worked iron, iron vs zinc, iron vs copper wire and subsequently vs copper sheet of much larger area.

1. Observe the corrosion couples prepared at least six hours in advance. The advance preparation allows for the indicator

reactions to develop fully. The cells are prepared using the following recipe. To make 250 ml, adequate to cover nails in three Petri dishes, dissolve 5 grams of agar in 250 ml of 3% NaCl solution. Place one nail in each Petri dish. Pour agar solution evenly into three Petri dishes. The first dish should contain an ordinary iron nail. The second should contain a nail dipped half its length for two minutes into the copper sulfate displacement solution (200 g/L H_2O). The third should contain a nail electroplated for ten minutes over the tip half with zinc (200 g/L potassium chloride, 32g/L zinc chloride, galvanized nail anode, and current density of 1 A/dm²). Check these specimens occasionally to observe any changes. Record the observations. Other small objects of interest to the individual student may be placed into the solution <u>not in contact with the nail</u>.

2. Fill a 400 ml beaker approximately half full with 3% NaCl solution (NOTE: This is about the concentration as in seawater and about three times more concentrated than in blood.). Clip multimeter leads to the selected pairs of electrodes and dip the electrodes (but not the clips) into the NaCl electrolyte. Measure the voltage and current, noting the polarities. Prior to immersion, estimate the approximate areas of each electrode so that current densities can be calculated. Describe any visible effects in the solution while the electrodes are immersed. Note any changes in the surface of the electrode after they are removed from the electrolyte and washed. The electrode pairs are: (a) iron nail vs deformed iron nail; (b) iron nail vs copper wire and copper sheet; and iron nail vs a zinc coated nail.

3. Questions: Answer the following questions in the report.
   (a) In what order of electrochemical activity should iron, copper, and zinc be placed? Illustrate by the quantitative emf differences recorded in your measurements.
   (b) How does the magnitude of the emf generated by the difference in cold work compare with the emf of the galvanic couples?
   (c) What is the cathodic reaction and why does it cause phenolphthalein to turn red only in those regions?
   (d) For each of the cells in the beakers, calculate the approximate current densities for cathodes and anodes.
   In which case is the most rapid corrosion taking place? Why? What is the effect of the ratio of cathode to anode area and why is there an effect?
   (e) Would you use zinc-coated roofing nails on aluminum flashing?
   (f) How could you eliminate the emf between the shank of the nail and its head or tip?

   DISCUSSION: Corrosion in aqueous electrolytes arises because of electrochemical differences of conducting solids that are coupled through an electronically conducting external circuit. Dissolution of metallic ions (or oxidation) takes place

at the anode while reduction (of O_2, hydrogen, metal ions, cations) occurs at the cathode in a galvanic cell.

The experiments illustrate the contributions of differences in the amount of cold work and chemical composition differences to the establishment of electromotive forces that cause corrosion to take place. Reactive indicators locate anodes and cathodes by color changes. The deep blue-black color of the ferro-ferricyanide ion identifies the anode where iron dissolves. A less distinct white color is formed by zinc ferrocyanide. In either case, the increasing alkalinity or pH at the cathodic areas causes phenolphthalein to turn red.

Using the same basic materials dipped into a sodium chloride solution in a beaker, the emf difference and the total corrosion current can be measured approximately with a high impedance multimeter. A "zero-resistance" ammeter is used by the corrosion engineer, since a normal ammeter has appreciable resistance, which could limit the current flow appreciably. For instance, the difference between the "true" short circuit current and the one actually read by the multimeter can be as much as 20%, depending on the quality and method of current measurement employed in the multimeter. The recording of the polarity is equally important and indicates the anodes and cathodes. An uncoated iron nail should be measured against a copper nail and copper sheet and against a zinc-plated nail. Also, an undeformed iron nail should be measured against a heavily deformed nail. In each case, both voltage and current should be recorded. Using the sizes of the immersed areas of anodes and cathodes allows the experimenter to estimate current densities. Verify that the ratio of cathode to anode area is important for the measurements of the iron nail vs a smaller copper wire or nail and against a larger area copper sheet. <u>Keep the clip contacts out of the electrolyte at all times</u>.

THE JUNIOR HIGH SCHOOL EXPERIMENT

Under the auspices of a National Science Foundation Grant for teaching junior high school students math and science, the Electrical Engineering Department at Western New England College has developed a set of three experiments taught at two different levels. These experiments are developed by E.E. professors to be taught to the junior high school students by assigned, mentor junior level electrical engineers at the College, during the summer and after school during the regular year. Some of the experiments are also performed by the college junior class in their Materials Science course during the regular school year in a different context and at a higher level. The experience has proven to demonstrate corrosion, qualitatively and quantitatively to younger, potential engineers and to provide learning experiences for the student-teacher as well as the college students at a higher level.

The three experiments chosen were: 1. POTATOES, LEMONS, NAILS, AND MONEY; 2. CORROSION IN EVERYDAY LIFE: ANODES AND CATHODES; and 3. CORROSION PREVENTION: MINDING YOUR A's AND C's. The first of these experiments is included in the following section.

BATTERIES:
POTATOES, LEMONS, NAILS, AND MONEY

Name_____   Date_____

INTRODUCTION

Often, many people think that there are two kinds of electricity - static electricity and current (or moving) electricity. Actually, they are really the same. The difference is that the electrons (negative charges), ions (negative or positive), or positive charges are not moving in static electricity, while current electricity is made up of moving charges. When electrons move and produce an **electrical current**, they develop a **magnetic field**. To understand electricity, it is necessary to know something about the relationship of electricity and magnetism. The two subjects are closely related. Electricity can produce magnetism and magnetism can produce electricity. This understanding has led us to many useful devices such as motors, generators, pacemakers, automobiles, batteries, electroplating, etc.

Electrochemical energy works for us and against us. It works against us when we have **corrosion**, such as the rust on a car or the rotting of gutters with nails of different materials than the gutter. It works for us when we see the action of a battery or an electroplating bath (like when we chromium plate a bumper on a car).

EXPERIMENT OBJECTIVES

As a result of this experiment you should be able to:
1. Predict when things will corrode;
2. Understand the electromotive series;
3. Make and measure the voltage of batteries using different materials;
4. Predict what voltage a particular battery will have

MATERIALS AND EQUIPMENT

1-POTATO
1-LEMON
1-VOLTMETER
1-AMMETER
1-COPPER NAIL
1-GALVANIZED NAIL
1-PIECE OF ALUMINUM FOIL
1-PIECE OF COPPER FOIL
SOME VINEGAR OR LEMON JUICE

1-STEEL NAIL
SOME PAPER TOWELS
TEN PENNIES
TEN DIMES OR NICKELS
A SMALL LIGHT BULB

132

PROCEDURE

Insert one end of the steel nail into one end of the potato and stick one end of the copper nail into the other end of the potato as shown. Connect the negative probe of the meter to the copper nail. The meter should read about 1/2 volt d.c. A lemon can be substituted for the potato. Try moving the nails closer together to see if the voltage changes. Do the same with all the combinations of materials you have available. Now measure the current produced by these materials, noting the changes with the size of the material used. Fill out the tabular chart below to see what the results are for various pairs of materials tested. What did you notice about the voltage change with distance? What did you notice about the voltage change with electrolyte?

_____

_____

_____

_____

What did you notice about the current change with size of the materials?

_____

_____

Now use lemon juice or mix a tablespoon of vinegar with a glass of water. Then soak a paper towel in the solution. Tear it into coin-sized pieces. Place a penny on the table and lay a wet piece of paper towel on top as shown in the next figure. Place a dime on top of that and then another piece of paper towel. You want a stack of alternating pennies and dimes, with each coin separated by a wet paper towel. Start the stack with a penny and end with a dime. Connect a voltmeter to the bottom penny and the other lead to the dime. What is the voltage?

What is the current?_____
What can you conclude from some test you can perform on this setup as to how the voltage and current vary with the number of penny/dime pairs? _____

Multimeter with lemon battery

NAILS

LEMON

1.354
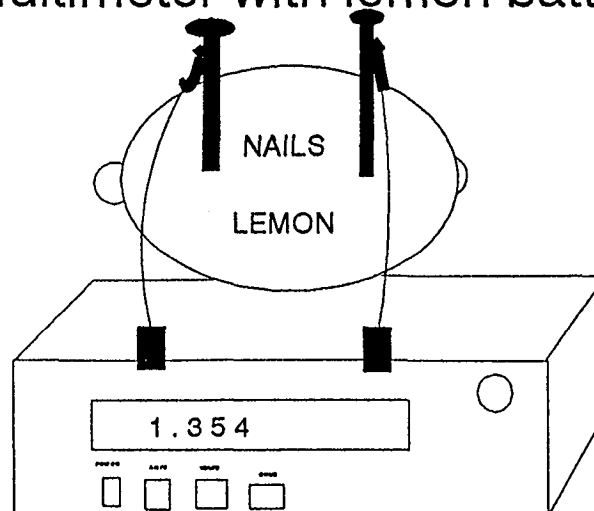
+ LEAD \ − LEAD	COPPER NAIL	STEEL NAIL	GALVANIZED NAIL	ALUMINUM NAIL/FOIL
COPPER NAIL				
STEEL NAIL				
GALVANIZED NAIL				
ALUMINUM NAIL/FOIL				

How many penny/dime pairs do you need to light the bulb supplied with the setup? _____

What kind of results would you get if you did the same thing with alternating layers of copper and aluminum?

_____
_____
_____

What could you make with this setup?

_____
_____
_____

Stack of coins as a battery

PAPER TOWEL

COINS

+ 3.812

MULTIMETER
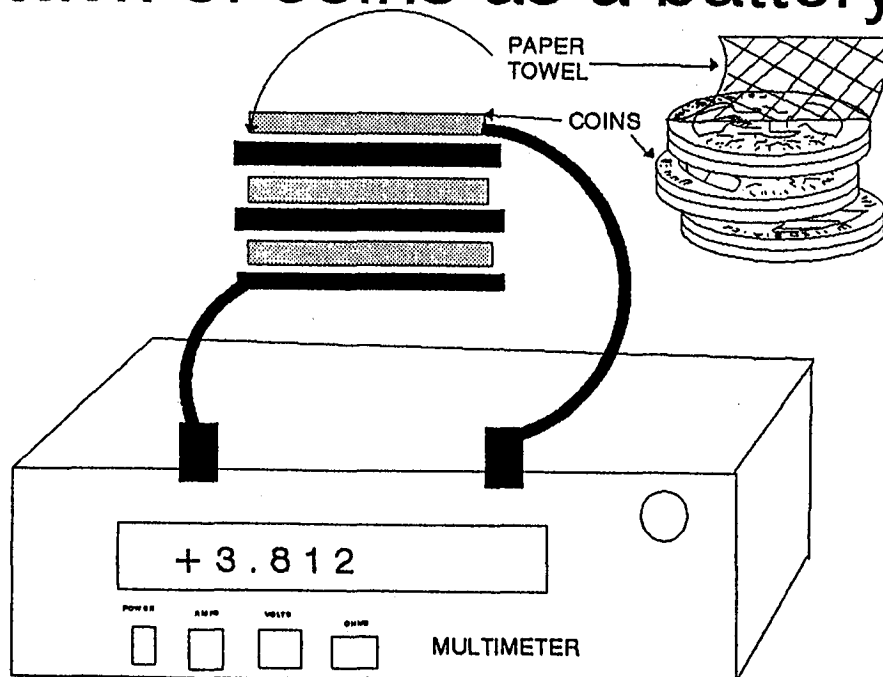
REFERENCES

1. Fontana, M. G., **Corrosion Engineering**, McGraw-Hill Book Co., New York, NY. 1986.

2. Barrett, C. R., Nix, W. D., Tetelman, A. S., **The Principles of Engineering Materials**, Prentice-Hall, Inc., New Jersey. 1973.

3. Wood, R. W., **Physics for Kids**, Tab Books, New Jersey. 1990.

Electromotive Force Series

Electrode Reaction	Standard Potential ϕ°(in volts) at 25°C
$Au^{3+} + 3e^- = Au$	1.50
$Pt^{2+} + 2e^- = Pt$	ca. 1.2
$Pd^{2+} + 2e^- = Pd$	0.987
$Hg^{2+} + 2e^- = Hg$	0.854
$Ag^+ + e^- = Ag$	0.800
$Hg_2^{2+} + 2e^- = 2Hg$	0.789
$Cu^+ + e^- = Cu$	0.521
$Cu^{2+} + 2e^- = Cu$	0.337
$2H^+ + 2e^- = H_2$	0.000
$Pb^{2+} + 2e^- = Pb$	−0.126
$Sn^{2+} + 2e^- = Sn$	−0.136
$Mo^{3+} + 3e^- = Mo$	ca. −0.2
$Ni^{2+} + 2e^- = Ni$	−0.250
$Co^{2+} + 2e^- = Co$	−0.277
$Tl^+ + e^- = Tl$	−0.336
$In^{3+} + 3e^- = In$	−0.342
$Cd^{2+} + 2e^- = Cd$	−0.403
$Fe^{2+} + 2e^- = Fe$	−0.440
$Ga^{3+} + 3e^- = Ga$	−0.53
$Cr^{3+} + 3e^- = Cr$	−0.74
$Cr^{2+} + 2e^- = Cr$	−0.91
$Zn^{2+} + 2e^- = Zn$	−0.763
$Nb^{3+} + 3e^- = Nb$	ca. −1.1
$Mn^{2+} + 2e^- = Mn$	−1.18
$Zr^{4+} + 4e^- = Zr$	−1.53
$Ti^{2+} + 2e^- = Ti$	−1.63
$Al^{3+} + 3e^- = Al$	−1.66
$Hf^{4+} + 4e^- = Hf$	−1.70
$U^{3+} + 3e^- = U$	−1.80
$Be^{2+} + 2e^- = Be$	−1.85
$Mg^{2+} + 2e^- = Mg$	−2.37
$Na^+ + e^- = Na$	−2.71
$Ca^{2+} + 2e^- = Ca$	−2.87
$K^+ + e^- = K$	−2.93
$Li^+ + e^- = Li$	−3.05

Participants

A MINIATURE FATIGUE TEST MACHINE

Steven M. Tipton

Mechanical Engineering Department
The University of Tulsa
600 S. College
Tulsa, Oklahoma 74104

Telephone 918-631-2994

A Miniature Fatigue Test Machine

Steven M. Tipton
Mechanical Engineering Department
The University of Tulsa, Tulsa, Oklahoma

KEY WORDS: Fatigue, wire, strain−life, fatigue data reduction, statistics

PREREQUISITE KNOWLEDGE: This experiment requires a basic knowledge of strength−of−materials bending stress−strain relations and basic fatigue concepts (S−N or ε−N). Also, an introduction to physical metallurgy and material microstructures is helpful.

OBJECTIVES: To enable the student to generate statistically sound fatigue data sets on wire specimens of varying diameter, microstructure or material. The student can then assess the effect of these parameters of fatigue resistance. The student can also be exposed to ASTM techniques for fatigue data reduction and presentation. Experiments involving variable amplitude block loading are also easily conducted.

EQUIPMENT AND SUPPLIES: A miniature fatigue testing apparatus and wire ranging in size from 14 to 22 gauge.

PROCEDURE: This experiment represents a refinement of the "paper clip demonstration" many professors use to demonstrate the concept of fatigue. Numerous mechanisms could be used to obtain *deflection controlled bending*. An example experimental set up is illustrated in Fig. 1. A wire specimen is mounted in a cantilevered support. The other end of the wire is oscillated transverse to its undeformed axis. When a wire of a particular diameter, d, material and microstructure, is displaced a constant distance, H, above and below the support centerline, the severity of bending is dependent only on the distance, L, from the fixed end of the wire to the moving end.
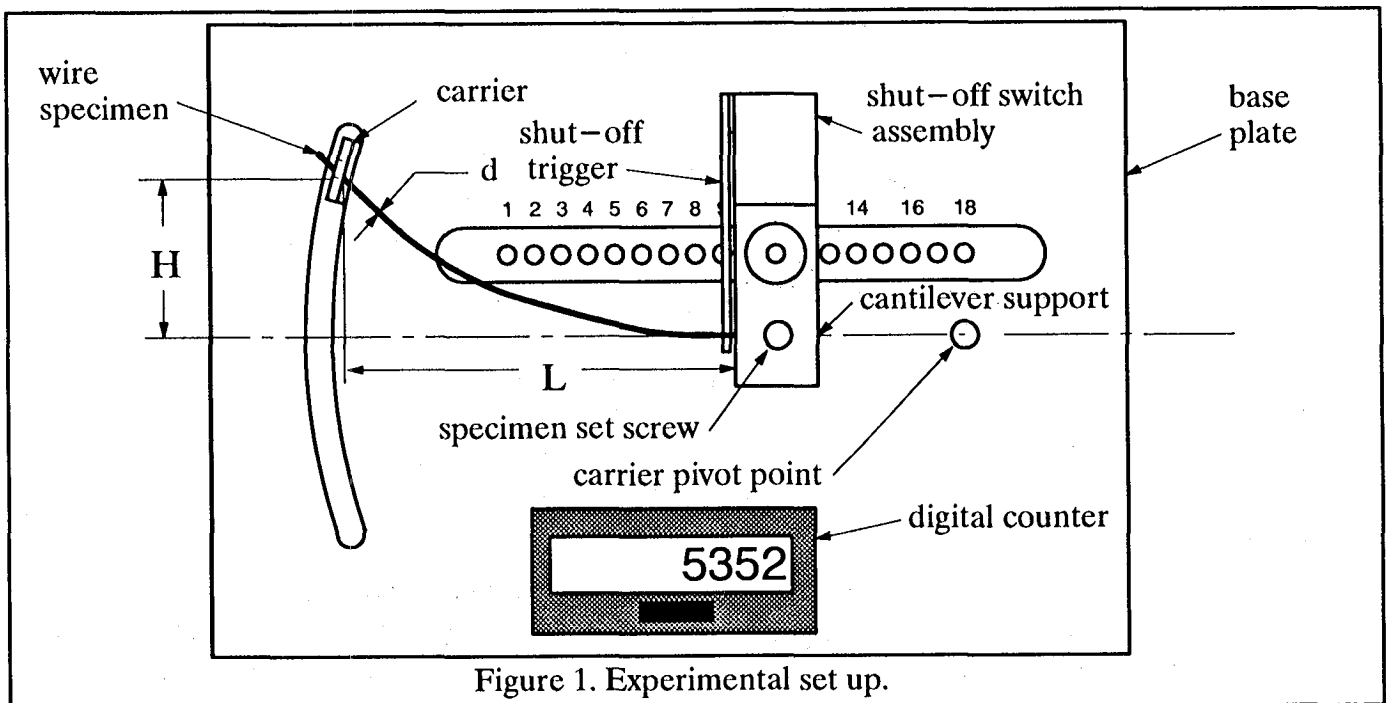

Figure 1. Experimental set up.

The carrier moves in an arcuate path, since it is fixed to the end of a pivoting member that oscillates underneath the support plate about a pivot point as shown in Fig. 1. An AC motor drives the pivoting member via a scotch yoke mechanism. The motor operates at 1550 RPM, but the speed of the carrier is reduced to about 600 RPM using a timing belt and pulleys. This reduction is necessary to reduce inertial effects.

When a wire is mounted in the cantilever support, a trigger is depressed and held in place by the wire specimen. The trigger holds closed a switch that completes a circuit to the motor, and serves as an automatic shut−off. Since the specimen always fails at the grip, the trigger is released upon specimen failure, cutting power to the motor.

Since specimen deformation and damage are confined to the grip area, the design of the grip fixture can significantly influence results. However, as long as a consistent gripping configuration is used from test to test, this effect is less important in comparing data sets. In the apparatus presented here, cylindrical brass inserts were fabricated with holes bored through their center corresponding to a clearance fit for wires of a particular gauge. A transverse set screw hole was drilled radially at the center of each insert to secure the specimen. Contact stresses between the specimen and insert at the failure site could be diminished if a tough polymeric material (e.g., nylon or polycarbonate) were used instead of brass. Figure 2 illustrates the specimen support and shut−off switch configuration.
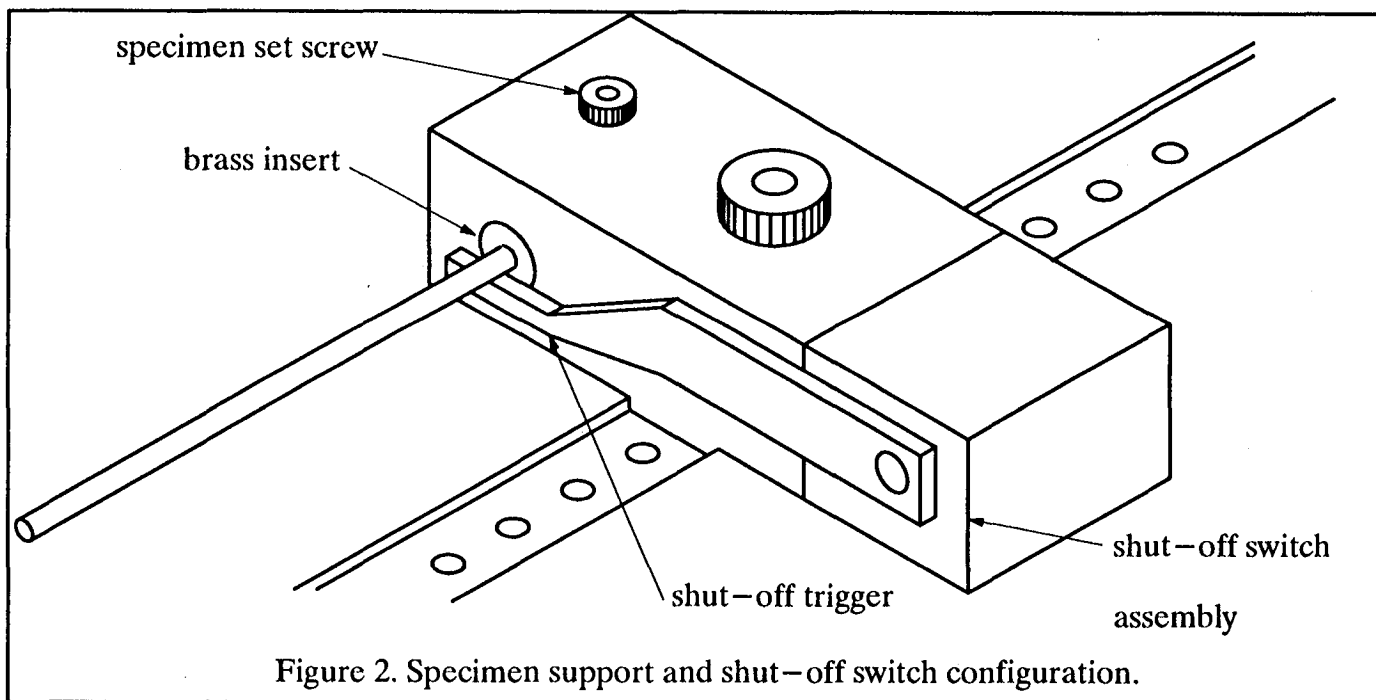
Figure 2. Specimen support and shut−off switch configuration.

A digital counter is used to record cycles. This electronic counter is battery operated and triggered by a magnetic reed switch. A magnet on the pivoting member closes the reed switch to record one count each cycle. A pushbutton reset is located on the front of the counter.

In order to correlate data from different diameter wires, a consistent damage parameter is required. For instance, in a conventional axial fatigue test or rotating−bending fatigue test, the stress amplitude is usually plotted versus fatigue life. However, deformations associated with conventional fatigue experiments are much smaller. Forces are controlled and therefore stresses are straightforwardly calcu-

lated. For the wire samples tested in this experiment, a more involved analysis is required to develop a stress or strain relation. This, in itself can provide an interesting aspect to the experiment for undergraduate or graduate level students.

INSTRUCTOR NOTES:

Fatigue is a complex subject. To convey fatigue concepts in the classroom, the subject is often oversimplified to the point where the methodology grasped by a student is too simple to be applicable to any serious fatigue problems. Experience is the best teacher when it comes to fatigue and a good way to gain experience is to conduct fatigue testing. However, the cost and time involved in generating meaningful, statistically sound fatigue data is usually prohibitive in a student laboratory setting. Rotating—bending tests make it possible to rack up cycles quickly, but even then specimens are not inexpensive or easy to obtain. Students usually generate one or a few points each, then blame scatter on the dubious nature of their lab partners. The majority of undergraduate students never gain the experience of generating and reducing their very own fatigue data set.

To make up for this, many students have been required to bend paper clips back and forth, by hand, controlling the degree of bending as closely as possible. In this way, crude but useful lessons can be learned about very low cycle fatigue. The experimental apparatus demonstrated in this experiment represents a refinement of the paper clip exercise.

The main difficulty with the apparatus is the complexity in characterizing the exact state of stress and strain at the failure site. However, this is overcome by the consistency between tests, by the repeatability of the data and by the extreme ease of "specimen preparation."

The embodiment of the miniature fatigue testing apparatus can take on any number of forms. With such an apparatus, a student can gain first—hand experience in fatigue testing and data reduction. A machine that is simple and safe to operate can be used for a wide range of experiments, from extremely simple in concept for underclassmen, to quite refined for graduate students.

SAMPLE DATA SHEETS:

A summary of potential experiments that could be undertaken with this apparatus is listed below:

- **Fatigue Damage Correlation Parameters:** As a wire is displaced back and forth in fully—reversed deflection, the state of stress—strain at the failure site fluctuates. It is possible to investigate several potential damage parameters to find the most suitable. For instance, for a given wire diameter, d, horizontal displacement, H and lateral position, L, approximate expressions can be derived for the stress amplitude, S_a, or strain amplitude, ε_a. Both of these have been used extensively to correlate fully reversed fatigue data. However the derivation of these expressions can be a formidable task. A simple approach is to plot elastically calculated stress amplitude,

$$S_a^e = \frac{3}{2} \frac{H \, d \, E}{L^2}$$

  (where E = the elastic modulus) versus life. Even though the value of this parameter usually greatly exceeds the yield stress of the material, the parameter is likely

to provide a relative measure of the bending strain amplitude at the failure site. To refine the analysis, data from tests conducted on wire of identical material, but varying diameter would be extremely useful. Some factors that could be considered are: *Plastic Hinging* (larger diameter wire or higher amplitude deflections can result in the formation of a plastic hinge at the grip), *Dynamic Effects* (the inertia of the moving wire can add to the stress–strain at the support point), *Contact Stresses* (these could be reduced if a tough polymeric material were used for the specimen mounting insert) and *Overall Machine Geometry* (such as the carrier arc radius and the width of the opening in the carrier).

- **Effect of Microstructure on Fatigue Life:** Wire samples could be prepared by applying varying heat treatments to initially identical material. Figure 3 depicts data for 1090 steel music wire in three heat treat conditions. These data are correlated using elastically calculated bending stresses (just discussed). (The data were generated by a freshman student in one afternoon.)

Figure 3. Data from 1090 steel wire in three different heat treat conditions. These data were generated using a hand powered prototype in one afternoon by a freshman student.
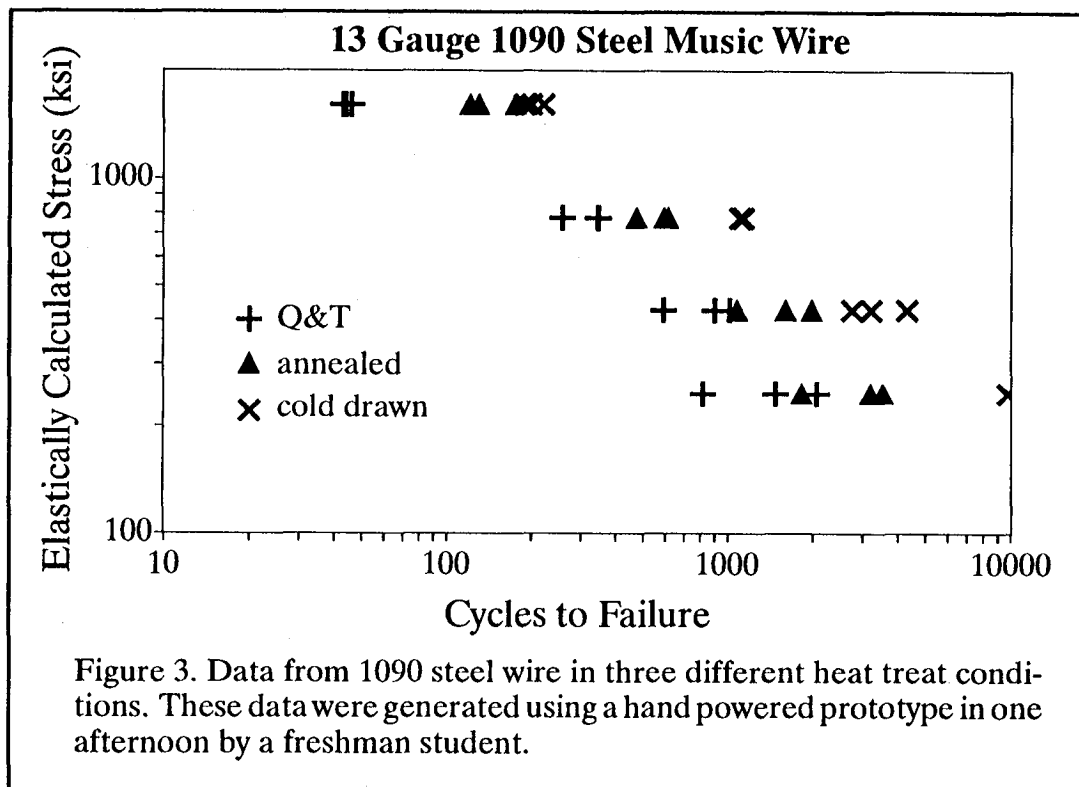
Another example would be to quench sets of steel wire samples, then temper at varying times or temperatures to produce a range of microstructures/hardnesses. For comparison, an additional set could be austempered. Microhardness tests could be used to find the hardness of each set. The question could then be addressed: Do the data from austempered samples correlate with the data from tempered martensite samples at similar hardness?

- **Relative Fatigue Behavior of Different Materials:** Wire made from several materials (steel, aluminum, copper and brass) can be obtained from any hardware store. Music wire also is readily available.

- **Cumulative Damage in Variable Amplitude Block Loading:** A small set of constant amplitude baseline fatigue data could be generated, for instance, by testing several samples each at two different bending deflections (corresponding to two different hole settings in Fig. 1). The most severe deflection would cause samples to fail at a mean life of $\overline{N}_1$, while the less severe setting would result in a longer mean life of $\overline{N}_2$. Variable amplitude block loading could then be generated at follows: at the most severe deflection, use the machine to apply $\overline{N}_1/2$ cycles to a new specimen. Next, change to the less severe hole setting and run until failure. Miner's rule would predict the wire to break in $\overline{N}_2/2$ cycles, but how well does the rule work for this *high—low block loading* sequence? The procedure should be repeated several times, then reversed by applying the less severe bending first, followed by the more severe loading (a *low—high block loading* sequence). It has been demonstrated that high—low block loading has been found to be more severe than low—high load blocks [1,2]. To demonstrate this experiment, consider the baseline data for dark annealed wire (purchased at a hardware store) as presented in Fig. 4.

Figure 4. Data from 19 gauge dark annealed wire. There are four data points per load level.
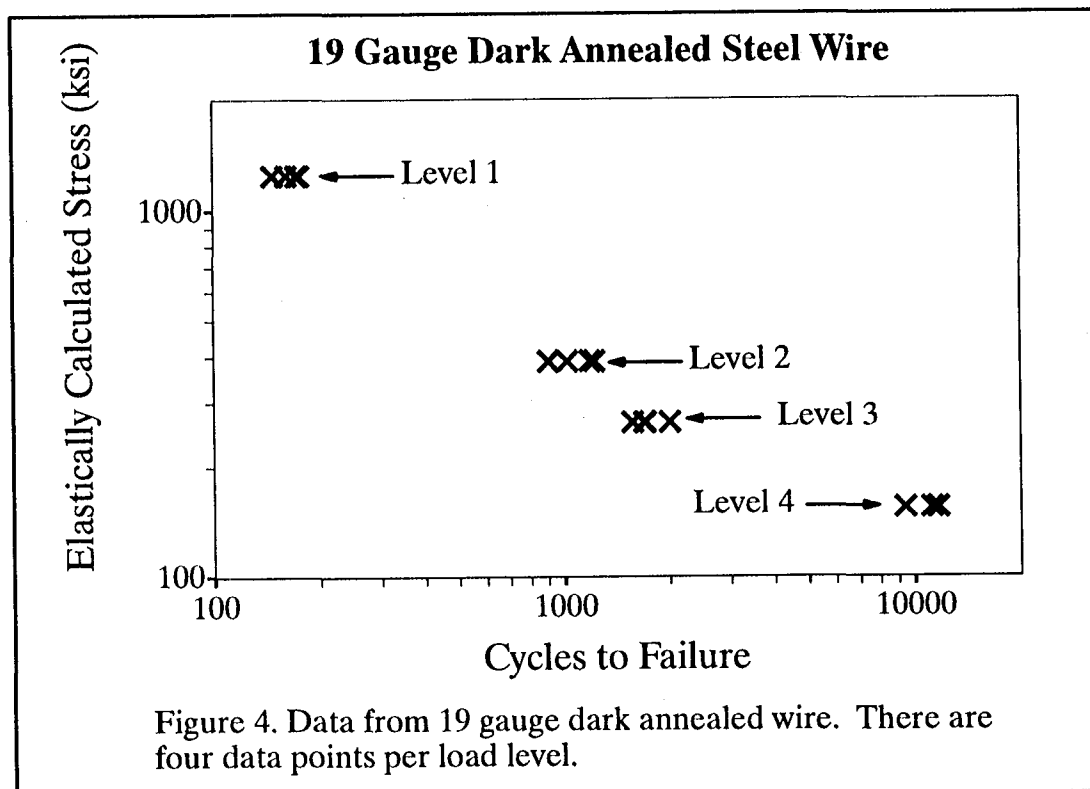
In addition to this baseline data, additional block loading tests were run as summarized in table 1 on the next page:

Table 1 – Block Loading Test Data 19 Gauge Dark Annealed Steel Wire	
Level 2 Mean Life, $\bar{N}_2$ = 1,080 cycles ($\bar{N}_2/2$=540 cycles) Level 4 Mean Life, $\bar{N}_4$ = 10,945 cycles ($\bar{N}_4/2$=5472 cycles)	
HIGH–LOW BLOCK: Apply 540 cycles at Level 2 Next: Apply loading at Level 4 Leads to failure in: 3640 cycles 3942 cycles 3394 cycles	**LOW–HIGH BLOCK:** Apply 5472 cycles at Level 4 Next: Apply loading at Level 2 Leads to failure in: 422 cycles 389 cycles 252 cycles

In the high–low tests, the mean number of less severe (level 4) cycles following the 540 applications of level 2 loading is 3658 cycles. This represents a cycle fraction of 0.336, considerably less than the 0.5 cycle fraction predicted by Miner's rule (which corresponds to a predicted remaining life of 5472 cycles). A similar result is demonstrated by the low–high blocks. Loading at level 2 following 5472 cycles of level 4 loading, the mean life was 357 cycles (a cycle fraction of .328).

This test could be repeated with different cycle ratios and between different load levels to demonstrate sequence effects on cumulative fatigue damage.

Any of the assignments just presented could be supplemented with the following tasks or follow–up experiments:

- **Correlation of Fatigue Strength with Tensile Strength:** Wire could be tested in an axial testing machine. Strength, ductility and microhardness could be compared with a material's fatigue behavior.

- **Fractography:** Fracture surfaces from an *entire set* of specimens can be mounted on a single stage for examination under a light microscope or a scanning electron microscope.

- **Statistical Reduction of Fatigue Data:** The ASTM Book of Standards, Volume 03.01 (Metals Test Methods and Analytical Procedures) contains several standard practices pertaining to the analysis and presentation of fatigue data. Among these are:

E 468–90, "Presentation of Constant Amplitude Fatigue Test Results for Metallic Materials" and

E 739–91, "Statistical Analysis of Linear or Linearized Stress–Life (S–N) and Strain Life (ε–N) Fatigue Data."

Students could gain valuable, first hand experience in the applications of these standards.
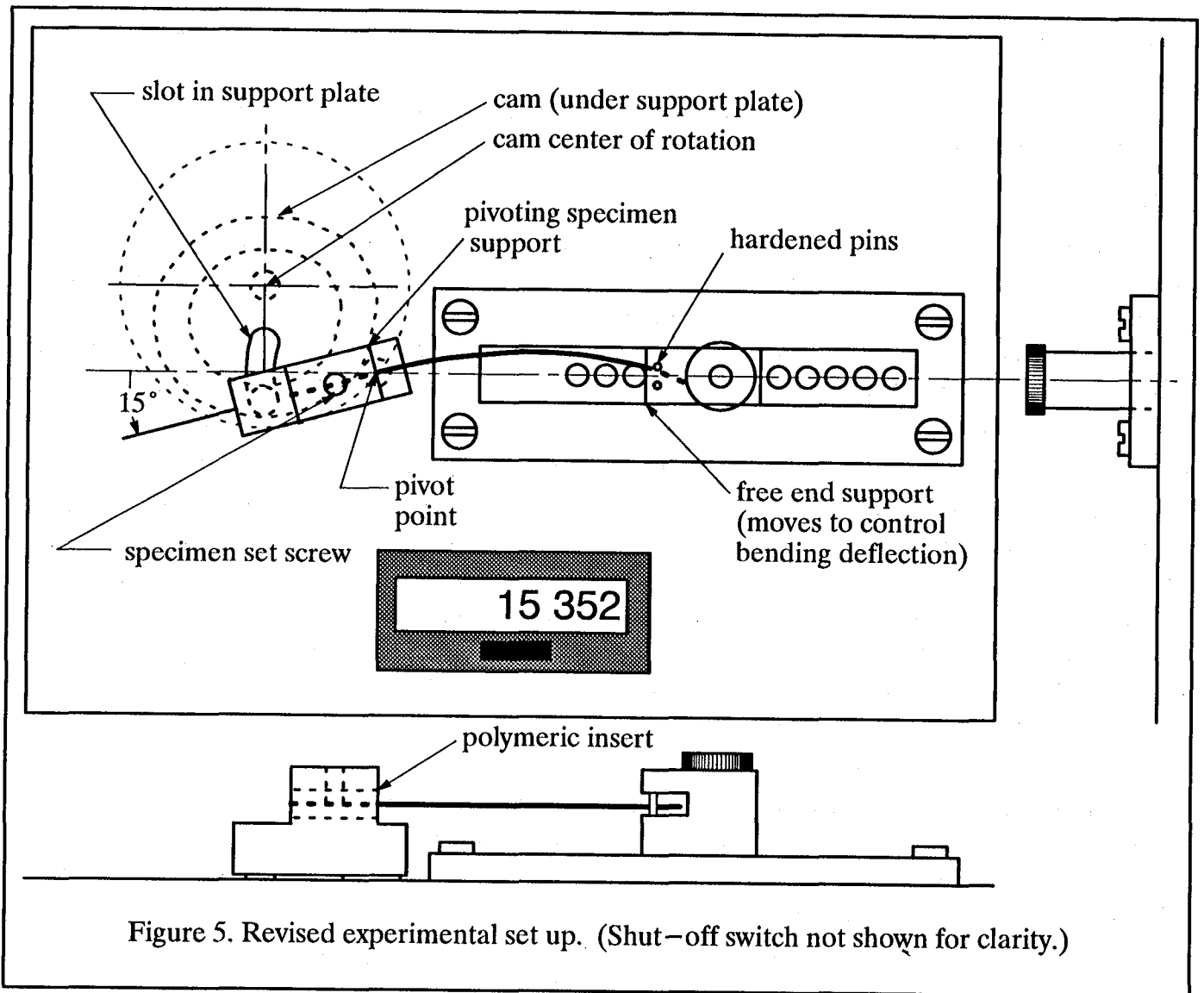
REFERENCES:

1. Fuchs, H.O. and Stephens, R.I., *Metal Fatigue in Engineering*, John Wiley and Sons, New York, N.Y., 1980.

2. Mitchell, M.R., "Fundamentals of Modern Fatigue Analysis for Design," *Fatigue and Microstructure*, Society of Automotive Engineers, 1977, pp. 385–437.

SOURCES OF SUPPLY:

An experimental set up like the one depicted in this paper can require a considerable amount of development time. For instance, safety must be considered since the carrier can do damage if encountered by the operator. Electrical switches and wiring must be isolated and well grounded. For a fully enclosed apparatus, the heat generated by an electric motor must be accounted for, since the machine can conceivably run for long periods of time. The development of such an apparatus could make an excellent student design project.

The earliest version of this machine to be investigated by the author was powered by a hand–cranked fishing reel. This was followed by a prototype similar to the one presented in this paper, powered by an electric motor. Although the results were useful, the prototype revealed two main difficulties that must be addressed. First, the AC motor (1/25 hp) used for the device develops a great deal of heat and would not be suitable for long term testing in an enclosed device. Second, the scotch yoke mechanism utilized to oscillate the carrier moves more quickly one direction than the other. This leads to uneven inertial loading on specimens. How to achieve fully harmonic oscillation, with minimal inertial loading on the motor, is not as trivial a design problem as it first appears.

A refined, more portable version is currently being designed and is depicted in Fig. 5. The new machine is to be mounted in a carrying case with a transparent lid. A fan is included for cooling the motor and a new mechanism is incorporated to provide uniform, harmonic oscillation. The mechanism is a cam that drives a follower mounted to the wire cantilever support. This oscillates the wire support while fixing the free end of the wire between two ground and hardened pins (as opposed to moving the free end, as in Fig. 1). The harmonic oscillation ensures that inertial loading on specimens is the same in both directions. The new mechanism further reduces dynamic effects on sample loading by decreasing the overall motion of the wire samples. Furthermore, vibration of the machine itself is reduced since the moving parts are smaller and oscillate over a much smaller amplitude. For safety sake, the closing of the lid activates a switch that sets the machine into operation. The machine is inexpensive enough that a number of them could be obtained for considerably less than the cost of a single rotating–bending machine. Students can utilize the machine in a laboratory or could check the machines out for use in their rooms.

Figure 5. Revised experimental set up. (Shut–off switch not shown for clarity.)

The figure labels include: slot in support plate, cam (under support plate), cam center of rotation, pivoting specimen support, hardened pins, 15°, pivot point, specimen set screw, free end support (moves to control bending deflection), polymeric insert. Display reads: 15 352.

INTRODUCTION TO HIGH PERFORMANCE COMPOSITES

Norman J. Johnston

National Aeronautics & Space Administration
Langley Research Center
MA-226
Hampton, Virginia

Telephone 804-864-4260

INTRODUCTION TO HIGH PERFORMANCE COMPOSITES

Norman J. Johnston
NASA Langley Research Center
Mail Stop 226
Hampton, Virginia 23681

ABSTRACT

THE TALK WILL ADDRESS THE FOLLOWING QUESTIONS:
- WHAT ARE HIGH PERFORMANCE COMPOSITES?
- HOW ARE THEY USED TODAY? (i.e., WHY ARE THEY IMPORTANT TO YOU AS USERS AND AS TEACHERS?)
- WHAT ARE THEIR PROPERTIES?
- HOW DO YOU MAKE THEM?
- WHAT ARE THE FUTURE TECHNOLOGY NEEDS FOR COMPOSITES? (i.e., WHY SHOULD YOU TEACH STUDENTS THIS TECHNOLOGY?)

IN ADDTION, SAMPLES OF COMPOSITE REINFORCEMENTS SUCH AS GLASS, CARBON AND KEVLAR FIBERS, MATRIX MATERIALS AND FABRICATED COMPOSITE PARTS WILL BE DEMONSTRATED AND MADE AVAILABLE.

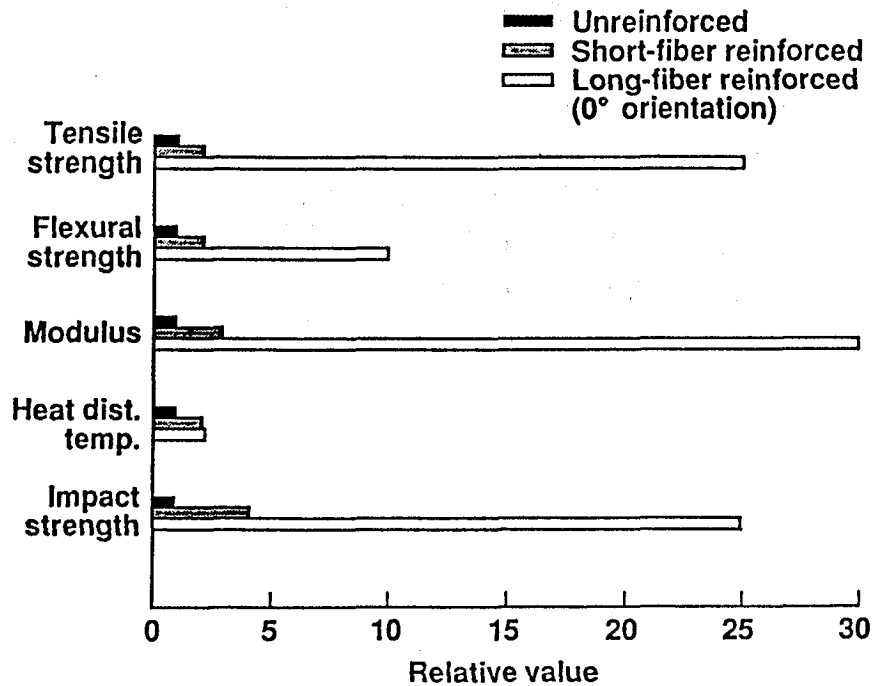# STRUCTURAL BUILDING MATERIALS

HISTORICAL PERSPECTIVE

WOOD

STONE

ICE

CLAY/CERAMIC

METAL

SYNTHETIC POLYMERS

COMPOSITES

NOMINAL RELATIVE PROPERTIES OF THERMOPLASTIC MATERIALS

Legend:
- Unreinforced
- Short-fiber reinforced
- Long-fiber reinforced (0° orientation)

Bar chart, horizontal axis "Relative value" (0 to 30):
- Tensile strength
- Flexural strength
- Modulus
- Heat dist. temp.
- Impact strength

POLYMERIC COMPOSITE MATERIALS

Reinforcement

Glass
Boron
Graphite
Kevlar

Matrix

Epoxy
Bismaleimide
Polyimide

Pre-impregnated tape

Fiber

Matrix

Laminated structure

Improvements

Strength Stiffness Weight Cost

COMPOSITES

FILAMENTS

MATRICES

GLASS

GRAPHITE

KEVLAR

BORON

GRAPHITE-EPOXY

EPOXY

POLYIMIDE

ALUMINUM
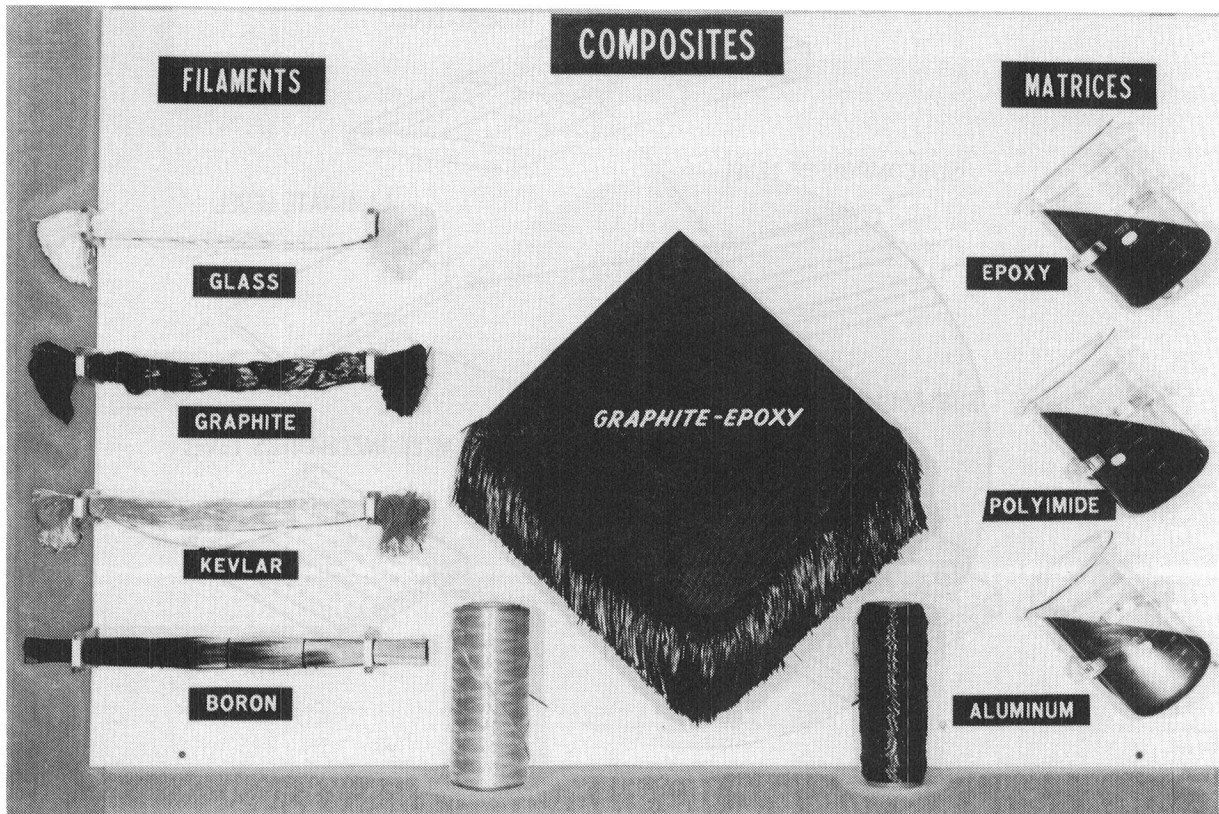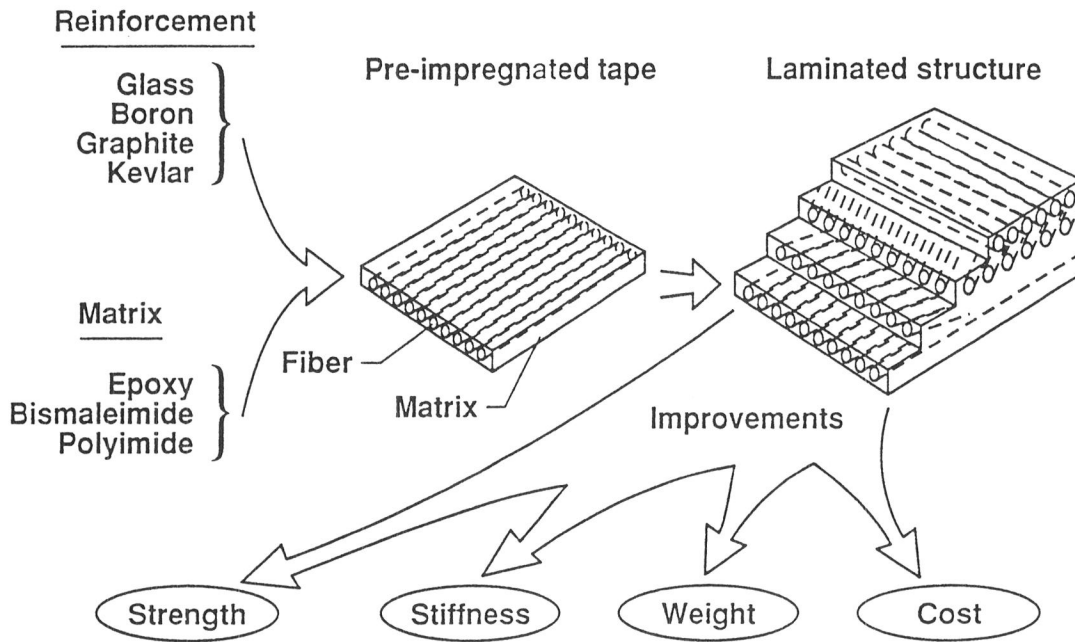
ROLE OF FIBER

- CARRIES IN-PLANE LOADS: PROVIDES STIFFNESS AND STRENGTH

- REDUCES THERMAL COEFFICIENT OF EXPANSION

ROLE OF MATRIX

- BONDS AND HOLDS FILAMENTS IN PLACE

- PROTECTS FILAMENTS

- PROVIDES TRANSVERSE STRENGTH

- ACTS AS A LOAD TRANSFER MEDIUM

- PROVIDES INTERLAMINAR TOUGHNESS

- PROVIDES DURABILITY

SOME DIFFERENT STRUCTURAL LEVELS FOR COMPOSITES

152
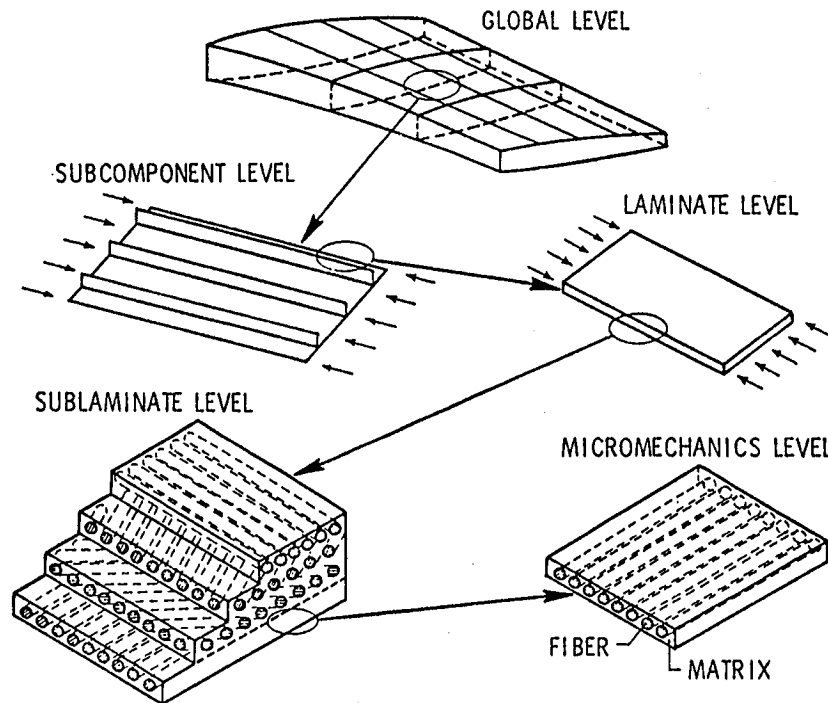
POTENTIAL BENEFITS OF COMPOSITES

<u>SUPERIOR TO METALS</u>
- DESIGN FLEXIBILITY
- CORROSION RESISTANCE
- HIGH SPECIFIC STRENGTH/STIFFNESS
- LOW THERMAL EXPANSION
- HIGH FATIGUE RESISTANCE

<u>UNPROVEN POTENTIAL</u>
- LOWER COMPONENT COSTS
  - o FABRICATION COSTS
  - o QUALITY ASSURANCE COSTS
  - o BUY-TO-FLY RATIO

- DAMAGE TOLERANCE
  - o COMPRESSION AFTER IMPACT
  - o OPEN HOLE STRENGTH
  - o FRACTURE TOUGHNESS

- REPAIR/MAINTENANCE

- RELIABILITY

OUTLINE

- WHAT ARE HIGH PERFORMANCE COMPOSITES?

- HOW ARE THEY USED TODAY? (i.e., WHY ARE THEY IMPORTANT TO YOU AS USERS AND AS TEACHERS?)

- WHAT ARE THEIR PROPERTIES?

- HOW DO YOU MAKE THEM?

- WHAT ARE THE FUTURE TECHNOLOGY NEEDS FOR COMPOSITES? (i.e., WHY SHOULD YOU TEACH STUDENTS THIS TECHNOLOGY?)

APPLICATIONS FOR CARBON FIBER REINFORCED COMPOSITES

Airframe Components
- Lightly-Loaded Structure
  - Control Surfaces
  - Fairings
  - Doors
- Heavily-Loaded Structure
  - Wing
  - Fuselage
- Engine Components

- Empennage (Horizontal and Vertical Stabilizers)
- Floor Panels

- Helicopter Blades

Missiles
- Fins, Tubes

Sporting Goods
- Fishing Rods and Boxes
- Tennis Rackets

- Golf Club Shafts

Recreational Boats
- Hulls

- Masts

APPLICATIONS FOR CARBON FIBER REINFORCED COMPOSITES

Automotive
- Drive Shafts
- Frames

- Small Engine Components (pistons rods, etc.)
- Leaf Springs

Industrial
- Pressure Vessels
- Housings, Covers
- Piping and Ducting Components

- Offshore Drilling Platforms and Cables
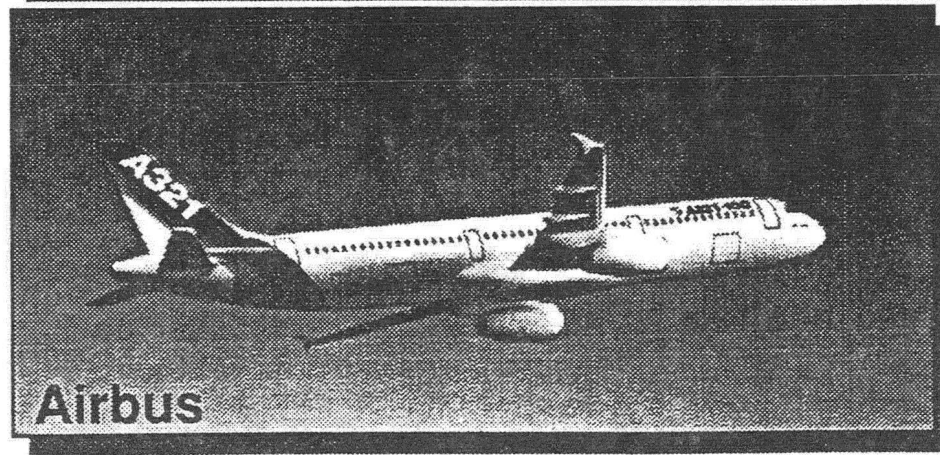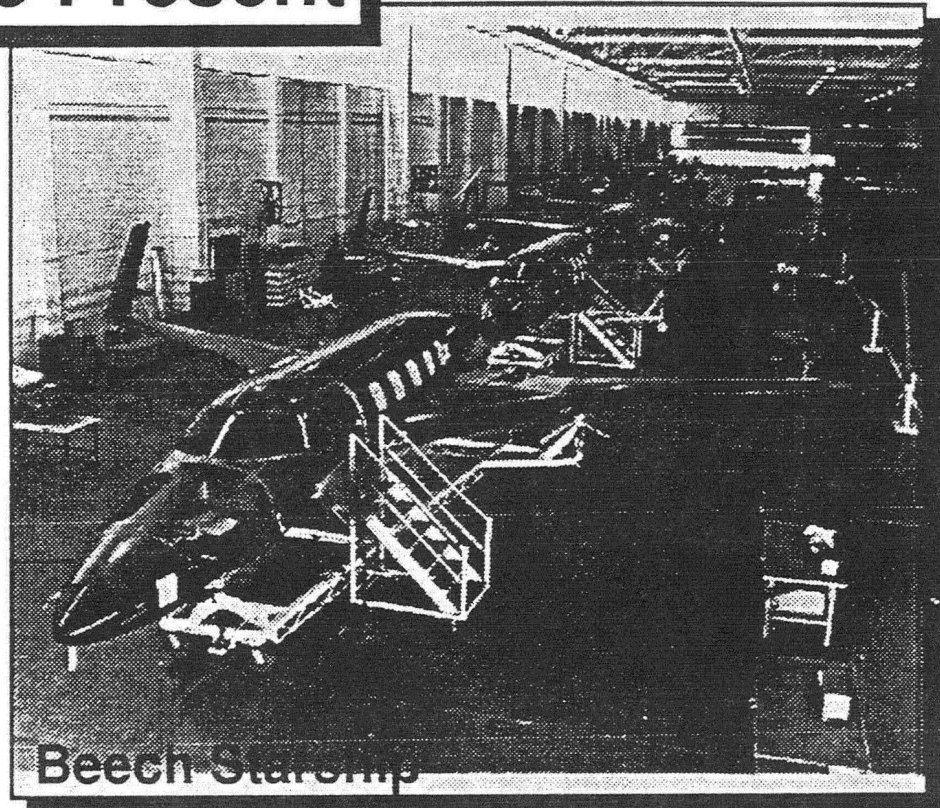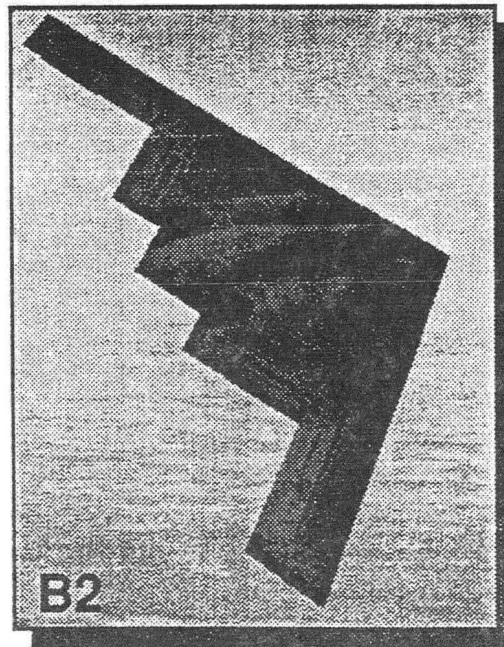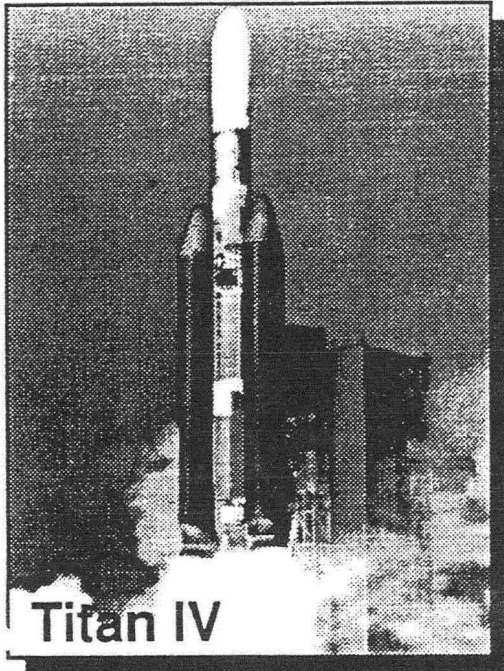- Downhole Drilling Equipment

Submarines
- Hulls

- Dry Deck Shelter

Ordnance
- Shelters
- Weapons

- Personnel and Vehicle Armor
- Bridging and Portable Structures

154

The Present

Primary Structures

Titan IV

B2

Beech Starship

Airbus
A321

Composite Components

737

Elevator

150-lb weight savings per airplane
(26% weight savings)

727

Stabilizer (NASA)

116-lb weight savings per airplane
(22% weight savings)
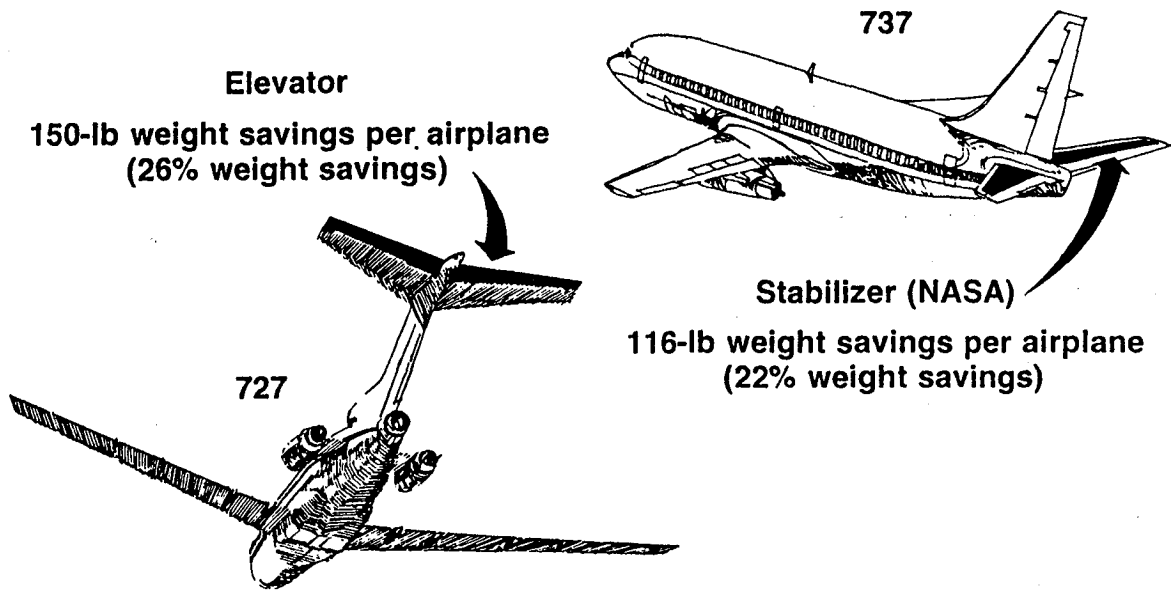
AIRCRAFT ENERGY EFFICIENCY (ACEE)
COMPOSITE PRIMARY AIRCRAFT STRUCTURES

TRANSPORT SECONDARY COMPONENTS

DOUGLAS DC-10 UPPER AFT RUDDERS

L-1011 COMPOSITE GROUND TEST AILERON

727 GRAPHITE-EPOXY ELEVATORS
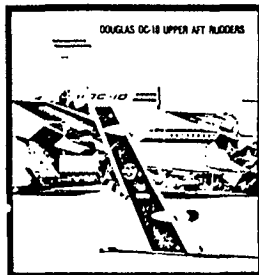
26.4% WEIGHT SAVED	23.6% WEIGHT SAVED	24.6% WEIGHT SAVED
12 UNITS IN FLIGHT SERVICE	8 UNITS IN FLIGHT SERVICE	10 UNITS IN FLIGHT SERVICE
SIZE: 3.2' X 13.2'	SIZE: 4.2' X 7.7'	SIZE: 3.4' X 17.4'
WEIGHT: 67#	WEIGHT: 107#	WEIGHT: 98#

AIRCRAFT ENERGY EFFICIENCY (ACEE) COMPOSITE PRIMARY AIRCRAFT STRUCTURES

TRANSPORT MEDIUM PRIMARY COMPONENTS
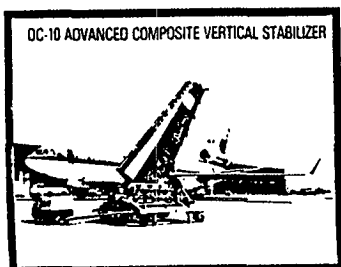
SIZE: 7' X 23'
WEIGHT: 780*
WEIGHT SAVED: 22.6%

SIZE: 9' X 25'
WEIGHT: 620*
WEIGHT SAVED: 28.4%
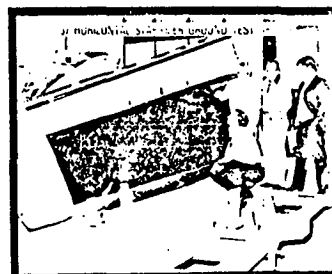
SIZE: 4' X 17'
WEIGHT: 204*
WEIGHT SAVED: 22.1%

BOEING 767 COMPOSITE STRUCTURE APPLICATIONS

HYBRID COMPOSITE (KEVLAR/GRAPHITE)
GRAPHITE COMPOSITE

STABILIZER TIPS
RUDDER
FIXED T. E. PANELS
ELEVATORS
SEAL PLATES
FIXED T. E. PANELS
SPOILERS
INBOARD AILERONS
WING TO BODY FAIRING
OUTBOARD AILERONS
NOSE LANDING GEAR DOORS
MAIN LANDING GEAR DOORS (BODY)
COWL COMPONENTS
LEADING EDGE ACCESS DOORS
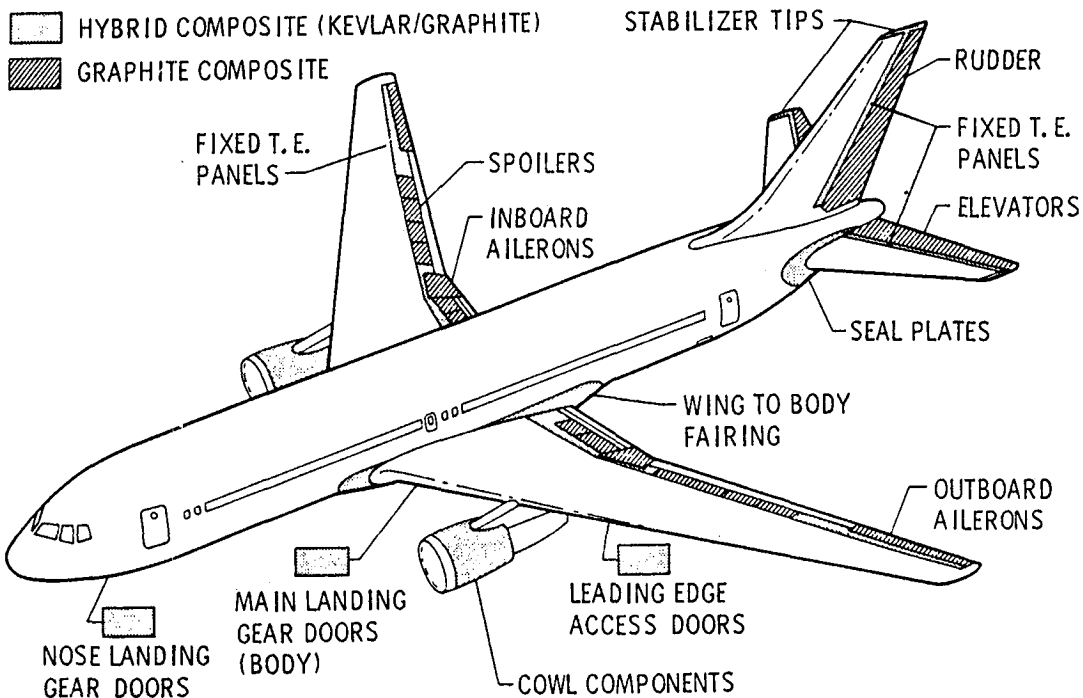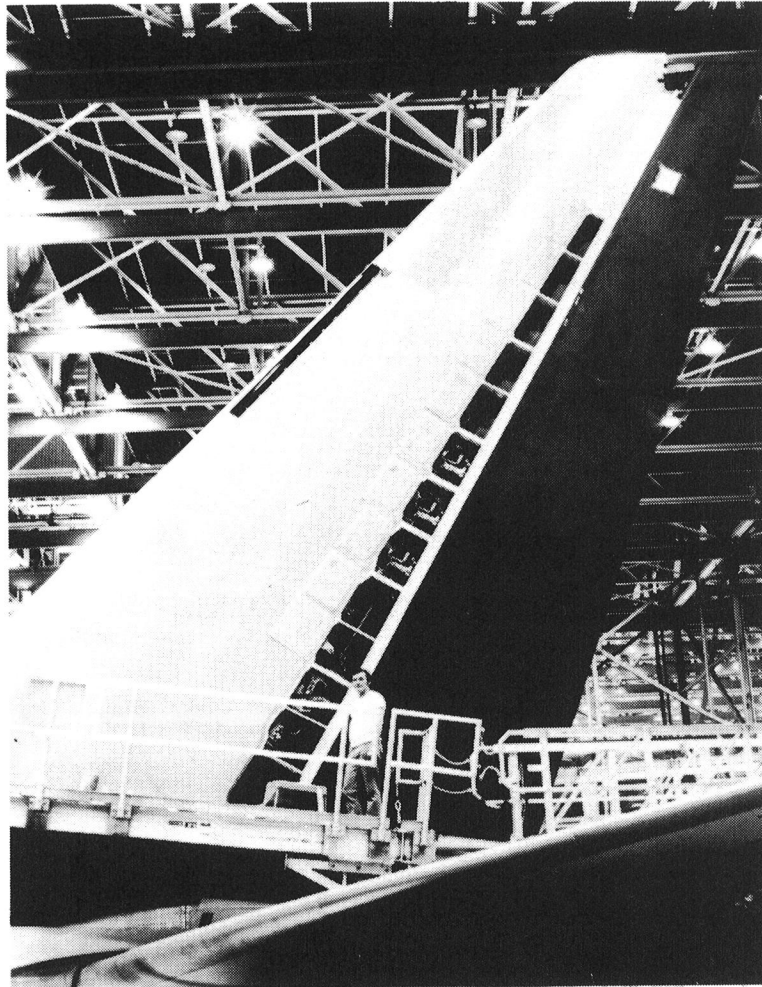
Advanced Composite Structural Applications Are Continually Expanding

ATF
40% of Structure
- Fuselage Substructure
- Inlet Structure
- Integral Tankage
- Bulkheads
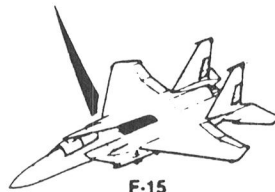
F-15
2% of Structure
- Secondary Structure
- Empennage Applications
- Full Depth Honeycomb
- Co-Cured Assembly
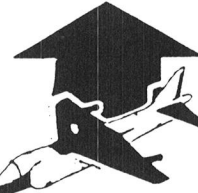
AV-8B
27% of Structure
- Wing Substructure
- Fuselage Applications
- Integral Stiffeners
- Strakes

F-18
10% of Structure
- Primary Structure
- Wing Applications
- Monolithic Laminates
- Bolted Assemblies
- Sandwich Panel Skins

A GLIMPSE OF THE FUTURE
- F-22 STEALTH FIGHTER -

Materials Development Critical To Successful HSCT Design

WASHINGTON

At cruise, a high-speed civil transport would experience skin temperatures from 200-400F, requiring advanced materials that are thermally stable at those levels. Pratt & Whitney and General Electric are cooperating to develop advanced alloys and castings for the aircraft's engines, which pose their own unique materials challenges.

Douglas Mach 2.4 Baseline Design

■ Titanium sandwich
▨ Composite sandwich
□ Composite stiffened sheet
■ Other
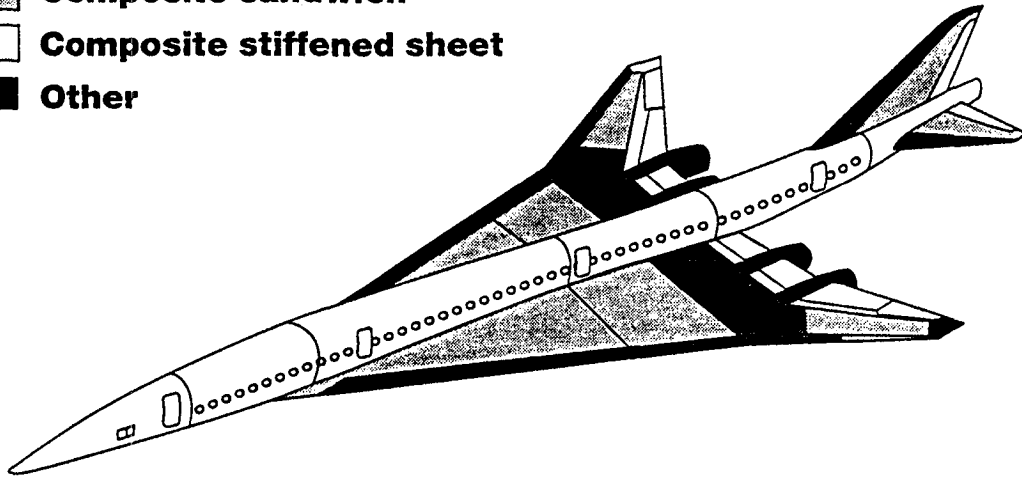
COMPOSITE STRUCTURE WEIGHT SAVING POTENTIAL

19%
5%

33%
38%

40%
6%

WEIGHT SAVINGS

PERCENT BASELINE STRUCTURAL WEIGHT

27%
4%

21%
33%

13%
14%

TOTAL
26%
SAVINGS
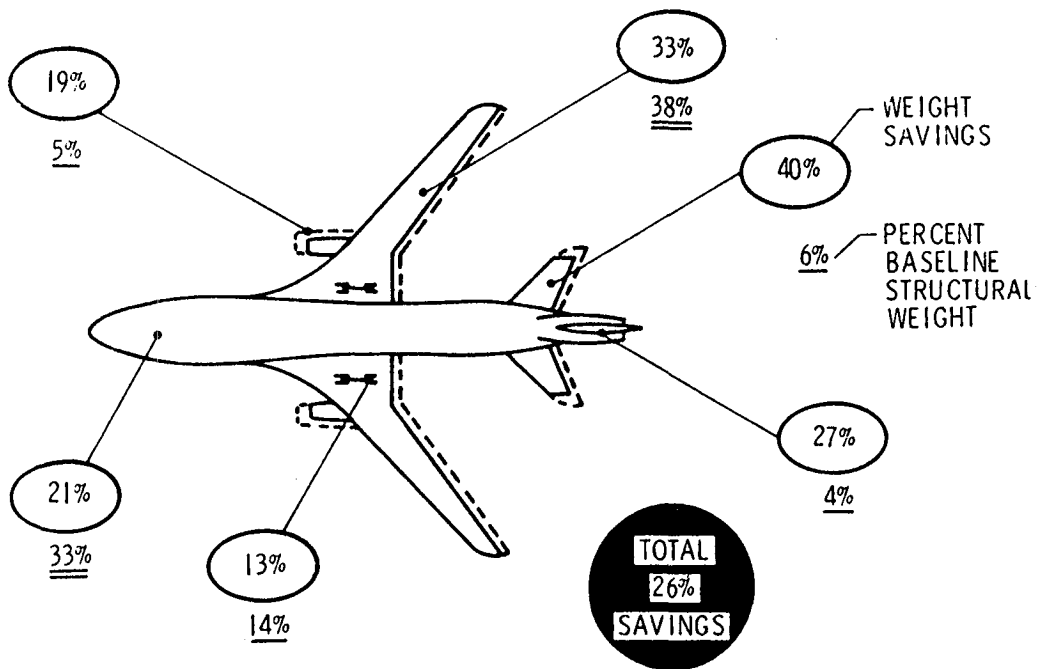
PERCENT WEIGHT SAVINGS IN TRANSPORT WINGS
BY 1990-1995

1980

2nd generation composite

32%

1st generation composite

22%

Advanced metals

10%

Δ 10% equals 25M gallons fuel per year*
*Assume 200 airplane fleet,
200 passengers per airplane,
1000 N. mi. flights

0   10   20   30   40

Weight savings, %
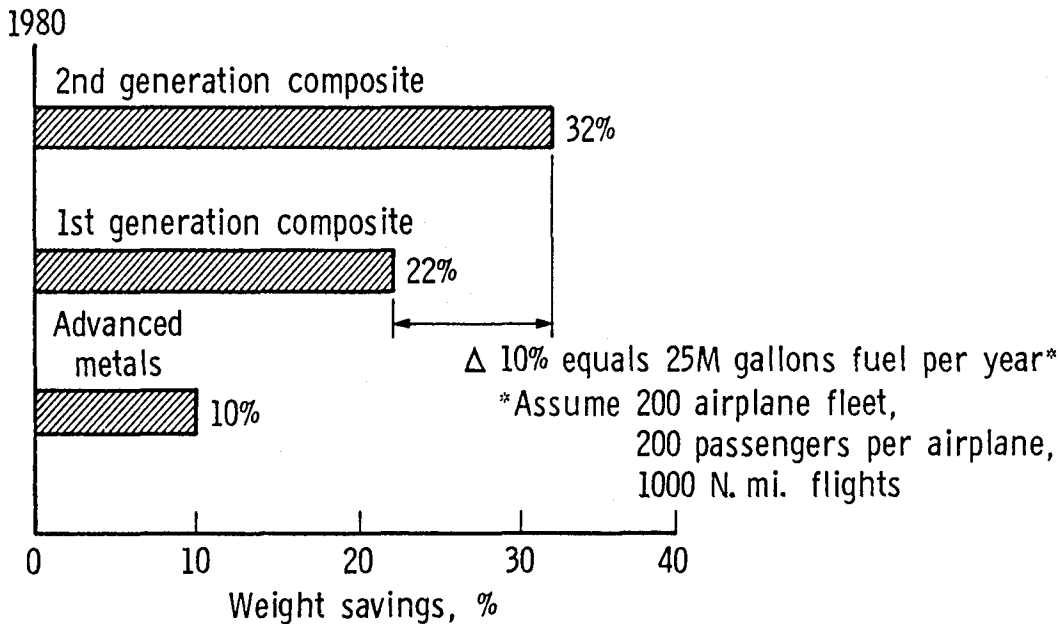
SUBSONIC TRANSPORTS
-COMPOSITES RATIONALE-

- 1990's Subsonic Commercial and Military Aircraft World Market is Projected to be > $200 Billion.

- Subsonic Aircraft Sector Contributes to U. S. Industrial Technology and National Security Base Comprising Over 15,000 Industrial Firms.

- Subsonic Aircraft Industry is Important to U. S. Economy, Accounting for Largest Positive Contribution of Any Manufactured Goods to Our Balance of Trade.

- U. S. Dominance Has Declined Dramatically in Recent Years.

- New Technology Can Triple the Fuel Economy of Today's Best Aircraft and Provide Substantially More Cost Effective Operation.

TRANSPORT AIRCRAFT COMPOSITE WING STRUCTURES
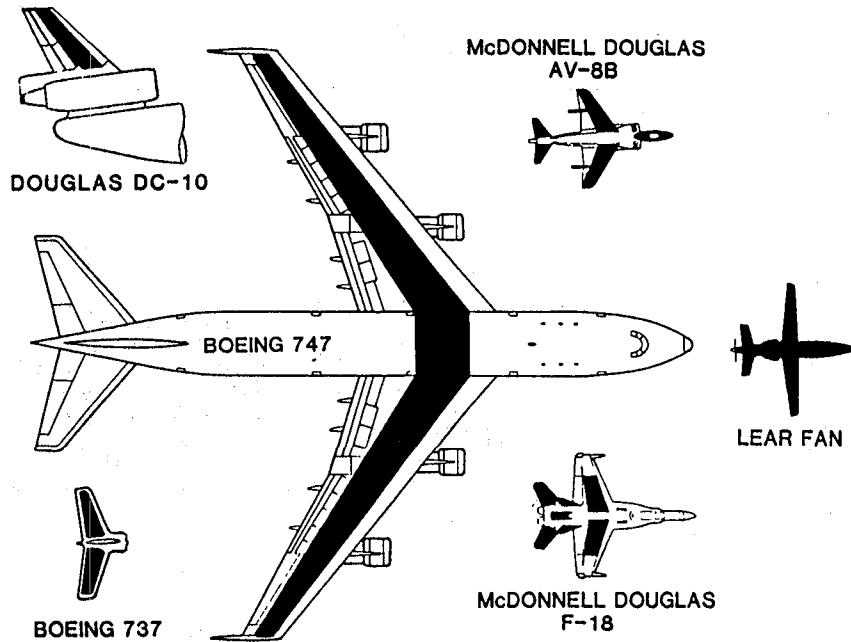
POTENTIAL WEIGHT SAVINGS TREND FOR FUTURE STRUCTURAL MATERIALS
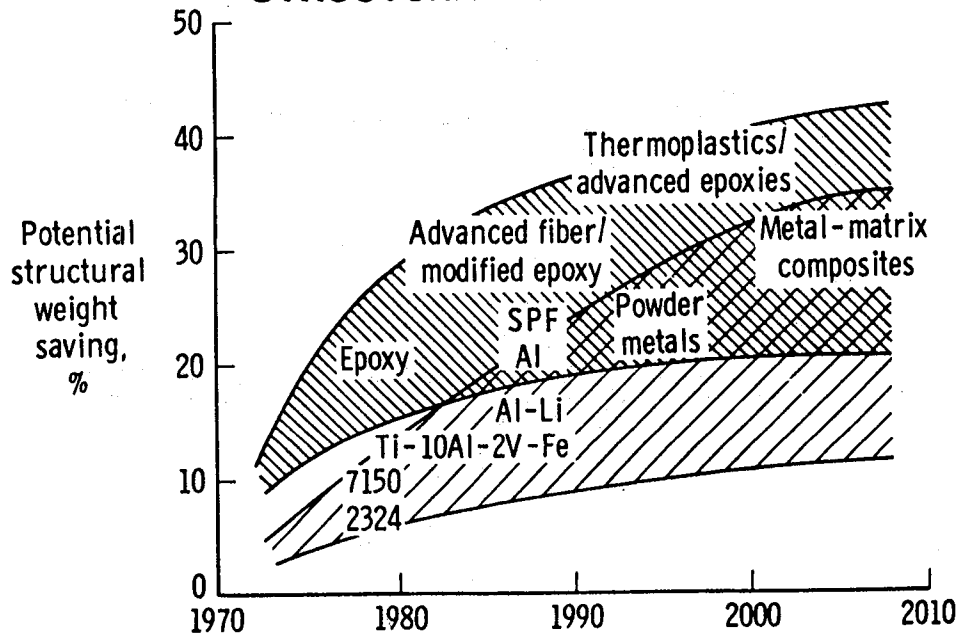
SCHEMATIC REPRESENTATION OF A PRINTED CIRCUIT BOARD

COPPER

BLIND OR BURIED VIA

DRILLED THRU HOLE

RESIN/ REINFORCEMENT

TOP VIEW

CROSS SECTION

Graphite Reinforced Tennis Racquets
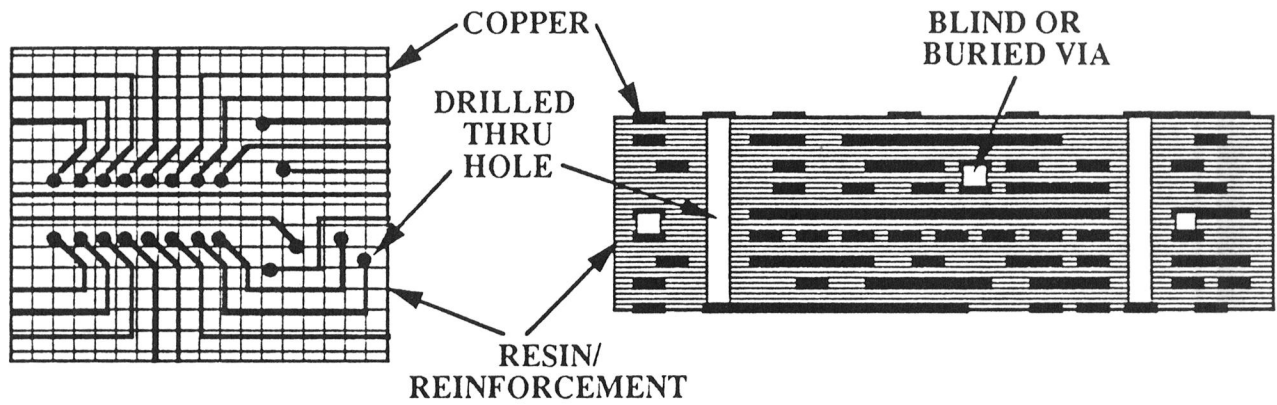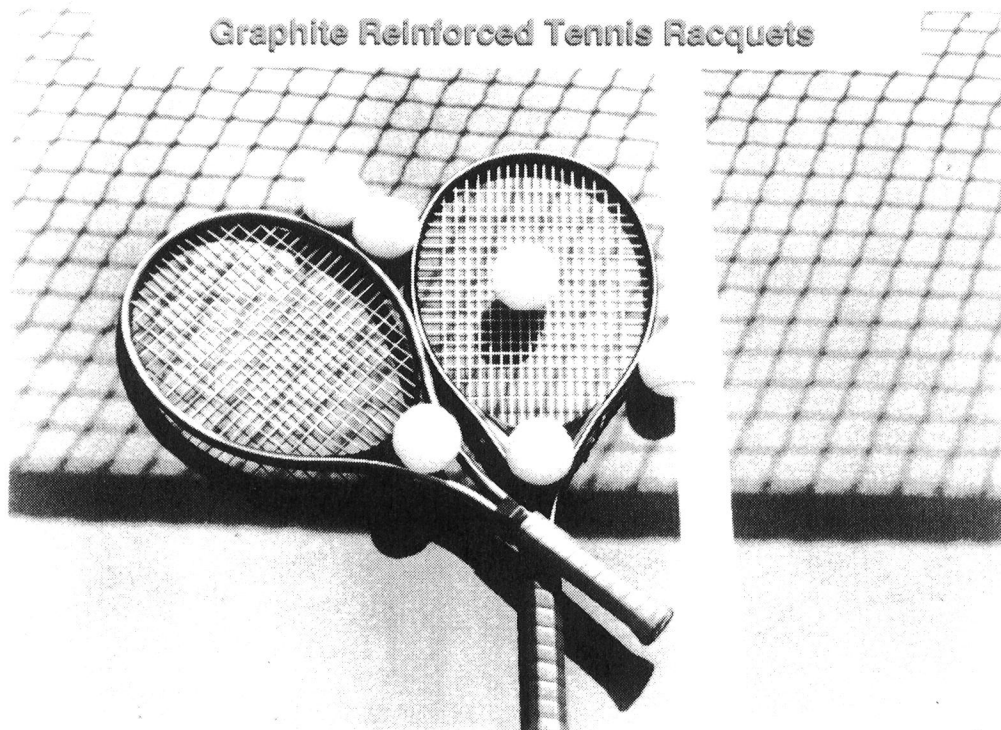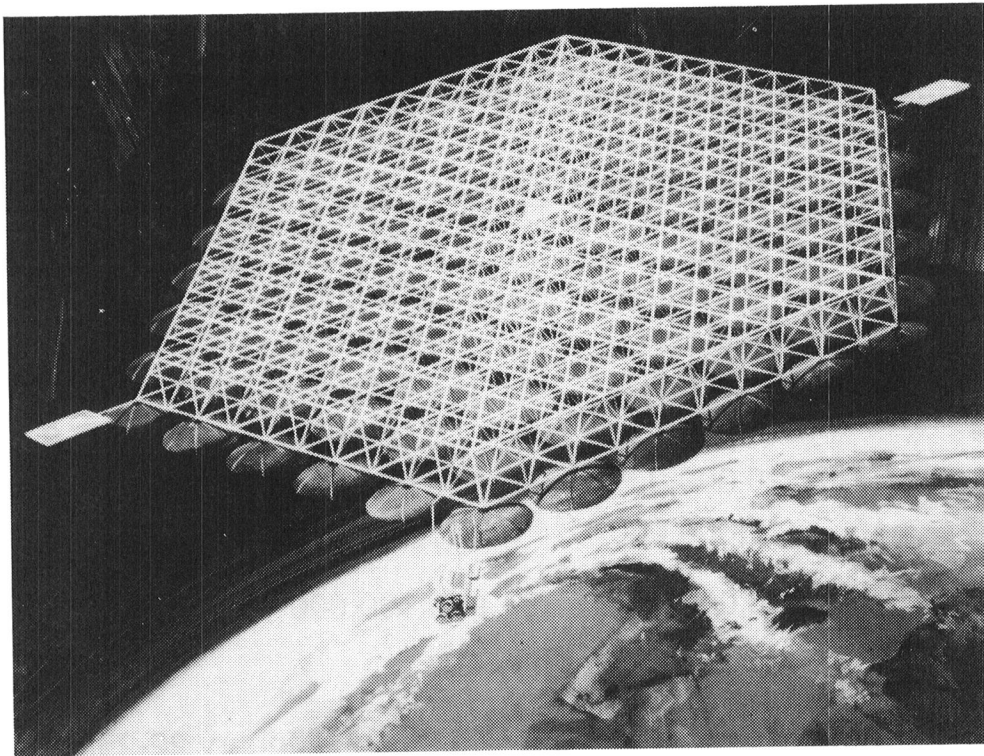
ADVANCED POLYMER COMPOSITES
- Kline Report, 1988 -

* Aerospace:
Commercial
Industry/NASA

Education/
Research
Universities

Recreational
1.0 M lb, $61 M
Industry

* Aerospace:
Military
DoD/NASA

U.S.
National
Composites
Program

11 M lb
$950 M } 1987

Industrial
3.2 M lb, $215 M
Industry

(* Aerospace
5.5 M lb, $586 M)

Automotive
0.3 M lb, $15 M
Industry

* Space
Structures
DoD/Industry/
NASA

Other
1.2 M lb, $72 M
DoD/Industry
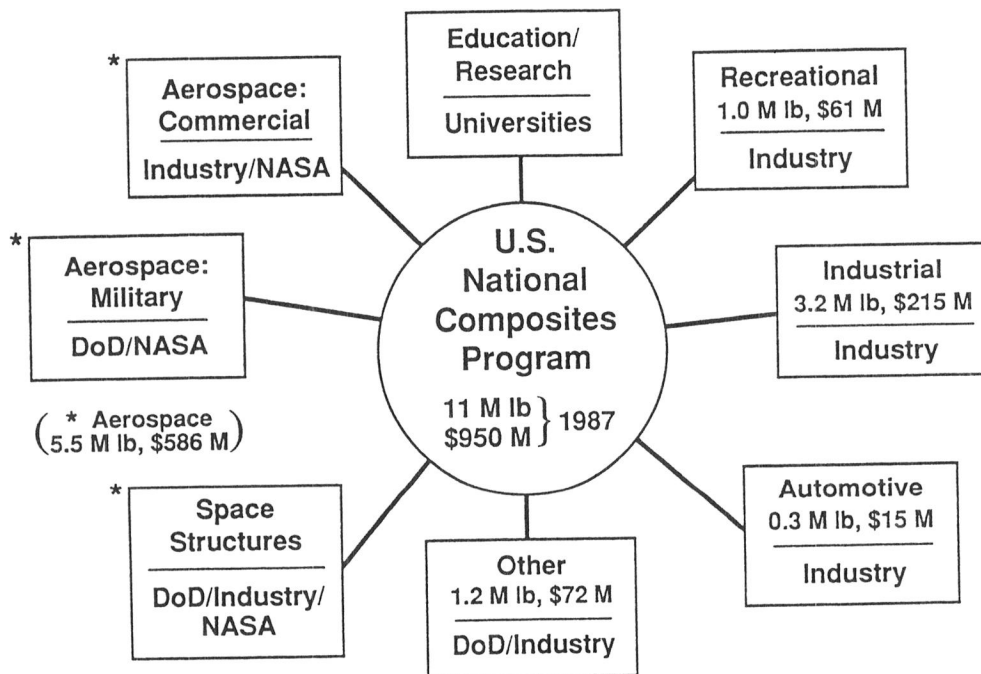
HIGH PERFORMANCE COMPOSITES
KEY GROWTH SEGMENTS FOR THE U.S.*

Market	Market Value		Annual Growth Rate
	1988	1993	1988-1993
Aerospace	$810,000,000	$1,560,000,000	14%
Recreation	40,000,000	50,000,000	5
Industrial	100,000,000	180,000,000	12
Automotive	10,000,000	15,000,000	8
Military	20,000,000	110,000,000	30
Other	40,000,000	55,000,000	5
Average	$1,020,000,000	$1,970,000,000	14

* P. W. Kopf, Polyimide Symposium, San Diego, CA, January 22-25, 1990.

SOME REASONS FOR ADVANCED COMPOSITES' SLOW PENETRATION OF THE OVERALL AEROSPACE MARKET*

- The extreme consequences of failure and the resulting conservativeness with respect to introducing new materials and technology.

- The need to develop new design technology specifically for composites.

- Labor-intensive and expensive methods of fabrication.

* P. W. Kopf, Polyimide Symposium, San Diego, CA, January 22-25, 1990.

INTRODUCTION OF NEW MATERIALS

The introduction of new materials is usually an *evolutionary* rather than *revolutionary* process.

— 10 to 15 years required to develop data base and assess potential and risk prior to committing to production

— new materials for extensive application about the year 2000 are in the laboratory today

OUTLINE

- WHAT ARE HIGH PERFORMANCE COMPOSITES?

- HOW ARE THEY USED TODAY? (i.e., WHY ARE THEY IMPORTANT TO YOU AS USERS AND AS TEACHERS?)

- WHAT ARE THEIR PROPERTIES?

- HOW DO YOU MAKE THEM?

- WHAT ARE THE FUTURE TECHNOLOGY. NEEDS FOR COMPOSITES? (i.e., WHY SHOULD YOU TEACH STUDENTS THIS TECHNOLOGY?)

Stress - Strain Curve
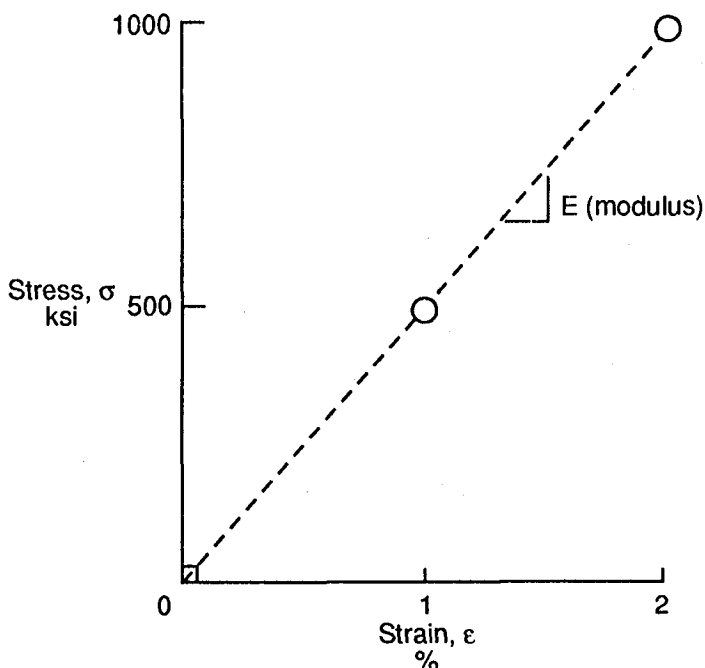
$$\frac{\sigma}{\varepsilon} = E$$

$$E = \frac{500,000 \text{ psi}}{0.01} = 50,000,000 \text{ psi}$$

or

50 msi

Stress, σ ksi (vertical axis: 500, 1000)

Strain, ε % (horizontal axis: 0, 1, 2)

E (modulus)

COMPOSITE MECHANICAL PROPERTY TESTS

(Strength, Modulus, Elongation)

LAMINA PROPERTIES (0°, 90°)

    TENSION
    COMPRESSION
    FLEXURE
    SHEAR
    SHORT BEAM SHEAR STRENGTH

LONGITUDINAL (0°)
TENSION

TRANSVERSE (90°)
TENSION
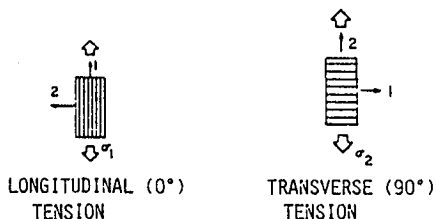
LAMINATE PROPERTIES

    TENSION
    COMPRESSION
    FLEXURE
    SHEAR

COMPRESSION

SHEAR

FRACTURE TOUGHNESS PROPERTIES

    DOUBLE CANTILEVER BEAM (DCB) - MODE I
    END NOTCH FLEXURE (ENF) - MODE II
    CRACKED LAP SHEAR (CLS) - MIXED MODE
    EDGE DELAMINATION (EDT) - MIXED MODE
    OPEN HOLE TENSION
    OPEN HOLE COMPRESSION
    COMPRESSION AFTER IMPACT

FLEXURE

168
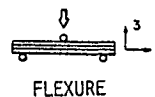
TYPICAL PROPERTIES OF THE CONSTITUENTS OF CONTINUOUS CARBON FIBER REINFORCED COMPOSITE MATERIALS VERSUS METALS

Fiber	Tensile Strength, Ksi	Tensile Modulus, Msi	Tensile Strain, %	Density, g/cc
REINFORCEMENT				
Carbon	600	34	1.6	1.8
Carbon (Intermediate Modulus)	800	44	1.8	1.8
S Glass	665	13	5.4	2.5
ARAMID	550	19	- -	1.5
Boron	510	60	0.8	2.5
PE	435	25	2.7	0.97
MATRIX				
Organic Polymers	15-20	0.4-0.6	1-60	1.2-1.4
METALS				
Steel	70-150	30	- -	7.8
Titanium	125	16	- -	4.5
Aluminum	70	11	- -	2.7

RULE OF MIXTURES FOR MODULUS CALCULATIONS

	Tensile Modulus	Volume Fraction	Theoretical Value
Fiber	34.00 Msi	0.60	20.40 Msi
Resin	0.45 Msi	0.40	0.18 Msi
		Total	20.58 Msi

TYPICAL PROPERTIES OF CONTINUOUS CARBON FIBER REINFORCED COMPOSITES

Property	Unidirectional	Quasi-isotropic
0° Tensile Strength, Ksi	250-300	110
0° Tensile Modulus, Msi	16-20	5-7
0° Tensile Strain, %	1.2-1.5	1.0
90° Tensile Strength, Ksi	7-12	- -
90° Tensile Modulus, Msi	1.0-1.5	- -
90° Tensile Strain, %	1-15	- -
0° Compression Strength, Ksi	150-250	100-120

SPECIFIC PROPERTIES OF MATERIALS
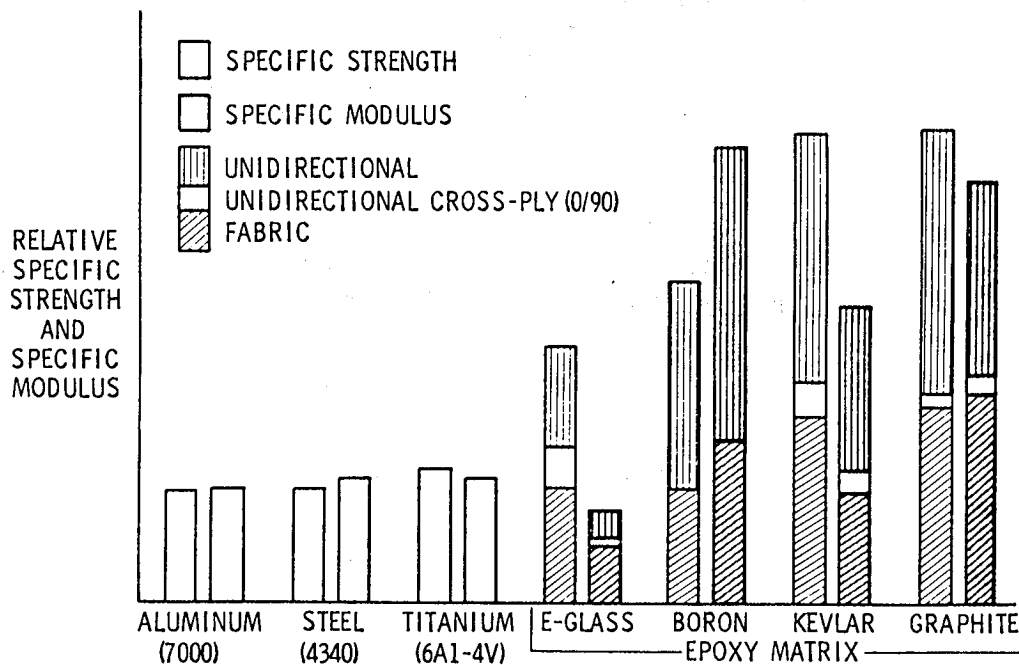
IMPACT INITIATED COMPRESSION FAILURE MODES

DELAMINATION

TRANSVERSE SHEAR

IMPACT

A-A

MATERIAL A (5208)

DAMAGE-TOLERANT RESIN
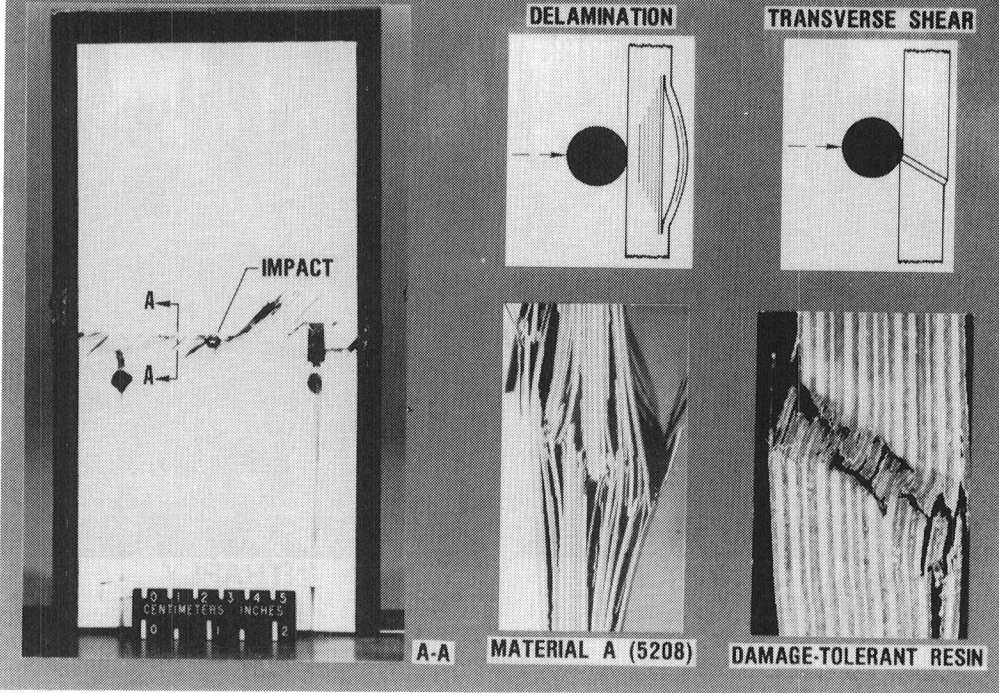
LAMINATE DAMAGE RESULTING FROM PROJECTILE IMPACT

IMPACTED SPECIMEN

FAILURE MODE

C-SCAN

1-INCH
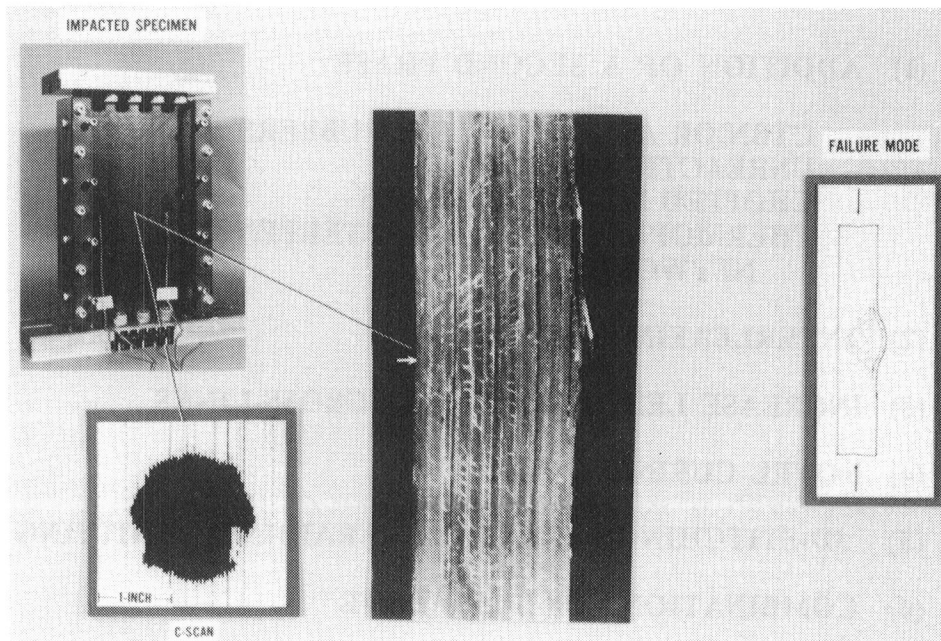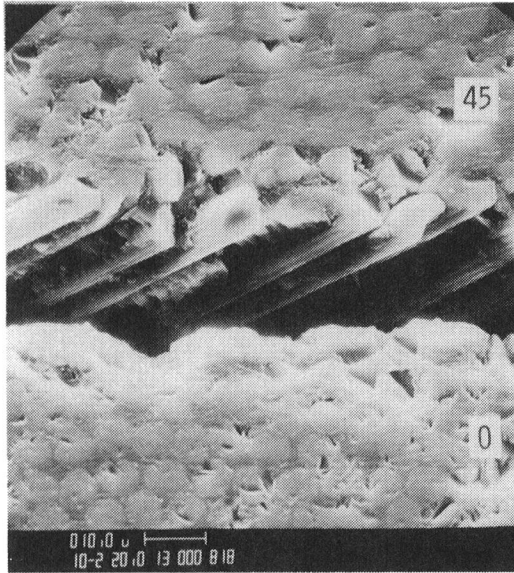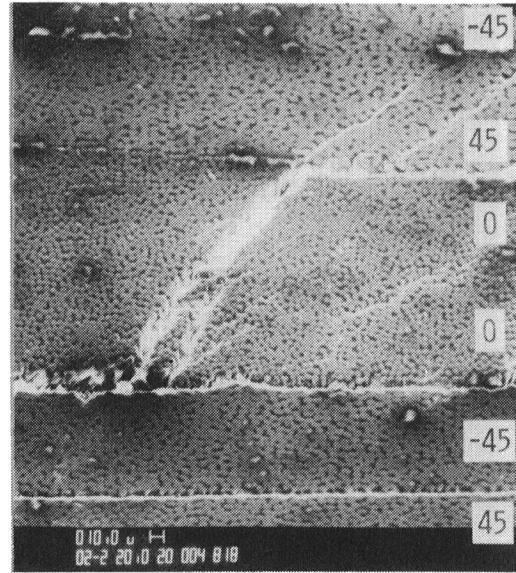
DELAMINATION   INTRAPLY

METHODS FOR TOUGHENING THERMOSET MATRICES

(1)   ADDITION OF A SECOND PHASE

      CTBN OR ATBN REACTIVE RUBBERS
      UNREACTIVE RUBBER
      CHOPPED FIBER OR FIBRILS
      THERMOPLASTICS/ SEMI-INTERPENETRATING
         NETWORKS (IPN'S)

(2)   INTERLEAFING

(3)   INCREASE LENGTH BETWEEN CROSS-LINKS

(4)   NOVEL CURING AGENTS

(5)   3D-STITCHING, -WEAVING, -BRAIDING, -KNITTING

(6)   COMBINATIONS OF THE ABOVE

IMPORTANT TESTS

- **RESIN FRACTURE TOUGHNESS**

- **COMPOSITE INTERLAMINAR FRACTURE TOUGHNESS**

- **COMPRESSION STRENGTH AFTER IMPACT (CAI)**

- **RESIN MODULUS**

HIGH PERFORMANCE COMPOSITES
Interleaf concepts for impact resistance

Graphite composite prepreg

Release paper

Graphite fibers in matrix resin with hot-wet strength

Discrete layer of high strain resin for "toughness"
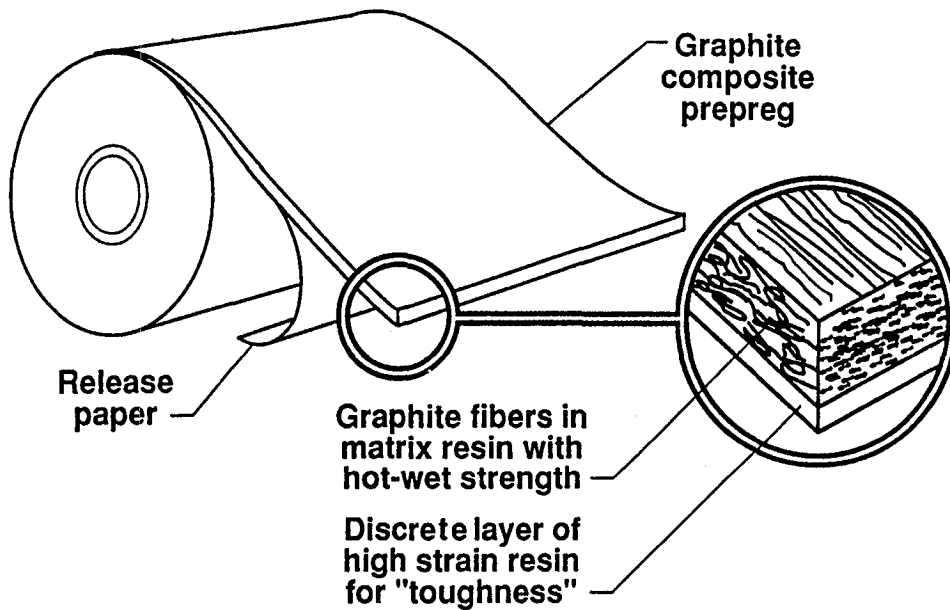
TOUGHENED EPOXY COMPOSITE PROPERTIES

RESIN/FIBER	RT COMPRESSIVE STRENGTH, KSI	RT COMPRESSIVE STRENGTH AFTER IMPACT, KSI	G_{Ic}, IN.LB/IN^2
BMS-8-276	200	45	NO SPEC.
TORAY 3900-2/ T800H	245	53	1.6
ICI 977/IM7	216	50	4.1
HERCULES 8551-7/ IM7	252	53	2.9

THERMOPLASTIC COMPOSITE PROPERTIES

RESIN/FIBER	RT COMPRESSIVE STRENGTH, KSI	RT COMPRESSIVE STRENGTH AFTER IMPACT, KSI	G_{Ic}, IN.LB/IN^2
BMS-8-276	200	45	NO SPEC.
ICI APC-2/AS-4	160	45	8.5
DUPONT AVIMID K/IM-6	144	38	8.1
PHILLIPS RYTON PPS/ AS-4	130	26	3.9/5.1
AMOCO RADEL C/ T650-42	159	45	----
AMOCO TORLON AIX-159/T650-42	230	45	7.5

Damage-Tolerant Stiffened Panel Concept

Basic 9-Ply subelement
AS4 Uniweave

0°
+45°
0°
-45°
0°
+45°
0°
-45°
90°

Stiffener

Eight 9-ply segments
stitched with 200d
Kevlar to form blade

Skin

Six 9-ply segments

Stiffened panel

Stringer flanges stitched to skin
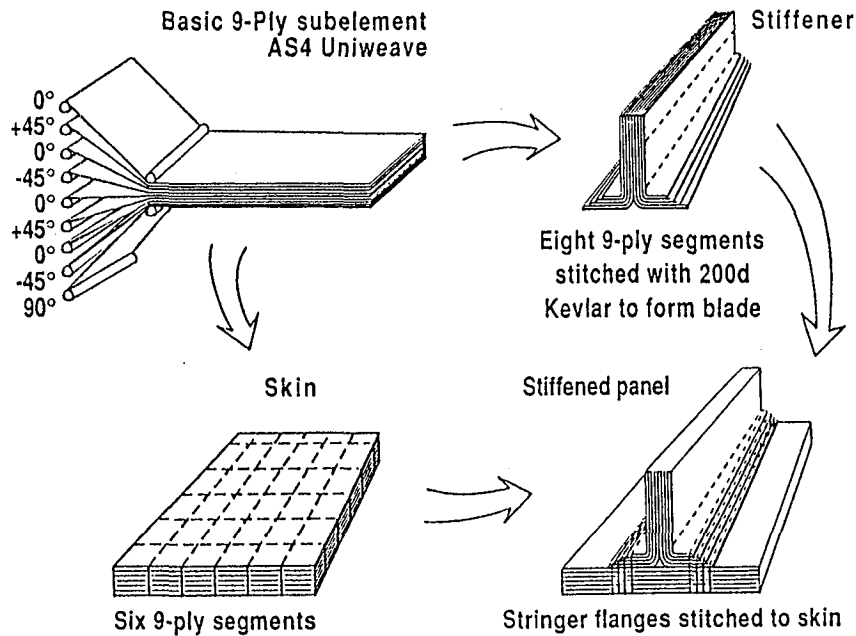
STITCHING CAN SIGNIFICANTLY IMPROVE DAMAGE TOLERANCE OF COMPOSITES

Details of stitched plates

Stitching spaced at 1/8 in.

Stitching pitch 8 per in.

Load direction
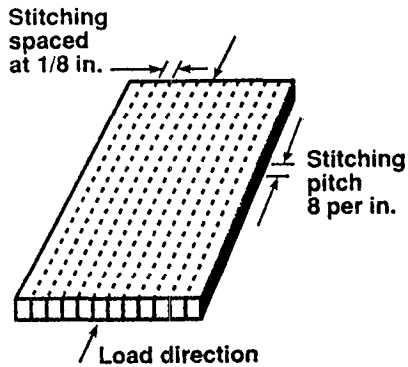
48 ply stitched laminate
$[+45/0/-45/90]_{6s}$

AS4 carbon fabric
3501-6 epoxy resin
S-2 glass stitching thread
Resin transfer molding

Compression after impact strength

A = Unstitched AS4/3501-6
B = Toughened matrix composites
C = Stitched AS4/3501-6

Comp. stress, ksi

Target value

Impact energy, ft-lb

175
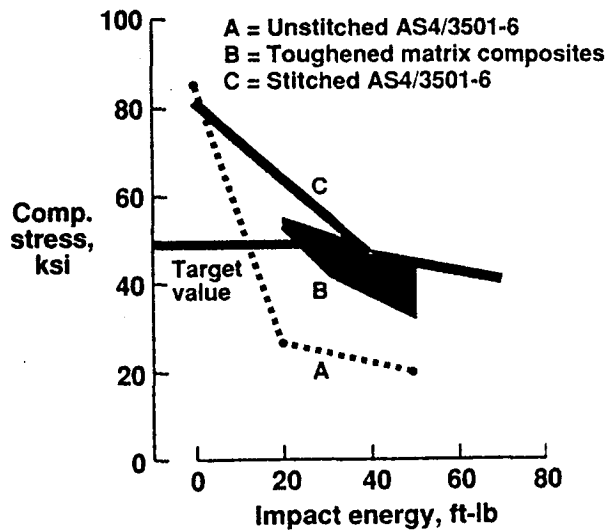
THROUGH THE THICKNESS REINFORCED TEXTILE FORMS
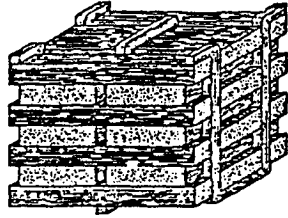
Stitched/woven fabric
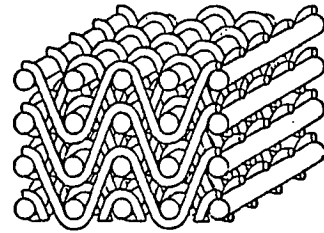
Layer-to-layer interlock weave
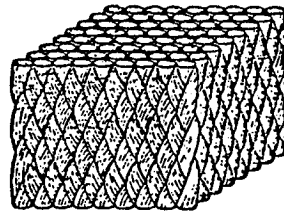
3-D braid

TEXTILE MATERIALS BEING EVALUATED
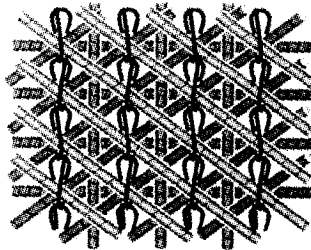
**Multiaxial warp knit
(stitched & unstitched)**

**2-D triaxial braid
(stitched & unstitched)**
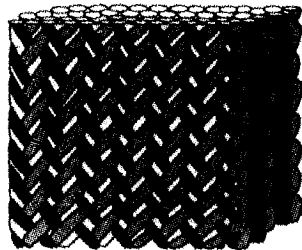
3-D braid
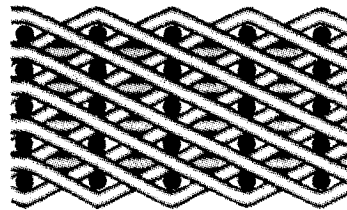
3-D interlock weave

SOME DESIRED PROPERTIES OF POLYMER MATRICES AND THEIR COMPOSITES

Resin	Property at RT	Composite
450 Ksi	0° tensile & compressive moduli	20 Msi
200 Ksi	shear modulus	1.0 Msi (G_{12})
16 Ksi	0° tensile strength	300 Ksi
16 Ksi	0° compressive strength	200 Ksi
16 Ksi	shear strength	16 Ksi (τ_{12})
8%	strain-to-failure	>1.5%
>4 in-lb/in^2 (700 J/m^2)	G_{Ic}	>4 in-lb/in^2 (700 J/m^2)
>50%	retention of RT properties at elevated temp wet	>50%
- -	compressive strength after 1500 in-lb/in impact on quasi-isotropic panel	50 ksi (0.6% strain)
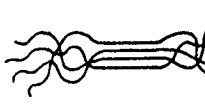
OUTLINE

- WHAT ARE HIGH PERFORMANCE COMPOSITES?

- HOW ARE THEY USED TODAY? (i.e., WHY ARE THEY IMPORTANT TO YOU AS USERS AND AS TEACHERS?)

- WHAT ARE THEIR PROPERTIES?

- HOW DO YOU MAKE THEM?

- WHAT ARE THE FUTURE TECHNOLOGY NEEDS FOR COMPOSITES? (i.e., WHY SHOULD YOU TEACH STUDENTS THIS TECHNOLOGY?)

POLYMER MATRIX COMPOSITES TECHNOLOGY

```
┌ ─ ─ ─ ─ ─ ─ ─ ─ ─ ─ ─ ┐
│  Computational        │
│  Materials            │              Textile  ────────►  Consolidation
│  (Proposed)           │              Preforms            Studies
└ ─ ─ ─ ─ ─ ─ ─ ─ ─ ─ ─ ┘                                    │
          │                                                   ▼
          ▼                                                Composites
  Matrix and                                               Characterization
  Adhesive                         Impregnation               │
  Synthesis                        Technology                 ▼
          │                            ▲              ┌ ─ ─ ─ ─ ─ ─ ─ ─ ┐
          ▼                            │              │ Structural       │
  Polymer                             │               │ Subcomponent    │
  Characterization                    │               │ Development     │
          │                            │              └ ─ ─ ─ ─ ─ ─ ─ ─ ┘
          ▼                            │                       │
  Prelim. Composites  ────►  Polymer                           ▼
  Screening                  Scale-up           ┌ ─ ─ ─ ─ ─ ─ ─ ─ ┐
  (liter quantities)                            │ Manufacturing    │
                                                │ Technology       │
                                                └ ─ ─ ─ ─ ─ ─ ─ ─ ┘
```
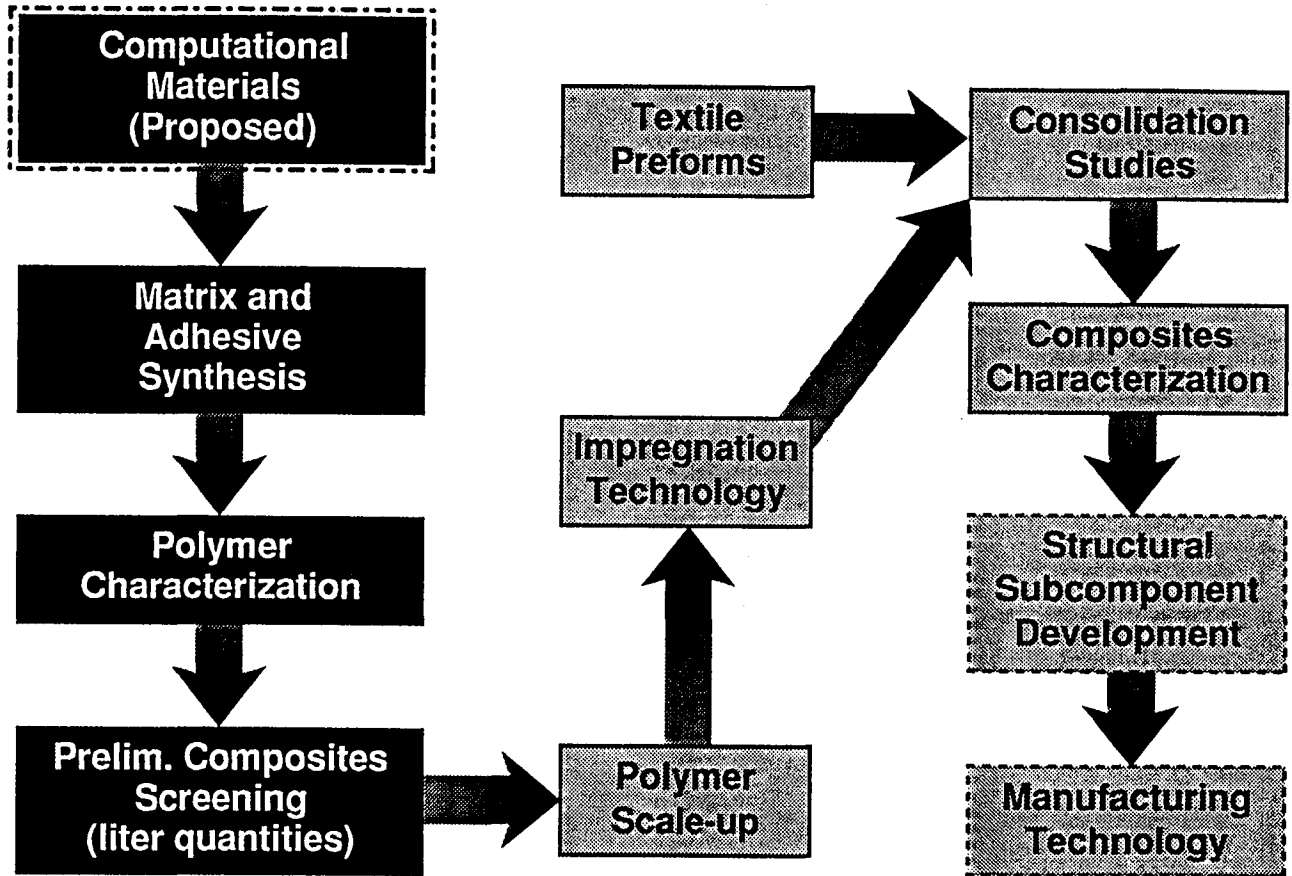
SYNTHETIC APPROACHES

● TOUGHENED THERMOSETS
    EPOXIES, BISMALEIMIDES+THERMOPLASTIC ADDITIVES

● LIGHTLY CROSSLINKED THERMOPLASTICS
    POLYSULFONES, POLYIMIDES + CROSSLINKERS

● CRYSTALLINE THERMOPLASTICS
    POLYESTERS, POLYARYLETHERS (PEEK, ETC.,)

● LINEAR THERMOPLASTICS
    POLYIMIDESULFONE, TPI

RTM RESINS FOR AEROSTRUCTURES

Current	Desired Properties
• Liquid epoxies/room temperature • Solid epoxies/elevated temperature • Solid BMIs	• Low viscosity liquid • Cure without evolution of volatiles at room or elevated temperatures • Acceptable hot/wet mechanical properties • Acceptable thermal performance

New Approaches

• Ring opening of low molecular weight cyclics:

Cyclic   High molecular weight polymer

• Addition polymerization of monomeric reactants:
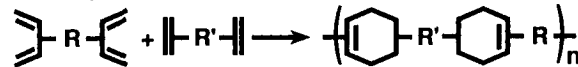
METHODS TO COMBINE RESINS AND FIBER

• SOLUTION: Standard for woven prepreg
Organic solvents undesirable

• HOT-MELT: Standard for epoxies
Difficult for thermoplastics

• RTM AND RIM: Mainly for preform technology

• INTERMINGLED
FILAMENTS: Costly fiber spinning
Difficult for large parts

• SLURRY: Versatile: insoluble powders, carrier liquids, binders, soluble polymers, blends

• POWDER: Solventless process in research stage
Yields boardy, tackless prepreg

• ELECTROPOLYM.,
VAPOR POLYM.
& DEPOSITION: In research stage, needs ideas

179

Polymer Powder Research

Dry powder prepreg equipment

Fiber feed → Tow spreader → Polymer deposition → Polymer fusion → Towpreg take-up

Powder prepreg

200 μm
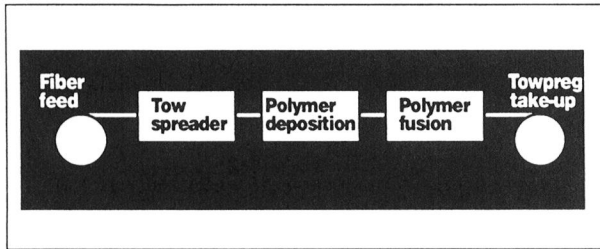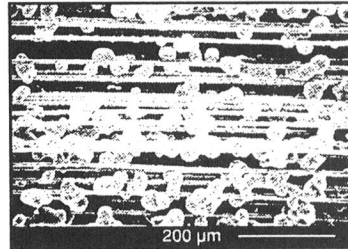
Woven powder towpreg

Composite properties

Short beam shear strength, ksi — Solution prepreg, Powder prepreg

Flexure strength, ksi — Solution prepreg, Film prepreg, Powder prepreg
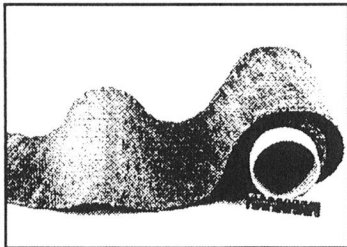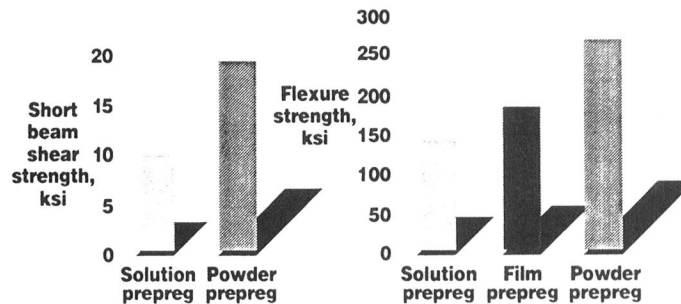
COMPOSITE PROCESSING TECHNOLOGIES

- RESIN TRANSFER MOLDING INTO TEXTILE PREFORMS

- PULTRUSION

- ROBOTIC PLACEMENT (FILAMENT WINDING, ADVANCED TOW AND TAPE PLACEMENT)

- THERMOFORMING

- HAND LAY-UP OF UNITAPE AND FABRIC PREPREG

- -

All require molds (or dies), temperature and pressure during the processing cycle

AUTOMATED COMPOSITE FABRICATION PROCESSES

Weaving/braiding
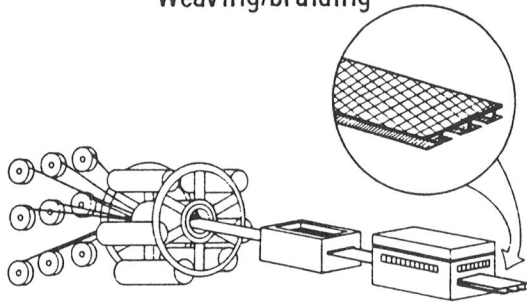
Material Placement
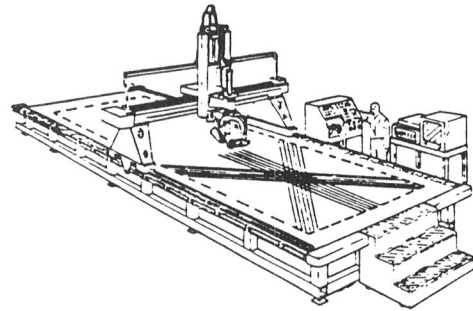
Pultrusion
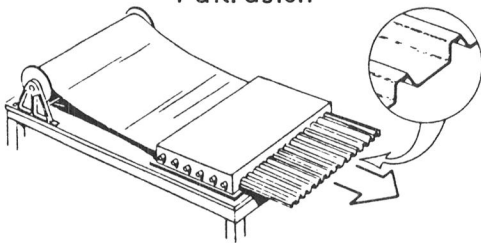
Filament Winding
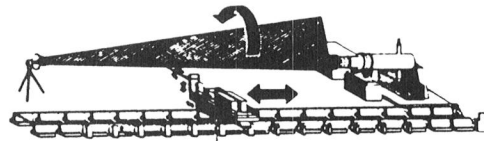
MILACRON'S THERMOPLASTIC/CARBON FIBER TAPE LAYER
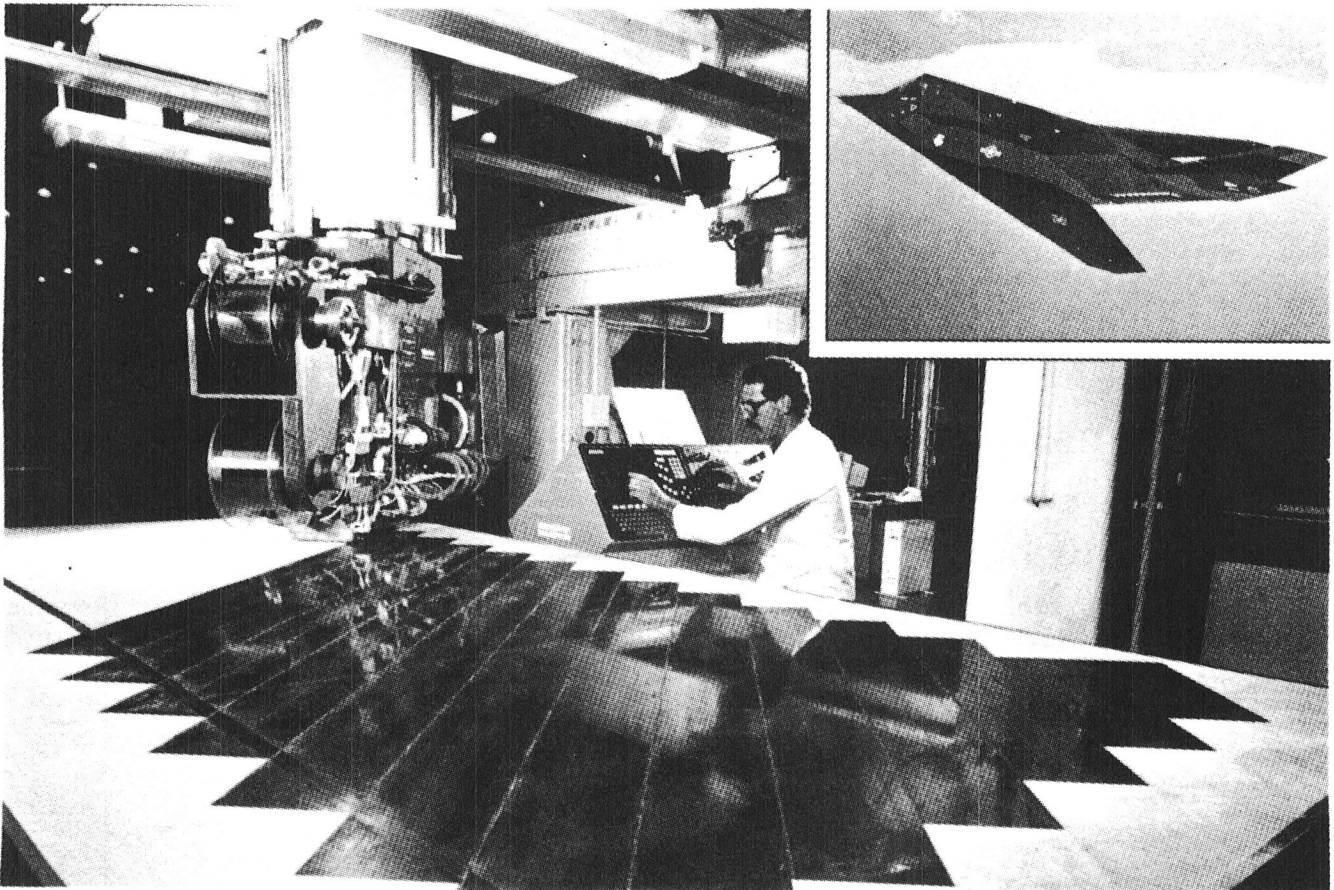
PROCESSING TECHNIQUES

PRESSURE:

- PRESS

- AUTOCLAVE

- VACUUM BAG

- INFLATABLE MANDREL

- EXPANDABLE TRAPPED RUBBER

TEMPERATURE:

- ELECTRICAL RESISTANCE

- HOT GAS

- MICROWAVE

- INDUCTION

OUTLINE

- WHAT ARE HIGH PERFORMANCE COMPOSITES?

- HOW ARE THEY USED TODAY? (i.e., WHY ARE THEY IMPORTANT TO YOU AS USERS AND AS TEACHERS?)

- WHAT ARE THEIR PROPERTIES?

- HOW DO YOU MAKE THEM?

- WHAT ARE THE FUTURE TECHNOLOGY NEEDS FOR COMPOSITES? (i.e., WHY SHOULD YOU TEACH STUDENTS THIS TECHNOLOGY?)

RESIN MATRICES
- Future Needs -

- <u>Conformational Chemistry</u>
    - **Predict Bulk Polymer Properties From Polymer Chemistry**

- <u>Improved Processability</u>
    - **Let's Get Rid of the Autoclave: Oven Cure Only**
    - **Thermoplastics That Cure Like Epoxies**
    - **Ring-Opening and Addition Polymerizations Without Volatiles**

- <u>Long Life Durability of High Temperature Matrices</u>
    - **60,000 Hours at 350°F Under Cycle Load**
    - **Volatile and Microcracking Issues**

- <u>Toughening Technology</u>
    Interleaving and Second Phase Morphology
    versus
    Stitching and Textile Technology

- <u>Preceramics</u>

- <u>Cost Consciousness</u>

183

KEY BARRIER TO APPLICATION

COST

TO DEVELOP

TO PRODUCE

COST COMPARISON OF GRAPHITE FIBERS AND FABRICATED STRUCTURES

| Graphite fibers | —— $20/lb |

| Prepregs | —— $40/lb |

| Fabricated structures | —— $200-500/lb |
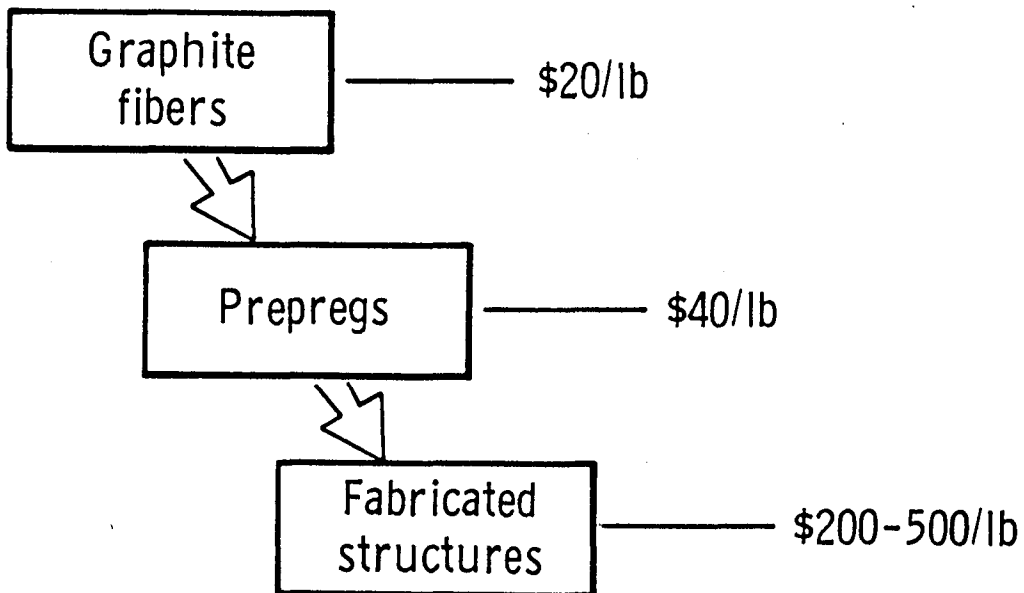
Factors That Influence Cost of Composite Structures

- **Cost of Materials**
    - -Fiber
    - -Resin
    - -Prepreg
    - -Preforms

- **Cost of Fabrication**
    - -Tooling
    - -Labor

- **Cost of Assembly**
    - -Equipment
    - -Labor

- **Cost of Design**

MULTI-AXIS FIBER PLACEMENT MACHINE

Pitch

Roll

Head elevation

Yaw

Longitudinal

Radial

Rotational

185
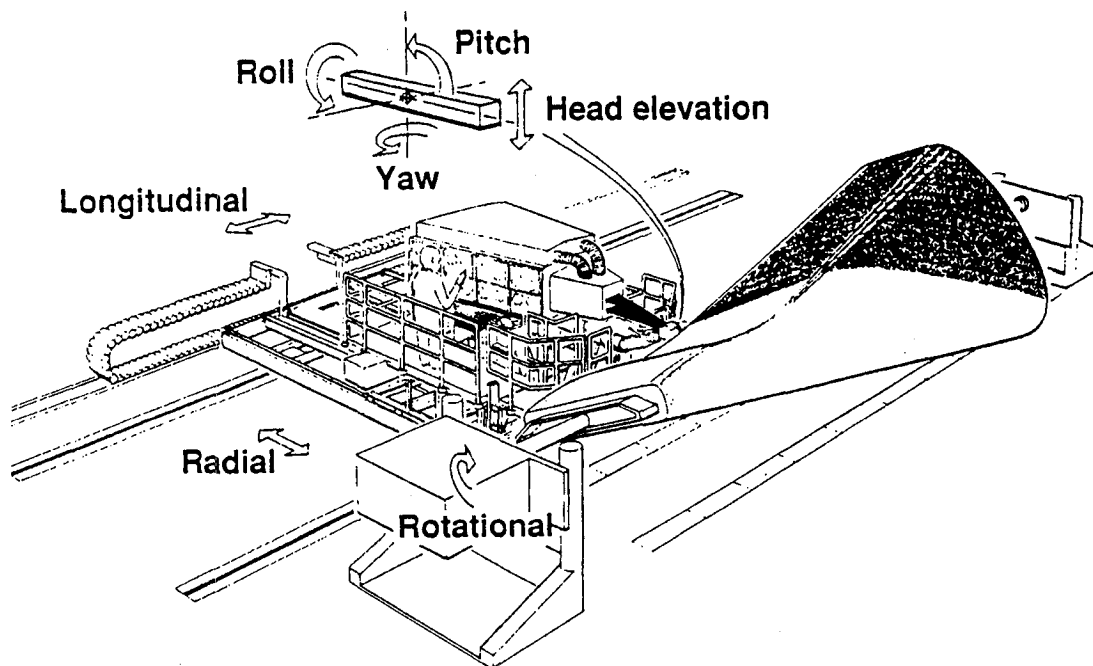
AUTOMATED FIBER PLACEMENT
Cincinnati Milacron Automates Fabrication of ATF Prototype Duct
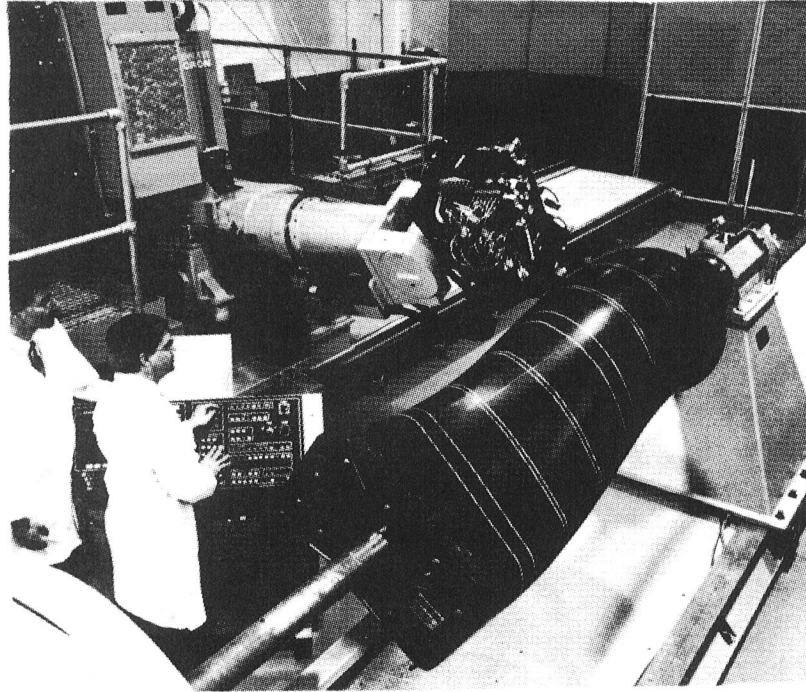
ROBOTICS
- Future Needs -

- Laydown to Net Shape

- Rapid (Pounds Per Hour)

- Versatile

- Quality Construction

- Application on the Factory Floor

Artist's Concept of
AFP Factory of the Future

Multineedle Stitching Station
(Textile Rivets)

Single Needle Stitching Robot

Multiple Interchangeable Thermoplastic Ribbon or
Powder Coated Tow Welding Heads

Multiple Interchangeable Staggered
Tacky Epoxy Tow Placement Heads
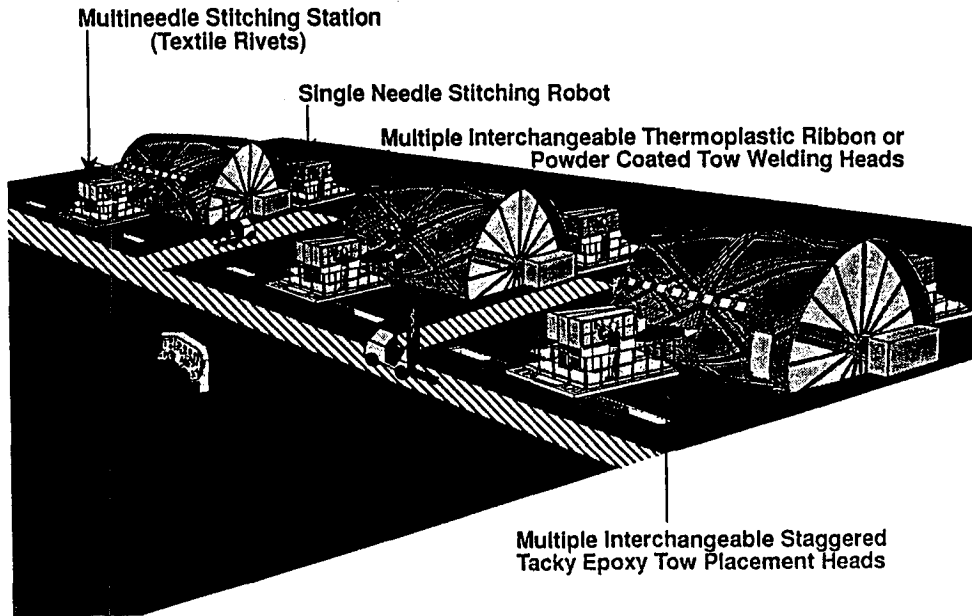
CURRENT OUTLOOK: CONCORDE AND HSCT
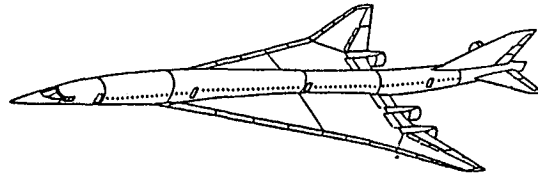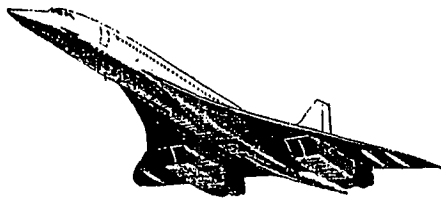
CONCORDE		HIGH-SPEED CIVIL TRANSPORT
3000	RANGE (n. mi.)	5000-6500
100	PAYLOAD (passengers)	250-300
400,000	WEIGHT (lb.)	750,000
EXEMPT	COMMUNITY NOISE STANDARD	FAR 36 - STAGE III
PREMIUM	FARE LEVELS	STANDARD

HSR AIRFRAME MATERIALS TECHNOLOGY

Key Issue

**No long-term, high-temperature
materials data base for HSCT airframes
(60,000-hr design life, 120,000-hr fatigue life)**
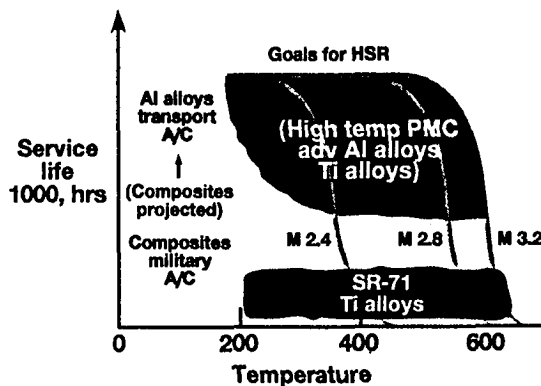
Key technology needs

- Life prediction methodology
  - Accelerated test procedures
  - Long-term flight
    simulation durability
- Demonstrated 300°- 500°F
  polymer matrices, adhesives and
  sealants for ≥60,000-hr lifetimes
- Demonstrated 300°- 600°F
  lightweight metals and
  metal matrix composites
  for ≥60,000-hr lifetimes

MAJOR HIGH TEMPERATURE STRUCTURAL RESIN REQUIREMENTS

- Acceptable Handlability (non-toxic, drape, etc.)

- Processable

- Volatileless or low volatile systems

- High Mechanical Properties (durable, damage tolerant, etc.) over
  temperature range-65° to 350°F, 60000 hours

- Environmental stability (moisture, fuel, etc.)

- Long shelflife

- Acceptable cost (final component)

- Amenable to different fabrication methods (automated tape laying,
  RTM, filament winding, etc.)

Candidate Resins for HSCT

- ° Bismaleimides including toughened versions

- ° PMR-15 including modified versions

- ° Polyimides (thermoplastics, semi-crystalline TP)

- ° Poly(arylene ether)s

- ° Emerging systems (e.g. benzocyclobutenes)

The Future

Decades To Go	Possible Composite Applications
1	Commercial aircraft wings and fuselage elements
	Dry deck shelter
	Space station
	Surface ships
	Cost parity with equivalent metal structure
2	Wide body commercial aircraft wings and fuselage
	High Speed Civil Transport
	Submarine elements
	Moon/Mars space vehicles/structures

Composites industrialization
- *Mil handbook/Alloy database*
- *Factories established*
- *Warehouse composite building block forms*

189

COMPOSITES FOR INFRASTRUCTURE RENEWAL

- **BRIDGES**
  * Use of >150,000 filament carbon fiber tow (small rope)

  * Use of low cost, environmentally durable and safe resin matrices

  * Use of very rapid, low cost fabrication techniques (such as pultrusion of large I-beams)

- **TRANSPORT VEHICLES**
  * Composite Railroad Freight Cars

  * Composite High Speed Passenger Railroad Cars

  * Composite Vans for 18-Wheelers

  * Composite Truck, Van and Passenger Car Bodies, Leaf Springs, Drive Shafts

NOMENCLATURE

B-STAGE:	AN INTERMEDIATE CURE STAGE.
STRAND (TOW):	A BUNDLE OF CONTINUOUS FILAMENTS COMBINED INTO A SINGLE COMPACT UNIT WITHOUT TWIST, E.G., 6000 FILAMENT STRAND. A TOW IS GENERALLY 10,000 OR MORE FILAMENTS.
YARN:	FORMED BY COMBINING TWO OR MORE CONTINUOUS FILAMENTS INTO AN ASSEMBLAGE OF TWISTED STRANDS; GENERALLY FEWER THAN 10,000 FILAMENTS.
ROVING:	A COLLECTION OF BUNDLES OF CONTINUOUS FILAMENTS EITHER AS UNTWISTED STRANDS OR TWISTED YARNS.
WOVEN FABRICS:	THOSE PRODUCED BY INTERLACING STRANDS AT MORE OR LESS RIGHT ANGLES.
WARP:	IN A WOVEN FABRIC, YARN RUNNING LENGTHWISE.
FILL (WEFT):	IN A WOVEN FABRIC, YARN RUNNING FROM SELVAGE TO SELVAGE (CROSSWISE) AT RIGHT ANGLES TO THE WARP.
SIZE:	A SUBSTANCE APPLIED TO A YARN OR FIBER DURING ITS FORMATION TO PROTECT ITS SURFACE AND AID HANDLING AND FABRICATION. STARCH, UNCURED EPOXY, WAX, OIL.
COUPLING AGENT: (FINISH)	PROMOTES A STRONG BOND BETWEEN FIBER AND MATRIX.
SURFACE TREATMENT:	CHEMICAL TREATMENT (USUALLY OXIDATIVE ON CARBON FIBER) PRIOR TO APPLICATION OF A SIZE OR FINISH.
DENIER:	WEIGHT IN GRAMS OF 9,000 METERS OF YARN OR FILAMENT.
TENACITY:	DENOTES BREAKING STRENGTH OF A YARN OR FILAMENT IN G/DENIER (PULLED AT A RATE OF 12 INCHES PER MINUTE).
PREPREG:	WOVEN OR CONTINUOUS FIBER TAPE SHEETS IMPREGNATED WITH RESIN AND READY TO MOLD; RESIN CAN BE UNCURED OR PARTIALLY CURED.

FIBER AREAL WEIGHT: IN A PREPREG OR COMPOSITE, WEIGHT OF FIBER PER UNIT AREA; USUALLY CITED IN
(FAW) G/M^2.

PLY: ONE LAYER IN A COMPOSITE.

UNIDIRECTIONAL   ONE WHICH HAS ALL FIBERS ORIENTED IN THE SAME DIRECTION.
LAMINATE $(0)_x$:

CROSSPLIED LAMINATE: ONE WHICH HAS FIBERS ORIENTED IN VARIOUS DIRECTIONS IN THE PLANE OF THE
                     LAMINATE. USUALLY HAS BALANCED CONSTRUCTION ABOUT THE CENTER LINE OF THE
                     THICKNESS OF THE LAMINATE.

STACKING SEQUENCE: ORDER OF PLY ORIENTATION IN A LAMINATE
                   $(0/\pm45/90)_s$ = 0/+45/-45/90/90/-45/+45/0
                   $(\pm30/\pm30/90/\overline{90})_s$ = +30/-30/+30/-30/90/90/90/-30/+30/-30/+30

ISOTROPIC LAMINATE: ONE IN WHICH THE STRENGTH PROPERTIES ARE EQUAL IN ALL DIRECTIONS.

ANISOTROPIC LAMINATE: ONE IN WHICH THE STRENGTH PROPERTIES ARE DIFFERENT IN DIFFERENT DIRECTIONS;
                      E.G., UNIDIRECTIONAL LAMINATE.

FABRIC DESIGNATIONS

FABRICS ARE GENERALLY DESCRIBED ACCORDING TO THE TYPE OF
WEAVE AND THE NUMBER OF YARNS PER INCH, FIRST IN THE WARP
DIRECTION (PARALLEL TO THE LENGTH OF THE FABRIC), THEN IN
THE FILL DIRECTION (PERPENDICULAR TO THE WARP). FOR
EXAMPLE, A "20 X 18" FABRIC HAS 20 YARNS/IN. IN THE WARP
DIRECTION AND 18 YARNS/IN. IN THE FILL DIRECTION.
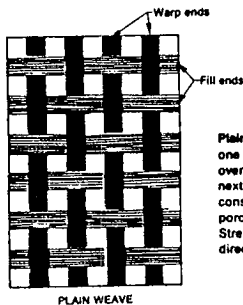
Plain Weave—In this construction, one warp end is repetitively woven over one fill yarn and under the next. It is the firmest, most stable construction, which provides for porosity and minimum slippage. Strength is uniform in both directions.

PLAIN WEAVE

Satin Weave—In this construction, one warp end is woven over several successive fill yarns, then under one fill yarn. A configuration having one warp end passing over four and under one fill yarn is called a five-harness satin weave. Similarly, in an eight-harness satin fabric, one warp end passes over seven fill yarns, then under one fill yarn. The satin weave is more pliable than the plain weave. It conforms readily to compound curves, and can be woven to a very high density. Satin weaves are less open than other weaves; strength is high in both directions.

FIVE-HARNESS SATIN WEAVE
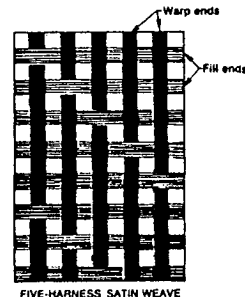
SHEPLER, TOWN AND SAYLOR, MACHINE
DESIGN, MAY 24, 1979.

REFERENCES

O HANDBOOK OF COMPOSITES, G. LUBIN, ED., VAN NOSTRAND CO., 1982
O ASTM STPs
O VENDOR DATA SHEETS
O JOURNALS
    * COMPOSITES
    * J. COMPOSITE MATERIALS
    * SAMPE J.; QUART., PREPRINTS
    * J. MATERIALS SCIENCE
    * INTERNAT. J. ADHESION AND ADHESIVES
    * J. ADHESIVES
    * J. REINFORCED PLASTICS
    * AIAA JOURNAL
    * J. COMPOSITES TECHNOLOGY AND RESEARCH
    * COMPOSITES SCIENCE AND TECHNOLOGY
    * COMPOSITE STRUCTURES
O GOVT. PUBLICATIONS
    * NASA: CR, TR, TM, CP, RP
    * AFWAL: TR, CR
    * ADVANCED COMPOSITES DESIGN GUIDE
O MODERN COMPOSITE MATERIALS, L. J. BRAUTMAN AND R. H. KROCK, ED.,
   ADDISION-WESLEY PUB. CO., 1967
O ASME, AIAA, SEM, ASC, AHS, ETC. AND PREPRINTS OF MEETINGS
O EXPERIMENTAL CHARACTERIZATION OF ADVANCED COMPOSITE MATERIALS, L. A.
   CARLSSON AND R. B. PIPES, PRENTICE-HALL, INC., 1987
O EXPERIMENTAL MECHANICS OF FIBER REINFORCED COMPOSITE MATERIALS, J. M.
   WHITNEY, I. M. DANIEL, AND R. B. PIPES, PRENTICE-HALL, INC. AND THE SOCIETY
   FOR EXPERIMENTAL STRESS ANALYSIS, MONOGRAPH NO. 4, 1982
O INTERNATIONAL SAMPE TECHNICAL CONFERENCE SERIES (FALL)
O SCIENCE OF ADVANCED MATERIALS AND PROCESS ENGINEERING SERIES (SPRING)

192

MATERIALS EDUCATION ACTIVITIES

Heidi R. Ries, Moderator, Norfolk State University
Jonice Harris, National Institute of Standards and Technology
Woodrow W. Leake, American Society for Engineering Education
L. Roy Bunnell, Battelle-Pacific Northwest Laboratories
Robert Berrettini, Materials Education Council

INTEGRATING MANUFACTURING AND ENGINEERING EXAMPLES INTO SCIENCE TEACHING

Heidi R. Ries
Department of Chemistry and Physics
Norfolk State University

Last year, at NEW: Update '91, a panel discussion was held to address the unique difficulties of "Attracting and Retaining Minorities and Women in Technical Studies" Unfortunately, retention in technical majors is a problem of varying proportions for the entire student population [1], and must be improved in order to maintain the strength of the nation's industrial base.

To investigate the cause of student attrition in technical majors, in-depth interviews of both current and former (non-graduating) engineering students at four colleges and universities in Colorado were conducted by Hewitt and Seymour [2]. They found that there was no significant difference in the level of high school preparation and undergraduate academic performance in these two groups, despite the prevailing faculty perception that most students who switch from technical to nontechnical majors were "underprepared". The majority of engineering students who changed majors reported that they were "turned off by science", while one-third complained of poor teaching.

Since most of these students transferred to other majors during the first two years in college, this suggests the need to examine the content of the introductory curriculum. The first year of a technical program generally includes basic mathematics and science courses, with little or no exposure to engineering or manufacturing applications. The abstract nature of these initial courses and the lack of instructor interest in "real world" examples may contribute to the loss of student interest in technical careers.

The Industrial and Management Systems Engineering Department at Penn State University, University Park Campus, elected to improve instruction in introductory mathematics and science courses by providing faculty members who teach these courses with experiences and materials which will enable them to incorporate appropriate manufacturing and engineering examples into their teaching. With National Science Foundation funding, a "Teaching Enhancement Program on Applications of Science and Mathematics to Manufacturing for Undergraduate Faculty" was offered during the summer of 1992. Over 50 mathematics and science instructors from various colleges attended, and enthusiastically participated in the metal casting, circuit board manufacturing, and machining modules, which included both lecture and laboratory experiences. A summary of concepts demonstrated in the modules was made, and implementation ideas were developed and discussed. The Teaching Enhancement Program will be repeated in the summer of 1993 [3].

At Morgan State University, a more direct approach is being used to address the entry-level curriculum, through the use of a "Phenomena-Driven Engineering Curriculum" (ECSEL program). In this effort, engineering problems (such as designing an electric vehicle or a bridge) are introduced in the first year of the program. This problem then

becomes the unifying theme in all courses, including introductory physics, chemistry, mathematics, and English. Since this program was initiated in Fall, 1991, the full impact on retention is not yet clear.

Norfolk State University is also pursuing integration of the topics in the technical curricula. Currently, chemistry, engineering, physics, and mathematics majors are enrolled together in a one semester hour orientation/seminar class. Faculty members from all programs present general information about careers and research in the various fields. A more expanded course is being developed which will emphasize interdisciplinary topics, "real world" problem solving, and visitations to research and/or industrial facilities. It is anticipated that students will gain a better understanding of the relevance of their introductory coursework to their ultimate career goals.

1. "A Profile of Undergraduates in the Sciences" Kenneth C. Green American Scientist 77 (475) 1989

2. "A Long, Discouraging Climb" Nancy M. Hewitt and Elaine Seymour ASEE Prism February 1992, p. 24

3. For further information and application materials, contact:
   Dr. Clayton Ruud
   Dept. of Industrial and Management Systems Engineering
   The Pennsylvania State University
   207 Hammond Building
   University Park, PA 16802-1401

IMPROVED MEASUREMENT OF THERMAL EFFECTS ON MICROSTRUCTURE

Mansur Rastani

Department of Manufacturing Systems
NC A&T State University
Greensboro, North Carolina 27411

Telephone 919-334-7585

Improved Measurement of Thermal Effects on Microstructure

Mansur Rastani, P.E., C.Mfg.E.
Department of Manufacturing Systems
NC A&T State University, Greensboro, NC

Key Words: partially and fully recrystallized microstructure, unrecrystallized microstructure, spring elongation number, elastic recovery factor, ohmic-resistance heat treatment.

Prerequisite Knowledge: elementary knowledge of material elasticity, metal structure, heat treating, and some quantitative metallographic measurements on microstructure.

Objectives: To introduce a simple methodology which could be used to replace the time-consuming and expensive conventional methods of metallographic and quantitative analysis of thermal treatment effect on microstructure.

Equipment & Supplies: The experiment itself needs ten standard 60 or 75 or 100 W light bulbs, a lamp holder and stand hooked up to an electric wire, a chronometer, a scale for measuring distance and two tweezers. However, in order to compare the results of this method with the ones of metallographic analysis, specimen preparation station, a fast curing epoxy mounting, and an optical metallurgical microscope are required.

Introduction: Metallurgical analysis continually calls for the evaluation of thermal treatment effects on microstructure. This commonly demands metallographic sample preparation and microscopic examination, which are time absorbing and costly. These drawbacks are burdensome when large numbers of samples must be levied fast. Mechanical testing can sometimes be substituted, but sample size and shape frequently make these methods impractical. The experiment described here is ideal for the microstructural evaluation of lamp filaments and other wire samples such as copper wire which can be conveniently coiled.

Procedure: In this experiment, a common coiled incandescent lamp filament is used. The coil body was about 12.5 mm long, and it was made from standard grade tungsten lamp wire. The samples were heat treated by ohmic resistance; simply each light bulb is placed in an electric current circuit and is lighted for a fraction or a multiple of seconds. The treatment took place in steps of 0.8 seconds duration at temperatures which were expected to span the recrystallization range. Ten samples were treated so

that each was removed from this process at a progressively higher step, table 1.

Specimen	1	2	3	4	5	6	7	8	9	10
H.T. Duration (sec)	–	0.8	1.6	2.4	3.2	4.0	4.8	5.6	6.4	7.2

Table 1. Ohmic-resistance heat treatment on ten specimens at time duration steps which are expected to span the recrystallization temperature range.

The recrystallization temperature of the tungsten filament is around 2000 °C. When the lamp is lighted for the first time, filament temperature rises quickly to about 2500 °C. At this temperature, the tungsten filament readily recrystallizes and the fibrous grain structure of the filament, figure 1, is replaced by recrystallized grains. Figures 2 and 3 show the fracture surfaces of the cross sections of the filaments with no heat treatment and with heat treatment respectively.

After treatment, the samples were evaluated in the elastic recovery test. Using a scale and tweezers each sample was carefully stretched to a coil length of 40 mm and then allowed to return to a relaxed length. Then, the deflection recovered (e) was measured. The recovered portion of the deflection (e) is

$$e = L - l'$$

where L is the stretched length, 40 mm, and l' is the length after elastic recovery, as indicated in figure 4.
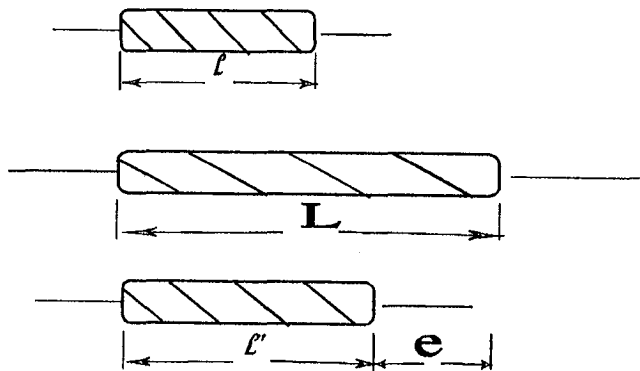
Figure 4. The recovered portion of the deflection (e) is shown in an elastic recovery test on a filament

200
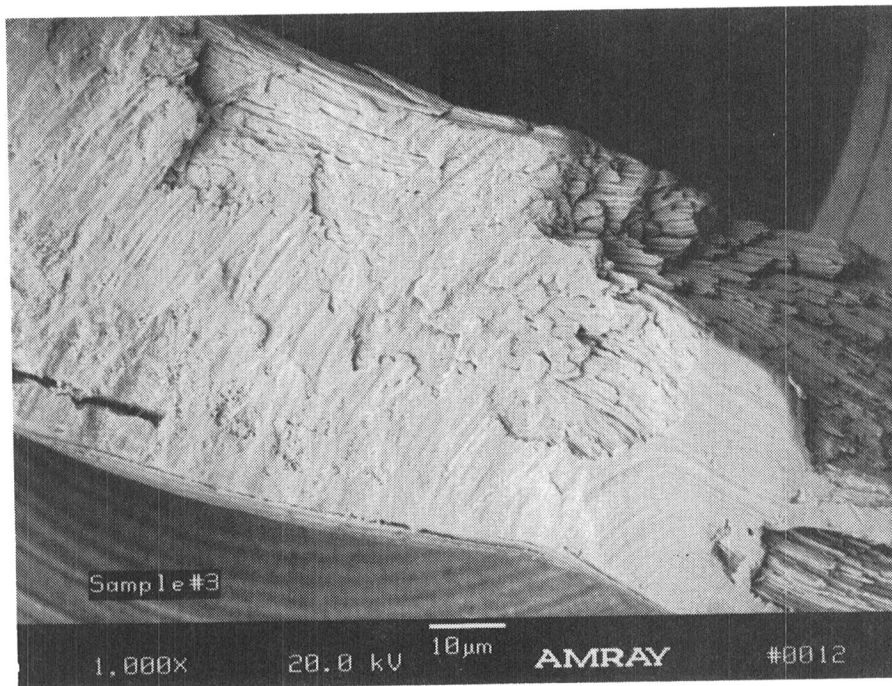
Figure 1. SEM micrograph of the fibrous microstructure of an unrecrystallized filament, 1000X.
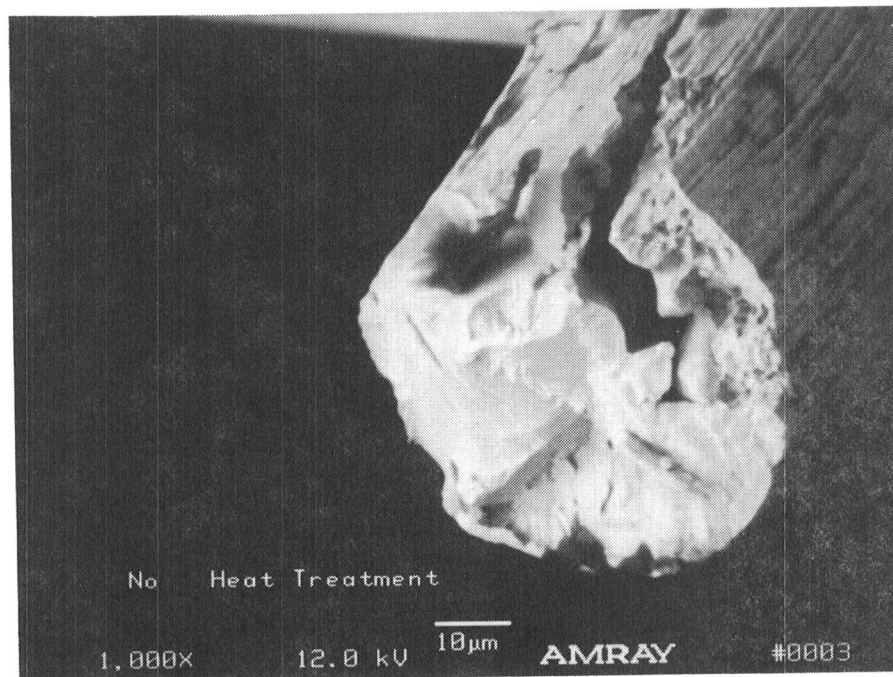
Figure 2. SEM micrograph of the fracture surface of an uncrystallized filament, 1000X.

1 Sec. Heat Treatment

1,000X   18.0 kV   10 µm   AMRAY   #0006
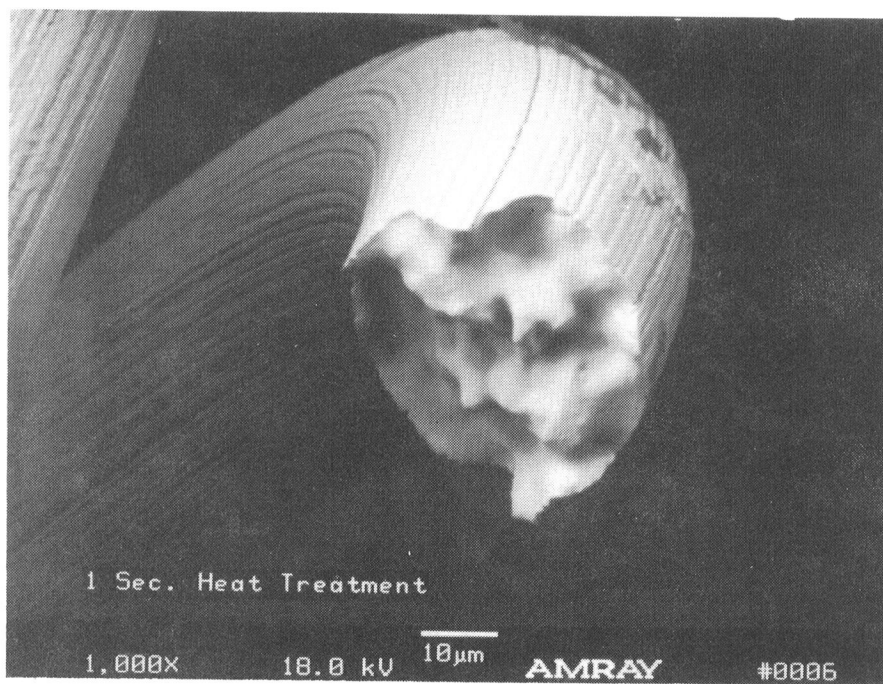
Figure 3. SEM micrograph of the fracture surface of a crystallized filament, 1000X.

The normalized elastic recovery factor (erf) is defined in terms of deflections as:

$$erf = (e-e_{min})/(e_{max}-e_{min}) \qquad (1)$$

where e is the deflection of a specimen of unknown degree of recrystallization, e_{min} is the minimum value of recovered deflection presumably for the fully recrystallized material and e_{max} is the maximum deflection value for the totally unrecrystallized structure. In the following, the results on three specimens illustrate how computations are made.

Results: In the elastic recovery test, amount of stretch was 40 mm, the calculated erf for three specimens are listed in table 2.

Specimen	l (mm)	e (mm)	erf (mm)
Partially Rec.	20	e = 20	50%
Fully Rec.	26	$e_{min}=14$	0%
Unrecryst.	14	$e_{max}=26$	100%

Table 2. Results of elastic recovery test on three specimens.

In order to evaluate the amount of crystallized and uncrystallized portion in different filaments by the conventional metallography method, the specimens are metallographically prepared. The samples were carefully placed in a mounting cup and encapsulated in EPO-KWICK fast curing epoxy. Each sample was then ground and polished with care. The polished samples were etched with Murakami's[*] etch to reveal the microstructure of the wire cross-section. Figures 5, 6, show the optical micrographs of filaments' cross sections with partial recrystallization which illustrate some of the problems associated with quantitative measurement of the partially recrystallized microstructures. A full recrystallized filament is shown in figure 7. The microstructure of the region of the wire which remained unrecrystallized, consists of long, thin fibers having longitudinal axes parallel to the axis of the wire. Corresponding sections of the recrystallized portions of the wire usually show no grain boundaries. Along the length of

---

[*] Murakami's etch consists of 10 gr of potasium iron cyanide and 10 gr of potasium hydroxide in 100cc water
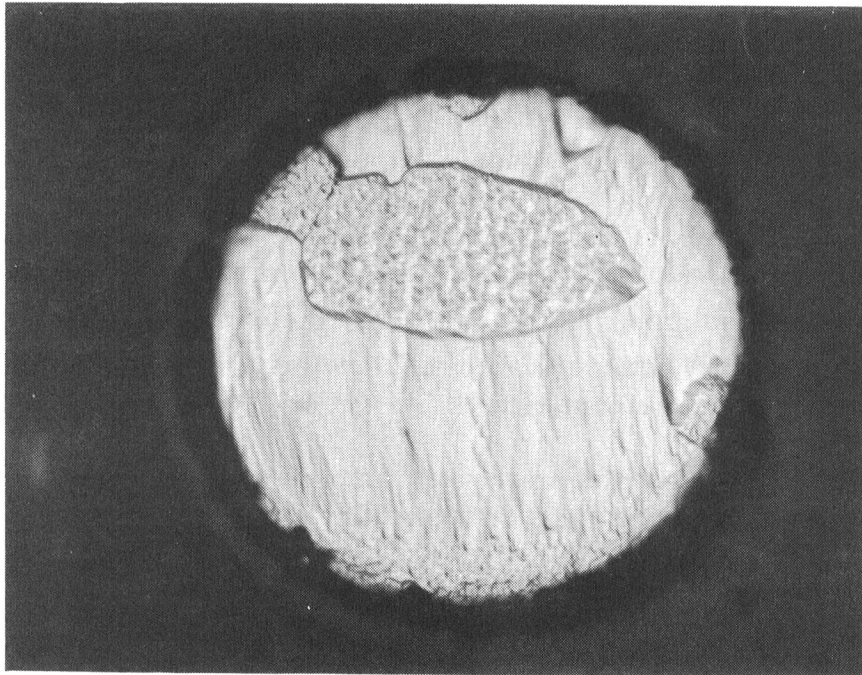
Figure 5. Optical micrograph of partially-crystallized filament section, 1 sec heat treated, murakami's etch, 1000X.
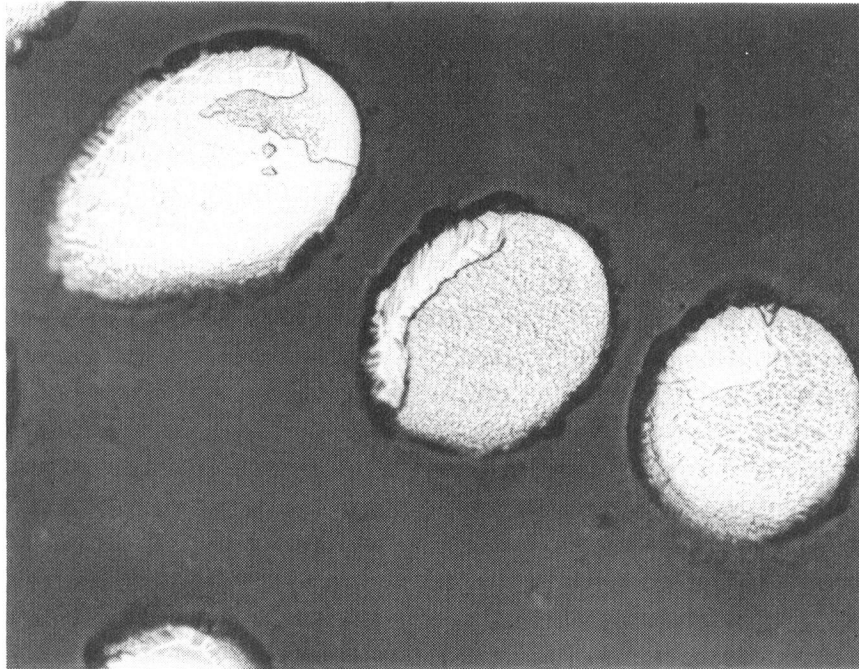
Figure 6. Optical micrograph of partially-crystallized filament sections, 5 sec heat treated, murakami's etch, 1000X.
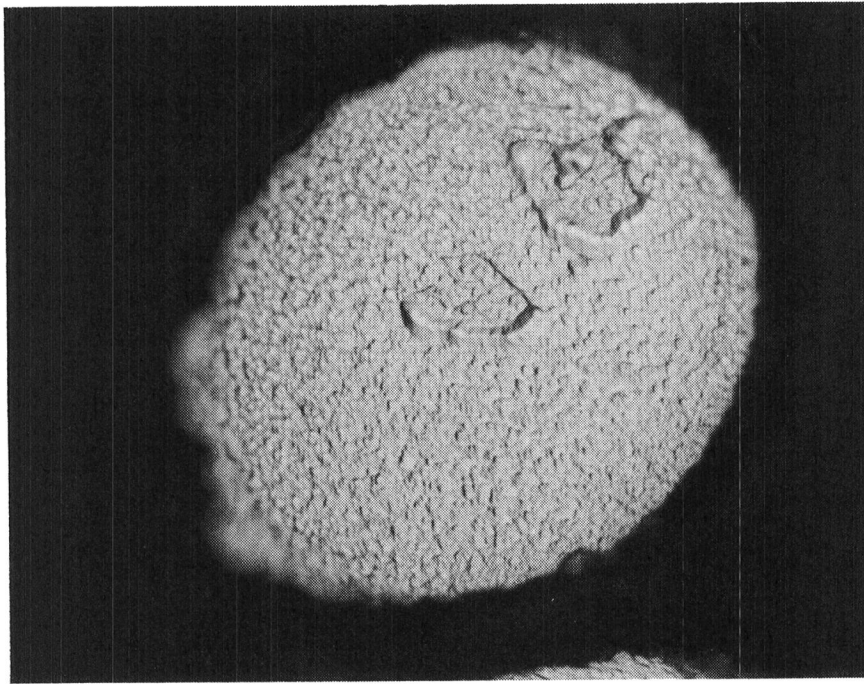
Figure 7. Optical micrograph of fully-crystallized filament section, 7.2 sec heat treated, murakami's etch, 1000X.

the coiled wire there may be variations in relative proportions of recrystallized and unrecrystallized structures. The elastic recovery factor and the fraction of uncrystallized material determined metallographically are both plotted as a function of the heat treating duration on the same diagram, figure 8. Altogether, five comparisons were made, and the correspondence was always good.
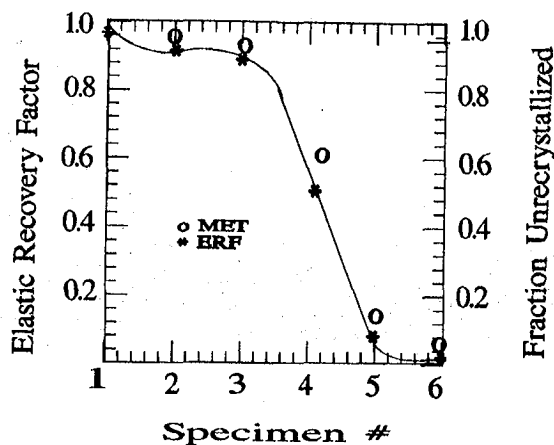
Figure 8. Elastic recovery factor (ERF) and fraction of unrecrystallized material, determined metallographically (MET), as a function of heat treatment duration.

The elastic recovery factor versus the fraction of unrecrystallized material is plotted in figure 9 for five different heat treated filaments which had different recrystallization behavior. The fraction of unrecrystallized materials as determined metallographically appears to be consistently lower than would be predicted from the elastic recovery factor data.
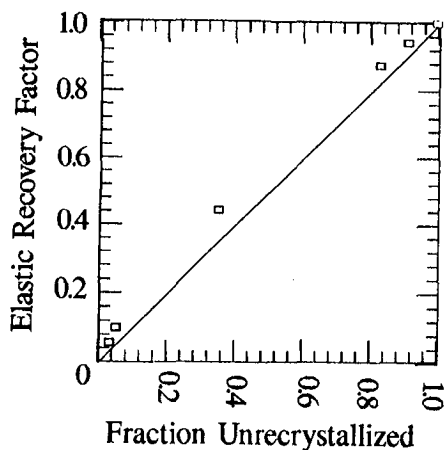
Figure 9. Elastic recovery factor vs fraction recrystallized material as determined metallographically.

206

Conclusion: Experimentally it has been shown that elastic recovery factor depends on the degree of recrystallization, i.e.; those sections of the filament where most recrystallization had taken place showed the most coil deformation. Theoretically, the reason for this is perhaps obvious. As yield strength is diminished by the progress of recrystallization, since the elastic modulus is not affected much by the heat treatment, it can be concluded that the extent of recovery after deflection, e, is also proportionally diminished. Because the elastic recovery method examines the whole filament rather than just one section through the filament, as in the metallographical method, it more accurately measures the degree of recrystallization. The method also takes a considerably shorter time and cost compared to the conventional method. The elastic recovery method may be applied to other metals and alloys which could be formed into coil so that after heat treatment they could be stretched to obtain measurable plastic elongation and elastic recovery.

Analogous Tests: The Following People Used a "Spring Elongation Number" Test on Copper Wire For Different Purposes as Follows:

R. Nilsson (J. Inst. Metals, 1960) :
To Differentiate Between Grain Sizes.

S. Harper (J. Inst Metals, 1965):
To Differentiate Cooling Rates.

S. Carlen (J Inst Metals, 1960):
To Measure the Effect of Finish Temperature.

A. Smith (Inst of Min & Metall. Trans., 1966):
To Demonstrate Variation in Drawing Practice.

References: 1. S. Harper and A. Goreham, Factors Affecting the Springiness of Copper Wire, J of the Inst. of Metals, 1965, Vol. 93, pp. 409-17.

2. F. Schuckher and R. Nilsson, A Method for Assessing the Suitability of Copper Wire for Enamelling, J of the Inst. of Metals, 1960, Vol. 88, pp. 7-14.

3. K. MacKay and G. Smith, Quality Control of Electrolytic Tough Pitch Copper, Inst. of Min. & Mer. Trans., 1966, Vol 75, PP. 269-85.

DIRECT TENSION EXPERIMENTS ON COMPACTED GRANULAR MATERIALS

Steven W. Perkins

Assistant Professor of Civil Engineering
College of Engineering
Montana State University
Bozeman, Montana 59717-0007

Telephone 406-994-2111

DIRECT TENSION EXPERIMENTS ON COMPACTED GRANULAR MATERIALS

Steven W. Perkins
Department of Civil and Agricultural Engineering
Montana State University, Bozeman, Montana

KEY WORDS: granular materials, tensile strength, low mean stress, material modeling.

PREREQUISITE KNOWLEDGE: The student should have an understanding of soil mechanics, concepts of stress and strain, and the formulation of ideally elastic stress-strain behavior in loading and unloading.

OBJECTIVES: The objective of this experiment is to determine the level of tensile strength of uncemented, dry, granular materials. The experimental apparatus does not lend itself to a direct measurement of the material's tensile strength, but must be analyzed as a stress field problem in order to arrive at a tensile strength value. The experiment, and subsequent analysis, serve to instruct the student on the influence of gravitationally induced stresses in frictional granular materials, the importance and difficulty of accurately describing the entire failure envelope for granular materials in the low mean stress range, and the fundamental principles of material modeling.

BACKGROUND AND THEORY: Granular materials, such as highly angular dry sands and silts, are known to contain a small but significant level of cohesive strength. It has been shown that a dry, silty, highly angular sand, prepared to near 100% relative density, possesses a cohesion of approximately 2.5 kPa (1). Cohesive strengths in these materials are believed to arise mainly from interlocking of highly angular particles.

By virtue of the continuous nature of a material's failure envelope, materials containing a cohesive strength must contain a small, but finite, level of tensile strength. This is illustrated schematically in Figure 1, where the tensile strength is represented by the symbol "T" and the cohesion by "c", where compression is taken as positive and tension as negative. This tensile strength is typically much smaller than the corresponding cohesive shear strength, which implies a high degree of non-linearity in the failure envelope in this low range of mean stress. In the absence of tensile strength information it has been common practice to extrapolate the failure envelope back to the intersection with the tensile mean stress axis. This fails to account for the dramatic curvature of the failure surface in the region of low mean stress. In addition, the tensile strength of a material is often times overestimated by this technique. To avoid these problems it is necessary to determine the material's tensile strength, no matter how small this strength may be.

Problems of low mean stress confinement have received considerable attention in conjunction with plans for developing facilities on the surface of the moon. The low gravity level on the moon, coupled with the light weight of proposed structures, requires that the properties of lunar soil be examined in the low mean stress regime. The study of the mechanics of granular materials at low mean stress levels also has terrestrial applications in the study of liquefaction problems and the performance of roadway bases.

Engineering problems associated with this low mean stress range are significantly impacted by the assumptions made with regard to the level of tensile strength of the material. For example, the soil behind a retaining wall of conventional height, erected in a low gravity environment such as that on the moon, will experience relatively low levels of mean stress confinement. A condition of active failure will produce stress paths in the various soil elements which progress towards tensile states of stress. An accurate description of the tensile strength of the material is necessary to evaluate the active earth pressure acting on the wall. This problem is more significant in a low gravity environment where a greater proportion of the material experiences lower levels of mean stress confinement. Overestimation of the tensile strength by extrapolation techniques can result in an overprediction of the capacity of structures with loadings in the low mean stress

211
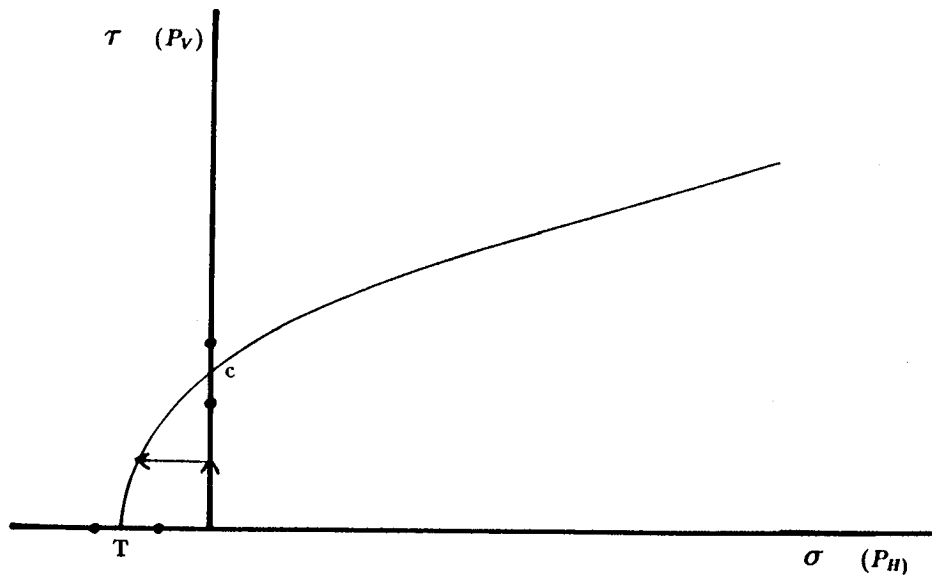
Figure 1: Schematic Failure Envelope

range.

In addition to conventional geotechnical engineering solutions, modern constitutive models often rely on the assessment of the isotropic tensile strength as an input parameter. The proper identification of this parameter is essential when using the material model in conjunction with finite element codes to determine the response of complex loadings involving initially low levels of mean stress confinement. The problem then lies in developing an appropriate experimental device to determine the tensile strength of a weakly cohesive material.

EXPERIMENTAL PROCEDURE: A new apparatus has been designed and built for measuring the tensile strength of uncemented silty sands (1). This device is shown schematically in Figure 2. The device consists of a mounting plate (not shown), loading system (consisting of a motor support block, motor, load cell and screw mechanism), horizontal travel rails and ball bearing blocks, split specimen box, and horizontal restraint rails (vertical guide rails). The device is designed to contain a 17.8 cm cuboidal specimen in a box split along a vertical plane. The box is split to form two equal halves. The front half of the box is mounted to two lateral guide rails by roller bearing (pillow) blocks attached to its underside. The rear half of the box rests on two aluminum blocks to position it to the same vertical height as the front. The rear half of the box is restrained from horizontal movement by two vertical guide rails. It is noted that these guide rails may serve to translate the rear half of the box upwards. This can allow the box to be modified to impose a shearing force on the plane of failure.

With the soil specimen in place, the front half of the box is pulled in a direction perpendicular to the vertical plane of split by a motor as shown in Figure 2. The load required to split the sample is measured with a load cell attached to the front of the box. This load cell has a range of 0-222 N and a resolution of +/- 0.0555N. Lateral displacement is measured with LVDT's having a linear range of +/- 1.27 mm (not shown). The force required to overcome rolling resistance between the pillow blocks and the guide rails is estimated by placing a weight inside the front box and operating the motor at the same speed used for the experiments. This force is negligible compared to the resistance of the material itself.

Specimens of silty sand were prepared by closing the two boxes together and attaching the loading system so that no gap existed between the two boxes. This required driving the motor and screw mechanism in reverse until the boxes mated. Known masses of material were then placed in the box in

212
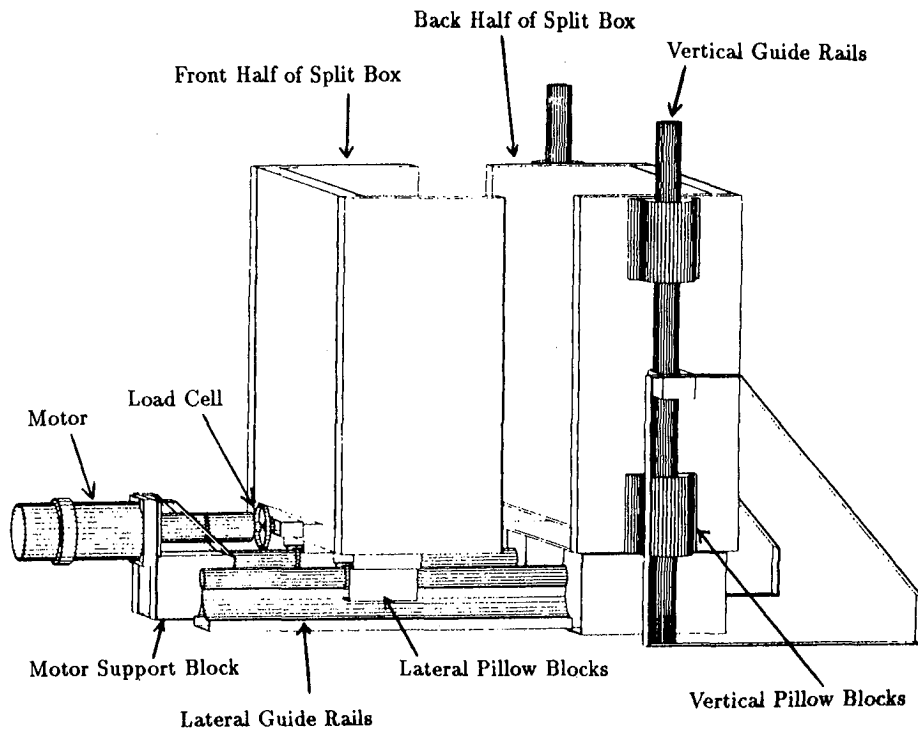
Figure 2: Direct Tension Device (Perkins, 1991)

several lifts and compacted with a small (4cm x 5.5cm) flat metal plate attached to a commercial metal etcher. The metal etcher served to vibrate the plate to provide compaction to the underlying material. Packings approaching 100% relative density have been achieved using this technique. Specimen uniformity is obtained by employing the method of "undercompaction" (2). The lateral earth pressure induced in the sample during preparation was monitored by recording the voltage output from the attached load cell. The specimen is "gripped" by the sides and bottom of the box by lining the inside of the box with coarse sand paper and relying on shear stresses developed between the sand paper and the sand specimen.

Experimental results are expressed as the average stress on the vertical plane of failure versus the displacement of the front box. The average stress on the vertical plane of failure is computed by dividing the measured load from the load cell by the cross sectional area of the plane of split. Results from three experiments on a dense silty sand are shown in Figure 3. The average horizontal stress on the plane of split is compressive at the beginning of the tests due to the lateral earth pressure within the soil mass. As the test proceeds, the average stress tends to decrease towards zero. For materials containing an appreciable tensile strength, it would be expected that the average stress would reach negative values.

The initial state of stress in the specimen depends on the depth within the sample as well as the level of compaction, which determines whether the horizontal stress is less or greater than the vertical stress. Therefore, the initial state of stress is far from uniform. When a uniform tensile load is applied, the soil in the upper portion of the box will experience tensile failure long before the bottom elements. This process is discussed and illustrated in the following section. It will be evident that the peak response from the experimental results is not necessarily the corresponding tensile strength of the material. Furthermore, it is clear that to determine this value one must analyze this experiment while taking into account the influence of the gravitationally induced material stresses and the progressive nature of the tensile failure.

DISCUSSION AND ANALYSIS OF RESULTS: The design of the apparatus and the method of sample preparation allow for the lateral earth pressure (σ_H) in the direction normal to the plane

213
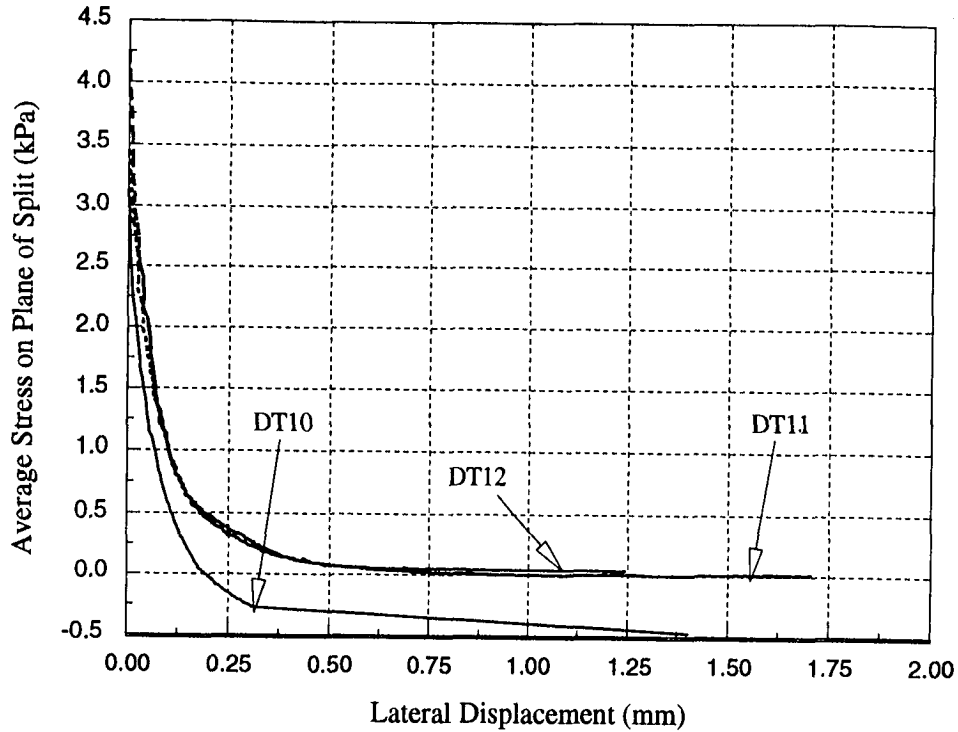
Figure 3: Direct Tension Results (Perkins, 1991)

of split, to be monitored during sample preparation. This was accomplished by using the loading frame assembly to hold the front box against the rear box. As soil was deposited in the box and compacted by vibration, the lateral stress in the direction of travel of the front box was resisted by the loading frame. The load necessary to resist any movement was monitored by the load cell. The coefficient of lateral earth pressure ($K_o = \sigma_H/\sigma_V$) could be calculated assuming a linear distribution of vertical and lateral stress with depth. The load cell reading at the end of sample preparation could be converted to lateral stress by using the vertical cross-sectional dimensions of the box along with the assumption of a linear distribution of stress with depth. This is illustrated in Figure 4. The variation of vertical stress with depth is given by:

$$\sigma_V = \rho g h \tag{1}$$

where ρ is the mass unit weight of the soil, g is the acceleration of gravity and h is the depth below the surface of the soil. The vertical stress in the soil at the bottom of the box is given by:

$$\sigma_V = \rho g H \tag{2}$$

where H is the depth of the box. The average lateral stress perpendicular to the plane of split is given by:

$$\sigma_{H_{avg}} = \frac{P}{A} \tag{3}$$

where P is the load on the front half of the box and A is the cross sectional area of the plane of split. The distribution of σ_H with depth is then:

$$\sigma_H = \frac{2P}{A}\frac{h}{H} \tag{4}$$

so that at the bottom of the box σ_H is given by:

$$\sigma_H = \frac{2P}{A} \tag{5}$$

214

The figure shows stress distribution with depth. Labels in figure: H, h, $\sigma_V = \rho g h$, $\sigma_V = \rho g H$, $\sigma_H = \frac{2P}{A}$, $K_o = \frac{\sigma_H}{\sigma_V}$
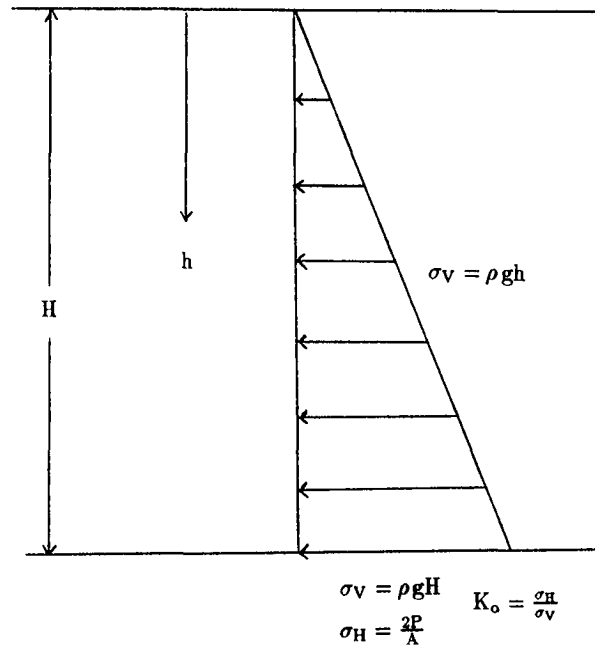
Figure 4: Assumed Distribution of Vertical and Lateral Stress With Depth In The Direct Tension Device

The lateral earth pressure coefficient is then calculated from:

$$K_o = \frac{\sigma_H}{\sigma_V} = \frac{2P/A}{\rho g H} \tag{6}$$

From the above discussion it has been shown that the initial state of stress (immediately following sample preparation) in the direct tension specimen mass is one where one of the principal stresses is directed in the vertical direction (due to the material self-weight) while the other two principal stresses lie in the horizontal plane and are equal and due to the lateral earth pressure condition. If K_o is greater than one then the two lateral principal stresses will be the major and intermediate principal stresses while the vertical stress will be the minor principal stress. If K_o is less than one then the two lateral principal stresses will be the minor and intermediate principal stresses while the vertical stress will be the major principal stress. These conditions are shown in Figure 5 for an element of soil adjacent to the plane of split.

As the load applied to the front of the box is reduced the assumption is made that this reduction in load is applied uniformly to the plane of split. This process is illustrated in Figure 6. In order for this assumption to hold there must be a no-slip condition between the sides of the box and the soil. The sand paper lining on the interior of the box should ensure this condition. This condition would also create shearing stresses in the soil at the soil-wall interface so that the directions of the principal stresses discussed above would apply only to elements sufficiently far from the box walls.

From Figure 6 it is immediately noticed that the upper portion of the specimen will be subjected to tensile stresses long before elements located at the bottom of the box. This suggests that failure in the specimen will progress from the top of the plane of split down to the bottom. This concept is further illustrated in Figure 7 where possible stress paths for various points along a vertical line along the plane of split are sketched on a $p - q$ diagram, where p is defined as the average mean stress $[p = (\sigma_1 + \sigma_2 + \sigma_3)/3]$ and q is defined as the principal stress difference ($q = \sigma_1 - \sigma_3$). The principal stresses are taken as shown in the upper right portion of Figure 7 (i.e. $K_o > 1$). Since the two horizontal stresses (σ_1 and σ_3) are equal at the beginning of the test, q is zero for all points along a vertical line, denoted by varying levels of h. As a uniform load is applied to the plane of split, through the front box, q begins to increase by the same
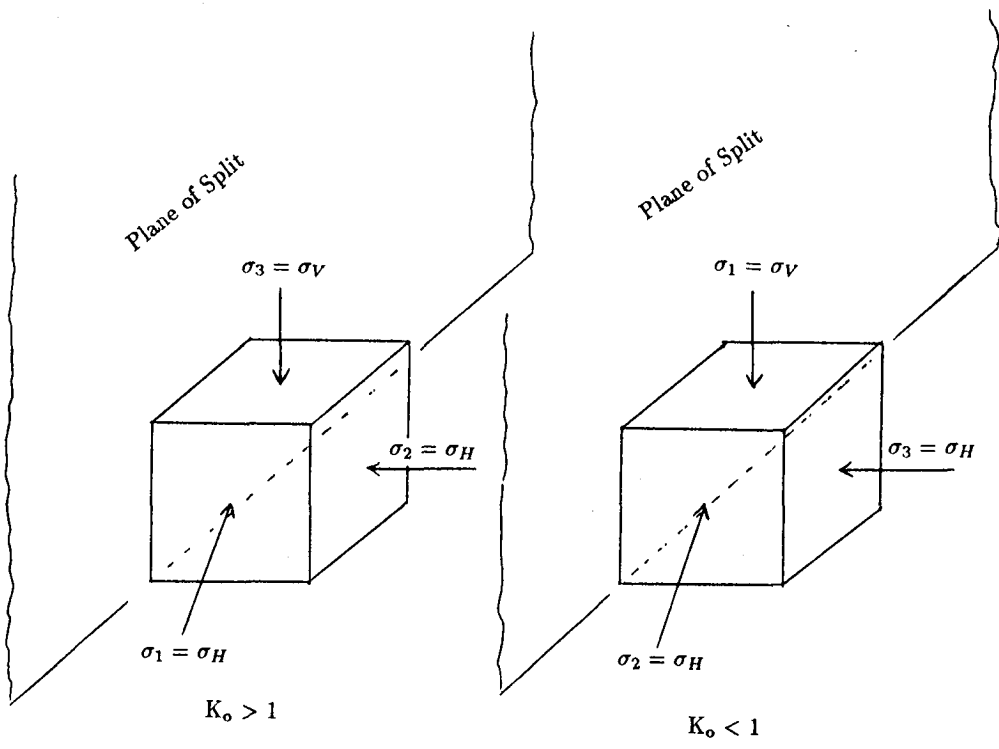
Figure 5: Initial State of Stress in the Direct Tension Specimen
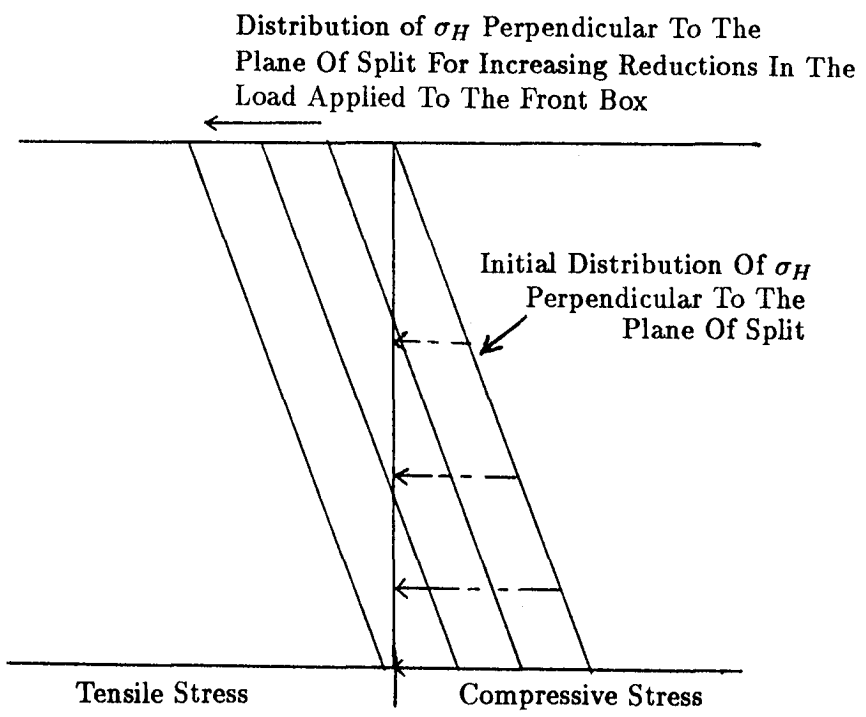
Figure 6: Mechanism of Load Application To The Plane of Split
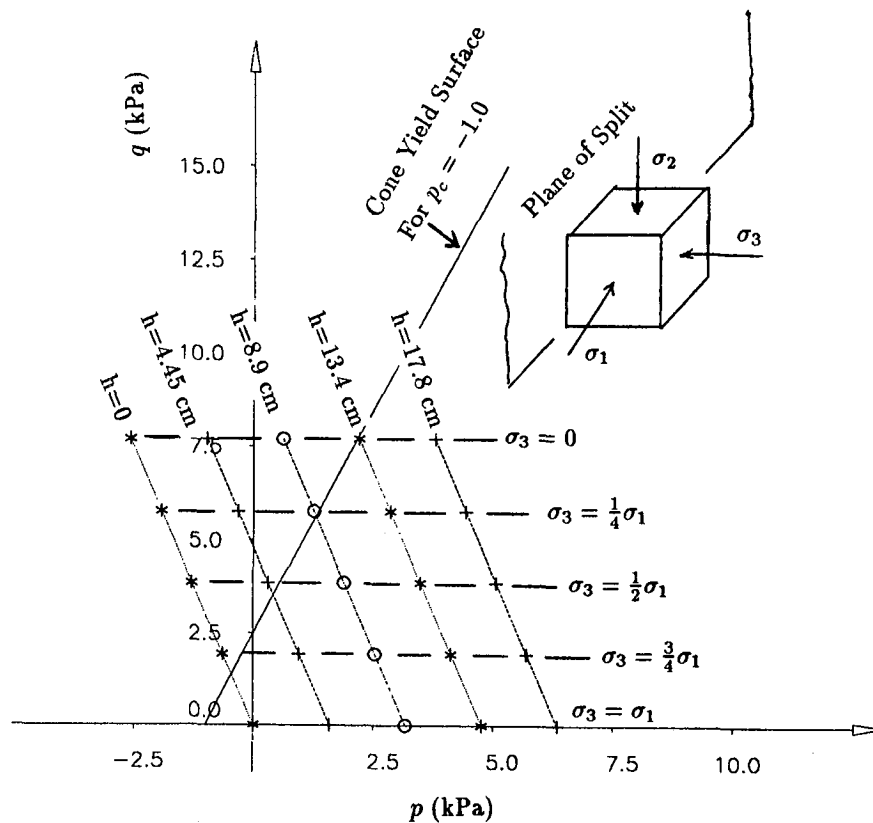
Figure 7: Stress Paths for Direct Tension Loading

amount for all points along a vertical line so that the load steps can be portrayed as horizontal lines on Figure 7. Superimposed on this diagram is a possible failure envelope. This failure envelope was derived from conventional triaxial compression experiments conducted within this range of mean stress. The initial levels of σ_1 and σ_3 in Figure 7 were derived from actual test results. The loading sequence again illustrates that the top elements reach the failure envelope far before elements at the bottom of the box.

A simplistic, mechanistic approach is used to describe the loading and failure conditions present during the direct tension test. The soil specimen is treated as a number of layers whose material properties are identical but whose initial state of stress is governed by the relative vertical position in the soil mass. A simple material model is used to describe the soil's stress-strain characteristics. This model describes the relationship between the stress and strain perpendicular to the plane of split by the elastic modulus in compression and tension (assumed to be equal) and a softening elastic modulus applicable beyond the tensile strength of the material as demonstrated in Figure 8. It is assumed that the material can be described in terms of these elastic parameters for the range of loads considered. Clearly this is an idealization of the true non-linear, elastic-plastic nature of the material, but nevertheless is useful in describing the mechanisms associated with this experiment.

It is assumed that this material model applies to each layer in the divided soil mass. The upper most infinitesimal layer has an initial stress acting perpendicular to the plane of split equal to zero and is denoted as the point at $h = 0$ in Figure 8. Successively deeper layers are treated as elastically preloaded elements and are denoted on Figure 8 as points along the stress-strain curve at successively higher levels of stress and strain. As a uniform displacement is applied to the box, each of these points moves downward in equal increments along the stress-strain curve until the maximum tensile strength (σ_t) is reached, after which the element in the layer softens until the stress perpendicular to the plane of split is zero.

This process can be illustrated by an analogy given by a simple set of springs in parallel where each
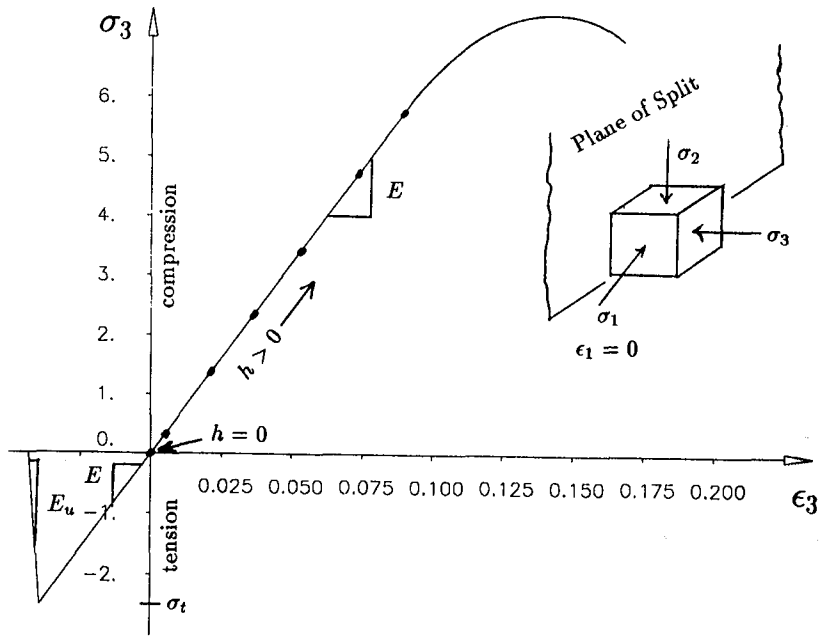
Figure 8: Idealized Stress-Strain Behavior of Soil in Compression-Tension

spring represents a layer of soil, as shown in Figure 9a. Each spring is preloaded by a compressive load, P_i, as shown in Figure 9b. Each spring, having the same spring constant, is then uniformly unloaded by an equal displacement, Δ_j, until each spring reaches its maximum tensile carrying capacity, P_t, after which the spring relaxes according to the spring constant K_u until the spring carries no load. It is seen that this is a progressive process with the upper most springs reaching "failure" before the lower springs.

In Figure 8, if we assume that σ_2 remains constant and that there exists a condition of plane strain in the direction of σ_1, then the stress and strain in the direction of σ_3 are related by:

$$\Delta\sigma_3 = \Delta\epsilon_3 \frac{E}{1 - \nu^2} \tag{7}$$

Assuming values for E, ν, E_u, and σ_t, it is possible to predict the response of direct tension experiments using the density of the soil from these tests to determine initial distributions of σ_3. The response is strain-driven by applying equal increments of strain to each soil layer. As each soil layer reaches the assumed level of σ_t the soil softens along the unloading branch until the stress in the element is zero.

A program was written to perform this analysis where the number of soil layers was included as a variable. The soil mass was divided into 10, 100 and 500 layers. The response appeared more smooth when the number of layers was increased to 100 but little difference was observed by increasing this number further. The initial conditions from an experiment were first used to perform this analysis. An elastic modulus of $E = 6000$ kPa and $\nu = 0.25$ were found to produce results which matched experimental results during the initial part of loading. A tensile strength value of $\sigma_t = -0.1$ kPa was selected at first. The analysis was performed for five values of the unloading modulus, namely $E_u = -E/100$, $E_u = -E$, $E_u = -E * 100$, $E_u = -E * 1000$ and $E_u = -E * 100,000$, corresponding to increasingly brittle behavior. By increasing the absolute value of the modulus E_u the observed effect is to increase the brittleness of the material so that a net negative stress on the plane of failure is never observed. The difference between the response curves for the various values of E_u was insignificant, due primarily to the small level of σ_t. Additional analyses demonstrated greater differences in the softening behavior for larger levels of σ_t. In either case, the behavior was virtually unchanged above levels of $E_u = -E * 100$.
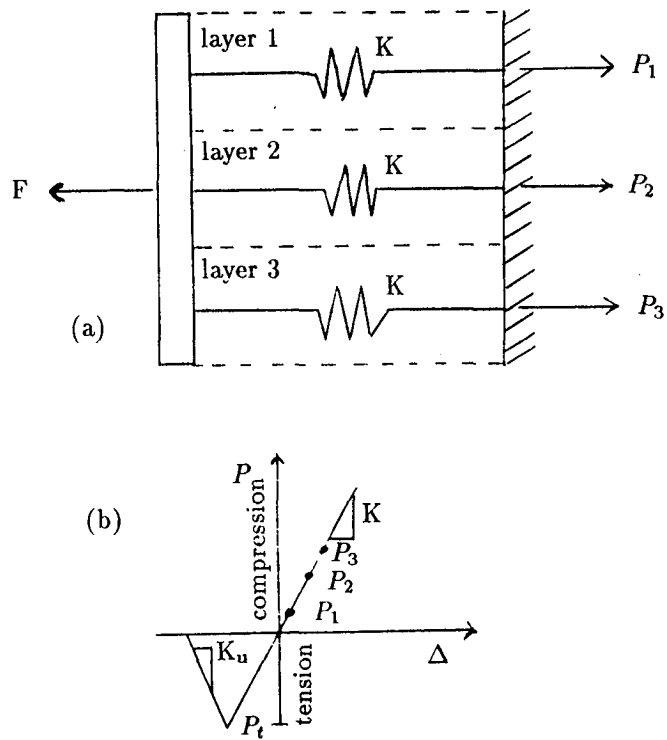
Figure 9: Elastic Spring Model for Layered Soil in Tension
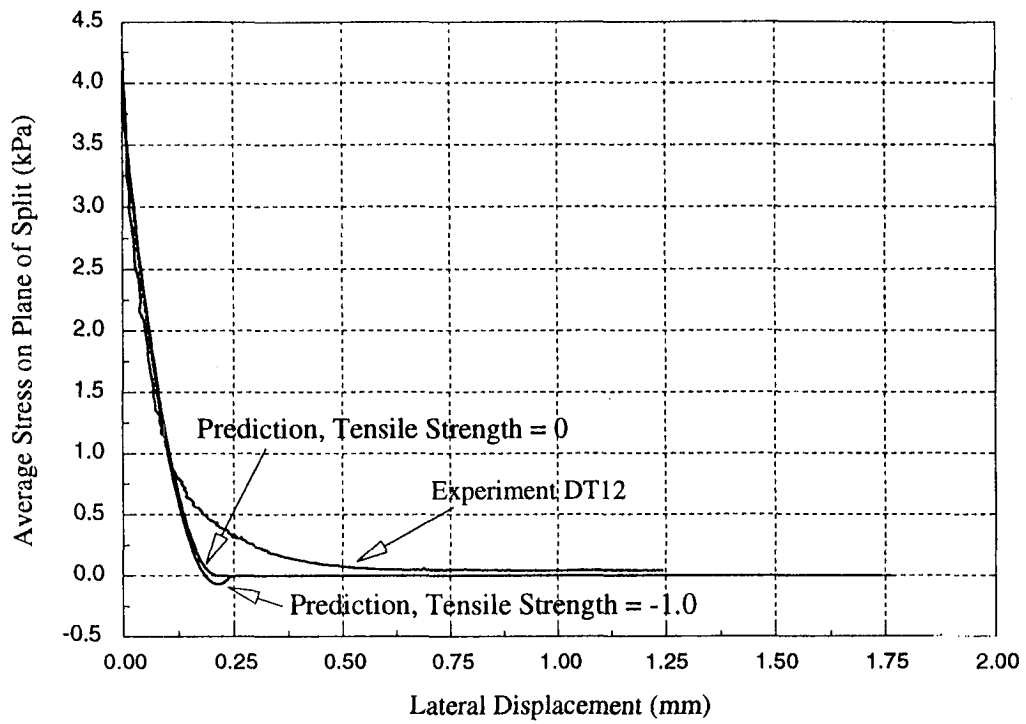
Figure 10: Predictions of Direct Tension Tests for Varying Levels of σ_t

Figure 10 shows predictions for different assumed levels of σ_t for $E_u = -E * 100$. For $\sigma_t = -1.0$ kPa a noticeable peak in the response is observed. Little difference is observed between the results for $\sigma_t = -0.1$ kPa and $\sigma_t = 0$. In these cases the material begins to soften as it approaches the zero average stress level on the plane of split with no peak response being observed. The initial load-displacement curve is matched reasonably well by the predictions as is the final state at large displacements. The softening behavior, however, is not matched very well for this material model. For low levels of tensile strength the response curve approaches the zero stress line rather abruptly. The predictions tend to show far more brittle behavior than the experiments.

CONCLUSION: The above direct tension experiment and analysis approach serves to illustrate important fundamental material behavior of frictional granular materials. The material model proposed for the analysis of the experiment relies on simple linear elasticity principles. In addition to this material model, the student can try other models, some of which might include a parabolic shaped stress-strain curve in compression and tension, or elastic moduli that vary from each material layer.

REFERENCES:
(1) Perkins, S.W. (1991) "Modeling of Regolith Structure Interaction in Extraterrestrial Constructed Facilities", Ph.D. Thesis, University of Colorado at Boulder, 324 p.
(2) Ladd R.S. (1978), "Preparing Test Specimens Using Undercompaction", *Geotechnical Testing Journal*, GTJODJ, V.1, No.1, pp.16-23.

APPLICATION OF HARDNESS TESTING IN FOUNDRY PROCESSING OPERATIONS: A UNIVERSITY AND INDUSTRY PARTNERSHIP

Donald H. Martin

School of Manufacturing Technology
Tri-State University
300 South Darling
Angola, Indiana 46703

Telephone 219-665-4265

and

Bruce Lash

Q. A. Manager
AL-FE Heat Treating, Inc.
Columbia City, Indiana 46725

APPLICATION OF HARDNESS TESTING IN FOUNDRY PROCESSING OPERATIONS: A UNIVERSITY AND INDUSTRY PARTNERSHIP

Donald H. Martin, Associate Professor
School of Manufacturing Technology
Tri-State University, Angola, IN 46703
and
Bruce Lash - Q.A. Manager
AL-FE Heat Treating, Inc.
Columbia City, IN 46725

KEY WORDS: Partnership, Brinell Hardness, Hardness, ASTM Standards, Brinell Scope, Hardness Equation, Hardness Conversion Scales, Tensile Strength.

PREREQUISITE KNOWLEDGE: The student should understand the concept of tensile strength of materials either previously or concurrently presented with the experiment.

OBJECTIVES:

1. Plant tour of local manufacturing facility to observe hardness ·testing methods used and how they support the manufacturing process today.

2. To learn the operation of Brinell <u>Hardness</u> Testing, equipment set up with samples of accessory equipment for testing of various materials.

3. Use of <u>Brinell Scope</u> (hand magnifier) to measure the diameter of the test indentation (in millimeters).

4. Use of the <u>hardness equation</u> to determine the spherical area of the indentation and the calculation of the Brinell Hardness Number.

5. Use of standard charts for <u>ASTM standard</u> size indenters to find the hardness number.

6. Method of <u>conversion</u> of the Brinell number to other hardness scales, their common usage, and also to convert the hardness number to the approximate <u>tensile strength.</u>

EQUIPMENT AND SUPPLIES: Selection of metal test samples; Brinell hardness tester; hand held magnifier (Brinell Scope); ASTM reference hardness charts.

PROCEDURE:

PHASE I

Tour of Foundry or Foundry Support Manufacturing Facility:
Tour of AL-FE Heat Treating, Inc., Columbia City.

1. RECEIVING

When material is received at the Columbia City division, it
is held at the dock until the following is accomplished:
Identified
- a.   by alloy
- b.   by quantity
- c.   by any damage
- d.   by parts matching Bills of Lading
- e.   by serialized work order identification tag:
  1.   Al-Fe Heat Treating, Columbia City
  2.   customer name
  3.   packing slip number if any
  4.   customer ID #
  5.   work order number for each container
  6.   part number
  7.   date received
  8.   container 1 of 1
  9.   quantity

2. STORAGE

The material is then placed in the as-cast area. There are
two divisions of as-cast materials, 1. regular process and
2. special process.

3. HEAT TREAT CONTAINER LOADING

All material is loaded into heat treat containers using the
following criteria:
- a.   alloy specific
- b.   process temp.
- c.   process time
- d.   specific quench requirements
- e.   damage prevention
- f.   weight limitations

4. SOLUTION TREATING

To take advantage of the precipitation hardening reaction,
it is necessary first to produce a supersaturated solid

solution. The process by which this is accomplished is called solution treating. It consists of soaking the alloy at a temperature sufficiently high to achieve a nearly homogeneous solid solution and then quenching fast enough to retain the solute in solution. The temperature is kept low enough so that eutectic melting does not occur.

5. QUENCHING (i.e. controlled cooling)

The quench portion of the process can be accomplished by either room air cooling, forced air cooling, water, or polymer. To avoid the type of precipitation detrimental to mechanical properties or corrosion resistance, the solid solution formed during solution treating must be rapidly cooled to produce a supersaturated solution at room temperature, the optimum condition for subsequent precipitation and hardening. This is usually accomplished by immersing the parts in cold water.

6. ROOM AGE

Room age is part of the process that is time dependent as specified by the customer and this specification then becomes part of our process. The length of time can be 15 min. minimum to any number of days.

7. ARTIFICIAL AGE

This part of the process, which is an accelerated age cycle, is dependent on time and temperature. Through this process we achieve the customer's required specific hardness.

8. HARDNESS CHECKING

In our Heat Treating process, we'll use the following hardness testing methods: Brinell, Rockwell, and Impression.

9. SHIPMENT

All material is packaged to prevent damage in transit, and the material is identified with an "OK-TO-SHIP" tag providing the batch number, inspector name, and date of inspection. Material is CERTIFIED, per customer request, stating the process performed.

PHASE II

1. After the professor has demonstrated the hardness test, measured the specimen, calculated the hardness number, and

made an equivalent chart determination, all class members will take turns repeating the measurement.

2. Before testing each specimen, measure the thickness and record on a data sheet; then insert the specimen in the tester and build up to the specified pressure shown on Chart 1. Hold pressure the specified time and release.

3. Remove specimen from tester, and with magnifier, (Brinell Scope) measure the indenter diameter in millimeters.

4. Calculate the Brinell Hardness Number and record on the data sheet. Check this number with the thickness in the Chart II, to see if an anvilling error exists. ie: If the hardness number is less than that of the table, you are "testing the hardness of the anvil" instead of the specimen (must use a thicker material for a valid reading).

5. Utilizing the wall chart and additional conversion charts, fill in the remaining columns of the data sheet.

6. The far right hand column is reserved for comments if difficulty is experienced. If specimen is too thin and reading is INVALID, write ANVILLING in this space.

This table shows that a single Brinell Number represents a specific hardness. (Thus, using different loads on the same material gives different indentations, but gives the same Brinell Number for the one material!)	Examples of use of ASTM E-10 Table:			
		LOAD		Spec.
	BHN	3000	1500	500	No.
	341	3.30	2.35		1
	302	3.50	2.50		2
	262	3.75	2.70		3
	223	4.05	2.90		4
	159	4.75	3.40	2.00	5
	128	5.25	3.80	2.20	6
	101	5.85	4.25	2.50	7
	81	6.45	4.70	2.77	8

Diameter is shown in millimeters
Load is in Kgf

HARDNESS CONVERSIONS

FOR CONVERSIONS TO TENSILE STRENGTH AND TO OTHER HARDNESS SCALES, USE APPROXIMATE CONVERSION CHART ON NEXT PAGE.

From a Brinell hardness reading, read from the scale at the
top, go down to the Brinell "curve" and then horizontal to the
left for the approximate ultimate tensile strength.

From this horizontal line, intersecting other curves, go to
the respective scale to read the approximate hardness conver-
sion to that scale.

```
RULES FOR ESTIMATING TENSILE
STRENGTH FROM BRINELL HARDNESS:
   (For steel)
Under 175 HB:
 HB x 515 = Tensile (psi)
Over 175 HB:
 HB x 495 = Tensile (psi)
```

PSI = Pounds per square inch

GRAPH SHOWING APPROXIMATE CONVERSIONS OF DIFFERENT HARDNESS SCALES
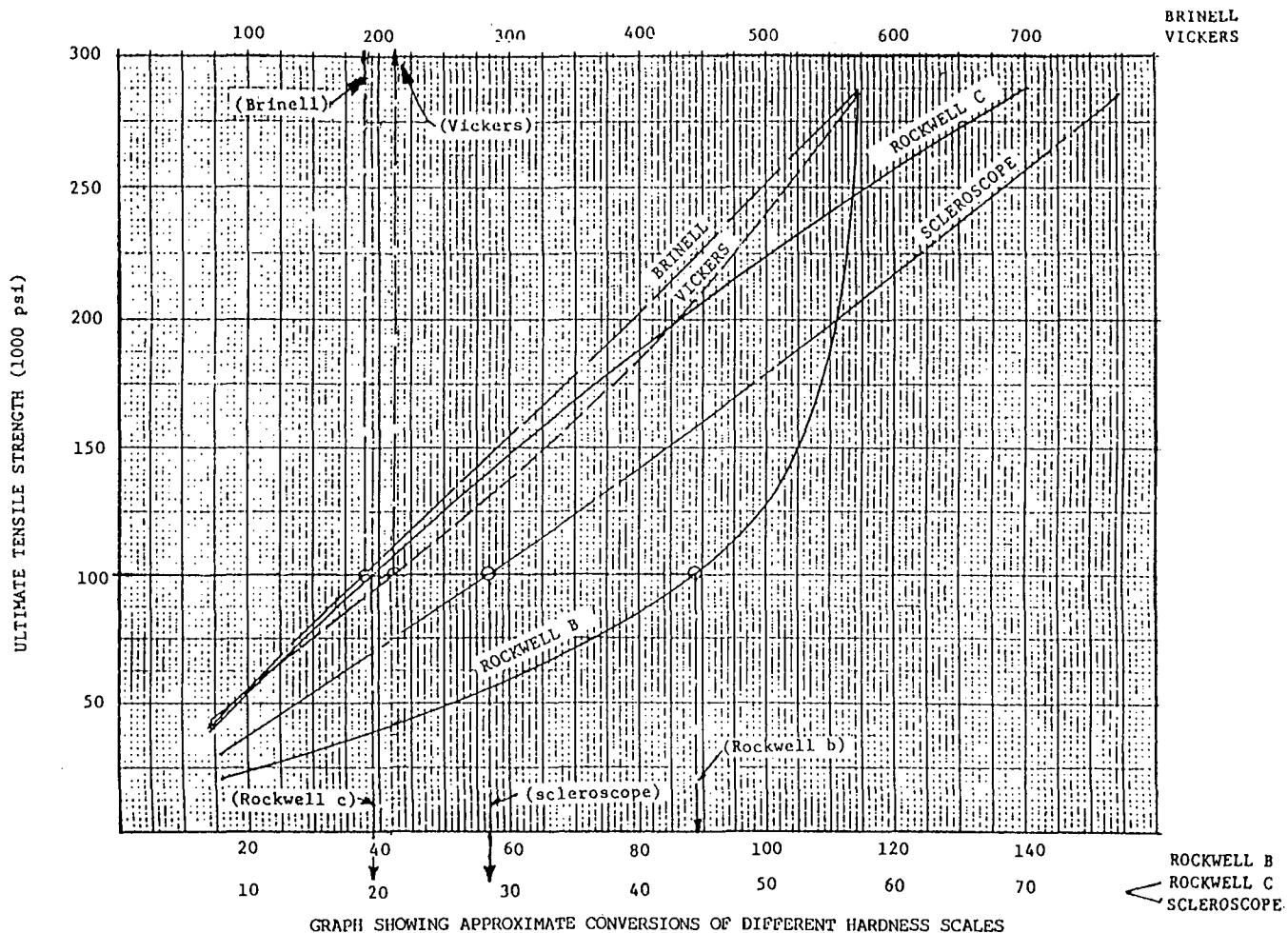
CHART I.

BRINELL HARDNESS EQUATION:

$$HB = \frac{2\ P}{\pi\ D\ (D - \sqrt{D^2 - d^2})}$$

Where:

P = Load in kilograms K_{gF}

D = Ball diameter (10 mm $\pm$.005 mm)

d = Indentation (mean diameter in mm)

HB = Hardness Brinell in Kgf/mm^2

INDENTERS: Steel ball (Vickers hardness 850) for use under 450 HB of specimen. Hultgren ball for use in specimens with hardness less than 500 HB Carbide ball for use with specimens of hardness less than 630 HB. (Impression diameter must be 2.50 to 6.00 mm and 25-60% of ball dia.) (Load duration shall be between 10-15 seconds, at full load).

HARDNESS SPECIFICATION: Example: 63 HB 10/3000/12 means 63 Brinell hardness measured using a 10mm ball and a load of 3000 kg_F for 12 seconds. (If the load is not specified, 3000 kg_F shall be assumed.)

INDENTATION READING TOLERANCE (per ASTM): diameter to 0.1 mm and estimate to .02 mm.

SPACING OF INDENTATIONS: Spacing of two adjacent readings or spacing to a corner shall be a minimum of two and one half times the diameter of the indentation (2 1/2 d).

CHART II

LOAD APPLICATION AND ANVILLING EFFECTS (ASTM Standard and Scott modification)

BRINELL HARDNESS RANGE: (Overlapping ranges) 2.00 mm d to 6.99 mm d	96 to 600 HB	48 to 300 HB	16 to 100 HB
Kg (F)	3000 Kg$_f$	1500 Kg$_f$	500 Kg$_f$
Pound (Equiv.)	6613.85 #	3306.93 #	1102.31 #
Scott Pressure Gauge (Compr. Spec.) w/ .372 in^2 Area (.6882 dia RAM)	(17,779. psi) Beyond Range of Scott	8,890. psi	2,963. psi
Best Relation of Load to ball dia.	$\frac{P}{D^2} = 30$ (or $P = 30D^2$)	$\frac{P}{D^2} = 15$	$\frac{P}{D^2} = 5$
Best Ball Dia.	10 mm	10 mm	5 mm
ANVILLING EFFECTS: Min. Thickness Metal Sample	Minimum HB for thickness of specimen to prevent mushrooming far side.		
Reqd. 1/16 inches	602	301	100
Reqd. 1/8 inches	301	150	50
Reqd. 3/16 inches	201	100	33
Reqd. 1/4 inches	150	75	25
Reqd. 5/16 inches	120	60	20
Reqd. 3/8 inches	100	50	17

(Anvilling gives incorrect data by reading partial hardness of anvil, instead of specimen.)
Softer loads of 250, 125 and 100 Kg$_F$ are standard and are occasionally used.

230

DATA LOG TABLE   Date:_____

P LOAD	MATERIAL	SKETCH	THICK-NESS	Dia. D mm.	BRIN-ELL HB	Vickers	Mohs	TENSILE STRENGTH p: i	COMMENTS (Evidence of Anvilling)

INSTRUCTOR NOTES: "Hardness" is a term that has different meanings to different people. It is resistance to penetration to a metallurgist, resistance to wear to a lubrication engineer, a measure of flow-stress to a design engineer, resistance to scratching to a mineralogist, and resistance to cutting to a machinist. Although these several actions appear to differ greatly in character, they are all related to the plastic flow-stress of the material.

To avoid misapplication of Brinell hardness testing, the fundamentals and limitations of the test procedure must be clearly understood. Further, to avoid inaccuracies some general rules should be followed:

1. Indentations should not be made on a curved surface having a radius of less than 1 inch.

2. Spacing of indentations should be correct, as outlined in the ASTM section, "Spacing of Indentations."

3. The load should be applied steadily to avoid overloading caused by hand-inertia on the weights.

4. The load should be applied in such a way that the direction of loading·and the test surface are perpendicular to each other within a 2° angle.

5. The thickness of the workpiece being tested should be such that no bulge or mark showing the effect of the load appears on the side of the workpiece opposite the indentation. Very soft samples are unsuitable.

6. The surface finish of the workpiece being tested should be smooth, so the indentation diameter is clearly outlined.

REFERENCES:
ASM, "Hardness Testing", Materials Park, OH, 1987.
ASM, "Metals Handbook, Desk Edition", 1985 - Metals Park, OH; Boyer, H.E. & Gall, T.L., editors, pp. 33-4.
American Society For Testing and Materials (A.S.T.M.), Standards E 6, E 10, A 370, E 110.

Budinski; "Engineering Materials; Properties and Selection", 3rd ed.; Prentice-Hall, Englewood Cliffs, N.J., 1989.

Jacobs, J.A. & Kilduff, T.F. "Engineering Materials Technology", Prentice-Hall, Englewood Cliffs, N.J., 1985.

Van Vlack, L.H., "A Textbook of Materials Technology", Addison-Wesley, Reading, MA 1973.

LABORATORY EXPERIMENTS IN INTEGRATED CIRCUIT FABRICATION

Thomas J. Jenkins
and
Edward S. Kolesar

Professor of Electrical Engineering
Department of Electrical and Computer Engineering
(AFIT/ENG Bldg. 640 Area B)
Air Force Institute of Technology
Wright-Patterson Air Force Base
Ohio 45433-6583

Telephone 513-255-3708; 4960; 6027

LABORATORY EXPERIMENTS IN INTEGRATED CIRCUIT FABRICATION

Thomas J. Jenkins, Capt, USAF

Edward S. Kolesar, PhD, P.E., Lt Col, USAF

Air Force Institute of Technology

Department of Electrical and Computer Engineering

(AFIT/ENG, Bldg 640, Area B)

Wright-Patterson Air Force Base, Dayton, OH 45433-6583

KEY WORDS: cross-bridge test structure, diffusion, integrated circuit (IC), metallization, metal-oxide-semiconductor (MOS) capacitor, metal-oxide-semiconductor field-effect transistor (MOSFET), oxidation, photolithography, pn-junction diode, semiconductor, silicon, transfer length method (TLM) test structure.

PREREQUISITE KNOWLEDGE: The student should understand the concepts associated with silicon integrated circuit (IC) fabrication, such as oxidation, photolithography, diffusion, and metallization. Also, the student should understand the theory of operation of metal-oxide-semiconductor (MOS) devices and pn-junctions. The fabrication concepts can be presented in advance of, or concurrently with, the experiment. However, the theory of operation of the devices must be mastered prior to implementing the laboratory experiments.

OBJECTIVES: The objectives of the experiment are fourfold: 1) to provide practical experience implementing the fundamental processes and technology associated with the science and art of IC fabrication, 2) to afford the opportunity for the student to apply the theory associated with IC fabrication and semiconductor device operation, 3) to motivate the student to exercise engineering decisions associated with fabricating integrated circuits, and 4) to complement the theory of n-channel MOS and diffused devices that are presented in the classroom by actually fabricating and testing them. Therefore, a balance between theory and practice can be realized in the education of young engineers, whose education is often criticized as lacking sufficient design and practical content[1].

EQUIPMENT AND SUPPLIES: The equipment required to implement this laboratory experiment is listed in Table I. The equipment list is partitioned into two principal categories. The first category is associated with the fabrication process. The second category is related to process characterization and testing the fabricated devices.

Table I. Laboratory Materials and Equipment

Fabrication Process:

Convection Ovens
Model Imperial IV, Lab-Line Instruments, Inc., Melrose Park, IL
Crystal Thickness Monitor
Model TM-100R, Maxtek, Inc., Torrance, CA
Diffusion/Oxidation Furnace
Model 4100, Thermco Products Corp., Orange, CA
Mask Aligner
Model MJB3, Karl Suss America, Inc., Waterbury Center, VT
Metallization System
Model DV602, Denton Vacuum, Cherry Hill, NJ

Process Characterization and Device Test:

Ellipsometer
Model L117, Gaertner Scientific Corp., Chicago, IL
Four-Point Probe
Model AP-150, Veeco Instruments Inc., Plainview, NY
Low-Frequency Impedance Analyzer
Model HP 4192 A, Hewlett Packard, Palo Alto, CA
Micromanipulators and Probe Station
Model 6200, Micromanipulator Co., Inc., Carson City, NV
Multimeter
Model HP 3478 A, Hewlett Packard, Palo Alto, CA
Optical Microscope Interferometer
Model 255574, Wild Heerbrugg Ltd., Heerbrugg, Switzerland
Photoresist Spinner
Model 1-PM101D-R790, Headway Research Inc., Garland, TX
Profilometer
Model Dektak IIA, Sloan Technology Corp., Santa Barbara, CA
Semiconductor Parameter Analyzer
Model HP 4145 B, Hewlett Packard, Palo Alto, CA

PROCEDURE: For a typical ten-week academic quarter, the student accomplishes five distinct, two-week fabrication and testing exercises: oxidation, photolithography, diffusion, metallization, and test. While some of the exercises are obviously repeated throughout the laboratory, such as photolithography, the student's introduction to a distinct process is emphasized during each of the two-week exercises. For example, oxidation is initially introduced during the first meeting of the laboratory. In the next exercise, the student explores photolithography and the conditions required for optimal exposure and development of the photoresist. However, during subsequent exercises, the results of both the initial oxidation and photolithography exercises are reinforced and utilized, but the emphasis shifts toward exploring other process control variables, such as optimal etch times and etch rates.

To implement the laboratory experiments, the student uses a four-level photomask set, which is illustrated in Figures 1-6. Successful implementation of the individual exercises in this laboratory experiment yields *pn*-junction diodes, cross-bridge test structures, transfer length method (TLM) test structures, metal-oxide-semiconductor field-effect transistors (MOSFETs), and MOS capacitors.

1. Initial Oxidation Exercise.

The first laboratory exercise provides the students' orientation with the IC fabrication facilities, as well as a closely supervised oxidation experiment. During the orientation, the students receive specialized instructions concerning the proper operation of the laboratory equipment. The instructions also include specific safety concerns appropriate for the equipment or process. After the students have demonstrated their proficiency with the laboratory equipment or a specific process, only minimal supervision is required. This situation affords the student the opportunity to exercise engineering design and decision skills. This general administrative process is repeated during the later exercises, as required.

Each student is furnished with one copy of the photomask set and ten silicon wafers at the beginning of the laboratory experiment. The silicon wafers are prime grade, (100)-oriented, p-type (boron doped) with a nominal resistivity of 6-18 Ω·cm. Before transferring the wafers to the students, they are thermally oxidized at 1100°C for 485 minutes with dry oxygen by the students (in conjunction with close supervision by a laboratory technician) during the first meeting of the laboratory. Since these oxidized wafers will serve as the starting material for the subsequent phosphorus diffusion exercise, the oxide thickness needs to be approximately 450 nm.

Before initiating the photolithography exercise, the student estimates the oxide thickness on a representative wafer using an oxide color chart and measures it with an ellipsometer. With this information, the student can correlate the measured oxide thickness with the
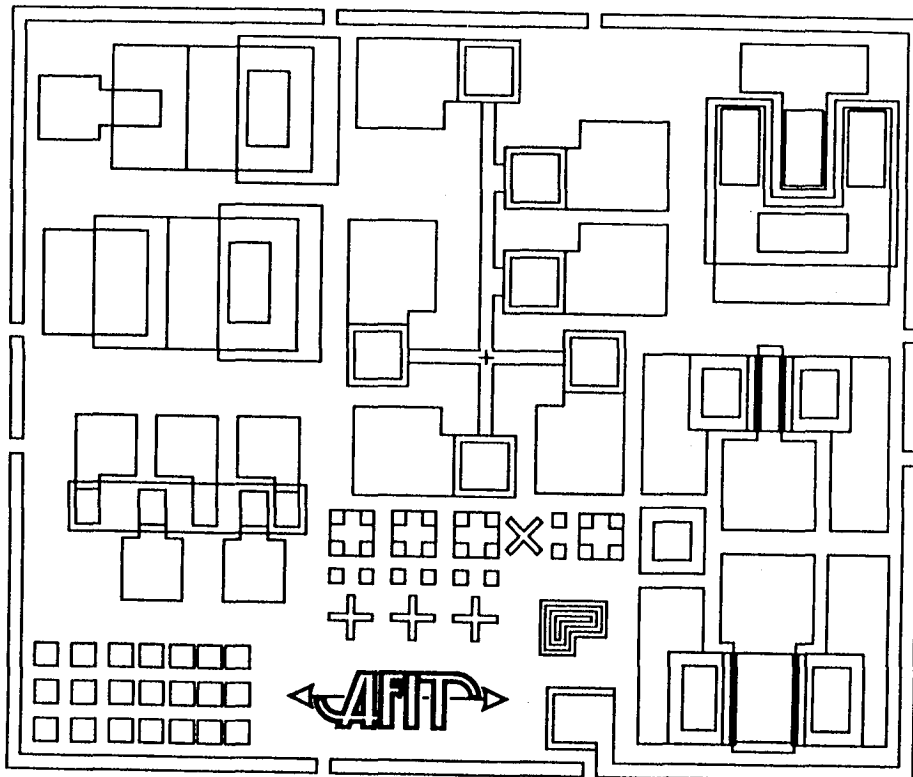
Figure 1. Composite view of the four-level photomask reticle.
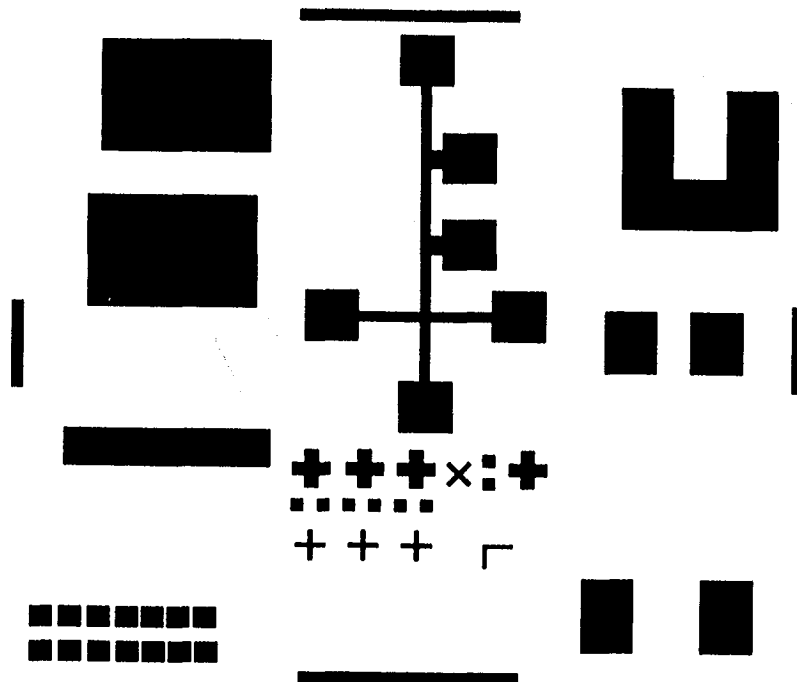
Figure 2. Level-one photomask reticle used during the diffusion exercise.

238
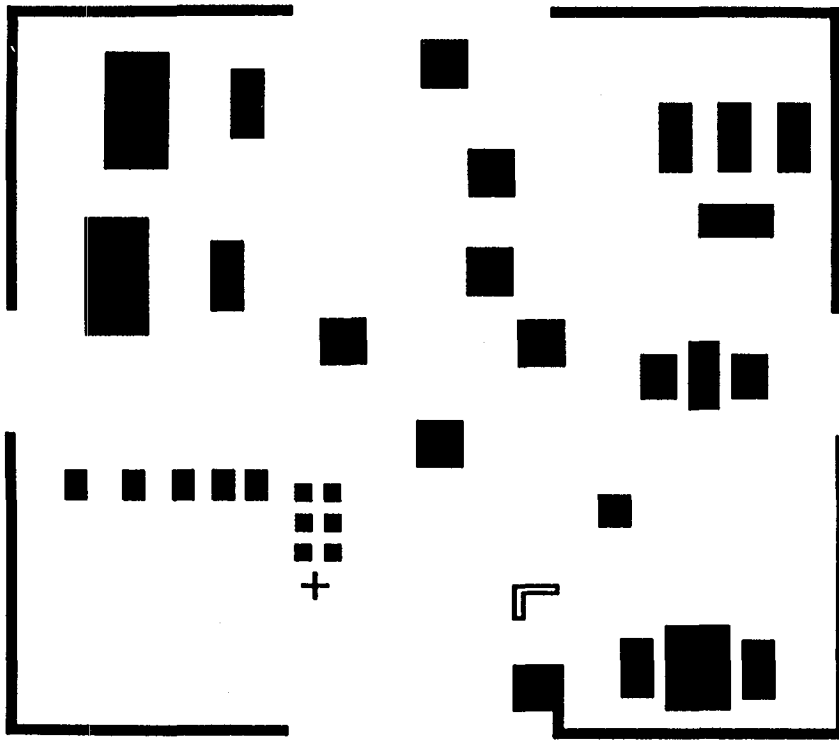
Figure 3. Level-two photomask reticle used during the gate-oxidation exercise.
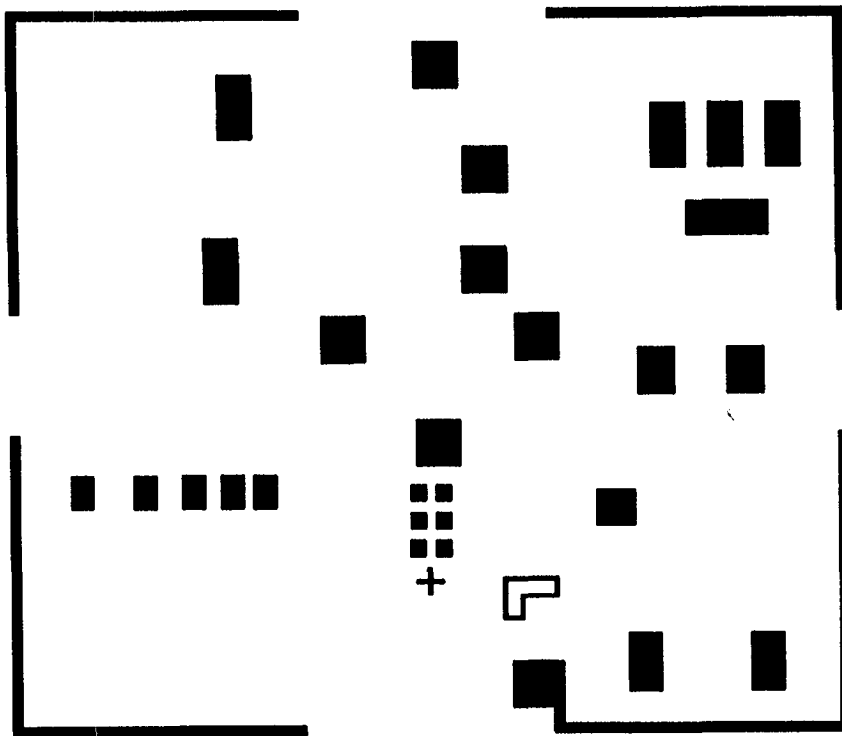
Figure 4. Level-three photomask reticle used to define the semiconductor-metal contacts.

239
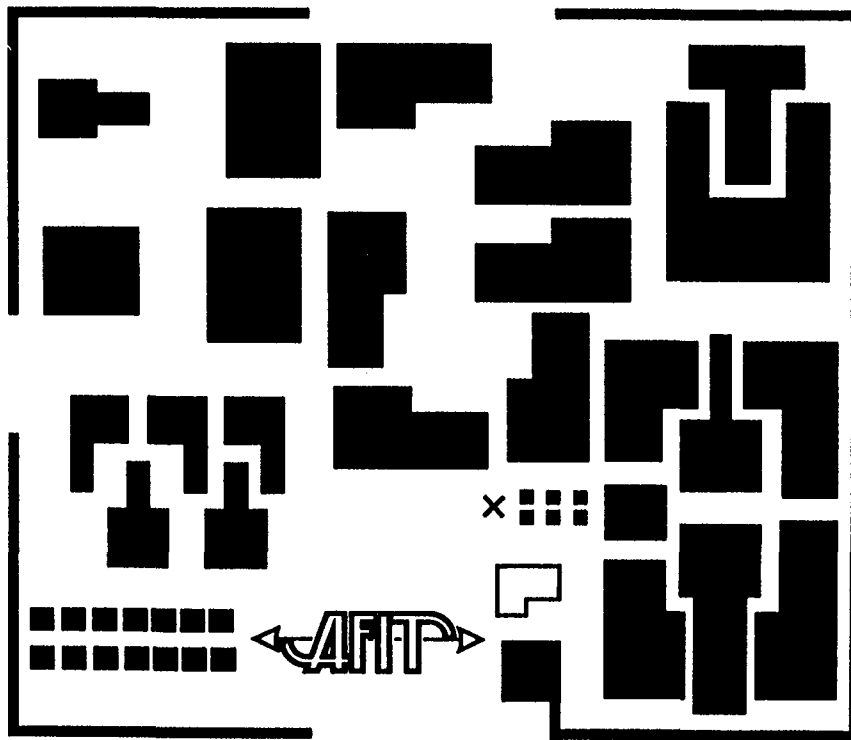
Figure 5. Level-four photomask reticle used during the metallization exercise.
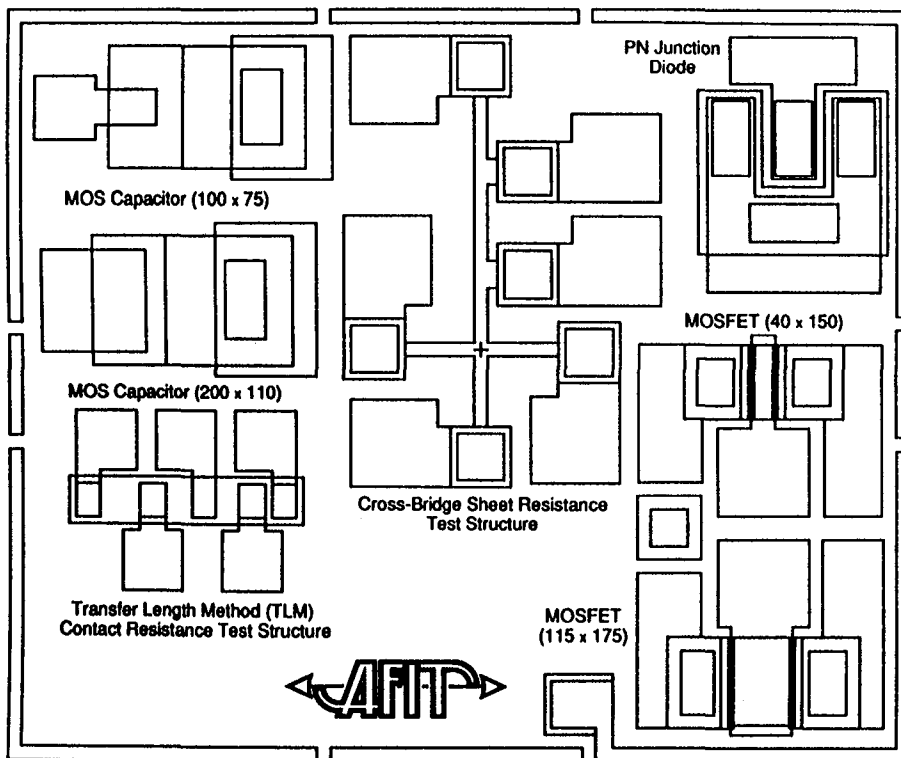
Figure 6. Relative location of the fabricated devices within the photomask reticles.

processing conditions actually utilized during the initial oxidation exercise and the predicted results obtained by simulating it with the *TSUPREM-4* (Technology Modeling Associates, Inc., Palo Alto, CA) software[2]. In a supplemental appendix to the student's laboratory hand-out, an introductory guide to using *TSUPREM-4* is provided. The results of the simulated oxidation process are depicted in Figure 7a.

2. Photolithography Exercise.

In this exercise, the student prints the Level-One Diffusion Photomask pattern on the pre-oxidized silicon wafers. This pattern will subsequently be etched through the oxide. The etched oxide is used to provide a mask for the subsequent diffusion of the n-type (phosphorus) dopant. The reticle of this photomask is depicted in Figure 2.

Having previously characterized the thickness of the oxide, the student is directed to complete the following steps:

(1) The pre-oxidized wafers have been stored in a photoresist post-bake oven to prevent moisture absorption; therefore, the N_2 gas supply is turned-off before the wafers are removed. To prepare the wafers for the first negative photoresist printing, they must be cleansed of organic surface contaminants. To accomplish this task, either,

(a) Immerse each wafer into a beaker of acetone and mechanically agitate it for 30 seconds and follow this step with an immersion into a methyl alcohol ultrasonic bath for 1 minute, or,

(b) Immerse the wafers into a modified piranha solution composed of H_2SO_4 : H_2O_2 (3:2), whereby the exothermic reaction makes it self-heating. For safety reasons, this solution must be prepared by adding the H_2O_2 to the H_2SO_4. The wafers should be cleaned for 20 minutes.

(c) After accomplishing either step (a) or (b), the wafers should be rinsed in deionized (DI) water, blown dry with N_2, and pre-baked at 200°C for 45 minutes to remove surface moisture.

(2) After the wafers cool to room temperature, the HR200 negative photoresist, manufactured by Waycoat, Inc., is deposited on the wafers using a photoresist spinner. To implement this step, the student should flood the center of the wafer with the photoresist which is dispensed from an eyedropper. There should be a two-inch diameter puddle of photoresist in the center of the wafer. The wafer should be spun at 5000 rpm for 15 seconds to uniformly distribute the photoresist.

(3) The wafers should then be pre-baked in the photoresist oven at 65°C for 15 minutes to evaporate the solvents from the photoresist and harden its surface.

Etched Diffusion Mask
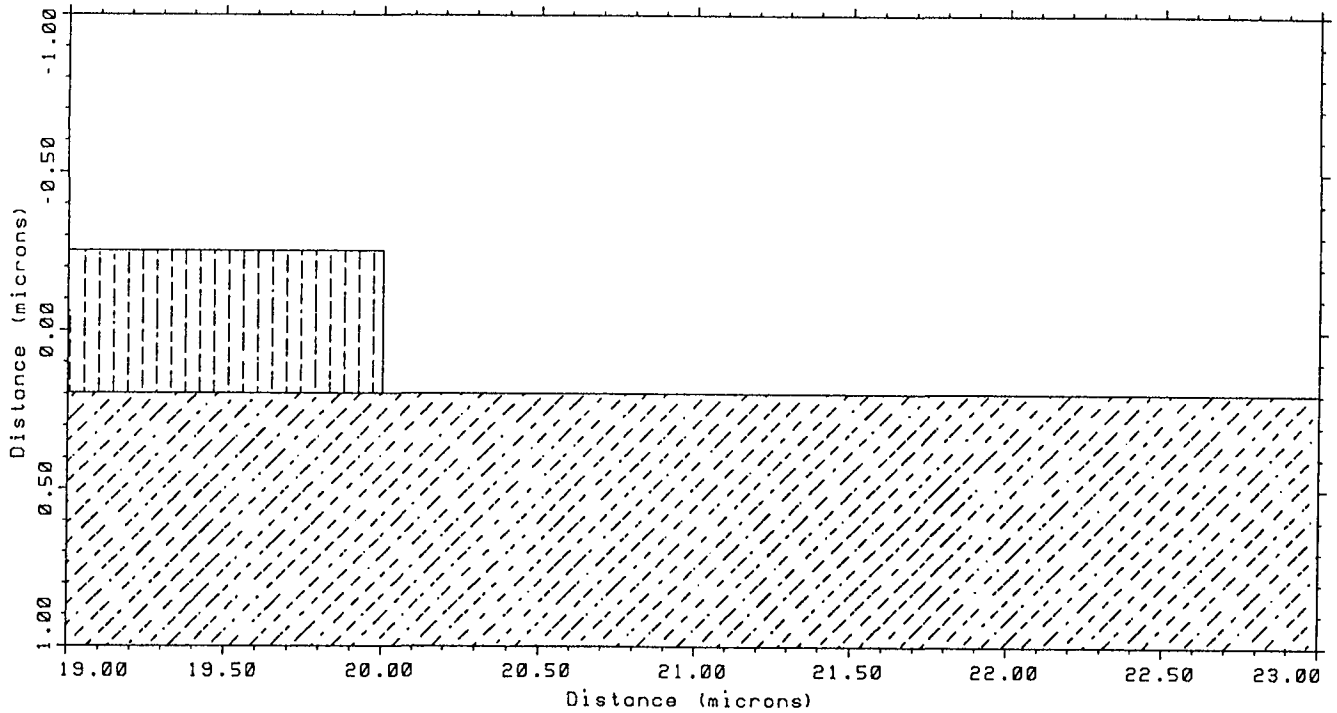
Figure 7. Samples of the simulation results using the *TSUPREM-4* software.
a) Diffusion-mask oxide thickness. b) Junction depth resulting from the diffusion and
the gate-oxidation processes. c) Gate-oxide thickness. d) "Small-Gate" MOSFET
cross-section.

(4) Each photoresist-coated wafer should be printed using a mask aligner and the level-one Diffusion Mask reticle that is depicted in Figure 2. The photomask and photoresist coated wafer "sandwich" should be exposed to the UV light source for 10-30 seconds. Due to the number of variables involved, the student will have to determine the optimum exposure duration experimentally. However, due to the geometries of the devices, the negative photoresist can be overexposed without seriously jeopardizing the chances that the student can realize functional devices.

(5) The exposed photoresist covered wafers should be developed by implementing the following procedure: a wafer is positioned on the vacuum chuck of the photoresist spinner configured for developing, and while being spun at 500 rpm, xylene is sprayed onto it from a squeeze bottle for 30 seconds; next, butyl acetate is sprayed for 30 seconds; and finally, the wafer is blown dry with an N_2 purge for 30 seconds.

(6) The printed wafers should then be inspected under an optical microscope to confirm proper image alignment and pattern definition. However, since the level-one Diffusion Photomask is the first photomask, proper image alignment is only a concern for those photomasks which follow the level-one Diffusion Photomask. If the photoresist is underdeveloped, step (5) should be repeated. If the image features are misaligned, the remaining photoresist should be stripped using the plasma asher, cleaned, pre-baked, and the process should be repeated beginning with step (2). An example of an acceptable image alignment of the "L-shaped" alignment mark is depicted in Figure 8.

(7) The satisfactorily processed wafers should be transferred to a post-bake oven set at 135°C for 15 minutes to further harden and promote the adherence of the patterned photoresist. The photoresist product literature and a stylus profilometer can be utilized to determine the final thickness of the photoresist on a representative control sample wafer.

(8) The wafers should be inspected with an optical microscope (dark-field mode). If the photoresist has pinholes, it must be stripped, and the process should be restarted with step (2).

(9) The wafer's oxide that is exposed through the open photoresist windows should be etched using a buffered HF (NH_4F : HF, 4:1) solution.

   (a) Fresh etchant should be mixed sufficiently early to let it stabilize (2 hours) before it is used. Nevertheless, it must also be used within 6 hours after mixing.

   (b) The wafers should be individually etched. The introduction of bubbles into the etchant should be avoided.

   (c) Periodically (30 second intervals), each wafer should be removed from the etchant, rinsed thoroughly in deionized (DI) water, blown dry with N_2, and inspected for etch
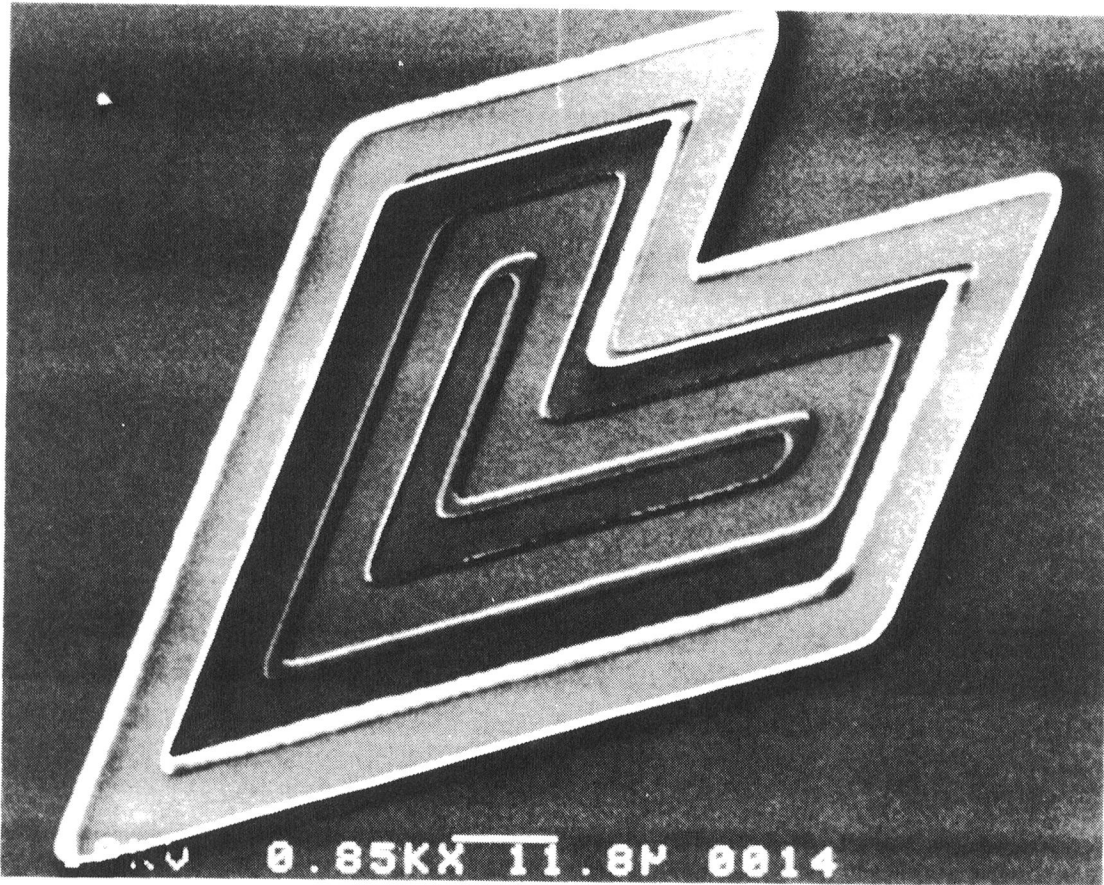
Figure 8. Example of an acceptable image alignment using the *"L-shaped"* alignment feature.

completion. The open photoresist windows will appear light-gray, and the wafer's surface will become hydrophobic when the silicon dioxide (SiO_2) has been completely etched away.

(d) Etching should be continued as necessary. From the total etch time, the etch rate should be calculated. The student should anticipate an etch rate of 110-150 nm/minute.

(10) After this etching process, the student should remove the remaining photoresist in the plasma asher (approximately 15 minutes, or until all traces of the photoresist are removed). At this point, the student should verify the thickness of the oxide mask, which was previously measured with the ellipsometer and calculated using the *TSUPREM-4* software for the process variables implemented during the initial oxidation exercise. The thickness of the oxide between two adjacent windows on one of the control wafers should be measured using a mechanical stylus profilometer.

(11) Finally, the student should inspect the wafers with the optical microscope in the dark-field illumination mode to verify that all of the photoresist has been completely removed.

3. Diffusion Exercise.

In this exercise, the student will perform a two-step dopant diffusion process. The student will also evaluate the resultant diffusion profile. To accomplish the evaluation, two control wafers (not patterned and not oxidized) are required. These control wafers are supplied by the instructor during this exercise. To begin, the student should measure the resistivity of the control wafers with a four-point probe to determine the initial conditions prior to diffusion. To implement the diffusion process, the following steps should be accomplished:

(1) Cleaning:

Since undetectable traces of contaminants can be catastrophic to both the wafer and the diffusion furnace, proper cleaning is essential before exposing the wafers to the elevated temperatures in the diffusion furnace.

(a) The wafers should be immersed in the modified piranha solution (H_2SO_4 : H_2O_2, 3:2). The wafers should be cleaned for 20 minutes and rinsed thoroughly with DI water.

(b) After mixing a DI H_2O : HF (10:1) deglaze solution; the wafers should be dipped in this bath for 30 seconds, rinsed with DI water (to a 10 MΩ·cm standard), and blown dry with N_2.

(c) The wafers should then be transported to the diffusion furnace in a covered carrier.

(2) Predeposition:

(a) The dopant source boat should be loaded with the polished wafer surface facing the PhosPlus TP360-7130 phosphorus-dopant source wafers, manufactured by OI-NEG TV Products, Inc.

(b) A furnace setting of 900°C, and a gas flow of one lpm of N_2 should be verified.

(c) The wafer boat should then be slowly pushed into the furnace's hot zone (1 inch per minute), diffused for one hour; and then slowly withdrawn (1 inch per minute).

(3) Deglaze:

To terminate the introduction of impurities, the phosphosilicate glass phase formed during the predeposition step must be removed. This procedure also prevents contaminating the diffusion furnace's drive-in tube with impurities which could make subsequent diffusions unpredictable.

(a) The wafers should be immersed for 30 seconds in the DI H_2O : HF (10:1) bath, rinsed with DI water (10 $M\Omega{\cdot}cm$ standard), and blown dry with N_2. A control wafer's sheet resistance should be measured using a four-point probe instrument.

(4) Drive-in:

(a) The wafers should be transported to the diffusion furnace in a covered container. The drive-in boat should be loaded with the wafers; a furnace setting of 1100°C and an O_2 gas flow of one lpm should be verified. In addition, the steam bubbler should be verified to be operating with a setting of at least 95°C.

(b) The boat should be slowly pushed (1 inch per minute) into the furnace's drive-in tube. After 30 minutes in dry oxygen, the steam atmosphere should be switched into the furnace for 30 minutes, and then the nitrogen atmosphere should be switched into the furnace for 60 minutes to anneal the silicon/silicon dioxide interface and complete the diffusion process. Then, the boat should be slowly withdrawn (1 inch per minute).

(c) After the wafers cool, the student should store them in the post-bake oven.

(5) Evaluation:

Using a control wafer processed along with the working device wafers, the student should measure the resulting sheet resistance and junction depth. In addition, the student should calculate the diffusion profile using conventional Irvin curves[3] and the *TSUPREM-4* software.

(a) Using the four-point probe instrument, the student should measure the sheet resistance, ρ_s; it can be assumed that the phosphorus concentration at the silicon wafer's surface is solid solubility limited.

(b) After carefully scribing a small piece of silicon from a control wafer, it should be attached with hot wax to a grinding chuck, and a bevel should be polished approximately 1 mm wide. The beveled sample should be stained with several drops of a HNO_3 : HF : CH_3COOH (3:1:10) solution under strong illumination to delineate the junction. An optical microscope interferometer should be used to measure the junction's depth.

(c) Using the wafer's initial resistivity (before diffusion), the student should select the proper curve from Irvin's data, assume a Gaussian diffusion profile, and calculate N_0, and plot $\log_{10}$ of N(x) with respect to the junction's depth (x), where N(x) is the spatial distribution of the dopant's concentration.

(d) Using the *TSUPREM-4* software and the process parameters employed, the student should calculate and plot the spatial distribution of the dopant's concentration. A representative result is depicted in Figure 7b.

(e) From the processing schedule and the oxide's color, the student should determine the net silicon dioxide thickness.

(f) Using the *TSUPREM-4* software and the process parameters employed, the student should calculate the results of the oxidation process implemented during the drive-in process.

4. Gate Oxide Exercise.

In order to realize the MOS capacitors and the gate oxide region in the MOSFETs, the student employs the level-two Gate Oxide Mask that is depicted in Figure 3. In order to realize an electrically-functional thin gate oxide (for this exercise, a nominal thickness of 600 Å), the student must oxidize the wafers to minimize pin-holes. Therefore, the student will accomplish the thermal oxidation process in a dry oxygen environment. The student is required to establish the conditions necessary to realize the required gate oxide. Their solution for the process variables becomes part of the "recipe". The required oxidation conditions can be estimated using the reference material provided to the student in the laboratory handout and verified with the *TSUPREM-4* software.

(1) To ensure success with the subsequent exercises in this laboratory experiment, the student is also required to select one or more of the wafers from the group that has been successfully processed with the diffusion's "drive-in" step. However, because of the critical nature of this particular process, the student should not initially implement the Gate Oxide Exercise with the wafers that have just been selected. Rather, the student should only process these selected wafers after the gate oxidation process has been practiced and experimentally verified. If time permits, the effect of a variable gate oxide thickness can be investigated using those wafers that were set aside.

Dopant Concentration Following Drive-in
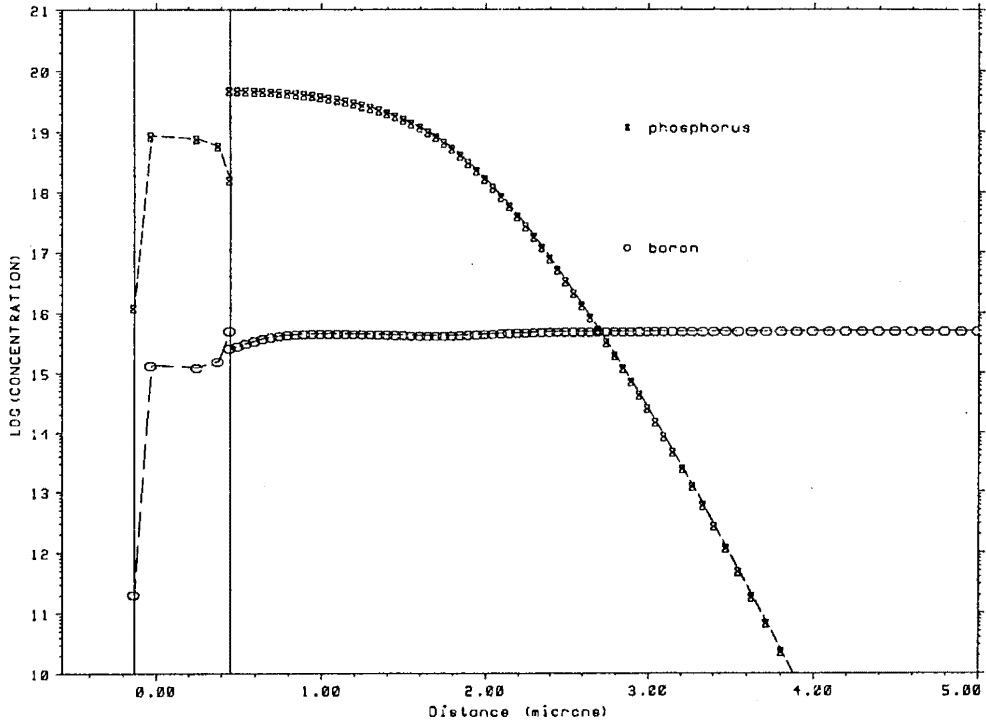
Results of The Gate Oxidation
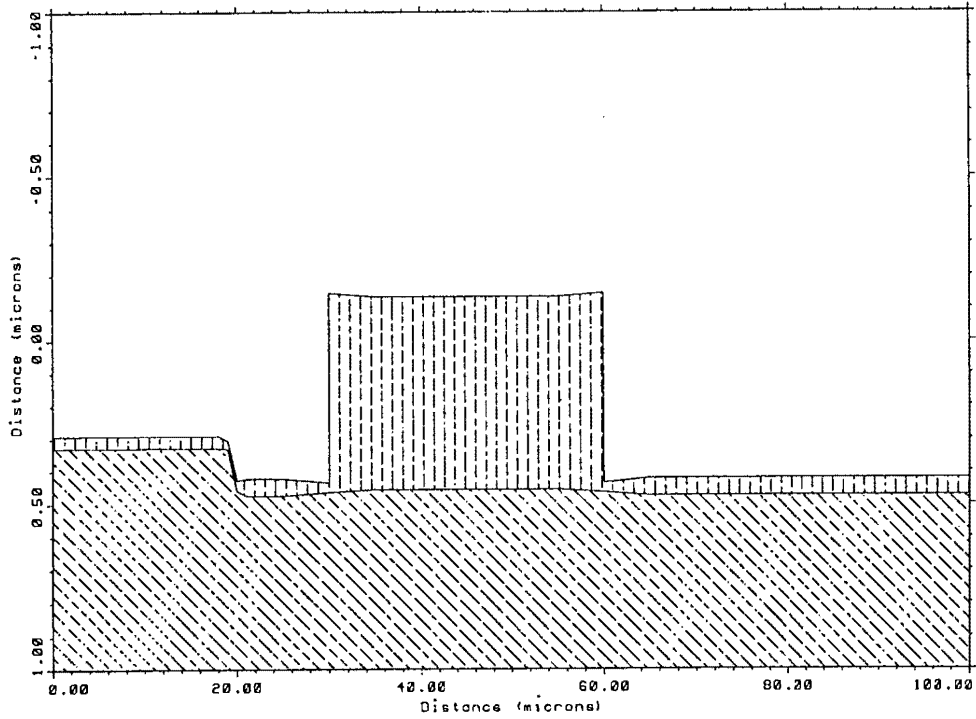
Small-Gate MOSFET
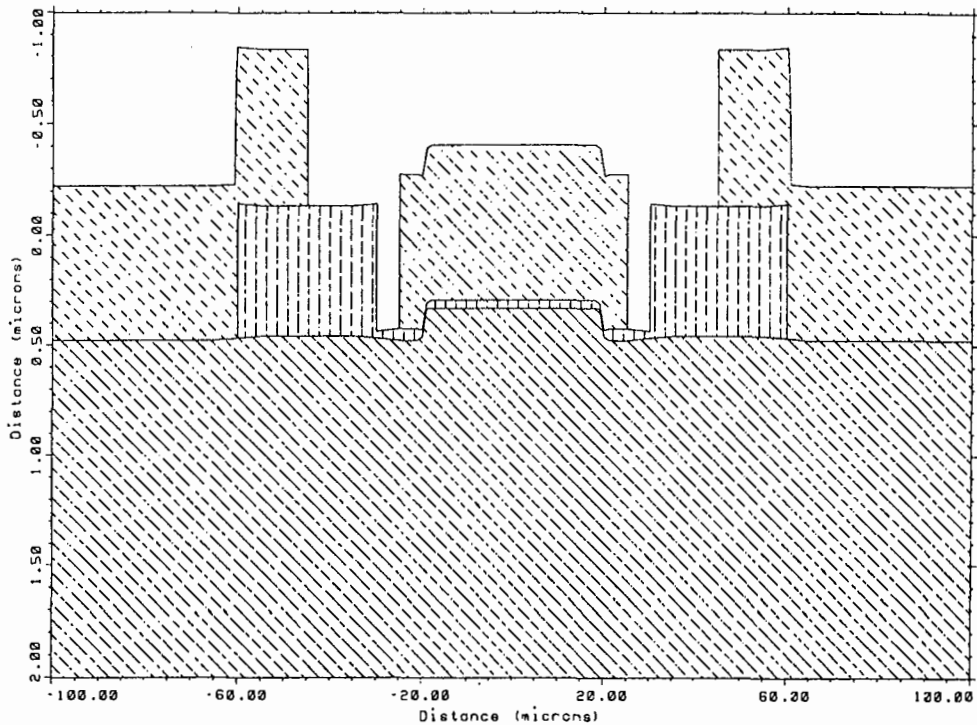
(2) Using negative photoresist, the student should implement the photolithographic steps utilized earlier (Photolithography Exercise).

(3) The student should properly clean the wafers before using the oxidation/drive-in furnace. Two hours in a dry oxygen atmosphere with a furnace setting of 900°C and gas flow of one lpm should be sufficient.

(4) As before, the student should verify the thickness of the resulting gate oxide. A control wafer is useful for this measurement.

(5) Using an ellipsometer, the student should measure the final oxide thickness of the field oxide on one of the wafers.

5. Metallization Exercise.

Thermal evaporation and sputtering are two simple processes employed to coat substrates with thin films (especially nonrefractory metals). Patterning the metallization can be accomplished using a metal-etch process or a metal lift-off process. In this exercise, the student thermally evaporates aluminum (Al) onto those wafers which have been processed with a patterned positive photoresist, followed by a "recipe" to implement a metal lift-off process. The student is also encouraged to explore the option of a direct metal-etch process. The industrious student will realize that this simple alternative procedure, which utilizes the same photomask that was used for the lift-off process, can be accomplished using negative photoresist applied to an Al coated wafer to pattern the metal film. A simple Al etch solution comprised of phosphoric acid is commonly used for this purpose. This alternative metallization process affords the student the opportunity to exercise engineering decisions and to explore alternatives within a structured environment.

Whichever process the student implements, the objectives of the metallization exercise are twofold: 1) the locations of the metal-semiconductor contacts are photolithographically defined and etched, and 2) a metal film is deposited and defined using either a lift-off or a conventional wet chemical etch process.

To implement the metallization exercise, the student is provided the following process description:

(1) Bake the wafers at 200°C for 45 minutes to remove surface moisture after they have been cleaned.

(2) Using the level-three Contact Mask that is depicted in Figure 4, etch windows in the wafer's surface oxide so that ohmic metal contacts and vias can be realized. The photolithography steps (Photolithography Exercise, steps 1-8 inclusive) are repeated using negative photoresist.

(3) Etch the wafer's oxide that has been exposed through the open photoresist windows using a buffered HF (NH_4F : HF, 4:1) solution. Verify that all the windows are clear of oxide before proceeding.

(4) After etching, remove the photoresist in the plasma asher; verify that all traces of the photoresist have been removed before proceeding.

(5) Clean the wafers by immersing them in acetone, rinse them in a methyl alcohol ultrasonic bath, rinse with DI water, and blow dry with N_2. Before continuing, bake the wafers at 200°C for 45 minutes to remove surface moisture.

(6) A positive photoresist and the lift-off technique can also be used to pattern the aluminum metallization. To optimize the yield of the positive photoresist process, an adhesion promoter, hexamethyl disilazane (HMDS), should be spin-coated onto the wafers at 4000 rpm for 30 seconds to realize a homogeneous thin film. Next, the S135OJ positive photoresist, manufactured by Shipley, Inc., is liberally applied to the wafer and spun at 5000 rpm for 30 seconds.

(7) Then, the wafers are placed in a pre-bake oven at 70°C for 20 minutes.

(8) The level-four Metallization Mask that is depicted in Figure 5 is printed. Exposure to a UV light source for a duration of 30 to 70 seconds should be adequate (The student will need to establish the optimum exposure duration experimentally, similar to the process practiced in the initial Photolithography Exercise). The exposed wafers are immersed in a bath of chlorobenzene for 2 minutes and then soft baked at 90°C for 15 minutes to prepare them for development.

(9) Develop the exposed wafers with the Shipley Microposit 351 developer (DI H_2O: developer solution, 3:1). Development times on the order of 45 seconds to one minute are typical. After development, rinse the wafer with DI water and blow-dry with nitrogen. Examine the wafers under an optical microscope to verify the quality of the procedure.

(10) Post-bake the printed wafers at 90°C for 15 minutes to harden the remaining photoresist.

(11) Before metallizing the wafers, etch them in a DI H_2O : HF (10:1) solution to remove any remaining oxide within the previously patterned metal-semiconductor contact regions. A 3 to 5 second etch should be sufficient. Follow with a brief rinse in DI water and blow dry with N_2.

(12) Mount the photoresist coated wafers in the vacuum deposition system.

(13) Evacuate the chamber (typically, 10^{-6} torr pressure) and deposit the Al film. Use the piezoelectric quartz crystal thickness monitor to determine the Al film's thickness. (A thickness of at least 7000 Å is required for subsequent wire bonding and probing).

(14) Vent the chamber and remove the wafers.

(15) Using an acetone filled ultrasonic bath, the lift-off procedure is completed when the undesired metal and photoresist float away from the wafer. The process can be assisted by periodically removing the wafer from the bath, and blowing high pressure N_2 across the wafer's surface.

(16) Finally, sinter the Al metallization at 450°C for 30 minutes in a nitrogen atmosphere to realize ohmic quality contacts.

6. Final Testing and Analysis.

Upon completion of the Metallization Exercise, the student can begin probing the semiconductor devices. The variety of fabricated devices permits the student to accomplish a wide range of electrical characterizations. The particular electrical tests can be tailored to the previous theoretical courses that the student has completed. The student conducts the electrical tests by probing the diffused resistor test structures, MOS capacitors, a *pn*-junction diode and several MOSFETs. Having recorded the characteristics of the devices, the student comments on the results. To assist with the analysis, the student may utilize *TSUPREM-4*, *PISCES-2B* (Technology Modeling Associates, Inc., Palo Alto, CA), and *HSPICE H9007* (Meta-Software, Inc., Campbell, CA), as well other theoretical techniques from prerequisite knowledge.

The student initiates the electrical characterization phase by examining the transfer length method (TLM) test structure. This structure, which is depicted in Figure 9, is examined first to establish the quality of the ohmic contacts, and then to determine the actual contact resistance. If the TLM exhibits a nonlinear current versus voltage characteristic, the student should sinter the wafer for an additional 15 minutes at 500°C (not to exceed the Al/Si eutectic point) and then re-examine the contact quality.

Contact resistance (R_c) can be estimated by fitting a linear least-squares line to the measured resistance values with respect to the contact spacing[6], as depicted in Figure 9. As depicted in Figure 9, the measured resistance between pads 4 and 5 can be approximated as the sum of the R_c associated with pad 4, the length-dependent resistance (proportional to the spacing d_{45}), and the R_c associated with pad 5. That is, in general:

$$R = 2R_c + (R_{sh}) \cdot d \tag{1}$$

where R is the measured resistance, R_c is the contact resistance, R_{sh} is the sheet resistance normalized to the effective width of the contact, and d is the spacing between contacts. The function described in (1) is a simple linear function of the dependent variable R and the inde-
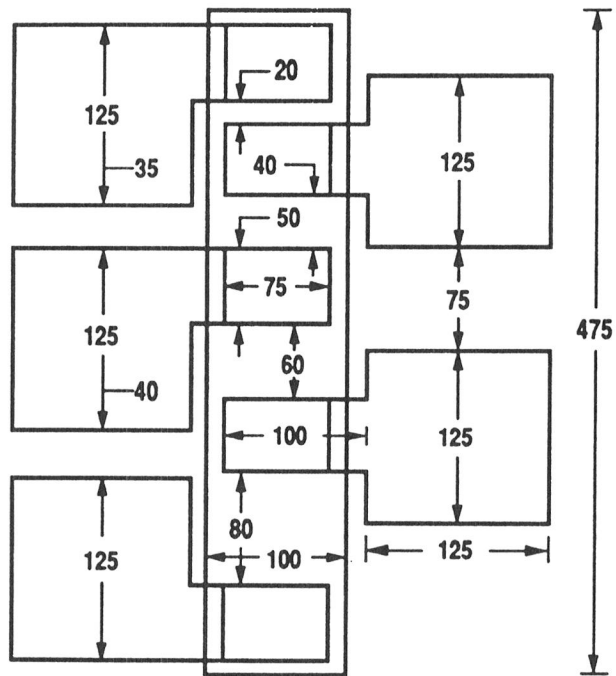
Figure 9. a) Transfer Length Method (TLM) contact resistance test structure (dimensions in microns).
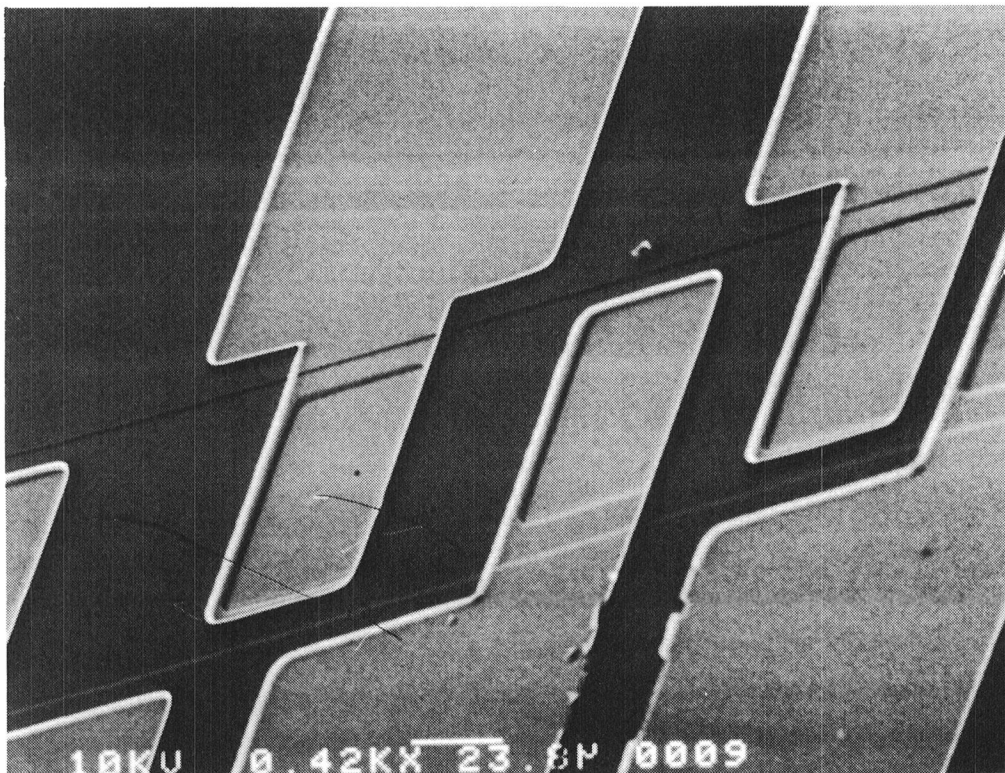
Figure 9. b) Photograph of a fabricated TLM contact resistance test structure.
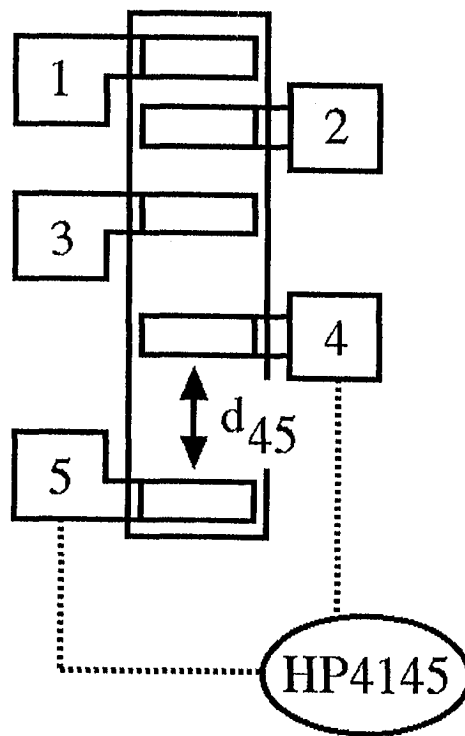
Figure 9. c) Test configuration for the TLM contact resistance test structure.

$$y = 25.8 + 0.298\ x \qquad R^2 = 0.993$$
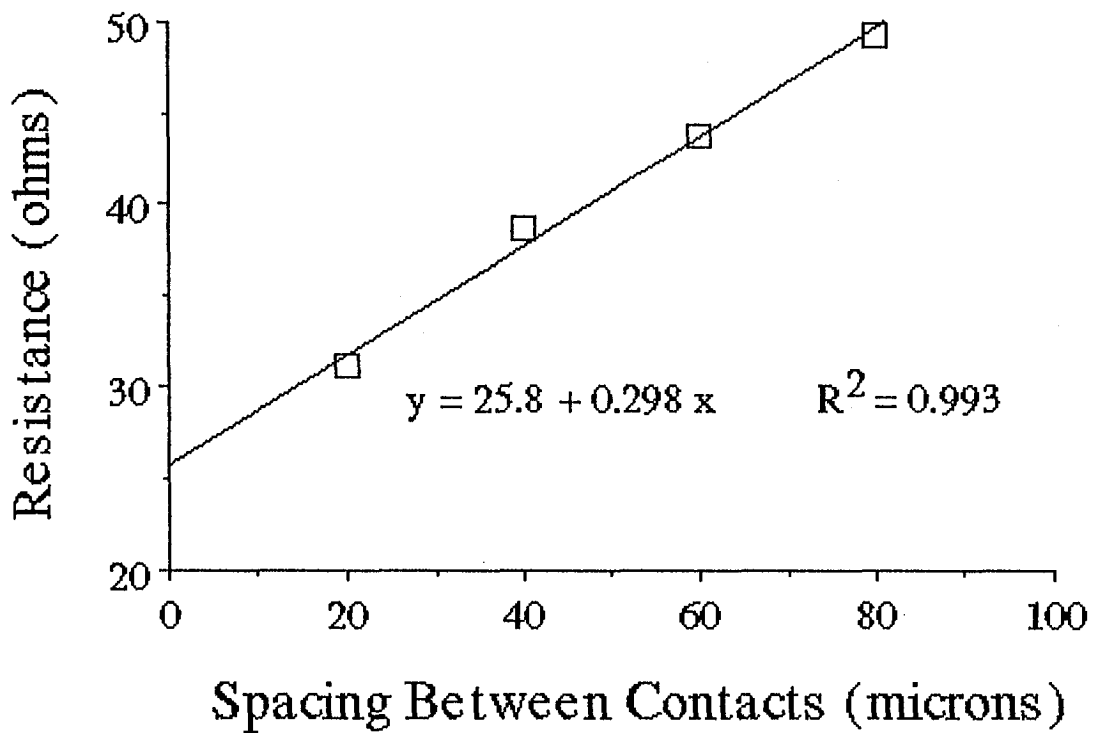
Figure 9. d) Sample of the measured results for the TLM contact resistance test structure.

pendent variable d. Hence, the R-axis intercept is equal to $2R_c$. The measurements can be accomplished by sequentially connecting a semiconductor parameter analyzer (model HP 4145 B, Hewlett Packard, Palo Alto, CA) between each pair of the pads (1-2, 2-3, 3-4, and 4-5 as depicted in Figure 9c) in the TLM structure. As depicted in Figure 9d, the contact resistance (R_c) is 12.9 Ω.

The specific contact resistance (ρ_c) can be approximated using the relation:

$$\rho_c = R_c L_T W \tag{2}$$

where L_T is the transfer length of the electrical contact, and W is the width of the contact. L_T can be determined from the linear least-squares line described in (1) as one-half of the horizontal d-axis intercept. That is, L_T is the distance over which the electrical potential arising from the current flowing from the semiconductor to the metal has been attenuated to $1/e$ of its maximum value. For the data illustrated in Figure 9d, the calculated specific contact resistance is 4×10^{-4} $\Omega \cdot cm^2$.

The student accomplishes sheet resistance and line-width measurements using the cross-bridge sheet resistance test structure[7]. This structure is illustrated in Figure 10. The sheet resistance (ρ_s) can be measured by applying a current of I_{12} between pads I_1 and I_2, and then measuring the voltage potential V_{12} which is produced between pads V_1 and V_2. This measurement can be accomplished using a semiconductor parameter analyzer as the current source and the voltage detector. The sheet resistance can be calculated as:

$$\rho_s = \frac{\pi}{\ln (2)} \left[\frac{V_{12}}{I_{12}} \right] \tag{3}$$

Using the cross-bridge sheet resistance test structure, ρ_s has been calculated to be 23.5 Ω/square.

Having determined the sheet resistance, the line-width W can be determined with additional electrical measurements using the semiconductor parameter analyzer, as depicted in Figure 10. By applying a current of I_{13} between pads I_1 and I_3, and measuring the induced potential of V_{23} between pads V_2 and V_3, the line width W is simply

$$W = \rho_s L \frac{I_{13}}{V_{23}} \tag{4}$$

255
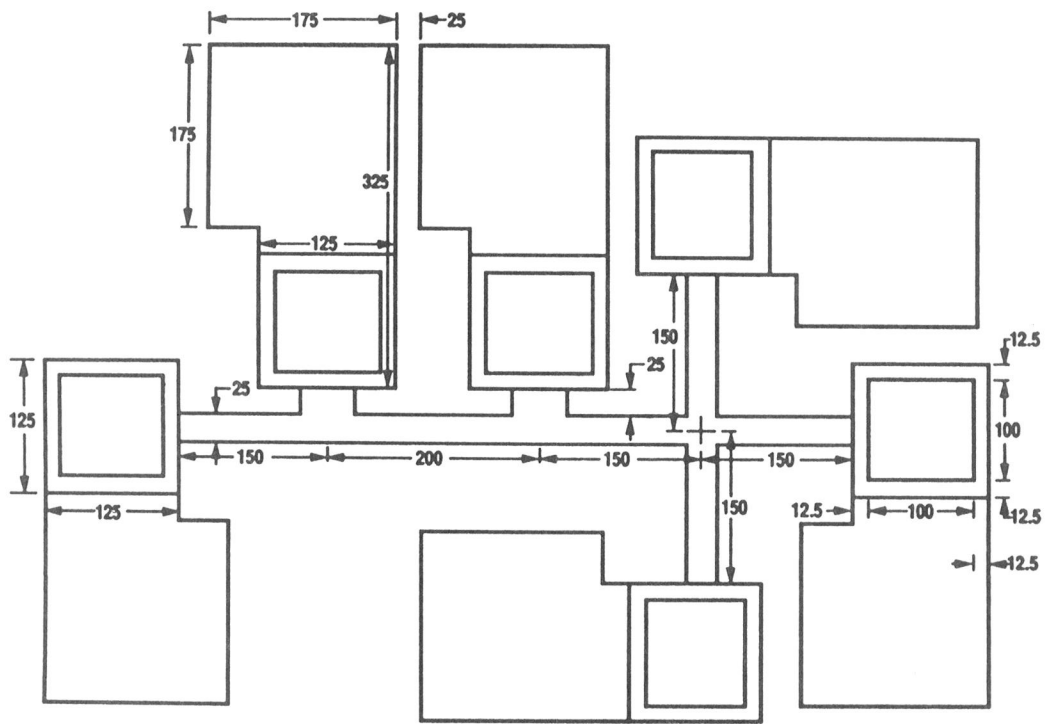
Figure 10. a) Cross-bridge sheet resistance and line-width control test structure (dimensions in microns).
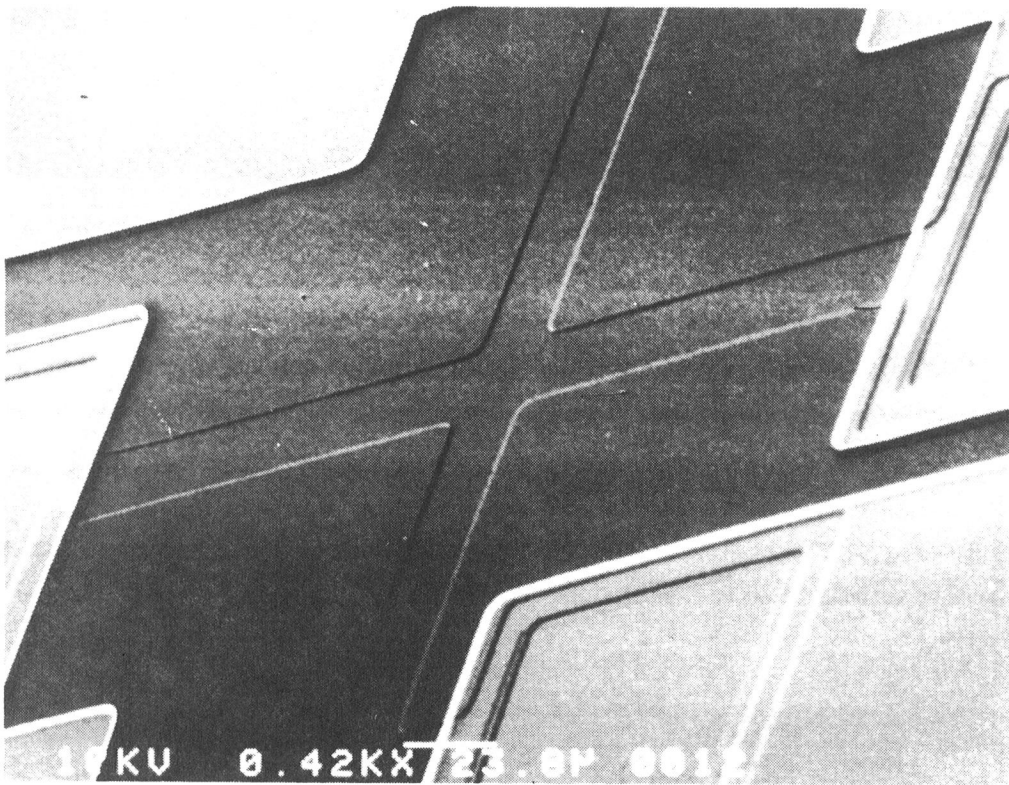
Figure 10. b) Photograph of the cross region of a fabricated cross-bridge test structure.

256
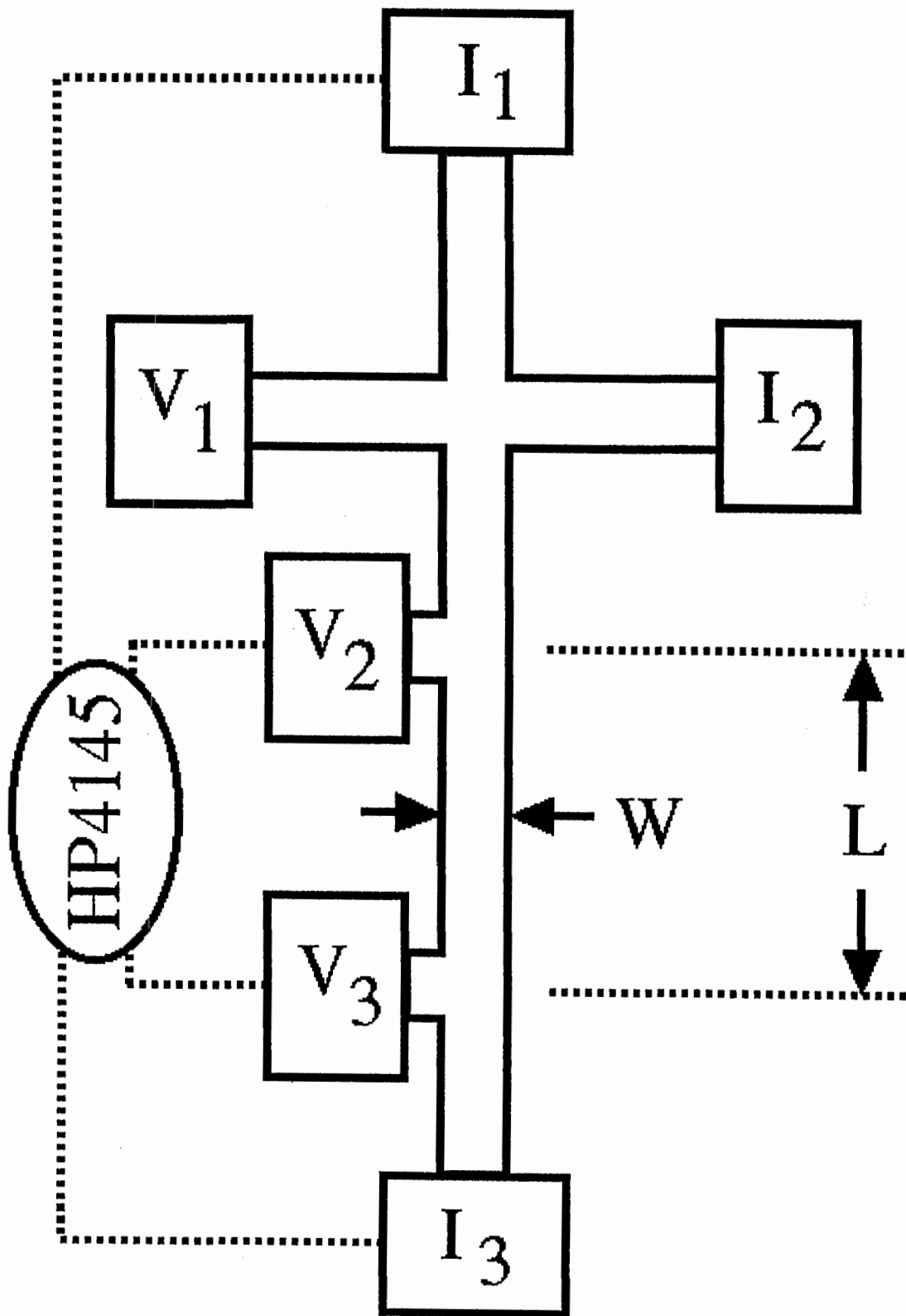
Figure 10. c) Test configuration using the cross-bridge test structure.

where L is the center-to-center spacing between pads V_2 and V_3. Since L is physically very large, errors associated with its estimate are relatively small. Thus, by using electrical measurements, the width W can be measured relatively accurately. For example, a width of 25.7 microns has been calculated from the experimental data which employed a mask whose feature width was 25 microns.

A variety of measurements can be accomplished by the student using the pn-junction diode[8] (which is depicted in Figure 11), MOS capacitors[9] (which are illustrated in Figures 12 and 13), and the MOSFETs[10] (which are depicted in Figures 14 and 15). For example, in the case of the *pn*-junction diode, the student may measure the reverse-bias depletion capacitance with respect to the applied voltage. This measurement can be accomplished with a low-frequency impedance analyzer (model HP 4192 A, Hewlett Packard, Palo Alto, CA). Using the impedance analyzer, a variable dc voltage bias can be applied while simultaneously biasing the junction with a 1 MHz, 50 mV (peak amplitude) ac signal. Also, the student can measure the current-voltage (I-V) characteristics of the diode with a semiconductor parameter analyzer. For the MOS capacitors, the student may characterize the silicon dioxide dielectric properties using a low-frequency impedance analyzer. Finally, the student can implement a nearly endless ensemble of electrical tests devoted to the MOSFETs[11] with a semiconductor parameter analyzer and low-frequency impedance analyzer, as depicted in Figure 15c. For example, the gate capacitance of the MOSFET can be estimated with the impedance analyzer by probing the device with a series connection from the gate electrode to the shunted combination of the source, drain, and substrate electrodes.

SAMPLE DATA SHEETS: Self-Evident.

INSTRUCTOR NOTES: The laboratory experiment is readily partitioned into four distinct exercises, that consist of oxidation, photolithography, diffusion, and metallization. Therefore, the laboratory experiment, or portions thereof, can readily be incorporated concurrently with a silicon IC fabrication theory course. In addition, the series of distinct exercises can each begin with a pre-processed wafer supplied by the instructor; thus, the cumulative effect of student errors can be avoided.

The experiment affords the student an opportunity to experiment and explore within a structured environment. Therefore, the student should be encouraged to experiment with alternative solutions to the challenges presented in the laboratory. Upon completion of the laboratory experiment, the student should be able to assess the compatibility of their laboratory skills with the requirements associated with an experimentally-based senior project or graduate thesis topic.
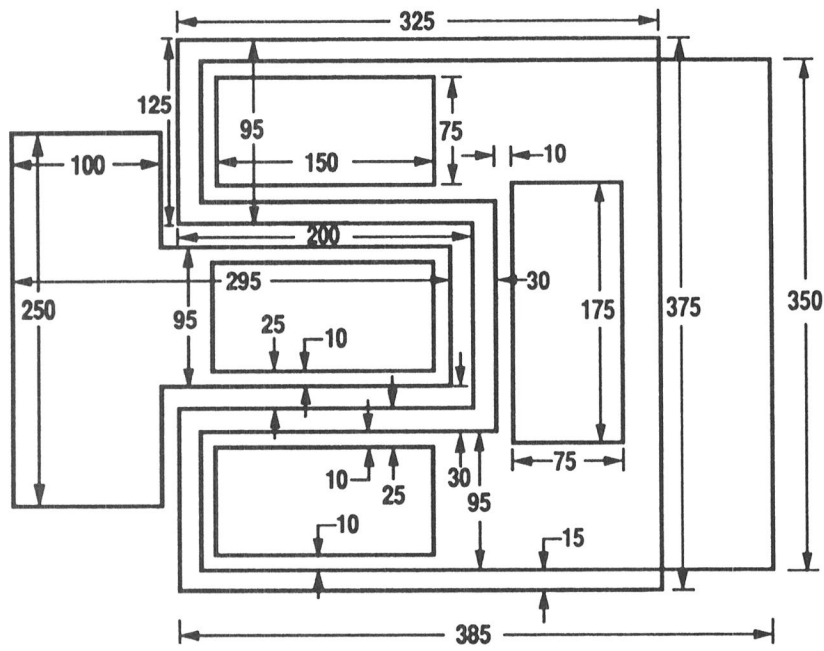
Figure 11. a) PN-junction diode structure (dimensions in microns).
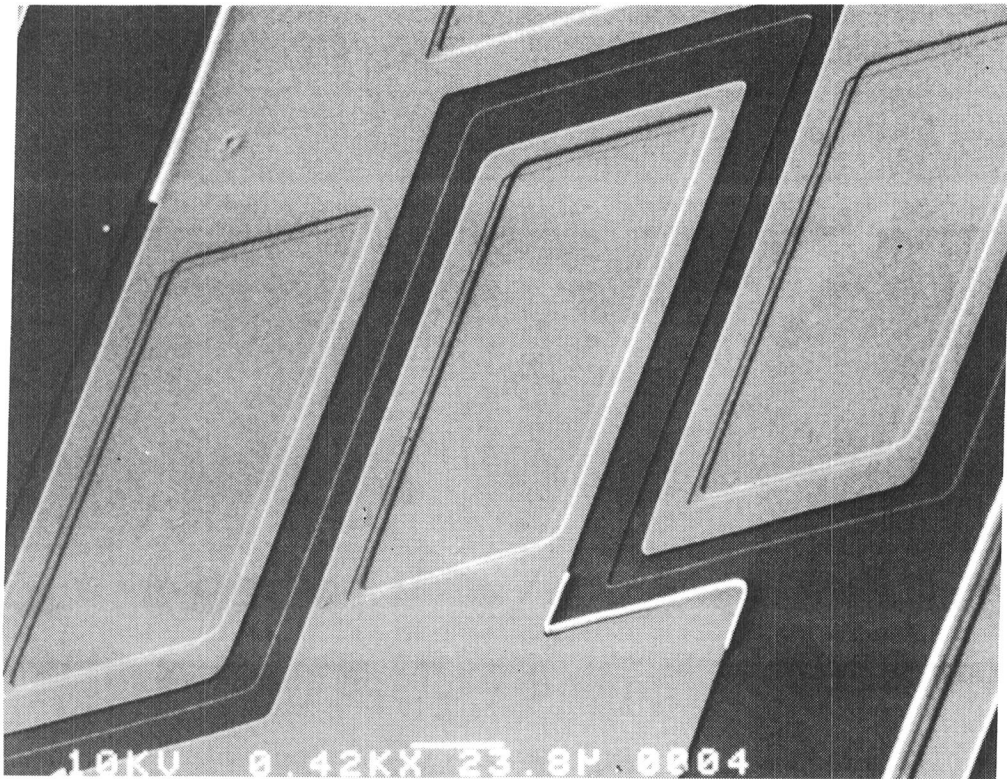
Figure 11. b) Photograph of a fabricated pn-junction diode structure.
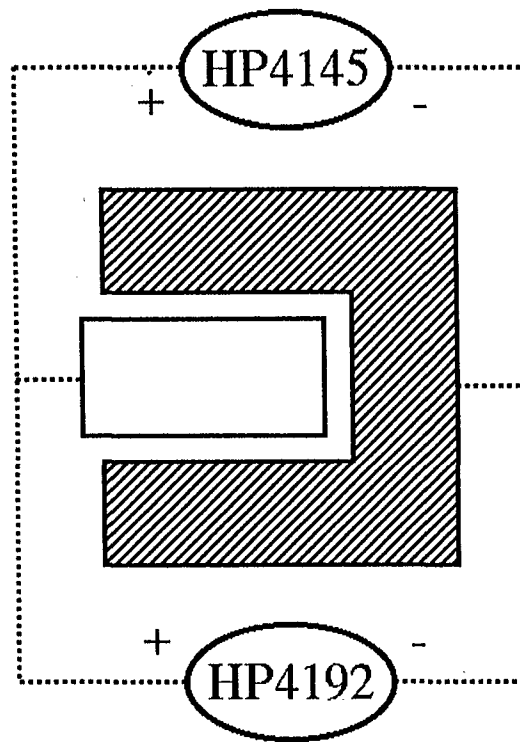
Figure 11. c) Test configuration for the pn-junction diode structure.
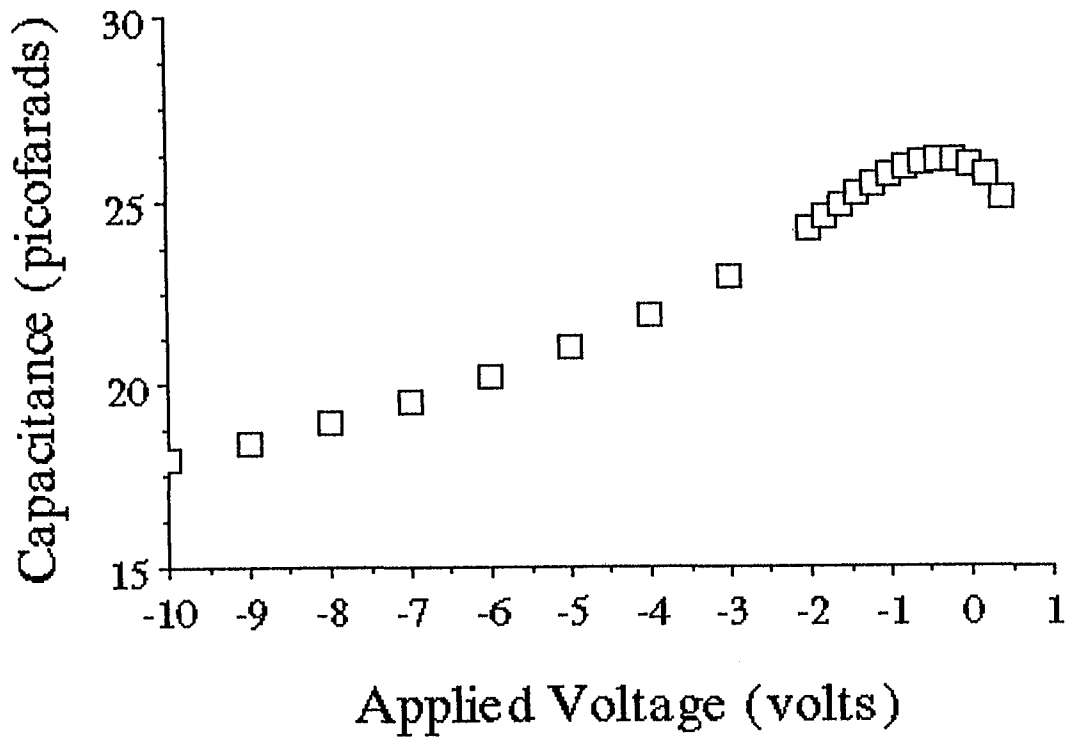
Figure 11. d) Sample of the measured results for the reverse-bias capacitance.
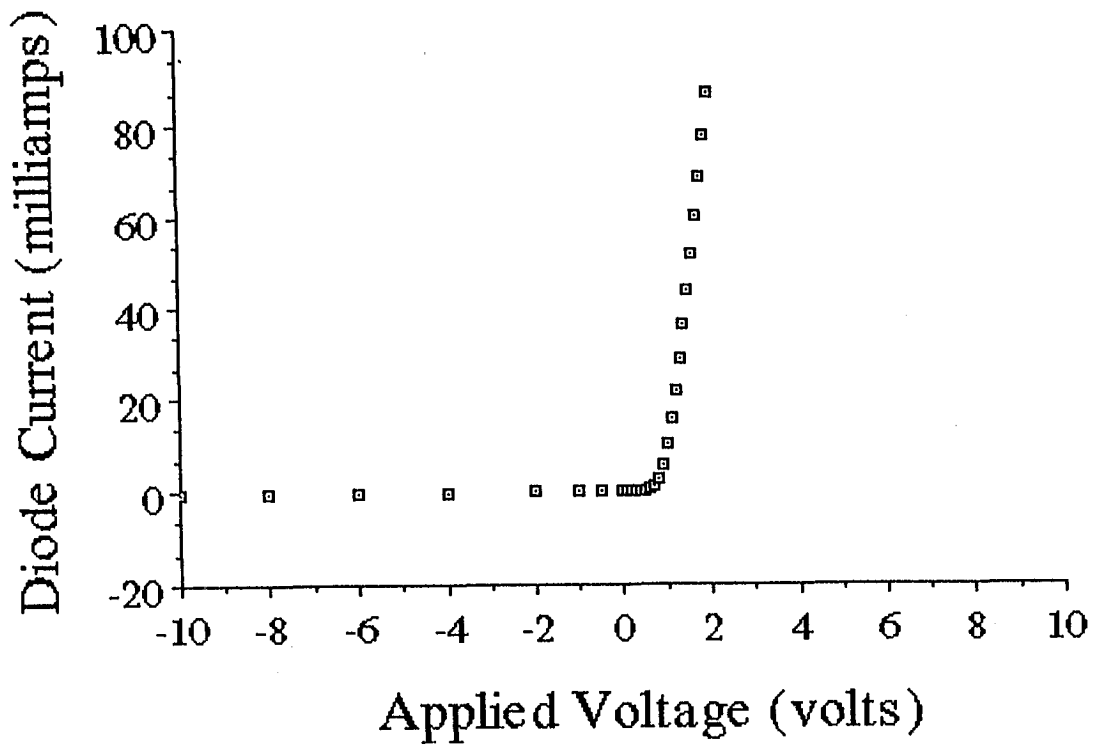
Figure 11. e) Sample of the current-voltage characteristics for a pn-junction diode structure.
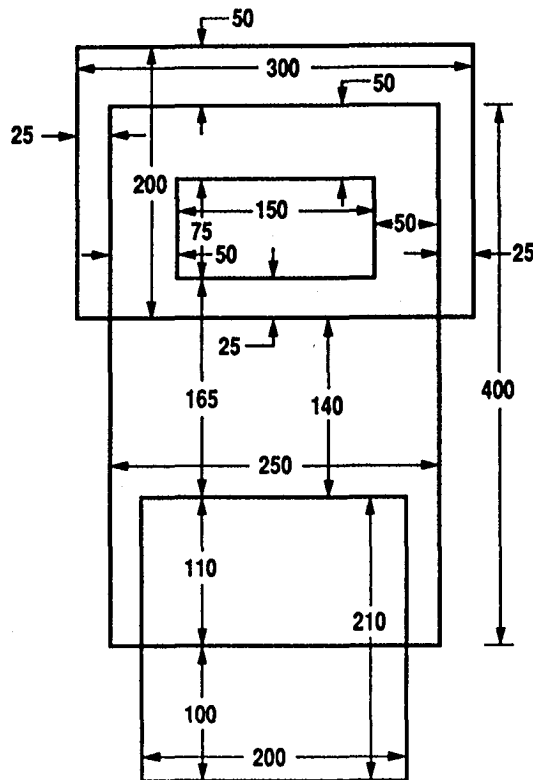
Figure 12. "Large" MOS capacitor structure (dimensions in microns).
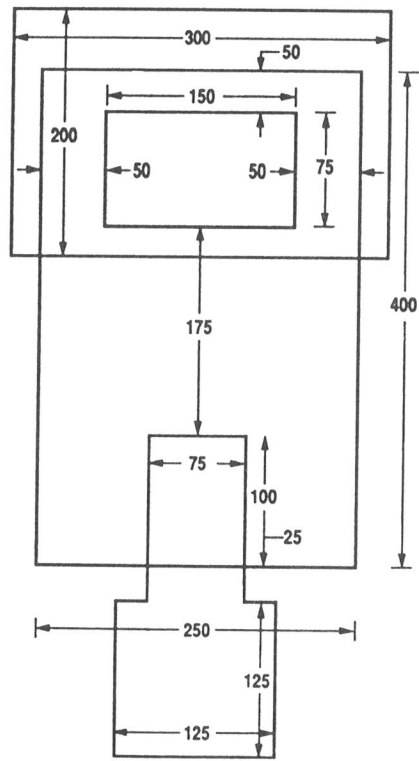
Figure 13. a) "Small" MOS capacitor structure (dimensions in microns).
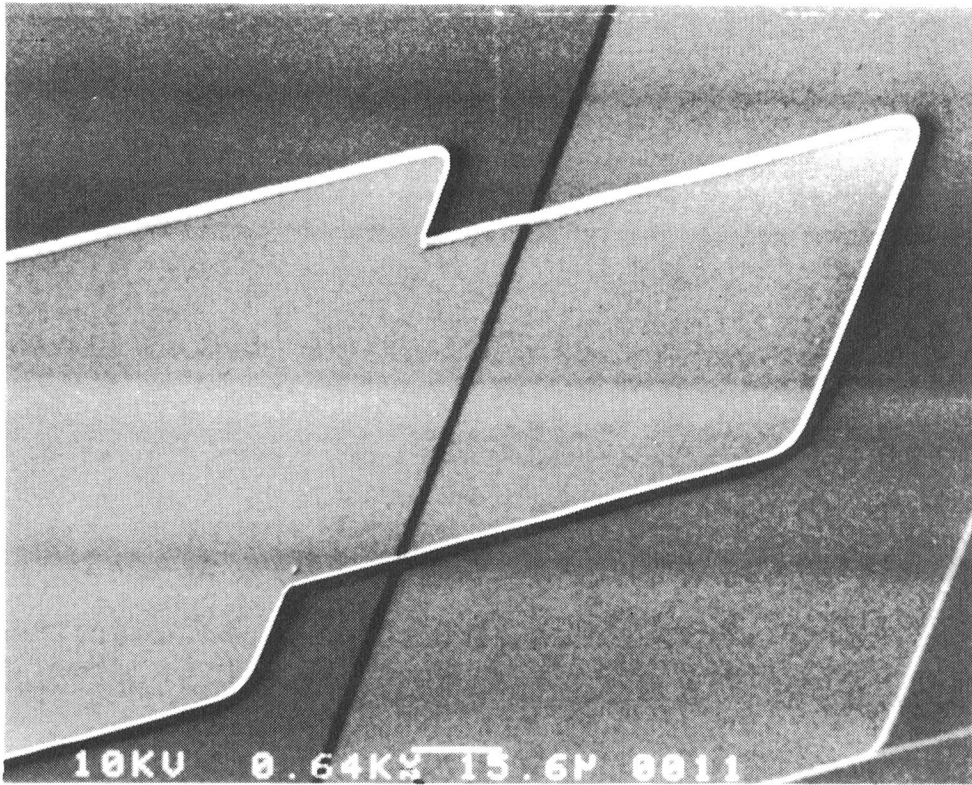
Figure 13. b) Photograph of a fabricated "Small" MOS capacitor structure.
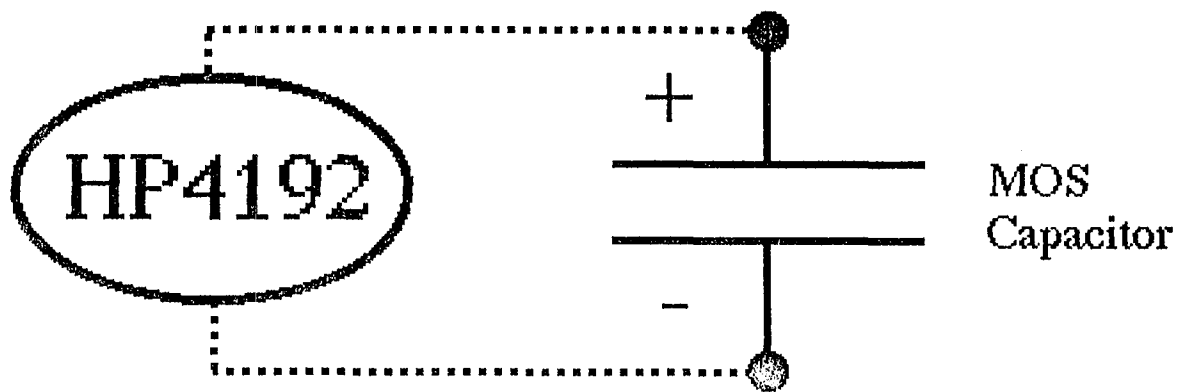
Figure 13. c) Test configuration for the MOS capacitor structure.
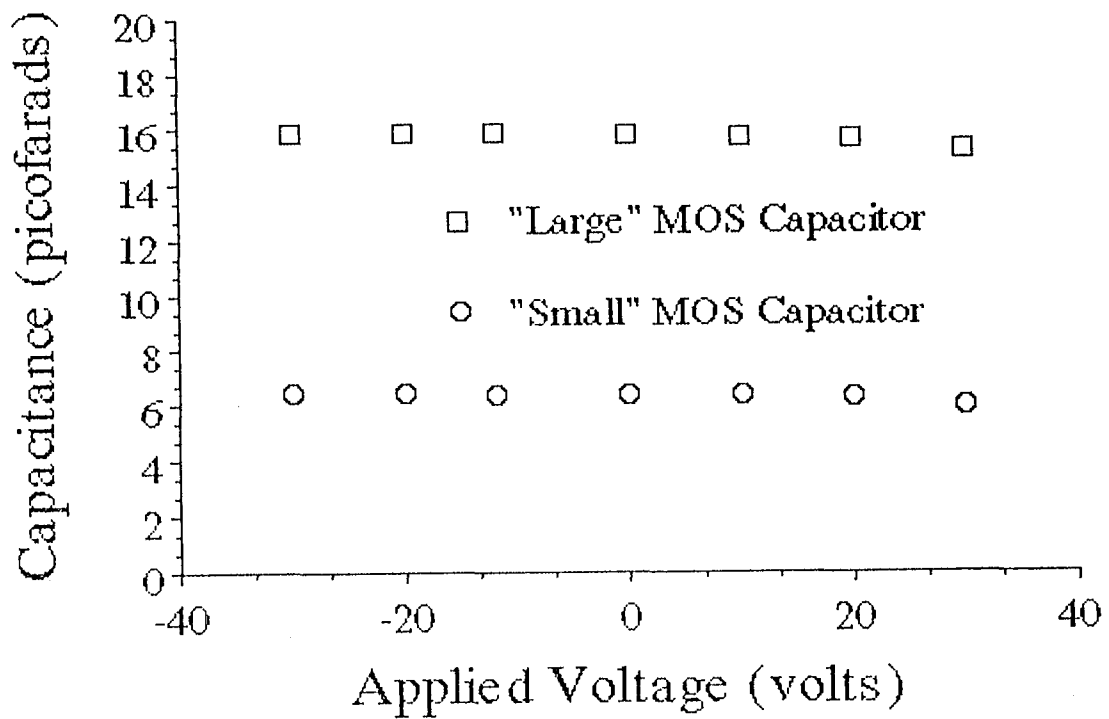
Figure 13. d) Sample of the capacitance measurements for "Large" and "Small" MOS capacitor structures.
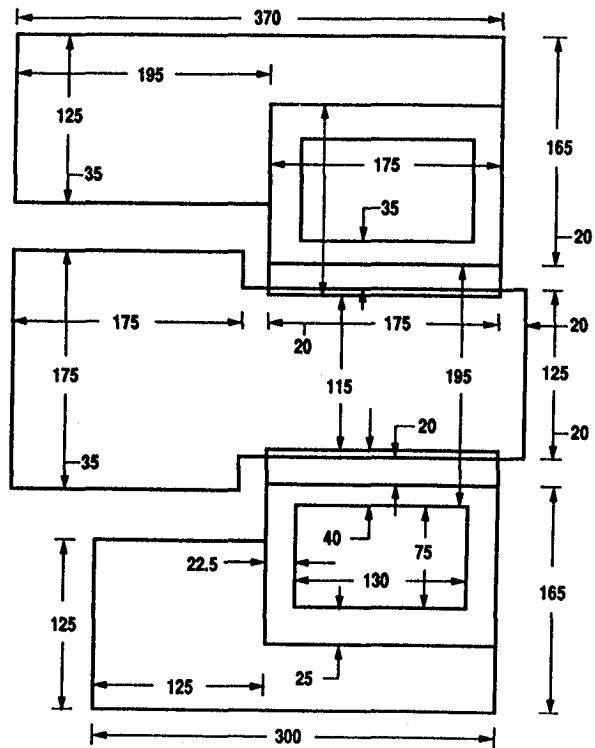
Figure 14. "Large-Gate" Metal-Oxide-Semiconductor Field-Effect Transistor (MOSFET) structure (dimensions in microns).
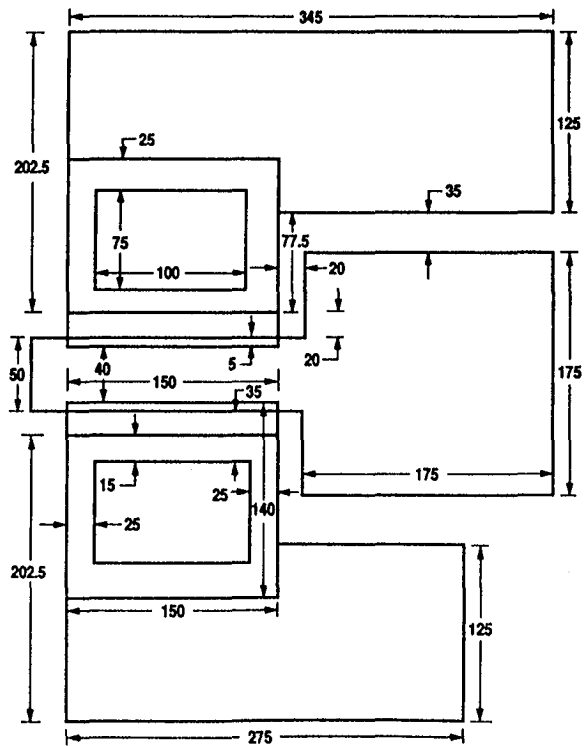
Figure 15. a) "Small-Gate" Metal-Oxide-Semiconductor Field-Effect Transistor (MOSFET) structure (dimensions in microns).
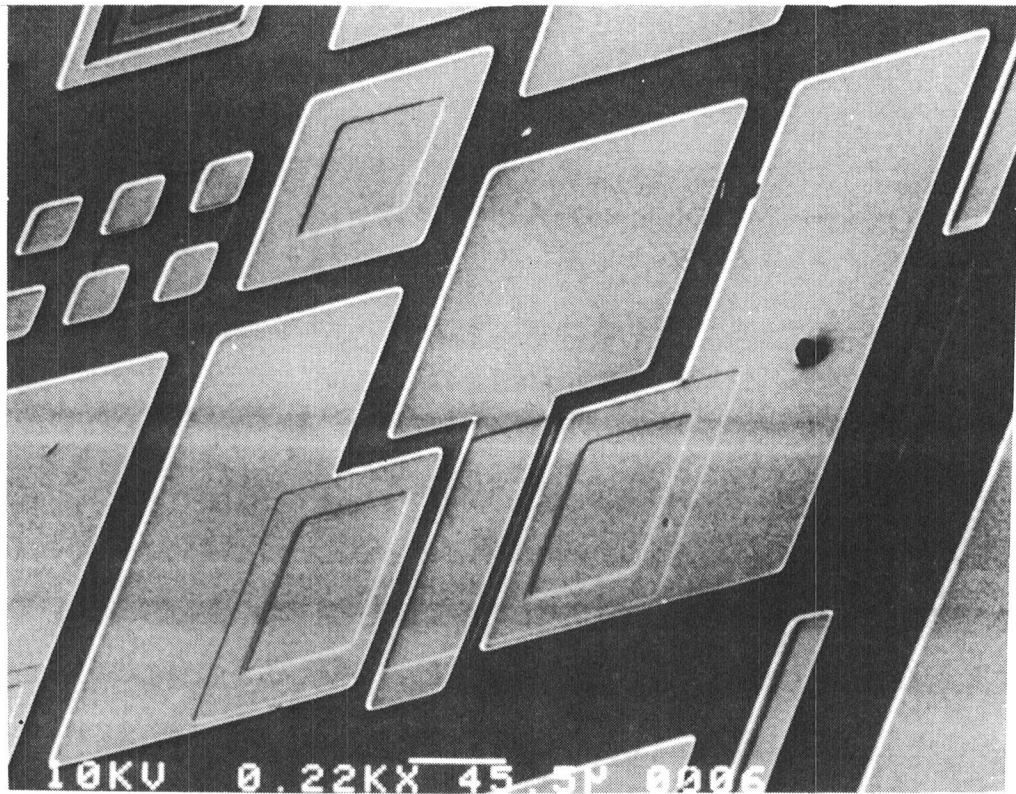
Figure 15. b) Photograph of a fabricated "Small-Gate" MOSFET and a substrate contact.
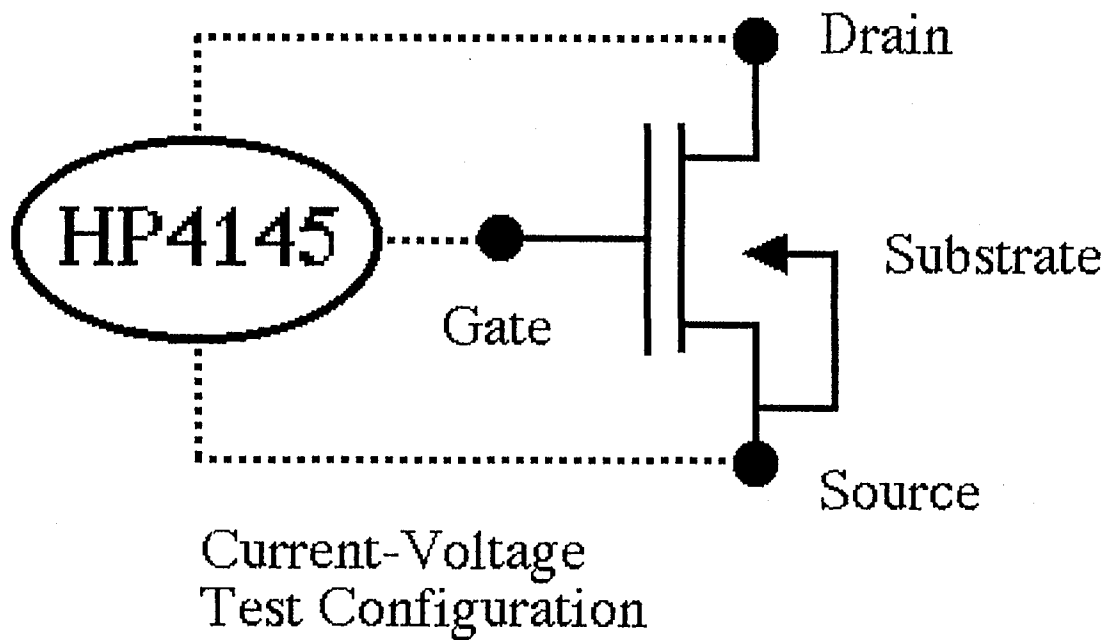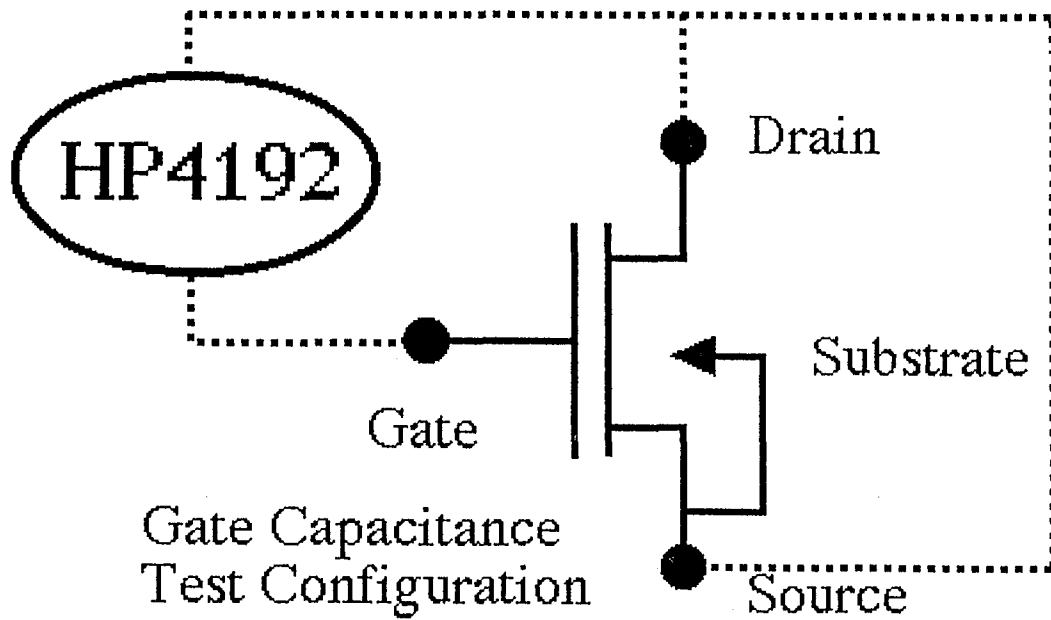
Figure 15. c) Test configuration for measuring the MOSFET characteristics.
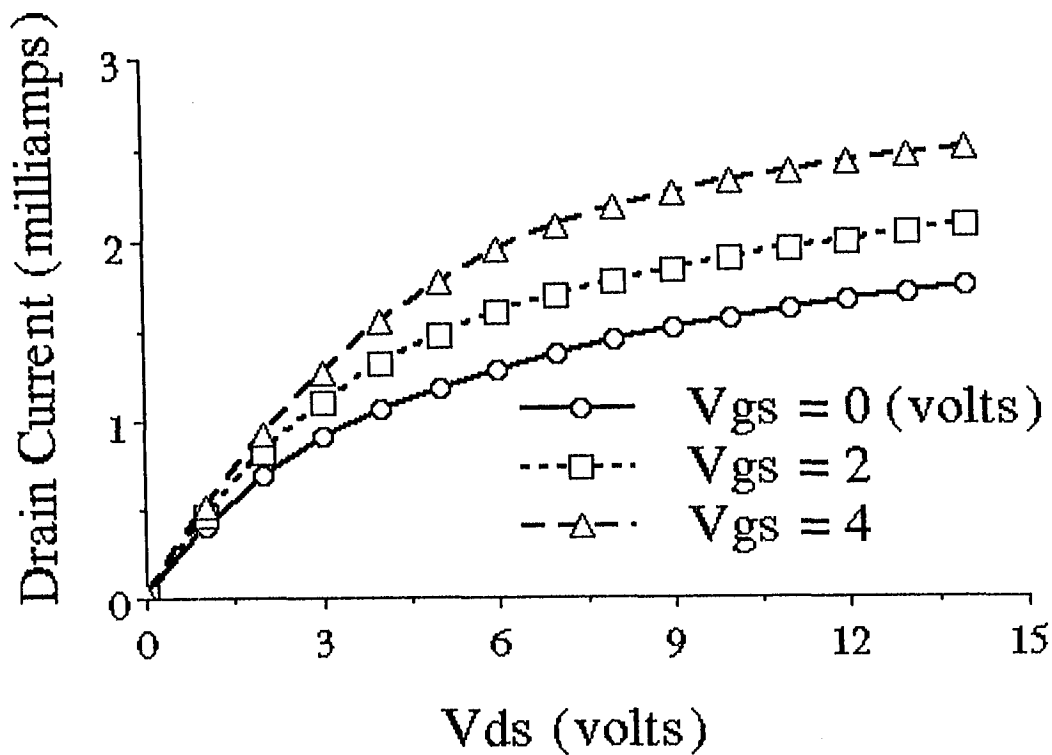
Figure 15. d) Sample of the measured results for the current-voltage characteristics of a "Small-Gate" MOSFET where Vds is the drain-to-source potential and Vgs is the gate-to-source potential.
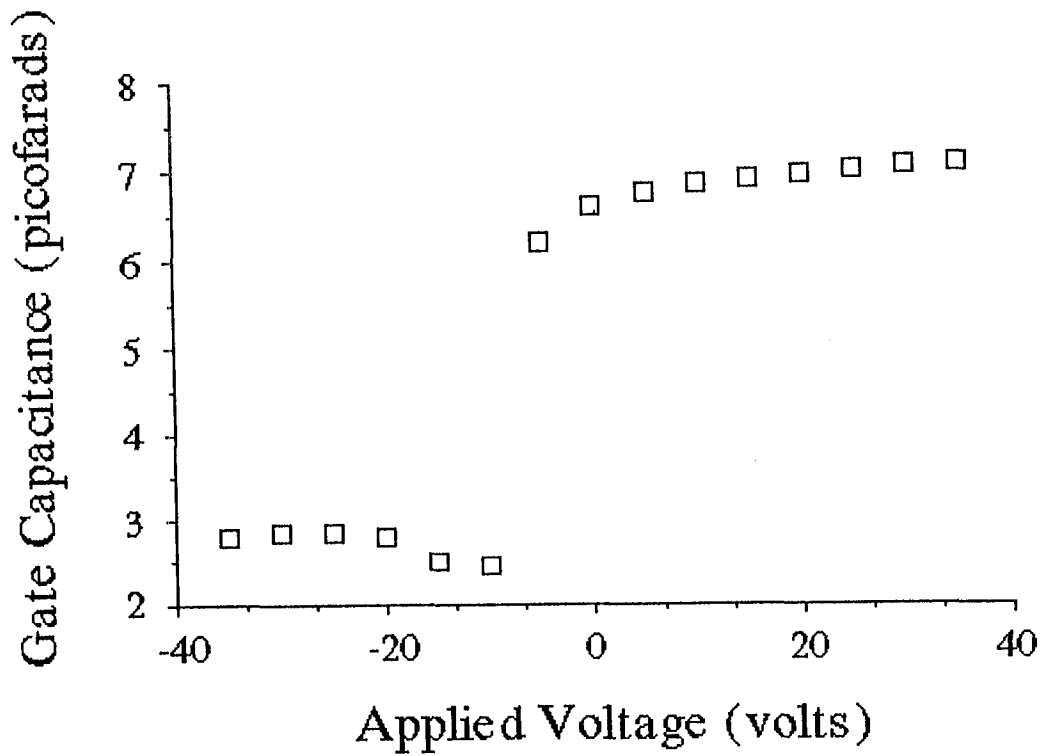
Figure 15. e) Sample of the gate capacitance measurement for a "Small-Gate" MOSFET.

In addition, the student should be required to complete a written report that reflects their laboratory experiences. The written report will reinforce the need to effectively communicate within a technical community. The suggested format of the report is flexible, but should include the following: 1) summary of the theory underlying the physical or chemical process being employed, and how it is monitored and controlled, 2) critical parameters associated with the structure, pattern, or process which facilitates the desired outcome of the fabrication step, 3) steps implemented in the fabrication process and evaluation scheme, and 4) results, problems encountered, and related discussion; including experimental data, measurements, and their analysis.

To ensure the timely completion of the experiment, a suggested milestone schedule is provided in Table II. This schedule has worked successfully during a ten-week academic quarter. The laboratory time has been scheduled using four-hour periods, and it has been accomplished by individual students, as well as with teams composed of two or three students. However, since the prerequisite knowledge was presented during the previous academic quarter, the student could focus on the practical implementation of fabrication with the benefit of having already mastered the theoretical concepts.

REFERENCES:

1. Donald Christiansen: New Curricula. *IEEE Spectrum*, vol. 29, no. 7, July 1992, p. 25.

2. User's Manual: *TMA TSUPREM-4 Two-Dimensional Process Analysis Program*, Version 9035. Technology Modeling Associates, Inc., 300 Hamilton Avenue, Third Floor, Palo Alto, California 94301, September 1990.

3. John C. Irvin: Resistivity of Bulk Silicon and of Diffused Layers in Silicon. *Bell System Tech. J.*, vol. 41, no. 2, March 1962, pp. 387-410.

4. User's Manual: *TMA PISCES-2B Two-Dimensional Process Analysis Program*, Version 9033. Technology Modeling Associates, Inc., 300 Hamilton Avenue, Third Floor, Palo Alto, California 94301, November 1990.

5. User's Manual: *HSPICE*, Version H9007. Meta-Software, Inc., 1300 White Oaks Road, Campbell, California 95008, 1991.

6. Dieter Schroder: *Semiconductor Material and Device Characterization*, John Wiley & Sons, New York, 1990, pp. 119-121.

7. Dieter Schroder: *Semiconductor Material and Device Characterization*, John Wiley & Sons, New York, 1990, pp. 12-14.

8. Dieter Schroder: *Semiconductor Material and Device Characterization*, John Wiley & Sons, New York, 1990, pp. 147-151.

9. Simon Sze: *Semiconductor Devices Physics and Technology*, John Wiley & Sons, New York, 1985, p. 471.

10. Dieter Schroder: *Semiconductor Material and Device Characterization*, John Wiley & Sons, New York, 1990, pp. 169-180.

11. Simon Sze: *Semiconductor Devices Physics and Technology*, John Wiley & Sons, New York, 1985, pp. 200-219.

SOURCES OF SUPPLY: All laboratory chemicals required for this experiment are available from Mallinckrodt, Inc., Science Products Division, Paris, Kentucky. The phosphorus diffusion sources can be obtained from OI-NEG TV Products, Inc., Toledo, Ohio, and the silicon wafers are available from Ziti, Inc., 14755 Preston Road, Suite 421, Dallas, Texas.

Table II. Laboratory Milestone Schedule

Week	*Activity*
1	Lab staff demonstrates the bulk oxidation of silicon wafers. Laboratory and safety orientation.
2	Photolithography: Negative photoresist: apply, pre-bake, expose, develop, rinse, and post-bake.
3	Diffusion: Etch diffusion mask, remove photoresist, clean, and pre-deposition.
4	Strip pre-deposition, clean and drive. Four-point probe. Bevel and stain.
5	Photolithography: Negative photoresist, etch gate oxide region.
6	Oxidation: Grow the gate oxide. Four-point probe. Bevel and stain.
7	Photolithography: Negative photoresist, pattern contacts, etch, and clean.
8	Metallization: Positive photoresist. Deposit metal, lift-off, and sinter.
9	Test: Probe wafer and test functional devices.
10	Complete laboratory report.

Participants
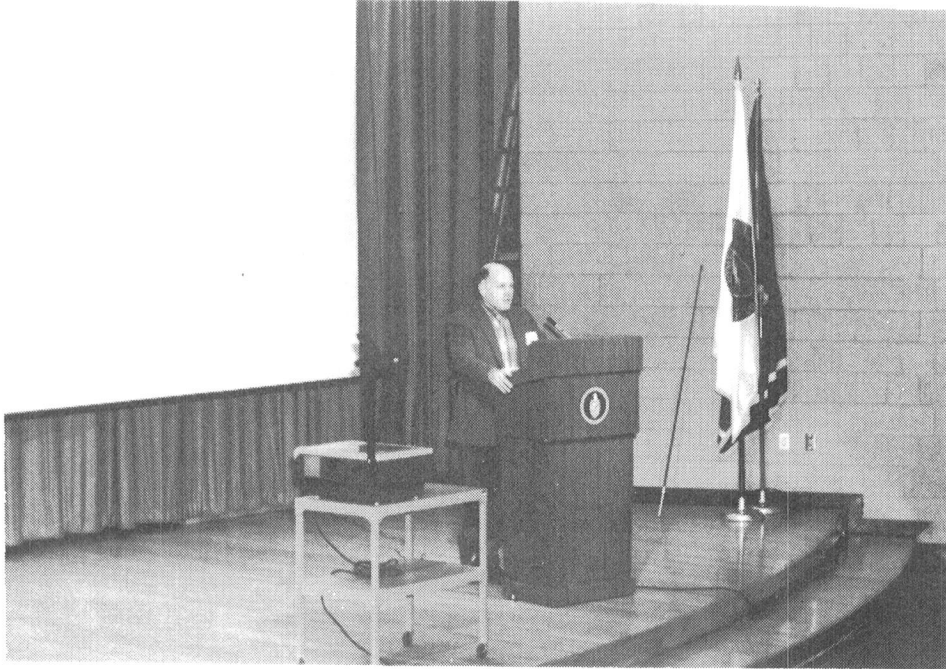
A 69 CENT LOOK AT THERMOPLASTIC SOFTENING

Linda S. Vanasupa

Materials Engineering Department
California Polytechnic State University
San Luis Obispo, California 93407

Telephone 805-756-1537

A 69 CENT LOOK AT THERMOPLASTIC SOFTENING

Linda S. Vanasupa
Materials Engineering Department
California Polytechnic State University
San Luis Obispo, California 93407

KEY WORDS: thermoplastic, glass transition temperature, brittle, ductile, polyethylene, stiffness, van der Waals bonding, covalent bonding

PREREQUISITE KNOWLEDGE: The student should be familiar with the microstructure of a thermoplastic. He or she should know that thermoplastics consist of long polymeric chains (molecules) which are held to one another by physical bonds. The student should also understand the concept of heat energy.

OBJECTIVES: To demonstrate the change in mechanical properties of a thermoplastic polymer when the polymer is heated above the glass transition temperature.

EQUIPMENT AND SUPPLIES: (1) transparent toothbrush (colored or clear) (2) hot plate (3) 250 ml pyrex beaker or Erlenmeyer flask (4) washcloth or rag

PROCEDURE: The instructor or student can perform this demonstration. In preparation for the demonstration, fill the flask or beaker 3/4 full with water and bring the water to a boil.

First observe the initial stiffness of the toothbrush by slightly flexing it. Note that it is fairly stiff and retains its initial shape when the forces are removed. If you were to apply enough force, the toothbrush would break in a somewhat brittle fashion. Now place the toothbrush in the boiling water for 2 minutes. After the 2 minutes are up, remove the toothbrush from the boiling water with the washcloth. At this time you will be able to bend the toothbrush easily. When it cools it will retain this bent shape. You've just demonstrated heating the polymer above the glass transition temperature, demonstrating thermoplastic softening.

INSTRUCTORS NOTES:

The mechanical properties of thermoplastics...
Thermoplastic polymers consist of long chains of a repeating chemical unit called a *mer*.[1] Figure 1 below illustrates polyethylene, the polymer made from the repeating mer, ethylene. The central element of the mer is usually carbon. The carbon-based units are bonded to one another through strong

covalent bonds. These long chains, the polymer molecules, are bonded to one another by weak physical bonds, such as van der Waals bonds.

$$
\begin{array}{ccccccccccc}
H & H & H & H & H & H & H & H & & H & H \\
| & | & | & | & | & | & | & | & & | & | \\
-\,C & -\,C & -\,C & -\,C & -\,C & -\,C & -\,C & -\,C & -\cdots & C & =C \\
| & | & | & | & | & | & | & | & & | & | \\
H & H & H & H & H & H & H & H & & H & H
\end{array}
$$

polyethylene   ethylene
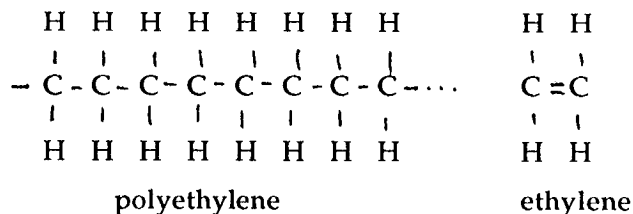
Figure 1. Schematic illustration of polyethylene.

The stiffness of the molecule is due, in the case of polyethylene, to a combination of the covalent bonding along the backbone of the polymers and the van der Waals bonding. The long molecules are essentially tangled with one another. The force that you apply is not large enough to overcome the "friction" of the molecules against one another. A typical transparent toothbrush is made of a polymer similar to polyethylene. Figure 2 shows the infrared spectrum for your everyday toothbrush.
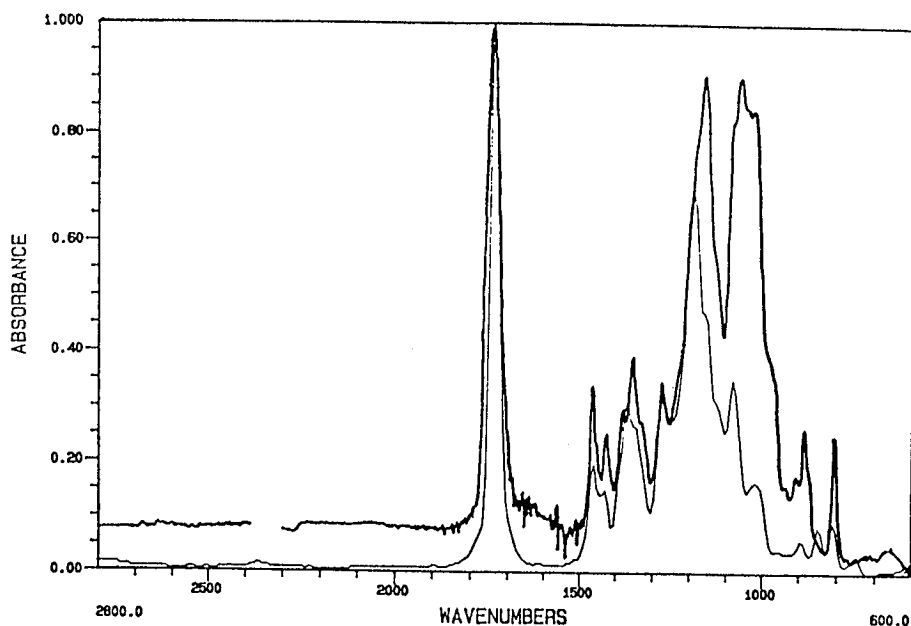
Figure 2. The infrared spectrum for a transparent toothbrush. (Toothbrush spectrum is the thicker, jagged curve. The other curve is the reference spectrum for poly(vinyl propionate: acrylate).

A note about infrared spectroscopy...
Infrared spectroscopy is a technique that can be used to identify polymers. In this technique, a beam of infrared light of varying wavelengths is passed through the sample. The beam emerging from the sample is analyzed to see which wavelengths passed through and which were absorbed by the sample. The results are then plotted, showing the relative beam intensity of the emerging beam for each wavelength of light that was incident on the specimen. An alternate way of plotting the information is by showing the absorbance as it varies with wavenumber ("wavenumber" is 1/wavelength) as shown in Figure 2.

It turns out that the wavenumber range of infrared light is the same energy range within which covalent bonds vibrate. The wavenumbers that are absorbed correspond to a particular covalent bond, for example, the C-H bond has a particular wavenumber which is different from that of the C=O bond. The wavenumber depends on the strength of the bond and the mass of the atoms involved in the bond. So, the infrared spectrum serves as a "fingerprint" for polymers, giving us an indication of the covalent bonds that exist.

Back to the toothbrush...
If you apply a large enough force to the toothbrush, it will fracture, rather than deform. By putting the toothbrush in boiling water, you are supplying enough energy from the water to allow the molecules to slide past one another when the same force is applied.

The glass transition temperature, T_g, in the polymer is the temperature below which the polymer is rigid, a "frozen liquid." Above T_g, the polymer is first rubbery and then becomes a viscous liquid as it nears the melting temperature. (A more complete explanation can be found in any introductory materials engineering text[2],[3]) This demonstration shows the change in mechanical properties for a polymer when it is heated above T_g.

REFERENCES

[1]Callister, W.D. Jr., *Materials Science and Engineering: An Introduction, 2nd Ed.* , John Wiley and Sons, 1991.

[2]Shackelford, J.F., *Introduction to Materials Science For Engineers, 3rd Ed.* , Macmillan Publishing Co, 1992.

[3]Smith, W.F. , *Principles of Materials Science and Engineering, 2nd Ed.*, McGraw Hill, 1990.

Participants
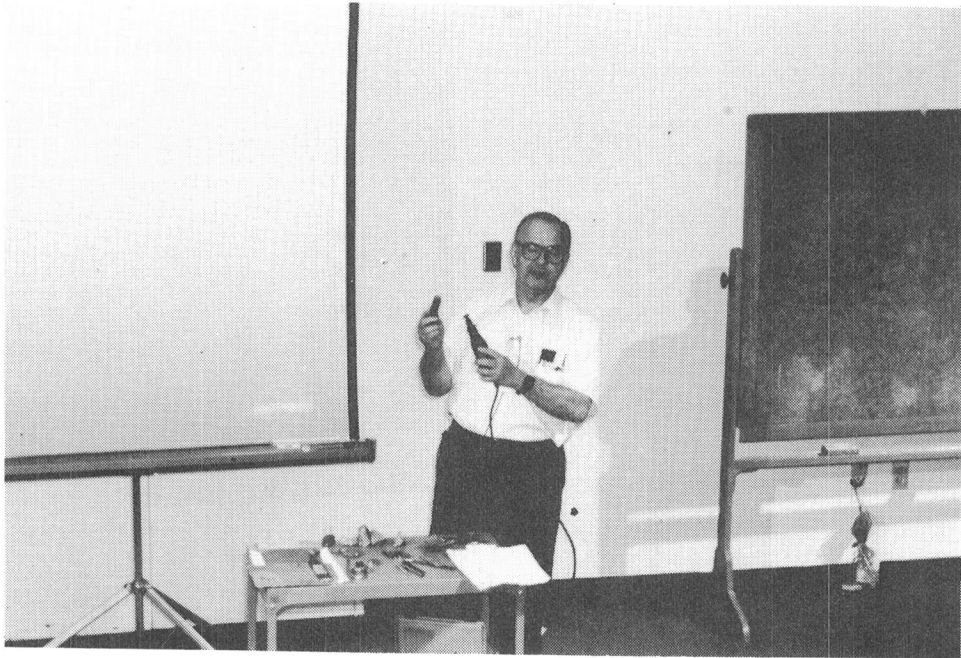
SOLVING A PRODUCT SAFETY PROBLEM USING A RECYCLED HIGH DENSITY POLYETHYLENE CONTAINER

Ping Liu
and
T. L. Waskom

School of Technology
Eastern Illinois University
101 Klehm Hall
Charleston, Illinois 61920

Telephone 217-581-6267/3226

SOLVING A PRODUCT SAFETY PROBLEM USING A RECYCLED HIGH DENSITY POLYETHYLENE CONTAINER

P. Liu and T. L. Waskom
School of Technology
Eastern Illinois University
Charleston, IL 61920

KEY WORDS: high density polyethylene (HDPE), milk jug, safety evaluation, stress, safety factor, material strength, permissible stress

PREREQUISITE KNOWLEDGE: The student should understand the concepts of load, stress, material strength, safety factors and basic engineering design as well as material testing techniques.

OBJECTIVES: To introduce basic problem-solving techniques for product safety including problem identification, definition, solution criteria, test process and design, and data analysis.

EQUIPMENT AND SUPPLIES: (1) recycled one gallon milk jug; (2) utility knife; (3) tensile test machine.

PROCEDURE: The students are given a recycled milk jug made of high density polyethylene (HDPE) by blow molding. Their objectives are to design and perform proper material test(s) so they can evaluate the product safety if the milk jug is used in any of the following working conditions:
   (a) Holding a gallon of water;
   (b) Holding a gallon of mercury.
It is assumed that the above media do not have any significant chemical effect on the mechanical behavior of the plastics and no stress corrosion cracking is expected.

The following steps are used to approach the problem:
   I. Find the density of the two liquids and calculate the weight of one gallon of each liquid;

   II. Calculate the expected maximum stress exerted by either water or mercury on the milk jug;

There are two ways of calculating the maximum expected stress on the milk jug.
   a. Stress exerted by the weight of liquid:
When the container holding one of the liquids is lifted, the maximum stress exerted by the liquid weight is the total weight of the liquid divided by the smallest cross section areas of the container, as in Figure 1.

By water:
$$S_{max.1} = W_{water} / (A_1 + A_2) \tag{1}$$

By mercury:
$$S_{max.2} = W_{mercury} / (A_1 + A_2) \tag{2}$$

b. Thin-wall pressure vessel model [1]:

When the milk jug holds the liquid statically (not lifted), the fluid pressure causes stress on the container according to the thin-wall pressure vessel model as indicated in Figure 2

$$\text{Hoop Stress, } S_{hoop} = P_{max} \, r/t \qquad\qquad (3)$$

where r is radius of the container and t its thickness. P_{max} is the maximum hydraulic pressure of the fluid, governed by

$$P_{max} = pgh_{max} \qquad\qquad (4)$$

$g = 9.80 \text{ m/s}^2$ (gravity constant) .

where h_{max} is the maximum depth and p is the density of water or mercury.

$$P_{water} = 1.00 \times 10^3 \text{ kg/m}^3$$

$$P_{mercury} = 13.6 \times 10^3 \text{ kg/m}^3 \, [2]$$

III. Determine necessary test(s) to ensure the product safety; note that the strength of any material should be greater than the expected stress in relation to the safety factor.

After the analysis of working conditions, it is believed that tension stress is a potential problem for the product safety. Therefore, it is necessary to determine the tensile strength of the plastics by performing a tension test.

IV. Design a material test and determine the specimen dimensions according to ASTM standards;

ASTM standards on plastics testing [3] were consulted to set up the tensile test and to prepare specimens from the milk jug.
The specimen dimensions are shown in Figure 3.

V. Prepare the specimens and perform the designed test(s);

VI. Analyze the test results and compare the material strength with the permissible stress on the milk jug in relation to the safety factor.

It is recommended that for continuous loading no more than 10% of the material strength be used for plastic product design criteria [4]. That is, the expected stress should not be higher than 10% of the plastic strength to ensure the product safety.

VI. Draw a conclusion on product safety.

SAMPLE DATA SHEETS:

A. Density and weight of 1 gallon of water or mercury:

The density of water is 1.00×10^3 kg/m^3 and that of mercury (Hg) is 13.6×10^3 kg/m^3 [2].

1 gal. $= 3.79$ L $= 3.79 \times 10^{-3}$ m^3

The weight of 1 gallon water is:

$W_{water} = 3.79 \times 10^{-3} \times 1.00 \times 10^3 = 3.79$ kg

1 kg $= 9.8$ N

or $W_{water} = 3.79 \times 9.8 = 37.1$ N

1 kg $= 2.20$ lb.

or $W_{water} = 3.79 \times 2.20 = 8.3$ lb.

The weight of 1 gallon mercury is:

$W_{mercury} = 3.79 \times 10^{-3} \times 13.6 \times 10^3 = 51.54$ kg

or $W_{mercury} = 51.54 \times 9.8 = 505.1$ N

or $W_{mercury} = 51.54 \times 2.20 = 113.4$ lb.

B. Expected stress on the container:

1. By weight:
The measured results for A_1 and A_2 are:

Wall thickness t $= 0.015$ in

$A_1 = (0.75$ in. $+ 0.875$ in. $) \times 2 \times 0.015$ in.

$= 0.049$ in^2

$= 3.16 \times 10^{-5}$ m^2

$A_2 = (0.75$ in. $+ 1$ in.$) \times 0.015$ in.

$= 0.053$ in^2

$= 3.42 \times 10^{-5}$ m^2

Maximum stress by water per equation (1)

$S_{max.1} = W_{water} / (A_1 + A_2)$

$= 37.1 / (3.16 \times 10^{-5} + 3.42 \times 10^{-5})$

$$= 0.56 \times 10^6 \, P_a$$

$$= 0.56 \, MP_a$$

Maximum stress by mercury per equation (2):

$$S_{max.2} \quad = W_{mercury} / (A_1 + A_2)$$

$$= 505.1 / (3.16 \times 10^{-5} + 3.42 \times 10^{-5})$$

$$= 7.7 \times 10^6 \, P_a$$

$$= 7.7 \, MP_a$$

2. Pressure vessel model:

The average milk jug height:
$h_{max.} = 8.5 \, in. = 0.22 \, m$

The average radius of a milk jug:
$r = 2.5 \, in. = 0.0635 \, m$

Wall thickness:
$t = 0.015 \, in. = 3.81 \times 10^{-4} \, m$

Maximum pressure of water per equation (4)

$$P_{max.1} = \rho g h_{max} \quad = 1.0 \times 10^3 \times 9.8 \, m/s^2 \times 0.22$$

$$= 2.16 \times 10^3 \, P_a$$

$$= 2.16 \times 10^{-3} \, MP_a$$

Maximum hoop stress by water per equation (3)

$$S_{hoop,1} = P_{max} \, r/t$$

$$= 2.16 \times 10^{-3} \times 0.0635 / (3.81 \times 10^{-4})$$

$$= 0.36 \, MP_a$$

Maximum pressure of mercury per equation (4)

$$P_{max.2} = \rho g h_{max} \quad = 13.6 \times 10^3 \times 9.8 \, m/s^2 \times 0.22$$

$$= 2.93 \times 10^4 \, P_a$$

$$= 2.93 \times 10^{-2} \, MP_a$$

Maximum hoop stress by mercury per equation (3)

$$S_{hoop,2} = P_{max} \, r/t$$

$$= 2.93 \times 10^{-2} \times 0.0635/(3.81 \times 10^{-4})$$

$$= 4.88 \, MP_a$$

3. The maximum expected stresses on the milk jug are the larger values on the above two situations, thus;

By water:

Maximum Stress, $S_{water} = 0.56 \, MP_a$

By mercury:

Maximum Stress, $S_{mercury} = 7.7 \, MP_a$

C. Average tensile strength of a high density polyethylene (HDPE) specimen cut from the milk jug is 2200 psi, i.e.

Material strength, $S_{HDPE} = 2200 \, psi = 15.2 \, MP_a$

D. Comparison of material strength with maximum expected stress on the milk jug in relation to the safety factor (10). The permissible stress [5] S_p of high density polyethylene is the material strength divided by the safety factor or multiplied by 10% [4] in this case:

$$S_p = 10\% \, S_{HDPE} = 10\% \times 15.2 = 1.52 \, MP_a$$

$$S_{water} = 0.56 \, MP_a < S_p = 1.52 \, MP_a < S_{mercury} = 7.7 \, MP_a$$

All the necessary data and calculated results used for the safety evaluation are listed in Table I.

Table I. Data for Safety Evaluation of a Milk Jug

	Water	Mercury
Density, kg/m^3	1.0×10^3	13.6×10^3
Weight per gallon, N	37.1 (8.3 lb.)	505.1 (113.4 lb.)
Expected maximum stress, MP_a	0.56 (81.2 psi)	7.7 (1116.8 psi)
Material strength (S), MP_a	15.2 (2200 psi)	15.2 (2200 psi)
Permissible stress (S_p), MP_a	1.52 (220.5 psi)	1.52 (220.5 psi)

E. Conclusion:

Since the permissible stress of the high density polyethylene (HDPE) is higher than the expected stress by water but lower than that by mercury, it is concluded that the milk jug is safe to hold 1 gallon of water but unsafe to hold 1 gallon of mercury.

INSTRUCTOR NOTES: (1) The experiment gives students comprehensive practice in materials testing theory and methods as well as the application of material testing to product design and evaluation. (2) The engineering design approach needs to be introduced in the beginning of the materials testing course. (3) There are different methods of solving product safety problems and students should be encouraged to seek various ways to tackle the problem. For example, some students approached the problem by pressure-testing the container and comparing the results with the expected pressure on the container exerted by different liquids. Be aware that pressure tests should be performed in an approved safety chamber. (4) For those students not having enough background in mechanics, the instructor should encourage them to estimate the stress based on common sense and a basic definition of stress.

REFERENCES:

1. Gere, J. M.; and Timoshenko, S. P.: *Mechanics of Materials*, third ed., PWS-KENT Publishing, Boston, 1990, pp 411 - 413.

2. Serway, R. A.: *Physics for Scientists and Engineers*, second ed., Saunders College Publishing, Philadelphia, 1986, pp 316.

3. Standard Test Method for Tensile Properties of Plastics (Metric), *Annual Book of ASTM Standards*, ASTM, Philadelphia, vol. 08.01, 1989, pp 168 - 176.

4. Wendle, B. C.: *What Every Engineer Should Know About Developing Plastics Products*, Marcel Dekker, Inc. New York, 1991, pp 26 -27.

5. Shigley, J. E.; and Mitchell, L. D.: *Mechanical Engineering Design*, fourth ed., McGraw-Hill Book Co. New York, 1983, pp 226.

SOURCE OF SUPPLY: The milk jugs were recycled by faculty at no cost. This type of recycling reduces the amount of solid waste going to landfills.
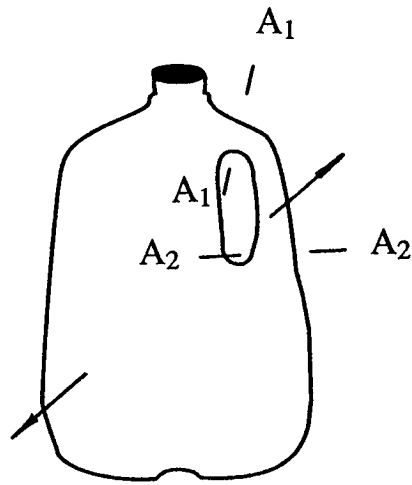
Figure 1. Schematic of milk jug subjected to weight loading when it is lifted by the handle. A_1 and A_2 are the two smallest cross section areas.
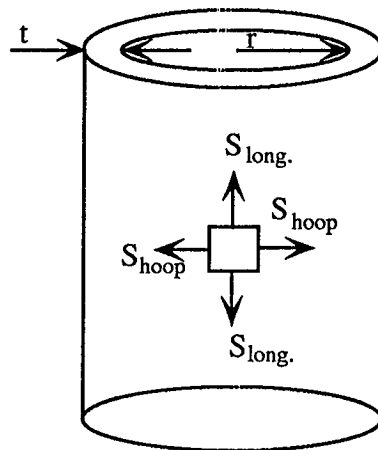
$$S_{hoop} = \frac{p\,r}{t}$$

$$S_{long.} = \frac{p\,r}{2t}$$

p = internal pressure
r = radius of the container
t = wall thickness

Figure 2. Stresses on thin-wall pressure vessel, caused by internal pressure.
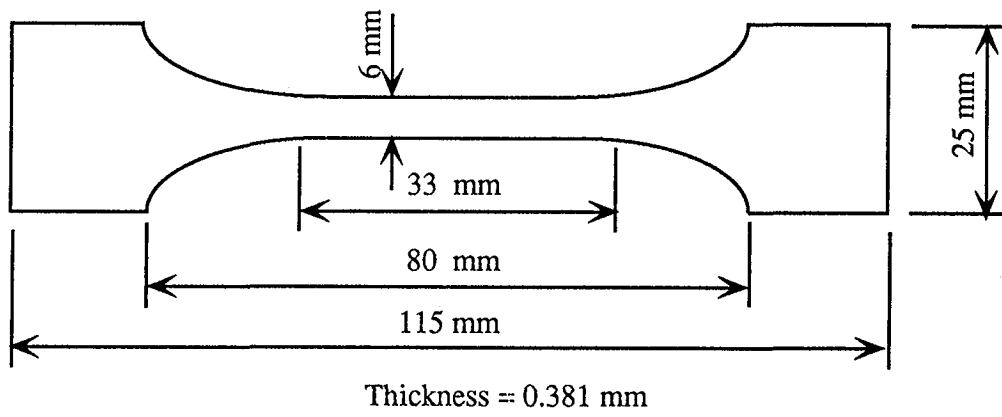
Figure 3. Dimensions of the tensile test specimen for high density polyethylene.

Participants
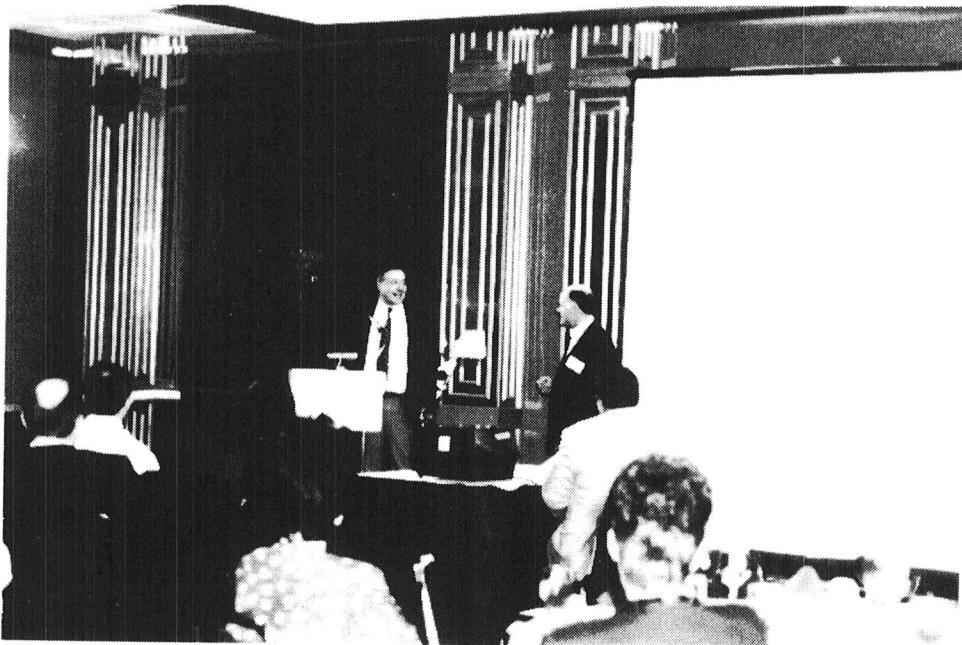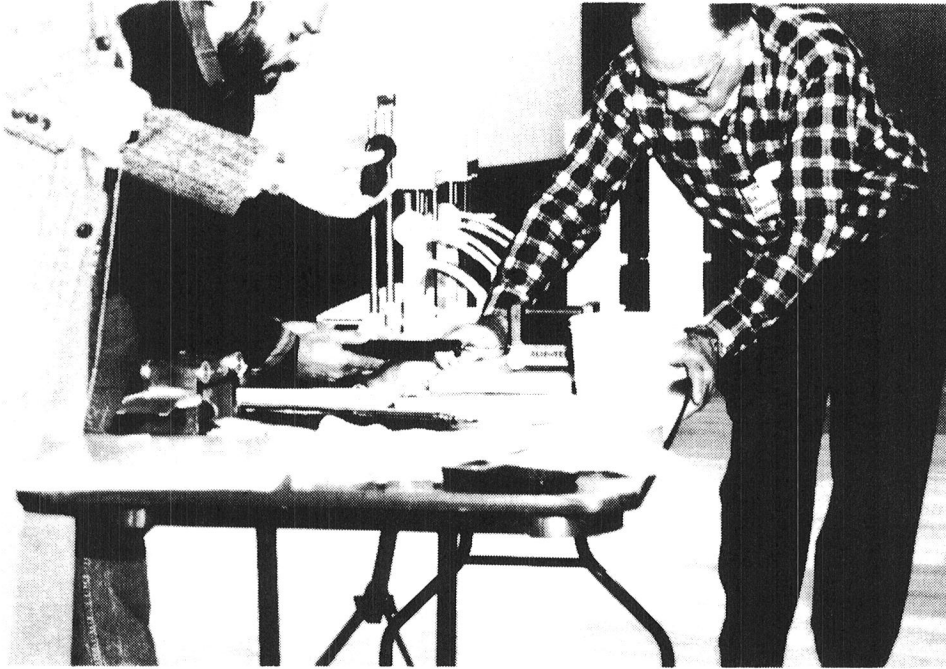
TRIBOLOGY: FRICTION, LUBRICATION, AND WEAR TECHNOLOGY

Peter J. Blau

Metals and Ceramics Division
Martin Marietta Energy Systems, Inc.
Oak Ridge National Laboratory
P. O. Box 2008
Oak Ridge, Tennessee 37831-6063

Telephone 615-574-5377

FRICTION, LUBRICATION, AND WEAR TECHNOLOGY

Peter J. Blau

Metals and Ceramics Division

Oak Ridge National Laboratory

<<< Lecture Outline >>>

<<< 1.0 Introduction and Definitions >>>

Friction, lubrication, and wear problems are extremely common in everyday life.

Many other technologies depend strongly on solving friction, lubrication, and/or wear problems. (e.g., transportation, utilities, computers, material processing, construction, and many others)

Despite the importance of friction, lubrication, and wear, *the education of engineers on the classical aspects of these subjects is rarely attempted in U.S. colleges and universities.* (Problem-driven, on-the-job training and short courses are the main sources of such information.)

Friction, lubrication, and wear, and their principles and applications, are all part of a multi-disciplinary field which we will call "tribology."

<<< 2.0 Friction Concepts >>>

Most students' exposure to friction problems is from physics or mechanics courses which stress problems like sliding boxes up inclines, looping ropes around pulleys, and deciding when a ladder will slip down a wall.

Mechanics-type approaches generally do not address the root causes for friction since they begin with an assumed value(s) for the friction coefficient(s). Little or no attention is given to the proper use of friction coefficients or to understanding of the origins of friction on real surfaces. (These are *"beyond the usual scope of the course."*)

Knowing how friction behaves in a wide range of circumstances will avoid costly errors in design and help analyze machinery problems.

Friction is not exclusively a property of the two contacting materials!

CONTRIBUTIONS TO THE TOTAL FRICTION LOSS
IN ENGINES VARY WITH ENGINE RPM

Bar chart categories (top to bottom): AUXILLIARY SYSTEMS (belts, etc), CONNECTING ROD SYSTEM, CRANKSHAFT SYSTEM, VALVE TRAIN, PISTON SYSTEM

Legend: 5000 rpm, 2000 rpm

X-axis: ENGINE FRICTION LOSS (% OF TOTAL), scale 0 10 20 30 40 50 60
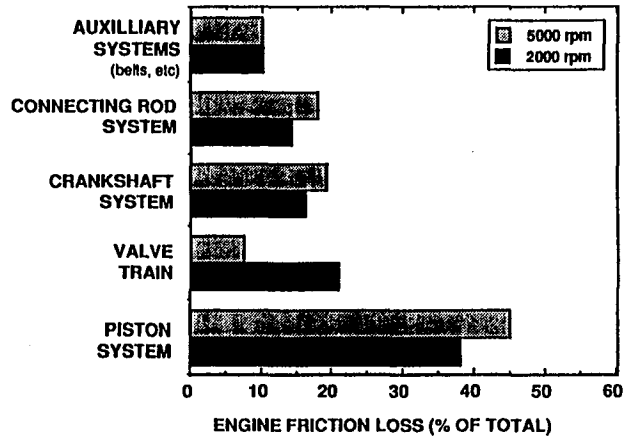
Reference: M. Hoshi, *Tribology International* (1984), Vol. 17(4), p. 185
Data: Subaru 4 cyl, OHV engine, SAE 10W-30 oil, 80o C, motored

Classical Definitions of the Friction Coefficient and Some Misunderstandings About Them

$$\mu_s = \frac{F}{N}$$

Static (impending motion)

$$\mu_k = \frac{F_v}{N}$$

Kinetic (while moving)

THE ABOVE DEFINITIONS ARE NOT UNIVERSAL LAWS OF SOLID FRICTION

FRICTION IS NOT INDEPENDENT OF VELOCITY, NORMAL FORCE, TEMPERATURE, ETC., AS THE EQUATIONS MIGHT OTHERWISE IMPLY

THE STATIC FRICTION IS NOT ALWAYS GREATER THAN THE KINETIC FRICTION

FRICTION IS NOT EXCLUSIVELY A "MATERIALS PROPERTY"

FRICTION IS FAIRLY EASY TO MEASURE, BUT NOT EASY TO PREDICT FROM BASIC PRINCIPLES.

BLOCK-on-RING SLIDING FRICTION
(Tests in Ar Gas at 5.0 cm/s)
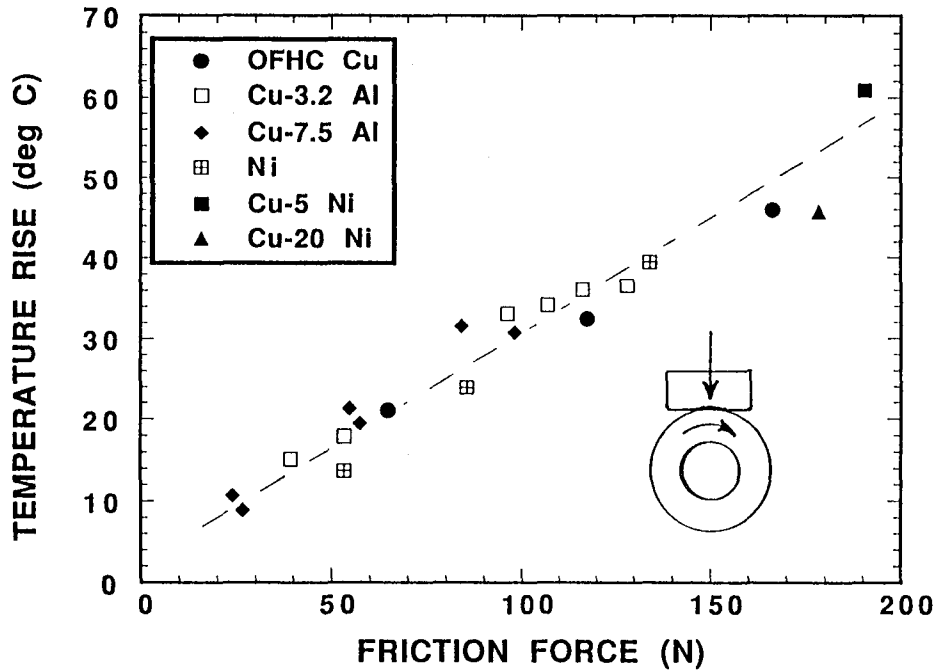
FRICTION EXPERIMENTS HAVE BEEN CONDUCTED FOR OVER 500 YEARS

Leonard da Vinci, applied mechanics studies (1493-1497)
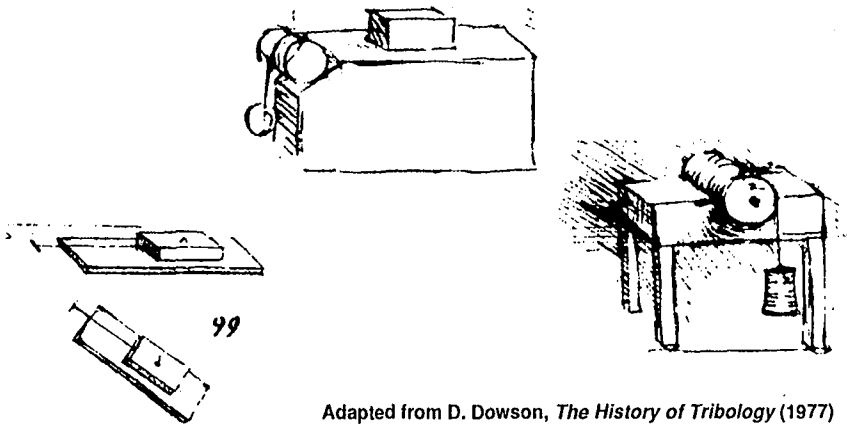
Adapted from D. Dowson, *The History of Tribology* (1977)

DOE, OTM, TRIBOLOGY - BY - DESIGN

298

TIME (s)

PIN-ON-DISK TEST
0.1 m/s, 1.0 N load
alumina ball on aluminum disk
no lubrication used

REVOLUTIONS ➝
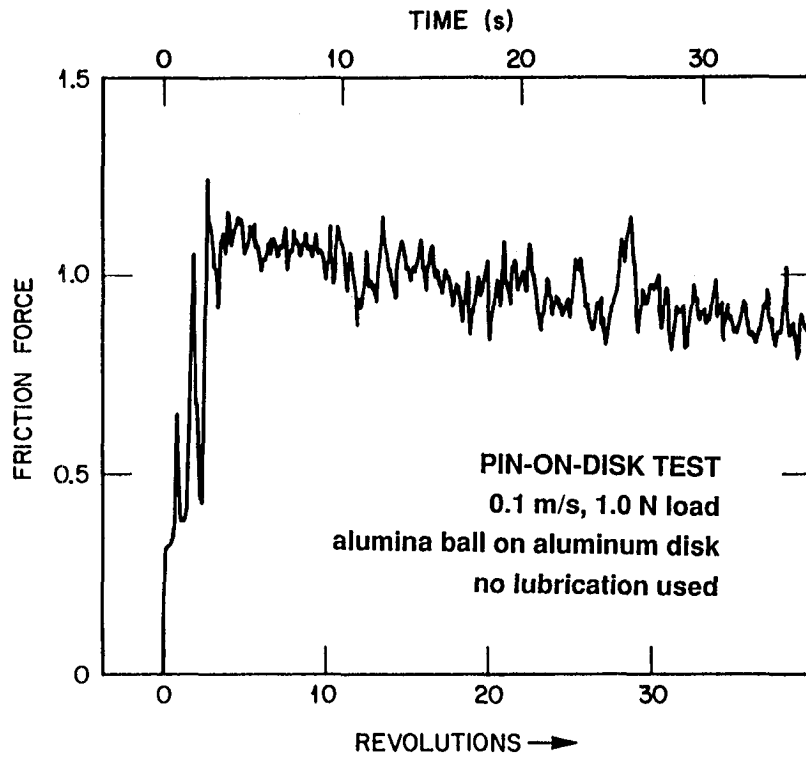
Pin-on-Disk Tests of Two Ceramics Show That
"A Sliding on B" ≠ "B Sliding on A"

ALUMINA SPHERE
SILICON CARBIDE DISK

SILICON CARBIDE SPHERE
ALUMINA DISK
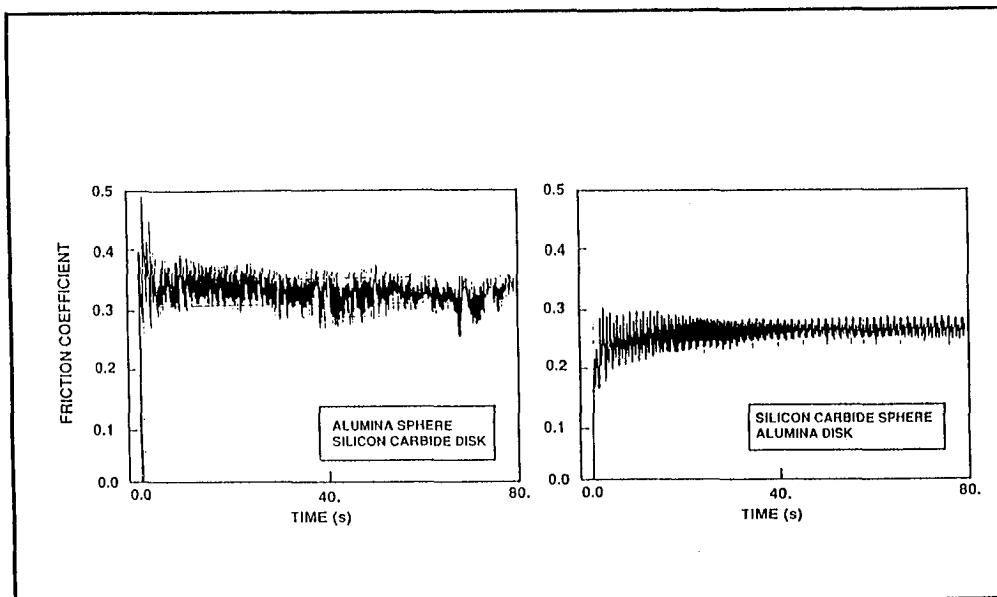
A SURVEY OF FRICTION COEFFICIENT COMPILATIONS

Ref. #	Source(s) of Data	Description of Test Conditions	Number of COF Values Static	Kinetic
1	Rankin (1858)	not given	14	19
2	Rankin (1858)	not given	31	31
3	not given	partial (incomplete)	233	34
4	23 references	not given in table		
		"dry"	29	34
		"greasy"	26	44
5	Marks	(same table as in Ref. 4, above)		
6	2 references	not given	16	0

References:

1) <u>Mining Engineers Handbook</u>, 3rd Ed., Vol. II John Wiley (1952) p. 36-42
2) <u>Handbook of Chemistry and Physics</u>, 35th Ed., CRC Press (1953) p. 1972
3) <u>Handbook of Chemistry and Physics</u>, 51st Ed., CRC Press (1971) p. F-15
4) <u>Marks Standard Handbook for Mechanical Engineers</u>, 9th Ed., McGraw Hill (1987), p. 3-26.
5) <u>Handbook of Lubrication</u>, Vol. II, Ed. Booser, CRC Press (1984), p. 46.
6) <u>SME Tool and Manufacturing Engineers Handbook</u>, 3rd Ed.,McGraw-Hill (1976), p. 41-12.

DOE, OTM, TRIBOLOGY - BY - DESIGN

Evolving Concepts of "Surface" Strongly Influenced the Development of Friction and Wear Models
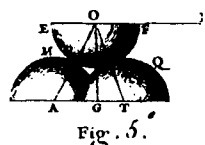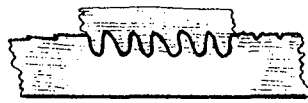
Belidor (1737)　　　*Coulomb (1875)*　　　*Goodman (1886)*
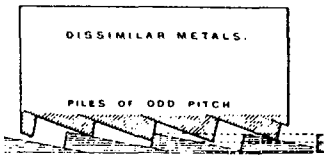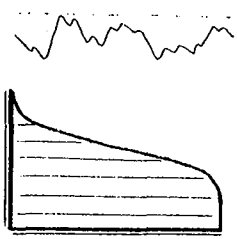
Abbott and Firestone (1933)　　*Samuels (1982)*　　*Nano-probe instruments (1981)*
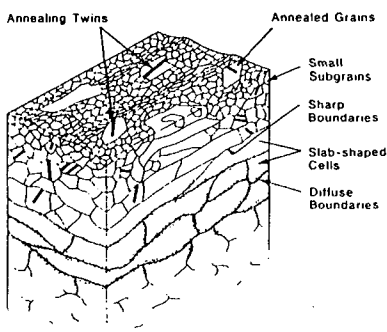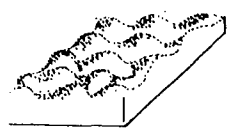
300

SENSIBLE FRICTION
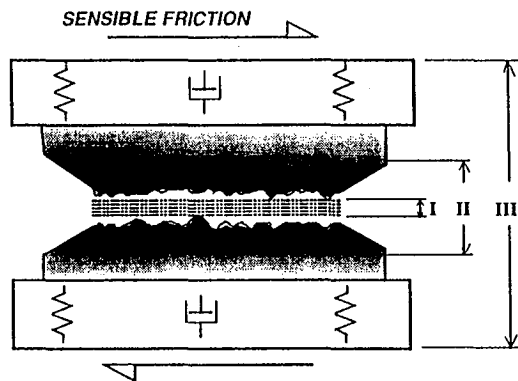
HIERARCHY OF INTERACTION LEVELS

I - INTERFACIAL MEDIA

    LUBRICATION THEORIES
    TRIBOCHEMICAL FILMS
    TRIBOPARTICULATES

II - BOUNDING SOLIDS

    DEFORMATION AND FRACTURE
    FATIGUE
    MATERIAL/ENVIRONMENT INTERACTION
    WHITE-LAYERS AND TRANSFER

III - MACHINE AND ITS ENVIRONS

    DYNAMICS OF THE CONTAINMENT

<<< 3.0 Lubrication Technology Concepts >>>

Functions of Lubricants

1. Reduce sliding friction
2. Support and distribute the contact load
3. Protect surfaces for excessive wear or seizure
4. Cool sliding surfaces
5. Carry away wear particles (debris)

Types of Lubricants

1. Liquid lubricants
2. Greases
3. Solid lubricants (graphite, teflon, soft metals, chalcogenides)
4. Gases (air bearings)

REGIMES OF LUBRICATION: THE STRIBECK CURVE

η = viscosity

v = velocity

p = pressure

HYDRODYNAMIC

DRY

BOUNDARY

MIXED

EHD

μ

1.0

0.1

0.001

$\dfrac{\eta\, v}{p}$

FILM THICKNESS

$\dfrac{\eta\, v}{p}$

Ref: J. A. Schey, Tribology in Metalworking (1983)
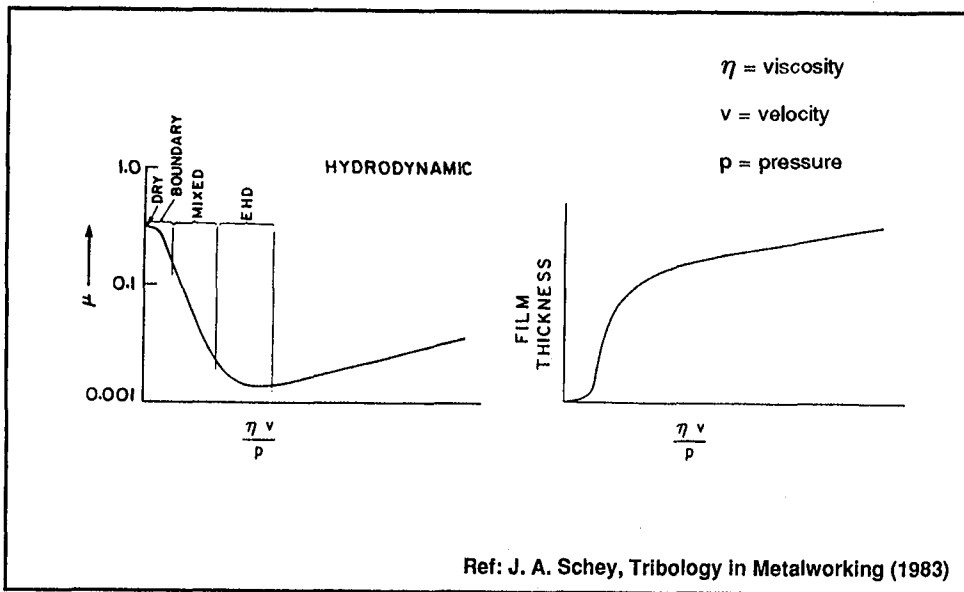
FILM THICKNESS RATIO, $(\lambda) = [\, h / (\, \sigma_1^2 + \sigma_2^2\,)^{1/2}\,]$

SOME COMMON SOLID LUBRICANTS

PTFE (TeflonTM)

graphite (powder and foil)

molybdenum disulphide

talc

Pb, Sn, Ag

SOME LESS-COMMON SOLID LUBRICANTS

barium fluoride / calcium fluoride

boric acid

tungsten diselenide

tungsten disulphide

titanium oxide

ornl tribology

302

SOLID LUBRICATION:

Simple models for frictional behavior

It is generally assumed that the frictional behavior of a solid
lubricant is proportional to its shear strength.

$$F = \tau A$$

F = friction force, t = shear strength of the solid, and
A = area of interfacial contact

But, the shear strength of [Bridgeman] solids can be affected by

the pressure on them, and τ is modified as follows:

$$\tau = \tau_0 + \alpha P$$

τ_0 = shear strength at ambient pressure, α = a constant, and
P = contact pressure

ornl tribology

SOLID LUBRICANT FILM PROPERTIES:

Pressure Dependence of the Shear Strength

$$\tau = \tau_0 + \alpha P$$

Test conditions: glass hemispherical slider, glass
substrate, 0.24 mm/s sliding speed, 1-300 mN load,
40-150 MPa mean contact pressure

	τ_0, (MPa)	α
molybdenum disulphide: commercial grade	2.0	0.15
molybdenum disulphide: research grade	2.0	0.17
oleophilic, high-purity graphite	4.0	0.09
high-density polythene	2.5	0.10
low-density polythene	6.0	0.14

[Ref.: B. J. Briscoe and A. C. Smith, ASLE Transactions (1981)]

ornl tribology

```
┌─────────────────────────────────────────────────────────────┐
│              SELF-LUBRICATING COATINGS:                       │
│      Current Applications and Technology Needs                │
│  ─────────────────────────────────────────────────────       │
│                                                               │
│  (1)   ceramic engine parts - valve guides, piston ring grooves, etc. │
│  (2)   diesel turbocharger bearings - high-temperatures       │
│  (3)   seals for non-CFC-containing refrigeration systems     │
│  (4)   bearing element retainers (spacers between balls and rollers) │
│  (5)   cryogenic bearings (Space Shuttle turbopump, etc.)     │
│  (6)   moving parts in advanced gas turbine engines (seals and bearings) │
│  (7)   gimbals and pointing control systems in orbital guidance systems │
│  (8)   dry-lubricated bearings for cruise missile engines (elevated temp.) │
│  (9)   machine tool spindles  (grinders, high-speed drills, honing machines) │
│  (10)  moving parts in hard-to-lubricate locations in industrial machinery │
│  (11)  small parts in computer magnetic storage systems       │
│  (12)  mechanical parts in office copiers and other business machines │
│  (13)  small parts in motorized cameras                       │
│  (14)  aircraft auxilliary power units (APU's)                │
│                                                               │
│                                        ──── ornl tribology ──┘
└─────────────────────────────────────────────────────────────┘
```

<<< 4.0 Wear Technology Concepts >>>

Wear Modes (c.f. wear mechanisms)

There are numerous ways to classify wear. Here is one scheme that depends on the relative motion and the geometry of contact:

1. Abrasive wear (2- and 3-body)
2. Erosive wear (impinging particles; solid or liquid)
3. Cavitation erosion
4. Impact wear
5. Fretting wear (fretting fatigue; fretting corrosion)
6. Sliding wear ("adhesive wear")
7. Rolling contact wear (rolling contact fatigue; fatigue wear)
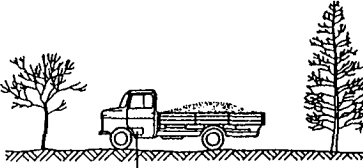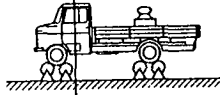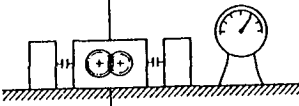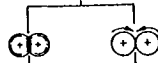
[Note: Galling and scuffing are not strictly forms of wear since they do not always involve *progressive loss of material.*]

304

THERE IS NO UNIVERSAL, "STANDARD" WEAR TEST

WEAR TESTS ARE DESIGNED OR SELECTED FOR THE FOLLOWING REASONS

(1) TO SIMULATE A SPECIFIC SET OF CONDITIONS IN AN APPLICATION

(2) TO ISOLATE A PARTICULAR TYPE OF WEAR PROCESS (ABRASION, SLIDING, ETC.) FOR RESEARCH PURPOSES

(3) TO SCREEN MATERIALS AS TO THEIR RELATIVE WEAR RESISTANCE UNDER SPECIFIED CONDITIONS.

Tabelle 2. Kategorien der Verschleißprüfung bei einem Nutzkraftwagen-Getriebe

Kategorien	Art des Versuches		Symbol
I	Betriebs- bzw. betriebsähnliche Versuche	Betriebsversuch (Feldversuch)	
II		Prüfstandsversuch	
III		Prüfstandsversuch mit Aggregat oder Baugruppe	
IV	Versuche mit Modellsystem	Versuch mit unverändertem Bauteil oder verkleinertem Aggregat	
V		Beanspruchungsähnlicher Versuch mit Probekörpern	
VI		Modellversuch mit einfachen Probekörpern	

FRICTION AND WEAR DEVICES

Second Edition

1976

Revised and Enlarged Report

of

Subcommitte on Wear
Lubrication Fundamentals Committee
American Society of Lubrication Engineers

Authors

R. Benzing
I. Goldblatt
V. Hopkins
W. Jamison
K. Mecklenburg
M. Peterson

Printed in the United States of America

A list of 234 different testing machines

THERE IS NO UNIVERSAL UNIT FOR WEAR

UNITS FOR WEAR DEPEND ON THE REASON FOR TESTING:

(1) DIMENSIONAL CHANGE (increase in clearance in a bearing or seal)

(2) WEIGHT CHANGE (generation of contaminating debris)

(3) DISTANCE (guarantees on automobile tires)

(4) MANY OTHER UNITS (volume, volume loss per unit time, weight loss per unit distance slid, relative wear, etc., etc., etc....
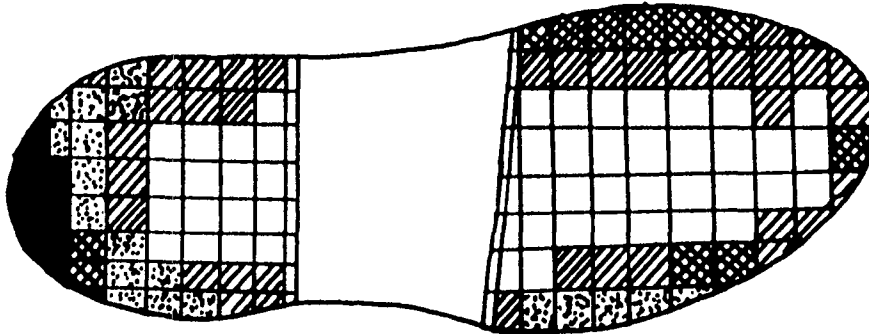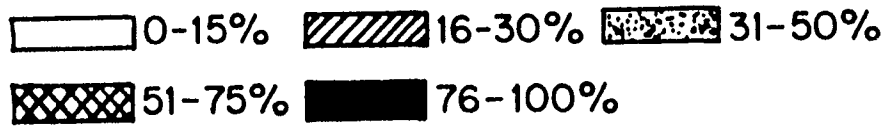
Topology of wear of a shoe. Between 76 and 100% of the shoes examined showed wear of the edge of the heel. (James, D. I. (Ed.) (1967). "Abrasion of Rubber", Rubber and Plastics Research Association of Great Britain, London.)

<<< 5.0 Tribological Transitions >>>

Definition

tribological transition, n. - a change in friction or wear behavior produced by either an external change in the operation of a tribosystem, or by the aging of materials or components during use.

Some Examples and Manifestations

1. running in a new set of brakes
2. a bearing suddenly begins to smoke and rattle
3. a valve begins to leak after operating satisfactorily for a year
4. your engine starts to burn oil
5. increasing the sliding speed during a test causes friction to drop

Controlling friction or wear transitions can be vitally important to the effective design and long-term operation of machines of all kinds.

To model friction or wear, a comprehensive definition of the tribosystem is needed.

All relevant variables must be specified.

☞ *Load-related variables:* direction, magnitude, distribution (pressure), history, vibration, contact stiffness

☞ *Contact geometry-related variables:* size of the nominal contact, surface roughness, macro-geometry (Hertz arguments)

☞ *Materials variables:* composition, surface micromechanical properties, processing history

☞ *Thermal variables:* ambient temperature, frictional heating contribution

☞ *Chemical variables:* reactivity of the environment, tribo-chemistry

☞ *Cleanliness and effects of particles:* initial surface cleanliness, wear debris, contaminating particles

☞ *State of lubrication:* boundary, dry, mixed, hydrodynamic, intermittent

---

<<< 6.0 Summary >>>

Friction, lubrication, and wear technology impacts everyday life.

Friction and wear are properties of the system, not just the contacting materials.

Friction is not easy to predict, despite deceptively simple definitions for the friction coefficient given in introductory texts on physics and mechanics of materials. *Measuring friction is usually easy, but understanding it is not.*

Lubrication technology is the key to transportation, manufacturing, utilities, defense, and many other sectors.

The regimes of lubrication can be controlled to alter the effectiveness of friction reduction.

Solids, liquids, and gases can all lubricate. Lubricant formulation is both a science and an art.

There are various ways to classify and measure wear. Methods of wear measurement should suit the desired application.

Tribological transitions can be affected by intentional changes in operating parameters or by aging of the tribosystem.

Friction, lubrication, and wear technology should be a part of the academic training of every undergraduate mechanical engineer, industrial engineer, and materials engineer because *tribology is an enabling technology.*

*** BIBLIOGRAPHY ***

Books:

D. Dowson, <u>History of Tribology</u>, Longman Pub. (1979).

<u>ASME Wear Control Handbook</u>, ed. W. O. Winer and M. B. Peterson, ASME, New York (1980).

<u>Friction, Lubrication, and Wear Technology</u>, ASM Handbook, 10th Ed., Vol. 18 (1992).

E. Rabinowicz, <u>Friction and Wear of Materials</u>, John Wiley (1965).

<u>Handbook of Lubrication</u>, Vol. I (Applications and Maintenance) and II (Theory and Practice of Tribology), ed. R. Booser, CRC Press (1984).

F. P. Bowden and D. Tabor, <u>The Friction and Lubrication of Solids</u>, Clarendon Press, Oxford (1986).

K. C. Budinski, <u>Surface Engineering for Wear Resistance</u>, Prentice Hall (1988).

P. J. Blau, <u>Friction and Wear Transitions of Materials</u>, Noyes Pub. (1989).

Journals:

Journal of Tribology, ASME (formerly *J. of Lubrication Technology*)

Wear, Elsevier Sequoia Pub.

Tribology International, Butterworth-Heineman

Lubrication Engineering, STLE

Tribology Transactions, STLE

WALKWAY FRICTION: EXPERIMENT AND ANALYSIS

Mark I. Marpet

Associate Professor of Quantitative Analysis
St. John's University
Staten Island Campus
300 Howard Avenue
Staten Island, New York 10301

Telephone 718-390-4545

and

Robert J. Brungraber

Bucknell University
Lewisburg, Pennsylvania

WALKWAY FRICTION: EXPERIMENT AND ANALYSIS

Mark I. Marpet, Ph.D., P.E.
St. John's University, New York City, New York
and
Robert J. Brungraber, Ph.D., P.E.
Bucknell University, Lewisburg, Pennsylvania

KEY WORDS: friction, walkway safety, tribology, articulated strut.

PREREQUISITE KNOWLEDGE: The student should either be familiar with the classical (Amontons-Coulomb) friction model or, alternatively, this model should be presented concurrently with the experiment.

OBJECTIVES: To explore the utility and the limitations of the Amontons-Coulomb friction model. To explore Design of Experiments issues which underlie competent testing.

EQUIPMENT AND SUPPLIES:

(1) Two test devices: a drag sled tester and an articulated strut tester must be fabricated. If friction versus test foot[1] velocity is to be tested, obtain a suitable small, variable-speed gear-motor.

(2) Walkway surrogates (test surfaces). Test surfaces can include steel, wood, vinyl tile, ceramic tile, and carpet (glued to a substrate).

(3) Foot-bottom surrogates can include various leather and synthetic shoe bottoms (taken from old shoes), standard leather, neolite, steel, and silicone elastomer.

(4) A calibrated dynamometer (or a pull scale) is used to weigh and pull the drag sled.

(5) Double-sided carpet tape is needed to affix a test surface to the table for the drag sled tests.

(6) A stopwatch may be used to time the residence time[2] for the drag sled tester.

(7) 400 grit wet/dry sandpaper is needed to prepare the test feet.

(8) An engineering calculator is needed to convert the articulated strut readings to friction coefficients. Alternatively, a computer program can be written to automate the conversions; this is an excellent student project.

(9) A commercial statistical analysis program will be needed to perform Multivariate general linear hypothesis[3] tests. We use MyStat. It retails for under $20 (DOS or Macintosh).

(10) A computer to run the software is needed.

---

[1] Friction is an interface property. It is normally considered to be a property relating to two surfaces in contact, perhaps with lubricants or contaminants at the interface. Walkway friction has a natural orientation which is not present when one talks in general about friction: the pedestrian's foot contacts the walkway surface, and not the other way around. Walkway friction concerns include what kind of foot surrogates can be used to test walkway surfaces, what types of floor surrogates can be used to test shoe or foot bottoms, and what suites of interface conditions are relevant to real-life pedestrian walking. In order to avoid ambiguity, we will in this paper denote that material that stands in for whatever is on the bottom of the foot as the *test foot* or the *foot-bottom surrogate* (or just *foot surrogate*) and whatever stands in for the walkway surface as the *test surface* or *walkway surrogate*. We will denote any interface lubricants (e.g., water) or contaminants simply as contaminants.

[2] The time between the application of the normal force and the initiation of slip

[3] A technique which combines regression analysis (curve fitting) and analysis of variance (multi-family tests of hypotheses)

BACKGROUND: Pedestrian accidents have been shown to be the leading cause of direct and morbidity accident costs in the United States. Thus, the analysis and prevention of pedestrian slips is a high priority if fall-induced injury costs are to be minimized.

Many of the walkway friction testing methodologies used today are based upon the 'classical friction model,' that is, upon the Amontons-Coulomb friction axioms: that friction is independent of pressure, temperature, humidity, velocity, and residence time. In fact, these assumptions are not, in general, strictly correct. More to the point, these axioms are unjustified in many walkway situations, especially if the friction interface is wet or contaminated, as is often the case.

The purpose of this experiment is to discuss design of experiments issues in an information-gathering experiment, to investigate the variation in friction with respect to the above parameters, and to explore the envelope of the Amontons-Coulomb friction model. The tests illustrate how using inappropriate tests will obtain anomalous results (for example, drag sled tests of wet leather against wet tile often exhibit higher friction results than do tests of dry leather against the same (dry) tile) and — in contrast — show that if appropriate methods are employed, one obtains results consistent with common sense.

PROCEDURE:

Introduction: The two friction testers can be fabricated according to the designs given in this paper. Both testers have been designed to use the same test foot mounting scheme. If the drag-sled is to be motorized, the dynamometer can be rigidly mounted to the sled (as low as possible) and the pull wire fastened between the motor pulley and the dynamometer. The pull wire should be 'axially stiff'. A strain gauge apparatus with appropriate instrumentation may be substituted for the dynamometer. Students may design their own testers. In the case of the articulated strut tester, this is a non-trivial exercise.

Before the equipment can be utilized for testing, an experimental design must be developed and the test sensor set must be prepared.

Experimental Design: The test plan, or experimental design, is formulated in advance so as to explicitly consider and effect reasonable compromises in the number of tests, the amount of information gathered, and the amount of test replication. Replication helps ensure reliability of results, but only at the price of a substantially increased number of tests. And the number of tests can mount factorially if too much is attempted. For example, if one wanted to conduct a complete test suite: the two test devices with steel, leather, neolite, and silicone test feet against steel, wood, vinyl tile, and carpet test surfaces at two contact pressures, two velocities, and wet and dry, one would need to conduct

$$2_{machines} \cdot 4_{sensors} \cdot 4_{surfaces} \cdot 2_{pressures} \cdot 2_{velocities} \cdot 2_{wet \& dry} = 256 \text{ tests} \qquad (1)$$

without any replication. Four replications are often conducted for each set of test conditions. Each replication is conducted in a different compass point orientation, i.e., the test surface (or the tester) is rotated 90° between each test. That implies that the test design would require $256 \cdot 4 = 1024$ tests![4]

The first element in the test design is to estimate how many tests can reasonably be run by dividing how long each test will take (time tests conducted on each machine to get an estimate of the time needed) into a realistic estimate of how many hours can be

---

[4] Now you know why the mathematical symbol for the factorial operation is '!' .

devoted to testing. Once that number of tests is determined, the compromises needed to fit the experiment into the real world should become clear.

The general linear model should be used for the analysis of the significance of test results. Essentially, one starts with a set of baseline conditions, e.g., articulated strut tester, neolite test surface, vinyl tile, low contact pressure, low velocity. Each modification to the baseline is accounted for, first, by a linear categorical constant attached to a dummy variable and, if desired, by compound (non-linear) terms which quantize the factor interaction effects:

$$\mu_s = b_0 + b_1 x_1 + b_2 x_2 + \cdots + b_i x_i + \cdots + b_n x_n + b_{12} x_1 x_2 + \cdots + b_{ij} x_i x_j + \cdots \tag{2}$$

where

μ_s = static coefficient of friction

b_0 = the static friction coefficient under baseline conditions

b_i = the marginal friction increase or decrease for condition i

x_i = a dummy variable. $x_i = \begin{cases} 0; \text{ if condition is absent} \\ 1; \text{ if condition is present} \end{cases}$

b_{ij} = the marginal increase in friction when both
conditions i and j are present

Similarly, b_{ijk} and higher-order interactions can be defined. b_{ijk}, for example, is the marginal friction factor when i, j, and k are all present. Higher-level interactions will likely overpower all but the most powerful statistical analysis programs.

The data should be collected in tabular form.

Machine	f_i or θ	Sensor	Surface	Wet/Dry
Strut	32°	Neolite	Steel	Dry
Strut	75°	Neolite	Steel	Wet
...				

Figure 1. A sample data collection format.

Test Sensor Preparation: An adequate number (this can be determined by reference to the experimental design) of steel test-foot brackets must be fabricated. Test feet from old shoe soles can be prepared by cutting a 3-inch square (or smaller, as the experimental design dictates) from the heel or sole of the shoe, and trimming and sanding the back of the sole or heel until it is smooth and level. Small heels, as those found on high-heeled shoes, may be used in pairs (or in groups of three) for stability. Each foot bottom surrogate is glued to a test-foot bracket.

Before each test, the sensor is prepared for use by sanding it lightly — four times in each of two orthogonal directions — with 400 grit wet-or-dry sandpaper.

The Drag Sled Tester: The drag sled tester is utilized by mounting a test surface to the table using double-sided carpet tape. A test foot is held to the weight bottom by the magnetic tape adhered to the bottom of the weight. The drag sled/test-foot assembly is weighed; the weight, f_n, is recorded. The drag sled/test-foot assembly is placed on the test surface. If residence time is to be monitored, a stopwatch is started when the weight is placed upon the test surface. An increasing horizontal force is then applied to the sled, either manually or through a motor arrangement. When the sled moves (breaks away), the lateral force,

f_l, is recorded. If residence time is monitored, the stopwatch is stopped when the sled first moves. It is essential to keep the pull wire horizontal. The motor or the dynamometer can be shimmed with wood or another material to ensure this. The static friction coefficient, μ_s, is computed as the ratio of the lateral to the weight force:

$$\mu_s = \frac{f_l}{f_n}. \tag{3}$$

The articulated strut tester: It is easy to see that, if the static friction coefficient is defined as the ratio of the lateral and normal forces, it is equivalently characterized by the tangent of the angle at which slip occurs:
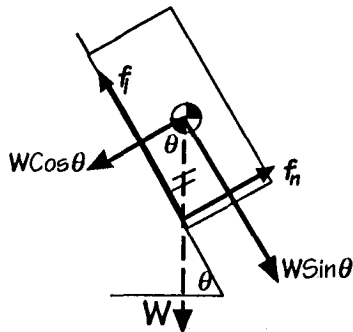
$$\tan\theta = \frac{W\mathrm{Sin}\theta}{W\mathrm{Cos}\theta} = \frac{f_l}{f_n} \tag{4}$$

is, by reference to the diagram on the left, the ratio of the lateral force to the normal force. That ratio is the definition of the static friction coefficient.

Figures 2 and 3. Idealized and actual free body diagrams of an articulated strut tester.
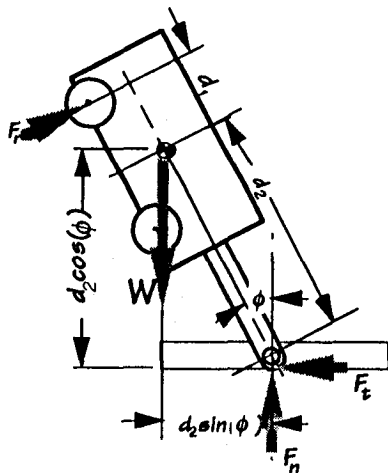
The tester described in the sequel has a somewhat more complex mathematical model because the strut is cantilevered to the weight/transport assembly, and not hinged, as in the more complex commercial articulated strut devices. Noting that, at slip, there is no weight on the forward wheel, that the reaction at the rear wheel is perpendicular to the strut axis, and that the line of action of the strut passes, by construction, through the center of gravity, we can determine the formula for the static friction coefficient by summing moments about the center of gravity:

$$d_2\mathrm{sn}\phi F_n = d_2\cos\phi F_t + d_1 F_r \tag{5}$$

and

$$\frac{d_2\sin\phi F_n}{d_2\cos\phi F_t} = 1 + \frac{d_1 F_r}{d_2\cos\phi F_t} \tag{6}$$

It follows that

$$\frac{1}{\mu_s} = \frac{F_n}{F_t} = \frac{1}{\tan\phi} + \frac{d_1 F_r}{d_2\cos\phi F_t \, \tan\phi} = \frac{1}{\tan\phi} + \frac{d_1}{d_2\cos^2\phi\tan\phi} = \frac{1}{\tan\phi}\left(1 + \frac{d_1}{d_2\cos^2\phi}\right) \tag{7}$$

$$\mu_s = \tan\phi\left(\frac{d_2\cos\phi}{d_2\cos\phi + d_1}\right) = \tan\phi\left(\frac{\cos^2\phi}{\cos^2\phi + \frac{d_1}{d_2}}\right) \tag{8}$$

It is clear that, to minimize the correction factor, d_1 should be made as small as possible by moving the back wheels close to the center of gravity of the strut assembly.

316

The articulated strut tester is operated by clamping the test surface onto the baseboard, setting the angle board at a specific angle: the ramp angle measured from the vertical, dropping the weight, and seeing if the articulated strut assembly 'breaks away.' For the tester design described here, breakaway detection is visually obvious.
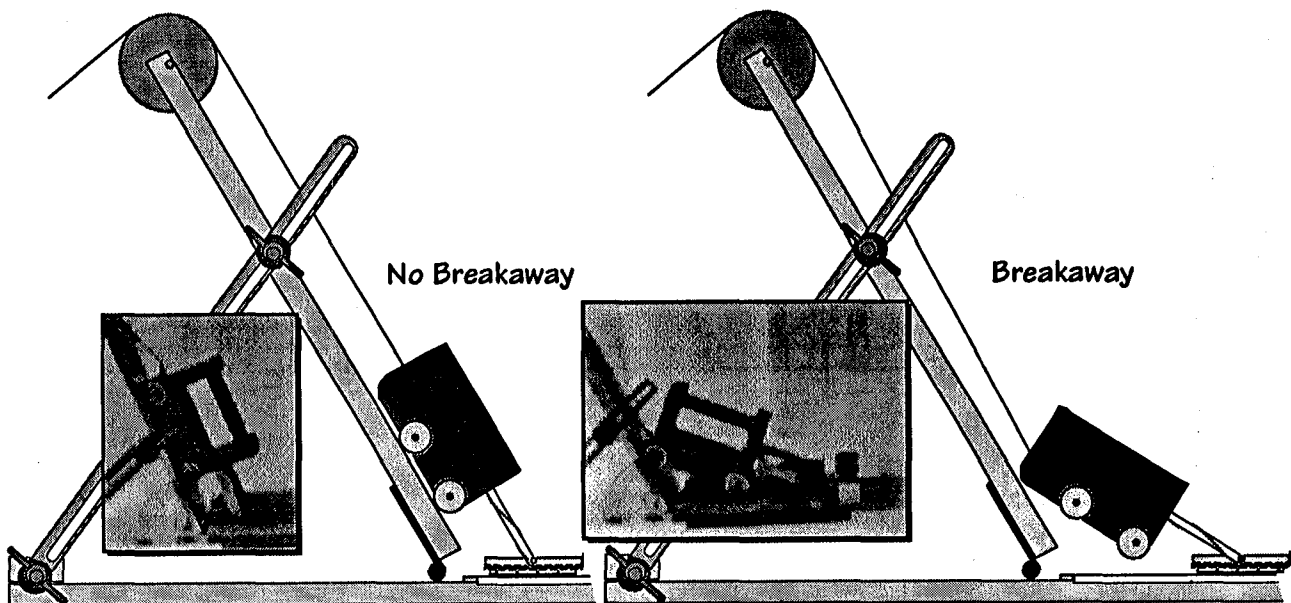
Figure 4. Side views of the articulated strut tester, depicting how breakaway is detected.

If there is no breakaway, the coefficient of friction is greater than the adjusted tangent of ϕ, the ramp angle. The test foot does not need to be re-sanded. The angle board is then adjusted with the wing nuts to a larger ramp angle, the weight is raised, and the strut assembly is again released.

If the articulated strut breaks away, the friction coefficient is less than the adjusted tangent of ϕ, the ramp angle. The test foot is re-sanded, the ramp angle is reduced, and the test sequence is repeated.

Repeated tests home in upon the breakaway angle. Using the articulated strut tester, it is customary to record the full sequence of test angles for each test set, circling those angles which result in sensor breakaway, e.g., in the simulated results below,

$$25°, 30°, 35°, 40°, 45°, 41°, 42°, 43°$$

the slip angle lies between 42° and 43°. The tangent of that breakaway angle is the desired friction coefficient. In this simulated example, $\theta = 42°–43°$ corresponds to $\mu_s = 0.46–0.47$. (Use the formula above, with $d_1/d_2 = .525$, for our tester.)

Data Analysis: The use of computerized statistical analysis is essential. (This example uses MyStat.) The example below is based upon real data obtained in walkway friction testing. The following factors were accounted for in the experimental design:

- *LATFORCE* (These results are from drag sled tests; lateral force is more convenient to work with than the friction coefficient derived directly from it.)
- *WETDRY* (1 = dry, 2 = wet)
- *SENSOR* [i.e., the test foot] (1 = neolite, 2 = leather, 3 = rubber)
- *TILE* [i.e., the test surface] (1 = 'brand A' tile, 2 = 'brand X' tile, 3 = 'brand Z' tile)
- *DIRECTIO*[n] (1 = 'North', 2 = 'East', 3 = 'South', and 4 = 'West')

The analysis is started by inputting the data into the data editor, which appears to be a spreadsheet, but is not. (In the example below, only 12 of the 72 cases are shown.)

	LATFORCE	WETDRY	SENSOR	TILE	DIRECTIO
1	41.000	1.000	1.000	1.000	1.000
2	42.000	1.000	1.000	1.000	2.000
3	38.000	1.000	1.000	1.000	3.000
4	40.000	1.000	1.000	1.000	4.000
5	41.000	1.000	1.000	2.000	1.000
6	43.000	1.000	1.000	2.000	2.000
7	41.000	1.000	1.000	2.000	3.000
8	39.000	1.000	1.000	2.000	4.000
9	40.000	1.000	1.000	3.000	1.000
10	43.000	1.000	1.000	3.000	2.000
11	39.000	1.000	1.000	3.000	3.000
12	43.000	1.000	1.000	3.000	4.000

Figure 5. A computer screen 'snapshot' of the MyStat (Macintosh) data editor. The factor names are first entered into the top row. The data are then entered, one case at a time, row by row. The numbers in the left-hand column are the 'case' numbers, and are not entered by the experimenter. By way of example, test 4 had a lateral force of 40 lbs., and was conducted dry, with a neolite sensor on a brand A tile in the 'West' direction. The triple-digit accuracy is a software artifact; ignore it.

After all the data were entered into the editor, they were saved, and the regression tool was selected. In regression, LATFORCE was first selected as the independent variable. The rest of the variables were specified to be *categorical*; all were utilized as dependent variables. No interactions were examined. The fact that all the dependent variables are categorical implies that MyStat will use analysis of variance (ANOVA).

```
                    Analysis of Variance
Dependent variable: LATFORCE                          N: 72
Multiple R: 0.499             Squared Multiple R: 0.249

Source      Sum-Squares  DF  Mean-Square  F-Ratio  P-Value
WETDRY         6.125      1      6.125      0.345    0.559
SENSOR       241.750      2    120.875      6.815    0.002
TILE          95.083      2     47.542      2.680    0.076
DIRECTIO[N]   28.486      3      9.495      0.535    0.660
Error       1117.431     63     17.737
```

Figure 6. These results of the ANOVA are slightly rearranged for clarity.The dependent variable and the number of cases analyzed (72) are presented first. Multiple R is the overall correlation coefficient. Squared multiple-R is the proportion of experimental variation explained by the ANOVA. (This ANOVA explained 25% of the variation, a rather poor showing.) The remainder of the results is the ANOVA table, shown in canonical form.

The first and last columns of the ANOVA table are of interest to the experimenter. The first column lists the factors (WETDRY, SENSOR, ...)controlled in the experimental design. The last table column gives, for each line, the P-$value$ of the factor in that line. The P-value is the probability that one will be wrong if one ascribes *significance*, i.e., causality, to that factor. (The opposite of significance is, of course, non-significance: that any effects which can be attributed to a given factor are, in fact, due to chance.)

For example, if one asserted that WETDRY — whether the tile floor surface was wet or dry — was a significant factor, one would be wrong over half of the time. Clearly, if you accept these experimental results, any observed effect of water on the tile surface is due to chance! In other words, no confidence can be placed in the assertion that WETDRY is a significant factor. (The notion that wet tile surfaces are neither more nor less slippery than dry tile surfaces should fly in the face of your experience. That's because these tests were conducted with a drag sled, which is completely unsuitable for testing in the wet because of sensor/test surface adhesion effects: the test foot literally suction-cups itself to the test surface.)

Similarly, if you asserted that the sensor material was a significant factor in the lateral force, you would be wrong only 0.2% of the time. Great confidence can be placed in the hypothesis that the sensor material was a significant determinant of lateral force and in the corresponding static friction coefficient.

In the United States, it is customary to ascribe significance to P-values at or below 5%, and non-significance to P-values above 5%. In the given example, only the SENSOR material was a significant determinant of friction. WETDRY, DIRECTIO[N], and TILE would not be considered statistically significant.

Other Considerations:

Average contact pressure: While average, i.e., bulk contact pressure, can be varied by changing the weight, it is simpler to vary the size of the sensor. For example, changing from the standard 3 inch-square sensor to a 1½x3 inch sensor *cet. par.,* doubles the average contact pressure.

Velocity: If velocity is used as a factor in the experimental design, the sled (or the strut assembly) should be driven by a variable-speed motor. If velocity is not used as a factor in the experimental design, operators should practice with the equipment, endeavoring to operate the testers at a uniform velocity so as to eliminate velocity as a factor in the experimental results. Better yet, motorize the instruments.

REFERENCES & BIBLIOGRAPHY:

Hale, Robert L., *MYSTAT Statistical Applications,* Available in *Macintosh and DOS Editions*], Course Technology, Inc., 1990.

Adler & Pierman, *A History of Walkway Slip-Resistance Research at the National Bureau of Standards* (NBS Special Publication 565), U. S. Department of Commerce, 1979.

Anderson & Senne, ed., *Walkway Surfaces: Measurement of Slip Resistance* (ASTM STP 649), American Society for Testing and Materials, 1978.

Brungraber, Robert J., The Measurement of Slip-Resistance and the Setting of Standards, *Educational Workshop on Building Safety,* Georgia Inst. of Tech., April, 1992.

Brungraber, Robert J., *An Overview of Floor Slip-Resistance Research With Annotated Bibliography* (NBS Technical Note 895), U. S. Department of Commerce, 1976.

Brungraber & Templar, Controlled Slip Resistance in *Progressive Architecture,* March, 1991.

Ekkebus & Killey, Measurement of Safe Walkway Surfaces in *Soap/Cosmetics/Chemical Specialties,* February, 1973.

James, D. I., A Broader Look at Pedestrian Friction, in *Rubber Reviews: Rubber Chemistry & Technology,* 1980.

Marpet, Mark I., Gait Dynamics and Walkway Safety, *Educational Workshop on Building Safety,* Georgia Inst. of Tech., April, 1992.

Irvine, Charles, A New Slipmeter for Evaluating Walkway Slipperiness in *Materials Research and Standards,* December, 1967.

Figure 7. Articulated Strut Tester (Side view).

Guide Wire Pulley

Guide Wire

Slotted Bar

Wing Nut & Washer

Angle Board

Articulated Strut Assembly

Protractor- Ensure that the protractor center is aligned with the Angle Board Hinge Pivot Center

Wing Nut & Washer

Test Foot Support Struts

Test Foot Assembly

Test Surface

Stationary Stop

Angle Board Hinge Pivot Center

Angle Board Hinge

Moveable Stop Assembly

Baseboard. Place on horizontal surface.

Protractor Index Mark. Place index mark on Angle Board. Ensure that index mark is radial with respect to the hinge pivot and that it reads correctly.

Weight

Figure 8. Drag-Type Tester.

Axially-Stiff Pull Wire: Keep horizontal

Dynamometer: Pull horizontally

3" sq. adhesive Magnetic "Tape"

Test Foot Glued to Test Foot Bracket

Steel L-shaped Test Foot Bracket

Block to keep dynamometer horizontal

320

Moveable Stop Assembly

Threaded Stop Bolt (round head corners)

Slip fit pin with head

Moveable stop block

Guide wire

1/2 " Radius

Articulated Strut Assembly

Baseboard

Holes on 1" centers

Figure 9. Articulated Strut Tester Details.

Press fit both Sensor Support Struts into weight.

Weight

Align the holes in the two struts so the Sensor Support Base does not bind.

Test Foot Support Pivot Shaft

Sensor Assembly

Vari-speed Motor

Motor Installation Detail

Test Foot Glued to Sensor Bracket

Steel L-shaped Test Foot Bracket

3" sq. adhesive Magnetic 'Tape'

Sensor Support base

Walkway Friction: Experiment & Analysis
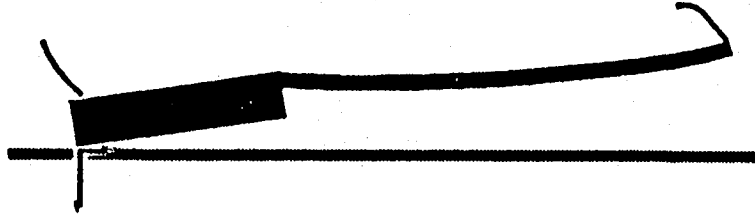
- Robert Brungraber, Ph.D., P.E.
  - Bucknell University, Lewisburg, Pennsylvania
- Mark Marpet, Ph.D., P.E.
  - Saint John's University, New York City, New York

Walkway Friction?
So What?
(Why explore walkway friction?)

- The high $$ losses from walkway accidents
- Interesting Real-World deviation from the classical (Amontons-Coulomb) friction model
- Interesting design of experiments issues

Walkway Friction

v.

Amontons-Coulomb Friction

- Anomalous results vis à vis Amontons-Coulomb
- Resilient v. non-resilient surfaces
- Violations of the assumptions of independence of friction with respect to:
  - Contact pressure
  - Temperature
  - Humidity
  - Velocity
  - Residence time

Walkway Friction Testing Instruments

- Drag sled
- Inclined plane
- Pendulum
- Articulated strut
- Inclined strut

The Design of Experiments:
An exploration of the minefield between the rock and the hard place

- THE ROCK—A linear increase in the factors requires a geometric increase in the number of tests.
- THE HARD PLACE—If the test design is not complete, confounding (aliasing) of results can occur.
- STEP WITH CARE—
  - explicitly consider the goals of the testing
  - explicitly consider the testing "budget"
  - explicitly consider confounding
- A horror story

The General Linear Model
(It's not *really* linear, but it sure is general)

- $\mu_\bullet = b_0 + b_1 X_1 + b_2 X_2 + \ldots + b_i X_i + \ldots + b_n X_n + b_{12} X_1 X_2 + \ldots + b_{ij} X_i X_j + \ldots + \text{H.O.T.}$
- The first line of the equation *is* linear
- Without replication, the number of experiments in the full model grows with the product of the factor levels.
- Replication
- Canned software
  - General math engines: MathCAD, Mathematica
  - Statistical software: MyStat, MiniTab, SPSS, ...

Setting up the data for analysis

- Design a form to record your data

Machine	fl or θ	Sensor	Surface	Wet/Dry
Strut	32°	Neolite	Vinyl Tile	Dry
Strut	75°	Neolite	Vinyl Tile	Wet
...				

- Enter the data into the program

Analyze the data
(The Horror Story, Continued)

- Analysis of Variance

- Dependent variable: LATFORCE   N: 72
  Multiple R: 0.499   Squared Multiple R: 0.249

Source	Sum-squares	DF	Mean-square	F-ratio	P-Value
WETDRY	6.125	1	6.125	0.345	0.559
SENSOR	41.750	2	20.875	6.815	0.002
TILE	95.083	2	47.542	2.640	0.076
DIRECTIO[N]	28.486	3	9.495	0.535	0.660
Error	1117.431	63	17.737		

Participants

THERMOFORMING FROM A SYSTEMS VIEWPOINT

Jerry L. Wickman

Director Plastics Research and Education Center
College of Applied Sciences and Technology
Department of Industry and Technology
Ball State University
Muncie, Indiana 47306-0255

Telephone 317-285-5648

and

Nikhil Kundu

Purdue University

THERMOFORMING FROM A SYSTEMS VIEWPOINT

J.L. Wickman Ph.D.
Ball State University
Nikhil Kundu
Purdue University

KEY WORDS: thermoforming, statistical process control, metrology, fixture design, gage R&R, processing variability

PREREQUISITE KNOWLEDGE: The student should understand the concepts of thermoforming, statistical process control, metrology, and be familiar with ASTM standards as related to manufacturing.

OBJECTIVES: To be able to select and manipulate control charts to adequately reflect processing characteristics and variation. Understand how a manufacturing process can be broken down into its basic components and subsequently analyzed. Understand how statistics, standards, and metrology are critical to manufacturing.

EQUIPMENT AND SUPPLIES: Standard tooling and gages available to the students should include but not be limited to a(n):

infrared thermometer	portable contact thermocouple
calipers	height gages
dial indicators	micrometers
surface plates	DataMyte data collection units
stop watches	melt index unit

ASTM standards
universal test equipment (Instron model 1011)
statistics package for process control
AAA model MB-5 thermoforming unit with 24" x 24" capacity

INTRODUCTION:

Thermoforming can be one of the processes that meets the objectives and allows for an in depth manufacturing study. This type of experiment has the potential to involve/combine any or all of the following topical areas:

Quality control
Heat transfer
Parts handling
Materials testing
Materials design
Data collection
Data analysis
Statistics
Materials processing
Standards
Fixture design
Metrology
Gage R&R (repeatability & reproducibility)
Material selection

Berins (1991) indicates that thermoforming is the process of heating a plastic material in sheet form to its particular processing temperature and forming the hot and flexible material against the contours of a mold by mechanical or pneumatic means. When held to the shape of the mold and allowed to cool, the plastic retains the shape and detail of the mold. Thermoforming of plastic sheet stock has been used extensively to produce inexpensive disposable containers. Recent developments have focused on sophisticated material and processing developments that meet microwaveable, ovenable, barrier type packaging demands. Thermoforming as a system has come into its own and is beginning to produce engineered products that effectively compete with other more expensive plastics processing techniques.

The students will be working in groups of 3 in order to complete the project in the approximate time interval of 5 to 7 weeks. Cooperation by all members is critical. The students will be asked to quantify and to provide all documentation necessary to identify all possible sources of variability; this includes incoming material, all components of the process, operator caused variation, and operational methods. They are then requested to select and use appropriate tools to begin to control variation. The use of ASTM E 178-Standard Practice for Dealing With Outlying Observations is encouraged. A log book will be essential to each laboratory report submitted. Appropriate written operating, setup, gaging, data collection, data analysis policies and procedures will be required for the entire operational sequence.

Input, process, and output represent a logical breakdown of the process into critical components. Additional divisions may be necessary as the project continues. It is safe to assume the students have had some contact with all of the issues. This is the first time that a manufacturing system of this type is being addressed.

Flowcharts of the process must be developed. Flowcharts display the various stages in the process and, through the use of different types of symbols, demonstrate the flow of a product or service over time. Extensive detailing will be required of the flowchart before the project is allowed to begin. Mistakes will occur on paper and should be minimized in the experiment.

Cause-and-effect diagrams (Ishikawa diagrams) will also be required. Juran and Gryna (1980) indicate that this will force organization of all known causes into general categories such as methods, materials, machine, and human, illustrating the common relationships. Its impact on the students comes from the graphic representation of the relationships between problems and their sources.

Documentation and traceability are critical to this project. Everything that is used or input into or out of the process should be measured and evaluated as per the appropriate ASTM standard. If no standard exists then an appropriate mutually acceptable, logical

procedure should be documented and followed as closely as possible.

INPUT:
Incoming material to be thermoformed should have a particular molecular orientation as a result of the former extrusion process. It is important that the molecular orientation for all sheets be kept as a constant, all being placed in the machine in the same direction.

ASTM D 1898, Recommended Practice for Sampling of Plastics, will be used to select appropriate samples for additional testing.

ASTM D638, Standard Test Method for Tensile Properties of Plastics, will be used to evaluate tensile properties in the extruded direction and perpendicular to the extruded direction of the sheet. Test number, sample number, and material type will be documented. All data collection forms for all documentation will be developed prior to running the experiment.

ASTM D 1238, Standard Test Method for Flow Rates of Thermoplastics by Extrusion Plastometer, will be used to determine flow rates. Flow rate is an empirically defined parameter critically influenced by the physical properties and molecular structure of the polymer and the conditions of measurement. Melt flow is one of the most often used tests of this nature. This measurement may later be correlated with processing problems that may occur within or between lots.

A sampling procedure and fixture must be developed to evaluate the thickness of incoming material. It is assumed that incoming material will have a particular target dimension but it is the students' obligation to determine how much variation exists in the incoming product. Six data points will be measured per sheet, 1 data point per cavity. The number of data points required per sheet is a function of the shape and number of cavities of the thermoforming tool being used. Appropriate statistics and control charts as selected, and defended by the student, should be used to indicate sheet thickness and variation. Control charts can be developed from attribute or variable data. Although attribute control charts are easier to use, variable control charts will provide more insight into the process under consideration. Hayes and Romig (1982) have developed one of the more complete sources for applications with and without standards. The fixture or gage used to measure sheet thickness should take gage R&R (repeatability and reproducibility) and their implications into consideration. The DataMyte Handbook (1989) references the formulas for gage R&R. It is the opinion of the authors that the issue of gage R&R needs to be addressed in this experiment but actual calculations might be a more appropriate topic if taken as a separate study. Documented procedures should at least exist relative to the design and use of the fixture to minimize operator error.

PROCESS:
Thermoforming is a process whereby the sheet material is loaded into a frame and moved into a heated enclosed box and subjected to elevated temperatures to soak for a predetermined amount of time. Heat sources are located above and below the sheet material in an effort to uniformly bring the plastic to temperature. Time and temperature are the critical processing variables. For a particular processing tool, processing standards will be developed along with documented procedures. It will be the students' obligation to develop statistics and control charts with documentation to reflect processing characteristics over a production run of 60 good parts. Subgroup size if used, will also be determined by the student.

Procedures developed by the students will document all necessary information so that a person familiar with the process could reproduce the experiment. It can not be over emphasized that tools, gages, times, locations, machine settings, and other items must be documented. Part removal from the thermoformer and placement on a cooling fixture needs documentation and standards to minimize the introduction of operator error.

OUTPUT:
The resultant product that is to be evaluated is a function of the thermoforming tool being used. The tool being used in this experiment is a 6 cavity tool that allows the students to consider within cavity and between cavity variation.

Kennedy et al. (1987) contend that the metrology fixture is also a function of the tool being used. The most desirable tool would have 1 cavity, but with 6 cavities the student can concentrate on several or all cavities. Documentation, time invested, and number of measurements required increase considerably with multiple cavity tools. If the student wants to capture 6 data points from each part in a 6 cavity tool, there is a total of 2160 data points for the 60 part run. That's a dilemma that the students will have to resolve. It is also their responsibility to determine where to take measurements, how many measurements per part, how to take measurements (fixture design), control charting procedure, and other items, but the process they develop must represent the critical characteristics of the part and process. Once again gage R&R is an important factor. Given the limitations of the gaging, the measurement process can be destructive of the part.

SYNTHESIS:
Webster defines synthesis as the putting together of parts or elements so as to form a whole. The individual components of the project need to be assembled into a cohesive unit that best describes where variation may be taking place, how to minimize variation and how to hold to the new levels of productivity. Material input, material testing, process control, fixtures and fixture design, gaging, statistics, operators, documentation, standards, output, variations of all those articles mentioned above and others need to be assembled to form a whole that best represents typical manufacturing. A statistically quantifiable

relationship exists and must be shown between input, process, operators, and output.

SUMMARY:
Using the thermoforming unit gives us the flexibility to develop a complete manufacturing process. The manufacturing students, cooperating within a group, should be able to look at a process and break it down into critical components that can be easily understood and manipulated. The student should be able to take the processing components and use whatever statistics, gaging, recognized standards, and other tools that are available to analyze the components as they relate to the whole, reduce variability and improve upon the process. The manufacturing student must be able to identify the various sources of variability and how they might impact the system.

Modern manufacturing will not exist without the use of statistics. We must improve the students' understanding and appreciation for statistics and the use of statistics. The use of statistics should become second nature as should the use and familiarity with the science of measurement (metrology) and all associated standards (ASTM/ANSI/ASQC/ISO/Others).

REFERENCES:
Berins, M.L., Editor, Plastics Engineering Handbook, Fifth Edition, 1991,Van Nostrand Reinhold, New York

Annual Book of ASTM Standards, 1986, American Society For Testing and Materials, Philadelphia

Juran, J.M., and F.M. Gryna Jr., Quality Planning and Analysis, Second Edition, 1980, McGraw Hill, Inc., New York

Hayes, G.E., and H.G. Romig, Modern Quality Control, Revised Edition, Glencoe Publishing Co., Inc. California

DataMyte Handbook, Fourth Edition, 1989, DataMyte Corporation, Minnesota

Kennedy, C.W., et al., Inspection and Gaging, Sixth Edition, 1987, Industrial Press., New York

Neufeldt, Victoria. Editor, Webster's New World Dictionary, Third Edition, 1988, Simon Shuster, Inc. Ohio

THE CHARACTERIZATION OF MATERIALS USING X-RAY DIFFRACTION

A. F. Sprecher, Jr.
Harvey A. West
and
A. A. Fahmy

Department of Materials Science & Engineering
North Carolina State University
Raleigh, North Carolina 27695-7907

Telephone 919-515-2377

THE CHARACTERIZATION OF MATERIALS USING
X-RAY DIFFRACTION

A. F. Sprecher, Jr., H. A. West, and A. A. Fahmy

Department of Materials Science and Engineering
North Carolina State University
Raleigh, NC 27695-7907
Telephone: (919) 515-2377
FAX: (919) 515-7724

Key Words

X-ray, diffraction, Debye-Scherrer, crystallography, Miller indices, Bragg's law

Prerequisite Knowledge

This laboratory requires a general knowledge of crystal structure and wave diffraction phenomena.

Objectives

1. Familiarize the student with X-ray techniques for diffraction pattern generation.
2. Show the student how to utilize X-ray diffraction data for crystal structure determination.
3. Illustrate systematic and random errors associated with experimental data.

Background

Crystalline materials, by definition, are composed of atoms arranged in a periodic array; such a configuration can also be viewed as regularly spaced planes of atoms. The properties of the plane, such as atoms per unit area or interplanar distance, depend upon the crystal structure as well as the angles the plane makes with the axes of the unit cell. The orientation of a plane is given by its Miller Indices (hkl) which are the reciprocals of the axial intercepts of the plane. For a cubic system the interplanar distance d_{hkl} is given by:

$$d_{hkl} = \frac{a}{\sqrt{h^2+k^2+l^2}} \qquad (1)$$

where a is the length of the side of the cubic unit cell.

When X-rays of wavelength λ are reflected off of these parallel planes of atoms, a measurable signal will only be produced when constructive interference of the reflected

waves takes place. By geometry, this condition will result if the path difference (depicted in Figure 1) is equal to an integral number of wavelengths. This condition for *X-ray diffraction* can be expressed by *Bragg's Law:*

$$n\lambda = 2d_{hkl}\sin\theta \tag{2}$$

where θ is the angle that the incident X-rays make with the planes and n is the integral number of wavelengths difference in the diffracted X-rays. When θ is such that this equation is first satisfied ($n=1$), a strong X-ray signal will be emitted from the specimen at a similar angle θ. In practice, the signals diffracted for $n=1$ are the strongest, which is primarily due to absorption of X-rays in the material. By measuring the intensity of X-rays as a function of θ, a pattern of diffraction peaks will be produced which yields information about the material's atomic structure.

Figure 1 - Diffraction of X-Rays from Atomic Planes

Substitution of equation (1) into equation (2) yields:

$$\lambda = \frac{2a}{\sqrt{h^2+k^2+l^2}} \sin\theta \tag{3}$$

340

By squaring both sides and substituting Q^2 for $h^2+k^2+l^2$, equation 3 becomes:

$$\sin^2\theta = \frac{\lambda^2}{4a^2}\left(Q^2\right) \qquad (4)$$

This relationship shows that for a given crystal rotated in a columnated beam of monochromatic X-rays (constant wavelength), diffracted radiation will occur at certain values of θ, the sine squares of which are directly proportional to the Q^2 value for the reflecting plane. So how does this render information about the placement of atoms in the unit cell?

Not all crystal planes will produce a diffracted beam, even if Bragg's Law is satisfied. For instance, assume that Figure 1 represents a set of (100) planes in a body-centered cubic material. The "body center" atoms make another set of planes (200) exactly half way between the (100) planes. More importantly, these intermediate planes will have the same number of atoms per unit area (planar density) as the (100) planes. Therefore, the beam reflected off of the (200) planes will be of equal intensity and exactly $\lambda/2$ out of phase with the beam reflected off of the (100) planes and no net signal will be detected. Hence, there will not be a diffraction peak at that angle. However, at a higher value of θ, there will be a primary ($n=1$) diffraction corresponding to the distance between (200) planes as there does not exist a set of populated (400) planes to cancel these reflections. (Note: The diamond cubic structure does have such a set of planes and, consequently, diffraction does not occur here either.) This condition, known as *"systematic extinction"*, exists for different sets of planes for each type of crystal structure, and, if it can be determined exactly which planes are producing the primary diffracted beams, the structure of the crystal can be determined. The rules for the existence of diffraction peaks for any plane (hkl) in the common crystal structures are given in Table I.

Table I - Conditions of Diffraction for Various Crystal Structures

Crystal Structure	Conditions for Diffraction
Simple Cubic	all planes
FCC	h,k,l are all even or odd (zero is considered even)
BCC	$h + k + l$ = even number
HCP	$(h + 2k) \neq 3n$ (n is an integer) **and** l is even

From the information in Table I, it is possible to predict the increasing values of Q^2 corresponding to diffraction peaks as θ is varied from 0° to 180°. Furthermore, the values of $sin^2\theta$ obtained from actual diffraction data should follow the same proportional scheme as the Q^2 values. In other words, dividing the $sin^2\theta$ of the first observed peak by the first possible Q^2, and the second peak by the second Q^2, etc., should all result in a constant number if the proper crystal structure is chosen. By employing equation 4, this constant number can be used to calculate the lattice parameter a for the particular material.

The Production of Diffraction Patterns

One of the most common methods of obtaining X-ray diffraction data is the Debye-Scherrer "powder method". As shown in Figure 2, a polycrystalline sample, usually a powder of the material covering a glass fiber, is exposed to an incident beam of monochromatic radiation (for instance CuK_α radiation, λ=1.5418Å). The random orientation of the planes in the sample coupled with physical rotation of the sample, gives rise to diffraction from every possible set of planes in the specimen. The "cones" of diffracted radiation will expose the film and cause a pattern of concentric arcs to be formed. As will be discussed in the proceeding section, the location of these arcs gives the value of 2θ for each set of planes causing diffraction.

Figure 2 - Debye-Scherrer Diffraction Geometry

Other methods of obtaining X-ray diffraction information are:

Diffractometer - a polycrystalline specimen is placed at the center of a circle and exposed to monochromatic radiation. A detector is swept around the perimeter of the circle and intensity vs. angle is recorded.

Laue method - a single crystal is exposed to polychromatic radiation and the diffracted beams produce spots on a flat piece of film located behind (transmission) or in front (back-reflection) of the specimen.

Errors Associated with the Debye Technique

Several sources of error exist when using the Debye-Scherrer powder technique. These lead to inaccuracies in determining the lattice parameter. Aside from the obvious *random errors* in measuring the locations on the film, four sources of *systematic error* in the diffraction angle θ are as follows:

1. Film shrinkage
2. Incorrect camera radius
3. Off-centering of specimen
4. X-ray absorption of specimen

These errors act to systematically shift the observed diffraction angles on the film. They are experimental effects and not true variations of the diffraction angles found in the Bragg equation. Rather, the geometry inherent in the Debye-Scherrer technique acts to shift the measured angles. It can be shown that the shift in line distance on the film is given by:

$$\Delta d/d = K\cos^2\theta \qquad (5)$$

where $\Delta d/d$ is the relative line shift and K is the constant of proportionality due to all sources of error. This relation of accumulated errors is known as the Nelson-Riley function. It follows that:

$$\Delta d/d = \Delta a/a = (a - a_0)/a_0 = K\cos^2\theta \qquad (6)$$

upon rearranging:

$$a = a_0 + a_0 K\cos^2\theta \qquad (7)$$

It can be seen that in order to get the true lattice parameter a_o, equation 7 can be used. Each angle θ measured corresponds to a unique set of *(hkl)*. By using equation 4, a value for a can be calculated. This is not the true lattice parameter a_o, but includes all the aforementioned errors associated with this technique. By plotting equation 7, a versus $cos^2\theta$, the value a_o can be obtained. Referring to Figures 3-6, the intercept represents a_o while the slope is equal to a_oK. This known as a *back extrapolation technique* and is common in many experimental situations where measurements are subject to real, unavoidable errors.

Experimental Procedure

Debye-Scherrer diffraction patterns for five unknown materials are provided (Figure 7). These materials are elements (rather than compounds) and their crystal structures are restricted to one of the following systems: SC, BCC, FCC, or HCP. The overall goal of the experiment is to identify each material from its pattern. In order to accomplish this goal, the following steps are performed on each pattern.

1. Measure all 2θ diffraction lines from the patterns presented in Figure 7. Place the diffraction pattern with the tab situated in the upper right hand corner. Begining with the hole on the left side, set the ruler on the first ring to the left side of the hole. Then measure all the diffraction rings to the right in millimeters (one millimeter = one degree). Stop measuring when the opposite hole is reached. The angle θ is determined through the formula:

$$\theta_n \; (°) = \text{Diff. Line}_n - (\; \text{Diff. Line}_1 + \text{Diff. Line}_2)/2 \qquad (8)$$

2. Generate tables for $sin^2\theta$ and take ratios of these values. Compare them to the ratios for the values of Q^2, as described in the previous section, for all the possible crystal structures. By matching the two sets of ratios, a crystal structure determination can be made.

3. Once the crystal structure has been identified, calculate the lattice parameter a for **each** plane using Bragg's law.

4. Employ the back extrapolation technique in order to determine the true lattice parameter a_o for each pattern. This is done by plotting a versus $cos^2\theta$ and extrapolating the value of a_o at $cos^2\theta = 0$.

5. Once a_o and the crystal structure are known, a material identification can be made by comparing these values with those tabulated for the elements listed in the reference given at the bottom of Table II.

Instructor notes

The pattern for the HCP material requires a slightly different approach and is usually not a required pattern but is given for potential extra credit in order to stimulate the more imaginative or motivated student.

The problem with the HCP pattern is that it has two independent lattice parameters, a and c, making it impossible to take ratios of $sin^2\theta$ as with the other crystal structures. The problem can be circumvented in the following manner.

1. Measure all diffraction lines and generate values of 2θ.

2. Assume the pattern is HCP. This can be done by inspection since the students have identified the other crystal systems and know what they look like.

3. Prove the pattern is HCP. Taking the first two θ values, θ_1 and θ_2, and using Bragg's law and equation 9 below, generate two equations with two unknowns, a and c. Solve both equations simultaneously to obtain values for the two lattice parameters. Using these values of a and c, check the rest of the pattern. Do the calculated values of θ from Bragg's law match those that are measured directly from the diffraction pattern? They of course will match, thereby making the crystal structure and lattice parameters determination.

$$d_{hkl_{hex}} = \frac{a}{\sqrt{\frac{4}{3}\left(h^2 + hk + k^2\right) + l^2\left(\frac{a}{c}\right)^2}} \qquad (9)$$

Table II summarizes the data obtained from the diffraction patterns and Figures 3-6 represent values of a_o attained from the data.

Table II - Data Summary for Diffraction Patterns

Pattern #	1	2	3	4	5
Material	Ni	W	Cu	Nb	Zn
Crystal Structure	FCC	BCC	FCC	BCC	HCP
Lattice Parameter, a_o* (Å)	3.5239	3.1653	3.6148	3.3067	$a_o = 2.6650$ $c_o = 4.9470$
Diffraction Angles, θ	22.15	20.05	22.00	19.55	18.30
	26.00	29.40	25.45	27.95	19.80
	38.20	36.95	37.15	35.05	21.75
	46.60	43.85	45.10	41.45	27.35
	49.30	50.55	47.65	47.70	35.45
	61.20	57.85	58.45	54.05	38.60
	72.15	65.95	68.10	60.95	41.35
	77.80	77.40	72.30	69.05	43.30
					45.45
					47.65
					54.70
					58.20
					62.30
					63.75
					69.55

* Cullity, B.D. *Elements of X-Ray Diffraction*, Addison-Wesley, 1978.

Figure 3 - Back Extrapolation for Nickel Data

Figure 4 - Back Extrapolation for Tungsten Data

Figure 5 - Back Extrapolation for Copper Data

Figure 6 - Back Extrapolation for Niobium Data

348

Figure 7 - Debye-Scherrer Patterns

FRACTURE OF GLASS

John M. Henshaw

Assistant Professor
Department of Mechanical Engineering
University of Tulsa
Tulsa, Oklahoma 74104

Telephone 918-631-3002

Fracture of Glass

John M. Henshaw
Department of Mechanical Engineering
University of Tulsa, Tulsa, Oklahoma 74104

KEY WORDS: glass, fracture, bending, stress/strain, static fatigue, delayed fracture, fracture mechanics, residual stress.

PREREQUISITE KNOWLEDGE: The student should understand the fundamentals of beam bending - as would normally be obtained in an introductory mechanics of materials course. Some understanding of elementary statistical concepts, such as mean and standard deviation, is also helpful. Some elementary concepts of fracture mechanics are introduced in this lab, although no previous knowledge of this subject is required.

OBJECTIVES: To observe and understand the fracture behavior of a brittle material. To quantify the effects of various treatments on that material designed to modify its strength.

EQUIPMENT AND SUPPLIES:

(1) Glass microscope slides (1" by 3" - approx. 12 per student)
(2) Three-point bending loading fixture (see attached drawing)
(Note: Item (2) is not intended to be constructed by the student)
(3) Continuous loading mechanism: Small solenoid valve and 12V battery, two 2-liter plastic water reservoirs and fixture, misc. lengths of tubing and wiring, tap water (see attached drawing)
(4) Calibrated weights (1000, 500, 200, 100g)
(5) Anhydrous HF acid (*not* to be handled by students)
(6) Bench-top metallurgical heat treating oven
(7) Mass balance (4 kg capacity)
(8) Micrometer (preferably) or dial calipers
(9) Diamond-point scribe
(10) Straight edge
(11) Computer spreadsheet (preferably) or hand calculator

INTRODUCTION: Common plate glass, such as is used to make laboratory microscope slides, is a very brittle material. Such materials exhibit large variations in fracture stress. These variations can be due to very small surface defects (to which brittle materials are highly sensitive), or to residual stresses in the material.

Beam Bending: To understand the role of the surface in determining the fracture strength, it is necessary to examine the state of stress within the glass slide as it is loaded in three-point bending. The equations below should be familiar from your background in mechanics of materials. The deflection at the center of a simply supported beam with a single concentrated load at mid span (i.e., a beam in three-point bending) is

$$y = \frac{Fl^3}{48EI} \tag{1}$$

where y is deflection, F is the load, l is the distance between the outer supports, I is the moment of inertia (= $wh^3/12$ for a beam of rectangular cross-section, where w is the width of the beam and h is the thickness), and E is the modulus of elasticity of the material. Since glass is a homogeneous isotropic material, there is a linear distribution of stresses through the specimen thickness, with compression at the top surface, zero stress at the mid plane, and tension at the bottom surface, as illustrated in Figure 1.

Figure 1. Distribution of tensile (+) and compressive (-) stresses through the thickness of beam in bending.

The maximum normal stress occurs at the top (compressive) and bottom (tensile) surfaces of the slide and equals

$$S_{max} = \frac{3Fl}{2wh^2} \qquad (2)$$

Fracture Mechanics: Since the maximum stress of a beam in bending is at the surface (tensile at the bottom and compressive at the top), and since glass is a brittle material, we would expect the bending strength of glass to be very sensitive to surface flaws.

The science of fracture mechanics tells us that the more brittle a material is, the more sensitive it will be to smaller and smaller flaws - even flaws that may be too small to see with the unaided eye. This relationship is quantified through a quantity called "stress intensity" (K) as follows:

$$K = \sigma\sqrt{\pi a} \qquad (3)$$

where σ is the applied stress and a is the length of a crack oriented perpendicular to the applied stress. When the stress intensity reaches a critical value, fracture mechanics theory predicts that the material will fracture. This critical stress intensity value varies for different materials and is known as the "fracture toughness" (K_{Ic}), a material property. Very tough materials such as some steels have high K_{Ic} values (say, 75-100 MPa(m)$^{1/2}$), whereas brittle materials like glass have extremely small values of K_{Ic} (say, 0.5-1.5 MPa(m)$^{1/2}$).

The exact form of equation (3) will vary with the shape of the specimen, the location of the crack, and the type of loading, but what doesn't change is this: if the material property K_{Ic} is very low, then the critical combination of stress and crack length necessary to cause fracture is also very low. For materials like glass, even if the stress is not very great, a "crack" in the form of an "invisible" surface scratch can induce fracture.

Investigating the Influence of Surface Flaws: The influence of surface condition on the fracture stress of glass may be investigated by testing specimens whose surfaces have been altered. One simple way to alter the surface is by introducing a sharp scratch with a glass-cutting instrument. The scratch thus produced is clearly much deeper than any of the slight imperfections that might have pre-existed on the surface. Equation (3) predicts that since the crack length a has increased, the stress necessary to reach the critical stress intensity (K_{Ic}) will decrease. This prediction can be easily verified experimentally. We can also investigate the influence of crack *location*, by testing specimens with the crack oriented down (crack in tension) or up (crack in compression).

Another way to alter the surface of the glass is by chemically removing the surface layer (along with any scratches that might be on the surface). This can be accomplished by immersing the glass in HF acid, which readily attacks glass. *NOTE: HF acid is an extremely dangerous chemical. Thus, all HF acid etching will be done ahead of time by the lab assistant.* After the acid has been allowed to remove the surface layer, the specimens are thoroughly rinsed and dried. The acid-treated specimens may then be tested, and the fracture strengths obtained should allow conclusions to be drawn about the presence or absence of surface flaws on the "as received" (straight out of the box) glass specimens.

Residual Stresses: Another factor that can influence the fracture properties of a material is the presence of residual or "locked-in" stresses. The beam theory stress distribution shown above assumes that the material is in the unstressed state prior to application of the bending load. This may or may not be true. Glass can be processed so as to induce compressive residual stresses at the surfaces - this process is known as "tempering" (and is quite different from the tempering of steel!). Tempered glass is much stronger than untempered. This is because extra force is required to overcome the compressive residual surface stresses. The stresses due to external loading are added to any residual stresses present. Conversely, glass, if it is improperly processed, could end up with harmful residual *tensile* stresses at the surfaces. These stresses, when added to the stresses due to external loading, should result in an observed reduction in strength.

By annealing glass (heating it hot enough to relieve the residual stresses, then cooling it very slowly to ensure that no new residual stresses are created) and then testing its strength, we should be able to draw conclusions regarding the state of residual stress in the as-received specimens. Since the annealing treatment is somewhat time-consuming, the annealed specimens will be prepared ahead of time by the lab assistant.

Static Fatigue: One factor that complicates the strength testing of glass is a phenomenon known as "static fatigue". Static fatigue, or delayed fracture, is the tendency exhibited by many glasses to withstand a given static load for a short period of time, say 30 seconds, before suddenly fracturing without warning. In order to ensure that static fatigue is not adversely affecting our results, it is important to apply load to the specimens slowly, and to repeat the same loading procedure for each specimen (see below). In addition, we can investigate the influence of static fatigue on strength by carefully varying the loading rate (N/min.).

PROCEDURE:
Safety considerations:
1. Be very careful around the glass loading fixture, especially when the glass is under load! The broken glass fragments will of course be very sharp.
2. Protective eye wear is mandatory for all those in the lab area.
3. Please clean up all glass fragments after each specimen fractures, and before you test the next specimen.
Specimen Preparation: Each student will test 12 glass specimens:

Specimen Condition	# Specimens to be tested by each student[4]
"as received"	4
annealed[1]	2
acid-etched[2]	2
scratch UP[3]	2
scratch DOWN[3]	2
TOTAL	12

1. Heat treated at 600°C for 10 minutes and slow cooled (inside furnace) to room temperature.
2. Soaked in 5% HF acid for 20 minutes to remove surface layer.

3. The glass specimens will be scratched by the students. The scratch should be centered across the width of the specimen (i.e. a one-inch wide scratch!) Try to be as consistent as possible from one scratch to the next! (Obviously, this is a potential source of error.) Use the diamond point scribe and straight edge to scratch your specimens.
4. As described below, ALL data generated by all the students in your lab should be averaged in order to obtain accurate strengths for the various specimen conditions.

The heat treated and acid-soaked specimens will be prepared ahead of time by the lab assistant. This is in the interest of saving time (in the case of the heat treating) and safety (in the case of the HF acid, which is very dangerous).

Measure and record the thickness and width of your specimens. Because of the importance of the thickness in calculating the maximum stress, at least three measurements of the critical thickness dimension should be taken and averaged. The thickness should be around 1 mm, or approximately 0.040 in. (Thickness should be reduced for the acid-etched specimens.)

Specimen testing: There are two ways to accomplish the loading of the glass specimens in this lab. The first loading method involves continuous loading of the specimens, while in the second method the specimens are loaded manually in discrete stages.

In the continuous loading method, Figure 2, the glass specimens are loaded by draining tap water from a reservoir suspended above the loading fixture, through a solenoid valve, and into a second container positioned on the three-point bending fixture. As the level of water in the second container goes up, the load on the specimen increases. When the specimen breaks, the upper arm of the loading fixture drops down, making contact with the base of the machine, and closing a circuit through which the solenoid valve is automatically shut. The water in the container on the fixture is then weighed and added to the (predetermined) weights of the container and arm of the fixture to determine the load at fracture of the glass. The fracture stress is then calculated using equation (2).

In the manual loading method, the glass specimens are loaded by placing calibrated masses on the loading pan one-by-one. Weights should be placed on the pan at 30 second intervals. (This is done to reduce the influence of static fatigue - see Introduction.) When the specimen breaks, the fracture load is determined by adding the weight of the masses on the pan to the weight of the loading arm. The fracture stress is then calculated using equation (2).

Statistical Treatment of Data: All the students in your lab should share all the fracture data generated. One way to do this easily is to enter all the data directly onto a computer spreadsheet during the lab period. At the end of the period, each student can copy the data file onto a floppy disk for analysis and report writing. The mean fracture strength for each specimen condition is determined by summing all the individual data points, s_{max}, for that condition, and dividing by the number of data points, n:

$$\bar{s}_{max} = \frac{\sum s_{max\,i}}{n} \tag{4}$$

The standard deviation for each condition is determined as follows:

$$std.\,dev. = \sqrt{\frac{\sum (s_{max\,i} - \bar{s}_{max})^2}{n-1}} \tag{5}$$

Figure 2. Schematic of glass fracture test fixture showing the continuous loading method

SAMPLE DATA SHEETS: Each student should complete by hand a data table similar to the one shown below. If a computer spreadsheet is being employed, this data should also be entered into the spreadsheet.

Specimen Condition	max. load (N)	l (m)	w (m)	h (m)	s_{max} (MPa)
as received					
as received					
as received					
as received					
annealed					
annealed					
acid-etched					
acid-etched					
scratch UP					
scratch UP					
scratch DOWN					
scratch DOWN					

INSTRUCTOR NOTES:

1. *Extreme* care should be taken during the HF acid etching of the glass. Eye protection and elbow length gloves should be worn at all times - of a type designed for use with HF. One drop of this material on your skin will give you a burn you will not soon forget! Observe proper disposal procedures for this material.

2. One of the most important lessons the students can get from this lab relates to the "significance" of the results. Students have been known to write long paragraphs explaining why "condition A", with a mean strength of 70 MPa and lots of scatter, was "stronger" than "condition B" with a mean strength of 69 MPa! Depending on the background of the students in statistics, one can introduce the subject of significance tests as a means of determining which of the conditions are significantly different from each other. Otherwise, students can simply be asked to use their best "engineering judgment" to determine the significance of the results.

3. Because of the large statistical variation in the strength of a brittle material like glass, it is very important in this lab for all the students in the lab to share their data. An added benefit of this is that it requires a fair amount of cooperation among the students.

4. The influence of static fatigue on the strength of the glass can be investigated using the continuous loading (water) setup. By using a set of valves with varying flow rates, and testing a sufficient number of specimens with each, the influence of loading rate on strength can be determined.

5. It is a simple matter in this lab to determine the modulus of elasticity (E) of the glass. This can be done by measuring deflections using a dial indicator and then calculating E from equation (1). Or, E can be determined directly if a strain gage is centered on the bottom surface of a glass specimen. Stress/strain data are then gathered, from which E is determined. It can be an interesting addition to the experiment to allow the students to investigate the influence of the various glass treatments on modulus.

REFERENCES:

1. Hertzberg, R.W., *Deformation and Fracture Mechanics of Engineering Materials*, 2d ed., John Wiley and Sons, 1983.

2. Kingery, W.D., Bowen, H.K., and Uhlmann, D.R., *Introduction to Ceramics*, 2d ed., John Wiley and Sons, 1976.

SOURCES OF SUPPLY: Glass microscope slides may be obtained from the Biology department of most schools or from a biological supply store. The solenoid valves and batteries may be purchased at most industrial/commercial equipment and supply stores. Most of the rest of the equipment is easily obtained at a hardware store.

PHASE TRANSITION STUDIES IN BARIUM AND STRONTIUM TITANATES AT MICROWAVE FREQUENCIES

Jai N. Dahiya

Southeast Missouri State University
One University Plaza
Cape Girardeau, Missouri 63701

Telephone 314-651-2390

PHASE TRANSITION STUDIES IN BARIUM AND STRONTIUM TITANATES AT MICROWAVE FREQUENCIES

J. N. Dahiya
Physics Department
Southeast Missouri State University

KEY WORDS

Phase transition, crystal lattice, simple cubic, dielectric behavior, frequency shift, Q-change

OBJECTIVES

1. To understand the phase transformations in barium and strontium titanates as the crystals go from one temperature to the other.

2. To study the dielectric behavior of barium and strontium titanate crystals at a microwave frequency of 9.12 GHz and as a function of temperature.

SUMMARY

Phase transition studies in barium and strontium titanate are conducted using a cylindrical microwave resonant cavity as a probe. The cavity technique is quite successful in establishing the phase changes in these crystals. It appears that dipole relaxation plays an important role in the behavior of the dielectric response of the medium loading the cavity as phase change takes place within the sample. The method of a loaded resonant microwave cavity as applied in this work has proven to be sensitive enough to monitor small phase changes of the cavity medium.

INTRODUCTION

The dielectric constant of single crystals of barium titanate has been measured at different frequencies (Ref. 1 and 2). In this investigation a microwave resonant cavity is used to study the dielectric behavior of barium and strontium titanate ceramics at a microwave frequency of 9.12 GHz. The cavity technique used is very successful in monitoring the phase changes in a fine crystal of barium titanate as it goes from the paraelectric cubic phase to the ferroelectric tetragonal phase, to the orthorhombic phase, and to the rhombohedral phase successively. The heating and the

cooling methods involved are very effective in maintaining a certain temperature of the sample under investigation for some time. The details of the microwave spectrometer used for this study along with the heating and cooling methods are given elsewhere (Ref. 3-7). This technique is also applied to study the dielectric properties of a sample of a mixture of 75 percent barium titanate and 25 percent strontium titanate.

EQUIPMENT, THEORY AND PROCEDURE

A microwave spectrometer operating in the x-band of frequencies was used to study the dielectric properties of barium and strontium titanate at a fixed frequency of about 9.12 GHz. The spectrometer involved has a tunable klystron with a frequency range of 8.4 to 11.0 GHz. The block diagram of the microwave spectrometer is shown in Figure 1 and the details of its components and operation are given in other papers (Ref. 5 and 6). In ferroelectric substances, the static dielectric constant varies with temperature as follows.

$$\varepsilon_s = B + \frac{C}{T - T_c} \qquad for \ T > T_c \qquad (1)$$

In Eq.(1), B and C are constants that do not depend on temperature, C is the Curie constant and T_c is known as the Curie temperature. As shown in Eq.(1), the behavior of the dielectric constant is valid for temperatures that are more than the Curie temperature. At temperatures less than the Curie temperature, the ferroelectric material develops a spontaneous electric polarization. As the material is brought to this temperature (T_c), there is a phase transition from the paraelectric cubic phase to the ferroelectric tetragonal phase. There is a very strong field produced in the material because of the interaction of dipoles below this temperature and because of this there is a perfect alignment of the dipoles and the material exhibits a very strong polarization. The polarization is related to the electric field as shown below.

$$P = \alpha E \qquad (2)$$

where α is the polarizability. The total polarizability has contributions from dipolar, ionic and electronic polarizabilities. The contributions to the polarizabilities are functions of the frequency of the applied field. At microwave

frequencies the dipolar contributions to the total polarizability are very weak and the complex permittivity has contributions from ionic and electronic polarizations.

The strong polarization effects in ferroelectric substances like barium titanate below the Curie temperature are responsible for a very high value of the dielectric constant of the material. Ferroelectric materials also exhibit piezoelectricity. According to the piezoelectric effect, a pressure applied to the ends of a crystal of barium titanate for example will produce a very large potential difference between the ends of the crystal. This is mainly because of the coupling between the polarization and the shape of the sample. The stress will change the shape of the sample, which induces the change of polarization and produces a very strong charge density at the ends of the crystal. On the other hand, if a potential difference is applied between the ends of the same crystal, the crystal will have mechanical oscillations because of this electro-mechanical coupling.

Above temperature T_c (120°C), barium titanate has a perfect cubic structure as shown in Figure 2. The barium ions occupy the corners of the cube, the oxygen ions are on the faces and the titanium ion at the body center of the cube. In other words, above the Curie temperature, also called the critical temperature, barium titanate has a body center, face center cubic structure. Below this temperature T_c there is a small shift of about 0.15A° in the ions. The titanium ions at the center of the cubic structure shift about 0.006 nm with respect to the barium ions that are at the corners of the cube. The shift for the oxygen ions is in the opposite direction. The net shift in these ions produces a very strong polarization in the material as it goes through the critical temperature of 120°C.

At microwave frequencies, the dielectric constant ε becomes a complex quantity $\varepsilon^* = \varepsilon' - j\varepsilon''$ where ε' and ε'' are the real and imaginary parts of the complex dielectric constant. According to the Slater's perturbation equations the real and imaginary parts of the complex permittivity are related to the frequency shift and the Q-changes of the signal as shown below (Ref. 4).

$$\frac{\Delta f}{f_0} = -\frac{\varepsilon'-1}{2} \frac{\int \vec{E_s} \cdot \vec{E} \, dv}{\int \vec{E} \cdot \vec{E_a} \, dv} \tag{3}$$

and

$$\Delta\left(\frac{1}{Q}\right) = \varepsilon'' \frac{\int \vec{E}_s \cdot \vec{E} \, dv}{\int \vec{E} \cdot \vec{E}_a \, dV} \qquad\qquad \textbf{(4)}$$

where $\vec{E}_s$, $\vec{E}$ and $\vec{E}_a$ are the field of the sample, the unperturbed cavity and the microwave field as applied to the cavity respectively, and v is the volume of the sample with V being the volume of the cavity.

Also

$$\Delta\left(\frac{1}{Q}\right) = \frac{\sqrt{3}\,\Delta W}{f_o} \qquad\qquad \textbf{(5)}$$

where ΔW is the width of the signal at half power points and f_o is the resonant frequency of the system.

According to Debye's theory, the relaxation time τ is related to ε' and ε'' as shown below.

$$\frac{\varepsilon_s - \varepsilon'}{\varepsilon''} = \omega\tau \qquad\qquad \textbf{(6)}$$

where $\omega = 2\pi f_o$ and ε_s is the static permittivity of the material.

The fine crystalline samples of barium and strontium titanate are placed in capillary tubes. The capillary tube is then placed in the microwave field of the resonant cavity. This causes a perturbation in the microwave field of the cavity and the corresponding perturbations in the signal are recorded in terms of the frequency shift and width change of the signal. This becomes the initial reading of the measurement of dielectric constant. The sample under investigation is then allowed to go through a temperature change from lower to higher temperatures and the corresponding values of frequency shifts and width changes are recorded. Slater's perturbation equations (3 and 4) are used to calculate the real and imaginary parts of the complex dielectric constant of the material.

EXPERIMENTAL RESULTS AND CONCLUSION

Figures 3 and 4 show the behavior of the dielectric constant of barium titanate as determined in this investigation. The frequency shifts ($\Delta f/f_o$) and the Q-changes [$\Delta(1/Q)$] are plotted as a function of temperature. From Eqs. 3 and 4 these correspond to the real and imaginary parts of the complex dielectric constant. As the temperature is reduced below the critical value of 120°C, barium titanate changes from the paraelectric cubic phase to the ferroelectric tetragonal phase. This change is very dramatic and is visible with a very high value of the dielectric constant around 120°C. As the temperature is further lowered to approximately 0-10°C, this material changes from tetragonal to the orthorhombic phase and finally around -100°C it goes from orthorhombic to rhombohedral phase.

Figures 5 and 6 show the dielectric relaxation in a sample containing 75 percent barium titanate and 25 percent strontium titanate. The frequency shifts and Q-changes are plotted as a function of temperature at a microwave frequency of 9.12 GHz. As can be seen from Figure 5, $\Delta f/f_o$ that corresponds to ε' increases dramatically around 34°C and then it lowers to a value between 70-110°C. The corresponding curve for $\Delta(1/Q)$ or constant ε'' also exhibits a similar behavior except it has a higher value around -40°C. As we know that the Curie temperature for a pure crystal of barium titanate is 120°C, in comparison the Curie temperature for a composition of 75 percent barium titanate and 25 percent strontium titanate changes dramatically.

The microwave resonant cavity technique as applied in this investigation was very successful in monitoring the phase changes in barium titanate as it goes from paraelectric cubic phase to the ferroelectric tetragonal phase, to the ferroelectric orthorhombic phase, and to the ferroelectric rhombohedral phase respectively. The heating and the cooling methods involved in this technique were very effective in maintaining a certain temperature. Data was taken at a microwave resonant frequency of 9.12 GHz and the experiment was repeated several times to observe the dielectric behavior of barium titanate and also a mixture of 75 percent barium titanate and 25 percent strontium titanate.

The reason that barium titanate has a high dielectric constant is because of the Ba^{2+} ion that is so large as compared to the very small Ti^{4+} ion that is sitting in the middle of the crystal structure. The oxygen and barium ions are so large, they push each other apart, leaving the titanium ion in an octahedral hole where it can rattle around. Therefore, when an electric field is applied to a crystal of barium titanate, the titanium ions are repelled by this field and are drawn over to one side of their octahedral hole. Because of this very strong displacement of titanium ions, the crystal of barium titanate becomes highly polar in nature and the total polarization of the material increases dramatically around 120°C. As shown in Figures 5 and 6, an addition of 25 percent strontium titanate to 75 percent barium titanate changes the Curie point dramatically and there is also a change in the dielectric behavior of the crystal.

ACKNOWLEDGEMENTS

REFERENCES

1. Lurio, A., and Stern, E.: Measurements of the Dielectric Constant of BaTiO$_3$ Single Crystals in the Paraelectric Region at X-band. J. Appl. Phys., 31, 1960, p. 1805.

2. Arlt, G., Hennings, D., and de With, G.: Dielectric Properties of Fine-grained Barium Titanate Ceramics. J. Appl. Phys., 58 (4), 15 August 1985, p. 1619.

3. Dahiya, J. N., and Freeman, R. W.: Computer Interfacing of Microwave Resonant Cavity for Temperature Measurements During Dielectric Relaxation. Computers in Physics, July/Aug. 1989, p. 49.

4. Dahiya, J. N., Jani, S. K. and Roberts, J. A.: Phase Transition Studies in Polar and Non-Polar Liquids at Microwave Frequencies. J. Chem. Phys. 74(6), 1981, p. 3609.

5. Dahiya, J. N.: Dielectric Behavior of Superconductors at Microwave Frequencies. NIST Special Publication 822, 1990, p. 145.

6. Dahiya, J. N.: Dielectric Properties of Germanium and Silicon as Determined in the Microwave Field. J. Mater. Educ., 13, 1991, p. 367.

7. Hong, K. H., and Roberts, J. A.: Microwave Properties of Liquids and Solids Using a Resonant Microwave Cavity as Probe. J. Appl. Phys., 45(6), 1974, p. 2452.

1. Block diagram of the microwave spectrometer used in this investigation.

2. Structure of barium titanate above T_c.

3. Microwave loss Δ(1/Q) as a function of temperature for a sample of barium titanate.

4. Frequency shift $\Delta f/f_o$ as a function of temperature for a sample of barium titanate.

5. Microwave loss $\Delta(1/Q)$ as a function of temperature for a sample containing 75 percent barium titanate and 25 percent strontium titanate.

6. Frequency shift $\Delta f/f_0$ as a function of temperature for a sample containing 75 percent barium titanate and 25 percent strontium titanate.

EXPERIMENTS IN MATERIALS SCIENCE FROM HOUSEHOLD ITEMS

F. Xavier Spiegel

Department of Engineering
Loyola College
4501 N. Charles Street
Baltimore, Maryland 21210

Telephone 410-617-2515

EXPERIMENTS IN MATERIALS SCIENCE FROM HOUSEHOLD ITEMS

F. Xavier Spiegel
Department of Electrical Engineering & Engineering Science
Loyola College, Baltimore, Maryland

ABSTRACT: Everyday household items are used to demonstrate some unique properties of materials. A coat hanger, rubber band, balloon, and corn starch have typical properties which we often take for granted but can be truly amazing.

KEY WORDS: Polymer, Coat Hanger, Rubber band, Balloon, Corn Starch.

PREREQUISITE KNOWLEDGE: Curiosity.

OBJECTIVES: The purpose of these demonstrations is to illustrate some interesting properties of household items. The following demonstrations have been performed by the author for many years and have been received enthusiastically by audiences of all ages.[1,2]

EQUIPMENT AND SUPPLIES:
1) Metal Coat Hanger
2) String
3) Rubber Band
4) Balloon
5) Corn Starch

THE COAT HANGER: A metal coat hanger can be used to demonstrate the ability of string to transmit sound better than air. Sound travels more efficiently in a more dense medium than a rarefied medium. If a metal coat hanger is inverted and a piece of string approximately three feet long is tied to each end of the coat hanger, and then it is moved to strike a wall or some other solid, a rather dull thud will be heard. However, if the ends of the strings are placed close to the ears (by holding the strings against each ear with a finger) and then the experiment is repeated, a resounding tone will

be heard that is much more beautiful than the dull thud. Different types of string, twine or monofilament will produce different qualities of the sound.

THE RUBBER BAND: A rubber band is a polymer which consists of long bulky chain molecules. These molecules are tangled and not strongly bound to each other, similar to a bowl of spaghetti noodles. When the rubber band is stretched, the long chain molecules rearrange to line up along the direction of the stretching and the rubber band becomes warm. This warming is caused by internal friction as the molecules slide over one another and can be readily observed by touching the stretched rubber band to the lower portion of the upper lip (a very sensitive temperature sensor of the body).[3]

THE BALLOON: A balloon is also a polymer and can be used to show the different behavior of a stretched polymer as opposed to an unstretched polymer. If a balloon is inflated and touched by a sharp object such as a skewer it will burst. However, if the skewer is inserted carefully from the bottom of the balloon and then into the top from the inside the balloon will stay inflated for some time. The reason the balloon bursts in the first instance is that the molecules have been stretched apart and cannot inhibit the burst. In the latter case the molecules are relatively unstretched and hence, as jumbled molecules, "grab" the skewer and prevent air from escaping. A variation on the above is to skewer the balloon before inflation and show that the balloon can still be inflated.[1,2,3]

CORN STARCH: Corn starch is used in cooking for thickening gravies. However, if corn starch is mixed with water to about the consistency of pancake batter, it will be noticed that if it is moved slowly, for instance by pouring or trying to slowly stir the corn starch "batter", it will behave normally as most fluids do. However, if you try to stir the "batter" rapidly or drop something into it the "batter" will behave more like a solid. The "batter" is known as a non-Newtonian fluid. Variations of the above can be tried by mixing the "batter", freely pouring from one glass to another, and then

374

suddenly trying to throw the "batter" from the glass by a jerk of the wrist. Please note, experiment with your mixes before trying this towards an unsuspecting audience. Unfortunately the "batter" has a very limited shelf life.

CONCLUSIONS: The author has had enthusiastic response from audiences of all ages. With each of these demonstrations, quantitative results can be measured and each can be expanded and/or altered. You are only limited by your imagination and curiosity.

REFERENCES:
1. Fellers, William O.: *Materials Science, Testing and Properties for Technicians,* Prentice-Hall 1990.

2. Jacobs, James A. and Kilduff, Thomas F.: *Engineering Materials Technology,* Prentice-Hall 1985.

3. Spiegel, F. Xavier: *Five Experiments in Materials Science for Less than $10.00,* NASA Conference Publication 3151 November 1991 263-265.

AN AUTOMATED DATA COLLECTION SYSTEM FOR A CHARPY IMPACT TESTER

Bernard J. Weigman

and

F. Xavier Spiegel

Department of Engineering

Loyola College

4501 N. Charles Street

Baltimore, Maryland 21210

Telephone 410-617-2515

AN AUTOMATED DATA COLLECTION SYSTEM
FOR A CHARPY IMPACT TESTER

Bernard J. Weigman and F. Xavier Spiegel
Department of Electrical Engineering and Engineering Science
Loyola College, Baltimore, Maryland

ABSTRACT: A method for automated data collection has been developed for a Charpy impact tester. A potentiometer is connected to the pivot point of the hammer and measures the angular displacement of the hammer. This data is collected with a computer and through appropriate software accurately records the energy absorbed by the specimen. The device can be easily calibrated with minimal effort.

KEY WORDS: impact, Charpy, potentiometer, fracture energy, potential energy, computer, analog to digital converter.

PREREQUISITE KNOWLEDGE: The student should understand the concepts of fracture and the use of a computer for automatic data collection.

OBJECTIVES: This experiment is intended to familiarize the student with the technique of automated data collection using a Charpy Impact Tester, a potentiometer, and a computer.[1,2,3,4,5]

EQUIPMENT AND SUPPLIES: (1) Charpy impact tester; (2) Potentiometer; (3) Computer; (4) Analog to Digital Converter; (5) Samples as desired.

EXPERIMENTAL PROCEDURE: A 10 KΩ potentiometer was fastened to the rotating arm of the Charpy impact tester so that as the arm of the tester rotated, the resistance of the potentiometer increased linearly with the angle (Figure 1). The voltage at the wiper arm of the potentiometer then also varies linearly with the angle of the tester arm. In the experiment, the tester arm is released from a known height which corresponds to a known angle which in turn corresponds to

379

a known voltage, V_1. The tester arm then breaks a piece of material, in this experiment wood, and keeps swinging until it reaches its final height, which corresponds to its final voltage, V_F. The difference in height from the initial position of the pendulum to the final position corresponds to a loss in potential energy. This loss in potential energy is equal to the energy used to break the piece of wood. The Charpy impact tester is calibrated, not in angle, but in inch-pounds of energy used to break the material placed at the bottom of the pendulum's swing.[6]

When the experiment is done without the use of a computer, an observer visually determines how high the hammer swings after it breaks the sample and relates this to the loss of potential energy in inch-pounds. When the computer is used in the experiment, the voltage output from the potentiometer, V_{out}, is measured by the computer by reading the output of an Analog to Digital Converter (ADC) every fiftieth of a second for the duration of the swing of the pendulum. The program then picks out the maximum voltage, which corresponds to V_F and calculates the loss of energy due to breaking the sample in inch-pounds.[7]

It is necessary to calibrate the Charpy impact tester before the experiment and sometimes during the experiment. This is done by measuring the voltage, V_1, at the beginning position, the voltage, V_2, at the bottom of the swing (the point of lowest potential energy), the voltage, V_3, when the arm makes a 90° angle with the vertical and the voltage, V_4, when the pendulum swings to its largest height with no sample present. The wiring of the potentiometer is set up so that $V_1 < V_2 < V_3 < V_4$. Once the differences between the four voltages are known, they will not change, even if all of the voltages rise or fall due to a twisting of the potentiometer shaft because of the sharp impact each time a sample is broken. Thus to re-calibrate, all we need to do is measure the voltage, V_1, when the pendulum is at rest.

THEORY:

$$\Delta E = Mg(H-h) \tag{1}$$

When h = 0 then ΔE = 50 in-lb
Therefore, MgH = 50 in-lb

$$V_{out} = \kappa\theta + V_2 \tag{2}$$

$$V_3 = \kappa\frac{\pi}{2} + V_2 \tag{3}$$

$$\kappa = \frac{2}{\pi}(V_3 - V_2) \tag{4}$$

$$\theta = \frac{V_{out} - V_2}{\kappa} \tag{5}$$

$$\theta = \frac{\pi}{2}\frac{V_{out} - V_2}{V_3 - V_2} \tag{6}$$

$$h = L(1-\cos\theta) \tag{7}$$

$$\Delta E = Mg(H - L + L\cos\theta) \tag{8}$$

h = H when $V_{out} = V_1$ and $\theta = \theta_1$

$$H = L(1 - \cos\theta_1) \tag{9}$$

θ is a function of V_{out}

$$\theta = \theta(V_{out}) \tag{10}$$

and

$$\theta_1 = \theta(V_1) \tag{11}$$

Then

$$\frac{L}{H} = \frac{1}{1 - \cos\theta_1} \qquad (12)$$

$$\Delta E = MgH(1 - \frac{L}{H}(1 - \cos\theta)) \qquad (13)$$

$$\Delta E = MgH\frac{\cos\theta - \cos\theta_1}{1 - \cos\theta_1} \qquad (14)$$

Finally,

$$\Delta E = 50\frac{\cos\theta - \cos\theta_1}{1 - \cos\theta_1} \qquad (15)$$

INSTRUCTOR'S NOTES: In this experiment, wooden samples of pine were fractured with and against the grain. The automated experiment provides much more consistent results than visual observation. Variations on the fracture of wood can be performed such as the fracture energy of wood as a function of water content, the effects of knots and/or notches, and the relative strengths of various types of glue by gluing the fractured pieces and repeating the experiment. Not to be overlooked is the appearance of the fracture surfaces.

REFERENCES:

1. Eggebrecht, L. C.: *Interfacing to the IBM Personal Computer*, Howard W. Sams & Co.

2. Thompson & Kuckes: *IBM-PC in the laboratory*, Cambridge University Press.

3. Krutz, Ronald L.: *Interfacing Techniques in Digital Design*, Wiley.

4. Stone, Harold S.: *Microcomputer Interfacing*, Addison Wesley.

5. Cripps, Martin: *Computer Interfacing - Connection to the Real World*, Edward Arnold Publisher, a division of Hodder & Stoughton.

6. Spiegel, F. Xavier; and Weigman, Bernard J.: "An Automated System for Creep Testing," NASA CP-3151, 1991.

7. Fellers, William O.: *Materials Science, Testing and Properties for Technicians*, Prentice Hall, 1990.
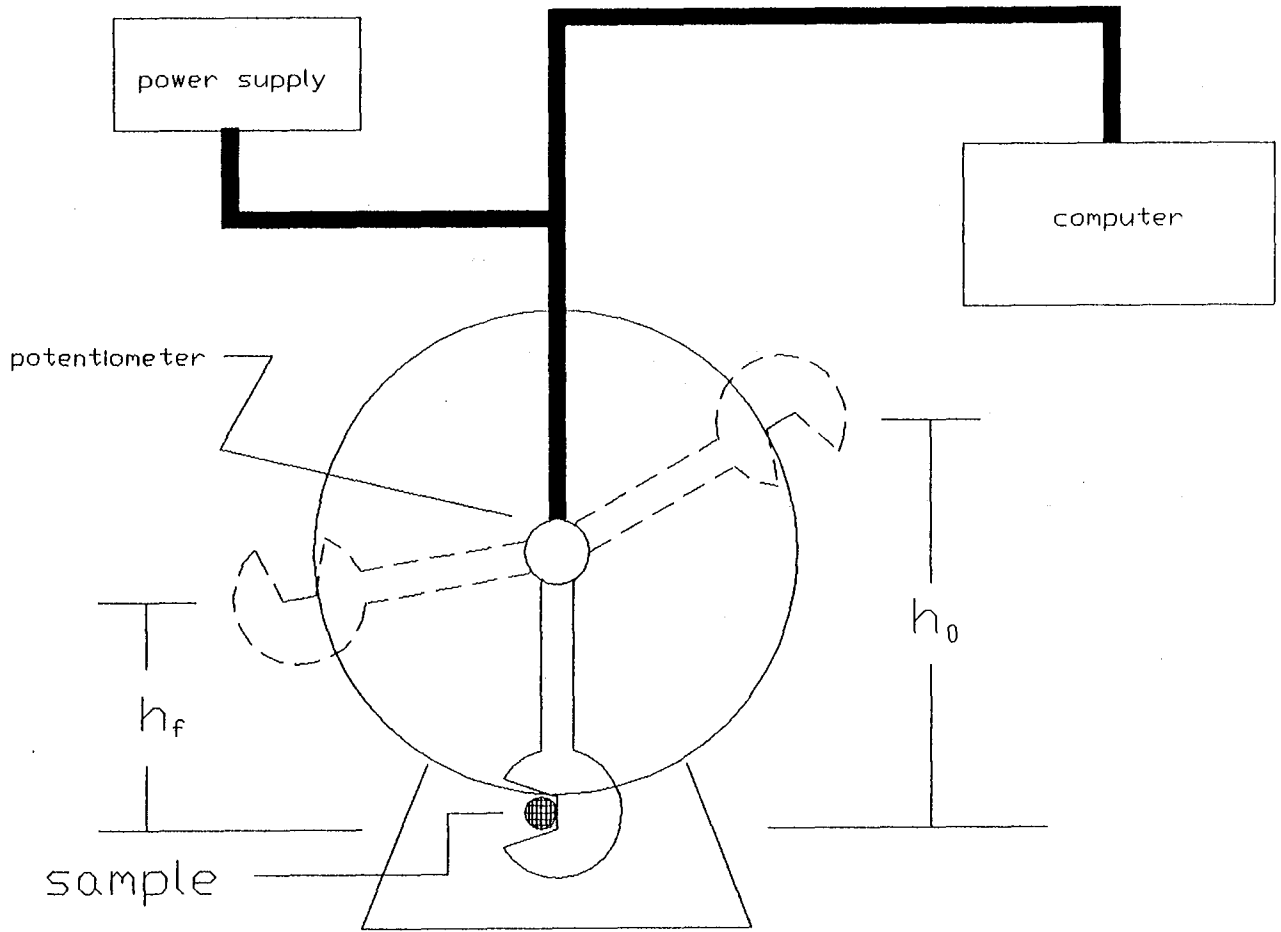
Figure 1
Charpy Impact Tester

VISUALIZING WELD METAL SOLIDIFICATION USING ORGANIC ANALOGS

Daniel W. Walsh

and

Gary Ray Rogers

Materials Engineering Department
School of Engineering
California Polytechnic State University
San Luis Obispo, California 93407

Telephone 805-756-2131

VISUALIZING WELD METAL SOLIDIFICATION USING ORGANIC ANALOGS

Daniel W. Walsh and Gary Ray Rogers
Materials Engineering Department
California Polytechnic State University
San Luis Obispo, CA

KEY WORDS: solidification, weld metal, solidification modes, equiaxed, columnar, cellular, dendritic, planar

PREREQUISITE KNOWLEDGE: The student should understand basic solidification theory and be familiar with the different types of solidification modes.

OBJECTIVES: To allow the student to observe the solidification of a low melting temperature transparent crystalline organic compound that exhibits behavior similar to that of weld metal.

EQUIPMENT AND SUPPLIES: (1) Cell assembly 2.00-in. x 6.00-in. brass plate with a 0.75-in. x 2.00-in. slot milled out of the geometrical center of the plate. (2) Two glass slides rest in this slot, serving to encapsulate the organic compound. The movable platform upon which the cell is mounted, (3) a 12.00-in. x 8.00-in. x 0.5-in. aluminum plate has a 2.00-in. x 6.00-in. slot milled out for insertion of the cell assembly. The movable platform is mounted on (4) four linear motion pillow block bearings which support the load. The pillow blocks run along (5) two 15.00-in. long AISI 1060 case-hardened and ground steel rails. The rails are in turn supported by (6) four malleable iron support blocks, and the entire assembly is mounted on a (7) 28.00-in. x 22.00-in. x 1.00-in. aluminum base plate to provide dimensional stability. (8) A Dayton 1/15 horsepower, variable speed electric motor is mounted on the base plate and drives the platform via a 1/2-20 UNF feed screw/nut assembly consisting of a (9) 1/2-20 UNF feed screw and (10) two

1/2-20 UNF nuts welded to the movable platform. The feed screw is connected to the motor through a (11) small flexible coupling. Below the cell a variable intensity light source is mounted to provide the necessary back light illumination for microscopic observation. This consists of (12) a sewing machine lamp with a bayonet-type 15 W bulb connected to a (13) standard dimmer switch. The filament assembly consists of a (14) 0.004-in. diameter AISI 304 stainless steel filament wire connected to (15) two quick release terminals on (16) 16 gage wire connected to a (17) 2-12 volt, 0-5 amp rated DC power supply. The filament assembly simulates the welding arc. The organic compound chosen for use in the apparatus is (18) Succinonitrile; a few grams will suffice. To view the solidification event a (19) low power stereomicroscope will be needed. This can be mounted directly to the base plate.

PROCEDURE: It is assumed that a student or technician has constructed the Organic Weld Solidification Analog (OWSA), as the experiment described here is intended to further the <u>understanding</u> of the organic simulator, not the <u>construction</u> of it.

The study of solidification often lacks immediacy. Akin to the paleontologist, researchers in materials scan the "fossil" remains of long past solidified pools to gain clues to the nature of the solidification event. This experiment provides a method to improve students' understanding of solidification by exposing them to in-situ solidification. The organic weld solidification simulator is a device that allows the observation of solidification at low temperature. The device takes advantage of the transparency and low melting temperature of several crystalline organic compounds. This system provides the students with visual reinforcement to concepts discussed in lectures, and is exciting and fun to use.

Direct observation of the solid liquid interface in metals is difficult; metals are not transparent and the temperatures associated with the interface prohibit simple visualization systems. The interface is a critical region, as much of the structure resulting from solidification depends on the interface morphology. The OWSA allows students access to this event.

Solidification processes depend upon the roughness, on an atomic scale, of the solid-liquid interface. Materials can be classified in terms of their freezing behavior according to their entropy of melting. Certain organic compounds exhibit entropies of melting that are very similar to those of metals. The availability of transparent materials for metallic analogs presents an opportunity to directly observe the phenomena that determine the structure of cast metals and fusion welds.

This device has been used to view many of the features associated with welds in metals. Direct observations of epitaxial nucleation, competitive growth, morphological changes and defect formation have been accomplished in the laboratory. Students experimentally verify the relations shown below.
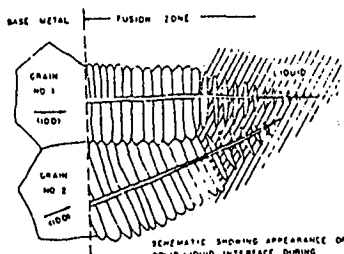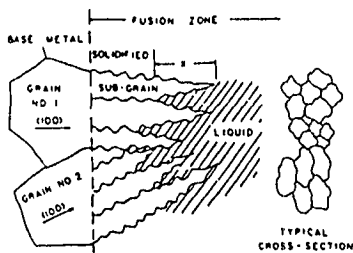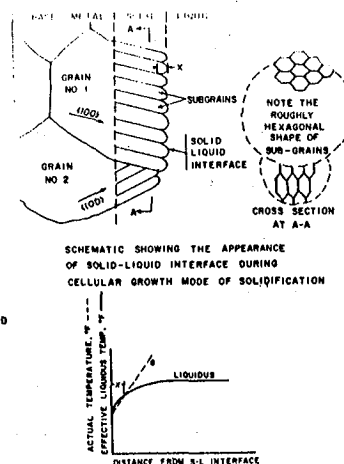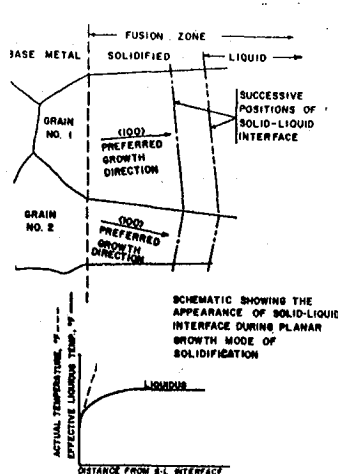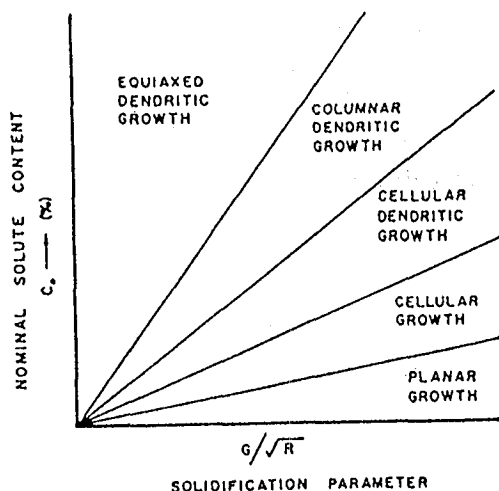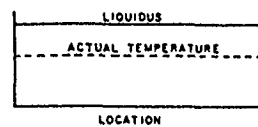
These drawings depict the relationships among solidification substructures, the process parameters (G/√R̄, where G is the thermal gradient and R is the rate of motion of the solidification front) and the production parameter (C_o), the nominal composition. One may view the diagram as providing limits for the breakdown of a planar solidification front based on the time necessary to redistribute matter by diffusion or heat by conduction.

As the student uses these diagrams, it should become apparent there is a basic philosophical conundrum involved with the microstructures thus generated. There is solid growth proceeding from the pool edge, where it is relatively cool, toward the pool center, where it is hot. How can this be? Why should bits of solids form as cells, or dendrites, and jut ahead of the planar interface? Solidification should proceed in a planar fashion, that is, as the liquid cools, the planar surface should move uniformly forward.

Once again, reality is more complex and beautiful than it is obvious. Neither solids nor liquids are homogeneous isotropic continua. This experiment demonstrates graphically that a solidification front engenders a solute gradient in the liquid ahead of that front.

We can derive an expression for the effective liquidus temperature as a function of distance from the solidification interface. We know

EQN 1 $C_1 = C_o[1 + \{(1-k)/k\} \exp(-R/D_1)x']$
and
EQN 2 $dT_e/dx' = (dC_1/dx') (dT_e/dC_1)$
Thus
EQN 3 $(dC_1/dx') = -(C_oR/D_1) \{(1-k)/k\}$ @ $x' = 0$
and
EQN 4 $dT_e/dC_1 = m_1$
Thus
EQN 5 $G_c = -(RC_o)/D_1 \{m_1[1-k]/k\}$

    where G_c denotes the effective thermal gradient induced by compositional variance.

If G_t, the thermal gradient, is greater than G_c solidification will proceed on planar fronts. If G_t is equal to or less than G_c, the planar front will become unstable. Depending on the magnitude of the difference between the two, any of the following substructures can occur: cellular, cellular dendritic, columnar dendritic or equiaxed dendritic growth. In effect, by altering the composition ahead of the interface, we have created a chemical supercooling. The physical thermal gradient (G_t), though positive, may be less severe than the chemical gradient (G_c), leading to virtual supercooling.

SAMPLE QUESTIONS:

1. Discuss the solidification of the succinonitrile analog in the context of weld solidification in general.
2. Discuss the macroscopic bead shape as affected by process parameters.
3. Relate macroscopic process parameters to resultant microstructures.
4. Relate microstructures to resultant properties.
5. Certain process parameters will give rise to centerline cracks and cracks at the edge of the pool. Discuss the changes in process and production parameters which cause the formation of these cracks.
6. How does the dynamic character of solidification change the composition and the phase distribution in an engineering material vis-a-vis its hypothetical equilibrium counterpoint?
7. Verify the relationships between the microstucture and the process and production parameters using the diagrams enclosed.
8. What ramifications does solidification have for corrosion properties, mechanical properties, and for magnetic behavior in ferromagnetic metals?
9. Develop a relationship between the velocity of the moving heat source and the velocity of the pool interface. What limits the stability of pool shape? Relate this to question 5.

SAFETY NOTE: The organic compound most suitable for this type of study is succinonitrile. This is readily available from most chemistry departments. This is a relatively safe compound at

temperatures below its boiling point. Nonetheless, basic chemistry lab rules should be followed. The Material Safety Data Sheet for succinonitrile should be available for all students to read as should the MSDS for all lab chemicals in the lab.

REFERENCES:

(1) Savage, W.F., Nippes, E.F., and Miller, T.W., "Microsegregation in 70Cu-30Ni Weld Metal", Welding Journal Research Supplement, Vol 55, No. 6, June 1976, pp. 165s-173s.

(2) Chalmers, B. Principles of Solidification, John Wiley and Sons, Inc., New York, 1967.

(3) Savage, W. F., Lundin, C. D. and Chace, T. F. "Technical Note: Direct Observation of Microstructural Changes Associated with Fusion Welding." Welding Journal Research Supplement, Vol. 47, No. 11, November 1968, pp. 527s -528s.

(4) Jackson, K. A. and Hunt, J. D. "Transparent Compounds That Freeze Like Metals." Acta Metallurgica, Vol. 13, 1965, pp. 1212 - 1215.

(5) Savage, W. F. and Hrubec, R. J. "Synthesis of Weld Solidification Using Crystalline Organic Materials." Welding Journal Research Supplement, Vol. 51, No. 5, May 1972, pp. 260s - 271s.

PERFORMANCE OF THERMAL ADHESIVES IN FORCED CONVECTION

Nikhil K. Kundu

Statewide Technology
Purdue University
2424 California Road
Elkhart, Indiana 46514

Telephone 219-264-3111

PERFORMANCE OF THERMAL ADHESIVES
IN FORCED CONVECTION

Nikhil K. Kundu
Purdue University
Elkhart, Indiana

ABSTRACT:

Cooling is critical for the life and performance of electronic equipment. In most cases cooling may be achieved by natural convection but forced convection may be necessary for high wattage applications. Use of conventional type heat sinks may not be feasible from the viewpoint of specific applications and the costs involved. In a heat sink, fins can be attached to the well by ultrasonic welding, by soldering, or with a number of industrially available thermal adhesives. In this paper the author investigates the heat transfer characteristics of several adhesives and compares them with ultrasonic welding and theoretically calculated values. This experiment was conducted in an air flow chamber. Heat was generated by using heaters mounted on the well. Thermstrate foil, Uniset A401, and Aremco 571 adhesives were tested along with an ultrasonically welded sample. Ultrasonic welding performed far better than the adhesives and Thermstrate foil.

This type of experiment can be adapted for a laboratory exercise in an upper level heat transfer course. It gives students an exposure to industrial applications that help them appreciate the importance of the course material.

KEY WORDS:
heat transfer, thermal conductivity, thermal interface, heat sink, ultrasonic welding

PREREQUISITE KNOWLEDGE:
The students should understand the concept of heat transfer by conduction and convection.

OBJECTIVES:
Cooling is critical for the life and performance of electronic equipment. Conventional heat sinks for high wattage applications consist of a well with fins attached with thermally conductive interface materials or ultrasonic welding. Any interface increases thermal resistance of the system. The objective of this experiment is to investigate the thermal effectiveness of a number of selected interface adhesives and ultrasonic welding.

INTRODUCTION:
Cooling devices for electronic equipment are generally rated by their thermal resistance. It is expressed by the temperature rise per unit of heat

395

transfer or power dissipated. The major goal of any cooling system is to lower thermal resistance of the heat sink. The heat sink is composed of a well, a thermal adhesive interface between heat source and well and between well and fins so the heat sink has three major locations of thermal impedance.

The aluminum well makes up approximately 25% to 30%, the adhesive makes up between 15 to 20%, and the fin convection resistance makes up between 50% to 60% of the total thermal resistance (fig 1).

The adhesives are often called thermal interface due to their conductive nature. A desirable adhesive interface should possess a high thermal conductivity and must be installed with uniform pressure yielding minimum film thickness. The area of contact is dictated by the fin geometry and the semiconductor device. The film thickness again depends on the viscosity and surface tension of the adhesive at installation temperature. Trapped air bubbles may cause significantly higher thermal resistance. Thermal conductivity is not a sufficient measure of the suitability of an adhesive. Adhesives have thermally conductive filler materials. High conductivity materials with large particles may be found to be thermally poor for bonding high conductivity materials as they gap the surfaces excessively.

Thermal resistance is given by $R = L/kA$ (1)
where L is the interface thickness, k is the thermal conductivity of the adhesive, and A is the contact area.

The convection resistance R_c is a function of the air flow rate, fin configuration and geometry. Temperature drop across the fins increases with decreasing fin thickness.

TEST EQUIPMENT
      An air flow chamber (fig 2) with fan and adjustable nozzles; heat sink well with four sets of fins, two sets attached with thermal adhesives, (Uniset A401 and Aremco- 571) one set with thermstrate foil, and one set with ultrasonic welding; two 300 watt heaters, and a power supply.

PROCEDURE:
      The sample heat sink consisted of a 3" x 1" aluminum channel with 2" high and .010" thick fins; two 300 watt heaters were mounted on the channel with thermally conductive grease between the heater and the channel. The heaters were securely held with C clamps. Thermocouples were soldered at eight locations. Two thermocouples were used for each sample interface, one on the heater side and the other on a fin (fig. 3).

The heat sink assembly was installed at the exit gate of an air flow chamber with a shroud (fig. 4). The tests were run at varying power levels and air flow. All tests were run at a well temperature of 130 °C.

Table I:
Thermal conductivities of selected adhesives and their curing temperature and time.

	Btu/hr. ft.$^\circ$F	curing time(hr)	curing temp($^\circ$C)
Thermstrate Foil	K= 2.395	—	—
Uniset A 401	K= 0.417	1/2	150
Silicon Grease 340	K= 0.430	24	25
Aremco 571	K= 18.082	—	—

Table II:
Temperature difference between well and fins at varying air flow.

	air velocity (fpm)	ΔT between well and fins ($^\circ$C)		air velocity (fpm)	ΔT between well and fins ($^\circ$C)
Thermstrate Foil	1300	77.5	Uniset A401	1300	70.0
	1800	61.0		1800	60.2
	2200	60.3		2200	57.8
	3000	51.8		3000	53.0
	3200	50.6			
Aremco 571	1300	64.9	Ultrasonic Welding	1300	53.5
	1800	56.5		1600	53.5
	2300	57.8		2100	52.0
	3000	53.5		2500	45.0
	3200	54.0		2600	45.0

RESULTS AND DISCUSSION:

Two sample adhesives tested were Uniset A401 and Aremco 571. These were compared against samples with thermstrate foils and ultrasonic welding. The temperature difference between the well and the fins at varying air flow was recorded for evaluation.

The curves in figure 5 for temperature differential between well and fins versus air flow demonstrate the heat transfer capability of the interface materials. Out of four samples ultrasonic welding performs the best. Ultrasonic welding maintains a temperature difference of approximately 10°C with other samples throughout the testing range. Thermstrate foil is least effective in heat transfer because of non uniform contact area between well and fins. The temperature differential between well and fins decreases with increased air flow for all four interfaces. All four curves tend to level off around an air velocity of 300 feet per minute.

The temperature differentials for Aremco and Uniset adhesives are not representative of their thermal conductivities. Aremco 571 was expected to be far better than Uniset A401, but they lie very close to each other. This explains the fact that there are other factors responsible for heat transfer through interface such as viscosity, surface tension, film thickness, applied pressure, particle sizes of filler materials, and chemistry of adhesives. The performance of interface materials also greatly depends on the cleanliness and roughness of both surfaces.

RECOMMENDATION:
Ideally there should be very little or no temperature difference between well and fins which would be the case of a unibody heat sink design (fig6). In a unibody heat sink, well and fins are machined from one block of metal. The number of fins in a unibody heat sink is less due to thicker fins and manufacturing limitations. This may not be economically attractive, but many times the design of cooling systems is dictated by the size or compactness of the electronic equipment.

REFERENCES:
1. Scott, A.W., "Cooling of Electronic Equipment", Wiley Interscience Publishing.
2. Thermalloy Inc., Engineering Information Releases on Thermal Interfaces.
3. Technical Data Sheet from Power Devices Inc., Masterbond Inc., Aremco Products, and Thermalloy Inc.

SOURCES OF SUPPLY:

Thermstrate Adhesive
Power Devices Inc.
Thermal Interface Products Group
27071 Cabot Road
Laguna Hills 114
phone: (714) 582-6712

Thermal Grease
Thermalloy Inc.
P.O.Box 810839
Dallas, TX 75381-0839
phone: (214) 243-4321

Aremco 571 Adhesive
Aremco Products
P.O.Box 429
Ossining, NY 10562-0429
phone: (914) 762-0685

Uniset A-401 Adhesive
Amicon Corporation
Polymer Products Division
25 Hartwell Avenue
Lexington, MA 02173

ACKNOWLEDGMENTS:
This research was conducted in the laboratory of Crown International in Elkhart, Indiana. The author wants to express his deep appreciation to Joe McGuire and Ross Brady of Crown International for their guidance and support.

Rs Conductive Sink Resistance

Ra Adhesive Resistance

Rc Convective Resistance
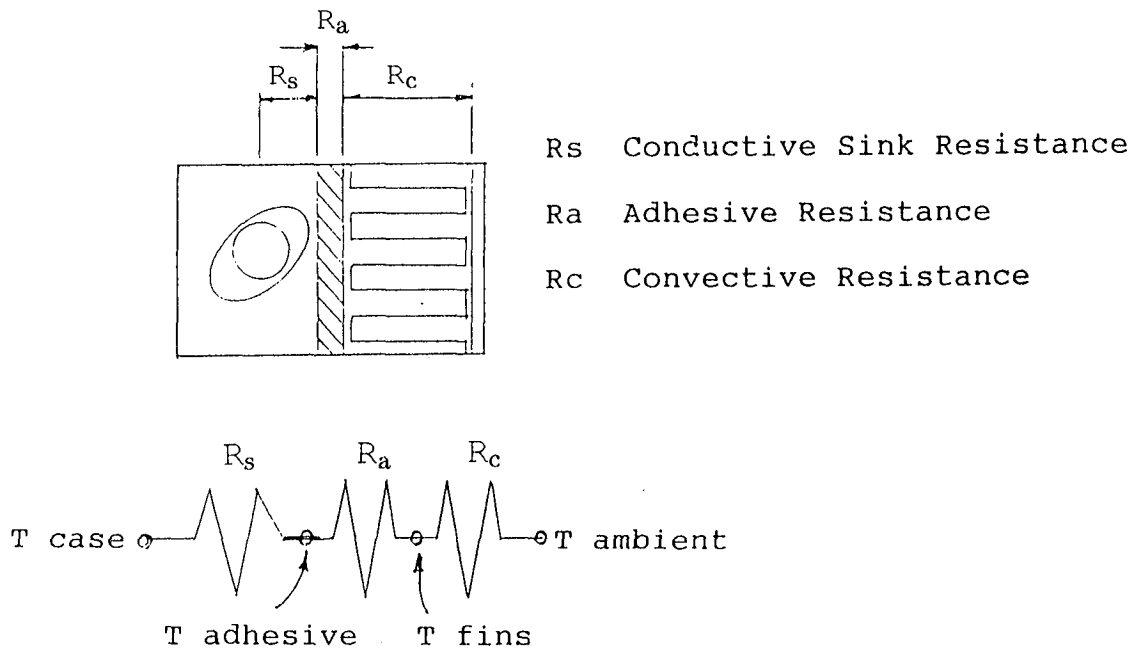
Figure 1: Heat sink thermal resistance
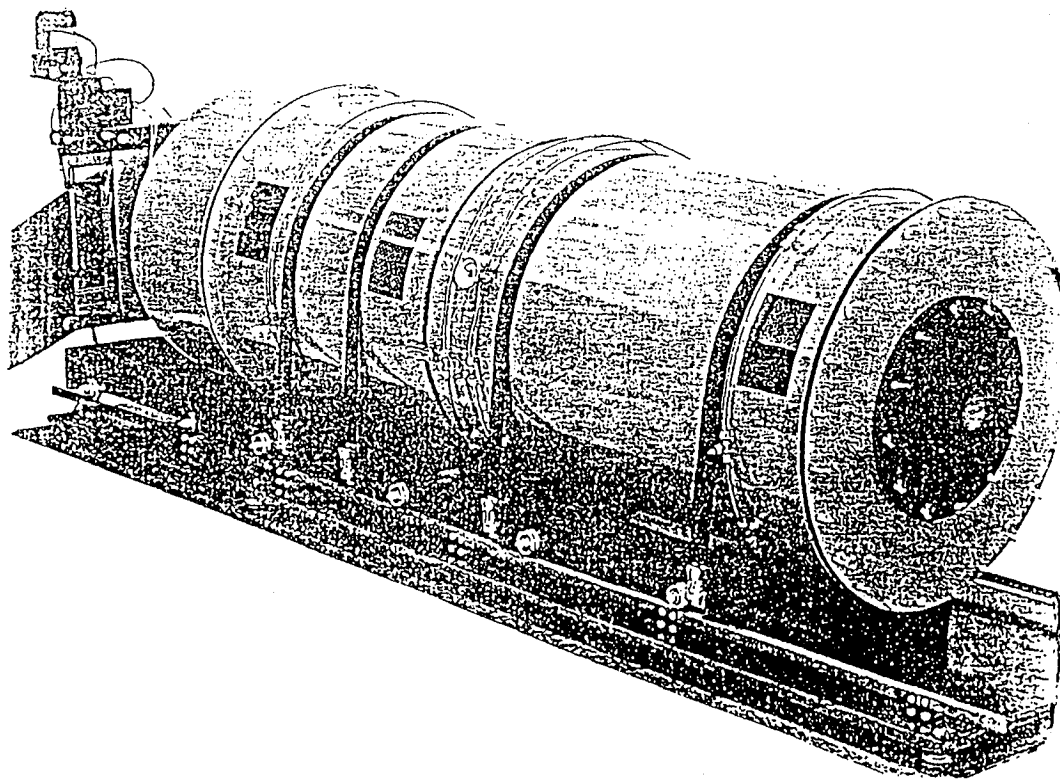
Figure 2: Air flow chamber

Thermstrate   Uniset   Aremco   Ultrasonic welding

Fins

Well
Heater
Thermocouple

Interface
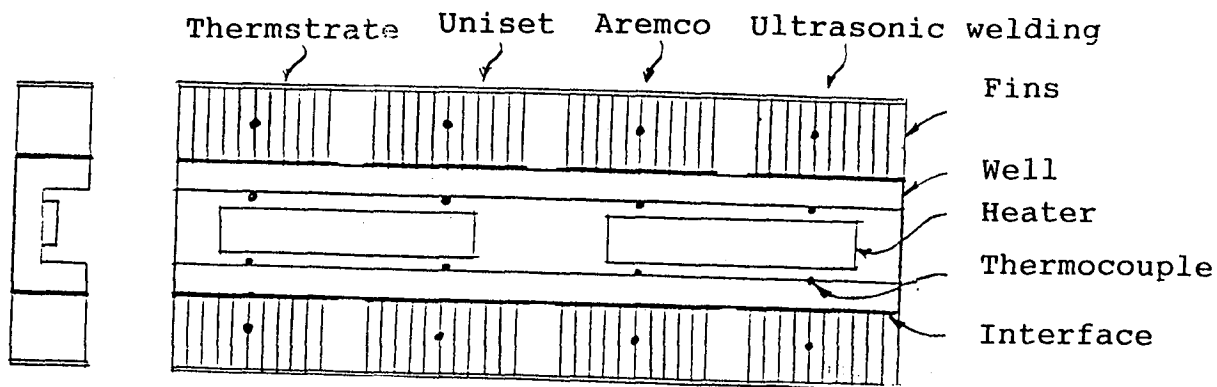
Figure 3: Heat sink assembly

Fins

Heaters

Air

Well

Interface

Shroud   Air flow chamber
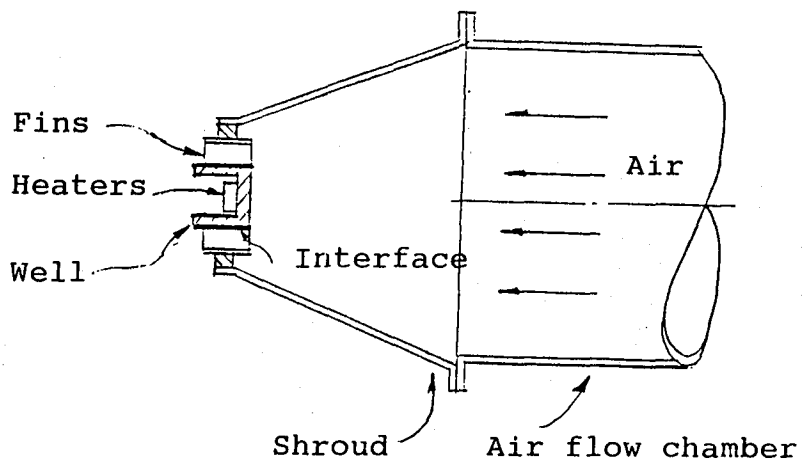
Figure 4: Test set up at air chamber
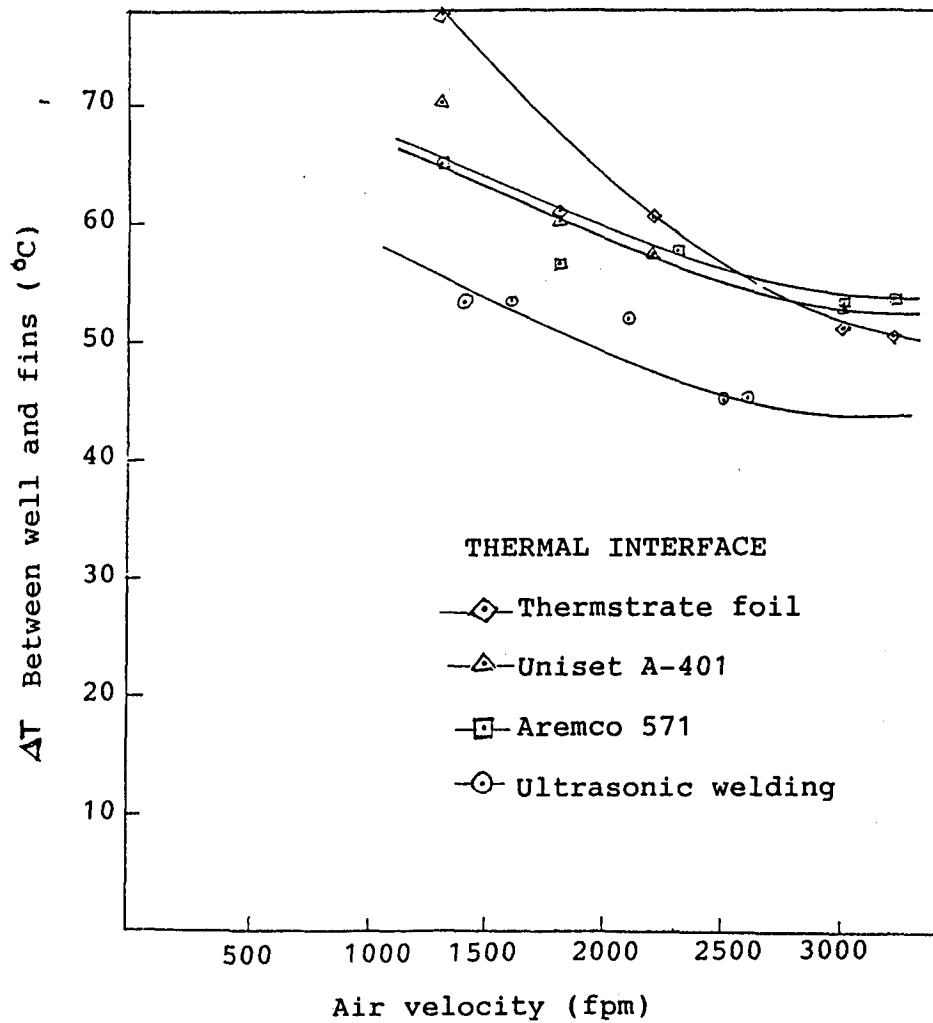
Figure 5: Temperature differential
between well and fins vs. air velocity
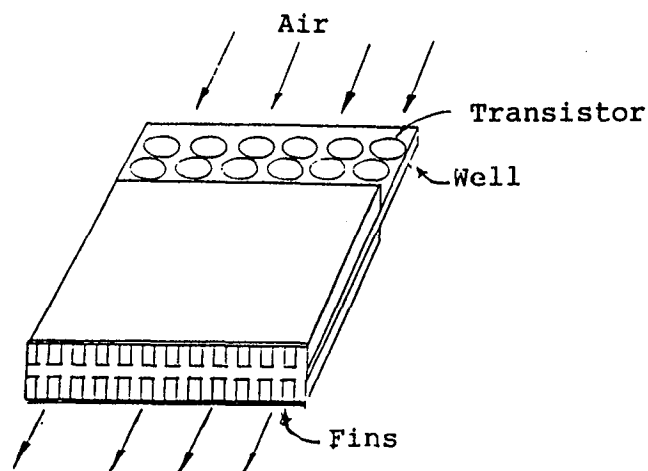
Figure 6: Unibody heat sink

TAGUCHI METHOD OF EXPERIMENTAL DESIGN IN MATERIALS EDUCATION

Martin W. Weiser

Mechanical Engineering Department and
Center for Micro-Engineered Ceramics
University of New Mexico
Albuquerque, New Mexico 87131

Telephone 505-277-2831

Taguchi Method of Experimental Design in Materials Education

Martin W. Weiser
Mechanical Engineering Department and
UNM/NSF Center for Micro-Engineered Ceramics
University of New Mexico, Albuquerque, NM 87131

Abstract

Some of the advantages and disadvantages of the Taguchi Method of experimental design as applied to Materials Science will be discussed. This is a fractional factorial method that employs the minimum number of experimental trials for the information obtained. The analysis is also very simple to use and teach, which is quite advantageous in the classroom. In addition, the Taguchi loss function can be easily incorporated to emphasize that improvements in reproducibility are often at least as important as optimization of the response. The disadvantages of the Taguchi Method include the fact that factor interactions are normally not accounted for, there are zero degrees of freedom if all of the possible factors are used, and randomization is normally not used to prevent environmental biasing. In spite of these disadvantages it is felt that the Taguchi Method is extremely useful for both teaching experimental design and as a research tool, as will be shown with a number of brief examples.

Introduction

The Taguchi Method of experimental design is a methodology that performs the minimum number of experiments necessary to determine the effects of three to as many as 63 independent variables on a response. It is a very efficient method that is well suited to use in Materials Science since it is conceptually quite simple and can be adapted to specific applications. In addition, the method meshes very well with Taguchi's loss function shown in Figure 1, which associates a cost with the response being away from the optimal value regardless of whether the error is due to the process being out of specification or the process being variable or noisy. However, as with all highly efficient methods, there are a number of problems with this technique that can result in erroneous results, particularly if a high degree of precision is required.
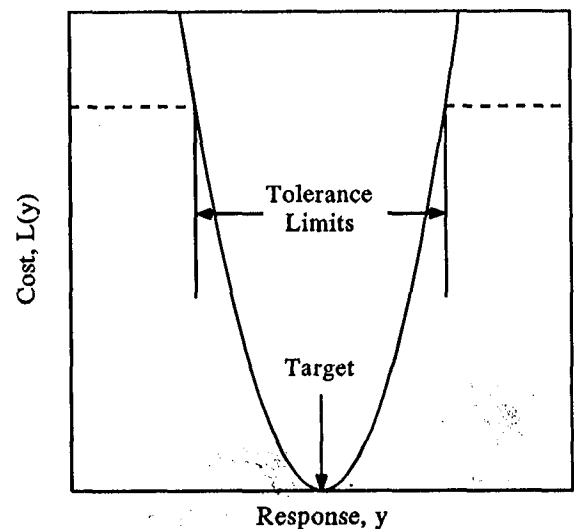
Figure 1 The Taguchi loss function.

Some of the advantages and disadvantages of the Taguchi Method are listed in Table I and are discussed in more detail below. Later, brief summaries of a number of examples where the Taguchi Method has proven very beneficial in Materials Science are presented. In addition, a number of comments on how the Taguchi Method can be employed in the typical Undergraduate Materials Laboratory and how it might be used to lead into other highly efficient methods of experimental design are offered.

Table I Advantages and Disadvantages of the Taguchi Method

High efficiency requires a minimum number of experimental trials
Error analysis is normally not exact
Can handle both continuous and discrete factors
Is conceptually very simple
Is computationally very simple
Easily incorporates the concepts involved in robust design
Does not handle factor interactions very well
Randomization is not commonly employed
Only a limited number of orthogonal arrays exist

High Efficiency

The Taguchi Method is very efficient in that it can be used to find as many factor effects as the number of trials that are performed, particularly the main factor effects. Use of carefully designed orthogonal arrays insures that the factor space is covered as uniformly as possible using the minimum number of trials. In addition, the arrays are at least pairwise orthogonal (the combination of levels A_1 and B_1 occurs as often as A_2 and B_2, etc.) so that any one factor interaction will not dominate the results.

This minimal number of trials results in a dramatic reduction in the amount of effort needed to obtain information about the system. For example, use of the L9 array, which examines four factors at three levels each, reduces the number of experimental trials from 81 for the full factorial design to nine for the Taguchi design. A consequence of this is that there are zero degrees of freedom in the system of equations that is used to calculate the main factor effects. This state is often referred to as "a statistician's bad dream[†]" because the response surface is required to pass through all of the data points. As such there are no degrees of freedom remaining for error variance analysis. This problem can be overcome by using one or more of the factors as a dummy variable to introduce additional degrees of freedom or to repeat the different trials. Repetition of the trials is particularly beneficial because it allows some examination of noise factors that cannot be controlled

Error Variance Analysis

Saturated orthogonal arrays with no degrees of freedom directly available for error variance analysis are normally used in the Taguchi Method. Error is therefore analyzed by assigning the factors that have the smallest effects on the response(s) to a pool. This can be done by simplistic Pareto analysis where the absolute magnitude of the effects is examined or by performance of the more detailed Analysis of Variance (ANOVA) which involves calculating the sum of squares of the effects due to each factor and then ranking

---

[†]   A negative number of degrees of freedom is known as "a statistician's nightmare" for very good reason.

them. Both of these methods of analysis are performed for the fired density in the powder metallurgy experiment presented elsewhere in this volume.[5] These results are displayed in Figure 2 (Pareto Analysis) and Table II (ANOVA) where it is readily seen that the consolidation pressure is the most significant factor, followed by the particle size, while the firing temperature and time were found to be relatively insignificant.
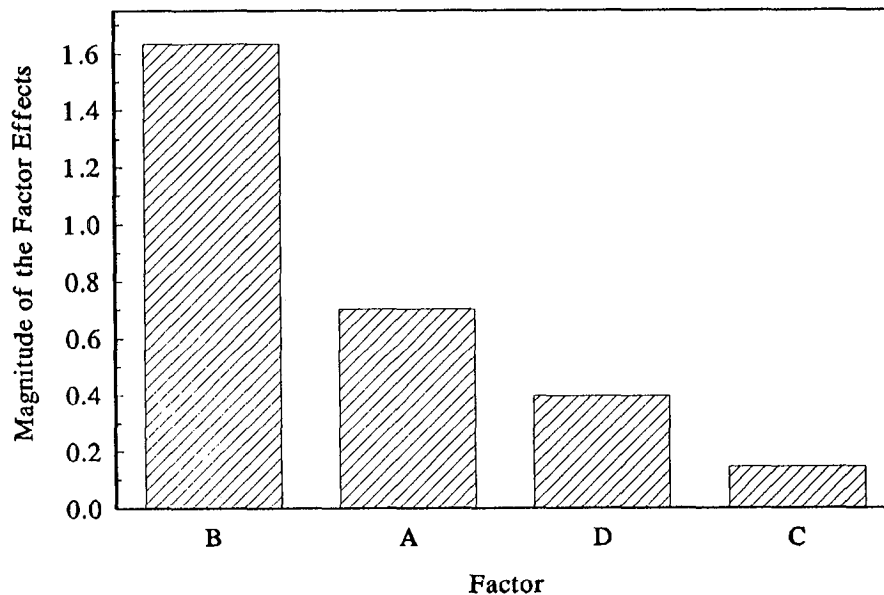
Figure 2 Pareto Diagram for the P/M experiment.

Table II ANOVA for the P/M Experiment

Factor	DOF[‡]	Sum of Squares	Mean Square	F[§]	% of Variation
B. Pressure	2	1.354	0.677	30.30	78.88%
A. Size	2	0.273	0.137	6.11	15.92%
D. Time	2	0.079	0.039		4.60%
C. Temperature	2	0.010	0.005		0.61%
Total	8	1.717			
Pooled Error	4	0.089	0.022		

The pooled factors are assumed to have effects that are comparable to the noise in the system. The use of one or more dummy factors will further improve the error variance analysis by including degrees of freedom that are devoted entirely to error analysis. In either case, a larger number of trials are required

---

[‡]   The degree of freedom is one less than the number of levels since the effects must sum to zero.

[§]   Mean square divided by pooled mean square error. Values greater than 1 indicate significance. Technically the F test cannot be applied unless the trials are fully randomized. This problem is handled in an unrandomized Taguchi experiment by stating that values of F between 1 and 2 are *probably* significant rather than definitely significant.

for most other experimental schemes to achieve the same level of error variance for each of the factors. For the L9 array, the process of progressively finding the best level for each of the four factors would require a total of 27 trials as opposed to the nine using the orthogonal array to achieve the same level of error variance. In addition, the true optimum might be missed since this approach is not pairwise orthogonal and an important factor interaction might be missed. The predictions from the Taguchi Method will not include the interaction, but it will show up as a discrepancy between the predicted optimum and the confirming trial result. The reader is referred to chapter 3 of Phadke[2] for a more complete discussion of this topic and how it can be related to Fourier analysis where the weaker harmonics are frequently classified as noise.

Continuous and Discrete Factors

The Taguchi Method is designed so that each of the factors is broken down into a small number of discrete levels and information is obtained about the factor effects only at these levels. This is very beneficial when one or more factors can only have discrete values such as a switch which can only be on or off. However, the discrete nature of the factor levels is not a problem when the factor is continuously variable, particularly if care is taken to systematically map the actual values of the factor to the factor levels.

The different factor effects from the Taguchi analysis are normally plotted versus the factor levels as shown by the filled circles in Figure 3 for a single four level factor. A solid line is traditionally used to connect the data points for a given factor to guide the eye. This line is not intended to present any information about the effect of the factor at any level between the experimental levels. In fact this line has absolutely no meaning if the factor can only have discrete values that correspond to the experimental levels. However, if the factor is continuous and systematic mapping has been done between the values of the factors and the levels, there must be factor effects corresponding to factor levels between those that were tested. The problem lies in determining what these factor effects are.
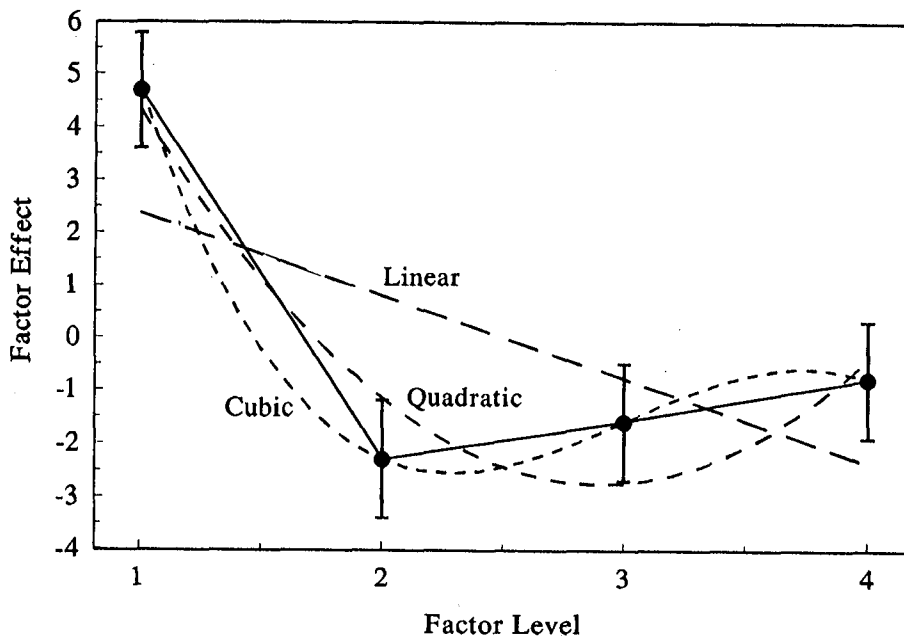
Figure 3 Different Fittings of the Factor Effects for a Four Level Factor

It is proposed that the solid lines, which are normally drawn to guide the eye, are actually a rather poor estimate of the intermediate factor effects since most systems respond to a continuous change in a factor with a continuous change in response rather than to the discontinuous response represented by the solid line. The most obvious solution to this problem is to use a continuous function that passes through all of the data points. This has been done using a cubic equation in Figure 3. The problem with this approach is that increasing the number of levels normally results in worse prediction of the factor effects at intermediate levels when noise is present in the experimental results since the curve must pass through all of the data points. This is contrary to the expectation that increasing the number of levels should improve prediction of the factor effects at intermediate levels.

Instead it is proposed that regression analysis should be used to fit a curve with fewer adjustable factors to the factor effects. This has been done using the least squares technique for both linear and quadratic functions in Figure 3. The quadratic function represents the experimental factor effects and the type of behavior that is expected by most systems fairly well, particularly when the error bars are considered. This method is quite similar to the approach employed in the various surface response techniques. However, it should be pointed out that this method of analysis should not be used for making predictions of the system response. Rather it should be used to gain additional information that will help guide further experimental exploration of the system. For example, if the goal is to minimize the response, a confirming trial with this factor set to level 2 would be required. However, the quadratic regression analysis indicates that the true minimum lies closer to a level of 2.9, so either additional confirming trials should be performed in this range or an another array experiment should be performed which covers a smaller range of factor values that are close to the indicated optimum.

Concept and Computation

The basic premise of the Taguchi Method is that a minimum number of trials are used to determine how a set of factors at a number of levels affect one or more responses. This is accomplished by arranging the levels of the factors in an array so that each level of a factor appears the same number of times and is paired with each of the levels of the other factors the same number of times. This array is a small subset of the full factorial experimental array in which all of the possible combinations of the factor levels are used. The result is an experimental array that is quite small and easily examined by the users.

The computations involved in the Taguchi Method are very simple and quite transparent to the practitioner. Determination of the effect of a factor at a given level is done by finding the mean response when the factor has this level and then subtracting the overall mean response. The optimal response is found by adding the effect for the most beneficial level of each factor to the overall mean response. This simplicity is extremely beneficial to students and instructors since it is not necessary to use complicated calculations or proprietary algorithms.

The conceptual and computational simplicity of the Taguchi Method allows students to quickly master the fundamentals of the analysis technique and then proceed to more complex issues in experimental design. This is of particular benefit in Materials Science where the underlying science is often quite complicated. The simplicity of the analysis makes it possible for the student to quickly begin to apply statistical methods of error variance analysis (particularly ANOVA) without having an extensive statistics background. The meaning of the statistics can be easily seen by comparing the results to those shown in a Pareto chart such as was described earlier.

The minimal number of experiments used in the Taguchi Method makes it feasible to use the first experiment to develop additional experiments to gain more insight into the process that is being investigated. The need to perform confirming trials at factor levels that are close to the predicted optimum is a first step in this development. The extreme simplicity of the technique makes it possible for the student to make modifications to the basic technique that make it better suited to studying their system. An example of this is the use of regression to fit the factor effects which is a simple surface response technique.

Robust Design

Robust design involves development of processes that are tolerant of perturbations in the controlled factors or the environment. This topic is of great interest from an industrial standpoint, but is often neglected in engineering education as science is currently deemed to be far more important in most programs. The Taguchi Method directly incorporates a number of aspects of robust design. Since only a small number of trials must be investigated to examine a system, it is possible to conduct each trial a number of times to examine the statistical nature of the process. Optimization of one of the Taguchi signal-to-noise functions, rather than the actual response, reinforces the concept that reproducibility is often as important as achieving the optimal response in an industrial setting. The quick determination of the near optimal factor settings via the Taguchi technique makes it possible to examine other aspects of robust design. This can include examination of how non-linear factor effects can be exploited to deal with inherently noisy factors.

Factor Interactions

One of the biggest problems that arises in the Taguchi Method is that of factor interactions. The technique relies upon the additivity of the main factor effects for both its efficiency and computational simplicity. Since there is at least a small amount of factor interaction in most real processes it is necessary to conduct confirming trials that involve the near optimal factor settings to make sure that the optimal settings are found. However, even strong factor interactions are not necessarily fatal to the successful application of the Taguchi technique.

Factor interactions are generally classified as synergistic and antisynergistic as shown in Figure 4. Synergistic interactions are such that the response varies in a consistent manner so that the Taguchi Method finds the optimal factor levels but does not predict the proper response since the interaction violates the additivity rule. Antisynergistic interactions result in inconsistent factor effects which can result in not finding the optimal factor levels.

The basic Taguchi Method cannot handle antisynergistic interactions since they violate the additivity rule. However, it is possible to modify the technique to account for the interactions by using one or more of the columns in the orthogonal array to incorporate a new factor based upon the type of factor interaction that is to be investigated, just as dummy factors can be used to improve error variance analysis. This technique is not as elegant as that used in some of the surface response techniques, but it is simply a modification of a technique that the students already understand rather than a brand new technique.

Randomization

Another major complaint about the Taguchi Method is that lack of randomization can lead to systematic errors. The method does not use randomization so that fewer errors are caused by constantly

410
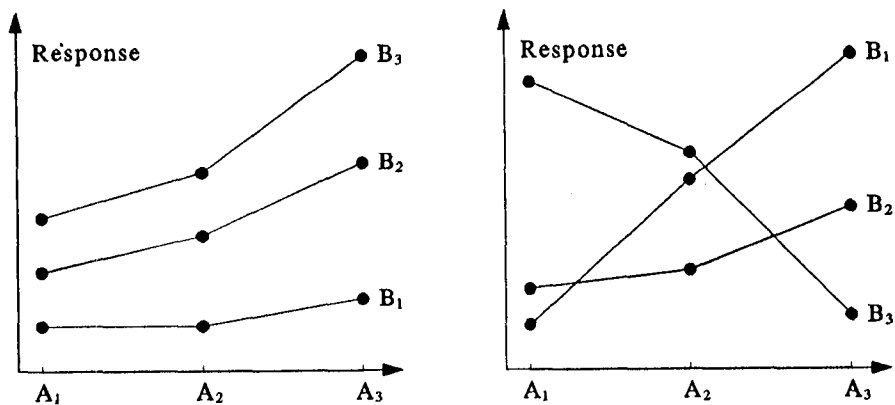
Figure 4 Synergistic (left) and antisynergistic (right) parameter effects for a two parameter system. After Phadke.[2]

setting and resetting the factor levels. The orthogonal arrays used in the Taguchi Method are designed so that the first factor is changed quite infrequently so a difficult to change factor can be associated with it. An example of this type of factor is a process temperature that requires a long time to stabilize. Constantly changing the process temperature will either result in inaccurate temperatures or a very long experimental procedure as the temperature is allowed to equilibrate.

Randomization can be employed in the Taguchi Method, particularly if none of the factors are difficult to change or control. The first type of randomization involves randomly assigning the factor letters and level numbers to the actual factors and levels. This procedure would allow a large series of experiments to be conducted using the same orthogonal array and factor levels without repeating any one experiment, which is very useful in a classroom setting. This type of randomization will not disrupt the mapping from the factor setting to the factor level since the levels can be rearranged for plotting. For example, if randomization yielded $B_1 = 125°C$, $B_2 = 150°C$, and $B_3 = 100°C$, the effects would be plotted in the order B_3, B_1, B_2 to more clearly show the relationships. The second type of randomization involves conducting the trials in a random order. This technique will help eliminate systematic biases due to instrument drift. However, it may cause problems with reproducibility since instrument drift is one of the factors that must be accounted for when developing a stable process.

Limited Number of Arrays

There are only a limited number of arrays that are pairwise orthogonal and suitable for use with the Taguchi Method. Phadke[2] lists 19 different orthogonal arrays involving four (four factors at two levels each) to 81 (40 factors at three levels each) trials. However, many of these involve a large number of factors so they are not particularly suitable to classroom use. Some of the smaller arrays that the author has found useful in an academic setting are listed in Table III. First examination of this table indicates that the possible number of factors and levels is quite limited. However, one or more of the factors can be used as a dummy factor to decrease the number of factors and improve the error analysis in any of the arrays. For example, if the last column of the L'16 array is a dummy, the experiment will examine four factors at four levels each. In addition, two columns can be combined in some of the arrays to yield a column with a larger number of levels. For example, the first and second columns of the L18 array can be combined to create a column with six levels.

411

Table III Nomenclature of Orthogonal Arrays

Name	Factors	Levels	Combinations	Conditions
L4	3	2	8	4
L8	7	2	128	8
L9	4	3	81	9
L12	11	2	2,048	12
L16	15	2	32,768	16
L'16	5	4	1,024	16
L18	6, 1	3, 2	1,458	18
L25	6	5	15,625	25

Examples

The Taguchi Method using an L9 array has been used for the past two years to study the processing of a semi-vitreous ceramic in the Mechanical Engineering Materials Science Laboratory Course at UNM as described elsewhere.[4] The experiment serves as a very good introduction to both designed experiments and ceramics processing. The students are told that the optimal product has both maximum strength and minimum density, which also introduces them to the idea that compromises in product requirements are often necessary. A total of seven different factors have been used during the four semesters so that the same experiment is never done two consecutive semesters. The ranges for the factors are selected so that they all have about the same effect on the response, which prevents the students from simply discarding a factor as unimportant.

During the fall 1992 semester exactly the same variable factors and settings were used as during the spring 1992 semester except that their assignment to the factor labels and levels were rearranged. This resulted in examination of the same factor space using two different L9 array experiments. The results from the two experiments were similar as shown in Figure 5. The differences between the results are primarily due to interactions between the factors that are not accounted for by the Taguchi method.
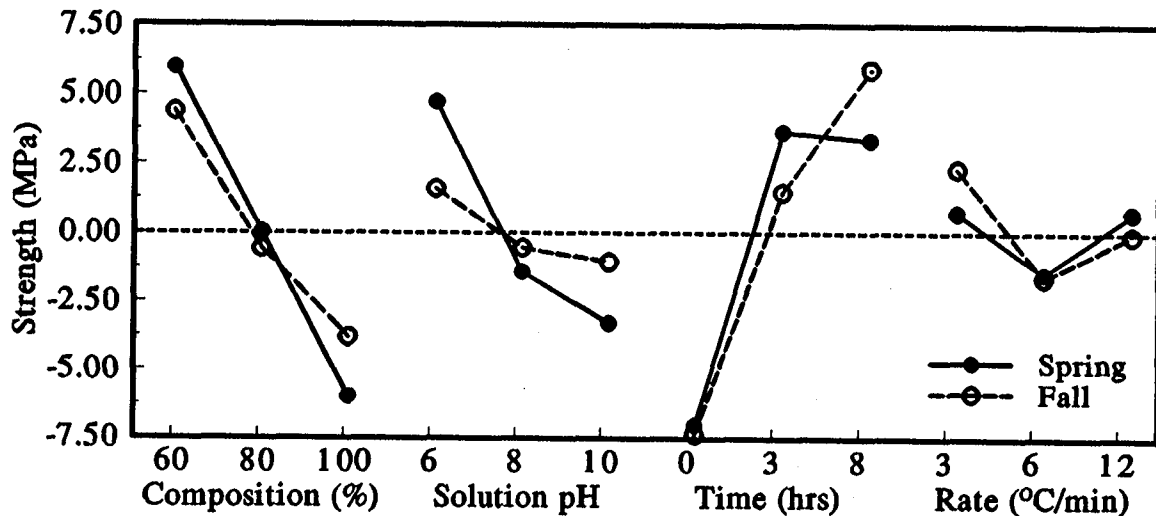
Figure 5 Both the spring and fall 1992 factor effects on the strength of the semivitreous clay bars where the composition is the percent of goldart clay used.

Confirming trials were run during both semesters to find the optimal processing conditions to maximize the strength of the ceramic. The results of these experiments are shown in Table IV where the labels list the semester, and if the trial was predicted, to give the first or second highest strength of the actual maximum. It is seen that the agreement between the measured and predicted values is fairly good particularly when the normal standard deviation of the strengths ($\approx$ 2-3 MPa) is taken into account. In addition, the results were used to extend the factor space during the fall semester to longer times and lower fractions of goldart clay. This resulted in some dramatically higher strengths as shown but the results were much more variable.

Table IV Results of the Confirming Trials

Experimental Conditions				Response (MPa)		η (dB)	
				Measured	Predicted	Measured	Predicted
Sp 1st	60	6	3	3	21.93	26.88	25.57	29.50
Sp 2nd	60	6	8	3	24.24	26.59	27.88	29.00
Sp Max	80	6	2	12	26.42		28.21	
Fa 1st	60	6	8	3	27.73	25.90	28.77	28.81
Fa 2nd	60	6	5¶	3	21.22	24.90	26.43	27.62
Fa Max	45	6	8	3	34.44	N/A	29.92	N/A

A powder metallurgy experiment which also uses an L9 array has recently been developed** and will be alternated with the ceramics experiment. It appears that this experiment will also serve as an excellent introduction to both designed experiments and the sintering of materials. The copper based system used is thermodynamically simpler than the semi-vitreous ceramic system so it will be possible to emphasize the sintering process more in this experiment.

Conclusions and Recommendations

The Taguchi Method of experimental design and analysis is strongly recommended as both an excellent tool to teach fractional factorial experimental design and as a research tool in Materials Science. The simplicity of the technique allows the students to concentrate on the concepts behind fractional factorial experiments and explanation of the experimental results rather than on the experimental design and analysis. The computational simplicity also insures that the students do not have to use complex or proprietary computer codes to design and analyze the results as is necessary with many other fractional factorial experimental designs. The simplicity of the method also makes it possible for the practitioner to use ANOVA to examine the quality of their results and to modify the method to adapt it to their particular application.

The Taguchi Method is not the best experimental design method for all applications. However, it is a very good method that is excellent for screening experimental factors to determine which ones merit further investigation. It suffers from a number of disadvantages such as limited number of experimental arrays, poor handling of factor interactions, and lack of explicit randomization that limit its utility. However, many of the competing fractional factorial experimental design methods suffer from some of the same

---

¶   Not one of the factor levels conducted in the L9 experiment. This effect was interpolated.
**   Described elsewhere in this volume.[5]

limitations or are less efficient or significantly more complex. The ability to use the experimental design system that is best suited to the investigation is a skill that must be taught to today's students. The Taguchi Method is a good start in this process. We are in the process of expanding our use of statistical design of experiments beyond the Taguchi Method to suit a variety of different applications.

References

1   Taguchi, G., Elsayed, E.A., and Hsiang, T.C.: *Quality Engineering in Production Systems,* McGraw-Hill, New York, NY 1989

2   Phadke, M.S.: *Quality Engineering Using Robust Design,* Prentice Hall, Englewood Cliffs, NJ 1989

3   Ross, P.J.: *Taguchi Techniques for Quality Engineering,* McGraw-Hill, New York, NY 1988

4   Weiser, M.W., Lauben, D.N., and Madrid, P.G.: Ceramics Processing: Experimental Design and Optimization, Gardner, J.E., Jacobs, J.A., and Stiegler, J.O., eds.: *National Educators' Workshop: Update 91,* NASA, Washington, DC 1992, pp. 67-95

5   Sheldon, R., and Weiser, M.W.: Powder Metallurgy: Solid and Liquid Phase Sintering of Copper, Craig, D.F. and Jacobs, J.A., eds.: *National Educators' Workshop Update 92,* NASA CP-   , 1993

6   Weiser, M.W., Lauben, D.N., Madrid, P.G., and Fong, K.B.: Ceramic Processing Using Designed Partial Factorial Experiments, to appear in *Ceram. Engr. Sci. Proc.,* Am. Ceram. Soc., Columbus, OH

7   Weiser, M.W. and Fong, K.B., Ceramics Processing Using Designed Fractional Factorial Experiments, to appear in *Am. Ceram. Soc. Bull.,* vol. 72, no 3, 1993

POWDER METALLURGY: SOLID AND LIQUID PHASE SINTERING OF COPPER

Rex Sheldon
and
Martin W. Weiser

Mechanical Engineering Department and
Center for Micro-Engineered Ceramics
University of New Mexico
Albuquerque, New Mexico 87131

Telephone 505-277-2831

Powder Metallurgy: Solid and Liquid Phase Sintering of Copper

Rex Sheldon[†] and Martin W. Weiser[‡]
Mechanical Engineering Department
University of New Mexico, Albuquerque, NM 87131

Abstract

Basic powder metallurgy (P/M) principles and techniques are presented in this laboratory experiment. A copper based system is used since it is relatively easy to work with and is commercially important. In addition to standard solid state sintering, small quantities of low melting metals such as tin, zinc, lead, and aluminum can be added to demonstrate liquid phase sintering and alloy formation. The Taguchi Method of experimental design was used to study the effect of particle size, pressing force, sintering temperature, and sintering time. These parameters can be easily changed to incorporate liquid phase sintering effects and some guidelines for such substitutions are presented. The experiment is typically carried out over a period of three weeks.

Key Words: Powder Metallurgy, Density, Copper, Solid State Sintering, Liquid Phase Sintering, Uniaxial Pressing, Hardness

Prerequisite Knowledge: The student should have some basic background knowledge of diffusion in solids and the microstructure of metals.

Objectives: The experiment demonstrates the fundamentals of powder metallurgy including the effect of many of the possible process variables. These effects are:
- a. effect of consolidation pressure on the density of the green compact,
- b. effect of sintering time on the sintered density,
- c. effect of sintering temperature on the sintered density,
- c. effect of liquid phase additions on densification.

The Taguchi Method of Experimental Design is used to demonstrate a simple, high efficiency experimental scheme. This allows both the experimental response and its reproducibility to be optimized concurrently.

Equipment and Supplies:

1. 8 to 15 mm diameter punch and die for compacting the powders[§]
2. Press capable of exerting enough force to yield a compaction pressure of 800 MPa (63 KN or 14,200 lb$_f$ for a 10 mm punch and die)
3. Programmable furnace capable of 1000°C with an inert atmosphere retort
4. Sieves to fractionate the copper powder. #325, (45 μm), #200 (75 μm), #100 (150 μm), #50 (300 μm) and #30 (600 μm) work quite well.

---

5. Scale capable of measuring up to 20 g with an accuracy of 0.01 g (0.001 preferred).
6. Vernier caliper accurate to 0.1 mm or better.
7. Standard metallographic equipment and supplies for mounting, grinding, and polishing non-ferrous specimens.
8. One kilogram of copper powder.
9. One hundred grams of lead, tin, zinc, or aluminum powders.
10. 100 cm^2 copper foil
11. Cylinder of forming gas (2 to 4% H_2 in N_2 which is non-flammable) and an appropriate regulator.
12. Lubricants and dispersants if desired (stearic acid, metal stearates, light machine oil, carbon powder, ethyl alcohol, etc.).

Introduction and Background

Powder Metallurgy (P/M) is an important production technique for a wide variety of products including inexpensive bronze bushings, W/Co cutting tools, and very expensive TiAl turbine blades. The P/M process is used to create these parts for a number of different reasons, including the ability to create a porous product that can contain a lubricant, a lower cost due to less waste material when creating complex shapes, and difficulty in melting the metal due to either a high melting temperature or incongruent melting. P/M techniques are very similar to the processes used to create many ceramic products since the ceramics frequently have quite high melting temperatures.

The understanding of powder metallurgy has expanded greatly during the past forty years after Kuczynski's pioneering study of the sintering of copper.[1] Not only have P/M techniques undergone a great deal of refinement, but new materials formed by P/M processes have been introduced. Metals that are difficult or impossible to alloy by casting, such as certain superalloys, can be successfully alloyed via P/M.[2] Cermets and cemented carbides, which are ceramics bonded together with a metal, are P/M products. Tool steels and specialty steels which depend on a fine dispersion of a second phase constituent can also be produced by P/M. Filtering mediums, self lubricating bearings, and friction materials depend upon P/M technology to create unique products.

Materials processed via P/M techniques offer several advantages compared to materials cast from the melt. Homogeneity and microstructural control are often superior for P/M processes compared to casting. Energy, time, and material use are frequently more efficient in P/M since parts are produced "near net shape". Scrap reduction and minimal finishing are particularly beneficial if the item is being manufactured from expensive stock or difficult to machine materials. P/M parts can be forged, extruded, heat treated, and machined like cast parts to achieve particular properties, but the operations are normally significantly faster and more economical for the P/M part.

The largest P/M segment by volume is for ferrous alloys, although there are other important materials that incorporate P/M in their processing. Since many of the basic considerations and parameters in P/M are quite similar for different alloys, a good grasp of the basics can be achieved by demonstrations with simple systems. Iron, aluminum, zinc, tin and copper powders, for instance, are relatively cheap, available, safe and easy to use. Insight into the fundamentals of P/M can be gained by using these metals.

Copper is a typical P/M system with wide application.[3] A wide range of physical properties become available through the proper use of P/M technology and copper powders. The list of copper based P/M applications is too extensive to list except for a couple of examples. Copper sintered with iron and steel powders produces a strong, corrosion resistant material with good machining qualities. Copper and tin are

used to produce porous bronze bushings. The pores are then impregnated with a lubricant to create a self lubricating bearing. The biggest advantages of copper based P/M from the standpoint of this experiment are that the processing is quite simple and a number of different alloying elements can be used to produce different products with different properties.

The Powder Metallurgy Process

The powder metallurgy process consists of four primary steps: powder preparation, consolidation, sintering, and finishing. A number of quite sophisticated powder preparation techniques are currently used to manufacture metal powders of very specific chemistry and morphology. However, these are beyond the scope of this experiment so commercial powders will be used. Compaction involves production of a preform from the loose powders by mechanically pressing them at high pressure. Sintering consists of a high temperature heat treatment to allow diffusion so that the particles can fuse together. The final step is finishing of the part by standard metal fabrication techniques to produce the desired final dimensions or surface finish. Limited details of the production, consolidation and sintering steps are given below with further information on all of the steps available in references 4 through 7.

Powdered metals can be produced in a variety of ways. Atomization, electrolysis, hydrometallurgy, solid state reduction and mechanical milling are the most important methods.[4] Each method results in a powder with different characteristics. Cleanliness, range of particle sizes, particle shapes, internal particle porosity, and surface oxides are functions of powder production and have a profound influence on the final product. Consequently, the desired properties of the final product will determine the method of powder production.

Powder consolidation can be done via a number of different techniques. In all cases the goal is to create a preform known as a green compact which has the proper shape, a reasonable level of porosity, and enough mechanical strength so that it can be handled. In all cases the powder is placed in a mold with the proper shape and then pressurized to push the particles closer together and eliminate the porosity. The most common consolidation techniques are uniaxial and isostatic pressing. The mold for uniaxial pressing is a rigid cavity of constant cross section known as the die. The pressure is then applied by a pair of punches which can have either smooth or contoured inner surfaces that just fit into the cavity. Either one or both of the punches can move during the pressing operation. A single action punch and die results when only one punch moves while a double action system involves movement of both punches.

The mold for isostatic pressing is a flexible bag in which the powder is placed. This bag of powder is then compacted by placing it in a chamber and applying the pressure via a fluid such as nitrogen, water, or oil. A lubricant such as a metal stearate can be used to reduce friction between the particles and tool wear in both techniques but this normally results in a loss of "green" strength for the compact. There are advantages and disadvantages to each technique. Uniaxial pressing is inexpensive and fast but it is limited to relatively simple shapes that are no taller than they are wide unless inhomogeneities in the powder packing can be tolerated. Isostatic pressing normally gives very homogeneous parts that can have quite complicated shapes, but it is expensive and slow.

Sintering is a diffusional process that fuses the particles together. The strength of the part is almost always increased dramatically (sometimes by 3 to 5 orders of magnitude) and the porosity of the part is frequently reduced. Sintering can be either a solid state process where none of the components melt or a liquid phase process where small portions of the powder melt. In either case the diffusion is driven by a reduction in the total surface energy of the system, which is normally accomplished by replacement of

solid/vapor surface by grain boundaries. The advantage of liquid phase sintering is that diffusion is normally a couple of orders of magnitude faster in a liquid than it is in the solid. However, there are a number of rules involving the relative melting points and solubilities of the different components along with the wetting behavior of the system that must be followed for the system to sinter well.[8]

In addition to enhancing the diffusion of the system, the liquid phase additive can dramatically enhance the properties of the powder compact after sintering. Solid solution and precipitation strengthening are common phenomena in metallic systems depending upon the solubility of the liquid phase in the solid phase. In cermets such as WC/Co the metallic liquid phase dramatically increases the ductility of the composite. Liquid phases that oxidize easily can leave fine oxide particles behind that both result in precipitation strengthening and help control grain growth. The melting points and the effects of some of the possible liquid phase additives for copper P/M are listed in Table I.

Table I Liquid Phase Additives for Copper P/M

Additive	T_m (°C)	Effects
Zinc	420	brass solid solutions and some intermetallics
Tin	232	bronze intermetallics
Aluminum	660	fine Al_2O_3 particles to control grain growth and intermetallics
Lead	328	lubrication only, very limited solubility and reactivity, toxic
Sn/Pb alloys	183	both long term lubrication and intermetallic strengthening

The sintering rate increases exponentially with temperature for both solid sate and liquid phase since diffusion is thermally activated. However, the rate of grain growth is also thermally activated (normally with a different activation energy) so it will also increase as the temperature increases. This gives rise to larger grains and potentially abnormal grain growth which can trap pores inside the grains. In nearly all P/M systems there is an optimal combination of time and temperature which results in best properties for the part. While theoretical considerations are useful for estimating the optimal time and temperature,[9] the P/M process is quite complicated and empirical techniques are needed to determine the true optimum.

Experimental Design

This experiment uses the Taguchi Method of Experimental Design to examine how a variety of factors affect the measured responses. This technique is used because it is very efficient and quite simple while incorporating the concept that improvements in the reproducibility of a process are often as important as improvements in the response. The largest disadvantages of the Taguchi Method are that randomization is not employed and can introduce systematic errors and that interactions between the parameters are ignored. However, the extreme simplicity more than compensates for these disadvantages, particularly with regard to performing screening experiments and teaching the fundamentals of experimental design.

A Taguchi array experiment involves conducting a number of experimental trials (called trials from here on) that each measure one or more responses for a given experimental condition (a particular combination of factor levels). This experiment is presented using an L9 orthogonal array which investigates the effects of four factors at three levels, each using a total of nine experimental trials rather than the $3^4 = 81$ trials needed for a traditional full factorial experiment. This smaller number of trials allows the different trials to be repeated to obtain information about the reproducibility of the process. Other orthogonal arrays such as the L'16 (16 trials using 5 factors at 4 levels each) and the L4 (4 trials involving 3 factors at 2 levels each) are also quite suitable to investigate the P/M process in either more or less detail respectively. In

any case, it will probably be necessary for the instructor and/or the student to consult additional references on the Taguchi Method. The authors would like to recommend Appendix A of reference 10 as a fairly simple treatment of the topic while reference 11 is much more detailed.

The L9 orthogonal array used in this experiment employs four factors at three levels each as shown in Table II where the factors are listed as A, B, C, and D and the levels are assigned values of 1, 2, and 3. The response or responses that will be measured and optimized will depend upon the nature of the experiment being performed and will always be some form of the mean of the results for all of the repetitions of each trial. One of the best responses to optimize is the Taguchi Signal-to-Noise function, η, which strives to maximize the reproducibility of a property while achieving the "best" value of the property. One of the most common cases is known as the more-is-better criteria where it is desirable to maximize the property. In this case the response to optimize is given by

$$\eta_{MB} = -10 \log_{10} \left(\frac{1}{n} \sum_{i=1}^{n} \frac{1}{y_i^2} \right) \tag{1}$$

where there are n repetitions of the trial each yielding an individual response y_i. A consequence of the formulation of Taguchi signal-to-noise function is that it is always desirable to maximize the value of η.

Table II The L9 Orthogonal Array

Trial	A	B	C	D	Response
1	1	1	1	1	y_1
2	1	2	2	2	y_2
3	1	3	3	3	y_3
4	2	1	2	3	y_4
5	2	2	3	1	y_5
6	2	3	1	2	y_6
7	3	1	3	2	y_7
8	3	2	1	3	y_8
9	3	3	2	1	y_9
Overall					$\bar{y}$

Regardless of whether the actual response, y, or the Taguchi signal-to-noise ratio, η, is to be optimized, the effect of each parameter at each level is found by subtracting the average overall response, $\bar{y}$ or $\bar{\eta}$ respectively, from the average response for the trials where the factor has been set to the level of interest. This is illustrated for the case of factor C at level 3 which is known as effect c_3. Factor C is set to level 3 in trials 3, 5, and 7 so the overall mean response is subtracted from mean response of these three trials as shown in Equation 2.

$$c_3 = \frac{y_3 - y_5 - y_7}{3} - \bar{y} \tag{2}$$

The predicted response for any combination of factor levels can be found by adding the effects of each of the factors at the desired level to the mean response. Selecting the smallest effect for each parameter will predict a minimum response, while selecting the largest effect will attempt to maximize the response. A

more accurate prediction is obtained when only the most significant factor effects are included in this calculation as illustrated in the example at the end of this paper.

In all cases it is necessary to perform one or more confirming trials to determine if the predicted optimal response is really the optimal response. The authors suggest that confirming trials be performed for the best two or three sets of experimental conditions to help insure that minor interactions between the factors do not result in a response that is less than optimal. Major interactions between the factors cannot be handled by the Taguchi Method without modification and will show themselves as predictions of impossible response values (negative strengths for example) and very poor correlation between the predicted and actual responses once the confirming trials are performed.

Experimental Procedure

1. Determine which orthogonal array will be used, which factors will be constants, and which ones will be varied. The factors that the authors have identified along with suggested ranges of values are listed in Table III. Determine the settings for the constant factors and the levels of the variable factors.

Table III Experimental Variables and Potential Values

Copper Particle Size	$45 - 1000~\mu m$
Sintering Time	0 - 12 hrs
Solid State Sintering Temperature	700 - 1050°C
Heating and Cooling Rates	1 - 200°C/min
Liquid Phase Additives	Al, Zn, Sn, Pb
Liquid Phase Fraction	0 - 20 vol% (solids basis)
Liquid Phase Sintering Temperature	$T_m \pm 100$°C
Consolidation Pressure	50 - 850 MPa
Consolidation Time	0 - 60 s
Lubricant	Stearic Acid, Metal Stearates, or Light Oil
Lubricant Fraction	0 - 1 vol% (solids basis)

2. Assign each of the variable factors a letter from those listed for the orthogonal array that is to be used. This can either be done by randomly selecting the letter for each factor or by using A for the most difficult factor to vary and so on. The former approach is favored when there are apt to be systematic errors, but the latter is favored when changing some of the factor levels is difficult or subject to error.

3. Determine the theoretical density of the solids in the green compact for each composition to be tested using the rule-of-mixtures. For example the density of solids in a compact composed of 90 vol% Cu ($\rho = 8.96$ g/cm³) and 10 vol% Zn (7.13 g/cm³) would be $0.9 \times 8.96 + 0.1 \times 7.13 = 8.78$ g/cm³.

4. Determine how much powder is needed for each pellet and then how much powder is needed for each trial based upon the number of repetitions to be performed (5 to 10 are recommended). If a cylindrical punch and die are used, the mass of each pellet will be

$$m_p = \frac{0.60 \, \rho \, \pi \, d^2 h}{4} \tag{3}$$

where ρ is the density of the metal powder in g/cm^3, d is the diameter of the pellet, h is the estimated height of the pellet which should be approximately equal to the pellet diameter, and the green density of the pellet is assumed to be roughly 60% of the theoretical density of the metal. Approximately 10 to 20% should be allowed for waste when the total powder mass is calculated.

5. Sieve the metal powders into the different size fractions desired. This is done by making a stack of sieves ranging from the smallest opening (largest size number) at the bottom to the largest opening at the top. A pan is placed at the bottom of the stack and one or two sieves that are larger than the size of the largest desired sieve are placed on the very top of the stack. The powder is then added to the top of the stack and the stack is shaken and tapped for a period of time to allow the finer particles to reach the bottom of the stack. The exact amount of time required depends upon the powder and the size of the smallest sieves. For metal powders that are larger than 45 μm a couple of minutes should suffice.

    Powders that have been classified by sieving are labeled as +(the smaller sieve) –(the larger sieve) to indicate that they passed through the larger sieve but did not pass through the smaller sieve. A powder sample that passed through a 200 mesh sieve and remained above a 325 mesh sieve would be labeled +325 –200 mesh. This can be stated as +45 –75 μm which yields more information about the actual size of the particle but it is not as precise since the listed size of a sieve is an average with a coefficient of variation of approximately 10%.

6. Mix the different metal powders together and disperse the lubricant around the particles. Dispersion of the lubricant is best accomplished by dissolving it in an appropriate solvent (typically an alcohol), mixing this solution with the metal powder, and drying the mixture.

7. Make tubes with one closed end out of copper foil to contain the powder if any low consolidation pressures (<300 MPa) are to be used. These tubes are best made by wrapping a rectangle of copper foil that is 5 × diameter by 4 × height around the end of a mandrel that is slightly smaller ($\approx$ 10 × the foil thickness) than the punch and then carefully folding the end of the tube over to close it. Do not be tempted to substitute aluminum foil for the copper foil as this will result in liquid phase sintering of the outer surface and constrained sintering of the interior of the pellet and will give erroneous results as the authors found out experimentally.

8. Place the bottom punch in the die and insert the copper tube with the open end up if it is being used. Use the mandrel to push the tube out against the inside of the die, pour in the proper mass of powder, and use a pointed rod to fold over the top of the tube. Insert the upper punch, place the punch and die set on the press, and load it to the appropriate force based upon the desired pressure and die size. Holding the pressure for roughly 15 seconds allows the powder particles to rearrange and results in more uniform pellets, but this is a factor that can be varied.

9. Eject the pellet from the punch and die by placing it on either a pair of blocks or a short piece of pipe and loading it to push the bottom punch and the pellet from the die. After the pellet has been

ejected the interior of the die and exterior of the punches must be cleaned to prevent the build up of film from the powder being pressed and will eventually result in seizure of the punch in the die.

10. Measure the green density of the pellets by either measuring the mass and outside dimensions of the pellets with vernier calipers or via Archimedes' method[12] if the copper tubes were not used. Archimedes' method is slightly more accurate but slower and can result in the pellets falling apart, particularly if a lubricant or lower consolidation pressures were used.

11. Fire the pellets in an inert atmosphere retort with a small flow of forming gas (2 - 4% H_2 in N_2). Heating and cooling rates of roughly 5 to 10°C/min can be maintained by most systems and result in experiments requiring a reasonable length of time. Rates of greater than 50°C/min almost always involve moving the pellets in and out of a preheated furnace which is slightly more difficult as copper will oxidize rather badly at temperatures above 400°C in air.

12. Measure the fired density of the pellets as in step #8. Archimedes' method is facilitated by grinding off at least a portion of the copper containment tube if it was used.

13. Grind off one end of the pellet to expose a surface that is more representative of the bulk of the pellet rather than the as fired surface of the pellet. This is particularly important if the pellets were encapsulated in copper foil.

14. Measure the hardness of the fired pellets to get an idea of their strength. The Rockwell A scale test is the best for this application since the indentor is big enough to measure the bulk hardness rather than the local hardness which depends upon whether the material under the indentor is in copper, alloy, alloying agent (Al, Zn, Sn, or Pb), or void. In addition, the load is low enough to avoid crushing the pellet. Three to ten measurements should be taken on each pellet to obtain a representative value. Measurement of the Vickers or Knoop hardness can be done to determine the relative hardness of the different phases that are present.

15. Mount, grind, and polish one of the ends of the pellet to obtain a surface that is representative of the bulk of the pellet. Mount the pellet with the ground end exposed in epoxy via vacuum impregnation to fill the pores with epoxy. The sample is then fine ground and polished using light pressure and adequate lubrication to avoid smearing the soft metal. Ultrasonic cleaning between the grinding and polishing steps helps to remove metal that has been smeared and better reveals the microstructure.

16. Calculate the factor effects from the responses for the different trials. The authors strongly suggest computation of the effects for both the actual response and the appropriate Taguchi signal-to-noise function to allow comparison of the effect of the different factors on these related responses.

17. Determine the combination of factors that results in the optimal response or responses and the second and third best responses. Remember that the Taguchi signal-to-noise function should always be maximized.

18. If the predicted optimal combinations of factors were not one of the initial trials (they rarely are) perform the confirming trials corresponding to these experimental conditions.

19. Compare the results for the confirming trials to the predicted results. If the values are fairly close the system can be assumed to abide by the additivity constraint impose by the Taguchi method. If

424

the results do not agree, there are probably strong factor interactions and further investigation will be necessary to determine the true optimal combination of factors. However, these results will be very useful in designing the additional experiments necessary to find the true optimum.

Preliminary Experimental Results

Mr. Rex Sheldon developed this experiment and performed it using an L9 orthogonal array during the fall 1991 semester. The factors that he varied and his experimental results are presented below to illustrate the type of results that might be obtained and a few aspects of the Taguchi analysis. It must be pointed out that the use of different variable factors and/or different factor levels may yield dramatically different results. This has the advantage of providing a different experiment each academic term so that a standard laboratory report cannot be developed but it can present some problems to the instructor who must explain results that occasionally make little or no sense, particularly if strong factor interactions occur.

The factors and the levels used in this version of the experiment are presented in Table IV where the four variable factors are labeled A, B, C, and D. The raw experimental results are presented in Table V while the Taguchi analysis is presented in Table VI and graphed in Figure 1. Only the density is presented in Figure 1 since the η_{MB} effects are very similar. It is seen that the finest particles densify the best as predicted by theory and that higher compaction pressures result in higher densities as predicted. Heat treating at 850°C gives the best densification, which is probably a result of the competition between densification and grain growth. Maximum densification after just one hour heat treatment is somewhat surprising since longer heat treatment normally results in better densification at these moderate temperatures.[5] This effect may be the result of factor interactions that will have to be investigated in more detail.

Table IV Experimental Factors and Levels

A - Particle Size (μm)	25 - 74, 149 - 250, 600 - 833
B - Consolidation Pressure (MPa)	113, 226, 252
C - Sintering Temperature (°C)	750, 850, 950
D - Sintering Time (hrs)	1, 2, 4
Liquid Phase Additive	None
Lubricant	0.1 vol% light machine oil
Consolidation Time (s)	15

Table V Experimental Data for the Fired Density of the Copper Compacts

	Levels				Replications						Mean	η_{MB}
Trial	A	B	C	D	1	2	3	4	5	6	(g/cm³)	(dB)
1	1	1	1	1	6.919	6.882	6.862	6.971	6.919		6.911	16.790
2	1	2	2	2	7.564	7.589	7.630	7.556	7.550	7.606	7.583	17.596
3	1	3	3	3	8.410	8.385	8.375	8.347	8.318	8.123	8.326	18.407
4	2	1	2	3	6.116	6.120	6.070	6.131	6.085	6.276	6.133	15.752
5	2	2	3	1	7.186	7.079	7.082	7.125	7.083	7.223	7.130	17.061
6	2	3	1	2	7.541	7.445	7.385	7.512	7.364		7.449	17.441
7	3	1	3	2	5.606	5.977	5.924	5.801	5.883	6.231	5.904	15.409
8	3	2	1	3	7.374	7.031	7.075	7.252	7.168		7.180	17.119
9	3	3	2	1	8.213	8.150	8.027	7.986	8.071	8.022	8.078	18.145
Overall Means											7.188	17.080

Table VI Taguchi Analysis of the Fired Density of the Copper Compacts

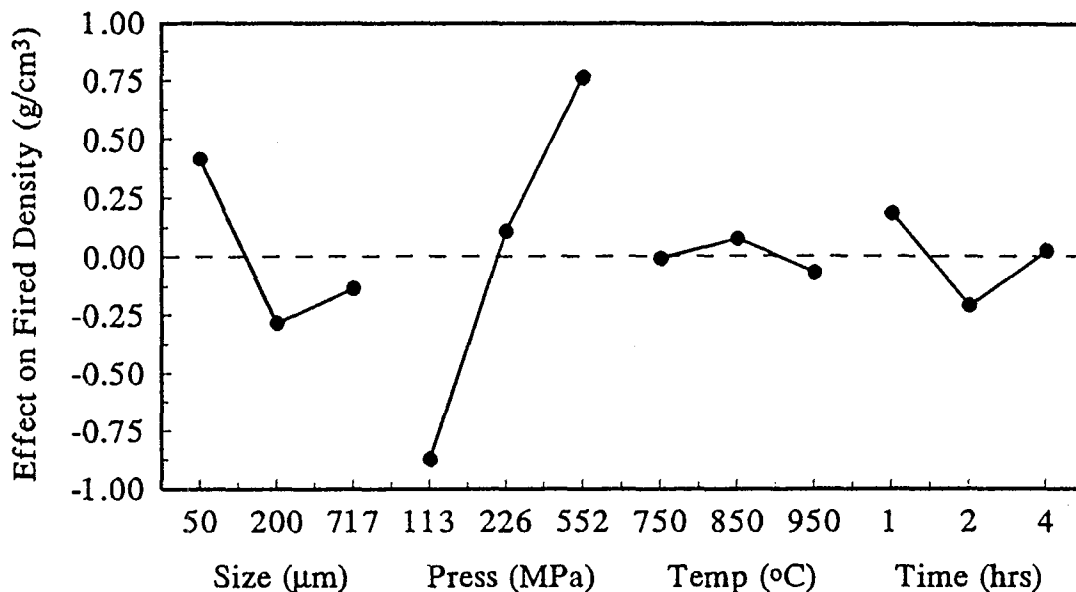| Factor	Fired Density (g/cm³)			η_{MB} (dB)		
	1	2	3	1	2	3
A	0.418	-0.284	-0.134	0.518	-0.329	-0.189
B	-0.872	0.109	0.763	-1.096	0.178	0.918
C	-0.008	0.076	-0.068	0.037	0.084	-0.121
D	0.185	-0.210	0.025	0.252	-0.264	0.013

426

Figure 1 The factor effects on the fired density of copper powder.

Examination of the data in Table VI and Figure 1 shows that the consolidation pressure and particle size are the most significant factors in this experiment. The relative significance of the factors is a function of the range of levels used for each factor so the relative significance can be changed by changing the range of levels. The maximum density and value of η_{MB} were predicted based upon this data using the overall mean and the maximum effect for factors A and B. The maximum effects for factors C and D were not used in this prediction even though these factors will be set to their best level for the confirming trial. Experimental condition $a_1b_3c_2d_1$ was predicted to give the largest values of both the density (8.369 g/cm³) and η_{MB} (18.516 dB).

This optimal experimental condition had not been investigated as one of the original nine trials so a confirming trial was required. Unfortunately, this trial was not performed due to time constraints. However, a series of three experiments examining the density as a function of particle size were performed. The results for these experimental conditions and the predicted density for each are presented in Table VII. It is seen that the predicted and experimental densities do not directly correspond. However, the lowest experimental and predicted densities both occur for condition $a_2b_3c_3d_3$ which is promising. This is a result of the moderate sized particles neither packing well in the green state due to their small size, or sintering well due to their large size.

Table VII Predicted and Experimental Density as a Function of Particle Size

Condition	Particle Size (μm)	Predicted Density (g/cm³)	Experimental Density (g/cm³)
$a_1b_3c_3d_3$	25 - 74	8.369	7.39
$a_2b_3c_3d_3$	149 - 250	7.667	7.27
$a_3b_3c_3d_3$	600 - 833	7.817	7.91

Conclusions

An experiment which explores many of the issues involved in powder metallurgy (P/M) has been presented. It utilizes the Taguchi Method of Experimental Design to allow both experimental repetition and a larger number of variables to be explored at one time than is possible using traditional full factorial experiments. The experimental results do not directly follow from theoretical considerations, which points out the complexity of the P/M process. Information on possible liquid phase additions to the copper system used is also included since liquid phase sintering is a very important issue in P/M.

References

1   Kuczynski, G.C.; Self Diffusion in Sintering of Metallic Particles, *Met. Trans.,* vol. 185, 1949, pp. 169-78

2   Lherbier, L.W. and Kent, W.B.; P/M Superalloys: Technical and Economic Considerations, *Int. J. Powd. Metall.,* vol. 26, no. 2, 1990, pp. 131-37

3   Everhart, J.L.: Copper and Copper Alloy Powder Metallurgy Properties and Applications, Technical Report: Copper/Brass/Bronze, Copper Development Assn. Inc., NY

4   Bradbury, S., ed.: *Sourcebook On Powder Metallurgy,* American Society for Metals, 1979

5   Hausner, H.H.: *Handbook of Powder Metallurgy,* Chemical Publishing Co., New York, NY, 1973

6   Klar, E.: *Powder Metallurgy - Applications, Advantages and Limitations,* American Society for Metals, 1983

7   Yarton, D. and Argyle, M.: *A Practical Course in Powder Metallurgy,* Cassel & Company, Ltd., London, 1962

8   German, R.M.: *Liquid Phase Sintering,* Plenum Press, New York, NY, 1985

9   Ashby, M.F.: A First Report on Sintering Diagrams, *Acta Metal.,* vol. 22, 1974, pp. 275-89

10   Weiser, M.W., Lauben, D.N., and Madrid, P.G.: Ceramics Processing: Experimental Design and Optimization, Gardner, J.E., Jacobs, J.A., and Stiegler, J.O., eds.: *National Educators' Workshop: Update 91,* NASA, Washington, DC 1992, pp. 67-95

11   Phadke, M.S.: *Quality Engineering Using Robust Design,* Prentice Hall, Englewood Cliffs, NJ 1989

12   Jordan, G.W.: Adapting Archimedes' Method for Determining Densities and Porosities of Small Ceramic Samples, Harris, J.S. and Jacobs, J.A., eds: *National Educators' Workshop: Update 90,* NIST, Washington, DC 1991, pp 175-82

Appendix Punch and Die

The design of the simple single acting punch and die set used in the Powder Metallurgy Experiment is presented here. This punch and die set is designed to be inexpensive and easily refurbished while maintaining tight tolerances using hardened steel for the wear surfaces. This is accomplished by making both top and bottom punches from drill rod and the die liner from a drill bushing while the support block and cap are machined from a medium carbon steel such as AISI 1040. The punch and die set are designed to yield a pellet that is nearly 1 cm in diameter. However, the dimensions can be changed to produce sets covering a wide range of pellet diameters.

There are five parts used to make the punch and die set that are described below. It is strongly recommended that the drill rod and drill bushing be obtained before the rest of the parts are machined so that the dimensions can be modified to account for different sized parts. In addition, the drill rod and bushing must be stored in a dry environment such as in a desiccator since they corrode quite easily.
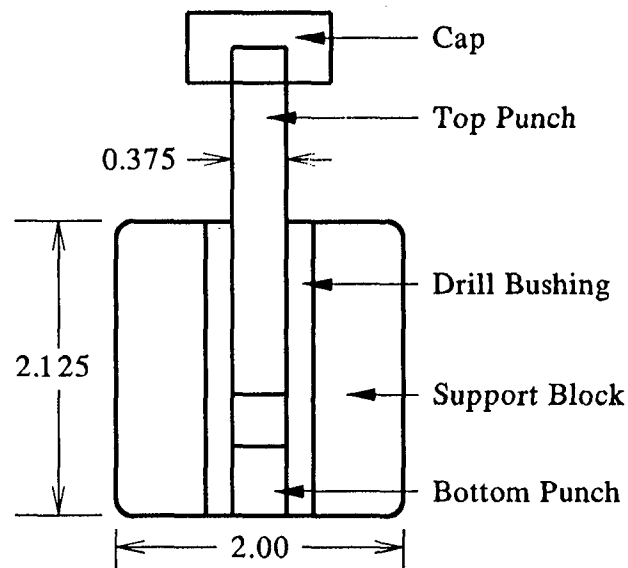

Figure A.1 The punch and die described in this Appendix and used in the experiment.

1. **Top Punch** 0.375" diameter × 2.5" long polished drill rod with both ends polished perpendicular to the axis of rotation. In addition, a flat should be ground on one end so that the cap can be affixed with a set screw.

2. **Bottom Punch** 0.375" diameter × 0.5" long polished drill rod with both ends polished perpendicular to the axis of rotation.

3. **Die Liner** 0.375" ID drill bushing (ours is 2.125" long) which is made from hardened steel with a polished interior surface. It is important that the drill bushing have a smooth interior rather than a stepped interior which is used to assist in chip clearance during drilling.

4. **Support Block** 2.0" diameter × 2.125" long low to medium carbon steel block. This should have a hole bored along its axis of rotation to press fit the drill bushing. Our drill bushing has an OD of

0.751" so the hole was bored 0.750". The precise amount of interference depends upon the diameter and can be found in most machining handbooks.

5. **Cap** 1.0" diameter × 0.5" long medium carbon steel with a 0.375" diameter × 0.25" deep hole in one face and a set screw (not shown in the figure) into this hole from the side. The cap should be hardened to prevent deformation by the upper punch at higher loads. The cap should be machined in an annealed or normalized state including chasing the threads for the set screw. The cap can then be hardened by heat treating at $\approx 900°C$ (orange-red) and quenching in oil. The cap can be made from any scrap of steel that can be hardened with the heat treatment temperature depending upon the material.

The punch and die must be kept clean to prevent contamination and galling even though they are made of hardened steel. Galling can be a major problem when hard powders such as ceramics are being pressed. One of the greatest advantages of the method of punch and die construction presented here is that it is relatively simple to replace the punches and the die liner when they become worn or galled. Replacement of the die liner is accomplished by pressing the old liner out of the support block and pressing in a new liner. Since the liners only cost a few dollars each this allows replacement when wear makes the punch and die difficult to use rather than having to try to get a few more pellets from the system. However, with care and cleaning the punch and die should last quite some time. Ours has been used to press in excess of 1000 pellets including many from hard ceramics.

HIGH THERMAL CONDUCTIVITY OF DIAMOND

Patrick M. Stephan

Business Development Manager
Norton Diamond Film
Goddard Road
Northboro, Massachusetts 01532-1545

Telephone 508-351-7600

HIGH THERMAL CONDUCTIVITY OF DIAMOND: DEMONSTRATION AND COMPARATIVE ANALYSIS

Patrick M. Stephan
Norton Diamond Film
Northborough, Massachusetts

KEY WORDS: diamond, copper, thermal conductivity, thermal diffusivity

PREREQUISITE KNOWLEDGE: The student should understand the principles of heat flow and thermal conductivity of materials, either previously learned or learned concurrently with the experiments.

OBJECTIVES: To demonstrate the high rate of heat flow from a synthetic diamond coupon and to compare it to a commonly used thermal conductor, such as copper. The principles of heat transfer by conduction and convection may also be demonstrated.

EQUIPMENT AND SUPPLIES: (1) Coupons of synthetic (chemical vapor deposited, or CVD) diamond and pure copper, approximately 12-25 mm long, 12 mm wide and 0.3-0.5 mm thick; (2) Voltmeter with digital readout and data collection and storage capability; (3) Low thermal input cable with bare wires on one end and voltmeter converter connection; (4) Two Type T thermocouples (copper-constantan) with 0.005 in. or 0.010 in. diameter, 12 in. long wires (apply teflon insulation to bare wires); (5) Temperature conversion table for Type T thermocouples; (6) Silver epoxy (having high thermal conductivity) for attaching thermocouples to coupons; (7) Beaker or cup of icewater; (8) Stand with clip to hold coupons during experiment; (9) Regular and two-cycle semi-log graph paper.

PROCEDURE: Some preparation is required prior to conducting the experiments. The thermocouples must be firmly attached to the diamond and copper coupons using the silver epoxy. The tip of the thermocouple should be placed against the coupon surface and should be 3 - 5 mm from either end of the coupon. The beaker of icewater should be prepared and its temperature should be stabilized.

The apparatus for the experiments may be arranged as shown in Figure 1. Note that the reference thermocouple junction must be immersed in the icewater. The copper thermocouple wires must be attached to the copper leads from the voltmeter cable and the reference thermocouple must be connected to achieve the correct polarity (this will be obvious from the voltmeter readout).
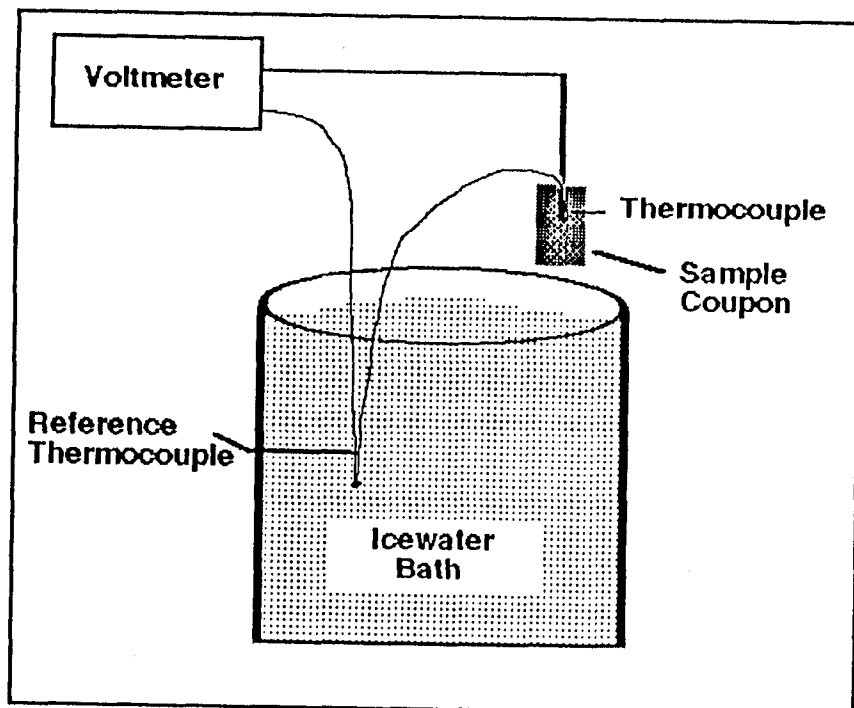

Figure 1. Experiment Setup

The sample coupon is held in a stand with an arm having vertical movement capability. The coupon should not be held above the beaker of icewater prior to data collection. The voltmeter should be set up for the diamond experiment to take data at 0.1 second intervals for at least 30 seconds after immersion of the coupon into the icewater. For copper, data may be collected for 60 seconds at 0.2 second intervals.

When the voltmeter is set up and ready to trigger for data collection, the sample coupon is rapidly positioned for immersion of one end, allowing a distance of 5-15 mm between the water and the thermocouple tip when immersed. The voltmeter is triggered for data collection, allowing no more than two seconds before the coupon is immersed 2-5 mm into the water. At the end of the data collection period, the sample is removed from the water and the data can be retrieved. The experiment can be enhanced for the students if they can

"feel" the coupon before and after the experiment and watch the digital readout change values during and after the experiment.

Data can be retrieved manually or digitally, if convenient. Data for the diamond and copper experiments may appear as shown in Figure 2 when plotted on regular graph paper or as in Figure 3, when plotted on two-cycle semi-log paper.
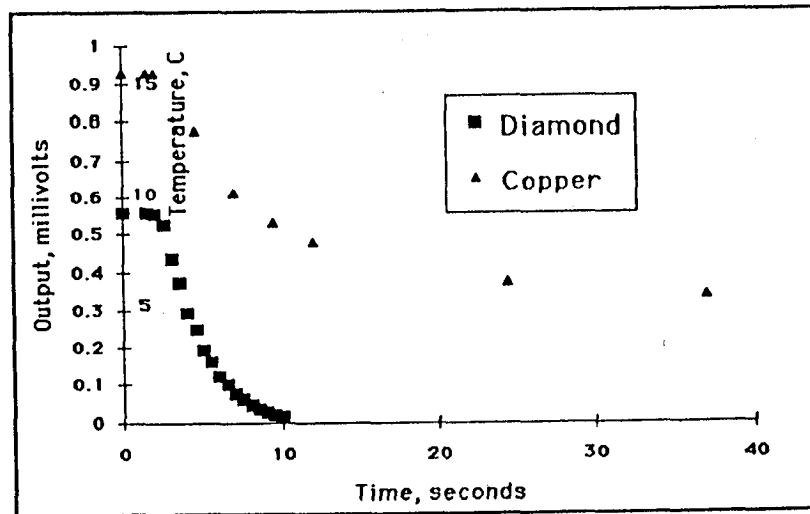

Figure 2. Thermocouple Output Versus Time for Sample Coupons Immersed in Icewater
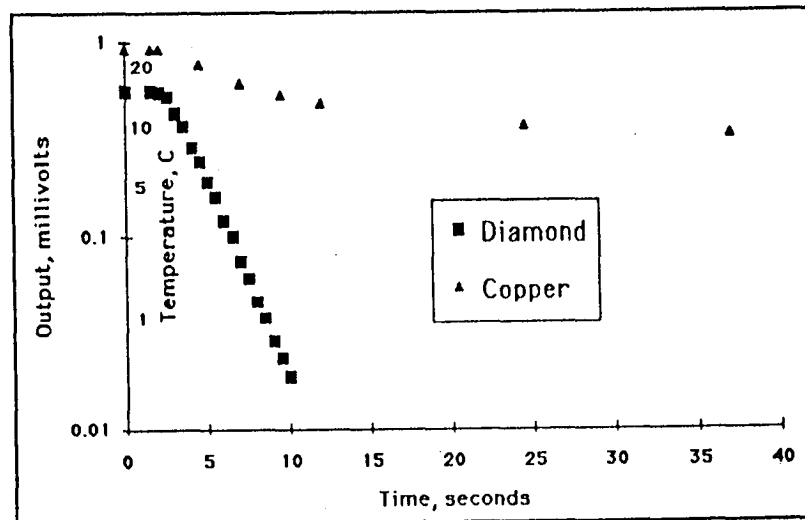

Figure 3. Thermocouple Output Versus Time for Sample Coupons Immersed in Icewater

This first experiment (diamond and copper coupons) demonstrates heat flow by conduction[1] according to the second law of thermodynamics and Fourier's simplified law of conduction:

$$q = kA \ (T_2 - T_1)/L \qquad\qquad (1)$$

Where q = heat transfer rate (in J sec^{-1})
k = thermal conductivity (in Watts cm^{-1} K^{-1})
A = cross-sectional area (in cm^2)
T = temperature (in degrees K)
L = path length of heat flow (in cm)

This equation assumes a steady-state condition where the material is surrounded by a perfect insulator except at two faces. Temperature T_2 is higher than T_1 at different locations along the heat flow path due to a thermal gradient. Since this is a steady state condition, there is no external thermal input to the material and there is no internal source of energy. It is also assumed that the material is isotropic, although the CVD diamond is anisotropic due to the directional nature of crystal growth during deposition.

Other simple experiments may be conducted to demonstrate the principles of heat transfer. Students should note their observations while conducting the following experiments.

Repeat the first experiment, while decreasing by one-half the distance from the water to the thermocouple tip. Plot the graphs and compare them to the graphs from the first experiment. Place an end of the diamond sample into the icewater and move the sample up and down in the water while observing the millivolt readings on the voltmeter. Data collection is not necessary.

Place a finger at various locations on the sample and notice the change and rate of change of temperature in the coupon, as determined from the voltmeter readings.

Convection of heat may be illustrated by simply blowing warm air (or breathing) onto the diamond coupon and observing the voltmeter readings. Also, by placing the diamond sample immediately above, but not touching the icewater bath, a change in temperature of the diamond may be observed due to convection.

DATA ANALYSIS: The data plots shown in Figures 2 and 3 indicate a substantial difference in the rate of temperature change for the

diamond coupon compared to that for a copper coupon of nearly the same size and with the same thermocouple location relative to the ice bath. One might assume that this observation is due to a fundamental difference in thermal properties for the two materials. In fact, equation (1) shows the relationship of thermal conductivity to heat flow and temperature gradient. While it is not the intent of this experiment to calculate the value of thermal conductivity for the diamond, based on the data collected, it is mathematically possible to do so from the data generated in this experiment.

From the literature and in-house measurements [2,3], Table 1 can be constructed for the thermal properties of diamond and copper. Thermal conductivity is often derived from thermal diffusivity data measured by laser flash techniques. Thermal conductivity is related to thermal diffusivity by the following equation:

$$\alpha = k/(\rho\, C_p) \qquad\qquad (2)$$

where

α = thermal diffusivity
k = thermal conductivity
ρ = specific gravity
C_p = specific heat

Table 1. Thermal Properties of Diamond and Copper

Material	Specific Heat $J\,g^{-1}K^{-1}$	Bulk Density $g\,cm^{-3}$	Thermal Diffusivity $cm^2\,sec^{-1}$	Thermal Conductivity $W\,cm^{-1}K^{-1}$
CVD Diamond	0.50	3.51	5.70	10.00
Pure Copper	0.38	8.92	1.10	3.88

The slope of the data curve for diamond in Figure 3 is nearly a straight line, indicating that the rate of temperature change is fairly constant according to an exponential equation. The slope for the copper data is not constant, perhaps indicating that factors such as convection of heat around the copper was significant compared to the the heat loss to the ice bath through conduction. Also note that the temperature registered by the thermocouple attached to the diamond approached the temperature of the icewater, while the asymptotic temperature for the

copper was nearly 5 degrees higher. This illustrates the rapid thermal transfer and "heat spreading" capability of diamond compared to another material more commonly used for heat transfer engineering solutions.

SAMPLE DATA SHEETS: In the case of manual data retrieval from the voltmeter, data sheets can be arranged with headings for data point number, seconds elapsed, millivolt readings and corresponding temperature (read from the conversion chart). The graphs are self-evident, being plots of millivolt readings versus time. It might be noted that data does not need to be written on the sheets for every data point in the register. Sufficient data is taken to plot a smooth curve by hand or computer. Programs such as Lotus 123 or Excel can be used to organize and plot data.

INSTRUCTOR NOTES: This experiment is simple enough to demonstrate the principles of heat transfer and thermal conductivity for materials having reasonably high thermal conductivity values. It should be obvious that the experiment would yield practically no data for materials having much lower thermal conductivity. Using another common material for the experiment, such as a glass microscope slide, would further illustrate the significant difference in thermal conductivity among engineering materials.

Many textbook cases[1,3] analyze the case of heat transfer or thermal conductivity for flat planes or slabs of materials through the thickness, rather than along a plane perpendicular to the thickness plane as considered in these experiments, although the approach and solutions are similar. Many different methods are used to measure thermal conductivity (or diffusivity) for materials having a wide range of thermal characteristics. Anisotropic materials, such as CVD diamond, are difficult to measure with consistency by different methods.

Touching the samples during the experiments and observing the sensitivity of the diamond to slight temperature changes is an important part of the experiment. While natural diamond is prohibitively expensive in large sizes, high purity synthetic diamond made by chemical vapor deposition having thermal, mechanical and optical properties similar to natural diamond is available in sizes up to 10 cm diameter and up to 2 mm thick. This is expected to revolutionize many industries, particularly the electronics industry, where thermal

438

management is critical to advancement of computing systems operating at higher power levels in smaller packages. A working knowledge of thermal characteristics of materials is used by many scientific and engineering disciplines, as well in everyday life!

REFERENCES:

(1) Sucec, J., *Heat Transfer*, Wm. C. Brown publishers, Dubuque, Iowa, 1985

(2) Weast, R.C., ed., *CRC Handbook of Chemistry and Physics*, CRC Press, Boca Raton, Florida, 1988

(3) Lu, G. and Swann, W.T., Measurement of Thermal Diffusivity of Polycrystalline Diamond Film By the Converging Thermal Wave Technique, Applied Physics Letters, 59 (13), Sept. 23, 1991, pp 1556-1558

SOURCES OF SUPPLY:

The diamond wafers were made by a DC Arc Jet Plasma CVD process by Norton Diamond Film in Northboro, Massachusetts.

The digital voltmeter (model 182) and cable used in these experiments were made by Keithley Instruments of Cleveland, Ohio. The thermocouples and wire insulation used were made by Omega Engineering of Stamford, Connecticut. The silver epoxy (DY 325) was made by Zymet in East Hanover, New Jersey.

The other materials are commonly available from supply houses.

TEMPERATURE-DEPENDENT ELECTRICAL CONDUCTIVITY OF SODA-LIME GLASS

L. Roy Bunnell

Battelle
Pacific Northwest Laboratories
P. O. Box 999 MSIN P8-44
Richland, Washington 99352

and

T. H. Vertrees

Kennewick High School
Kennewick, Washington

TEMPERATURE-DEPENDENT ELECTRICAL CONDUCTIVITY OF SODA-LIME GLASS

L. Roy Bunnell
Pacific Northwest Laboratory,[1] Richland, WA
T. H. Vertrees
Kennewick High School, Kennewick, WA

KEY WORDS: glass, ceramics, silicon carbide, electrical conductivity

PREREQUISITE KNOWLEDGE: This material is suitable as a demonstration for typical students of chemistry, physics or materials science at the high school level or above. Additional depth could be provided by comparisons of temperature-conductivity behavior with typical metals and other ceramics, or by using a DC power supply to observe polarization effects as described below.

OBJECTIVE: To demonstrate the difference between the electrical conductivity of metals and ceramics.

EQUIPMENT AND SUPPLIES: Listed below are the materials required to conduct the project.

- strips of ordinary window glass, either single or double strength, approx. 1 x 5 cm
- 10 to 12-gauge copper wire
- 75- or 100-watt light bulb
- socket mounted on wooden block
- wood screws to mount contact wires
- electrical cord and plug
- propane torch to heat glass

PROCEDURE: Begin by reviewing the principles of current conduction through water when ions are present. Next, discuss the difference between electrical conduction in a metal (free or delocalized electrons) and a glass or ceramic (in glass, ions; in other ceramics, either ions or electrons). Figure 1 or its equivalent should be used to clarify the great difference in the temperature dependence of electrical resistivity (the reciprocal of electrical conductivity) of metals and ceramics, resulting from these different
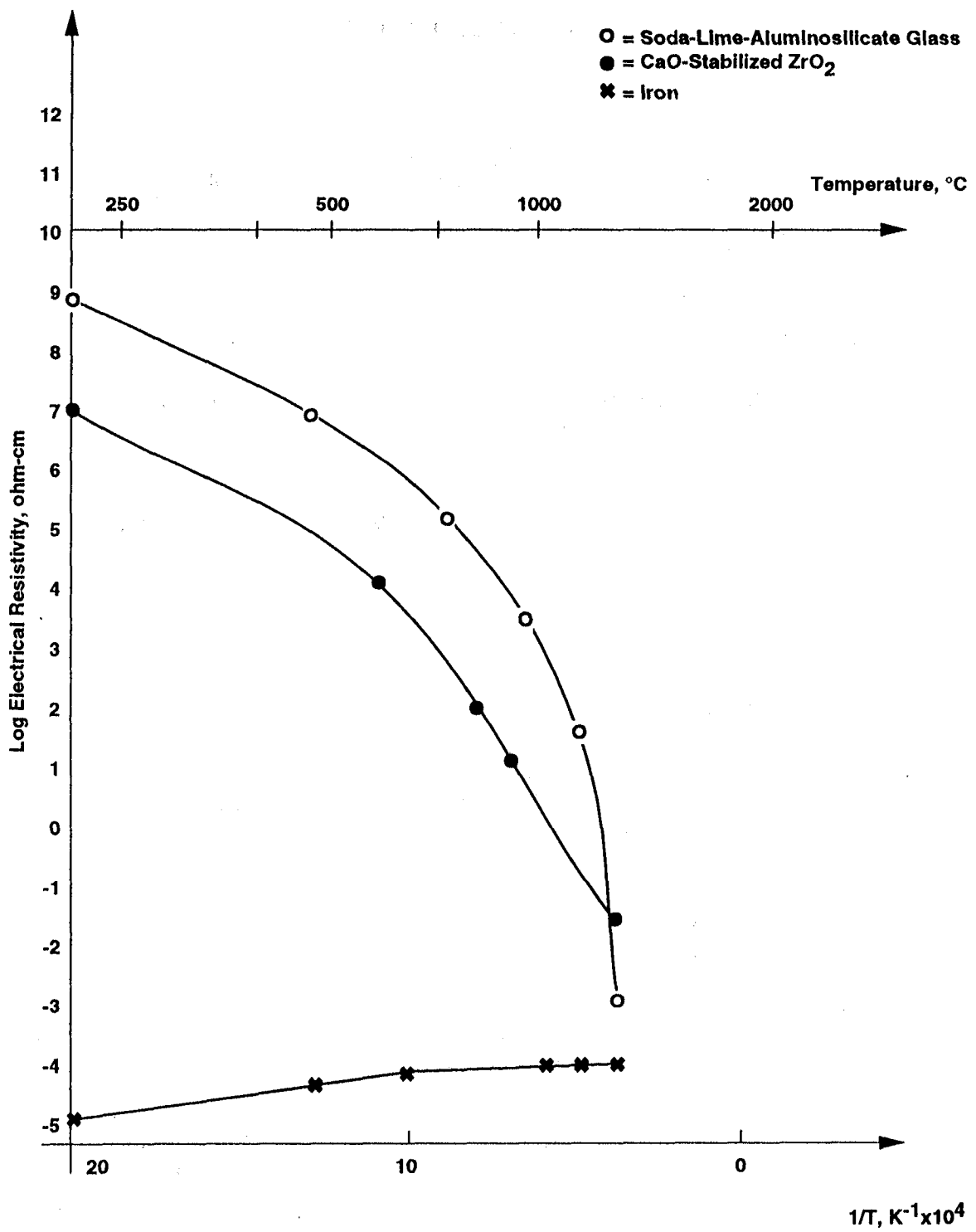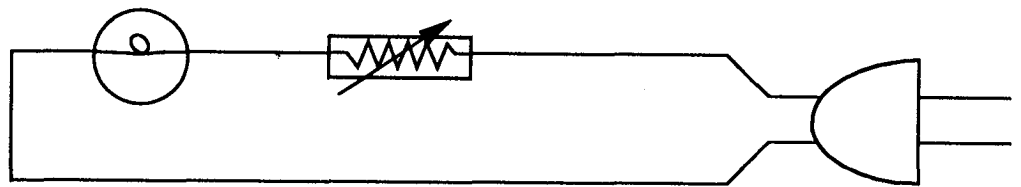

FIGURE 1.

mechanisms. Note the log scale on the resistivity axis, necessary to show the large change in the electrical resistivity of the glass or zirconium dioxide ceramic. The electrical resistivity of the metal increases by a factor of about 13 over the temperature range, although it is not obvious because of the log axis. This increase is caused when electrons are impeded by vibrating iron atoms; these vibrations increase with temperature. The current carriers present in ceramic materials are bonded too strongly to conduct much electricity at low temperature, but at higher energy (temperature) they become increasingly mobile and able to carry more current.

The instructor or students should build the simple apparatus shown in Figure 2. The light bulb, which is in the series circuit with the specimen, provides a visual indication that the resistance of the specimen has dropped enough that the current passing through the bulb filament is about 1 ampere. The bulb also provides a current limiter.

Insert the glass specimen into the wire contacts as shown in Figure 2, so that 1 to 2 cm of glass is between the contacts. Plug the tester into a 110-V outlet, and observe that the light bulb does not glow. Depending on the students' background, it may be useful to insert an AC ammeter into the circuit to provide another indication of current flow. The current through the light bulb is very low, because most of the voltage drop is across the glass specimen. Next, the instructor ignites the torch and carefully heats the glass, keeping the flame moving to avoid breaking the glass by thermal shock. The entire length of glass between the contacts should be heated, especially the contact areas. At about the time the glass begins to glow, the bulb will light. Increased heating will brighten the bulb, indicating that the glass is a better conductor as the temperature increases. If torch heating is discontinued, the bulb will continue to glow for a few minutes, indicating that the glass is being heated to some extent by its own electrical resistance to the current passing through it. The glass will finally cool to the point that it will no longer conduct sufficiently to light the bulb. As the glass cools, it may be possible to observe what appear to be tiny sparks inside the glass; these can be quite beautiful and are probably caused by plasma discharges across bubbles or cracks in the glass.

Ordinary window glass is a "soft" glass that contains a relatively large percentage of ions, such as sodium, that conduct current when the glass is heated. Other glasses have different temperature dependence of electrical conductivity; a borosilicate glass such as Pyrex, for instance, may be difficult to heat sufficiently to light the bulb. Fused silica contains no added fluxing agents, and so is a thousand times less conductive at 1000 Kelvins than the soda-lime aluminosilicate glass shown in Figure 1.

The temperature dependence of electrical conductivity in other ceramics can be demonstrated using the same apparatus as for the glass. A 0.3-cm rod

Circuit Schematic
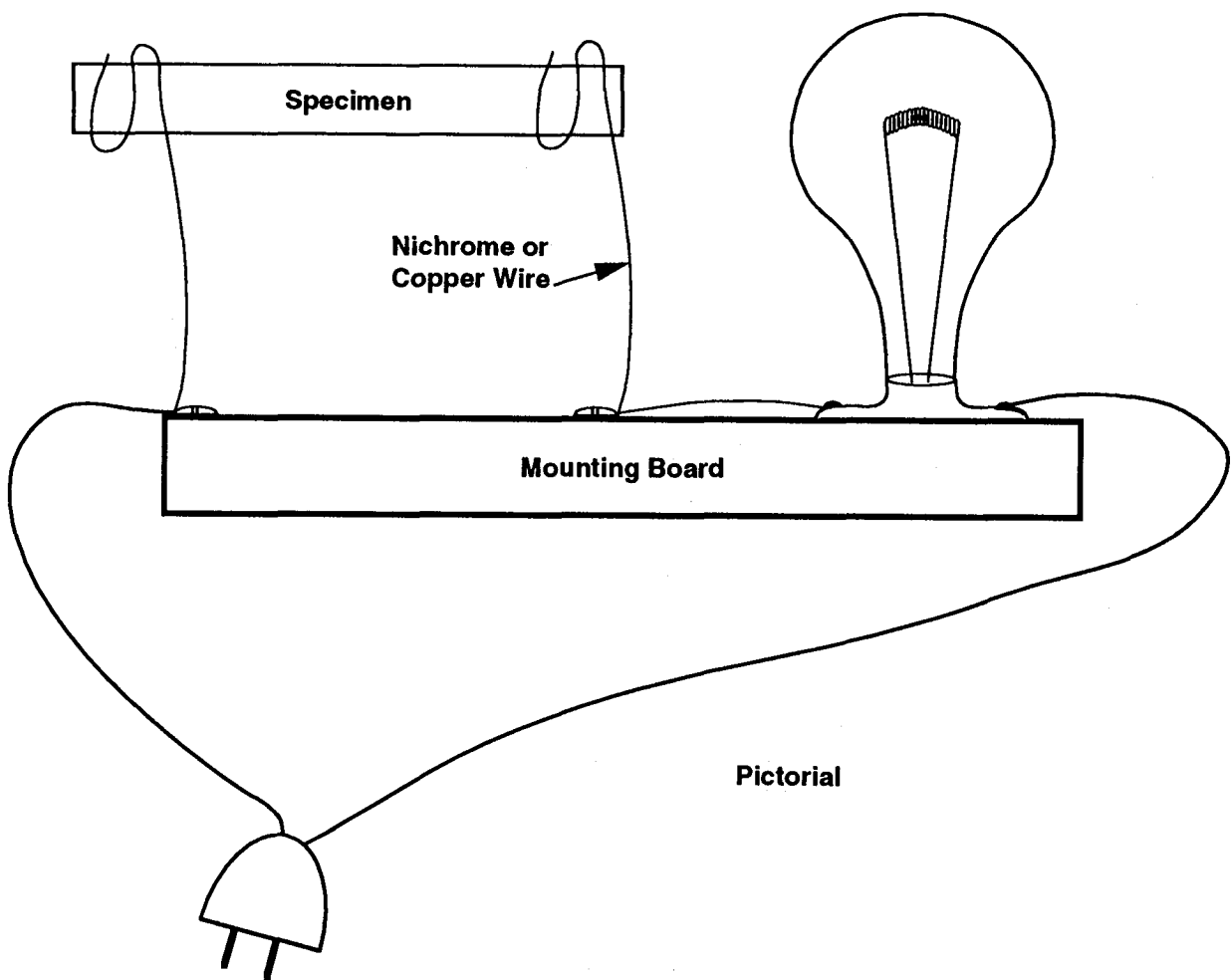
Pictorial

FIGURE 2.

446

of zirconium oxide, if carefully heated, will conduct sufficiently to light the bulb. The conduction mechanism in this case is the movement of oxygen ions between oxygen vacancies in the structure. Alternatively, a piece of silicon carbide heating element or furnace igniter can be used; in this case the conduction is by means of electrons that become able to move because of thermal energy supplied by heating. For another comparison, a steel nail of approximately 0.3-cm diameter will conduct over the entire temperature range, and the bulb will not dim perceptibly when the nail is heated.

If the AC electricity is replaced by a DC power supply capable of 110 V, 2 A, some interesting effects occur in the window glass. After the current flows for a few minutes, the glowing bulb will dim and will not conduct well even if the glass is heated strongly. The glass will now show a dark stripe at the negative contact and may show bubbles at the positive end. The bubbles are oxygen, and the dark stripe is caused by silicon ions in the glass that have been reduced to the metallic state. These effects occur because the glass is being electrolyzed by the current, just as a bath of water would be. If the glass is placed back in the contacts with its ends reversed (dark end is now connected to the positive contact) and heated, current will immediately flow upon heating because the polarized ends are now connected to oppositely charged contacts. Current will flow until polarization again occurs in the other direction.

SAMPLE DATA SHEETS: Not strictly applicable, though the demo would be good source material for students' journals.

INSTRUCTOR NOTES: Supervise the students closely while they are around live electrical circuits with bare wires. Always be certain that the apparatus is unplugged when working around the wires. If the copper wire contacts oxidize to the extent that contact resistance is too high for the bulb to light, the oxide can be reduced simply by heating the wire, the inner blue cone of the torch. The instructor may want to add this to the demonstration.

REFERENCES: Vertrees, T. H., "Ceramics Conductivity," Technology Focus, Fall/Winter 1991.

Touloukian, Y. S., ed., Thermophysical Properties of High-Temperature Solid Materials, Vol. 1 and Vol. 4. MacMillan, New York, 1967.

SOURCES OF SUPPLIES: Most items mentioned here should be available in a good hardware store.

Zirconium Oxide: One good source of the partially stabilized zirconium oxide tubing or rod that is most resistant to thermal shock is:

Advanced Ceramics Technology
990F Enterprise St.
Orange, CA 92667
(714) 538-2524
(Order several pieces, 0.64 cm (1/4") diameter x 10 cm long, cost unknown but likely less than $100 total).

Silicon Carbide: The most convenient and reasonable source of silicon carbide, except for pieces of discarded SiC heating elements, is furnace igniters made from the material. These are sized to operate on 110 volts, and include a suitable base and connector wires. Connect the two lead wires across the position normally occupied by the specimen in the test apparatus and heat the SiC with the torch to start current flowing. Igniters may be obtained for $25 or less from:

Igniter Systems, Inc.
12600 Clarence Center Rd.
Akron, NY 14001
(716) 542-5511

448

CONSTRUCTION AND TESTING OF SIMPLE AIRFOILS TO DEMONSTRATE STRUCTURAL DESIGN, MATERIALS CHOICE, AND COMPOSITE CONCEPTS

L. Roy Bunnell

Battelle
Pacific Norhtwest Laboratories
P. O. Box 999 MSIN P8-44
Richland, Washington 99352

and

Steven W. Piippo

Richland School District
Richland, Washington 99352

A DEMONSTRATION OF SIMPLE AIRFOILS: STRUCTURAL DESIGN AND MATERIALS CHOICES

L. Roy Bunnell
Pacific Northwest Laboratory,[a] Richland, Washington
Steven W. Piippo, Teacher
Richland School District, Richland, Washington

KEY WORDS: airfoils, composites, strength/weight ratio, structural testing

PREREQUISITE KNOWLEDGE: This unit is appropriate for a high school materials science class or lower-division college courses in structural engineering, materials science, or aeronautical engineering. Prepare for the project by explaining the following: the way that an airfoil shape generates lift (Bernoulli effect), the importance of airfoil shape regarding lift/drag ratio, and the structural requirements of a wing.

OBJECTIVE: Students will build and evaluate simple wing structures, and in so doing will learn about materials choices and lightweight construction methods.

EQUIPMENT AND SUPPLIES: Listed below are the materials required to conduct the project. The suggested quantities (see Table 1) should be sufficient material to construct three each of the six airfoil variations listed in Table 2,

TABLE 1. Materials for Building 18 Wings (including 50% excess)

Quantity, Each	Description[a]
36	Balsa sheet 1/16" x 3" x 36"
18	Balsa leading edge 3/8" x 5/16" x 36"
16	Balsa trailing edge 1/8" x 3/4" x 36"
12	Balsa 1/8" x 1/4" x 36"
9	Spruce 1/8" x 1.4" x 36"

(a) Wood is typically measured in English units.

TABLE 2. Wing Structural Variations

Variation	Description	Wt, g[a]
BW	Ribs 6 cm apart, balsa spars	38.9
BN	Ribs 3 cm apart, balsa spars	55.4
BWS	Ribs 6 cm apart, balsa spars, shear webs	53.0
SW	Ribs 6 cm apart, spruce spars	52.1
SN	Ribs 3 cm apart, spruce spars	56.9
SWS	Ribs 6 cm apart, spruce spars, shear webs	55.4

(a) Weights are those of the set built for this presentation, included here for reference. These were the weights used for the stiffness/weight and strength/weight ratios calculated below,

including 50% allowance for waste and mistakes. All required supplies can be purchased at any good hobby shop for under $200 (1991 prices).
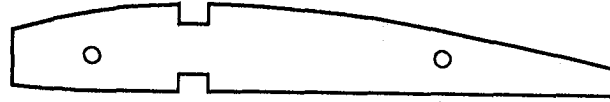
- a piece of fibrous ceiling tile about 60 x 120 cm, with a flat finish. Use back side if no flat tiles are available. (Before applying adhesive, the parts of the airfoil are pinned to the ceiling tile to ensure proper alignment; reference lines are used to control component orientation and spacing.)
- cyanoacrylate adhesive for model building; common brands are Zap or Hot Stuff
- bicarbonate of soda
- T-head pins, medium size
- transparent polyester covering material, Monokote (or equivalent) brand
- special iron designed for use in model construction
- special high-temperature heat gun designed for use in model construction
- steel templates, approximately 3 mm thick (cut to Clark Y airfoil shape, with notches for spars). X-Acto or equivalent hobby knives, with straight pointed blades

PROCEDURE: The various parts of a wing are illustrated and labeled for orientation in Figure 1. Figure 2 illustrates the actual airfoil size, which may be scaled larger or smaller using a photocopier. [Note that the two notches are placed to fit spars sized 0.64 cm by 0.32 cm (1/4 in. by 1/8 in.).] The six construction versions, all using the Clark Y airfoil, are listed in Table 2. The Clark Y was chosen for construction ease, since it is nearly flat-bottomed. These six versions are identical in cross section, but differ in the amount and placement

Shear Web - Vertical Grain Balsa

Section B-B' (without covering)

Clark Y

Section A-A'

B
B'

Leading Edge
Trailing Edge

Rib

A
A'

Rib Spacing

Shear Web

Spar

Top View of Wing Structure
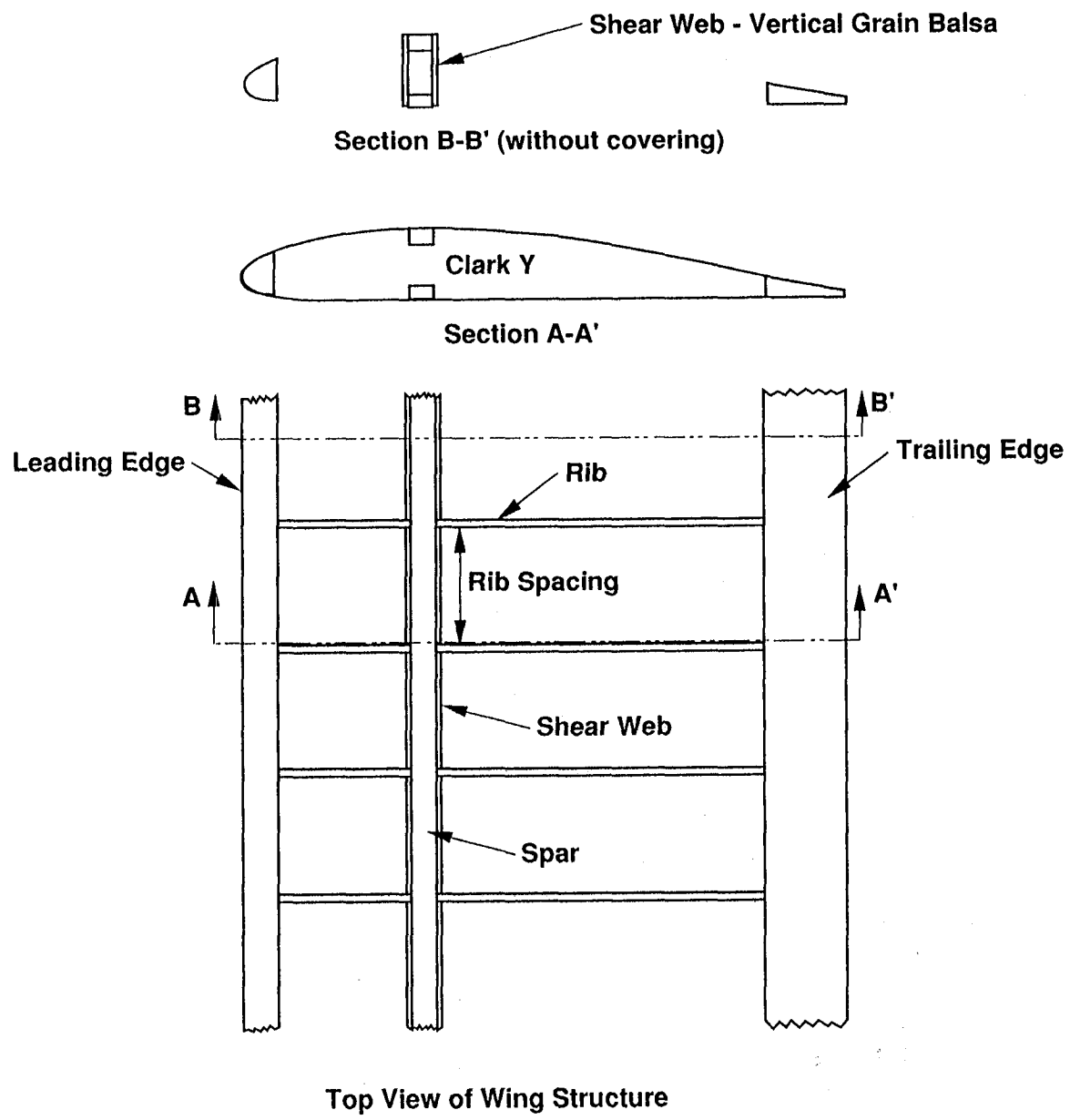
39208111.1

FIGURE 1. Construction Details of a Model Airplane Wing

39210034.1

FIGURE 2. Clark Y Airfoil, Actual Size Used in This Project

of internal reinforcements and in the use of either balsa or spruce as spar material. Assign each team of two or three students the task of constructing one of the six airfoils.

Construction: To make the ribs, the students will need to cut rectangles slightly larger than the templates from 1.6 mm (1/16-in.) sheets of balsa. Since the balsa rectangles will be clamped between the templates, oversized holes should be drilled in the balsa rectangles to match those in the templates. Next, carve and sand the ribs to the shape of the templates (avoid sanding the templates themselves). To make the notches for the spars, glue a 10-cm strip of 150-grit sandpaper to the 1/4-in. face of some scrap spruce spar wood. Sand the spar notches in the ribs, using care to avoid enlarging the notches in the templates.

Cover the building board (ceiling tile) with wax paper to prevent bonding the wing to the board. Pin the bottom spar in place on the building board. Pour bicarbonate of soda into a long narrow tray and dip each rib into the soda before placing it onto the bottom spar. The tiny amount of soda that clings to the rib accelerates the reaction rate of the cyanoacrylate and strengthens the bond. Hold each rib perpendicular to the building board, taking care that each closely follows its reference lines. Apply the cyanoacrylate; the bond will be complete in 2 to 3 seconds. (Use the cyanoacrylate in a well-ventilated area and avoid breathing the fumes.) Set the top spar securely into the notches, and apply cyanoacrylate to the joints. Pin leading and trailing edges in place using a 3-mm (1/8 in) shim under the leading edge, since the airfoil is not quite flat; then bond with cyanoacrylate.

If shear webs are to be attached to the spars, cut the webs so the grain is perpendicular to the building board, then bond to the front and back surfaces of the top spar with cyanoacrylate. The wing may now be removed from the building board and the shear webs bonded to the bottom spars. Glue a doubler of scrap spar material to the outer ribs at either end; this will prevent warpage as the covering material shrinks. Carefully sand the structure as necessary, and use a vacuum cleaner with brush to remove balsa dust. At this point, prepare the covering material by cutting it approximately 3 cm larger on
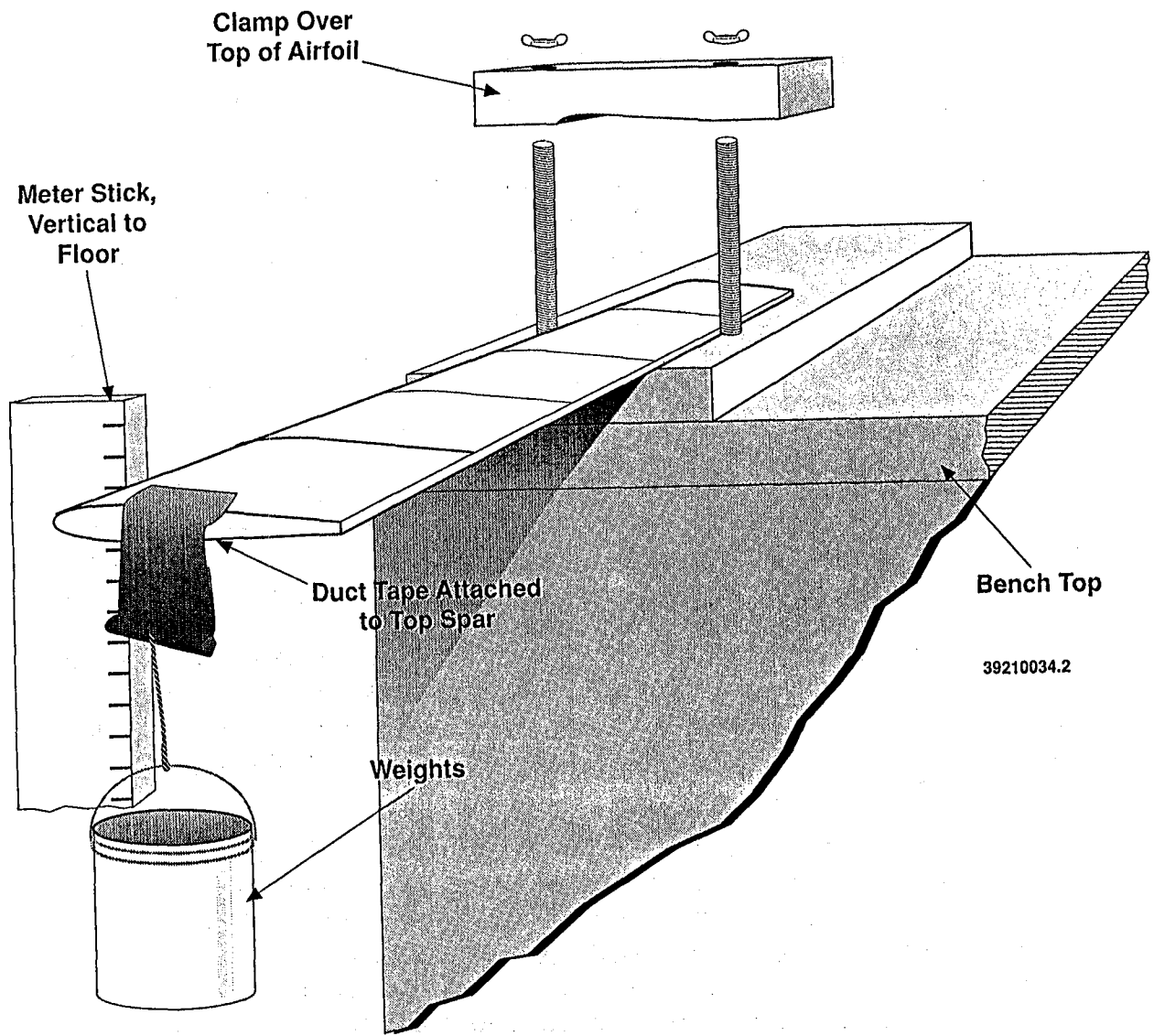
FIGURE 3. Arrangements to Test Stiffness and Strength of Airfoil Sections

all sides than the wing. Follow manufacturer's instructions for applying the covering, first tacking it in place using the iron, then using the heat gun to shrink the film.

Testing: Record the weight of each airfoil before testing for strength and stiffness. Then, using a clamp that fits the shape of the airfoil's top profile, fasten the airfoil to the edge of the workbench, allowing approx. 35 cm of the airfoil to hang free, like a cantilever. Since deflection under load is a cube function of length, the free length should be carefully controlled. Attach a plastic or cloth bag or small plastic pail to the top spar using strong string and duct tape. See Figure 3 for details. Using a meter stick fixed to a base, measure the distance to the nearest millimeter from the lower wing surface to the floor.

To measure the relative stiffness of the airfoil, apply weights (used wheel weights from a tire store will do) until a deflection of 1 cm is attained; weigh the container and weights, and record this weight. Continue to load the airfoil until failure occurs; record the failure weight and the approximate deflection at failure.

Be careful to avoid destroying the wing when failure occurs by suspending the weight container within 5 cm of the floor. When the airfoil fails, the distance the weight must drop to the floor is limited. After failure, examine the structure to locate the failure site, taking this information into consideration along with observations made during testing.

Discussion: In discussing cause for failure, students should speculate on what could have been done differently during construction. For instance, because all of our test structures failed in compression at the interface between the wing and the clamping fixture, a buttress at this point would be appropriate. If time permits, have students build and test a second airfoil (same cross section as the first) using their proposed remedies for increasing strength and stiffness and for minimizing weight. Alternatively, students may wish to simply duplicate their first airfoil, being more careful with wood selection and construction. Allow interested students to construct original designs, as long as their airfoils remain within the initial parameters of dimension, shape and material. An example of an original construction would be an airfoil cut from polystyrene insulation foam, using electrically heated wire and templates on each end. This airfoil could be covered with balsa sheeting bonded with epoxy. In spite of the weight penalty for such an airfoil, the improvements in strength and stiffness are impressive.

Plot the class's test results, using a simple bar graph like Figures 4 and 5. On the x-axis plot structure type; on the y-axis, plot either the weight to cause 1-cm deflection divided by the wing weight or failure weight divided by the wing weight. Observe and discuss scatter and trends. (Instructor should save results to use for comparison with subsequent classes.)

456

Based on tests conducted to prepare this presentation, Figure 4 shows the weight required to cause 1-cm deflection divided by the airfoil weight, which is proportional to the stiffness/weight of the various wing variations. On the strength of this single data set, the stiffness of wings built with either spar material appears to be substantially improved when shear webs are used. This is logical, because the combination of shear web and spar forms a box beam. The lightest structure, BW, shows stiffness/weight superior to airfoils built with spruce spars, except where shear webs were used. Finally, the airfoil with spruce spars had the highest stiffness/weight ratio, but only when shear webs were provided. Figure 5 shows the weight required to cause structural failure divided by the wing weight, for each of the six versions. The structures made with balsa spars and shear webs performed impressively for their weight, better than spruce-spar wings without shear webs. Although the shear-webbed wing made with spruce spars had the highest strength/weight, the difference was less than 10% more than the shear-webbed wing made with balsa
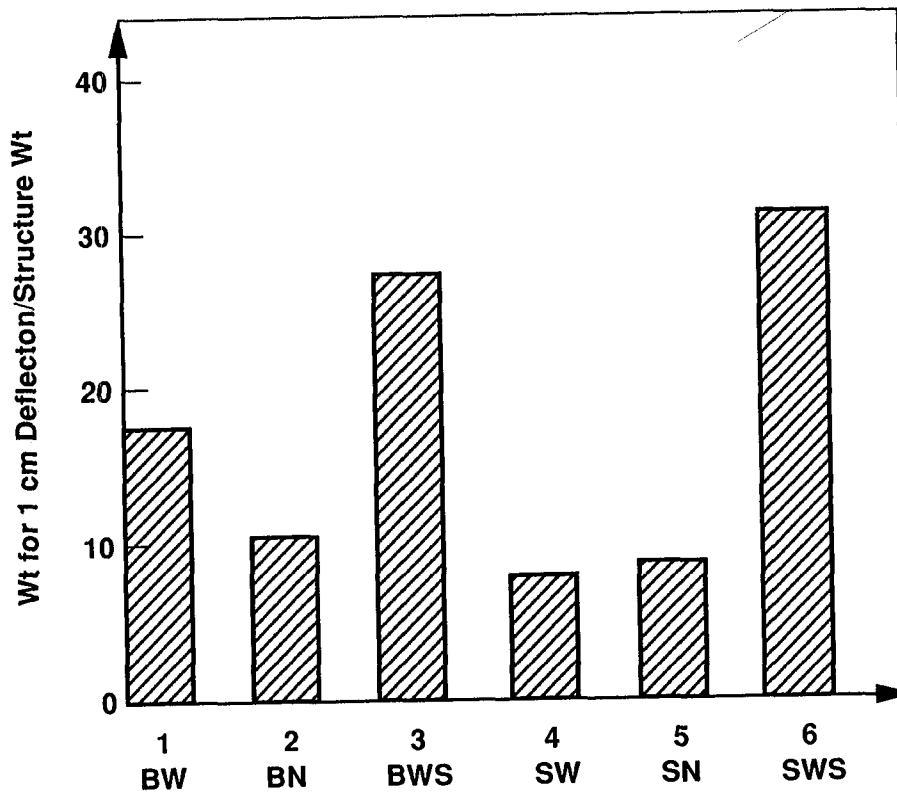
39210034.3

FIGURE 4. Stiffness/Weight Ratio of Six Structural Version of Same Airfoil
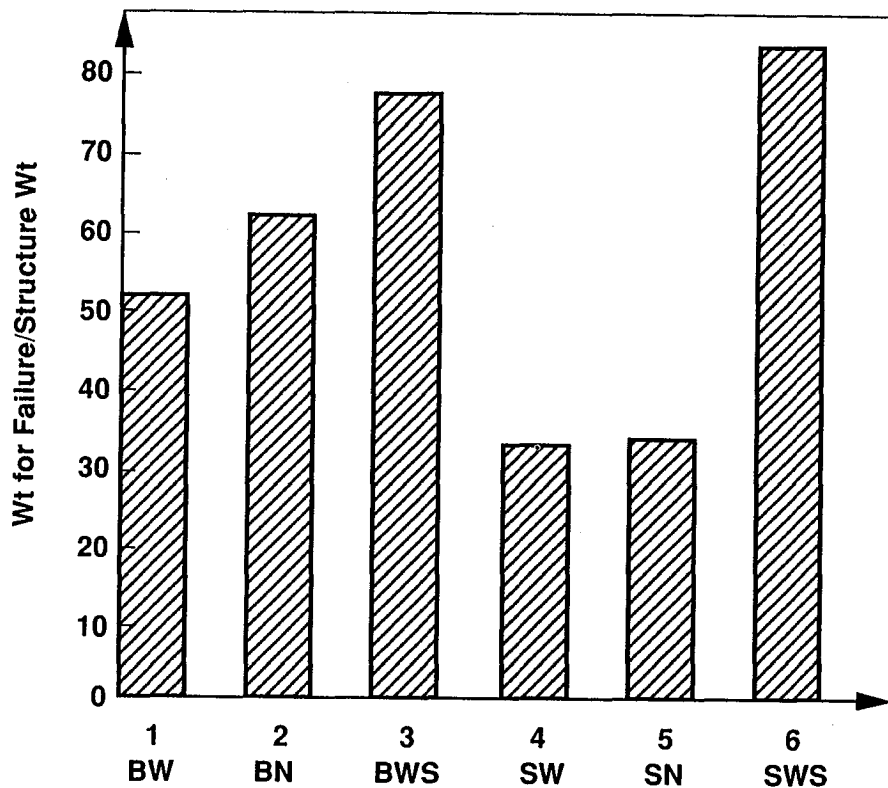
457

FIGURE 5. Failure Weight/Structure Weight Ratio for Six Structural Versions of Same Airfoil

spars. Of course, in an actual airplane wing design, the strength and stiffness would be critical factors in themselves and would only be divided by weight for purposes of comparison, as in this project.

INSTRUCTOR'S NOTES: The model airplane hobby offers students an excellent introduction to the basic techniques of producing the light, strong structures that make flight possible. Based on the principles of aircraft modeling, this project requires students to build an airfoil of constant cross section and to compare several variations of structural design and materials. Simple tests of the resulting airfoils enable comparisons of performance as a function of structural weight. Students should discuss whether the more elaborate construction methods are justified on the basis of added weight. Using modern materials and methods, airfoil construction and testing can be accomplished within the time and economic constraints of the classroom without requiring advanced craftsmanship of the students.

Note that the materials and construction techniques used to construct model airplanes may be unfamiliar to the average student. However, one or two students in many classes may have had experience in this particular hobby.

These students will be a valuable resource to the class, especially during the first round of airfoil construction; make use of such students.

SAFETY: Avoid breathing the fumes of reacting cyanoacrylate. In addition, take care not to bond fingers together with the cyanoacrylate, which adheres quickly and tenaciously to skin. If this should happen, use the debonding chemical available at hobby shops, or wait ten minutes before slowly <u>rolling</u> the bonded surfaces apart. Do not pull fingers directly apart or use sharp blades to cut skin surfaces apart. Take extra care to avoid getting glue into eyes.

REPORT DOCUMENTATION PAGE

Public reporting burden for this collection of information is estimated to average 1 hour per response, including the time for reviewing instructions, searching existing data sources, gathering and maintaining the data needed, and completing and reviewing the collection of information. Send comments regarding this burden estimate or any other aspect of this collection of information, including suggestions for reducing this burden, to Washington Headquarters Services, Directorate for Information Operations and Reports, 1215 Jefferson Davis Highway, Suite 1204, Arlington, VA 22202-4302, and to the Office of Management and Budget, Paperwork Reduction Project (0704-0188), Washington, DC 20503.

1. AGENCY USE ONLY(Leave blank)	2. REPORT DATE June 1993	3. REPORT TYPE AND DATES COVERED Conference Publication	
4. TITLE AND SUBTITLE National Educators' Workshop: Update 92 Standard Experiments in Engineering Materials Science and Technology		**5. FUNDING NUMBERS** 505-63-50-01	
6. AUTHOR(S) Compilers: James E. Gardner-NASA Langley Research Center, Hampton, VA; James A. Jacobs-Norfolk State Univ., Norfolk VA; Douglas F. Craig-Oak Ridge Nat. Lab., Oak Ridge, TN			
7. PERFORMING ORGANIZATION NAME(S) AND ADDRESS(ES) NASA Langley Research Center Hampton, VA 23681-0001		**8. PERFORMING ORGANIZATION REPORT NUMBER** L-17236	
9. SPONSORING/MONITORING AGENCY NAME(S) AND ADDRESS(ES) National Aeronautics and Space Administration Washington, DC 20546-0001; Norfolk State University, Norfolk, VA 23504; National Institute of Standards and Technology, Gaithersburg, MD 20899; United States Department of Energy, Oak Ridge, TN 37831-6132		**10. SPONSORING/MONITORING AGENCY REPORT NUMBER** NASA CP-3201	

11. SUPPLEMENTARY NOTES

Supporting Organizations: American Society for Engineering Education, ASM International, Battelle Pacific Northwest Laboratories, Martin Marietta Energy Systems, Inc., Materials Education Council of the United States, Westinghouse Environmental Management Company of Ohio, and American Society for Testing and Materials.

12a. DISTRIBUTION/AVAILABILITY STATEMENT Unclassified - Unlimited Subject Category 23	12b. DISTRIBUTION CODE

13. ABSTRACT *(Maximum 200 words)*

This document contains a collection of experiments presented and demonstrated at the National Educators' Workshop: Update 92 held at the Oak Ridge National Laboratory on November 11–13, 1992, in Oak Ridge, Tennessee. The experiments related to the nature and properties of engineering materials and provided information to assist in teaching about materials in the education community.

14. SUBJECT TERMS Materials; Experiments; Education		15. NUMBER OF PAGES 486
		16. PRICE CODE A21

17. SECURITY CLASSIFICATION OF REPORT Unclassified	18. SECURITY CLASSIFICATION OF THIS PAGE Unclassified	19. SECURITY CLASSIFICATION OF ABSTRACT Unclassified	20. LIMITATION OF ABSTRACT

NSN 7540-01-280-5500

National Aeronautics and
Space Administration
Code JTT
Washington, D.C.
20546-0001
Official Business
Penalty for Private Use, $300
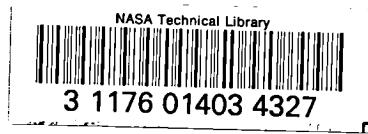
SPECIAL FOURTH-CLASS RATE
POSTAGE & FEES PAID
NASA
PERMIT No. G27

NASA

POSTMASTER: If Undeliverable (Section 158
Postal Manual) Do Not Return